Translational Investigation of Circadian Rhythm Modulating Drugs on Metabolic Disorder

A thesis submitted for the degree of Doctor of Philosophy at the University of Oxford

Trinity Term 2020



Zeinab Mohammad Wakaf

St. Cross College

Department of Pharmacology

Table of contents:

Acknowledgements.....6
Abstract.....7
Abbreviations.....8

CHAPTER 1: General Introduction **13**

1.1 Understanding Biological Rhythms.....***14***

1.2 The mammalian circadian system.....***16***
1.2.1 The SCN 16
1.2.2 The molecular clock 18
1.2.3 Peripheral oscillators 23
1.2.4 The photic pathway 24
1.2.5 Entrainment of peripheral clocks 26
1.2.6 *In vivo* and *in vitro* circadian rhythms 29

1.3 The metabolic syndrome.....***32***
1.3.1 Defining the metabolic syndrome 32
1.3.2 Pathophysiology of the MetS 35
1.3.3 Treatment of metabolic disorders 46

1.4 The role of circadian clock in metabolism.....***51***
1.4.1 Circadian regulation of glucose homeostasis 53
1.4.2 Circadian regulation of Lipid homeostasis 56
1.4.3 Cross-talk between metabolism and circadian clocks 58
1.4.4 Circadian disruption and the Metabolic Syndrome 60

1.5 Exploiting the clock to combat Metabolic syndrome.....***64***

1.6 Aims.....***68***

CHAPTER 2: Methods **70**

2.1 General Methods.....***71***
2.1.1 Cell culture technique 71
2.1.2 Differentiation of 3T3-L1 adipocytes 73
2.1.3 Luminescence detection experiments 75
2.1.4 mRNA Quantification 77
2.1.5 Cell viability assay 80
2.1.6 Pearson BCA Protein assay 80
2.1.7 Animals 81
2.1.8 General data analysis 81
2.1.9 General statistical analysis 82

2.2 Chapter 3- Methods.....***83***
2.2.1 Medium throughput screen 83
2.2.2 Assessing circadian rhythms 85

2.2.3 mRNA quantification of clock genes following drug treatment 85
2.2.4 Glucose uptake 86
2.2.5 Nile Red Staining of lipid droplets and its quantification in adipocytes 87
2.2.6 Nuclear staining and quantification in adipocytes 88
2.2.7 Quantification of mRNA adipogenic markers in adipocytes 89
2.2.8 Lipolysis 90
2.2.9 Assessment of Cellular Bioenergetics 91

2.3 Chapter 4- Methods 94
2.3.1 Assessing circadian rhythms 94
2.3.2 HRE-LUC assay 95
2.3.3 mRNA quantification 95
2.3.4 BC-STAR-PROM assay 96

2.4 Chapter 5- Methods 104
2.4.1 Linopirdine administration in a DIO-mouse model 104
2.4.2 mRNA quantification 104
2.4.3 Glucose and Insulin tolerance tests (GTT, ITT) 106
2.4.4 Plasma measurements 106
2.4.5 Histological staining of lipids in liver 107
2.4.6 *Ex-vivo* SCN cultures 108
2.4.7 Organotypic slices bioluminescence recording 109

2.5 Chapter 6- Methods 110
2.5.1 Reagents 110
2.5.2 Assessing circadian rhythms of CREB mutants 110
2.5.3 CREB/P-CREB quantification 111
2.5.4 cAMP-GloSensor and cGMP-GloSensor assays 112
2.5.5 CRE-LUC assay 112
2.5.6 Data analysis 113
2.5.7 mRNA quantification 113

CHAPTER 3: Identification and Evaluation of Circadian Modulators in Metabolism 114

3.1 Introduction 115
3.1.1 Aims 125

3.2 Results 126
3.2.1 Identification and validation of 3 circadian modulators. 126
3.2.2 Characterization of key circadian modulators in different cell lines 134
3.2.3 Validation of transcriptional change via mRNA 140
3.2.4 Investigating effects of lead circadian modulators on metabolic processes in adipocytes. 142

3.3 Discussion 159
3.3.1 Validation of the identified circadian modulators 159
3.3.2 Different circadian amplitude enhancers diverge in their metabolic phenotypes 160
3.3.3 Role of the clock in the observed metabolic phenotypes 168

3.4 Conclusion 171

CHAPTER 4: Investigating the Mechanism of Action of Linopirdine 173

4.1 Introduction 174

4.1.1 Background on Linopirdine 174

4.1.2 Could Linopirdine have a second target? 176

4.1.3 Hypoxia and circadian signalling 178

4.1.4 Aims 181

4.2 Results 182

4.2.1 Is Linopirdine's amplitude enhancing effect mediated by KCNQ inhibition? 182

4.2.2 Investigating PHD2-linked pathways as possible targets for Linopirdine 192

4.2.3 Investigating the mechanism mediating Per2 amplitude enhancement 203

4.3 Discussion 218

4.4 Conclusion and future work 230

CHAPTER 5: Investigating Linopirdine's *in vivo* actions in a DIO-Model of Metabolic Syndrome 232

5.1 Introduction 233

5.2 Results 238

5.2.1 Acute treatment of Linopirdine in vivo reduces blood glucose levels 238

5.2.2 Linopirdine exacerbates metabolic syndrome in DIO-mouse model 240

5.2.3 Linopirdine reduces XBP1s mRNA expression in hypothalamus 245

5.2.4 Linopirdine reduces markers of insulin sensitivity in visceral fat and liver, but significantly improves them in skeletal muscles 248

5.2.5 Linopirdine exacerbates inflammation of visceral WAT in DIO-mice 254

5.2.6 Linopirdine treatment does not cause peripheral clock desynchrony 256

5.2.7 Linopirdine treatment increases markers of MEIS1 upregulation in different tissues 260

5.3 Discussion 262

5.4 Conclusion 272

CHAPTER 6: Investigating the Mechanism of Action of Zaprinast 274

6.1 Introduction 275

6.1.1 Background on Zaprinast 276

6.1.2 Role of cGMP and cAMP in the circadian machinery 276

6.1.3 CREB- a key transcription factor regulating circadian rhythms 283

6.1.4 Aims 287

6.2 Results 288

6.2.1 Zaprinast showed high specificity for cGMP 288

6.2.2 cGMP elevation induces Bmal1-promoter expression and period elongation 290

6.2.3 Zaprinast's circadian phenotype was attenuated by PKG inhibition 292

6.2.4 Zaprinast's circadian phenotype was unaffected by blocking CREB phosphorylation 294

6.2.5 Zaprinast's circadian phenotype was unaffected by inhibition of CREB DNA binding 299

6.2.6 Zaprinast showed no effect on CRE activation 301

6.2.7 mTOR inhibition reduced Zaprinast's period elongation without affecting Bmal1-promoter expression. 303

6.2.8 ERK inhibition potentiated Zaprinast's amplitude effect in Bmal1-dLuc U2OS cells but reduced its period elongation 305

6.3 Discussion 309

6.3.1 Significance of cGMP signalling in peripheral circadian clocks 310

6.3.2 The mechanisms underlying cGMP's circadian modulation 313

6.4 Conclusion 320

CHAPTER 7: General Discussion 321

7.1 Understanding Linopirdine's mechanism of action - a novel circadian enhancing molecule 323

7.2 Role of cGMP in peripheral clock regulation 325

7.3 In vitro and in vivo metabolic investigations of circadian modulators 326

7.4 Final overviews 333

References 335

Acknowledgements:

First and foremost, I would like to extend my deepest gratitude to my supervisor, Dr Sridhar Vasudevan for his tremendous support and invaluable advice. This project would not have been possible without his unwavering encouragement and enthusiasm. He has given me the freedom to purse my interests, the opportunities to grow, and the much needed support and guidance throughout my entire DPhil journey, for which I feel incredibly grateful and fortunate!

I would also like to thank the amazing members of the Vasudevan lab: Dr Harshmeena Sanghani, Dragos Mosneagu, Dr Dorota Nawrot, Farid Ibrahimjee and Brooke Prakash, for their support and unparalleled encouragement. Our long chats, laughs and unforgettable memories will always be cherished. I have also received excellent advice and guidance from Prof. Aarti Jagannath and members of the Jagannath Lab, Steven Walsh, Dr Lewis Taylor, Dr Anna Ashton and Norbert Varga, for which I am very thankful. I would also like to extend my sincere thanks to Steve for all his help with the next-generation sequencing experiment. His contribution was instrumental, and I am very grateful for all his support. Special thanks goes to Dragos for keeping me sane throughout the long tiring *in vivo* experiment, to Harshmeena for her assistance in SCN *ex-vivo* and organotypic cultures, and to Dorota and Lewis for their help in tissue extractions, their inputs were instrumental. Another thank you goes to Dr Mehdi Olive for training me to do the seahorse assay, his input and guidance were invaluable.

A very special thank you is dedicated to my parents, Ahla and Mohammad. Their unconditional love and support, and their unyielding guidance have shaped me into who I am today. I am forever grateful for everything they have done for me and owe all my accomplishments to them. Special thanks goes to my brother Ali for always standing by me, my brother Ahmad for his encouragement, and my sister Maryam for always being a phone call away through the ups and the downs. Their unwavering love, support and positive attitude inspire me to dream bigger, grow stronger, and strive for a better and kinder version of myself.

Special thanks goes to my second family, Hala, Nizar and Louwai for their constant support, their unparalleled generosity and love, and the much needed family gatherings, for which I am very grateful. Finally and most importantly, I cannot begin to express my appreciation to my husband, Kinan. He is my rock, and none of this would have been possible without his unwavering support and encouragement. His late-night car journeys to the lab, his patience waiting for me while my experiments drag, his energy and enthusiasm, and his unparalleled love made it all possible, and for which I feel truly blessed.

In closing, I would like to express my deepest appreciation to the Said Foundation for believing in me, and for their generous contribution towards my studies. I am very grateful for the people I have met and for the friendships I have made, and I look forward to working together with the rest of the inspiring cohorts to make a difference in our region and in my beloved home, Syria.

Abstract

The metabolic syndrome represents a cluster of metabolic anomalies (including hyperglycaemia, obesity, hypercholesterolemia), that affects 25% of the world's population and is recognised as a major risk factor for development of diabetes and cardiovascular diseases. Several key enzymes identified in this disorder are directly under circadian regulation and evidence from both pre-clinical research and epidemiological studies strongly implicate disturbed circadian rhythms in metabolic disorders. Further, the recent demonstration that pharmacological enhancement of the clock ameliorate symptoms of metabolic syndrome suggests this could indeed be a novel therapeutic paradigm. In light of this, our study aimed to investigate the effects of three novel circadian modulators using a range of *in-vitro* models for metabolic syndrome and translate these findings to an *in-vivo* model of obesity.

Following a medium-throughput screen of ~5000 molecules using reporter cell-lines that track clock gene expression, 3 novel circadian modulators; Linopirdine, Diclazuril and Zaprinast were identified. Phenotypic characterization of these molecules in adipocytes demonstrated a lack of correlation between pharmacological amplitude enhancement of the adipocyte clock and metabolic phenotypes, despite displaying positive metabolic outcomes in *in-vitro* model system, thereby highlighting the significance of drug targets in metabolic outcomes. Using in-silico mining, followed by transcription-factor screening and siRNA knockdown, we identified a novel mechanism mediating Linopirdine's chrono-modulatory effect. We provide the first direct evidence of MEIS1 being a regulator of circadian clock expression and demonstrate Linopirdine as a novel modulator of MEIS1 and HIF. Furthermore, in a diet-induced obesity mouse model, Linopirdine mimicked HIF and MEIS1 activation *in-vivo*, emphasising the significance of the drug target in predicting *in-vivo* outcomes. Finally, using Zaprinast as a pharmacological tool, we provided new insight on the role of cGMP in regulating peripheral circadian clocks. Thus, this DPhil thesis provides original insight into the use of chrono-modulators in the treatment of metabolic syndrome and introduces novel targets for circadian modulation.

List of abbreviations:

2DG	2-deoxyglucose
2DG6P	2-deoxyglucose-6-phosphate
ACC	Acetyl-CoA carboxylase
AdipoQ	Adiponectin
Akt	Protein Kinase B
AMPK	AMP-activated protein kinase
ANP	Atrial natriuretic peptide
ATF6	Activating transcription factor 6
ATGL	Adipose triglyceride lipase
BAT	Brown adipose tissue
BMAL1/2	Brain and muscle ARNT-like protein 1, 2 (or ARNTL)
BNP	B-type natriuretic peptide
cAMP	Cyclic adenosine monophosphate
CBP	CREB binding protein
CCG	Clock-controlled genes
CD36	Platelet glycoprotein 4
CEBP	CCAAT-enhancer-binding proteins
CELF6	CUG-BP, Elav-like factor 6
cGMP	Cyclic guanosine monophosphate
Cidea	Cell death activator
CK	Casein kinase
CKe	Casein Kinase ε
CLOCK	Circadian locomotor output cycles kaput (CLOCK) and (BMAL1/2)
CNG	cyclic nucleotide-gated cation channels
CNP	C-type natriuretic peptide
CRE	cAMP binding element
CREB	Ca^{2+}/cAMP response element binding protein
CRY1/2	Cryptochrome 1, 2
CT	Circadian time
DBP	Albumin gene D-site binding protein

DD	Dark/dark cycle (constant darkness)
Ddit3	Pro-apoptotic DNA damage-inducible transcript 3
DEC1/2	Deleted in esophageal cancer 1/2 (also referred to as BHLHE40/41 or Basic helix-loop-helix family member E40/E41
DGAT2	Diacylglycerol acyltransferase 2
DIO	Diet-induced obesity
DMT-1	Divalent metal transporter 1
DNL	De novo lipogenesis
ECAR	Extracellular acidification rate
eNOS	Endothelial nitric oxide synthase
EPO	Erythropoietin
ER	Endoplasmic reticulum
ERK	Extracellular signal-regulated kinase
ERSE	ER-stress response elements
FABP4	Fatty-acid-binding protein 4
FAS	Fatty acid synthase
FFA	Free fatty acids
FHL1	Four And A Half LIM Domains 1
FIH	Factor inhibiting HIF
FOXO1	Forkhead box class O-1 transcription factor
FTN	Ferritin
FXR1	Fragile X mental retardation syndrome-related protein 1
GAPDH	Glyceraldehyde 3-phosphate dehydrogenase
GC	Guanylyl cyclase
GCK	Glucokinase
GFI1B	Growth factor independent 1B
GIP	Glucose-dependent insulinotropic polypeptide
GLP1	Glugacon-like peptide
Glut1-5	Glucose transporter 1-5
GR	Glucocorticoid receptor
HES5	Hes Family BHLH Transcription Factor 5
HEY2	Hairy/enhancer-of-split related with YRPW motif protein 2
HFD	High-fat diet

HIF1α	Hypoxia inducible factor α
HINFP	Histone H4 Transcription Factor
HK	Hexokinase
HRE	HIF response elements
HSL	Hormone sensitive lipase
HSPA1A	Heat Shock Protein Family A Member 1A
IH	Intermittent hypoxia
IL-6	Interleukin 6
iNOS	Inducible nitric oxide synthase
INSR	Insulin receptor
ipRGC	Intrinsically photosensitive retinal ganglion cells
IRE1	Inositol requiring enzyme 1
IRS1/2	Insulin receptor substrate 1, 2
JUN	c-Jun
KD	Knockdown
KID	Kinase inducible domain
LD	Light/dark cycle
LEPR	Long isoform leptin receptors
LFC	Logarithmic fold change
LPL	Lipoprotein lipase
MAFB	MAF BZIP Transcription Factor B
MAFG	MAF BZIP Transcription Factor G
MAX	myc-associated factor X
MBLN1	Muscleblind Like Splicing Regulator 1
MCP-1	Monocyte chemoattractant protein-1
MEF	Mouse embryonic fibroblasts
MEF2D	Myocyte specific enhancer factor 2d
MEIS1,3	Meis Homeobox 1,3 or Myeloid ecotropic viral integrations site-1
MetS	Metabolic syndrome
MKP-1	Mitogen-activated Protein Kinase (MAPK) Phosphatase 1
MPC	Mitochondrial pyruvate carrier
mTOR	Mechanistic target of Rapamycin
MTP	Microsomal triglyceride transfer protein

NAD	Nicotinamide adenine dinucleotide
NADP	Nicotinamide adenine dinucleotide phosphate
NAFLD	Non-alcoholic fatty liver disease
NASH	Non-alcoholic steatohepatitis
NEFA	Non-esterified fatty acids
NF-kB	Nuclear factor–kapa B
nNOS	Neuronal nitric oxide synthase
NO	Nitric oxide
NOS	Nitric oxide synthase
NPAS2	Neuronal PAS domain protein
NTC	non-targeting siRNA control
OCR	Oxygen consumption rate
PACAP	Pituitary adenylate cyclase-activating polypeptide
PAX2	Paired box protein 2
PDE	Phosphodiesterase
PDK1	Protein kinase 3-phosphoinositide-dependent protein kinase 1
PEPCK	Phosphoenolpyruvate carboxykinase
PER1/2/3	Period 1, 2, 3
PERK	PKR-like ER-resistance kinase
pGC	Particulate guanlyly cyclase
PGC1α	Peroxisome proliferator-activated receptor γ coactivator 1 α
PHD	Prolyl hydroxylase enzyme
PI(3)K	Phosphoinositide-3-kinase
PKA	Protein Kinase A
PKG	Protein kinase G or cGMP-regulated protein kinase
POMC	Pro-opiomelanocortin
PPRE	Peroxisome-proliferator elements
PRC	Phase response curve
Prdm16	PR domain containing 16
RBM42	RNA Binding Motif Protein 42
REV-ERBα	Nuclear receptor subfamily 1, group d, member 1 or NR1D1
RHT	Retinohypothalamic tract
RLS	Restless leg syndrome

RORE	Retinoic acid-related orphan receptor response elements
RORα	Retinoid-related orphan receptor α
RXRA	Retinoid X Receptor Alpha
RXRB	Retinoid X Receptor Beta
SCN	Suprachiasmatic nucleus
SCRD	Sleep and circadian rhythm disruption
sGC	Soluble guanylyl cyclase
SIRT1	Sirtuin 1
SNP	Sodium-nitroprusside
SP4	Specificity protein 4
SREBP-1C	Sterol regulatory element-binding protein 1
STAT2-4	Signal Transducers and Activators of Transcription
T2DM	Type 2 Diabetes Mellitus
TF	Transcription factor
TG	Triglyceride
TGH	Triglyceride hydrogenase
TGH	Triglyceride hydrolase
THRB	Thyroid hormone nuclear receptor beta
TNF	Tumour necrosis factor
TTFL	Transcription translation feedback loop
UCP	Uncoupling protein
UPR	Unfolded protein response
VEGF	Vascular endothelial growth factor
VIP	Vasoactive intestinal polypeptide
VLDL	Very low density lipoproteins
WAT	White adipose tissue
XBP1	X-binding protein 1 transcription factor
XBP1s	X-binding protein 1 splice variant
YY1	Yin Yang 1
ZT	Zeitgeber time

CHAPTER 1:

General Introduction

Modern societies are exhibiting a major rise in metabolic disorders (Batsis et al., 2007; Eckel et al., 2005; Julia et al., 2009). This rise is not unique to adults, but also extends to children and adolescents (Julia et al. 2009). Although genetics is a contributing factor (Groop 2005), the dramatic increase in production of high calorie foods that are nutritionally inadequate in addition to the general decrease in energy expenditure, most often linked to sedentary life-styles, have unquestionably added to the prevalence of metabolic disorders. Moreover, evidence from both human and mice studies show that circadian disruption induced environmentally and/or genetically (through alterations of circadian clock machinery) is a major risk factor for obesity, and can lead to significant metabolic anomalies. Therefore, the overall purpose of this DPhil thesis was to identify novel chrono-modulators and gain insight on how pharmacological modulation of circadian clock function influences the development of metabolic disorders.

1.1 Understanding Biological Rhythms

Since the beginning of life, some 3.8 billion years ago, the Earth has seen trillions of dawns and dusks. These daily solar cycles follow the Earth's rotation upon its axis, creating discrete periods of day and night, with predictable daily oscillations of approximately 24 hours. In order to optimise energy utilisation and sequester biological process to periods of day when they are needed most, organisms have evolved intrinsic biological and physiological rhythms that help anticipate and adapt to environmental changes. These internally generated daily rhythms are referred to as "circadian rhythms" (Latin for about a day, "circa" and "dies", respectively). Almost all organisms on Earth exhibit some form of rhythm, from cyanobacteria and plants to humans (Bell-Pedersen et al. 2005). The sleep wake cycle is a well-known target of

the circadian system. However circadian rhythms also control and modulate metabolic and physiological functions, including body temperature, blood pressure, glucose homeostasis, hormone secretions and even mood (Hastings et al. 2003).

The first ever report of circadian rhythms was made by Jean Jacques d'Ortous de Mairan, in 1729, who visually observed 24-hour recurrent changes in the *Mimosa pudica* plant. In his work, De Marian reported that Mimosa leaves exhibited daily patterns of movement, opening during the day and closing at night, and remarkably, these patterns continued under constant darkness (De Mairan 1729). This was the first evidence of an endogenous timekeeping rhythm in plants. Subsequently, in the 1930s, Erwin Bünning confirmed this finding by monitoring leaf movements using a kymograph, and proposed the term "biological clock" for these plant-based endogenous rhythms (Bünning 1971). Consequently, between the 1950s and 1960s, ground-breaking work by Jürgen Aschoff and Colin Pittendrigh showed that biological clocks can be re-set to environmental cues and exist in mammals including humans (Daan and Pittendrigh 1976; Aschoff 1965). Following decades of research, a criteria for circadian rhythms was established. An oscillation is thought to be circadian if it fulfils the following criteria: 1) the observed pattern fluctuates every 24 hours at approximately the same time each day 2) The rhythm continues in the absence of external cues (*zeitgebers*) such as light or food, and thus is endogenously generated 3) the rhythm is "entrainable", meaning it can be re-set upon stimulation and exhibits a specific phase relationship with the external environment, allowing a genuine depiction of the environmental status (Bünning 1971; Daan and Pittendrigh 1976).

1.2 The mammalian circadian system

1.2.1 The SCN

Mammals have evolved a hierarchical circadian system in order to maintain rhythmicity throughout their complex biology. The master synchroniser, or maestro, of this system is the suprachiasmatic nucleus (SCN) within the anterior hypothalamus (Weaver 1998). The SCN is a bilateral symmetrical nuclei, located lateral to the third ventricle just over the optic chiasm. The intricate neuronal network making up the SCN is enclosed within a diameter of 10 μm and comprised of approximately 45,000-50,000 neurones in humans and 15,000-20,000 neurones in rodents, and it is these neurones that make up the autonomous robust master clock (Hofman et al. 1988; Welsh, et al. 2010; van den Pol 1980).

The function and localisation of the master clock was established via a series of lesion studies. First, specific bilateral ablation of the nuclei significantly deteriorated rhythms in corticosterone, and drinking activity (Moore and Eichler 1972; Stephan and Zucker 1972). This provided the foundations for understanding SCN function, given only the SCN nuclei was specifically lesioned. Further studies by Ralph et al highlighted the robustness and autonomy of the SCN rhythms, where neural transplants from a fetal hamster donor not only restored behavioural rhythms in hamsters with ablated SCN, but also determined the period of the animal (Ralph et al. 1990). Furthermore, similar SCN lesion studies later confirmed that SCN provides an evolutionary advantage, given animals with arrhythmic circadian clocks as a result of

SCN ablation were at higher mortality risk from predators due to their unsuitably timed activity (DeCoursey et al. 1997; DeCoursey, Walker, and Smith 2000).

In animals, such as nocturnal rodents, which are active during the night and sleep during the day, *in vivo* spontaneous electrical activity within the hypothalamus monitored using electrophysiological techniques was shown to be completely opposite within the SCN, relative to the neighbouring regions (Inouye and Kawamura 1979), demonstrating that the phase relationship of the SCN to the light-dark cycle remains the same. This was shown by *ex vivo* and *in vitro* findings, where SCN rhythmic electrical activity was shown to peak during the subjective day, during which a nocturnal animal would be asleep and diurnal animal, awake, and trough at subjective night (Green and Gillette 1982; Shibata et al. 1982; Ding et al. 1994). This rhythmicity corresponded to light-mediated depolarisation of SCN cells via glutamate in mice (Castel et al. 1993).

The ability of the SCN to generate such robust rhythmic activity arises due to its incredibly strong intra-neuronal communication where the 50,000 or so neurones (in humans) couple to give a single unitary output. Using tetrodotoxin (a sodium channel blocker) on SCN neuron cultures eliminated cell-cell communication and subsequently desynchronised the rhythmic output, even though individual neuronal cellular rhythms were unaffected (Shibata and Moore 1993), suggesting maintaining SCN neuronal synchrony is key in its circadian timekeeping function. Furthermore, glial cells also contribute towards SCN rhythms, where astrocytes have been shown to exhibit antiphase activity to SCN (showing activity during circadian night-time),

thereby inhibiting SCN rhythms by regulating extracellular glutamate levels (Brancaccio et al. 2017).

1.2.2 The molecular clock

SCN neurones exhibit autonomous circadian properties capable of generating robust 24-hour rhythms. These rhythms are governed by diurnal fluctuations in clock gene expression, a mechanism uniformly found in the brain and the body alike, driven through a series of interlocking transcription translation feedback loops (TTFL) (Takahashi 2017). The ground-breaking work that led to our current understanding of the mammalian clock and shed light on the importance of this molecular clockwork, was acknowledged recently by the 2017 Nobel Prize in Physiology or Medicine, awarded to Hall, Rosbash and Young for their work on the molecular clock of *Drosophila melanogaster* (Dibner and Schibler 2018).

The principal driving force of the molecular clockwork is the primary TTFL, involving proteins that promote the expression of their own repressors (Figure 1.1). The positive arm of the clock, and the main transcriptional drive, consists of circadian locomotor output cycles kaput (CLOCK) and brain and muscle ARNT-like protein 1/2 (BMAL1/2) (which is also referred to as aryl hydrocarbon receptor nuclear translocator like or ARNTL), while the negative arm involves period 1/2/3 (PER1/2/3) and cryptochrome 1/2 (CRY1/2). At dawn, the rhythmically expressed BMAL1 and the constitutively expressed CLOCK heterodimerize and bind to E-box elements within target genes (at the canonical recognition sequence CACGTG), promoting transcription (King et al. 1997; Gekakis et al. 1998). Such function is possible as both components are part of the basic helix-loop-helix (bHLH)-PAS

transcription factor family, capable of protein-DNA and protein-protein interactions (Shearman et al. 1999). The CLOCK-BMAL1 dimer then drives rhythmic expression of thousands of genes, including their own repressors, *Per1-3* and *Cry1/2* genes (Gekakis et al. 1998; Kume et al. 1999; T. K. Sato et al. 2006). Indeed, approximately 43% of the mammalian protein-coding transcriptome is clock regulated and display 24-hour circadian rhythms in a tissue-specific manner (Zhang et al. 2014), emphasizing the significance of the biological clock in regulating physiology. Subsequently, *Per* and Cry mRNA levels increase during the day, and are translated into PER and CRY proteins, which can form complexes with themselves as PER-PER homomers PER-CRY heterodimers (Takahashi 2017). PER is then phosphorylated by the Casein Kinase 1 family of kinases (CK1) among other kinases marking it for degradation. Interestingly, formation of the PER-CK1 complex helps CRY binding, generating the CRY-PER-CK1 complex which stabilises PER and prevents its phosphorylation and degradation in the cytoplasm. CRY and PER within the CRY-PER-CK1, however, are phosphorylated by other kinases that allow its translocation into the nucleus where it inhibits CLOCK-BMAL1 transcription of the *Per* and *Cry* genes (Jagannath et al. 2017), forming the core negative arm of the TTFL. As a result, CRY-PER-CK1 complex levels start increasing during the day, peak at dusk, and trough the following dawn. The period of the clock is primarily set by the stability/degradation rate of the CRY-PER-CK1 complex and the reactivation of CLOCK-BMAL1 mediated transcription. PER proteins are phosphorylated and ubiquitinated by casein kinase 1ε/δ (CSNK1ε/δ) while at least two F-Box proteins target CRY proteins (FBXL3 and 11) (Lowrey et al. 2000; Akashi et al. 2002; Godinho et al. 2007), which allows CRY and PER proteins levels to trough just before dawn.

The robustness of the clock is also maintained by an interlocked secondary TTFL that regulates BMAL1 expression via the retinoid-related orphan receptor α (RORα) and nuclear receptors reverse erythroblastosis virus α (REV-ERBα) (referred to as NR1D1 or nuclear receptor subfamily 1, group d, member 1). These nuclear receptors compete over retinoic acid-related orphan receptor response elements (RORE) in the *Bmal1* promoter region, either inducing or repressing its transcription, respectively (Akashi and Takumi 2005; Guillaumond et al. 2005). Indeed, using gene knockout and RNA interference, RORα has been shown to control amplitude of *Bmal1* gene expression, while REV-ERBs are necessary for maintaining rhythmic *Bmal1* expression (Liu et al. 2008). Furthermore, *Rev-ervbα* and *Rorα* themselves are under the control of CLOCK-BMAL1 transcription, as they both hold E-boxes within their gene promoters. Their mRNA levels fluctuate in congruence with core clock oscillations, inducing or supressing *Bmal1* expression in a timely manner (Sato et al. 2004; Guillaumond et al. 2005) allowing BMAL1 protein levels to fluctuate in antiphase to CRY and PER proteins.

A tertiary TTFL has also been identified, which consists of the transcription factor deleted in esophageal cancer 1/2 (DEC1/2) (also referred to as BHLHE40/41 or basic helix-loop-helix family member E40/E41) which inhibit CLOCK-BMAL1 transcription of *Per* by competing over E-box binding, and/or through direct protein-protein interaction with BMAL1 (Honma et al. 2002) . *Dec1/2* transcription itself is also under clock control. It has been shown to be rhythmic, peaking during subjective day and its transcription is driven by both CLOCK-BMAL1 and RORα (Honma et al. 2002; Ozaki et al. 2012). Having such auxiliary loops is vital in maintaining robustness of circadian clocks, allowing them to be more resilient to changes from external stimuli.

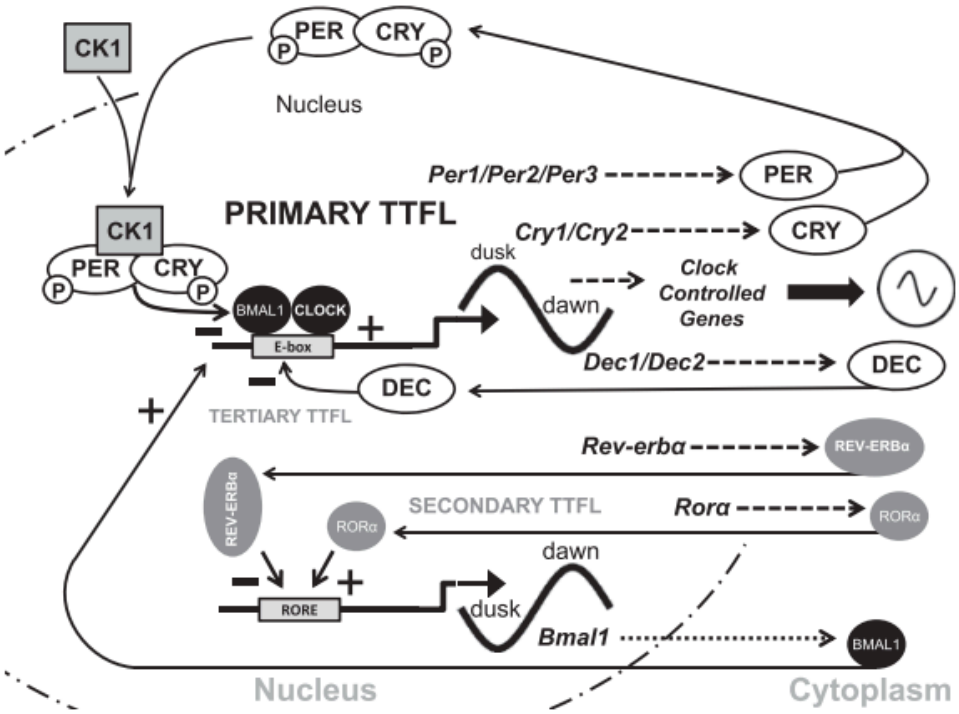


Figure 1.1. The mammalian molecular clock. (Adapted from Jagannath et al, 2017)

The main driving force of the mammalian molecular clock is provided by the transcriptional push initiated by CLOCK (Circadian Locomotor Output Cycles Kaput) and BMAL1 (Brain muscle arnt-like 1) protein dimerisation. CLOCK is constitutively expressed while *Bmal1* gene results in rhythmic production of BMAL1 protein. The formed CLOCK-BMAL1 heterodimer binds to E-boxes and promotes the rhythmic expression of Per1, Per2 and Per3 as well as Cry1 and Cry2. The different PER and CRY proteins also form complexes which, after binding with Casein Kinase 1 (CK1) and undergoing phosphorylation by other kinases, they then shuttle back into the nucleus and inhibit CLOCK-BMAL1 transcription, and thus their own transcription, forming the main negative arm of the transcription translation feedback loop (TTFL). The degradation rate of the CRY-PER-CK1 complex in the nucleus is a pivotal process in establishing the period of the clock and the net result of different kinases targeting and degrading PER and CRY is a rhythmic pattern of their expression, with their lowest transcriptional levels occurring just before dawn. Light is the most important zeitgeber (synchronizer) of SCN clock which is able to entrain the clock to the dawn/dusk cycle through up-regulation of Per1 and Per2 transcription.

A secondary TTFL exists as well, targeting BMAL1 expression. The nuclear receptors RORa and REV-ERB*α* cause activation and repression of BMAL1 expression respectively, via competitive binding at ROR elements (retinoic acid-related orphan receptor response elements/ROREs) in the Bmal1 promoter. Given both ROR*α* and REV-ERB*α* have E-boxes, they are rhythmically expressed in response to CLOCK-BMAL1 expression, with ROR peaking at dawn while REV-ERB*α* peaking at dusk- resulting in a combined effect of BMAL1 levels rising at dusk, peaking at dawn, then reaching its minimum just before dusk. As a result, BMAL1 rhythms are in antiphase to CRY and PER.

The tertiary TTFL is mediated by DEC1 and DEC2 proteins, which inhibit CLOCK-BMAL1 mediated transcription of clock controlled genes and reinforce the inhibitory effect of PER-CRY dimer. Finally, CLOCK-BMAL1 heterodimer binds to E-boxes in different clock target genes that possess E-boxes in their promoters, resulting in global circadian rhythms in behaviour and physiology.

Redundancy amongst the core clock genes has been revealed by the use of genetically modified mice. For instance, mice lacking either *Per1* or *Per2* display gradual arrhythmicity following extended periods of constant darkness, whereas deletion of *Per3* shows no effect on behavioural rhythms, placing the latter outside the core circadian machinery (Bae et al. 2001; Shearman et al. 2000). On the other hand, deletion of both *Per1* and *Per2* is associated with a direct onset of arrhythmicity, suggesting that these genes are somewhat functionally redundant (Bae et al. 2001). Equally, deletion of *Cry1* or *Cry2* genes cause a shorter period of 22.5 hours or a longer one of 24.6 hours, respectively, and introducing double *Cry1/Cry2* deletions trigger immediate arrhythmicity, therefore suggesting similar partial redundancy of the *Cry* genes (van der Horst et al. 1999; Vitaterna et al. 1999). Furthermore, *Clock* and its sequence-similar neuronal PAS domain protein (*NPAS2*) are functionally redundant; as *Clock* or *NPAS2* deficient mice both display normal behavioural circadian rhythms, while double knockout mice exhibit immediate arrhythmicity (DeBruyne, Weaver, and Reppert 2007; Landgraf et al. 2016). On the contrary, genetic deletion of *Bmal1* causes full arrhythmicity, therefore suggesting lack of functional redundancy between *Bmal1* and *Bmal2*. Given *Bmal2* expression is directly under the control of *Bmal1* and is 20% lower (Bunger et al. 2000), it's not surprising that deletion of *Bmal1* functionality would affect *Bmal2*.

1.2.3 Peripheral oscillators:

Autonomous molecular clocks are not unique to the SCN but are widely distributed throughout the body in peripheral tissues as well non-SCN neurones in the brain. As part of the hierarchical circadian system, oscillators can be divided into 2 main categories: master and slave oscillators (Balsalobre 2002), with the master oscillatory being the SCN. Subsidiary oscillators have been reported in most body parts including pineal gland, pituitary gland, heart, kidney, lungs, liver, muscle, skin and even cornea. Furthermore, cells in culture also maintain their circadian rhythmicity, stressing the conserved nature of molecular clocks throughout different tissues (Abe et al. 2002; Yoo et al. 2004; Balsalobre, Damiola, and Schibler 1998).

Despite the conservation of the molecular clockwork across different cells and tissue, cell-type specific differences have been reported. On one hand, relative to SCN, peripheral tissues oscillate for fewer cycles and gradually lose synchrony in the absence of SCN input. Although each cell exhibits autonomous 24-hour oscillations, lack of cell-cell communication could drift cells into desynchrony (Balsalobre, Damiola, and Schibler 1998). Moreover, different tissue cultures have been shown to display differential phase of their clock gene expression (Yoo et al. 2004). In addition, various cultured cell lines like human U2OS cells, murine NIH-3T3 fibroblasts, murine 3T3-L1 adipocytes and murine MMHD3 hepatocytes have been shown to display different circadian phenotypes following gene knockdown of core clock (*Bmal1, Clock, Npas2, Per, Cry*) or auxiliary genes (*Rev-erbα/β*, *Fbxl3*) (Ramanathan et al. 2014). Taken together, cell-type specific differences seem evident and could be associated

with differential cellular functions. Indeed, the molecular clock plays a vital role in regulating physiology and optimising tissue-specific functions in a timely manner. 3-16% of protein coding transcriptome display circadian rhythmicity in any individual tissue (Zhang et al. 2014), with numerous genes involved in neurotransmitter release (like monoamine oxidase A or tyrosine hydroxylase), hormones (like melatonin and glucocorticoids), glucose homeostasis (like Glut2, pyruvate kinase, glucagon receptor and glucose-6-phosphate transport protein 1) and lipid metabolism (like lipin1 and Hormone sensitive lipase) evidently under clock control (Cahill and Ehret 1981; Hampp et al. 2008; Weitzman et al. 1971; Lewy and Markey 1978; Panda et al. 2002). Thus, this highlights the significance of the molecular clock in regulating physiology.

1.2.4 The photic pathway:

Most organisms exhibit a genetically pre-determined endogenous circadian period of approximately 24 hours. Slight variations among organisms exist, with mice displaying a shorter period of 23.5 hours, and humans showing slightly longer free-running periods of 24.5 hours (Czeisler et al. 1999; Carskadon et al. 1999; Yoo et al. 2004). A *zeitgeber* represents any rhythmically occurring natural phenomenon that acts as a cue to entrain or re-set circadian clocks. Given the small degree of period deviation among different organisms from the 24-hour day, *zeitgebers* are vital in readjusting the endogenous rhythms to the external environment (van Esseveldt, Lehman, and Boer 2000).

The main *zeitgeber* relaying environmental cues to the SCN is light. Within the retina lies a small population of retinal ganglionic cells (RGC), making up 1-2% of all RGCs, which are highly specialised in communicating photic information from the external

environment (Berson, Dunn, and Takao 2002). These unique cells, known as the intrinsically photosensitive retinal ganglion cells (ipRGCs) contain melanopsin, a novel photopigment predominantly sensitive to blue light (λ_{max} =~480 nm) (Provencio, Cooper, and Foster 1998; Lucas et al. 2003). Their axons converge at the optic disk, forming the retinohypothalamic tract (RHT), which shapes the primary input pathway to the non-vision forming visual system (Hattar et al. 2002; Lucas et al. 2003). Cells from the RHT innervate SCN neurones, monosynpatically, interacting via glutamate and pituitary adenylate cyclase-activating polypeptide (PACAP) release at synapses (Castel et al. 1993; D. Chen et al. 1999).

The SCN consists of two anatomically and functionally distinct regions, the ventrolateral (or core) SCN and the dorsomedial (or shell) SCN. Differential neurochemical fingerprints of these two regions suggest they perform opposing functions (Abrahamson and Moore 2001; Mai et al. 1991). Owing to the close proximity of the SCN core to the optic chiasm, most of its neurones receive retinal input. The vasoactive intestinal polypeptide (VIP) is present in around 10% of all SCN neurones and is one of the major neurotransmitters in transmitting photic input (M. Tanaka et al. 1993; Welsh, Takahashi, and Kay 2010). VIP acts primarily on VPAC2 receptor and communicates time-of-day information to several brain regions, including the SCN core (with a third of its neurones expressing VPAC2) and the SCN shell, consequently promoting entrainment (Kalló et al. 2004; Piggins, Antle, and Rusak 1995; Reed et al. 2001). Shell neurones predominantly express arginine vasopressin, and act as output signals of the clock. These neurones relay SCN output into other brain regions, as a way of synchronizing different cells, tissues and organs throughout the body (Kalsbeek et al. 2010). Furthermore, 50% of shell neurones

express VPAC2 receptor, which allows for improved intra-SCN communication (Kalló et al. 2004).

1.2.5 Entrainment of peripheral clocks:

As the master synchroniser, the SCN establishes phase coherence across peripheral subordinate clocks through various direct and indirect routes. As summarised in Figure 1.2, these include rest-activity cycles driving feeding rhythms (Yamazaki et al. 2000; Damiola et al. 2000) and changes in body temperature (Brown et al. 2002) which are indirectly imposed by SCN through behavioural rhythms, as well as SCN-driven humoral and neuronal routes (Cailotto et al. 2009; Vujovic, Davidson, and Menaker 2008).

Indeed, daily feeding rhythms, which are normally in phase with rest-activity patterns, seem to be dominant *zeitgebers* for various peripheral organs (like the liver, heart, kidney and pancreas), as restricting feeding of nocturnal rodents to daytime has been shown to uncouple peripheral clocks from SCN, completely inverting their phase of gene expression (Damiola et al. 2000; Stokkan, Yamazaki, and Tei 1999). Moreover, changes in temperature also represent strong cues in mammals, *Neurospora*, and *Drosophila* (Cuninkova and Brown 2008). Mimicking body temperature fluctuations by imposing small rhythmic temperature changes in peripheral cells can maintain their rhythmicity and induce phase shifts, without affecting SCN phase (Brown et al. 2002), therefore highlighting its importance in establishing peripheral clock synchrony.

On the other hand, SCN has also been shown to drive rhythmic plasma glucocorticoid hormone levels via the hypothalamic-pituitary-adrenal axis (Oster et al. 2006). This is interesting, as the glucocorticoid receptor is prevalent in almost all cells except in the SCN (Balsalobre et al. 2000). Furthermore, *in vivo* evidence shows the glucocorticoid receptor (GR) agonist dexamethasone induces peripheral clock phase shifts without affecting the SCN (Balsalobre et al. 2000). In addition, hepatocytes lacking a functional GR entrain much faster to uncoupling daytime feeding than wildtypes (Le Minh et al. 2001), suggesting less responsiveness to SCN cues, and highlighting the importance of the glucocorticoid hormone as an entraining signal from the SCN.

The SCN also employs the autonomic nervous system as means of direct peripheral clock synchronization. Okamura and colleagues demonstrated a direct communication between the SCN and the adrenal cortex, where SCN lesioning abolished light-induced rhythmic corticosterone secretion (Ishida et al. 2005). Furthermore, disruption of liver innervation also abolished nocturnal light-induced effects on liver clock gene expression, stressing the role of the autonomic nervous system as a gateway for relaying SCN signals to peripheral clocks (Cailotto et al. 2009).

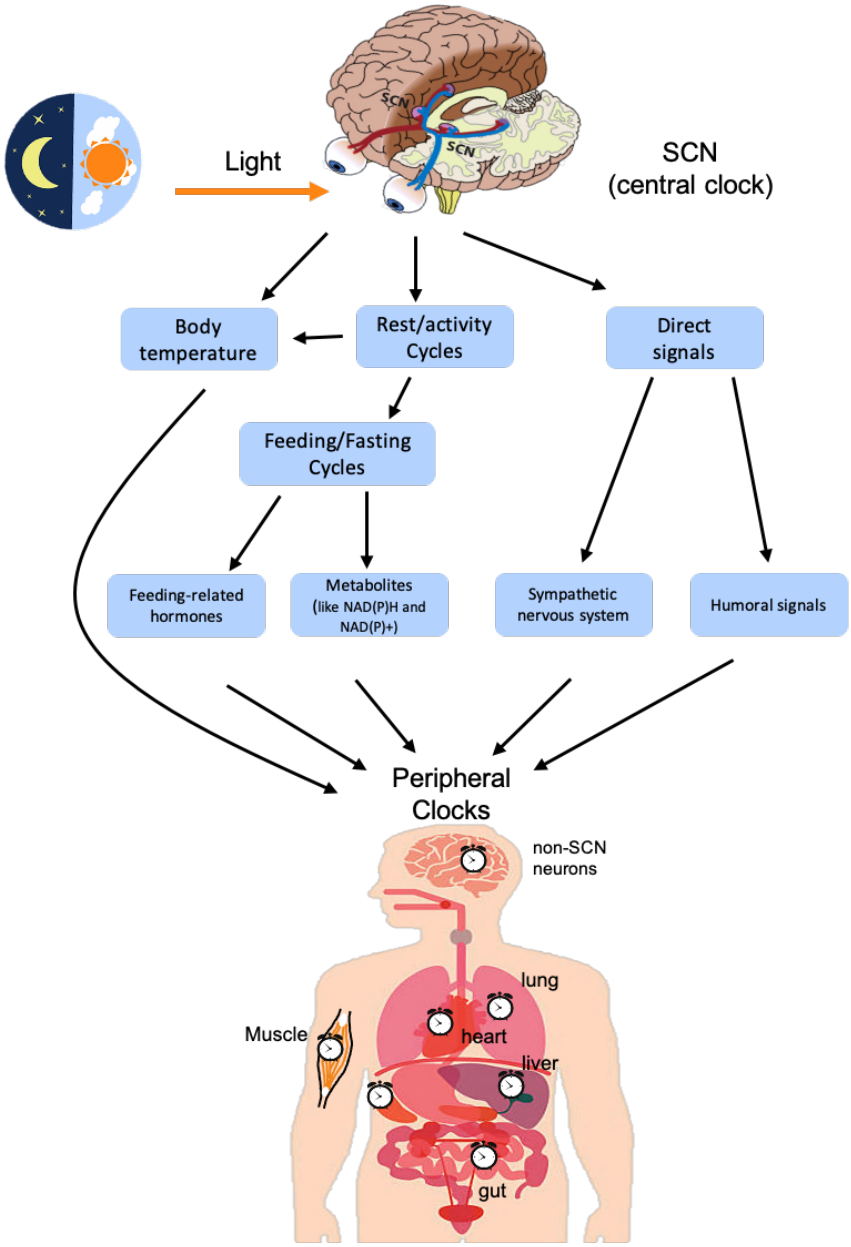


Figure 1.2. Schematic representation of SCN and peripheral clock entrainment pathways: (modified from Dibner et al. 2010).

Light from the environment enters the retina, where the ipRGCs reside, thereby transmitting this photic input via the RHT to the SCN. The SCN then relays time-of-day information to peripheral clocks across the body, including extra-SCN neurons, liver, lung, heart, etc. This is carried out indirectly through regulating rhythmic temperature changes that can sustain rhythmicity of peripheral clocks, or via behavioural rhythms of activity and rest that drive feeding/fasting cycles. The entrainment pathways from feeding/fasting can include hormones (like cholecystokinin, ghrelin, leptin and peptide YY) and food metabolite (like glucose and cholesterol) and redox-state markers (NAD(P)H/NAD(P)$^+$ ratio). Finally, SCN can also directly entrain peripheral clocks; either through sympathetic innervation of tissues like the liver and the adrenal glands, or through stimulation of hormonal secretions like glucocorticoids. Abbreviations can be found in the text.

1.2.6 In vivo and in vitro circadian rhythms:

Molecular clocks can be tracked through *in vivo* and *in vitro* means. Wheel-running locomotor activity corresponds to rodent behavioural rhythms and is one of the most widely used methods, as it accurately matches the SCN-driven endogenous rhythms of these animals (Jud et al. 2005). Owing to their small size, the capacity for genetic manipulation and their conserved circadian anatomy, mice are very valuable species for circadian research. Although, they are nocturnal and display most of their locomotor activity during dark phase, the phase of their molecular clocks is nonetheless consistent with diurnal species (Mrosovsky et al. 2001; Caldelas et al. 2003; Ripperger, Jud, and Albrecht 2011). The advancements in molecular genetics and the identification of peripheral clocks have enabled the development of bioluminescent reporters of core clock genes. This involved tagging different clock components, like *Per2*, to the luciferase (*Luc*) gene, and then monitoring photon emission from cells transfected with the novel *Per2::Luc* construct across 24 hours for several days. As a result, this enabled tracking of clock gene expression in real time (Ueda et al. 2002; Izumo, Johnson, and Yamazaki 2003). Similar principles were applied to generate the PER2::LUC fusion protein mouse model, which expresses *Per* gene flagged with luciferase (Yoo et al. 2004). These mouse models have enabled analysis of clock proteins within the SCN and all other clock-containing cells. Together, *in vivo* and *in vitro* models help us dissect and monitor the fundamental circadian parameters, like amplitude, period and phase (summarised in Figure 1.3) in different tissues and across whole animals.

Amplitude refers to the robustness of the biological rhythm, with greater amplitudes corresponding to stronger day/night differences. Assessing amplitude *in vivo* can be carried out by monitoring regularity of activity onset, where arrhythmic mice display different onset times, corresponding to lower amplitudes (Siepka and Takahashi 2005). *In vitro* assessments of amplitude can be more accurate and informative, and correspond to differences between peak and trough of an oscillation, where cells with stronger oscillators display larger amplitudes (Izumo, Johnson, and Yamazaki 2003).

Period of circadian rhythms can be assessed accurately using both *in vivo* and *in vitro* means as well. By monitoring daily locomotor activity of animals under constant darkness (DD), with the absence of light as a *zeitgeber*, the true endogenous free-running period *in vivo* can be assessed (Jud et al. 2005). On the other hand, *in vitro* evaluation of period is done by calculating the time difference between two peaks (or troughs), which corresponds to one complete cycle of the TTFL (Izumo, Johnson, and Yamazaki 2003).

Finally, the last parameter of interest is the phase of a circadian oscillation, which refers to the relationship between external *zeitgebers* and endogenous rhythms. To evaluate the light-phase relationship, animals should be placed under DD and their activity assessed following exposure to unnaturally timed light. Indeed, the timing of light pulses under DD conditions show different effects on activity. Subjecting animals to a pulse of light during their early subjective night (roughly endogenous circadian time (CT) 12-16) results in phase delay, where activity occurs later the following day as a result of photic input into the clock at a later time than expected. On the other hand, a pulse of light during the late night (or CT19) promotes a phase advance,

whereas light pulses during the animal's subjective day show no changes (Watanabe, Deboer, and Meijer 2001; Best et al. 1999; Takahashi et al. 1984). Together, these experiments have allowed the generation of the phase response curve (PRC) and propose the SCN has gating properties, where resetting is completely dependent on clock phase during stimuli. Moreover, *in vitro* assessments of phase advances and delays are also possible, by gauging leftward and rightward shifts in oscillation peaks, respectively (Brown et al. 2008).

All in all, monitoring these three parameters can facilitate a deeper understanding of circadian rhythms in cells and whole animals as well.

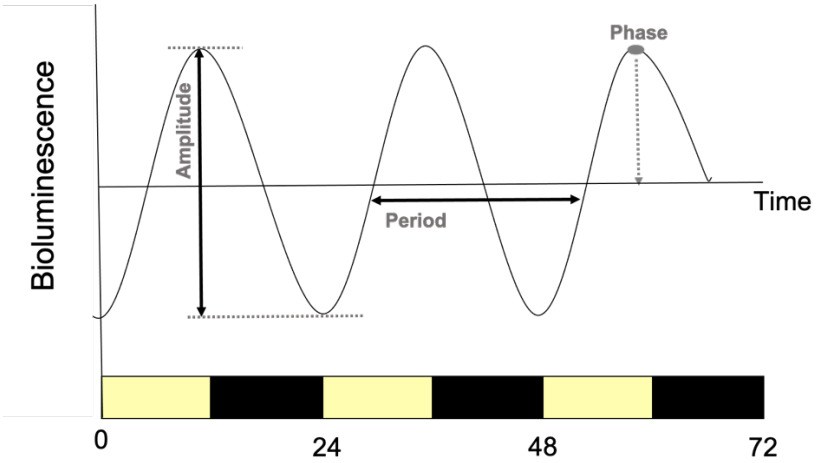


Figure 1.3. Parameters of circadian rhythms:

Amplitude: is the peak to trough difference
Period: or τ is the time taken to complete a full oscillation.
τ=24 h in circadian rhythm; and τ<20 h in ultradian rhythm
Phase: corresponds to the reference peak time of the circadian cycle (a reference point, for example, onset of sleep).
With relevance to biology, the period of a circadian clock is usually about 24 hours and represents the full cycle in response to day/night. Circadian period in humans spread across a spectrum, ranging from early bird chronotypes to night owls. The amplitude of the circadian clock represents the level of variation between day and night and corresponds to the expression level of the corresponding circadian genes. The phase represents the onset of the peak or trough of a rhythmic oscillation in relevance to the light/dark cycle

1.3 The metabolic syndrome:

1.3.1 Defining the metabolic syndrome:

The metabolic syndrome (MetS), also referred to as syndrome X (Reaven 1988), the insulin resistance syndrome (DeFronzo and Ferrannini 1991) or the deadly quartet (Kaplan 1989), involves a constellation of metabolic abnormalities which are believed to increase risk of developing cardiovascular diseases and type 2 diabetes mellitus (T2DM). The first report of this syndrome dates back to the 1920s, when the Swedish physician Kylin identified patients with a triad of gout, hypertension and hyperglycaemia (Kylin 1923). Thereafter, many studies correlated upper body obesity with similar metabolic abnormalities (Balkau 1999; Alberti and Zimmet 1998; Expert-Panel 2001). In 1988, Reaven's Banting lecture defined the onset of insulin resistance among obese and non-obese patients as syndrome X (Reaven 1988), where impaired fasting glucose and T2DM were regularly reported with concomitant onset of hyperlipidaemia, hypertension and other cardiovascular (CV) risk factors.

While MetS as a concept was widely accepted, efforts to develop a unifying internationally recognized definition were not made until 1998 (Alberti and Zimmet 1998). Discrepancies unfolded in the defining criteria of symptoms and thresholds amongst different health organisation, (summarised in Table 1.1). Nonetheless, all definitions agreed on 4 essential components; ***glucose intolerance, dyslipidaemia, hypertension*** *and* ***central obesity***, with the latter mostly linked to waist circumference (WC) and recognized based on ethnic and nation specificity (Table 1.2).

Table 1.1: Definitions of the Metabolic syndrome over time

Criteria	WHO (1998)	EGIR (1999)	ATPIII (2001)	AACE (2003)	IDF (2005)	AHA/NHLBI (2005)	Joint** (2009)
Obesity	BMI> 30kg/m^2 And/or WHR Men > 0.9 Women >0.85	WC: Men ≧ 94cm Women ≧ 80cm BMI not included	WC: Men > 103cm Women > 88cm	---	WC: country and ethnicity specific (**Table 1.2**)	WC: Men > 102 cm Women > 88cm (**Table 1.2**)	WC: country and ethnicity specific (**Table 1.2**)
TGs (mmol/L)	≧1.7	≧2.0	≧1.7	≧1.7	≧1.7	≧1.7	≧1.7
Blood pressure (mm Hg)	≧160/90	≧140/90	≧130/85	≧130/85	Systolic ≧130 and/or Diastollic≧85	Systolic ≧130 and/or Diastollic≧85	Systolic ≧130 and/or Diastollic≧85
Fasting glucose (mmol/L)	-*T2DM*: Fasting ≧7 -*Impaired glucose tolerance*: Fasting > 7 and 2-h post 7.8-11	Non-diabetics only: ≧6.1	≧6.1	Impaired fasting glucose ≧5.6 or 120min post 75g glucose ≧7.7	≧5.6 or previous diagnosis of T2DM	≧5.6 or on drug treatment for hyperglycemia	≧5.5
HDL-C (mmol/L)	Men ≦ 0.9 Women ≦ 1.0	< 1	Men < 1.03 Women < 1.3	Men ≦ 1.03 Women ≦ 1.3	Men ≦ 1.03 Women ≦ 1.3 or on drug treatment for reduced HDL-C	Men< 1.03 Women < 1.3 or on drug treatment for reduced HDL-C	Men < 1 Women < 1.3 or on drug treatment for reduced HDL-C
Insulin resistance	Assessed by clamp study; glucose uptake must be below lowest quartile of population	Fasting hyperinsulinemia	Not required	Risk factors for insulin resistance necessary [a]	----	Not required	Not required
Diagnosis Criteria	Glucose intolerance and 2 of the remaining criteria	Insulin resistance and 2 of the remaining criteria	3 of 5	At least 2 of 4	Central obesity and 2 others	3 of 5	All
References	(Alberti and Zimmet 1998)	(Balkau 1999)	(Expert-Panel 2001)	(Alberti et al. 2005)	(Alberti, et al. 2005)	(Grundy et al. 2005)	(Alberti et al. 2009)

TGs: Triglycerides. HDL-C: High density lipoprotein cholesterol. WHR: weight/height ratio. WC: waist circumference. [a]Diagnosis of CV, hypertension, NAFLD, family history of diabetes or glucose intolerance, Polycystic ovarian disorder, BMI>25kg/m^2, age>40 years **joint definition by: IDF Task Force on Epidemiology and Prevention; National Heart, Lung, and Blood Institute; American Heart Association; World Health Federation; International Atherosclerosis Society; and International Association for the Study of Obesity.

Table 1.2. Thresholds of waist circumference based on ethnicity

Ethnicity	Female	Male
Europid	≧88 cm	≧102 cm
South Asian	≧80 cm	≧90 cm
Central and South American	≧80 cm	≧90 cm
Middle Eastern/Mediterranean	≧80 cm	≧94 cm
Sub-Saharan African	≧80 cm	≧94 cm
Chinese	≧80 cm	≧90 cm
Japanese	≧80 cm	≧90 cm

1.3.2 Pathophysiology of the MetS:

The pathogenic mechanism underlying MetS are multifaceted and remain to be fully comprehended. Insulin resistance with fatty acid flux seems to be one of the most widely accepted mechanism, with visceral adiposity, leptin resistance, oxidative stress and low-grade chronic inflammation all proposed as contributing factors (Eckel, Grundy, and Zimmet 2005; McCracken, Monaghan, and Sreenivasan 2018). Understanding the pathophysiology of this condition provides the first step for identifying targeted therapeutic interventions.

1.3.2.1 Insulin resistance:

Insulin is one of the major anabolic hormones known, and is involved in induction of glucose uptake, glycogen and lipid synthesis and inhibition of glycogenolysis, gluconeogenesis and lipolysis. It is secreted by the β-cells of the pancreatic islets of Langerhans, and exerts its functions via insulin receptors located in insulin-sensitive tissues like the liver, adipocyte and skeletal muscles, amongst others (mechanism summarised in Figure 1.3).

The major pathway mediating insulin's metabolic actions is the phosphoinositide-3-kinase PI(3)K and protein kinase B (or Akt) pathway (see Figure 1.4). Indeed, transfection with dominant negative constructs of PI3K inhibits most metabolic actions of insulin, including glycogen and lipid synthesis and induction of glucose transport (Shepherd, Navé, and Siddle 1995; Saltiel and Kahn 2001). PI(3)K triggers a series of phosphorylation reactions culminating in Akt activation. PI3K mediated production of 3-phosphoinositides (PtdIns(3,4)*P*2 and PtdIns(3,4,5)*P*3), in

combination with protein kinase 3-phosphoinositide-dependent protein kinase 1 (PDK1) and another unidentified kinase tentatively named 3-phosphoinositide-dependent protein kinase 2, result in Akt activation. Activated Akt promotes insulin-mediated glucose transport, glycogen synthesis as well as lipolysis suppression. Indeed, overexpression of Akt has been shown to increase GLUT4 plasma membrane recruitment, and increase glucose uptake to a similar level to that induced by insulin in non-transfected cells (Hajduch et al. 1998; Foran et al. 1999). Similarly, over-expression of Akt in L6 muscle cells has also been shown to inhibit Glycogen-synthase kinase 3 (GSK3) and subsequently increase glycogen and protein synthesis (Hajduch et al. 1998; Ueki et al. 1998). Furthermore, Akt also inhibits protein kinase A (Choi et al. 2010), which is the main driver of lipolysis in adipose tissue, thereby supressing lipolysis.

Stimulation of glucose uptake by insulin also occurs via tyrosine-kinase phosphorylation of the Cbl protooncogene (Ribon and Saltiel 1997), which is associated with the adapter protein CAP (Ribon et al. 1998). Following phosphorylation, the CAP-Cbl complex translocates to lipid raft subdomains within the plasma membrane, recruiting the adapter protein CrkII. CrkII is associated with the guanyl nucleotide exchange protein C3G forming a constitutive complex, which once relocalised into the lipid raft, subsequently interacts with the G protein TC10, allowing exchange of GTP for GDP, thereby activating it. As a result, activated TC10 facilitates insulin-mediated glucose uptake by promoting GLUT4 translocation into the plasma membrane, in parallel with the PI(3)K pathway (Chiang et al. 2001; Baumann et al. 2000).

In addition to glucose storage, insulin promotes genetic transcription of glycolytic and fatty acid synthetic genes. Insulin inhibits gluconeogenesis and glycogenolysis through Akt-mediated phosphorylation of the forkhead box class O-1 transcription factor (FOXO1) which inhibits transcription and activity of gluconeogenic enzymes in the liver, but also via PGC1α (peroxisome proliferator-activated receptor γ coactivator 1 α), FOXO6 and cAMP responsive coactivator TORC2 (Kim et al. 2011; Dentin et al. 2007; Li et al. 2007; McCracken et al., 2018).

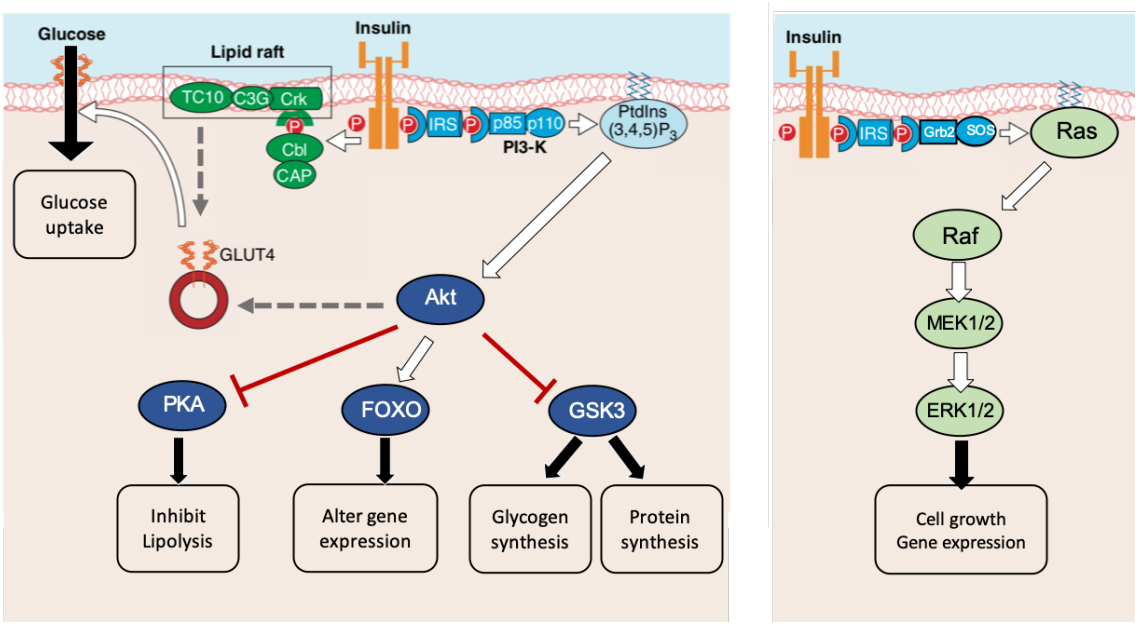


Figure 1.4. Insulin signalling:

The insulin receptor is a tyrosine-kinase receptor, consisting of two alpha subunits hosting the insulin binding site, and two beta subunits that traverse the cell membrane. As insulin binds, it induces a conformational change that activates the tyrosine kinase domain of the intracellular β subunit, promoting autophosphorylation of the tyrosine residues, and inducing full activation of the kinase activity. The phosphorylated tyrosines act as docking sites for proteins containing Src-homology-2 (SH2) domains, including the insulin-receptor substrate (IRS) family, which appears to mediate most insulin effects (White 2003; Taniguchi, Emanuelli, and Kahn 2006; Versteyhe et al. 2010). The activated kinase then drives a series of signalling pathways, including activation of the phsphoinosiditde-3-kinase PI(3)K and its downstream protein kinase B (or Akt), Ras and the MAP kinase cascade, as well as Cbl/CAP mediated TC10 activation, thus, leading to increased glucose uptake, inhibition of lipolysis, gluconeogenesis and glycogenolysis, induction of glycogen and protein synthesis, and enhancement of genetic transcription of glycolytic and fatty acid synthetic genes. Dashed arrows represent steps of the pathway that have not been fully elucidated. Red blunted arrow indicates inhibition.

When describing the pathophysiology of the MetS, insulin resistance remains the most unifying and widely accepted hypothesis.

One of the primary factors contributing to insulin resistance is the excessive abundance of circulating fatty acids. The main source of plasma free fatty acids (FFA) is the breakdown of adipose tissue triglycerides through induction of the hormone-sensitive lipase (also known as lipolysis). Lipoprotein lipase-mediated breakdown of triglyceride-rich lipoproteins in other tissues can also contribute (Eckel 1989). Consequently, excessive fatty acids can induce insulin resistance in tissues either due to increased substrate availability or as a result of pathway modification. For example, in muscles, fatty acid infusions have been shown to significantly impair insulin-mediated Akt1-phosphorylation and protein kinase C activation (Kim et al 2002). Similarly, in the liver, high-fat-diet induced insulin resistance in rats has been attributed to a reduction in insulin-mediated phosphorylation of the insulin receptor and insulin receptor substrate IRS1 (Samuel et al. 2004), thereby significantly ameliorating insulin downstream signalling. Furthermore, as suppression of lipolysis is one of the key functions of insulin signalling, development of insulin resistance can increase lipolysis and abundance of circulating fatty acids, which in turn can further exacerbate the insulin resistance.

Other mechanisms associated with insulin resistance include defects in the mitochondrial and endoplasmic reticulum (ER) function. Indeed, various studies on patients with T2DM and/or obese individuals with insulin resistance, their offspring as well as elderly participants have demonstrated increased accumulation of triglycerides and lipid molecules in muscles as a result of dysfunction in the

mitochondrial oxidative phosphorylation pathways (Kelley et al. 2002; Petersen et al. 2004; 2003). Similarly, in murine models of obesity, dysfunction of the ER was associated with hyperphosphorylation of IRS1 at the serine residue, resulting in insulin resistance (Ozcan et al. 2004).

Thus, the molecular mechanisms underlying insulin resistance are slowly emerging, but remain to be fully elucidated.

1.3.2.2 Obesity and increased waist circumference

Obesity has become a global epidemic, affecting over 650 million people worldwide (WHO obesity and overweight statistics, 2016). An individual is diagnosed with obesity if their body-mass index (BMI) is greater than 30, calculated as their weight (kg) divided by the square of their height (m^2). Obesity increases the risk of developing several diseases, including T2DM, dyslipidaemia, cardiovascular disease, hepatic steatosis and even cancer (Expert-Panel 1998), many of which are common with metabolic syndrome, and is therefore one of the key factors contributing to the latter's pathophysiology.

When defining the MetS, waist circumference is often included (Alberti and Zimmet 1998; Expert-Panel 2001; Balkau 1999). However, the cause of the large waist is still not well defined, debating an increase in visceral fat vs subcutaneous adiposity, which can only be determined using magnetic resonance imaging (MRI) or computed tomography (Lee, Janssen, and Ross 2004). Intra-abdominal or visceral adiposity is expected to elicit a higher FFA flux to the liver through the splanchnic circulation, whereas subcutaneous adipose tissue will more likely release lipolysis products

directly into the systemic circulation, thereby reducing effects on hepatic function (Aubert et al. 2003). Evidence from studies on Asians and Asian Indians (Bajaj and Banerji 2004) propose visceral fat to be more determinantal, given these populations have relatively higher prevalence of MetS compared to African-American men who predominantly display subcutaneous adiposity (Tanaka, Horimai, and Katsukawa 2003). Nonetheless, it has been shown that non-splanchnic upper body fat in obese women was the source of elevated postprandial FFA, not the visceral adipose tissue (Guo et al. 1999), which indicates that visceral adiposity is a key marker for FFA elevation, but is not the primary source.

A genetic basis for the syndrome is also evident. Indeed, single gene defects in adiponectin (Fumeron et al. 2004), the β-2 adrenergic receptor (Dallongeville et al. 2003) and peroxisome-proliferator activated receptor gamma (PPARγ) (Hegele 2003), which result in partial or complete lipoatrophy, have all been associated with insulin resistance and MetS. This highlights a role for genetics in the pathophysiology of MetS. Nonetheless, it is important to note that despite the importance of obesity in the pathophysiology of MetS, patients with normal weight can also suffer from insulin resistance (Ruderman et al. 1998).

1.3.2.3 Leptin and leptin resistance

Leptin is a peptide secreted by adipocytes at a level approximately proportional to their triglyceride (TG) content (Zhang et al. 1994; Frederich et al. 1995); therefore it acts as hormonal signal corresponding to body energy stores. It exerts its actions primarily on long isoform leptin receptors (LEPR) expressed in brain for the control of energy expenditure and feeding (Flak and Myers 2016) or on other short-isoforms

of that receptor in peripheral tissues for regulation of energy expenditure (de Luca et al. 2005). Mice exhibiting a mutation in the leptin gene (ob/ob mice) or in the long isoform of LEPR (db/db mice) are obese, hyperphagic and diabetic (Ingalls et al. 1950; Chua et al. 1996), stressing the crucial role of this peptide in maintaining energy homeostasis and in the progression of metabolic syndrome.

As discussed earlier, obesity is one of the main symptoms of MetS and has been shown to contribute to leptin resistance in various ways. Several studies show significant elevation of circulating leptin concentrations in obese human subjects or in diet-induced obese rodents that is proportional to their elevated adiposity (Frederich et al. 1995). In addition, exogenous leptin treatment fail to reduce food intake or weight, suggesting onset of leptin resistance in these obese subjects (El-Haschimi et al. 2000). Moreover, diet-induced obesity (DIO) and adipose tissue hyperplasia and hypertrophy significantly blunt the response of LEPR to leptin binding, which contributes to significant leptin resistance (Figure 1.5).

Hypothalamic inflammation has also been proposed as an underlying cause for leptin resistance. Indeed, intracerebroventricular TNF has been shown to promote food intake, increase weight and reduce energy expenditure (Romanatto et al. 2007), therefore supporting a role for hypothalamic inflammation in leptin resistance. Interestingly, DIO induces a state of low-grade inflammation in peripheral tissues, like adipose tissue (Lumeng and Saltiel 2011) as well as in hypothalamus (Thaler et al. 2012). It also promotes expression of pro-inflammatory cytokines (like TNF and interferons) in adipose tissue and enhances intracellular inflammatory signalling cascades in the hypothalamus (Lumeng and Saltiel 2011; Zhang et al. 2008; Benoit et

al. 2009), which supports a role for DIO-mediated hypothalamic inflammation in attenuating leptin action.

Furthermore, ER stress has been also implicated in the pathophysiology of leptin resistance and obesity. ER stress occurs when the level of protein and lipid synthesis in the ER overtakes its ability to process and export these molecules. This could happen as a result of increased misfolding of proteins (from infection or other associated alterations) or due to high rates of synthesis that increase ER demand. The inability of the ER to cope with this increased demand results in higher misfolded proteins, which trigger the unfolded protein response (UPR), that activates X-binding protein 1 (XBP1) transcription factor which reduces protein synthesis and increases expression of chaperons proteins that increase the protein folding capacity of the ER (Back and Kaufman 2012). Indeed, mice lacking XBP1 in nestin-positive neurones exhibit higher ER stress, profound hyperleptinemia, and weight gain (Ozcan et al. 2009). Furthermore, DIO has been associated with an increase in ER stress in peripheral tissues like adipose tissue, and several observations suggest a similar onset in hypothalamic neurones (Ozcan et al. 2009). On the other hand, constitutive expression of XBP1 in the pro-opiomelanocortin (POMC) neurones or treatment with chemical chaperons that reduce ER stress have been shown to protect against DIO (Ozcan et al. 2009; Williams et al. 2014). Similarly, two compound that decrease ER stress have been shown to reduce feeding and promote weight loss in DIO animals (Liu et al. 2015; Lee et al. 2016), all of which supports a role for hypothalamic ER stress in obesity and leptin resistance.

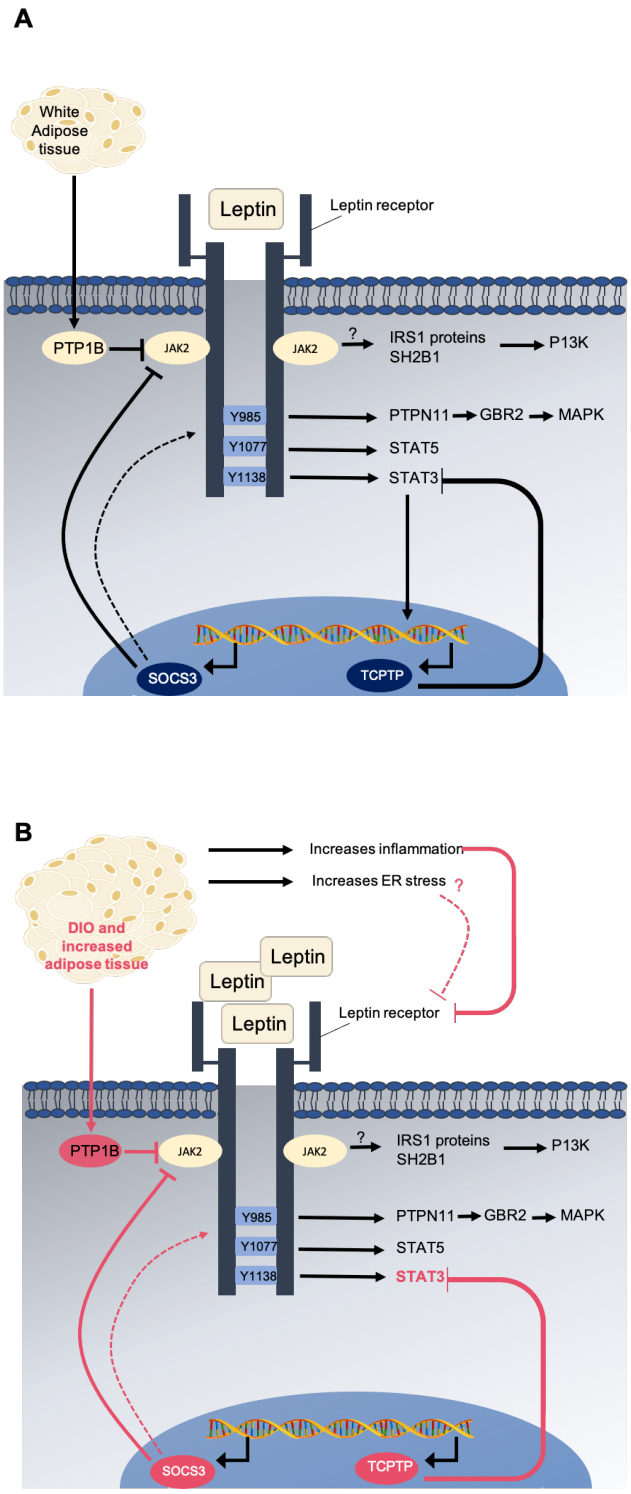


Figure 1.5. Leptin signalling in health and disease:
A) In normal body weight, circulating leptin released from white adipose tissue binds to its receptor (LEPR), activating the tyrosine-protein kinase JAK2, which subsequently phosphorylates the tyrosine residues Y985, Y1077 and Y1138 within the leptin receptor. Phosphorylated Y985 engages and enables the phosphorylation of tyrosine-protein phosphatase nonreceptor type 11 (PTPN11), which recruits the growth-factor-receptor-bound protein 2 (GBR2) and induces the mitogen-activated protein kinase (MAPK) pathway. Phosphorylated Y1077 recruits the signal transducer and activator of transcription (STAT5), which could play a role in leptin-mediated gene expression. Phosphorylated Y1138 engages and enables STAT3 phosphorylation, resulting in its translocation into the nucleus and its induction of gene expression. STAT3-mediated gene expression contributes to the control of energy balance by leptin, and also promotes the expression of cytokine signalling 3 (SOC3) which binds to phosphorylated Y985 and suppresses leptin signalling in the process.
The tyrosine phosphatases protein-tyrosine phosphatase 1B (PTP1B) dephosphorylates JAK2, while the T-cell protein-tyrosine phosphatase (TCPTP) dephosphorylates STAT3, thereby acting as feedback mechanisms. Leptin can also recruit the insulin receptor substrate (IRS) protein and Src homology domain 2 (SH2)-domain containing protein 1B (SH2B1) via a poorly understood mechanism (denoted by question mark).
B) In obesity, levels of circulating leptin increase as a result of elevated adipose mass, causing hyperactivation of LEPR signalling and increased SOCS3 and TCPTP expression. Obesity also enhances PTP1B expression and increases inflammation and ER stress. Together, these mechanisms suppress the normal responses to high leptin concentration and impair LEPR signalling, leading to resistance.
DIO: diet-induced obesity. P13K: phosphoinositide 3-kinase.

1.3.2.4 Non-alcoholic fatty liver disease (NAFLD)

NAFLD is defined as the presence of lipid in the liver (hepatic steatosis) independent of alcohol consumption or certain medications (like glucocorticoids, tamoxifen, tetracycline, etc) that induce such histology. It can be further characterized histologically into non-alcoholic fatty liver (NAFL), corresponding to hepatic steatosis with no hepatocellular injury or non-alcoholic steatohepatitis (NASH) where inflammation and hepatocyte injury with or without fibrosis progresses (Puri and Sanyal 2012). Despite NAFLD not being classified as a prerequisite for diagnosing MetS, intraabdominal obesity, hypertension and insulin resistance, all hallmarks of MetS have been identified as key risk factors for developing this condition (Bedogni et al. 2005; Marchesini et al. 2001; 1999). Furthermore, although the pathophysiology of NAFLD is still not fully clarified, insulin resistance seems to play a fundamental role (Figure 1.6).

Lipids accumulate in the liver as a result of imbalance between TG supply, formation and disposal. Lipids contributing to hepatic steatosis include plasma non-esterified fatty acids (NEFA) from adipose tissue, liver-derived fatty acids due to de novo lipogenesis (DNL) and dietary fat (either through uptake from intestinal chylomicrons or from spillover plasma NEFA). Interestingly, around 60-80% of liver TG comes from circulating FA. As mentioned earlier, insulin resistance reduces insulin's inhibitory action on lipolysis thereby increasing FFA. Furthermore, 20% of liver TG comes from DNL, whose mediating enzymes are under transcriptional regulation of the sterol regulatory element-binding protein 1 (SREBP-1C) (Donnelly et al. 2005). Given the latter is upregulated by insulin, it is therefore likely promoted

by hyperinsulinemia which consequently implicates insulin resistance in the pathogenesis of hepatic steatosis (Sanyal 2005). Finally, dietary fat intake accounts for 15% of FA liver supply, which are absorbed into intestinal epithelia, packaged in the ER as chylomicrons and then transported across the circulation to tissues like muscles, adipose and liver. Disruption in hepatic lipid export can contribute to hepatic steatosis. FA in the liver are normally exported as very-low-density lipoproteins (VLDL) which are generated through TG incorporation into apolipoprotein B (apo-B) by microsomal triglyceride transfer protein (MTP). Inhibition of MTP activity (Lettéron et al. 2003; Namikawa et al. 2004) or apoB synthesis or release (Charlton et al. 2002) may contribute to TG accumulation and suggest another mechanism leading to hepatic steatosis.

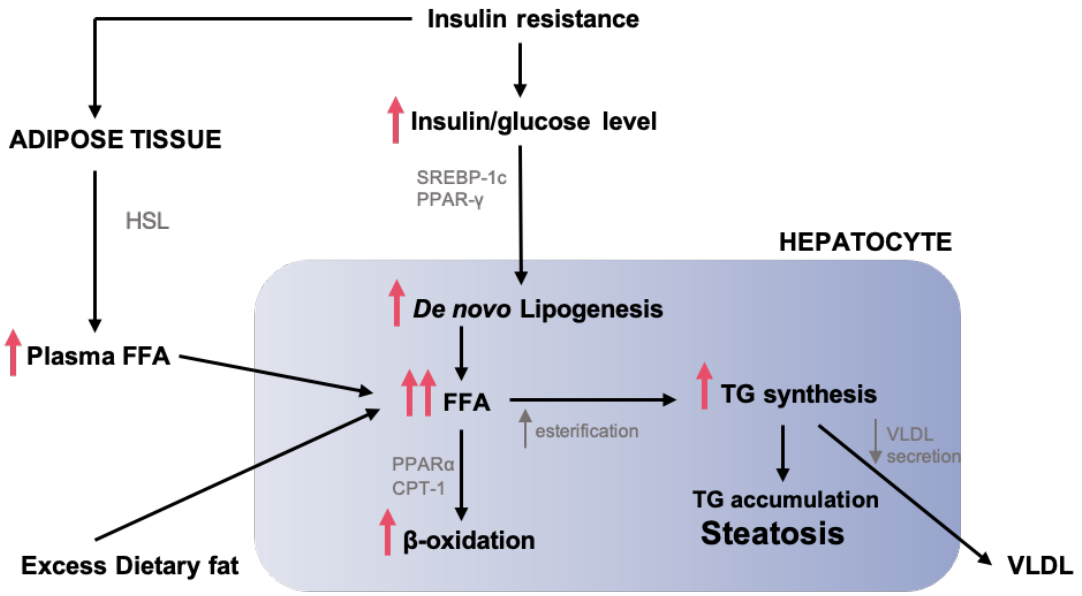


Figure 1.6. Pathophysiology of NAFLD: Adapted from (Paschos and Paletas 2009)

In adipose tissue, insulin resistance reduces the inhibitory effects of insulin on the hormone sensitive lipase (HSL), which consequently increases triglyceride (TG) lipolysis and promotes free fatty acid (FFA) release. This increases circulating levels of FFAs, which are subsequently taken up by the liver. Dietary fatty acids can also contribute to liver hepatosteatosis. During situations of excess dietary fat intake, FA enter the liver via spillover into the plasma NEFA pool and through uptake of intestinally derived chylomicron remnants. *In hepatocytes*, hyperinsulinemia increases production of FA through *de novo* lipogenesis. Insulin also upregulates lipogenic enzymes, such as peroxisome proliferator-activated receptor gamma (PPAR-γ) and sterol regulatory element binding protein 1 (SREBP-1). This, in addition to the increased hepatic FFA content, drives an increase in hepatic TG synthesis. The large hepatic pool of FFA also promotes mitochondrial FA β-oxidation by induction of PPAR-α and CPT-I. Meanwhile, TG export via very-low-density lipoproteins (VLDL) can be suppressed by the reduction of apolipoprotein B (apo B) synthesis or the decrease in TF incorporation with apo B by microsomal triglyceride transfer protein (MTP). HSL: hormone-sensitive lipase, TG: triglyceride, FFA: free fatty acid, PPAR-: peroxisome proliferator-activated receptor gamma, SREBP-1: sterol regulatory element binding protein 1, PPAR-α: peroxisome proliferator-activated receptor a, CPT-I: carnitine palmitoyltransferase I, VLDL: very-low-density lipoproteins, apo B: apolipoprotein B, MTP: microsomal triglyceride transfer protein).

1.3.3 Treatment of metabolic disorders:

1.3.3.1 Lifestyle changes:

Regular exercise and a maintaining a healthy diet are important for both prevention and treatment of MetS (Smith et al. 2011). Physical activity shows clear benefits in reducing risk of CV disease and improving insulin sensitivity and glucose tolerance (Wannamethee and Shaper 2001). Following weight loss, a reduction in visceral

depots can significantly improve insulin sensitivity. Indeed, overweight subjects displaying glucose intolerance showed an overall 58% reduction in incidence of diabetes relative to control group following a 3.2 year intervention aimed at increasing physical activity and fibre intake and reducing weight and overall fat consumption (Tuomilehto et al. 2001). Moreover, regular exercise improves insulin and leptin levels in overweight or obese patients (Frank et al. 2005) and when coupled with dietary restrictions, aerobic and resistance exercises significantly improve pre-prandial insulin levels and overall glucose tolerance (Rice et al. 1999).

Calorie restriction is a cardinal intervention for MetS prevention and treatment, however, increasing evidence suggests that the macronutrient composition of the diet is as important to achieve favourable effects. For example, the Mediterranean diet, which involves a high ratio of monounsaturated to saturated fats relative to the diets consumed in the US and northern Europe and greater consumption of fish and omega-3 fatty oils, has been shown to be superior to the standard low fat diets (Kris-Etherton et al. 2001; Esposito et al. 2004).

Bariatric surgery, or weight loss surgery, has shown the most effective in terms of reduction in body weight and comorbidity as well as improved survival (Kral and Näslund 2007; Sjöström et al. 2007). However, due to concerns of surgical complications and common need for reoperation, these procedures are reserved for morbidly obese individuals with poor prognosis only (Melnikova and Wages 2006).

Furthermore, with the busy 24/7 dynamics of the 21st century, lifestyle changes can be difficult to sustain or comply to and alone have failed to ameliorate the obesity

epidemic which is rapidly growing and remains to be a great socio-economic burden. Based on regional secular trends and population growth, a staggering 1.12 billion people are estimated to become obese by 2030 (Kelly et al. 2008). As a result, there is a pressing need for effective pharmacotherapeutic strategies.

1.3.3.2 Pharmacological interventions:

As a major contributor to MetS pathophysiology, tackling obesity is one of the first targets for combatting MetS. Current pharmacological candidates under development for obesity are categorized as follows: peripherally acting drugs that impair fat absorption from diet, centrally acting agents that reduce food intake and medications that enhance energy expenditure (Narayanaswami and Dwoskin 2017). According to Food and Drug Administration (FDA) guidelines, a drug is deemed effective against obesity if it results in a body weight reduction greater than 5% relative to placebo, or if at least 35% of participants show body weight loss >5% (FDA 2007). This is because a reduction in 5-10% of body weight has been shown to significantly reduce onset of T2DM and cardiovascular disorders (Avenell et al. 2004).

To date, there are 6 FDA-approved pharmacological anti-obesity medications (summarised in Table 1.3): Liraglutide (Davies et al. 2015), lorcaserin (Fidler et al. 2011), phentermine (Weintraub et al. 1992), extended release phentermine/topiramate (Aronne et al. 2013), sustained-release naltrexone/bupropion and orlistat (Van Gaal et al. 1998; James et al. 1997). While these drugs have shown clinical improvements, reducing weight by 3-7% (Srivastava and Apovian 2018b), their effects have been variable amongst different patients, with some people benefiting significantly less than others (Davies et al. 2015; Srivastava

and Apovian 2018a; James et al. 1997). Furthermore, adverse effects were common (as shown in Table 1.3), causing patients to abort therapy and swing between different anti-obesity drugs in pursuit of efficacy (Kang and Park 2012). In addition, many other anti-obesity medications have been launched over the last two decades yet withdrawn as a result of cardiovascular and psychiatric complications (Narayanaswami and Dwoskin 2017).

One of the major contributions for the failure of many anti-obesity medication is the complexity of the neuro-hormonal regulation of energy balance and the multifactorial aetiologies linked with metabolic syndrome. Despite the benefit observed with some anti-obesity medication, physiological redundancy and feedback pathways associated with appetite regulation and energy metabolism are multifactorial, and pose major limitations for drug development and efficacy (Rodgers, Tschöp, and Wilding 2012). Given the heterogeneity of the metabolic syndrome and its pathogenesis, a multi-target approach seems to be a better way of tackling this syndrome.

Table 1.3: Available FDA approved anti-obesity medication

Medication	Approval date	Mechanism of Action	Warnings and precautions	Side effects
Phentermine	1959	NE transport inhibitor, suppresses appetite via POMC neuron activation in arcuate nucleus	-Increases heart rate and blood pressure -Possible primary pulmonary hypertension	Insomnia, constipation, dry mouth, agitation
Orlistat	1999	A minimally absorbed agent; inhibits intestinal lipase thereby reducing dietary fat and TG absorption, inhibits gastric and pancreatic lipase and reduces dietary fat absorption	Reduces vitamin absorption	Diarrhoea, faecal urgency, oily spotting, flatus with discharge
Phentermine /topiramate	2012	Phentermine: like above Topiramate: GABA agonist, suppresses appetite by increasing GABA-A receptor activity, reducing AMPA/kainite glutamate receptor activity and modulating voltage gated ion channels	Fetal toxicity, cognitive impairment, metabolic acidosis	Dizziness, insomnia, constipation and dry mouth
Lorcaserin	2012	Serotonin 2C receptor agonist (mechanism unknown, but believed to reduce food consumption through activation of 5HT2C receptors in POMC of arcuate nucleus)	Risk of neuroleptic malignant syndrome-like reactions or serotonin syndrome	Non-diabetic patients: headache, fatigue, nausea, constipation, dry mouth Diabetic patients: hypoglycaemia, headache, cough, fatigue.
Naltrexone/ bupropion sustained-release	2014	Naltrexone: opioid receptor antagonist, prevents β-endorphin-mediated negative feedback on α-MSH release Bupropion: DA and NE transporter inhibitor; stimulates hypothalamic POMC neurons that release α-MSH resulting in decreased food intake and increased energy expenditure	Suicidal behaviour, Hepatotoxicity, Glaucoma, Increase heart rate and blood pressure	Nausea, constipation, headache, dizziness, insomnia, dry mouth, and diarrhoea.
Liraglutide	2014	GLP-1 agonist; reduces appetite	Serious hypoglycaemia when used with insulin, increased heart rate, Thyroid-tumours observed in rodents, rare incidence of acute pancreatitis ,renal impairment, suicidal behaviour	Hypoglycaemia, nausea, diarrhoea, constipation, headache, fatigue,

DA: dopamine, NE: noradrenaline, GABA: Gamma aminobutyric acid, POMC: Proopiomelanocortin, AMPA: α-amino-3-hydroxy-5-methyl-4-isoxazolepropionic acid, GLP-1: Glucagon-like peptide 1 , MSH: Melanocyte Stimulating Hormone
All counter-indicated in pregnancy

1.4 The role of circadian clock in metabolism

The circadian clock plays a pervasive role in regulating metabolism. Various studies examining gene expression profiles across the circadian cycle have reported 3% to 15% of the transcriptome in key metabolic tissues like liver, skeletal muscles, and white and brown adipose tissue (WAT, BAT, respectively), to be under strong circadian control (Ueda et al. 2002; Panda et al. 2002; Akhtar et al. 2002; Reddy et al. 2006; Storch et al. 2002). Remarkably, many of the identified rhythmic genes have roles in metabolic and biosynthetic pathways such as glycolysis and gluconeogenesis, oxidative phosphorylation, and cholesterol and lipid metabolism (Figure 1.7). Most notably, the rate-limiting steps in many of these processes are under circadian regulation (Panda 2002), suggesting a much broader impact on metabolism and energy homeostasis than anticipated by the number of rhythmic genes. Indeed, there is an evolutionary advantage of the circadian clock to sequester anabolic and catabolic mechanisms in a temporal fashion in order to meet activity cycles and energetic demands and increase efficiency, and a disruption in the alignment of these pathways has been linked to adverse metabolic effects (Figure 1.7). This section will shed light on the key metabolic pathways regulated by the clock, how they feedback into clock machinery and how different causes of circadian misalignment correlate to the metabolic syndrome.

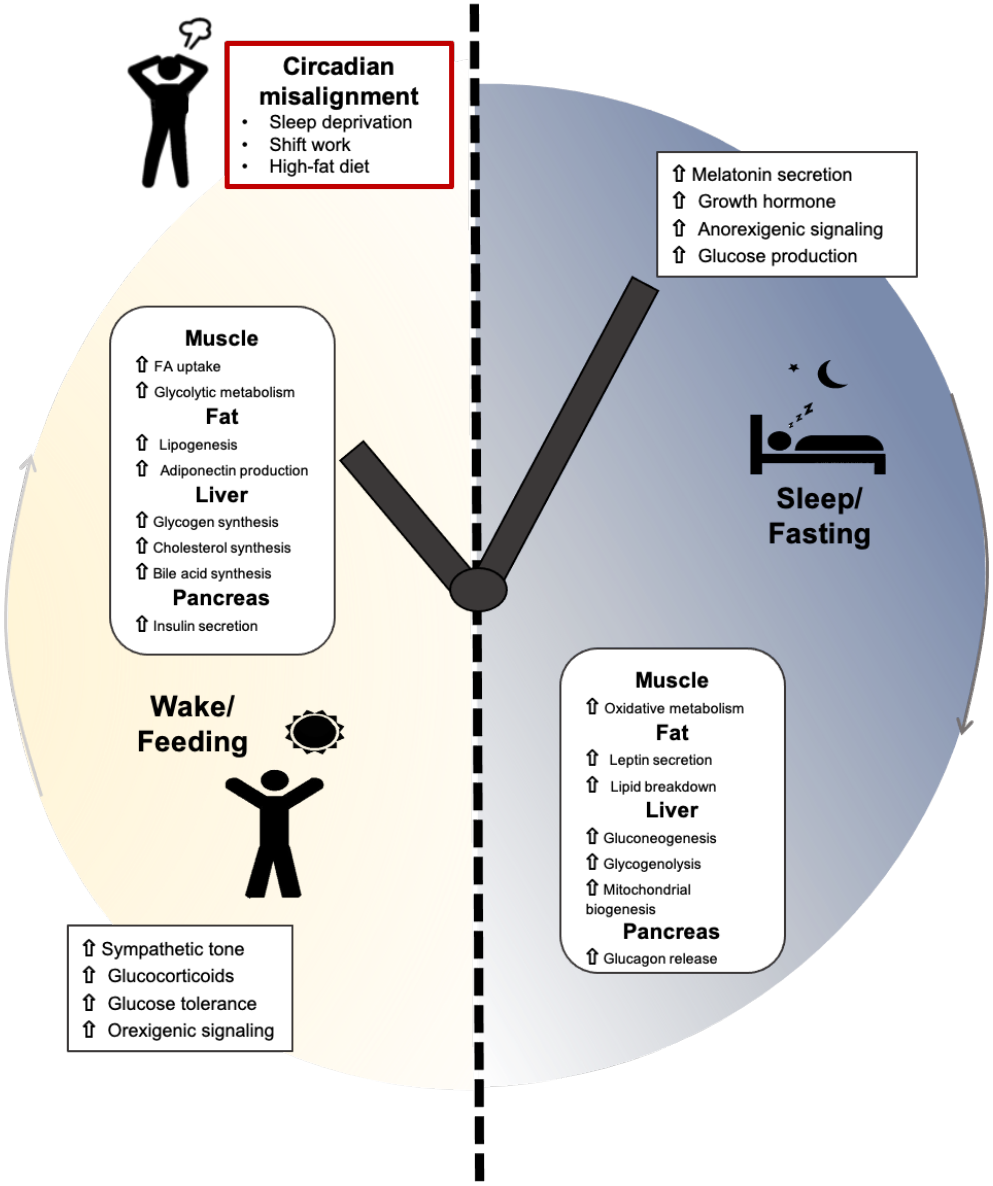


Figure 1.7. Circadian regulation of metabolism:

The circadian clock regulates suitable metabolic processes across the light/dark cycles, and enhances energetic efficiency by sequestering appropriate anabolic and catabolic pathways of peripheral tissues to the time of day they are needed most. When circadian misalignment occurs, as a result of sleep disruption, shift work or dietary changes, the circadian and metabolic alignments are disrupted which leads to adverse metabolic health outcomes. FA: fatty acids

1.4.1 Circadian regulation of glucose homeostasis

Glucose is the main fuel for biology, feeding into processes like glycolysis and oxidative phosphorylation to generate energy in the form of ATP. Plasma glucose levels are a function of the rate of glucose appearance (entering circulation) versus glucose disappearance (removal from circulation). Glucose enters the circulation through three processes: intestinal absorption following feeding, glycogenolysis involving breakdown of the polymerised glucose from glycogen stores, and gluconeogenesis involving glucose formation from amino acids and lactate (Aronoff et al. 2004). Glucose levels are tightly regulated within the narrow range of 3.3 and 8.8 mmol/L (or 60 and 160 mg/dl), despite daily fluctuations following exercise or food (Wahren, Felig, and Hagenfeldt 1978; Consoli et al. 1987). This is maintained via an intricate neuro-hormonal system involving hormones like insulin, amylin, glucagon, glucose-dependent insulinotropic polypeptide (GIP) and GLP1.

The circadian clock is strongly implicated in glucose regulation. Indeed, time-of-day dependent rhythms in glucose and insulin are observed in both humans and rodents. More importantly, these rhythmic levels are not merely linked to behavioural rhythms like feeding and exercise, as blood glucose rhythms persist when rats are fasted (La Fleur et al. 1999) and spike before waking, in both humans and rodents (Bolli et al. 1984). Furthermore, SCN lesions impair glucose and insulin tolerance (La Fleur et al. 1999; La Fleur et al. 2001), thus highlighting the impact of the circadian system in regulating key homeostatic mechanisms like glucose uptake, storage and release.

For instance, the influence of the clock on glucose uptake can be attributed to rhythmic levels of intestinal *Glut1* and *Glut5* and hepatic *Glut2* which are responsible for insulin-independent glucose uptake (Rhoads et al. 1998; Castelló et al. 1995; Panda et al. 2002). Similarly, insulin, which is a key regulator of glucose uptake, is secreted in a highly rhythmic manner that follows clock-controlled expression of secretory genes in the pancreas and its release is significantly diminished following tamoxifen-triggered loss of *Bmal1* in pancreas of adult mice (Perelis et al. 2015; Marcheva, Ramsey, et al. 2010). Furthermore insulin sensitivity also displays clock-regulated day-time dependence, as both insulin and glucose tolerance are disrupted following SCN lesions or in *Clock* mutant or *Bmal1* null mice (La Fleur et al. 2001; Rudic et al. 2004). Moreover, temporal regulation of other endocrine factors, like glucagon is also a key mechanism underlying clock-mediated regulation of glucose homeostasis, where glucagon plasma concentrations fluctuate with diurnal rhythms (Tasaka et al. 1980) and are regulated by feeding and the circadian machinery (Ruiter et al. 2003).

Incorporation of glucose into glycogen represents a vital depot for rapid storage/release of energy in the body, and interestingly, glycogen dynamics display clear circadian regulation. Glycogen levels fluctuate across the day and persist in fasted rodents independent of feeding cycles (Ishikawa and Shimazu 1976). Furthermore, enzymes involved in glycogen metabolism also oscillate across the day. For example, in rodents, glycogen synthase peaks during their active/dark phase while glycogen phosphorylase exhibits its maximal activity levels nearer the light phase (Peret, Chanez, and Pascal

1976; Ishikawa and Shimazu 1980). Furthermore, dampened circadian rhythms of hepatic glycogen content as well as mRNA and protein expression of glycogen synthase 2, that catalyses the rate-limiting step in hepatic glycogenolysis, have been reported in homozygous clock mutant mice ($Clock^{\Delta 19/\Delta 19}$) (Doi, Oishi, and Ishida 2010). These mice also develop hyperinsulinemia and hyperglycaemias as a result of their dysfunctional clock (Turek et al. 2005), emphasizing the role of the *Clock* gene in regulating glucose homeostasis.

Another key pathway in maintaining glucose levels is gluconeogenesis, which also displays rhythmicity. Indeed, higher rates of gluconeogenesis are reported in nocturnal rats *in vivo* during the evening and are matched with nocturnal oscillations in phosphoenolpyruvate carboxykinase (PEPCK) enzyme, which catalyses the irreversible conversion of oxaloacetate into phosphoenolpyruvate- the first step in gluconeogenesis (Kida et al. 1980). Moreover, several core clock genes have been implicated in glucose rhythms. Global loss of *Bmal1* disrupts glucose and triglyceride rhythms and significantly attenuates gluconeogenesis (Rudic et al. 2004) and hepatocyte-specific *Bmal1* knockdown completely abolishes rhythmic expression of gluconeogenic genes like PEPCK and Glut2 (Lamia, Storch, and Weitz 2008). Similarly, the negative regulator of Bmal1, Rev-erb*α*, also directly regulates expression of gluconeogenic enzymes like G6-phosphatase and PEPCK and knocking it down significantly suppresses their expression (Yin et al. 2007). Furthermore, the negative arm of the clock CRY attenuates hepatic gluconeogenesis, where hepatic expression of Pck1 and G6pc (Glucose-6-phosphate

catalytic subunit) and glucose production following glucagon were both increased following Cry1 and Cry2 knockdown. Whereas, on the contrary, CRY1 overexpression decreases fasting glucose and improves insulin sensitivity in diabetic mice (Zhang et al. 2010). In addition, CRYs also oppose glucocorticoid receptor activation and inhibit glucocorticoid-induced PEPCK expression and loss of both Cry1 and Cry2 induces glucose intolerance (Lamia et al. 2011).

Taken together, all of this evidence suggests a strong influence of cell autonomous circadian clocks on glucose homeostasis, through regulating gene expression of various key gluconeogenic or glycogenolytic enzymes, or via regulating release or sensitivity to endocrine factors.

1.4.2 Circadian regulation of Lipid homeostasis

Similar to glucose, it is well established that lipid metabolism exhibits robust time-of-day dependent rhythms. Increasing evidence supports a role for the endogenous circadian clock in the regulation of lipid absorption/digestion and metabolism.

Uptake of dietary fat involves emulsification, lipolytic breakdown and absorption into epithelial cells within the intestine. Interestingly, using isolated primary enterocytes, intestinal cholesterol and lipid absorption was shown to display rhythmicity that follows mice activity, with higher rates during the dark (active) phase and lower activity during light phase. More importantly, these rhythms were completely abolished in $Clock^{\Delta 19/\Delta 19}$

mice, supporting a role for the clock in regulating nutrient absorption (Pan and Hussain 2009). This comes as no surprise, as robust expression of clock genes within different cell types in the gastrointestinal tract have been widely reported (Pardini et al. 2005; Hoogerwerf et al. 2007; Sladek et al. 2007) and many key genes involved in lipid uptake and metabolism in the intestine, like apolipoprotein B and intestinal fatty acid binding protein (Fabp2) display circadian oscillations (Pan and Hussain 2009; Pan et al. 2010).

In addition to fat uptake, circulating NEFA, the main output of lipid metabolism, are known to fluctuate in a time-dependent manner. Human and rodent studies have reported higher NEFA levels during their corresponding inactive phases, as a result of increased lipolytic activity (Stavinoha et al. 2004; Shostak et al. 2013; Schlierf and Dorow 1973). Furthermore, human subjects under dim light maintain rhythmic plasma lipid levels, even when wakefulness and feeding were kept constant (Dallmann et al. 2012), therefore providing strong evidence that these observed lipid rhythms (and lipid metabolism by proxy) are not purely dependent on behavioural cycles.

Multiple studies have also shown circadian oscillations of triglycerides (TG) in plasma, which are partly attributed to rhythmic genes involved in TG biosynthesis (Shostak, Meyer-Kovac, and Oster 2013; Y Adamovich et al. 2014). Lipogenesis is regulated by the membrane bound sterol regulatory element-binding proteins (SREBP), a family of transcription factors that regulate expression of key lipogenic genes (Goldstein, DeBose-Boyd, and Brown 2006). Interestingly, REV-ERBα, the negative regulator of the clock

TTFL, directly influences activity and expression of SREBP as well as its downstream targets (such as fatty acid synthase and acetyl-CoA carboxylase a), independently of feeding behaviour (Martelot et al. 2009), therefore proposing evidence of clock regulation of lipid synthesis. Moreover, lipid turnover and fatty acid β-oxidation are also rhythmic. Indeed, enzymes such as carnitine palmitoyltransferase 1, medium-chain acyl-CoA dehydrogenase, adipose triglyceride lipase (ATGL), hormone-sensitive lipase (HSL), and diacylglycerol acyltransferase 2 (DGAT2) have all been shown to display rhythmic expression in various tissues (Alenghat et al. 2008; Shostak, Meyer-Kovac, and Oster 2013; Tsai et al. 2010; Filiano et al. 2013). In addition, oscillations in *Hsl* and *Atgl* are abolished in white adipose tissue from *Bmal1* null mice (Shostak, Meyer-Kovac, and Oster 2013) while Dgat2 rhythms are lost in cardiac tissue of $Clock^{\Delta 19/\Delta 19}$ mutant mice (Tsai et al. 2010), supporting a role of the clock in regulating their expression. Taken together, the cell autonomous circadian clock seems to play a vital role in regulating lipid metabolism at multiple levels.

1.4.3 Cross-talk between metabolism and circadian clocks

As discussed previously, a role for the clock in regulating metabolic function is evident. Interestingly, various metabolic pathways can feedback and interact with the clock, hence facilitating circadian and metabolic cross-talk. On one hand, AMP-activated protein kinase (AMPK), a catabolic energy sensing molecule that is primarily activated due to ATP depletion (Carling 2005), has been shown to interact with the clock machinery. Indeed, AMPK directly phosphorylate CK1ε, increasing its activity and

promoting PER degradation (Um et al. 2007). It also phosphorylates and destabilises CRY1 (Lamia et al. 2009). In addition, metformin, an indirect AMPK activator, has been shown to promote phase changes in a tissue-specific manner, inducing advances in liver and delays in muscles (Barnea et al. 2012), thus supporting the role of AMPK in linking the metabolic state to circadian clocks.

Similarly, peroxisome proliferator-activated receptor (PPAR) signalling serves as a key link between metabolism and the clock. PPARα expression is mediated by CLOCK-BMAL1, and it itself can bind peroxisome-proliferator elements (PPRE) and drive *Bmal1* expression (Oishi, Shirai, and Ishida 2005; Canaple et al. 2006; Inoue et al. 2005). FFA also bind PPARα which triggers transcription of genes involved in lipid and glucose metabolism (Lefebvre et al. 2006; Kersten, Desvergne, and Wahli 2000). Likewise, PPAR γ coactivator (PGC-1α), which is a key regulator of energy metabolism displays rhythmicity and can also reciprocally induce *Bmal1* and *Rev-erbα* expression through coactivation of ROR (Liu et al. 2007). Indeed, in their study, Liu et al showed abnormal expression of clock and metabolic genes in skeletal muscles and liver of PGC-1α null mice, which stresses its importance for cell-autonomous clock function (Liu et al. 2007).

In addition, SIRT1, a NAD^+ dependent histone deacetylase that catalyses transcriptional silencing (Cantó and Auwerx 2013), has also been shown to interact with the clock. In addition to targeting PPARY and PGC-1α which promote *Bmal1* expression, SIRT1 directly interacts with CLOCK and deacetylates BMAL1 and PER2 (Asher et al. 2008;

Nakahata et al. 2008), as a result, altering their stability. Furthermore, presence of NADH/NADPH promote efficient CLOCK-BMAL1 or NPAS2-BMAL1 heterodimerisation and therefore enhance their E-box binding, whereas on the other hand, NAD^+/$NADP^+$ inhibits it (Rutter et al. 2001). Hence, the levels of NAD^+ and rhythmicity of SIRT1 help maintain robustness of clock gene expression.

Therefore, cross-talk between the metabolic and circadian systems is evident, which acts as an extra layer of clock regulation for fine tuning circadian rhythmicity.

1.4.4 Circadian disruption and the metabolic syndrome:

One of the major contributions of the industrialised world has been the introduction of artificial light, which enabled night-time working, promoted voluntary sleep curtailment, and caused sleep and circadian rhythm disruption (SCRD) to become a ubiquitous feature in today's 24/7 society (Maury, Ramsey, and Bass 2010).

Interestingly, circadian disruption has been strongly associated with key features of MetS. Growing evidence from clinical epidemiological studies has shown shift work, such as night work or rotating shift work with irregular or unusual working hours, to be strongly associated with key symptoms of metabolic disorders like body weight gain and impaired glucose tolerance (Proper et al. 2016; Wang et al. 2011). Indeed, Sheer et al. demonstrated unfavourable metabolic and cardiovascular endpoints in human subjects as a consequence of forced circadian and behavioural misalignment. Mimicking shift

work and jet lag in this controlled clinical setting resulted in quantifiable significant reduction in leptin and an increase in glucose levels, despite insulin increase, demonstrating postprandial glucose responses within the typical prediabetic range which is indicative of worsened metabolic phenotype (Scheer et al. 2009).

Against this backdrop of clinical studies, mounting genetic evidence from human population studies have also uncovered a significant link between clock genes and symptoms of metabolic syndrome. For instance, two haplotypes of BMAL1 have been correlated to hypertension and type 2 diabetes (Woon et al. 2007), and polymorphisms in NPAS2 and PER2 gene have also been associated with hypertension and fasting hyperglycaemia, respectively (Englund et al. 2009). Similarly, CLOCK gene polymorphisms display higher predisposition to obesity (Scott, Carter, and Grant 2007; Sookoian et al. 2008). Furthermore, recent genome-wide association (GWAS) studies identified genetic variants in melatonin 1B receptor (*mtnr1b*) to be a major risk factor for developing T2DM (Bouatia-Naji et al. 2009; Prokopenko et al. 2009). This receptor corresponds to the nocturnal hormone, melatonin, which is a key output of the circadian machinery released from the pineal gland under direct control of the SCN and is inhibited by light (Pevet and Challet 2011). Interestingly, melatonin has been shown to regulate glucose-stimulated insulin secretion and its *mtnr1b* receptors are expressed in pancreatic β-cells (Lyssenko et al. 2009). Furthermore, in patients with T2DM, melatonin secretion is impaired (Radziuk and Pye 2006). Taken together, this suggests that

circadian disruption, either directly through impaired clock gene expression, or indirectly via melatonin, could actively contribute to the pathophysiology of MetS.

In addition to human studies, mutant mice provided compelling evidence for the role of the circadian clock in the development of metabolic syndrome. On one hand, homozygous *Clock* mutant mice (*Clock*$^{\Delta 19/\Delta 19}$), that show a loss of function of this gene, not only displayed arrhythmic feeding behaviour, but were also obese, hyperphagic and developed a pronounced metabolic phenotype characteristic of the MetS, which included hyperglycaemia, hyperinsulinemia, hepatic steatosis and dyslipidaemia (Turek et al. 2005). Furthermore, conditional knockdown of the *Clock* gene in pancreatic ß-cells has been shown to trigger diabetes mellitus (Marcheva, Ramsey, et al. 2010). Similarly, whole-body *Bmal1* knockout mice have reduced plasma insulin, impaired glucose tolerance and display fasting hypoglycaemia and increased adiposity (Rudic et al. 2004). Furthermore, obesity is one of the biggest hallmarks of metabolic syndrome, associated with adipocyte hyperplasia and hypertrophy, and *Bmal1* has been strongly implicated in adipose differentiation and lipogenesis. For instance, Bmal1 levels increase during adipose differentiation of 3T3-L1 mouse embryonic cells and its overexpression increases their lipid synthesis activity (Shimba et al. 2005).

On the other hand, aspects of metabolic syndrome like obesity and insulin intolerance have also been associated with signs of a disrupted clock. For example, obesity has been correlated to disruption of clock gene expression. In a small population of lean and obese

women, being obese altered adipocyte clock gene expression throughout the day and showed a significant upregulation of CRY2 and REV-ERBα, two key negative regulators of the TTFL, with the latter showing a clear positive correlation with BMI and waist circumference (Vieira et al. 2014). Similarly, patients with T2DM show a clear inverse correlation between their period length and the degree of hyperglycaemia exhibited, as represented by HbA_{1c} levels (Sinturel et al. 2019). All together, these findings highlight a clear overlap between the circadian clock and the pathophysiology of metabolic syndrome.

1.5 Exploiting the clock to combat metabolic syndrome:

The metabolic syndrome exhibits a multifaceted pathophysiology which would benefit from a multi-targeted therapeutic approach. As previously discussed, the circadian clock regulates vast aspects of metabolism and dysfunctions in its functionality are attributed to various symptoms of metabolic disorder.

Circadian robustness, or amplitude of clock gene expression, acts as an important physiological function and a dampened amplitude strongly correlates with chronic diseases, aging and aspects of metabolic syndrome (Schroeder and Colwell 2013; Gloston, Yoo, and Chen 2017). Indeed, shift work, known to be a prominent cause of metabolic syndrome, has been shown to reduce amplitude of blood pressure variation across the day (Eckel-Mahan and Sassone-Corsi 2013). Furthermore, pancreatic islets from patients with T2DM display significantly dampened circadian oscillations which also correspond to a reduction in clock-controlled secretion of endocrine hormones like insulin and glucagon (Petrenko et al. 2020). Moreover, sleep deprivation (which is linked to circadian disruption and metabolic consequences (Spiegel, Leproult, and Cauter 1999) has been shown to reduce circadian amplitude of core clock genes as well as metabolic genes and significantly dampen rhythmic transcriptomes in blood (Moller-Levet et al. 2013). And similarly, obesity associated with high fat diet has also been shown to

significantly impair clock function in metabolic genes, dampening rhythmic expression of clock genes in liver and adipose tissue (Kohsaka et al. 2007).

Hence, it could be hypothesized that a reduction in rhythmicity of metabolic processes from various contributing factors could predispose the individual to misalignment and consequent inefficiencies in maintaining metabolic homeostasis, whereas increasing the amplitude of clock gene expression would make peripheral clocks more resistant to desynchrony. Furthermore, increasing amplitude of CLOCK/BMAL1 on its own ,independently of circadian desynchrony, would drive greater timely expression of their downstream CCG such as key metabolic players like Hormone sensitive lipase (HSL), triglyceride hydrogenase (TGH), hexokinase (HK), Glyceraldehyde 3-phosphate dehydrogenase (Gapdh), etc which could enforce these metabolic pathways, improve efficiency and could possibly show benefit against different aspects of metabolic disorders.

Indeed, mice lacking *Nocturnin,* a circadian deadenyalse that is involved in clock-regulated posttranscriptional regulation of mRNA stability and/or translatability (Baggs and Green 2003), are resistant to diet-induced obesity and hepatic steatosis (Green et al. 2007). They also display significant enhancement in amplitude of mRNA expression of key metabolic hepatic enzymes involved in lipid and cholesterol synthesis (Stubblefield et al. 2018). This suggests that increasing metabolic flux via enhancing expression of metabolic genes can help protect against obesity. Similarly, pharmacological

enhancement of clock gene expression has also shown similar benefit. Nobiletin, a polymethoxyflavone extracted from orange peel and a potent ROR agonist, was shown to enhance amplitude of *Per2*-promoter expression in fibroblasts and pituitary explants (He et al. 2016). In parallel, *in vivo* nobiletin administration protected against diet-induced obesity and ameliorated symptoms of metabolic syndrome and, more importantly, these benefits were eliminated following loss of *Clock* gene function, suggesting a clock-dependent mechanism. Hence, taken together, these studies support a strong case for strengthening the clock gene rhythmicity in combatting metabolic syndrome.

Nonetheless, other circadian modulators that target the negative arms of the clock and affect amplitude and period differently have also shown benefit. For instance, CRY agonist KL001 significantly dampens amplitude of *Bmal1* and *Per2* expression in U2OS cells, fibroblasts and SCN explants and elongates their period length (Hirota, Lee, St. John, et al. 2012). More notably, it inhibits glucagon induced hepatic gluconeogenesis (Hirota, Lee, St. John, et al. 2012) and an improved CRY agonist also reported strong *in vivo* antidiabetic benefit (Humphries et al. 2016). Similarly, synthetic REV-ERB agonists (SR9011 and SR9009) dampen *Bmal1* promoter expression and *Per2* rhythms in SCN cultures (Solt et al. 2012). *In vivo*, they also reduce wheel running activity, increase energy expenditure, and significantly decrease fat mass and plasma lipids in diet-induced obese mice. However, despite displaying an overall improvement in metabolic genes, these *in vivo* observations are paralleled with differential effects on clock genes in the hypothalamus and liver.

Although both CRY and REV-ERB agonists significantly reduce amplitude of the clock, it cannot be ruled out that their actions could be target-specific, independent of the clock machinery. For example, in the case of REV-ERB agonists, despite liver core clock genes being unaffected, REV-ERB mRNA expression was significantly reduced, and that was correlated with a reduction in PPARy and shifts in Fasn and HMG-CoA. Furthermore, it is not clear what happens to the skeletal muscle and WAT clocks (Solt et al. 2012). Therefore REV-ERB specific effect independent of the clock cannot be ruled out. In addition, different tissues express various clock-controlled genes, and chrono-modulation might have varying effects based on tissue type and cell-specific stoichiometry. For instance, different patterns of expression of ROR and REV-ERB subtypes have been reported in nervous and peripheral tissues (Guillaumond et al. 2005). Similarly, differences in stoichiometry of core clock genes like PER and BMAL1 have also been reported in fibroblasts with PER being significantly less abundant, thereby acting as the limiting factor (Lee et al. 2011), which if altered, could therefore induce a bigger impact. This emphasises the influence of the clock target under consideration and the tissue-specific effects on outcomes of chrono-modulation.

All in all, it is clear that chrono-modulation displays profound benefit against metabolic syndrome, and in the search for new therapeutic interventions for this condition, targeting the clock seems to be a very promising area to pursue. However, which direction/form of chrono modulations is useful to manage MetS remains poorly

understood. Furthermore, tissue and target-specific effects of chrono-modulation still require further elucidation. The adipocyte is emerging as a key metabolic tissue with a pronounced endogenous clock (discussed in chapter 3). As a major contributor to metabolic syndrome and obesity, understanding how amplitude enhancement in this tissue can affect its metabolic profile will give a better understanding of how chrono-modulation can be used as a therapeutic strategy.

1.6 Aims

Therefore, the overall aims of this thesis can be divided into 4 key points:

1. A drug discovery investigation, to identify and validate novel chrono-modulators.
2. A metabolic investigation at the level of the adipocyte that screens the lead amplitude enhancing molecules on key pathways involved in metabolic syndrome, in order to understand the effects of amplitude enhancement on the adipocyte metabolic phenotype.
3. A mechanistic investigation to pinpoint the pathways via which our key leads interact with the clock and shed light on novel pathways via which the clock and metabolism interact.
4. An *in vivo* investigation for one chosen chrono-modulator in a model of diet-induced obesity to understand the influence of target vs clock effect in ameliorating development of MetS.

To address these points, the result chapters will be divided as follows:

- ◊ Chapter 3: This chapter will focus on identifying novel small molecules that increase amplitude of circadian clock expression. By setting up metabolic screens in an adipocyte *in vitro* model that correlate with key hallmarks of glucose intolerance and obesity and testing the validated chrono-modulators on them, this chapter aims to delve deeper into the effects of amplitude enhancers on metabolism, focusing purely on the adipocyte autonomous clock, away from humoral or neuronal influences and SCN inputs.
- ◊ Chapter 4: This chapter will investigate the mechanism of action underlying the circadian effects of Linopirdine, the most interesting lead from our circadian and metabolic screens.
- ◊ Chapter 5: This chapter will investigate the *in vivo* effects of Linopirdine in a diet-induced model of metabolic syndrome, to understand which mechanism holds stronger influence; its target-specific actions or its clock-enhancing properties.
- ◊ Chapter 6: Following the unbiased identification of a cGMP-specific phosphodiesterase inhibitor (Zaprinast) in our circadian screen, this chapter will aim to investigate the role of cGMP in peripheral clocks, and dissect the role of CREB in mediating its circadian effects.

CHAPTER 2: Methods

2.1 General Methods:

2.1.1 Cell culture technique:

All cell and tissue culture techniques were executed under sterile environments using a containment level II biological safety cabinet (Gelaire). Cells were maintained in 75 cm^2 or 25 cm^2 cell culture flasks (Greiner, Corning) in incubators (Panasonic) at 37°C under high humidity and 5% CO_2. All experiments were carried out in white clear-bottomed 96-well or 384-well plates (Greiner) unless mentioned otherwise.

2.1.1.1 Cell culture media

DMEM: Dulbecco's Modified Eagle's Medium (DMEM) with high glucose GlutaMAX supplement (ThermoFisher Scientific), 10% fetal bovine serum (FBS, Sigma), and 1% penicillin-streptomycin (P/S) (Sigma)

3T3-L1 MM media: Dulbecco's Modified Eagle's Medium (DMEM) with high glucose GlutaMAX supplement (ThermoFisher Scientific), 10% New born calf serum (NBCS, Sigma), and 1% penicillin-streptomycin (P/S) (Sigma)

RPMI: Roswell Park Memorial Institute (RPMI) media, supplemented with 10% FBS, 1% P/S, 1x GlutaMAX, 55ng/mL recombinant human epidermal growth factor (R&D systems), 16ng/mL insulin-like growth factor (Cambridge Bioscience), and 10 μg/mL human insulin (Roche Diagnostics).

MEF media: Dulbecco's Modified Eagle's Medium (DMEM) with high glucose GlutaMAX supplement (ThermoFisher Scientific), 10% FBS, 1% penicillin-streptomycin (P/S) (Sigma) and 1x Low Serum Growth Supplement (LSGS, Gibco)

Recording Media: For many experiments, low glucose DMEM (D2902 Powder) (Sigma) was used, which will be denoted as recording media. The recording media was supplemented with 9.5 mL/L 45% D-glucose solution (Sigma), 10mM HEPES solution (Sigma), 3.7 g/L NaHCO3 solution (Sigma), 0.5% P/S, 1x GlutaMAX and adjusted to pH 7.3 in 1L of water.

2.1.1.2 Maintenance of cell lines

The two main immortalised cell line used were the human U2OS osteosarcoma cells and the murine 3T3-L1 preadipocytes with and without stable *Per2*-d*Luc* or *Bmal1*-d*Luc* expression. These are promoter driven luciferase genes that allow photon detection following transcription factor binding to the *Per2* or *Bmal1* promoter regions. The U2OS-blank cells and the 3T3-L1 blank cells were obtained from the ATCC, the *Per2*-d*Luc* U2OS cells were gifted from Patrick Nolan (MRC Harwell, UK), and the *Bmal1*-d*Luc* U2OS cells were generated in-house.

U2OS cell lines were maintained in DMEM on standard tissue culture flasks, from passage 2-30, and were passaged when 80- 90% confluent and subcultured 1-2 times a week. The

3T3-L1 pre-adipocyte cells were maintained in DMEM with 10% NBCS (sigma) substituting the FBS and were kept under 50% confluency for 2-3 passages only.

Mouse embryonic fibroblasts (MEF) expressing stable PER2::LUCIFERASE fusion protein were (generated in-house), were also used and were maintained in MEF media for 1-3 passages.

The murine MMH-D3 pre-hepatocytes harbouring *Bmal1*-d*Luc* (generous gift from Hogenesch, University of Pennsylvania, USA), were also used for the drug screens. These cells were grown on rat tail collagen type 1 (Corning) pre-coated flasks, prepared as 50 µg/mL in 0.2 M acetic acid for a minimum of 5h, and maintained in RPMI media for 2-30 passages.

After washing with Dulbecco's phosphate-buffered saline (PBS) without magnesium or calcium (ThermoFisher Scientific), the cells were passaged using TrypLETM solution (ThermoFisher Scientific).

2.1.2 Differentiation of 3T3-L1 adipocytes:

3T3-L1 cells are mouse-derived fibroblast-like pre-adipocytes originally isolated from clones of Swiss 3T3 fibroblasts (Green and Kehinde 1974), which in the right conditions, can be differentiated into mature adipocytes. Following differentiation, these cells acquire an adipocyte morphology, with higher accumulation and synthesis of

triglycerides, and greater sensitivity to lipolytic and lipogenic hormones. They can also be manipulated molecularly and are responsive to drug treatments (Green and Kehinde 1975). To promote differentiation of 3T3-L1 preadipocytes, a cocktail of drugs must be supplemented to their culture media, which include: insulin, dexamethasone (a corticosteroid), and 3-Isobutyl-1-methylxanthine (IBMX). To achieve higher differentiation efficiency, a PPARG-agonist such as rosiglitazone could also be added (Zebisch et al. 2012). In our experiments, two protocols for adipocyte differentiation were followed. 3T3-L1 cells intended for differentiation must be grown on rat tail collagen type 1 (Corning) pre-coated flasks or plates.

ZenBio protocol: In this protocol, differentiation of 3T3-L1 cells was achieved following ZenBio (ZBM0009.06) instructions, where the full cocktail of drugs were used. 3T3-L1 preadipocytes were maintained in 3T3-L1 MM media and allowed to grow until 100% confluency. 48 hours after reaching confluency, differentiation was initiated (D0) by replacing 3T3-L1 MM media with differentiation media (DM-2-L1: containing, DMEM high glucose (Dulbecco), 10% FBS, and a final concentration of 1 µg/mL insulin (sigma), 500 µM IBMX (sigma), 1 µM Dexamethasone (sigma), and 2 µM Rosiglitazone (Abcam)). 3 days later (D3), media was replaced with adipocyte maintenance media and incubated for 2-3 days (AM-1-L1; containing final concentration of 1 µg/mL insulin and 1 µM Dexamethasone). Cells were fed every 2-3 days using AM-1-L1 media. At day 7-14 post differentiation using this protocol, 3T3-L1 adipocytes are suitable for most assays.

Promega protocol: Similar to the ZenBio protocol, induction of differentiation was commenced 48 hours after 3T3-L1 cells have reached confluency (D0). This was done by replacing the 3T3-1 MM media with DM-1 for 7 days (containing DMEM high glucose (Dulbecco), 3% FBS, and a final concentration of 1 µg/mL insulin (sigma), 500 µM IBMX (sigma), 1 µM Dexamethasone (sigma), and 2 µM Rosiglitazone (Abcam). Next (at D7), DM-2 media was used for 2 days (containing DMEM high glucose (Dulbecco), 3% FBS, and a final concentration of 1 µg/mL insulin (sigma)). At day 9, cells were maintained using maintenance 3T3-L1 MM media, fed every 2-3 days, until mature adipocytes were achieved at approximately Day 15-18. This protocol has the advantage of an insulin-free period which makes it more sensitive and reproducible for investigating insulin responses than the ZenBio protocol.

2.1.3 Luminescence detection experiments

Plate readers were used for detection of luminescence. Readers included: FLUOstar Omega and FLUOstar Optima (BMG Labtech), TriStar^2 LB 942 (Berthold Technologies), Tecan Infinite M200 Pro, and Tecan Infinite F200 (Tecan).

2.1.3.1 Transient transfection

Plasmid DNA was diluted to 1 µg per 100 µL of reduced serum Opti-MEM (ThermoFisher Scientific) with 4 µL of ViaFect transfection reagent (Promega) for U2OS cells. For cellular assays, reverse transfection in 96-well plates was carried out using 100 ng of DNA per well for 24 hours prior to use.

2.1.3.2 In vitro siRNA transfections

SMARTpool siRNA (Dharmacon) was assessed on human U2OS cells. The siRNA used in U2OS included: non-targeting control (NTC), *Hif1α, Rxrα , Rxrβ , Thrβ , Mef2d , Mafb, C/EBP*(α,β,γ,δ,ζ), *CKe, Jun, Stat2-4, Yy1, Fhl1, Celf6, Mbln1, Sp4, Gfi1B, Hinfp, Rbm42, Max, Hes5*, *Hey2, Meis1,3, Mafg, Pax2,* and *Fxr1*. All siRNA samples were resuspended and diluted to 2 μM concentrations using nuclease-free siRNA Buffer (Dharmacon). Cells were reverse transfected with 10-20 nM siRNA using lipofectamine RNAiMAX (Thermofischer) according to the manufacturer's instructions. This required diluting the siRNA in a final volume of 10 μL Opti- MEM, and 0.3 μL Lipofectamine RNAiMAX in a final volume of 10 μL Opti-MEM per well. The siRNA mix was next added to the transfection reagent (20 μL of whole complex), incubated at room temperature for 15 min and then subsequently added into corresponding wells. 15,000 cells suspended in 80 μL of DMEM media (lacking P/S) were then added per well. Cells were then incubated at 37^{o}C for 24h and synchronized with 200 nM dexamethasone prior to using them for circadian bioluminescence assays or real-time PCR analysis. RNA extractions were performed 48h after transfection.

2.1.3.3 Assessing circadian rhythms

Cells were seeded to 100% confluence in 24, 96- or 384-well plates and were synchronised using Dexamethasone, a glucocorticoid receptor agonist which allows observation of cellular rhythmic patterns by synchronising the clocks within individual cells. All cells were first treated with 200 nM dexamethasone (Sigma) in recording media

for 1.5h, then washed twice and finally treated with recording media supplemented with B27 (ThermoFisher Scientific), 400 μM D-luciferin potassium salt (Gold Biotechnology), with or without pharmacological compounds of interest. Bioluminescence was quantified for a minimum of 3 days in the micro-plate reader. The U2OS and 3T3-L1 were tested using a range of the above-mentioned micro-plate readers, however, MEF experiments were performed in the Tecan Infinite M200 Pro/ F200. Amplitude is reported in relative light units (RLU) or percentage change and period in hours.

2.1.4 mRNA Quantification

2.1.4.1 Cellular RNA preparation

RLT buffer (Qiagen) supplemented with 1% β-mercaptoethanol (Sigma), a reducing agent which degrades RNAases released as a result of cell lysis, was used for RNA extraction. RNA was obtained from U2OS cells and 3T3-L1 cells seeded in 24-well or 96-well plates and lysed using 350 μL or 100 μL per well RLT/β-mercaptoethanol mix respectively. RNeasy plus mini kit (Qiagen) was used for whole-cell RNA extraction based on manufacture instructions, with all centrifugation carried out at 13,000 g. In brief, cells in RLT mix were centrifuged in gDNA eliminator columns for 30 seconds. Next, flow-through was mixed at one volume with 100% ethanol (sigma) to precipitate the RNA, transferred to the RNeasy mini elute spin column to allow RNA to bind the column and centrifuged for 15s. Following that, columns were washed with buffers (RWI and RPE) before the addition of 80% ethanol, all of which were centrifuged for 15 s, 15 s, and 2 min respectively. Finally, RNA was eluted in 30 μL RNase-free-water following 1 min of

centrifugation and quantified using Nanordrop 2000 (ThermoFisher Scientific) prior to cDNA conversion.

2.1.4.2 Tissue RNA preparation

At the time of collection, tissue samples were cut at ≤ 0.5 cm in any single dimension and stored in 250 µL RNAlater (Invitrogen), which stabilizes and protects RNA. Tissues were then pelleted, supernatant discarded and samples were frozen at -80°C until needed. For total RNA extraction, TRIzol™ (ThermoFischer Scientific) was used following manufacture instructions. First, samples were homogenized in 1 mL of TRIzol™ using an electric homogonizer and then incubated for 5 minutes, to achieve full cell lysis and allow complete degradation of the nucleoproteins complex. 200 µL of chloroform (sigma) per 1 mL TRIzol™ were added, incubated for 5 minutes at room temperature, and centrifuged for 15 mins at 12,000 g at 4°C. This allowed the mixture to separate into a lower red phenol-chloroform containing protein, an interphase containing DNA, and a colourless upper aqueous phase containing RNA. The aqueous phase was then slowly transferred into a gDNA eliminator column and the RNeasy plus mini kit (Qiagen) was used for RNA-extraction, as mentioned earlier.

2.1.4.3 cDNA conversion

qScript cDNA Synthesis kit (Quanta Biosciences) was used for RNA to cDNA conversion following manufacture instructions. Per sample, 300 ng of RNA were converted to cDNA using 2 µL 5x qScript reaction mix and 0.5 µL qScript RT enzyme in a final volume of 10

μL water. The PCR protocol used, which in principle produces 1 copy of cDNA for 1 molecule of RNA, was as follows: 1 cycle of 22°C for 5min, 1 cycle of 42°C for 30min, and 1 cycle of 85°C for 5 min, before holding indefinitely at 4°C. cDNA samples were diluted in water to a final concentration of 2 ng/μL and stored at -80°C until real-time PCR was executed.

2.1.4.4 Real-time PCR

Real-time PCR was performed using the StepOne Real-Time PCR system (ThermoFischer Scientific) and SYBR green master mix (ThermoFischer Scientific). The SYBR-green intercalating fluorescent dye preferentially binds to dsDNA, hence as DNA denatures and is reformed and exponentially amplified during PCR, fluorescence can be used to interpret exponential increase in DNA. For the real-time PCR, 10ng of sample cDNA and 10 μL of master mix were loaded per well (96-well plate), the latter consisting of 2.2 μL water, 0.15 μL forward primer, 0.15 μL reverse primer and 7.5 μL 2x SYBR green. List of primers for each chapter could be found in their corresponding chapter methods. The PCR protocol involved 40 cycles of the following: an initial holding temperature of 95°C for 5min to activate the Taq polymerase, followed by 30 cycles of 95°C for 10s, 60°C for 30s, and 72°C for 12s. This was trailed by the production of a melt curve to validate primer specificity and quality.

2.1.5 Cell viability assay

Cell viability was assessed following termination of experiments using PrestoBlue™ cell viability assay (ThermoFisher Scientific). The reducing environment of live cells alters the non-fluorescent blue resazurin molecule found in this reagent into a very fluorescent resorufin molecule, which can be quantified using a plate reader. Viability assays were carried out by diluting the reagent to 1x in the respective cell-culture media, adding 50-100 µL per well of that, incubating at 37°C for 1h and finally measuring fluorescence intensity with the excitation and emission filters in a plate reader set at 544 nm and 590 nm, respectively. Empty wells containing no cells were used as negative control, and cell viability following treatment was determined by comparing to corresponding vehicle.

2.1.6 Pearson BCA Protein assay:

Protein levels were quantified using Pierce™ BCA Protein Assay Kit (ThermoFisher Scientific). This colorimetric assay utilises the well-validated reduction of Cu^{2+} to Cu^{1+} by protein in an alkaline environment (biuret reaction) and the subsequent sensitive and selective detection of Cu^{1+} using bicinchoninic acid (BCA). Two molecules of BCA chelate one Cu^{1+}, resulting in a purple-coloured reaction that displays strong absorbance at 562 nm. This reaction is nearly linear with ascending protein concentrations, allowing for protein detection and quantification. Briefly, the BCA working reagent is prepared by mixing 50 parts Reagents A with 1 part Reagent B (50:1). Then, in a 96-well plate format, 25 µL of unknown sample or standard are mixed with 200 µL of working reagent per well, and incubated at 37°C for 30min before measuring absorbance using a microplate

reader. A standard curve of known protein concentrations were used to determine concentrations of unknown samples.

2.1.7 Animals

All mice used in our experiments were reared and maintained under controlled ambient temperature of 20-22^{o}C, 40% humidity and 12:12h LD cycles. Standard chow was used as a source of food (unless stated otherwise) and together with water, were available ad libitum. For the DIO mouse models, ad libitum High-fat chow (Research diets, D12492: 60% Kcal Fat) or Diet-control chow (Research Diets, D12450J:10% Kcal Fat, matching sucrose to D12492) were used as a source of food. All animal experiments were implemented in agreement with the United Kingdom Animals (Scientific Procedures) Act of 1986.

2.1.8 General data analysis

Cell-based circadian analyses were done using a specialized software, MultiCycle (ActiMetrics). Unless specified otherwise, this software was used to compute the circadian amplitude and period of oscillations. MultiCycle calculates a baseline subtracted 24h running average of the raw luminescence data acquired from plate readers. It then smoothens the curve by 4h such that waveforms oscillate around Y=0, allowing comparison of various circadian parameters across wells and enabling the detection of subtle changes more accurately. Circadian parameters are then assessed by fitting a dampened sine wave on data, using a Levenberg-Marquardt algorithm. For all

cell-lines, the first 12-16 hours following synchronisation were excluded. Amplitude was then calculated for the first oscillation while period was calculated for 3 oscillations.

Circadian phase analysis was carried out manually following baseline-detrending using multicycle. Multicycle exported traces were plotted on excel and conditional formatting of traces was used to identify peaks and troughs. Subsequently, traces were adjusted to corresponding troughs and the start of the trough was set to time= 0h. Peaks were identified thereafter and their corresponding time denoted as phase (in hours). For this analysis, phase was calculated before and after drug treatment.

Real-Time PCR data was analysed using the Pfaffl-method. First standard curves for each primer-set were generated and used to estimate efficiency (E) of amplification (calculated as (1+ (-slope of standards)), which usually equates to 2. Then, CT values of all genes were converted to relative gene amount using the following equation:
$\mathcal{X} = E^{-CT}$ and then gene-of-interest (GOT) values were normalised to house-keeping genes (HKG) by dividing X_{GOT} by X_{HKG}. At least two HKGs were used for normalisation.

2.1.9 General statistical analysis

GraphPrad Prism 6 was used for all statistical analysis, where results were represented as average ± standard error of the mean (SEM). A one-way ANOVA with a Tukey or a Dunnett's post hoc test was performed when comparing multiple parameters, and an

unpaired two-tailed t-test was used when comparing two variables, unless specified otherwise. Significance was set at P<0.05. *P<0.05, **P<0.01, ***P<0.001, ****P<0.0001.

2.2 Chapter 3- Methods

2.2.1 Medium throughput screen:

Cells were grown to 100% confluency in 96 or 384-well plates, synchronised with dexamethasone, treated with drugs and bioluminescence was recorded in real-time to assess chrono-modulatory effects of different drug libraries on circadian rhythms (as described in **section 2.1.3.3.**). For the first round of screening, *Per2*-d*Luc* U2OS cells and *Bmal1*-d*Luc* MMH-D3 cells were seeded into 384-well plates and 10 μM of drug were used. The drug libraries used for the initial drug screen were: SPECTRUM, SCREEN-WELL FDA approved drug library V2 (Enzo Life Sciences, Inc) and NIH. For the second round of screening, interesting drugs were re-ordered (see **Table 2.1**) and *Per2*-d*Luc* U2OS cells were seeded in 384-well plates and treated with 5-doses per drug were used. Finally, *Bmal1*-d*Luc* and *Per2*-d*Luc* U2OS cells were used to validate key leads in 96-well plate format, as 5-point dose-responses per drug.

Table 2.1- Sources of drugs re-ordered for drug screen

No.	Drugs	Company
1	Enroflaoxacin 100mg	Sigma-Aldrich
2	Thiophene 99%	Alfa Aesar
3	Tetraethylthiuram disulfide 97%	Alfa Aesar
4	Enoxacin	Alfa Aesar
5	Tylosin tartrate 95%	Alfa Aesar

6	1-Benzhydrylpiperazine 97%	Alfa Aesar
7	Melphalan	Tocris
8	Dextrophan tartrate solution	Sigma-Aldrich
9	3-Trifluoromethylphenylpiperazine hydrochloride solution	Sigma-Aldrich
10	Levallophan tartrate salt 98%	Sigma-Aldrich
11	Riluzole (PK26124)	Abcam
12	Milnacipran hydrocholide	Abcam
13	Ondansetron hydrochloride	Abcam
14	Niflumic Acid	Fluorochem
15	Capsiacin	Sigma-Aldrich
16	Climbazole 5g	Fluorochem
17	Canrenone 1g	Fluorochem
18	Betamipron	Selleckchem
19	Moxifloxacin hydrochloride 50mg	Sigma-Aldrich
20	Linopiridine (Dup-996)	Abcam
21	Zaprinast	Abcam
22	Levocetirizine dihydrochloiride	Abcam
23	Milrinone	Abcam
24	Ampiroxicam	Abcam
25	Clopidol	Abcam
26	Xamoterol hemifumarate	Abcam
27	1'-hydroxy Midazolam	Cayman
28	Brimonidine (tartrate)	Cayman
29	Fasudil - HA-1077(hydrochloride)	Cayman
30	Idoxuridine	Cayman
31	Nicorandil	Cayman
32	Olmesartan Medoxomil	Cayman
33	Raloxifene (hydrochloride)	Cayman
34	Telmisartan	Cayman
35	Zileuton	Cayman
36	Oxaprozin	Cayman
37	Tenatoprazole	Cayman
38	Glycopyrrolate	Cayman
39	Todralazine (hydrochloride)	Cayman
40	Tenoxicam	Cayman
41	Melengestrol acetate	Insight Biotechnology
42	Propranolol hydrochloride	Insight Biotechnology
43	Sodium Phenylbutyrate	Insight Biotechnology
44	Cefalonium	Insight Biotechnology
45	Ceftazidime Pentahydrate	Insight Biotechnology
46	Epigallocatechin Gallate	Insight Biotechnology
47	Perindoprilat	Insight Biotechnology
48	Pinacidil	Insight Biotechnology
49	Venlafaxine hydrochloride	Insight Biotechnology
50	Carboplatin	Insight Biotechnology
51	2,3'-Dideoxyinosine	Insight Biotechnology
52	Amcinonide	Insight Biotechnology
53	Candesartan	Insight Biotechnology
54	Oxacarbazepine	Fluorochem
55	Mecillinam	Fluorochem
56	Dexchlorpheniramine Maleate	Sigma-Aldrich

57	Aprepitant	Biovision
58	Miglitol	Biovision
59	Chlorambucil	LKT Laboratories
60	Prednisone	Insight Biotechnology
61	Harmine hydrochloride	Insight Biotechnology
62	Nialamide	Insight Biotechnology
63	Deracoxib	LKT Laboratories
64	Carbadox 5g	Insight Biotechnology
65	Flutamide	Insight Biotechnology
66	Pentoxifylline	Insight Biotechnology
67	Triamcinolone	Insight Biotechnology
68	Diclazuril	Insight Biotechnology
69	Naltrindole Hydrochloride	Insight Biotechnology
70	Chlormadinone Acetate	Insight Biotechnology
71	3,7- dimethoxyflavone	Sigma-Aldrich
72	Cinnerazine	Sigma-Aldrich
73	Oxindole	Alfa Aesar
74	Chloroacetoxyquinoline	Alfa Aesar
76	Isoliquiritigenin	Cayman

2.2.2 Assessing circadian rhythms:

U2OS cells, 3T3-L1 cells were seeded in 96-well plates, whereas MEF were seeded in 24-well plates. Mature 3T3-L1 adipocytes were used following ZenBio differentiation protocol. Circadian rhythms were assessed similarly in all cell-lines, all of which were synchronized with dexamethasone, treated with drugs and their corresponding bioluminescence was recorded.

2.2.3 mRNA quantification of clock genes following drug treatment:

U2OS cells were grown to confluency in 24-well plates, synchronized with dexamethasone and then treated with Zaprinast, Linopirdine or Diclazuril at 3 μM each. mRNA was collected 16 hours later (time 0h), and 8 and 18 hours thereafter.

mRNA extraction and cDNA conversion were carried out as previously described in **section 2.1.4**, and quantification of *Per2* and *Bmal1* genes was done using qPCR. Primers used are listed in **Table 2.2**.

2.2.4 Glucose uptake

The Glucose Uptake-Glo™ assay (Promega) is a plate-based, bioluminescent approach that quantifies glucose uptake based on the detection of 2-deoxglucose-6-phosphate (2DG6P). When cells are incubated with 2DG, it is taken up by cells and phosphorylated to form 2DG6P via hexokinases. As a membrane-impermeable molecule that cannot be modified by enzymes that usually target G6P, 2DG6P accumulates intracellularly. An acidic detergent (Stop buffer) is then used to lyse cells, terminate uptake and eliminate any NADPH within cells. This is followed by a high-pH buffer to neutralise the acid (Neutralisation buffer) and a Detection Reagent to quantify the 2DG6P within the cells, as a proxy of a reaction that reduces $NADP^+$ to NADPH, which subsequently converts pro-luciferin to luciferin, and in the presence of luciferase, generates light (see **Figure 2.1**).

3T3-L1 cells were differentiated according to the Promega protocol in **Section 2.1.2**, and the assay was performed on day 15-19 of differentiation. To assess capacity of our key leads to alter glucose uptake, cells were treated with drugs in serum free media for 24 hours prior to the assay, and the next day, glucose and serum starved for 1h before the experiment was performed using the kit mentioned above. Luminescence was quantified

using a micro-plate reader and quantification of 2DG6P, as a proxy of glucose uptake, was done by removing the baseline and fitting the values on a standard curve.

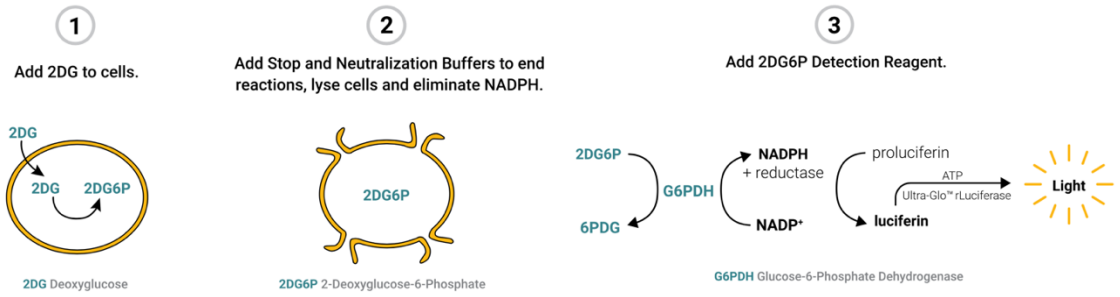


Figure 2.1 Schematic diagram of the Glucose-Uptake Glo™ assay principle.

2.2.5 Nile Red Staining of lipid droplets and its quantification in adipocytes:

For assessing adipogenic effects of the lead circadian-modulators in 3T3-L1 cells, Zaprinast (10 µM), Diclazuril (10 µM), Linopirdine (10 µM) or vehicle (DMSO 0.1%) were administered with the media throughout the differentiation process starting at D0. For *experiment 1*, the ZenBio differentiation protocol mentioned in **section 2.1.2** was used. In *experiment 2*, the same protocol was followed but without rosiglitazone in the cocktail. As a potent inducer of 3T3-L1 differentiation (Zebisch et al. 2012), rosiglitazone was removed to avoid masking any drug-mediated enhancement of differentiation.

Nile red (9-diethylamino-5H-benzo[alpha]phenoxazine-5-one, Sigma) was used to stain and quantify lipid droplet accumulation following the differentiation protocol. Nile red is a fluorescent lipophilic stain that is very soluble in lipids, therefore staining intracellular

lipids without dissolving them (Fowler and Greenspan 1985). It strongly fluoresces in a lipid-rich environment, with colours varying from deep red (in polar lipids like in membranes) to yellow-gold (in neutral lipids like intracellular storages) and exhibits an emission/excitation wavelengths of 515-560/>590 nM and 450-500/528 nM for these colour ranges, respectively (Greenspan, Mayer, and Fowler 1985). At day 9 of differentiation, cells were fixed with 4% Paraformaldehyde in PBS, for 15 minutes at room temperature, washed, and then stained with Nile red as per manufacture instructions. This involved diluting Nile red to a final concentration of 1 μg/mL in PBS and incubating for 5-7 min at room temperature followed by multiple washes to eliminate excess dye. Microscope images were taken using EVOS M7000 (ThermoFisher Scientific) at RFP channel (Ex 531/40, Em 593/40 nm) to ensure quantification of membrane lipids. Fluorescence intensity was subsequently quantified using Celleste™ image analysis software (ThermoFisher Scientific) and normalised to nuclei count (as stained by DAPI, mentioned below).

2.2.6 Nuclear staining and quantification in adipocytes:

DAPI (4',6-diamidino-2-phenylindole, Thermofischer Scientific) is a fluorescent dye able to stain both live and fixed cells, by binding adenine-thymine rich regions within DNA. DAPI can be used to stain and visualise nuclei by binding to dsDNA, with a maximal absorption at 358 nM (ultraviolet) and a maximal emission at 461 nM (blue) (Kapuscinski 1995). For nuclear staining, manufacture instructions were followed, which involved incubating fixed cells with 300 nM DAPI stain solution (in PBS) for 5

minutes, protected from light, and then washing 2-3 times with PBS to eliminate excess stain. Microscope images were subsequently taken using EVOS M7000 (ThermoFisher Scientific) at DAPI channel (Ex 357/44, Em 447/60 nm), and CellesteTM image analysis software (ThermoFisher Scientific) was used for quantification of DAPI-stained nuclei.

2.2.7 Quantification of mRNA adipogenic markers in adipocytes:

3T3-L1 cells were differentiated in the presence of Zaprinast (10 μM), Diclazuril (10 μM), Linopirdine (10 μM) or vehicle (DMSO 0.1%) throughout differentiation, following Zenbio protocol (ZBM0009.06). At day 9 of differentiation, mRNA was collected and qPCR was carried out as described in **section 2.1.4**., using mouse primers listed in **Table 2.2.**

Table 2.2- Sequences of the primers used in Chapter 3

Species	Gene	Forward/Reverse	Sequence 5'-3'
Homo Sapiens	*Bmal1*	Forward	GCCCATTGAACATCACGAGTAC
Homo Sapiens	*Bmal1*	Reverse	CCTGAGCCTGGCCTGATAGTAG
Homo Sapiens	*Per2*	Forward	AGTTGGCCTGCAAGAACCAG
Homo Sapiens	*Per2*	Reverse	ACTCGCATTTCCTCTTCAGGG
Homo Sapiens	*Gapdh*	Forward	AAGGTGAAGGTCGGAGTCAT
Homo Sapiens	*Gapdh*	Reverse	GAAGATGGTGATGGGATTC
Homo Sapiens	*β-Actin*	Forward	CATGTACGTTGCTATCCAGGC
Homo Sapiens	*β-Actin*	Reverse	CTCCTTAATGTCACGCACGAT
Mus Musculus	*UCP1*	Forward	GGCCTCTACGACTCAGTCCA
Mus Musculus	*UCP1*	Reverse	TAAGCCGGCTGAGATCTTGT
Mus Musculus	*Prdm16*	Forward	AGGAACACGCTACACGGATG
Mus Musculus	*Prdm16*	Reverse	ACTTTGGATGGGAGAGATGCTG
Mus Musculus	*Cidea*	Forward	CGTGGTGGACACAGAGGAGTT
Mus Musculus	*Cidea*	Reverse	CATTGAGACAGCCGAGGAAGT
Mus Musculus	*Ppary*	Forward	GGTGTGATCTTAACTGTCGG
Mus Musculus	*Ppary*	Reverse	TTCAGCTGGTCGATATCACT
Mus Musculus	*Pgc1a*	Forward	TGAATGACCTGGACACAGACA
Mus Musculus	*Pgc1a*	Reverse	ATCAAATGAGGGCAATCCGTC
Mus Musculus	*Hoxc9*	Forward	ACTCGCTCATCTCTCACGACA
Mus Musculus	*Hoxc9*	Reverse	AGGACGGAAAATCGCTACAGT

Mus Musculus	*Fabp4*	Forward	AAGGTGAAGAGCATCATAACCCT
Mus Musculus	*Fabp4*	Reverse	TCACGCCTTTCATAACACATTCC
Mus Musculus	*Leptin*	Forward	CTCCATCTGCTGGCCTTCTC
Mus Musculus	*Leptin*	Reverse	CATCCAGGCTCTCTGGCTTCT
Mus Musculus	*Adiponectin*	Forward	TGTTCCTCTTAATCCTGCCCA
Mus Musculus	*Adiponectin*	Reverse	CCAACCTGCACAAGTTCCCTT
Mus Musculus	*Glut4*	Forward	CCGGCAGCCTCTGATCAT
Mus Musculus	*Glut4*	Reverse	CCGACTCGAAGA TGCTGGTT
Mus Musculus	*β-Actin*	Forward	ACCAACTGGGACGATATGGAGAAGA
Mus Musculus	*β-Actin*	Reverse	CGCACGATTTCCCTCTCAGC
Mus Musculus	*Nono*	Forward	GCCAGAATGAAGGCTTGACTAT
Mus Musculus	*Nono*	Reverse	TATCAGGGGGAAGATTGCCCA

2.2.8 Lipolysis:

Lipolysis is the process of triglyceride hydrolysis into fatty acids and glycerol, which are then released into the surrounding environment, or culture media. The lipolysis assay kit (Abcam, ab185433) is a colorimetric assay that quantifies glycerol in media, at a wavelength >540 nm. By quantifying glycerol levels released over a 24h period in the presence or absence of drugs, changes in lipolysis activity can therefore be analysed (Schweiger et al. 2014).

To assess effect of circadian modulators on basal lipolysis of adipocytes, 3T3-L1 cells were differentiated using ZenBio protocol (ZBM0009.06) in 24-well plates, and at Day 10, Lipolysis assay was carried out following manufacturer instructions. This entailed changing the adipocyte maintenance media into phenol-less and serum-less DMEM, containing 2% bovine serum albumin (Fatty acid-free BSA, sigma) and the drugs in question (Zaprinast, Diclazuril, Linopirdine at a final concentration of 10 μM or vehicle (DMSO 0.1%)) and incubating the cells for 24h at 37°C in an incubator. Culture media

was then collected and assessed for glycerol concentration using the above mentioned kit relative to a standard glycerol solution, cells were lysed using RIPA buffer (Sigma), and protein content of cell lysate was quantified using BCA reagent (Sigma). Glycerol concentrations were then normalised to protein content to account for cell growth variability.

2.2.9 Assessment of Cellular Bioenergetics

To assess ATP production and mitochondrial bioenergetics of 3T3-L1 adipocytes, the Seahorse XF Analyzer assay (Agilent) was used. This assay measures oxygen consumption rate (OCR) (pmol/minute) and extracellular acidification rate (ECAR) (mpH/minute) of live cells, and assesses mitochondrial respiration and glycolysis using sequential addition of various inhibitors, such as oligomycin, carbonyl cyanide-4 phenylhydrazone (FCCP), rotenone and antimycin A, that enable quantification of ATP production, maximal respiratory, and non-mitochondrial respiration (NMR), respectively. Oligomycin inhibits ATP synthase (complex V), causing a decrease in mitochondrial respiration (OCR) which corresponds to ATP-production. FCCP uncouples the mitochondrial proton gradient and induces maximal electron flow and oxygen consumption by complex IV, which allows for maximal respiration and spare capacity measurements. Rotenone and antimycin A are complex I and complex III inhibitors, respectively, which shut down mitochondrial respiration and enable the calculation of NMR (**Figure 2.2).** Formulas used for the calculations are listed in **Table 2.3.**

Differentiated 3T3-L1 adipocytes were seeded at 20,000 cells/well in XF^{e}96 microplate pre-coated with collagen (see **section 2.1.2**), maintained in 3T3-L1 MM media for 2 days, and treated with drugs of interest for 24h (as described in (Isidor et al. 2016). The media was replaced with XF Assay medium containing 4.5 g/L glucose, 4.0 mM Glutamine and 1.0 mM Sodium pyruvate (pH adjusted to 7.35±0.05 using 1 mol/L NaOH). The plates were placed in a 37°C incubator without CO_2 for 1h prior to the assay. OCR and ECAR measurements were performed using Seahorse Biosciences XF^e Analyzer at 37°C following sequential addition of oligomycin(2.5 µM), FCCP(1 µM), rotenone/antimycin-A (0.5 µM/0.5 µM) and 2-deoxyglucose (2DG 100 mM).

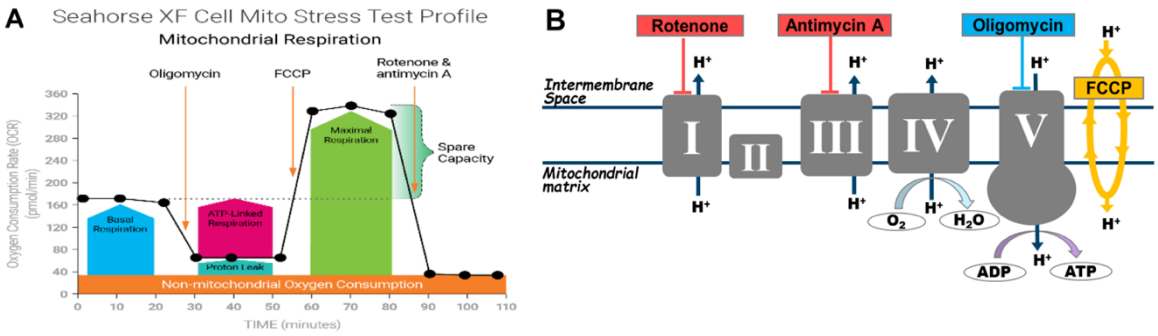


Figure 2.2. Seahorse XF Analyzer assay: (A) To assess mitochondrial respiration, basal OCR levels are quantified, then oligomycin, FCCP, Rotenone/AntimycinA are added sequentially, which inhibit different enzymes involved in the mitochondrial electron transport chain, and allow assessment of mitochondrial respiration and glycolysis **(B)** Targets for mitochondrial inhibitors used in assay.

Table 2.3. Calculations for mitochondrial and glycolytic parameters following OCR and ECAR measurements.

Parameter of interest	Calculation
Basal Respiration	First OCR before oligomycin injection
ATP-linked respiration	Last OCR after oligomycin injection - Basal OCR
Maximal Respiration	Last OCR after FCCP injection - Last OCR after oligomycin injection
Spare Capacity	Last OCR after FCCP injection - Basal OCR
NMR	Last OCR after rotenone/antimycin-A injection
MitoATP production (Basal)	[last OCR before first injection – Minimum OCR after oligomycin injection (but before Rot/Antimycin C)] * 2 * P/O *Where P/O is 2.75*
Proton Efflux Rate (PER)	ECAR x BF x Vol x Kvol *Buffer Factor (BF) if XF Assay medium used: 2.3* *Vol for 96-well plate: 2.28* *Kvol for 96-well plate: 1.6*
GlycoATP Production rate (Basal)	last Glyco PER measurement before Oligomycin injection
Total ATP production rate (Basal)	mitoATP + GlycoATP
XF ATP Rate Index (Basal)	MitoATP/GlycoATP
Glycolytic Metabolic potential	Stressed ECAR/Baseline ECAR) × 100 % Baseline ECAR: ECAR before Oligomycin Stresed ECAR: ECAR after oligomycin+FCCP
Mitochondrial Metabolic potential	Stressed OCR/Baseline OCR) × 100 % Baseline OCR: OCR before Oligomycin Stresed OCR: OCR after oligomycin+FCCP

2.3 Chapter 4- Methods

2.3.1 Assessing circadian rhythms:

U2OS cells were synchronized with dexamethasone, treated with drugs and their corresponding bioluminescence was recorded. Amplitude and period were analysed as described in **section2.1.3.3**.

2.3.1.1 Assessing circadian rhythms under hypoxia

Following synchronization, the circadian rhythms of *Bmal1*-d*Luc* and *Per2*-d*Luc* U2OS cells were measured in a micro-plate reader for 2 days. As the rhythms approached their nadir, the micro-plates were moved into a chamber and exposed to 6h of 1% O_2 (hypoxia) or 20% O_2 (normoxia). The plates were subsequently returned to the micro-plate reader, where measurement of bioluminescence was resumed. Amplitude and period analysis were performed for rhythms following the differential oxygen exposure.

2.3.1.2 Assessing circadian rhythms with siRNA knockdown

Before circadian rhythm assessment was performed, U2OS cells were transfected with siRNA libraries as described in **section 2.1.3.2**. Twenty-four hours after transfection, cells were synchronized with dexamethasone, and treated with Linopirdine or DMSO, and luminescence was recorded.

2.3.2 HRE-LUC assay

The HRE-LUC plasmid enables the detection of HIF transcription factor activity. The HRE consensus is fused to a firefly luciferase gene, such that HIF binding to HRE promotes an increase in luminescence. Following 24h of transfection, U2OS cells were serum-starved in recording media with 400 μM luciferin for 6h. Following baseline recordings, cells were treated with the drugs of interest and luminescence was recorded at 37°C for 16h. Data was analysed by calculating drug-induced percentage changes, comparing baseline measurements with peak luminescence values.

2.3.3 mRNA quantification:

Primers used in this section are listed in **Table 2.4**.

2.3.3.1 mRNA panel for early gene expression

U2OS cells were grown to confluency in 24-well plates and synchronized with dexamethasone. 16 hours later, cells were treated with 3 μM Linopirdine or DMSO (0.5%) and mRNA was collected at 0, 1, 2, 4, and 6 hours post treatment. mRNA extraction and cDNA conversion were carried out as previously described in **section 2.1.4**, and quantification of *Vegf* and *Glut1* genes was done using qPCR.

2.3.3.2 Temporal assessment of HIF1α expression relative to Bmal1 and Per2

Samples from **section 2.2.4** were used for this experiment. *HIF1α* mRNA was quantified as described previously in **section 2.1.4.**

Table 2.4- Sequences of the primers used in Chapter 4

Species	Gene	Forward/Reverse	Sequence 5'-3'
Homo Sapiens	*Vegf*	Forward	CTACCTCCACCATGCCAAGT
Homo Sapiens	*Vegf*	Reverse	GCAGTAGCTGCGCTGATAGA
Homo Sapiens	*Glut1*	Forward	CACTCCTGTTACTTACCTAA
Homo Sapiens	*Glut1*	Reverse	CACTTACTTCTGTCTCACT
Homo Sapiens	*HIF1α*	Forward	TCGGACAGCCTCACCAAACAGAGC
Homo Sapiens	*HIF1α*	Reverse	CATCCATTGATTGCCCCAGCAGTC

2.3.4 BC-STAR-PROM assay:

The barcoded synthetic tandem repeat promoter screening (BC-STAR-PROM) is a high-throughput screening tool for transcription factors (TFs) developed by Gosselin and colleagues (Gosselin et al., 2016). The BC-STAR-PROM library used consists of ~3000 luciferase-expression vectors, each containing a promoter and a unique barcode, with promoter sequences encompassing more than 400,000 base pairs (bp) of random DNA that generates a complexity sufficient to capture most transcription factors (TF). As shown in **Fig 2.3A**, each promoter consists of 6 tandem repeats of synthetic random DNA, which drives a luciferase gene, and associated with a unique barcode made of 20bp within the 3' untranslated mRNA region. Following stimulation (with a drug of interest), the upregulated TFs that respond to the drug treatment bind to their corresponding motifs within the barcoded promoters, thereby driving expression of the barcode, which is subsequently counted using next-generation sequencing. This enables tracking the activity of each of the ~3000 synthetic promoters, simultaneously, in a single experiment (**Fig 2.3B**). All primers used in this assay are listed in **Table 2.5** and SYBR green (ThermoFisher Scientific) was used for all qPCRs.

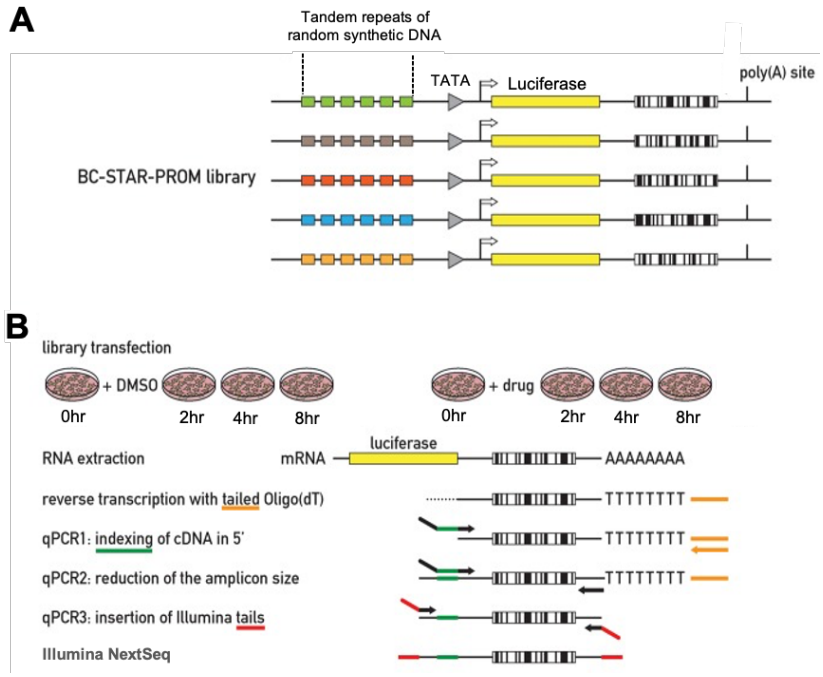


Figure 2.3. Overview of BC-STAR-PROM assay, adapted from *(Gosselin et al., 2016):*
(A) The BC-STAR-PROM library consists of ~3000 vectors, each holding a promoter (made of 6 tandem repeats of synthetic random DNA) that drives a luciferase gene, and associated with a unique barcode made of 20bp within the 3' untranslated mRNA region, generating a library of >400,000 bp of random DNA that is sufficient to capture most transcription factors.
(B) *Experimental procedure*: U2OS cells were transfected with the entire plasmid library containing >3000 BC-STAR-PROM plasmids. 48h later, cells were treated with vehicle (DMSO) or drug of interest, and total RNA was collected at specified time points. Non-treated (time 0h) and vehicle-treated cells were used as controls. RNA was reverse-transcribed using tailed Oligo(dT) primers and PCR was performed over a three-step process. The first qPCR involved amplifying the cDNA barcode regions using cDNA-specific primers with variable flying tails that introduced an index (6-nt identifier sequence) for every experimental sample. The second qPCR reduced the amplicon size by eliminating the polyA tail. And finally, the Illumina sequencing primers were inserted in the last qPCR. All barcode amplicons were pooled together, gel purified, and sequenced using Illumina NextSeq.

2.3.4.1 Transfection protocol

Plasmid DNA was diluted to 1 µg per 100 µL of reduced serum Opti-MEM (ThermoFisher Scientific) with 3 µL of ViaFect transfection reagent (Promega) for U2OS cells. Reverse transfection in 6-well plates was carried out using 2 µg of DNA per well in DMEM (lacking P/S, with 10% FBS) for 24h. Media was replaced to DMEM (with P/S and 0.5% FBS) for another 24h to serum starve the cells prior to drug and DMSO (0.1%) addition.

2.3.4.2 RNA extraction

Total RNA was collected at 0, 2, 4 and 8 hours post drug/DMSO addition, with 0h referring to no treatment. RNA was extracted with 1 mL TriZol (ThermoFisher Scientific) per well, as described in **section 2.1.4.2**. Following resuspension in water, RNA was purified using LiCl precipitation (LiCl 7.5M, EDTA 50mM, autoclave), at a ratio of 2:1 RNA to LiCl and centrifuged at 4°C (max speed) for 30min to obtain RNA pellet. The pellet was subsequently washed with ice-cold 75% EtOH, centrifuged again at 4°C (max speed) for 15min, dried and resuspended in 30 µL water prior to quantification.

2.3.4.3 Reverse Transcription with Oligo(dT) tail

2 µg of RNA were mixed with 1 µL of **Primer 81** (Nhel-Oligo(dT)-VN, 10 µM) and water to a final volume of 12 µL. To denature RNA secondary structures, samples were heated in thermocycler at 65°C for 10 min. Reverse-transcription was subsequently performed using SuperScriptII™/RNAseOUT™ Enzyme mix (ThermoFisher Scientific) with the following settings: 25°C for 10 min for annealing, 37°C for 20 min and 42°C for 30 min for elongation, 65°C for 10 min for inactivation, and finally cDNA was cooled and held at 4°C and stored at -20°C until RT-PCR was performed.

2.3.4.4 qPCR1- Inserting the left Illumina end (Index)

The first PCR amplifies luciferase fragments that contain the barcode using 1) forward primers that are specific for each sample and encompass an index sequence that enables their recognition inside the illumina reads, and 2) a reverse primer (**Primer 80**) that anneals to the Oligo(dT) tail and makes the amplification specific for cDNA without amplifying the plasmid DNA. To maximise library coverage, 1 µg cDNA was amplified in 4 separate reactions of 250 ng cDNA template each and the PCR was repeated twice (to utilize the full 2 µg of cDNA). The PCR run was aborted when amplification starts (~cycle 30) to maintain linear amplification (**Fig 2.3.1**)

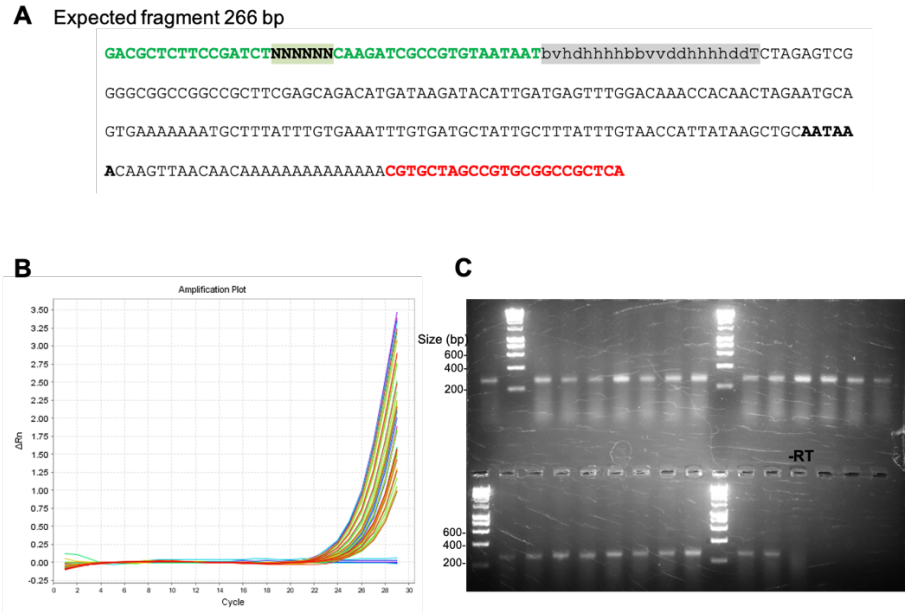


Fig 2.3.1 qPCR1- A) Expected fragment for qPCR product; Green represents the Forward primer index (unique for each sample), Red represents the reverse primer (Primer 80), Grey box represents the barcode. **B)** Representative qPCR amplification plots. **(C)** Representative bands produced per sample, -RT: denotes control sample with no reverse-transcriptase enzyme.

2.3.4.5 qPCR2- Inserting the right Illumina end

The products from PCR1 were used as a template for the second PCR2. The RT-PCR was performed using the same forward primers from PCR1 and a reverse primer (**Primer 40**) that introduces a docking site for the illumina. PCR run was aborted when amplification started (~cycle 10)- once annealing/extension is over to ensure the denaturation step has ended (**Fig 2.3.2**).

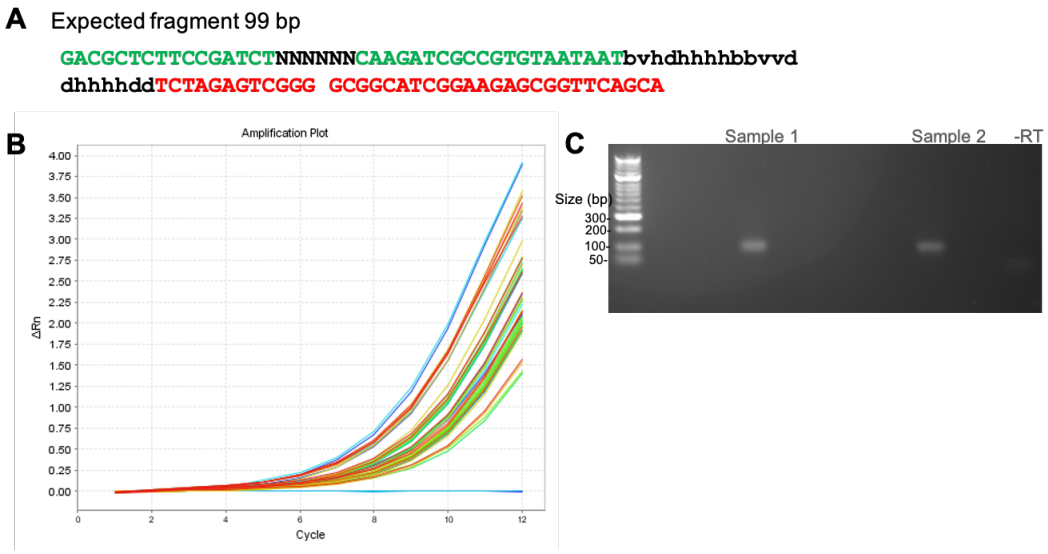


Fig 2.3.2 qPCR2- A) Expected fragment for qPCR product; Green represents the Forward primer index (unique for each sample), Red represents the reverse primer (Primer 42). **B)** Representative qPCR amplification plots. **(C)** Representative bands produced for 2 samples, -RT: denotes control sample with no reverse-transcriptase enzyme.

2.3.4.6 qPCR3- Inserting universal Illumina tails

All previous qPCR2 products (except -RT) were pooled, diluted (1:256 in Tris 10mM pH 8.0), and used for a third PCR to introduce the illumina tails using **Primer 44** and **Primer**

45. The PCR product was gel purified using QIAquick Gel Extraction Kit (Qiagen), eluted in 50 µL $T_{10}E_{01}$ and precipitated overnight at -20°C in sodium acetate 3 M pH 5.2 and 140 µL EtOH. Sample was centrifuged at max speed for 30min at 4°C, gently washed with 75% EtOH, and finally resuspended in 26.5 µL Tris 10 mM pH8, before being sent for sequencing (**Fig 2.3.3**).

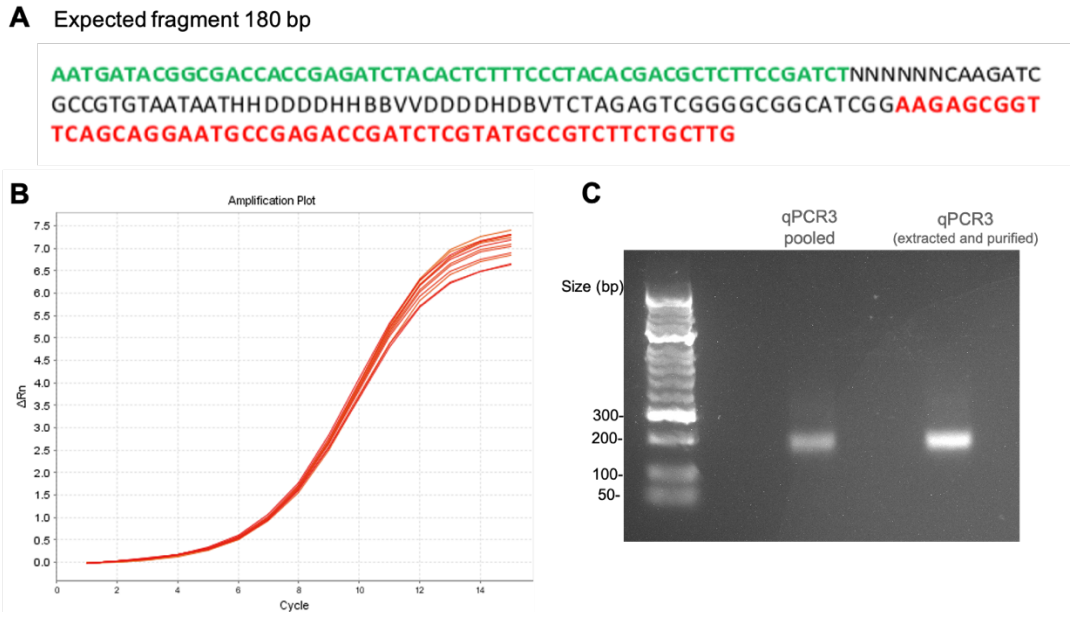


Fig 2.3.3 qPCR3- A) Expected fragment for qPCR product; Green represents the Forward primer index (Primer 44), Red represents the reverse primer (Primer 45). **B)** Representative qPCR amplification plots. **(C)** Representative bands produced for pooled product from the qPCR3 before and after gel extraction and purification.

2.3.4.7 Sequencing

Samples were prepared for NextSeq as per manufacture recommendations. In brief, sample was first denatured, by diluting it in 0.2N NaOH (1:1 vol/vol), incubating it at room temperature for 5min and subsequently adding 200mM Tris-HCl pH7 (1:1 ratio with library volume). Denatured sample was then diluted to 20pM, and then again to

1.8pM in prechilled HT1 buffer. Samples were spiked with 50% PhiX control v3 (Illumina), which is a well-characterized bacteriophage genome library with a balanced nucleotide composition, in order to increase the diversity and complexity of the library, avoid over clustering during sequencing and improve the overall run quality. The NextSeq 500/550 high output reagent v2 kit was used for sequencing on the NextSeq system.

2.3.4.8 Data analysis

R-studio was used for data analysis. Sequencing data was first reverse complimented, promoter and barcode sequences were read, samples were separated based on their indexing primers, and only barcodes present in BC-STAPROM list derived from Gosselin and colleagues were identified (Gosselin et al. 2016). DESeq2 was used for analysis, and up-regulated motifs with p-value<0.1 were selected. A heat map of all barcodes was also generated, and sequences from visual clusters of upregulated barcoded were retrieved. HOMER (Hypergeometric Optimization of Motif EnRichment) tool was used for Motif discovery and transcription factor identification of upregulated sequences. Only p-values of $1*e^{-10}$ generated by Homer de novo analysis were considered.

Table 2.5- Sequences of the primers used for BC-STAR-PROM

Step	Primer Name	ID	Sequence 5'-3'	Sample
RT	Tailed-Oligo(dT)-VN	81	ACGGCTAGCACGTTTTTTTTTTTTTTTVN	All samples
qPCR1	Forward indexing primers	1	GACGCTCTTCCGATCTATCACGCAAGATCGCCGTGTAATAAT	0h 1
		2	GACGCTCTTCCGATCTCGATGTCAAGATCGCCGTGTAATAAT	0h 2
		3	GACGCTCTTCCGATCTACAGTGCAAGATCGCCGTGTAATAAT	DMSO 2h 1
		4	GACGCTCTTCCGATCTGCCAATCAAGATCGCCGTGTAATAAT	DMSO 2h 2
		5	GACGCTCTTCCGATCTCAGATCCAAGATCGCCGTGTAATAAT	DMSO 4h 1
		6	GACGCTCTTCCGATCTACTTGACAAGATCGCCGTGTAATAAT	DMSO 4h 2
		7	GACGCTCTTCCGATCTGATCAGCAAGATCGCCGTGTAATAAT	DMSO 8h 1
		8	GACGCTCTTCCGATCTTAGCTTCAAGATCGCCGTGTAATAAT	DMSO 8h 2
		9	GACGCTCTTCCGATCTGTGAAACAAGATCGCCGTGTAATAAT	Lino 2h 1
		10	GACGCTCTTCCGATCTGTGGCCCAAGATCGCCGTGTAATAAT	Lino 2h 2
		11	GACGCTCTTCCGATCTGTTTCGCAAGATCGCCGTGTAATAAT	Lino 4h 1
		12	GACGCTCTTCCGATCTCGTACGCAAGATCGCCGTGTAATAAT	Lino 4h 2
		13	GACGCTCTTCCGATCTGAGTGGCAAGATCGCCGTGTAATAAT	Lino 8h 1
		14	GACGCTCTTCCGATCTGGTAGCCAAGATCGCCGTGTAATAAT	Lino 8h 2
		15	GACGCTCTTCCGATCTACTGATCAAGATCGCCGTGTAATAAT	NEC, NTC
qPCR1	Reverse tail RACE	80	TGAGCGGCCGCACGGCTAGCACGTT	All samples
qPCR2	Forward primers		(see qPCR1)	
qPCR2	Reverse primer	42	TGCTGAACCGCTCTTCCGATGCCGCCCCGACTCTAGA	All samples
qPCR3	Forward primer	44	AATGATACGGCGACCACCGAGATCTACACTCTTTCCCTACACG ACGCTCTTCCGATCT	Pooled qPCR2
qPCR3	Reverse primer	45	CAAGCAGAAGACGGCATACGAGATCGGTCTCGGCATTCCTGCT GAACCGCTCTT	Pooled qPCR2

Lino: Linopirdine, NEC: No enzyme control, NTC: No template control. Numbers 1 and 2 denote first and second experimental replicates.

2.4 Chapter 5- Methods

2.4.1 Linopirdine administration in a DIO-mouse model:

For diet-induced obesity, male C57BL/6 mice at 8 weeks of age were fed HFD (D12492; Research Diets) *ad libitum* until the end of the experimental protocol. The mice were treated with either vehicle (15% kolliphor HS15, Sigma) or Linopirdine (7.5 mg/kg body weight) via oral gavage **daily** (16 mice per group) in the time window of ZT8–ZT10, throughout the entire experimental period (14 weeks). Diet-control groups were fed sucrose matched diets (D12450J; Research Diets). Mice and food were weighed weekly.

2.4.2 mRNA quantification

At the end of the HFD experiment, mice were fasted for 6h before being culled by cervical dislocation. Tissues were then collected and mRNA was quantified as described in **section 2.1.4.2.** Primers used for qPCR are displayed in **Table 2.6**.

Table 2.6 Sequences of primers used in Chapter 5

Species	Gene	Forward/Reverse	Sequence 5'-3'
Mus Musculus	*CD36*	Forward	GATGACGTGGCAAAGAACAG
Mus Musculus	*CD36*	Reverse	TCCTCGGGGTCCTGAGTTAT
Mus Musculus	*Fasn*	Forward	CTGAGATCCCAGCACTTCTTGA
Mus Musculus	*Fasn*	Reverse	GCCTCCGAAGCCAAATGAG
Mus Musculus	*Ppar$_\gamma$*	Forward	CCACCAACTTCGGAATCAGCT
Mus Musculus	*Ppar$_\gamma$*	Reverse	TTTGTGGATCCGGCAGTTAAGA
Mus Musculus	*Dbp*	Forward	AATGACCTTTGAACCTGATCCCGCT
Mus Musculus	*Dbp*	Reverse	GCTCCAGTACTTCTCATCCTTCTGT
Mus Musculus	*Leptin*	Forward	CTCCATCTGCTGGCCTTCTC
Mus Musculus	*Leptin*	Reverse	CATCCAGGCTCTCTGGCTTCT
Mus Musculus	*Hspa1a*	Forward	TGGTGCAGTCCGACATGAAG
Mus Musculus	*Hspa1a*	Reverse	GCTGAGAGTCGTTGAAGTAGGC

Mus Musculus	*Xbp1s*	Forward	ACACGCTTGGGAATGGACAC
Mus Musculus	*Xbp1s*	Reverse	CCATGGGAAGATGTTCTGGG
Mus Musculus	*Ddit3*	Forward	GGAGCTGGAAGCCTGGTATG
Mus Musculus	*Ddit3*	Reverse	GGATGTGCGTGTGACCTCTG
Mus Musculus	*IRS1*	Forward	TCCTATCCCGAAGAGGGTCT
Mus Musculus	*IRS1*	Reverse	TGGGCATATAGCCATCATCA
Mus Musculus	*IRS2*	Forward	GTAGTTCAGGTCGCCTCTGC
Mus Musculus	*IRS2*	Reverse	TTGGGACCACCACTCCTAAG
Mus Musculus	*Glut1*	Forward	GGTGTGCAGCAGCCTGTGTA
Mus Musculus	*Glut1*	Reverse	CAACAAACAGCGACACCACAGT
Mus Musculus	*Glut4*	Forward	CCGGCAGCCTCTGATCAT
Mus Musculus	*Glut4*	Reverse	CCGACTCGAAGATGCTGGTT
Mus Musculus	*InsR*	Forward	TTTGTCATGGATGGAGGCTA
Mus Musculus	*InsR*	Reverse	CCTCATCTTGGGGTTGAACT
Mus Musculus	*Gck*	Forward	AGGGAACAACATCGTGGGAC
Mus Musculus	*Gck*	Reverse	TCACATTGGCGGTCTTCATA
Mus Musculus	*Il-6*	Forward	TAGTCCTTCCTACCCCAATTTCC
Mus Musculus	*Il-6*	Reverse	TTGGTCCTTAGCCACTCCTTC
Mus Musculus	*TNF α*	Forward	GCCTCTTCTCATTCCTGCTTG
Mus Musculus	*TNF α*	Reverse	CTGATGAGAGGGAGGCCATT
Mus Musculus	*Mcp-1*	Forward	TTAAAAACCTGGATCGGAACCAA
Mus Musculus	*Mcp-1*	Reverse	GCATTAGCTTCAGATTTACGGGT
Mus Musculus	*AdipoQ*	Forward	TGTTCCTCTTAATCCTGCCCA
Mus Musculus	*AdipoQ*	Reverse	CCAACCTGCACAAGTTCCCTT
Mus Musculus	*Resistin*	Forward	CCATCGACAAGAAGATCAAACAAG
Mus Musculus	*Resistin*	Reverse	GGAGACTGTCCAGCAATTTAAGC
Mus Musculus	*HIF1 α*	Forward	AAGAAACCACCCATGACGTG
Mus Musculus	*HIF1 α*	Reverse	CCACCTCTTTTGGCAAGCAT
Mus Musculus	*Sqle*	Forward	AAATCAGAGCCGTGGGCTAC
Mus Musculus	*Sqle*	Reverse	GGAAGTGACACAGTTCTATG
Mus Musculus	*18s*	Forward	GTAACCCGTTGAACCCCATT
Mus Musculus	*18s*	Reverse	CCATCCAATCGGTAGTAGCG
Mus Musculus	*Nono*	Forward	GCCAGAATGAAGGCTTGACTAT
Mus Musculus	*Nono*	Reverse	TATCAGGGGGAAGATTGCCCA
Mus Musculus	*β-Actin*	Forward	ACCAACTGGGACGATATGGAGAAGA
Mus Musculus	*β-Actin*	Reverse	CGCACGATTTCCCTCTCAGC
Mus Musculus	*GusB*	Forward	CCAGAGCGAGTATGGAGCAG
Mus Musculus	*GusB*	Reverse	TCGTCATGAAGTCGGCGAAA

2.4.3 Glucose and Insulin tolerance tests (GTT, ITT):

Glucose tolerance test (GTT) and insulin tolerance test (ITT) were performed on DIO-mice following 10 weeks on HFD and on age-matched Diet-control mice for the chronic study, and also on lean mice (14 weeks old) 3h after a Linopirdine (7.5 mg/kg weight) or vehicle oral gavage for the acute study. Following 16h and 5h fasting, GTT and ITT were conducted at ZT2 and ZT8, respectively. Glucose levels were quantified from tail blood before (time 0) and 15, 30, 60, 90 and 120 min following an oral gavage of 1 g/kg glucose or an i.p injection of 0.75 U/kg insulin (Sigma) at ZT2 and ZT8, respectively, using the AlphaTRAK2 blood glucose monitoring system. Quantified blood glucose levels were then plotted against time, and the area under the curve was calculated to estimate glucose and insulin tolerance.

2.4.4 Plasma measurements:

At week 10 of daily drug gavage and HFD, and in aged matched Diet-control mice, blood was collected from mice fasted for 5h through cardiac puncture in EDTA coated tubes. Samples were centrifuged at 2000x g and 4°C for 15 min and the plasma layer was collected and stored in aliquots at -20°C. Plasma insulin levels were measured using ELISA (ab100578, Abcam). Fluorometric assay kits were used for quantification of total cholesterol (Cell BioLabs, INC.), triglycerides (ab178780, Abcam) and non-esterified fatty acids (ab65341, Abcam). Fluorescence was quantified for each assay at its corresponding excitation/emission wavelengths in a micro-plate reader.

2.4.5 Histological staining of lipids in liver

For microscopic analysis of lipid accumulation in liver, tissue samples were collected and fixed in 4% paraformaldehyde for 48h. Samples were cryopreserved in 15% sucrose in PBS until tissues sank followed by 30% sucrose in PBS overnight. Samples were then embedded in OCT moulds and stored at -80°C. Samples were sectioned using Cryostat at 8 μm thickness and fixed with 4% paraformaldehyde for 1h. To stain lipid droplets and highlight cellular nuclei, Oil Red O and Mayer's Haematoxylin Solution (Merck Chemicals Ltd) were used according to their protocols. Liver sections were incubated in propylene glycol (2-5 min), immersed in pre-warmed Oil Red O (8-10 min), differentiated in 85% propylene glycol solution (2-5 min), rinsed in distilled water and finally counterstained with Mayer's haematoxylin (30 s). Samples were mounted using SlowFade™ Diamond Antifade Mountant (ThermoFisher Scientific) and imaged at magnification 40x using EVOS M7000.

ImageJ software was used for Oil Red O quantification. Images were first transformed in the YIQ colour space using the Colour Transformer plugin (by Maria E. Barilla, University of Birmingham, UK) and then converted into 8-bit image format. A threshold was applied by adjusting Q channel levels, allowing the Oil Red O staining to be visualized in a black and white contrast, and the black pixels that represented lipid droplets were quantified as a percentage of the total area of the image.

2.4.6 Ex-vivo SCN cultures:

Ex vivo SCN slice cultures were conducted using homozygous male and female PER2::LUC (mPer2^{Luc} knockin) C57BL/6J mice housed in 12:12 L/D cycles, belonging to the Foster Lab breeding colony at the University of Oxford. Adult mice between 8-10 weeks of age were used for all experiments.

Mice were euthanised by cervical dislocation and decapitation. The whole brain was enucleated and removed, and the caudal region was glued onto the stage and secured using 3% low melt agar (Sigma) to allow slicing of the coronal region using the Compresstome VF-200 semi-automatic slicer (Precision Instruments). 250 µm sequential brain sections (sliced in NMDG-HEPES recovery solution, **Table 2.7**) were obtained per mouse and the SCN-containing slices were micro-dissected to obtain intact bilateral SCN (~2mm in diameter).

Micro-dissected SCN slices were transferred to 0.6cm^2 Millicell cell culture inserts (Merk Millipore) located in a 24-well plate (Perkin Elmer), and supplemented with 300 µL recovery media (comprised of recording media, with 2.5MM AP-V (Tocris Biosciences), 100 nM MK-801 maleat (Abcam), and 3mM glutathione reduced ethyl ester (Sigma)) where they were incubated for 1hr at 37°C . Recovery media was then replaced with organotypic slice culture media (containing 1 part Eagle's Basal Media (Gibco) and 1 part Horse serum (Gibco), and supplemented with 1% Glucose, 1% Glutamax, and 1% P/S), and cultured for a minimum of one week before recording.

SCN slice cultures were moved into recording media supplemented with B27, 400 µM luciferin, and 5% FBS and bioluminescence was recorded using the TriStar^2 plate reader for 2-4 days before Linopirdine or DMSO (0.1%) were added as a partial media change and bioluminescence thereafter was further assessed. Data was gathered every hour by averaging photon emissions every 150 s. Period, amplitude and phase were calculated by comparing pre- and post-treatment oscillations.

Table 2.7. NMDG-HEPES recovery solution of SCN cultures

	mM	g/L
NMDG (sigma)	93	18.6
HCl	93	Adjust to pH 7.3
KCl (VWR International)	2.5	0.19
NaH_2PO_4 (Sigma)	1.2	0.17
$NaHCO_3$ (Sigma)	30	2.52
HEPES (VWR International)	20	4.77
Glucose (Sigma)	25	4.51
Sodium ascorbate (Sigma)	5	0.99
Thiourea (Sigma)	2	0.15
Sodium pyruvate (Sigma)	3	0.33
$MgSO_4$ (Sigma)	10	1.2
$CaCl_2.2H_2O$ (Merk Milipore)	0.5	250 µL (2 M stock)

2.4.7 Organotypic slices bioluminescence recording

Organotypic slices were prepared and bioluminescence assays were conducted as described in (Yoo et al. 2004). In brief, mice were culled by cervical dislocation and their organs were dissected and immersed in oxygenated ice-cold HBSS buffer (Gibco). The

different tissues were cut into ~1mm^2 slices, and each was transferred to 0.6cm^2 Millicell cell culture inserts (Merk Millipore) located in a 24-well plate (Perkin Elmer), and supplemented with 500 µL recording media (with B27, 400 µM luciferin, and 5% FBS). Bioluminescence was recorded in TriStar^2 plate reader.

2.5 Chapter 6- Methods:

2.5.1 Reagents

The compounds used for pharmacological investigations in this chapter were KT5823 (Sigma), Sildenafil (Abcam), CNP (Abcam), Rapamycin (Abcam), Torin1 (Sigma), PD98059 (Sigma) and SCH772894 (Sigma).

2.5.2 Assessing circadian rhythms of CREB mutants:

Before circadian rhythm assessment was performed, U2OS cells were transiently transfected with CREB^{S133A}, CREB^{S142A} or K-CREB plasmids as described in **section 2.1.3.1**. Twenty-four hours after transfection, cells were synchronized with dexamethasone, and treated with Zaprinast or DMSO, and luminescence was recorded.

2.5.3 CREB/P-CREB quantification

U2OS cells were seeded to confluency in 6-well plates and treated with Zaprinast (30 μM), Zaprinast (30 μM) with KT5823 (3 μM), or Forskolin (100 nM) for 1h. Following washing with PBS, cells were then lysed in pre-chilled RIPA lysis buffer (ThermoFisher Scientific) supplemented with 1:100 Halt Protease and Phosphatase Inhibitor Cocktail (ThermoFisher Scientific) and 1:100 0.5 M EDTA, which were incubated on ice for 30min. Inhibitors of proteases and phosphatases are critical to avoid unwanted protein modification, denaturation or proteolysis caused by the mass release of lysis-stimulated proteases and phosphatases. Equally, the divalent cation chelator EDTA reduces DNAse and proteases activity that require magnesium co-activation to function. Cell lysates were then sonicated for 3 pulses of 3s then centrifuged at 60,000g at 4°C for 20min. The supernatant was collected and total protein was quantified as specified in **section 2.1.6**. Cell lysates were mixed with 4x Laemmli buffer (Sigma) and 1:10 β-mercaptoethanol and heated in thermocycler to 95°C for 10min, before 30 μg/well protein were loaded into a 10% Tris-Glycine mini-gel (Invitrogen WedgeWell). 5 μL of Chameleon Duo protein ladder (Li-cor) was also loaded, and the western blot was run at 220 mV for 30 min before being transferred to a low-fluorescence PVDF membrane using the Trans-Blot Turbo™ kit (BioRad) for 7 min. Membrane was then blocked in Odyssey Blocking Buffer in PBS (Li-Cor) for 1h, washed 3 times in Tris-buffered saline containing 0.1% Tween (TBST) for 10min each, and finally incubated at 4°C overnight with primary CREB-Antibody (1:1000, Cell signalling) or PhosphoCREB (Ser133, 1:1000 Cell signalling), diluted in Blocking buffer. The membrane was washed 3x with TBST (10 min each) and

incubated for 1h with secondary antibody (1:10,000 IRDye 680CW Donkey-anti Rabbit, Li-Cor) diluted in Blocking buffer. After 3x TBST washes, membrane was visualised in the Odyssey gel imager (Li-Cor) and bands were quantified using ImageLight. Data was analysed as percentage change of P-CREB relative to CREB.

2.5.4 cAMP-GloSensor and cGMP-GloSensor assays:

The pGloSensor™22F cAMP and the pGloSensor™42F GAMP plasmids (Promega) allow high-sensitivity detection of intracellular changes in cAMP and cGMP. These plasmids contain a mutant luciferase biosensor (from *P.pyralis* firefly) attached to cAMP or cGMP binding domains. As cAMP/cGMP binds, the protein undergoes a conformational change that promotes photo emission. To assess intracellular cAMP or cGMP levels, U2OS cells were transfected with the corresponding plasmid (as reported in **section 2.1.3.1**). 24 hours later, cells were serum starved in CO_2-independent media with 5mM luciferin and various reagents for 2h at room temperature. Following baseline measurements, the cells were treated with forskolin (for cAMP) or SNP (for cGMP) and luminescence was recorded at 25^{o}C.

2.5.5 CRE-LUC assay

The CRE-LUC plasmid allows the detection of CREB activity. The CRE DNA sequence is attached to a firefly luciferase gene. As CREB binds CRE, the luciferase gene is expressed and increases in luminescence can be monitored. 24 hours after transfection, U2OS cells were serum starved in recording media supplemented with 400 μM luciferin and various

agents for 6h. After baseline measurements, cells were treated with forskolin or DMSO and luminescence was recorded at 37^{O}C.

2.5.6 Data analysis:

CRE-LUC, cAMP-GloSensor and cGMP-GloSensor transfection data was analysed by comparing baseline measurements with peak luminescence values, and then calculating drug-induced percentage changes relative to vehicle.

2.5.7 mRNA quantification

Samples from **section 2.2.4** were used for this experiment. *Mkp-1* mRNA was quantified as described in **section 2.1.4** using the primer displayed in **Table 2.8**.

Table 2.8- Sequences of the primers used in Chapter 4

Species	Gene	Forward/Reverse	Sequence 5'-3'
Homo Sapiens	*Mkp1*	Forward	CCATCTGCCTTGCTTACCTT
Homo Sapiens	*Mkp1*	Reverse	AGCACCTGGGACTCAAACTG

CHAPTER 3:

Identification and Evaluation of Circadian Modulators in Metabolism

3.1 Introduction

Obesity has become a global epidemic and a substantial socioeconomic burden, affecting over 650 million people worldwide (WHO obesity and overweight statistics, 2016). It has been shown to increase mortality rate and predispose individuals to a myriad of conditions, including T2DM, dyslipidaemia, cardiovascular disease, hepatic steatosis and even cancer (Expert-Panel 1998). Many of these conditions are common with metabolic syndrome, making obesity a major hallmark of this disease and a chief contributor to its pathophysiology (Kwok, Lam, and Xu 2016).

Over the past 20 years, the role of adipocytes as metabolically active endocrine organs has become more evident. Previously perceived as mere passive stores for excess lipids, increasing evidence has gradually transformed the adipose tissue into an important endocrine organ highly involved in regulation of glucose and lipid homeostasis, insulin sensitivity, non-shivering thermogenesis and inflammation (Saltiel and Kahn 2001; Tilg and Moschen 2006; Cannon and Nedergaard 2004). Therefore, it comes as no surprise that adipocytes play a major role in development of obesity and metabolic syndrome. Weight gain is a natural response to positive energy balance, however, when an imbalance of energy intake vs expenditure persists, excess accumulation of adipose tissue in the body occurs, which results in adipose tissue expansion and obesity. This is usually characterized with an abnormal increase in existing adipocyte size (hypertrophy) or increase in adipocyte number through differentiation from precursor

pre-adipocytes (hyperplasia) (Björntorp et al., 1966; Hirsch & Knittle, 1970). Differentiated adipocytes can undergo hypertrophy up to several micrometres in diameter, while the adipocyte number is generally predetermined early in life and remains typically stable throughout adulthood (Spalding et al. 2008) therefore, suggesting hypertrophy as the dominant cause of obesity in adulthood. Nonetheless, following long term calorific diets in rodents, formation of new adipocytes from precursors by *de novo* adipocyte formation (or adipogenesis) has also been reported, which can further contribute to obesity due to high-calorie intake (Wang et al., 2013).

In addition to being dependant on energy intake and expenditure, the development of obesity also occurs as a function of white adipose tissue (WAT) and brown adipose tissue (BAT) distribution and balance. These two structurally distinct adipose tissues exhibit opposing functions (Figure 3.1A). WAT serves as an energy reservoir and a storage site for triglycerides (TG) (Björntorp 1996). It is an important endocrine organ, secreting adipokines like leptin, adiponectin and resistin that act on both peripheral and central tissues to regulate appetite, energy expenditure and vascular function (Trayhurn and Beattie 2001). BAT on the other hand is a thermogenic organ. By expressing the uncoupling protein 1 (UCP1), BAT increases proton leakage across the mitochondrial membrane and reduces efficiency of energy production by converting energy to heat (Cannon and Nedergaard 2004). This reduction in efficiency of ATP production prompts cells to increase catabolic pathways to sustain ATP levels, thereby increasing energy expenditure. Although previously believed to be prominent in infant humans only, recent

studies have suggested BAT persisted in adults (Nedergaard et al. 2007), with both rodent and human BAT stimulated by cold exposure and epinephrine stimulation (Nedergaard, Bengtsson, and Cannon 2007; Cannon and Nedergaard 2004). While WAT is predominantly distributed in the subcutaneous and visceral fat depots, BAT can be found throughout the cervical, supraclavicular, axillary and paravertebral regions (Wehrli et al. 2007) (Figure 3.1B). WAT expansion can drive obesity, while higher levels of BAT have been shown to protect against obesity, insulin resistance and cardiovascular diseases (Mattson 2010). More recently, beige adipocytes have also been reported, which are developmentally close to WAT, but can functionally adapt to resemble the thermogenic potential of brown adipocytes (Harms and Seale 2013).

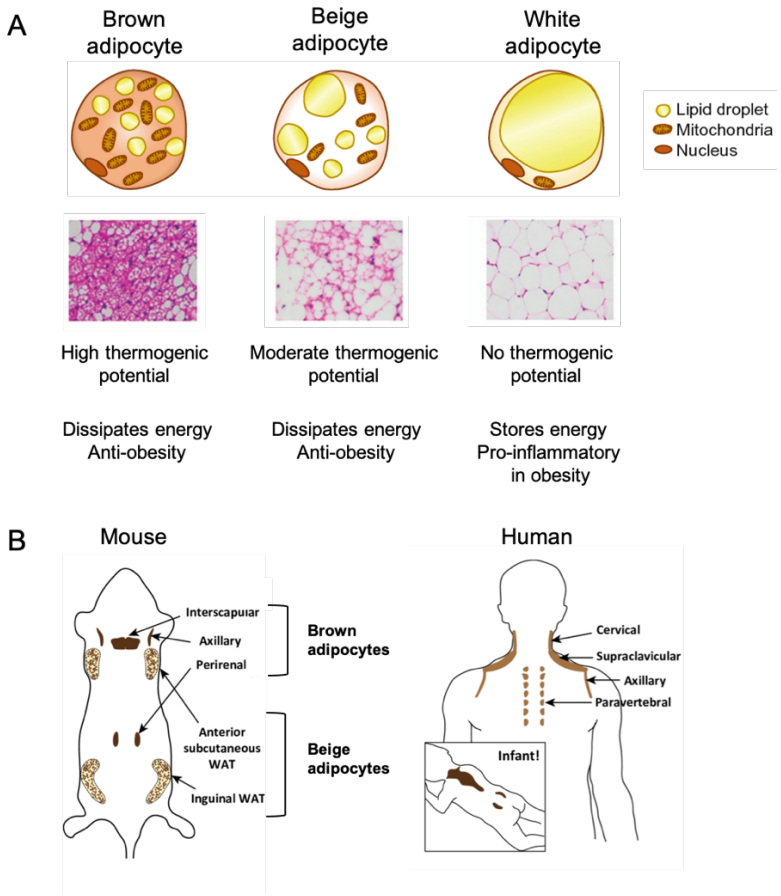


Figure. 3.1. Adipocyte classifications and distribution:
A) Brown adipocytes (BAT) are small, contain multiple small lipid droplets and pack numerous mitochondria and capillaries, due to their greater oxygen demand. White adipocytes (WAT) are larger spherical cells containing fewer large lipid droplets, where their size is functional to the size of the lipid droplets that they store. Beige adipocytes are developmentally close to WAT, stemming from the same lineage, but are functionally adaptive and express UCP-1 which allows them to dissipate energy. **B)** WAT are widely distributed in subcutaneous and visceral depots (not shown)**.** Classical BAT reside in dedicated depots in mice and infants, these include interscapular, axillary and perirenal regions while beige adipocytes are more sporadic, residing in subcutaneous WAT depots (like the anterior subcutaneous and inguinal WAT). In adult humans, BAT are distributed in multiple regions, including the cervical, supraclavicular, axillary and paravertebral depots. The deep neck regions contain thermogenic adipocytes that resemble murine classical BAT, while UCP1-expressing adipocytes residing in the supraclavicular region display a molecular signature similar to murine beige adipocytes.

Mammalian adipose tissue exhibit robust circadian clocks that regulate many aspects of its metabolic phenotype. Murine brown, inguinal and epididymal white adipose tissue have all been reported to display coordinated rhythms in core clock gene oscillators (like *Bmal1*, *Npas2*, *Per1-3* and *Cry1*-2) as well as downstream clock-controlled genes (such as *Reverba*, *Reverb*-b, *Dbp*) (Zvonic et al. 2006). Indeed, the adipose tissue circadian clock coordinates energy metabolism and lipid homeostasis through regulating rhythmic expression of adipokines, transporters and also via transcriptional control of rate-limiting enzymes (Figure 3.2). For example, circulating levels of major secreted adipokines, like adiponectin, leptin and plasminogen activator inhibitor 1 (PAI-1) demonstrate circadian rhythmicity with a 24-hour period (Maemura et al., 2000; Schoenhard et al., 2003; Yildiz et al., 2004) and mRNAs encoding the adipokine resistin also exhibit circadian oscillation in murine WAT (Oliver et al. 2006). Similar oscillatory profiles of the adipocyte-derived and macrophage derived inflammatory cytokines IL-6 and tumour necrosis factor-α (Vgontzas et al. 1999; 2002) have also been reported. As a key regulator of energy homeostasis and long-term energy storage (in the form of lipids), adipocytes shuttle between states of triglyceride (TG) synthesis ("lipogenesis") during times of energy surplus and TG breakdown into glycerol and free fatty acids ("lipolysis") when energy is in demand. Both these processes occur via choreographed sequence of enzymatic activity, and many of which are under circadian regulation (Figure 3.2). For example, activity of the adipocyte-derived circulating enzyme lipoprotein lipase (LPL) which clears TG from circulation to be taken up by adipocytes has been shown to display diurnal variation (Arasaradnam et al., 2002; De Gasquet et al., 1977) as has the fatty acid

synthase (FAS), the acetyl-CoA carboxylase (ACC) and the fatty-acid-binding protein 4 (FABP4) in murine adipose tissue (Kohsaka et al. 2007). Work by Shostak and colleagues have shed light on the ability of local adipose circadian clocks to drive lipolysis. The adipocyte triglyceride lipase (Atgl) and the hormone-sensitive lipase (HSL) are two of the key lipolytic enzymes, encoded by the *Pnpla2* and *Lipe* genes, respectively. Both *Pnpla2* and *Lipe* mRNA expression in WAT display circadian rhythmicity, and each of their promoters has been shown to associate with BMAL1 in chromatin immunoprecipitation assays (Shostak et al., 2013). This suggests the local WAT clock could be directly driving their expression. Similarly, the triglyceride hydrolase (TGH) enzyme (encoded by *Ces1d*) which also contributes to lipid release from adipocytes (Wei et al. 2010), seems to be under adipose tissue clock control as a direct target of BMAL1 (Koike et al. 2012; Paschos et al. 2012).

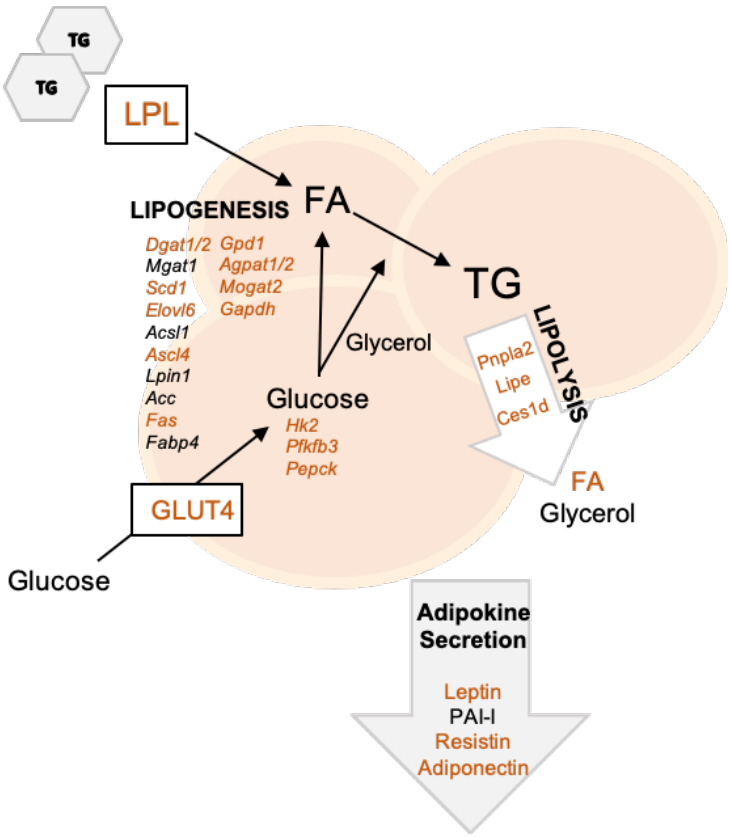


Fig 3.2. Circadian regulation of lipogenesis and lipolysis in adipose tissue, adapted from *Henriksson et al., 2015:*
As storage depots, adipocytes clear circulating TG by breaking them down to fatty acids (FA) and glycerol using the lipoprotein lipase (LPL) enzyme, which then allows their uptake into the cell. The FA taken up are then esterified and stored as TG. TG are also produced from other substrates, such as glucose, in a process called *de novo* lipogenesis. When other tissues demand energy, TG are hydrolysed in a process called lipolysis to generate soluble energy in the form of FA and glycerol (stimulated by catecholamines produced in the adrenal medulla). Furthermore, adipose tissue is an endocrine organ that secretes essential endocrine factors (called adipokines). The circadian clock coordinates different aspects of lipid metabolism and adipocyte function, partly through regulating expression of enzymes, adipokines and transporters. Genes and adipokines listed are reported to display diurnal oscillation. Those that are shown in orange font are direct targets of BMAL1/CLOCK complex and/or are impaired in mice with a disrupted intrinsic clock.

Abbreviations: Lpl, lipoprotein lipase; Dgat1/2, diglyceride acyltransferase 1/2; Mgat1, monoglyceride acyltransferase 1; Scd1, stearoyl-CoA desaturase-1; Elovl6, elongation of very long-chain fatty acids protein 6; Acsl1/4, acyl-CoA synthetase long-chain family member 1/4; Lpin1, phosphatidate phosphatase LPIN1; Ac1/2c, acetyl-CoA carboxylase 1/2; Fas, fatty acid synthase; Fabp4, fatty acid binding protein 4; Gpd1, glycerol-3-phosphate dehydrogenase 1; Agpat1/2, 1-acylglycerol-3-phosphate o-acyltransferase 4; Mogat2, monoacylglycerol acyltransferase 2; Gapdh, glyceraldehyde 3-phosphate dehydrogenase; Hk2, hexokinase 2; Pfkfb3, 6-phosphofructo-2-kinase/fructose-2,6-biphospatase 3; Pepck, phosphoenolpyruvate carboxykinase; Pnpla2 (Atgl), patatin-like phospholipase domain containing/adipose triglyceride lipase; Lipe (Hsl), hormone-sensitive lipase; Ces1d (Tgh), carboxylesterase 1D/triacylglycerol hydrolase; FA, fatty acid; GLUT4: glucose transporter type 4.

Interestingly, obesity has been shown to contribute to reduced circadian amplitude, particularly in adipose tissue. In a small population of human subjects, being obese altered adipocyte expression of core clock genes throughout the day, and caused notable upregulation of REVERBα and CRY2, two major regulators for the negative arm of the circadian clock (Vieira et al. 2014). Several obese mouse models have also been associated with a reduction in clock gene expression within adipose tissue. The obese *ob/ob* mice, which display loss of leptin function, exhibit attenuated activity rhythms and dampened core clock gene expression of *Clock, Bmal1, Cry1, Per1-2* and *Dbp* in adipose tissue and liver (Ando et al. 2011). Similar observations were reported in the *db/db* mice with mutant leptin receptor, which are also obese and hyperglycaemic and display impaired clock gene function in WAT (Caton et al., 2011). Furthermore, obesity associated with high fat diet has also been shown to significantly impair clock regulation of metabolic genes, dampening rhythmic expression of clock genes in adipose tissue and downstream clock-controlled genes involved in lipid metabolism, including *SREBP-1C*, and *FABP4* (Kohsaka et al. 2007). Since obesity generally correlates with a reduction in clock gene expression of adipose tissue, and given rate-limiting steps of key metabolic processes such as glucose, triglyceride and cholesterol are shown to be major sites of circadian regulation (Panda et al. 2002), it could be hypothesized that strengthening the rhythmic expression of clock genes in adipocytes could be of benefit. Increasing clock gene expression can drive higher expression of downstream clock-controlled genes at the correct time of day, which include key metabolic players like Hormone sensitive lipase (HSL), triglyceride hydrogenase (TGH), hexokinase (HK), Glyceraldehyde 3-

phosphate dehydrogenase (Gapdh), etc, which can potentially improve the function of these metabolic pathways and consequently aid in combatting symptoms of metabolic disorders.

Indeed, as reviewed in Chapter 1, small molecules that target the clock have been shown to ameliorate symptoms of MetS. However, chrono-modulators that target the negative and positive arms of the clock, and hence dampen or enhance circadian clock expression, respectively, have both been shown to be beneficial. On one hand, the circadian-amplitude enhancer nobiletin has been shown to restore dampened rhythms in clock mutant heterozygous mouse fibroblasts and increase amplitude in a dose-dependent manner in pituitary explants. Furthermore, when tested *in vivo*, nobiletin protected mice fed high fat diet from obesity and also improved their metabolic phenotype and their glycaemic state (He et al. 2016), which was entirely dependent on a functional clock, emphasizing the role of the circadian clock in mediating these benefits. On the other hand, a REVERB agonist which targets the negative feedback loop and inhibits *Bmal1* expression, was also shown to protect against weight-gain and hyperglycaemia associated with diet-induced obesity (Solt et al. 2012). Similarly, CRY agonists that significantly dampen *Bmal1* and *Per2* amplitude in U2OS cells, fibroblasts and SCN explants (Hirota, Lee, St. John, et al. 2012) also reported strong *in vivo* antidiabetic benefit (Hirota, Lee, St. John, et al. 2012; Humphries et al. 2016). However, in the absence of direct evidence of clock involvement, target-specific effects of these agents cannot be ruled out.

Of interest, from an adipocyte standpoint, both nobiletin and REVERB agonists, which play functionally opposing roles at the level of the circadian clock have shown to mediate similar phenotypic outcomes. Although nobiletin's effect on clock gene expression in adipocytes were not reported *in vivo*, *in vitro* examination in 3T3-L1 adipocytes has shown an increase in glucose uptake and lipolysis following its treatment (Onda et al. 2013), two processes, which as previously discussed, are under circadian regulation. On the other hand, despite the REVERB agonist's significant reduction in amplitude of clock gene expression in the hypothalamus, its protection against weight-gain was associated with an increase in energy expenditure, attributed to higher expression of metabolic genes like *UCP3*, *HK1*, *Fatp1*, *PPARy1b* and Cyc in adipocytes (Solt et al. 2012). This is particularly intriguing, as some of these genes are indeed under circadian control, suggesting tissue-dependent effects of this molecule. Hence, despite the inconsistency with regard to overall benefit of amplitude enhancement vs reduction of clock machinery, tissue-specific differences in these molecules' ability to enhance or reduce amplitude could be one way of explaining these differences.

3.1.1 Aims:

All in all, the adipocyte autonomic clock is emerging as a key contributor to the pathogenesis of metabolic syndrome, which makes it a very interesting peripheral cell for investigating the effects of circadian modulators. There is a clear evidence linking circadian clock disruption with exacerbated metabolic disorders and the use of small molecules that target the clock have shown promise as a therapeutic strategy against MetS. Although there has been reports of several circadian modulators showing benefit against metabolic syndrome, an adipocyte focused investigation of their effects on the adipocyte clock is still lacking. Thus, given the increasing interest in chrono-modulators and the emerging role of adipocytes as key metabolic organs linked to metabolic disorders, the first aim of this investigation was to i*dentify novel small molecules that increase amplitude of circadian clock expression*, focusing on adipocytes. Secondly, this investigation aimed to *set up metabolic screens that correlate with key hallmarks of glucose intolerance and obesity,* and test the validated chrono-modulators on them. This will allow us to delve deeper into the effects of amplitude enhancers on metabolism and help characterize the metabolic phenotypes associated with circadian enhancement, focusing purely on the adipocyte autonomous clock, away from humoral or neuronal influences and SCN inputs.

3.2 Results

3.2.1 Identification and validation of 3 circadian modulators.

For the purpose of identifying molecules that could act as circadian modulators, which alter amplitude and/or period of circadian clock gene expression, a screening platform was designed in the lab. Using different cell-lines expressing luciferase-reporters of key clock genes (namely, *Bmal1* and *Per2*) and then utilising a bioluminescent circadian assay (refer to methods section 2.1.3.3), *Bmal1* and *Per2* promoter expression could be monitored in real time for ~3-4 days, allowing for amplitude and period analyses following different drug treatments. By means of bioluminescent circadian assays, a medium-throughput screen was performed in the lab, using 3 small molecules libraries and a total of 5000 compounds. Figure 3.3 summarises the sequence of steps in the screening process.

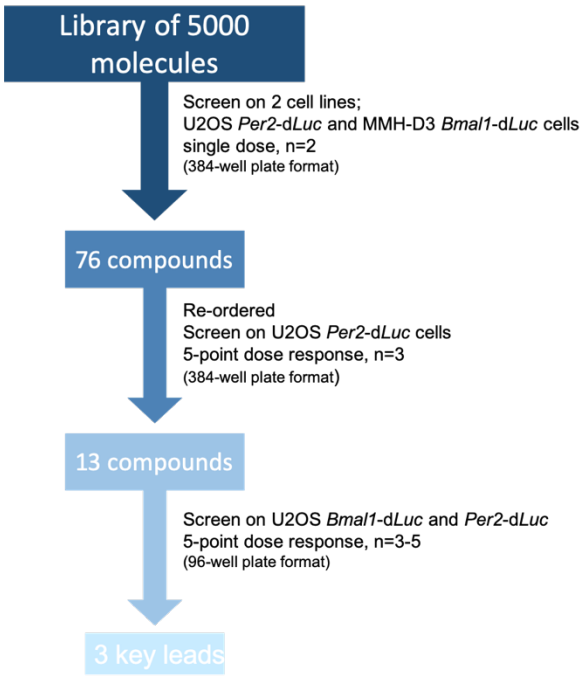


Figure 3.3 schematic flow chart for screening process

Firstly, 5000 molecules were screened in single doses on 2 distinct cell lines, human osteosarcoma U2OS *Per2*d-*Luc* and murine pre-hepatocytes MMH-D3 *Bmal1*-d*Luc* cells. From this, 76 compounds were chosen as hits for their amplitude and/or period altering effects. These compounds were re-ordered, to ensure reproducibility and eliminate batch-specific effects, and then tested in U2OS *Per2*-d*Luc* cells in 5-point dose responses for validation. Surprisingly, many of these compounds showed lack of effect, and primarily 13 compounds were selected to be taken forward to be validated on both *Bmal1* and *Per2* promoters in U2OS cells (represented in Table 3.1). To ensure the circadian modulatory effects are real, focus was set on molecules that increase both amplitude and period of promoter expression. The extent of amplitude and period potentiation of both *Bmal1* and *Per2* as well as the estimated EC50 of the drugs, which

corresponds to their potency, were taken into account. With that in mind, three drugs showed highest potential; Linopirdine, Zaprinast and Diclazuril (Table 3.1). The representative dose responses for the listed drugs are shown in Figure 3.4a-b, while the three lead molecules are reported in more detail in Figure 3.5 and 3.6.

Table 3.1: Top circadian modulators in *Bmal1*-d*Luc* and *Per2*-d*Luc* cells U2OS cells:

	Drug name	U2OS cells Reporter	Max Amplitude (% increase)	Amplitude EC50 (M)	Period Effect (Hours)	Period EC50 (M)
Drug 9	3-Trifluoromethylphenylpiperazine	Bmal1	48.64	3.48E-06	no change	X
Drug 9	3-Trifluoromethylphenylpiperazine	Per2	22.20	1.00E-06	no change	X
Drug 12	Milnacipran HCL	Bmal1	16.70	3.14E-07	0.45 decrease	***9.24E-13***
Drug 12	Milnacipran HCL	Per2	no change	X	no change	X
Drug 18	Betamipron	Bmal1	21.60	5.74E-06	no change	X
Drug 18	Betamipron	Per2	no change	X	no change	X
Drug 20	***Linopirdine (Dup-996)***	***Bmal1***	***25.60***	***1.87E-07***	***0.61***	***1.21E-07***
Drug 20	***Linopirdine (Dup-996)***	***Per2***	***93.49***	***7.40E-07***	***2.22***	***1.63E-06***
Drug 21	***Zaprinast***	***Bmal1***	***65.34***	***1.16E-06***	***1.36***	***1.08E-06***
Drug 21	***Zaprinast***	***Per2***	***15.20***	***8.34E-07***	***1.21***	***2.88E-06***
Drug 22	Levocetirizine dihydrochloiride	Bmal1	28.57	1.15E-07	no change	X
Drug 22	Levocetirizine dihydrochloiride	Per2	5.9	ambiguous	no change	X
Drug 28	Brimodine	Bmal1	26.73	5.82E-07	1.87	3.22E-08
Drug 28	Brimodine	Per2	13.40	2.05E-06	0.15	4.19E-07
Drug 30	Idoxuridine	Bmal1	25.70	1.70E-08	no change	X
Drug 30	Idoxuridine	Per2	9.25	ambiguous	no change	X
Drug 39	Todralazine (hydrochloride)	Bmal1	20.25	6.30E-08	no change	X
Drug 39	Todralazine (hydrochloride)	Per2	no change	ambiguous	no change	X
Drug 48	Pinacidil	Bmal1	19.06	7.47E-07	no change	X
Drug 48	Pinacidil	Per2	20.67	2.58E-07	0.30	1.18E-06
Drug 60	Prednisone	Bmal1	23.67	8.00E-06	0.3	6.10E-07
Drug 60	Prednisone	Per2	no change	X	no change	X
Drug 65	Flutamide	Bmal1	32.14	6.69E-07	0.62	1.46E-07
Drug 65	Flutamide	Per2	9.09	2.71E-07	0.76	~
Drug 68	***Diclazuril***	***Bmal1***	***56.29***	***1.03E-06***	***0.61***	***8.97E-07***
Drug 68	***Diclazuril***	***Per2***	***32.27***	***2.21E-06***	***no***	***X***

-The EC50 refers to the estimated concentration at which approximately 50% of a given compound's maximal amplitude or period effects were reached.
-X denotes no dose-dependent change and hence no estimated EC50.

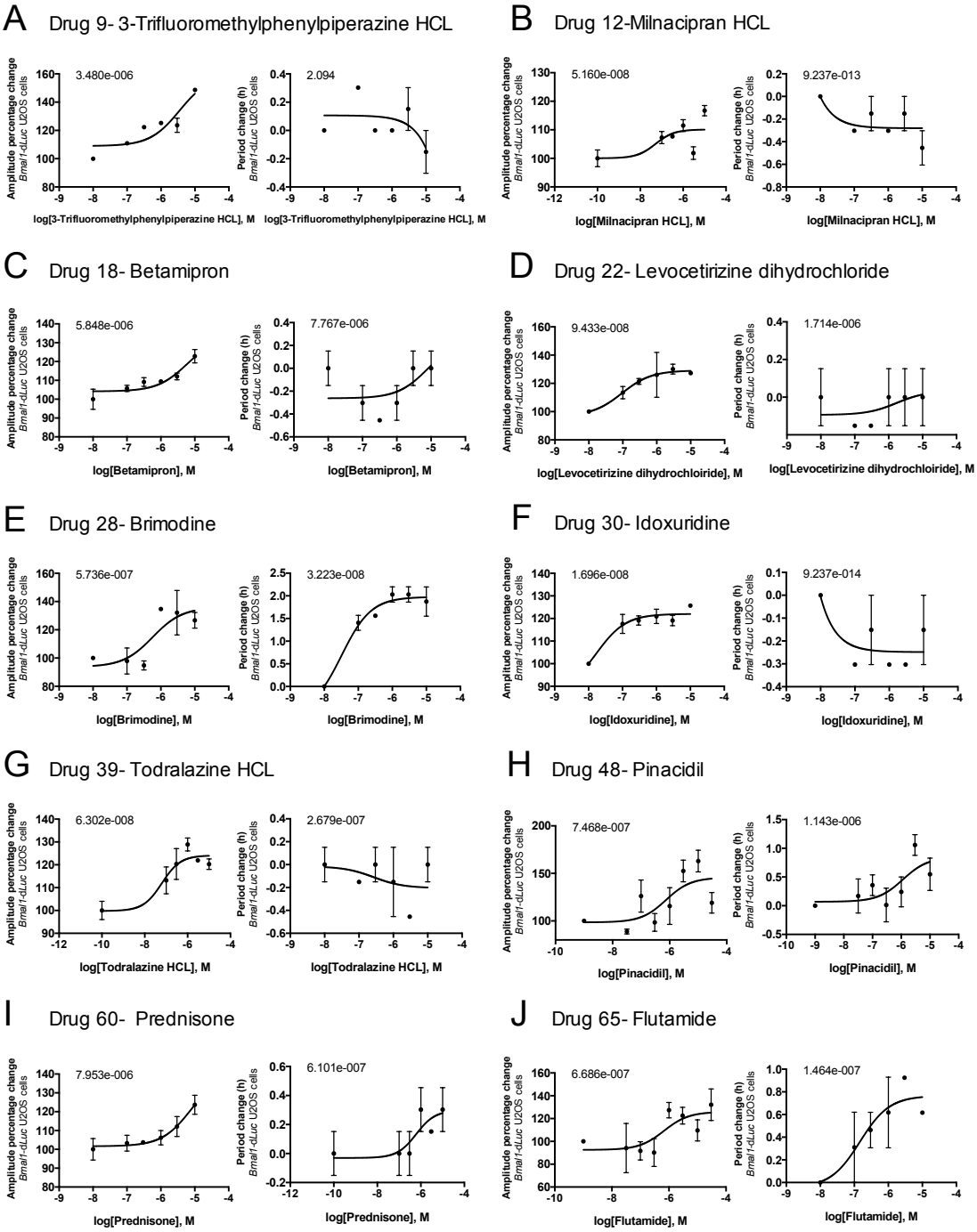


Figure 3.4a. Representative traces of real-time bioluminescence of *Bmal1*-d*Luc* U2OS cells: *Bmal1*-d*Luc* U2OS cells were synchronised with dexamethasone then treated with increasing doses of **(A)** 3-Trifluoromethylphylpiperazine, **(B)** Milnacipran HCL, **(C)** Betamipron, **(D)** Levocetrizine dihydhrochrolide, **(E)** Brimodine, **(F)** Idoxuridine, **(G)** Todralazine HCL, **(H)** Pinacidil, **(I)** Prednisone, and **(J)** Flutamide. Corresponding amplitude percentage changes analysis for the first day post drug administration and period change for each drug are displayed. Their corresponding EC50s are presented on each graph. Error bars denote ±SEM (N=3-5).

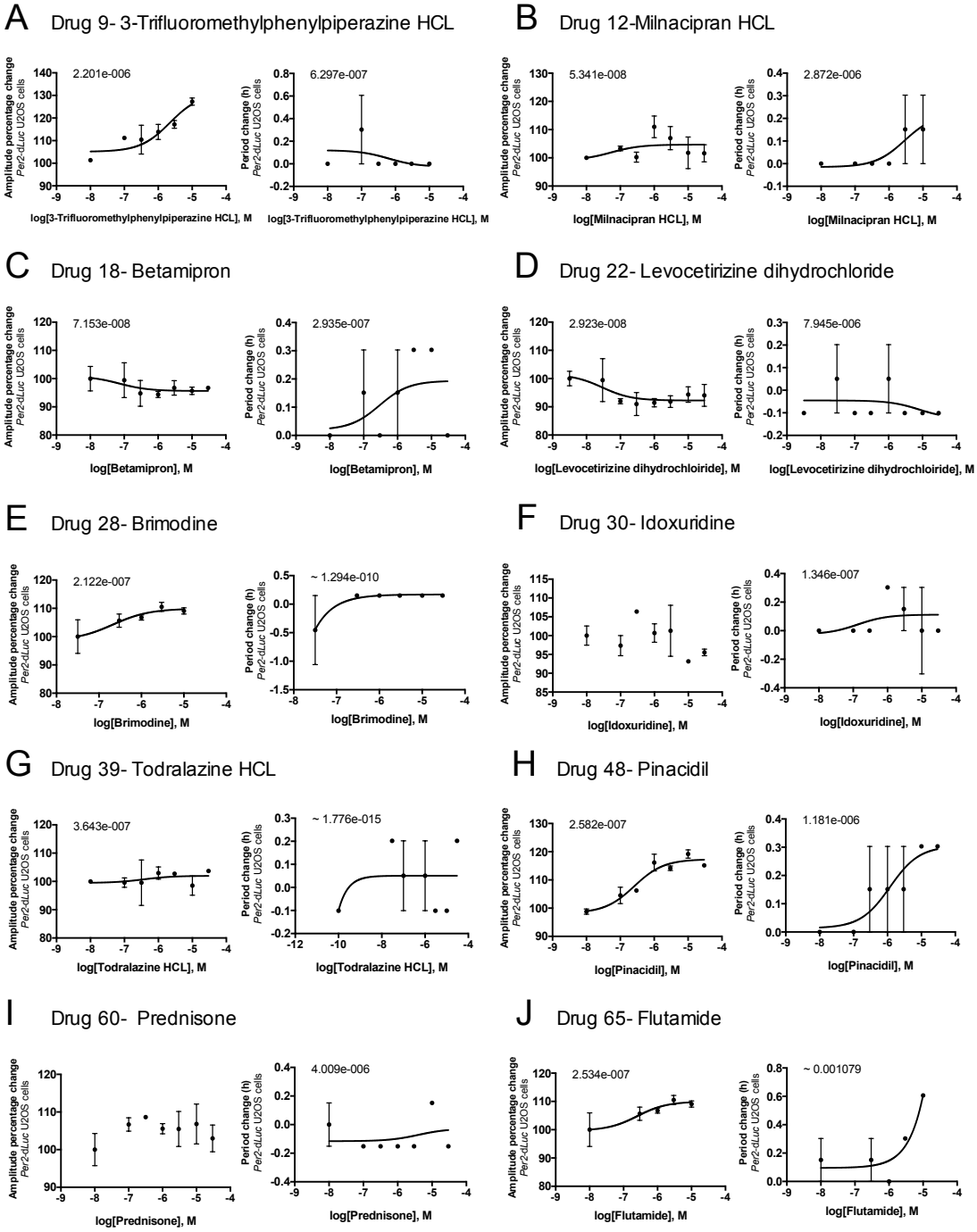


Figure 3.4b. Representative traces of real-time bioluminescence of *Per2*-d*Luc* U2OS cells:
Per2-d*Luc* U2OS cells were synchronised with dexamethasone then treated with increasing doses of **(A)** 3-Trifluoromethylphylpiperazine, **(B)** Milnacipran HCL, **(C)** Betamipron, **(D)** Levocetrizine dihydhrochrolide, **(E)** Brimodine, **(F)** Idoxuridine, **(G)** Todralazine HCL, **(H)** Pinacidil, **(I)** Prednisone, and **(J)** Flutamide. Corresponding amplitude percentage changes analysis for the first day post drug administration and period change for each drug are displayed. Their corresponding EC50s are presented on each graph. Error bars denote ±SEM (N=3-5).

Treatment with Zaprinast, a potent phosphodiesterase 5 and 6 inhibitor (PDE5) (Turko et al. 1999) resulted in a 65.3±1.4% increase in amplitude and 1.4±0.15 hours period elongation of *Bmal1*-d*Luc* expression in U2OS cells (Figure 3.5A, D, G), without affecting cell viability up to 10 μM (Figure 3.5J). Similar effects were observed in *Per2*-d*Luc* U2OS cells (Figure 3.6A, D, G), with comparable EC50s (834 nM for amplitude effect and 2.9 μM for period change). However the extent of amplitude enhancement was significantly lower, increasing amplitude of *Per2*-d*Luc* expression by 15.2±2.2%, with a similar period elongation of 1.21 hours.

Linopirdine is a well established blocker of KV_7 (KCNQ) voltage-gated potassium channels (Zaczek, Chorvat, and Brown 1997; Schnee and Brown 1998). In *Bmal1*-d*Luc* U2OS cells, Linopirdine increased amplitude and period by 25.6 ±2.75% and 0.61 ±0.15 hours, at an EC50 of 187 nM and 120 nM, respectively (Figure 3.5B, E, H), without affecting cell viability (Figure 3.5K). Interestingly, Linopirdine had a more prominent effect on *Per2*d-*Luc* U2OS cells, resulting in a 93.5±2.42% increase in amplitude and 2.32±0.1 hour period elongation, at an EC50 of 740 nM and 1.6 μM respectively (Figure 3.6B, E, H).

Diclazuril is a benzeneacetonitrile derivative used as a anticoccidial in animals, with no known mechanism of action or identified target (Matsuno et al. 1996). Diclazuril increased amplitude of *Bmal1*-d*Luc* expression by 41.9±3.8% and elongated period by 0.61±0.15 hours, with an EC50 of 620 nM and 914 nM respectively (Figure 3.5C,F,I). Diclazuril also had no effect on cell viability (Figure 3.5L). Similarly, Diclazuril showed an increase in amplitude of *Per2*d-*Luc* U2OS expression (32.9±2.0% increase) with a similar EC50 of 620 nM (Figure 3.6C,F), however showed no effect on period and had no effect on cell viability (Figure 3.6I,L).

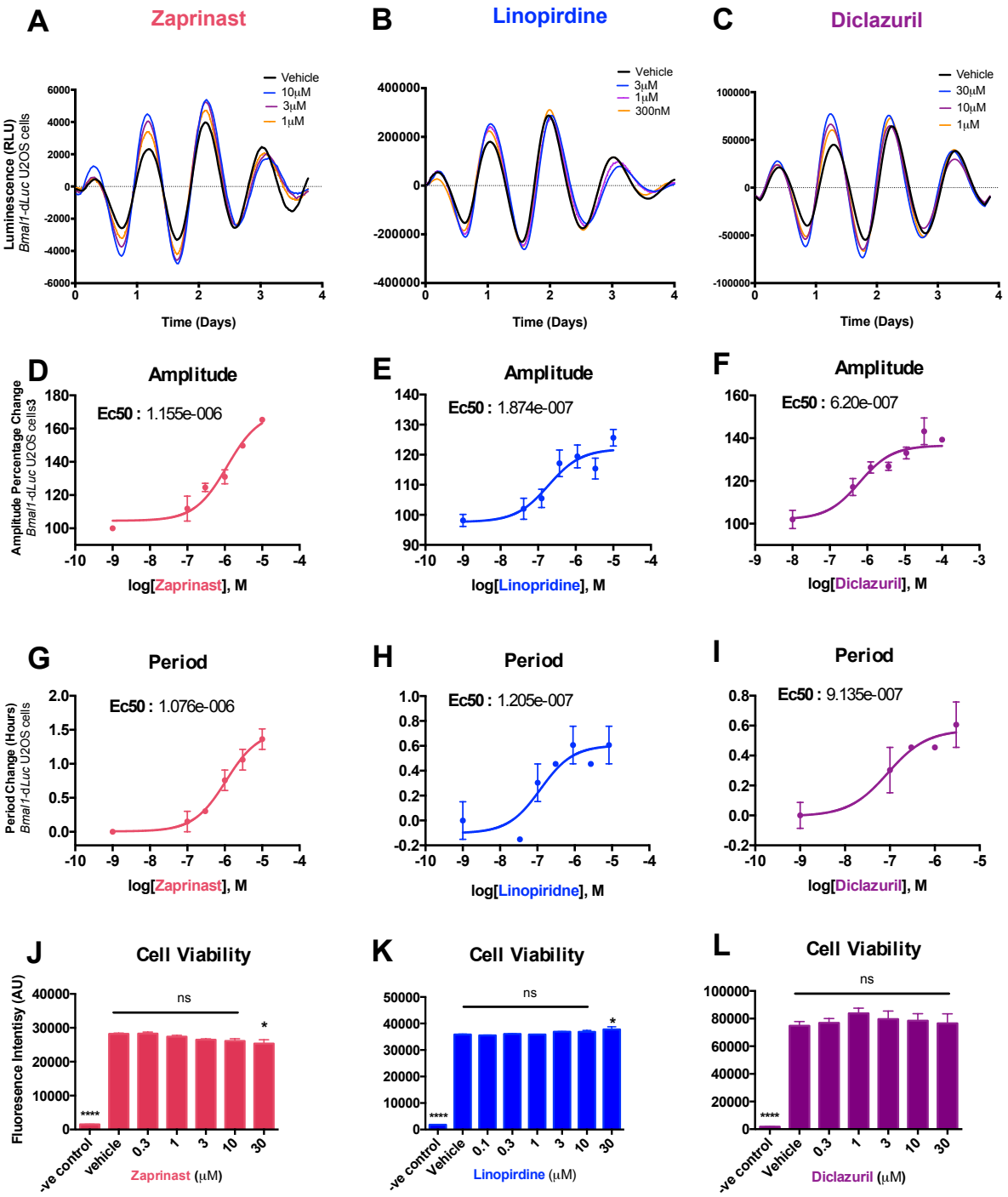


Figure 3.5. Identification of 3 potent circadian amplitude enhancers in *Bmal1*-d*Luc* U2OS cells: U2OS cells were synchronised with dexamethasone then treated with Zaprinast (red), Linopirdine (blue) or Diclazuril (purple) **A-C)** Representative traces of real-time bioluminescence of *Bmal1*-d*Luc* U2OS cells in the presence of drug treatments**. D-F)** Represent amplitude percentage changes analysis for the first day post drug administration (excluding first 16 hours post synchronisation). **G-I)** Represent period change following drug treatment. **J-L)** denote cell viability with increasing doses of drugs. Data shown is represented as mean ±SEM (N=3).

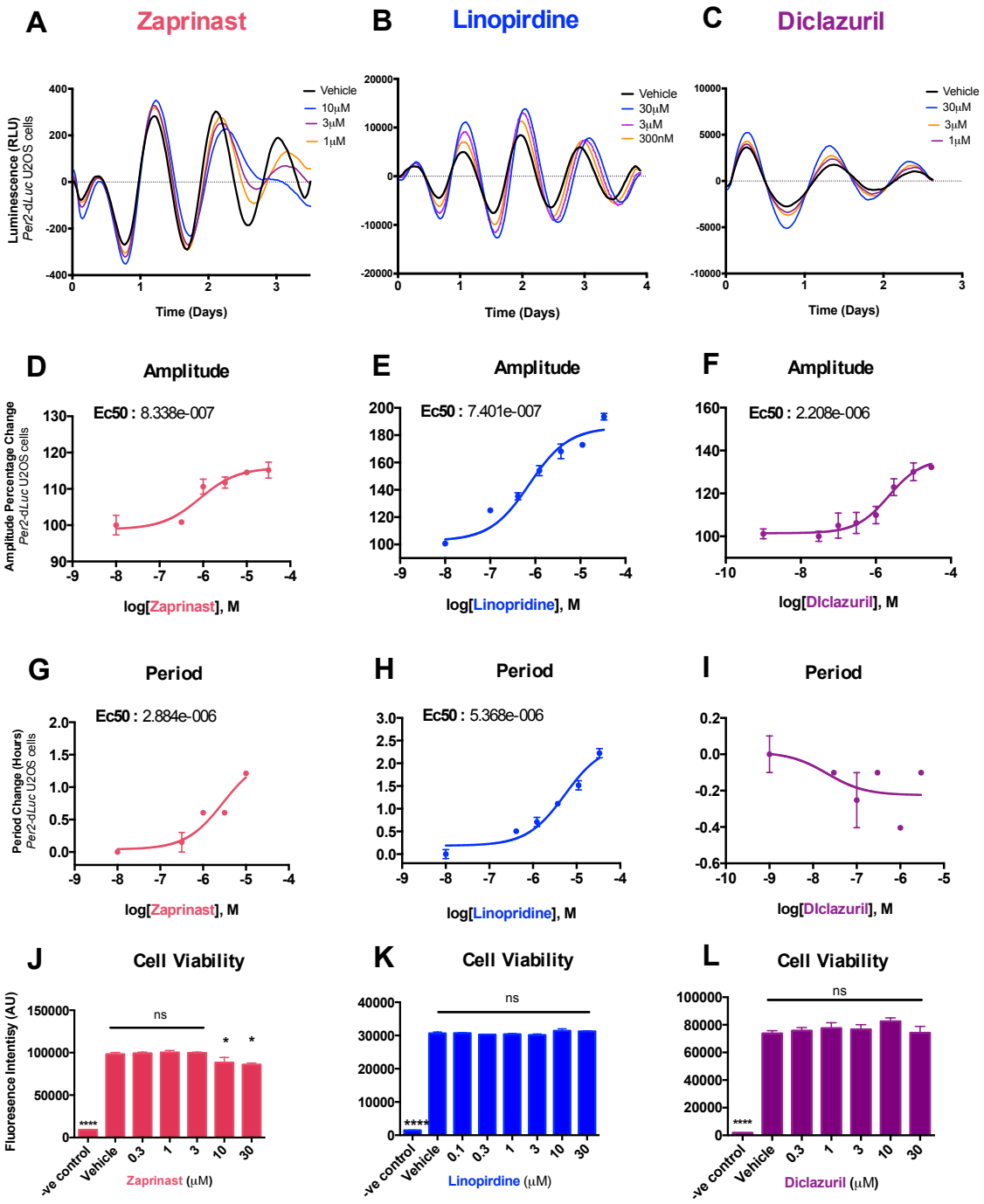


Figure 3.6. Identification of 3 potent circadian amplitude enhancers in *Per2*-d*Luc* U2OS cells: U2OS cells were synchronised with dexamethasone then treated with Zaprinast (red), Linopirdine (blue) or Diclazuril (purple) **A-C)** Representative traces of real-time bioluminescence of *Bmal1*-d*Luc* U2OS cells in the presence of drug treatments**. D-F)** Represent amplitude percentage changes analysis for the first day post drug administration (excluding first 16 hours post synchronisation). **G-I)** Represent period change following drug treatment. **J-L)** denote cell viability with increasing doses of drugs. Data shown is represented as mean ±SEM (N=3).

3.2.2 Characterization of key circadian modulators in different cell lines

To validate the amplitude effects of the drugs and gain confidence in the reproducibility of these observed effects, dose-response curves were generated in different cell lines. Keeping translatability into mice in mind, drugs were tested on murine adipocytes (Figure 3.7a-b) and mouse embryonic fibroblasts (Figure 3.8).

3.2.2.1 3T3-L1 adipocytes.

In line with our primary interest in metabolism, and given 3T3-L1 adipocyte cell line has been a pivotal tool in understanding basic cellular mechanisms associated with diabetes, obesity and other related disorders in thousands of studies (Green and Kehinde 1975; Kallen and Lazar 1996), the key drug leads were tested on this cell-line to validate their amplitude effects. Following differentiation of 3T3-L1 *Per2*-d*Luc* preadipocytes, mature adipocytes were synchronized and treated with increasing doses of Zaprinast, Linopirdine, or Diclazuril (Figure 3.7a) and bioluminescence was measured in real time over a period of ~4days. As observed in U2OS cells, all three drugs resulted in a dose-dependent increase in amplitude of *Per2*-d*Luc* expression; where Zaprinast caused a maximal increase of 104.2±21.7% with an EC50 of 2.2 μM, Linopirdine an increase of 39±22.1% with an EC50 of 4.37 μM, and Diclazuril caused a 60.4±26.5% maximal increase with an EC50 of 1.04 μM (Figure 3.7a-D-F). Linopirdine and Zaprinast had no effect on cell viability at any of the tested doses, while Diclazuril also had no effect up to 10 μM respectively (Figure 3.7J-L). Furthermore, Diclazuril resulted in a period increase

of 2.63±0.9 hours, with an EC50 of 734 nM, very similar to its amplitude effect (Figure 3.7a-I). Similarly, Linopirdine also increased period by 1.5±0.3 hours, at an EC50 of 613 nM, roughly 1 fold more potent than its amplitude effect (Figure 3.7a-H). Finally, although Zaprinast did increase period at 10 μM by 3.45±0.9 hours, its effect at other doses were ambiguous and so was the EC50 (Figure 3.7a-G). Similar increase in amplitude was observed when undifferentiated 3T3-L1 preadipocytes were treated with the drugs (Figure 3.7b), however the extent of the amplitude increase and the EC50s of the drug treatments were right shifted in the case of Linopirdine and Zaprinast, and left shifted with Diclazuril in these preadipocytes.

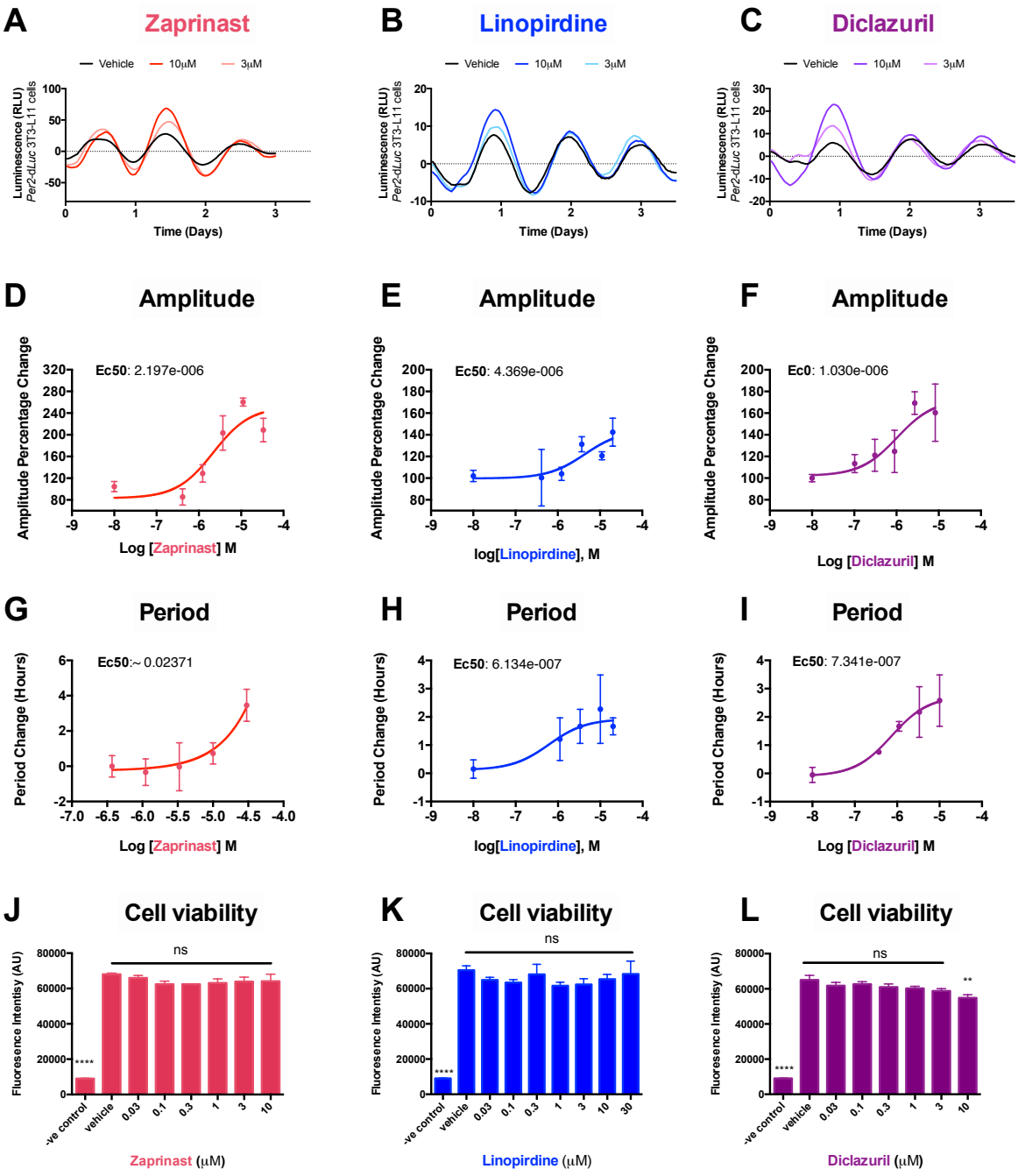


Figure 3.7a. The three leads from the drug screen increase amplitude of *Per2*-d*Luc* expression in mature adipocytes: Following differentiation and synchronisation, mature *Per2*-d*Luc* adipocytes were treated with increasing doses of Zaprinast, Linopirdine or Diclazuril and bioluminescence was measured in real-time. **A, B** and **C)** show representative traces. **D, E** and **F)** show analysis of amplitude percentage change of first day post-treatment. **G, H** and **I)** show period analysis post-treatment. **J-L)** Cell viability of *Per2*-d*Luc* 3T3-L1 cells post drug treatment. Error bars represent ±SEM, N=3 (each), significance determined by one-way ANOVA.

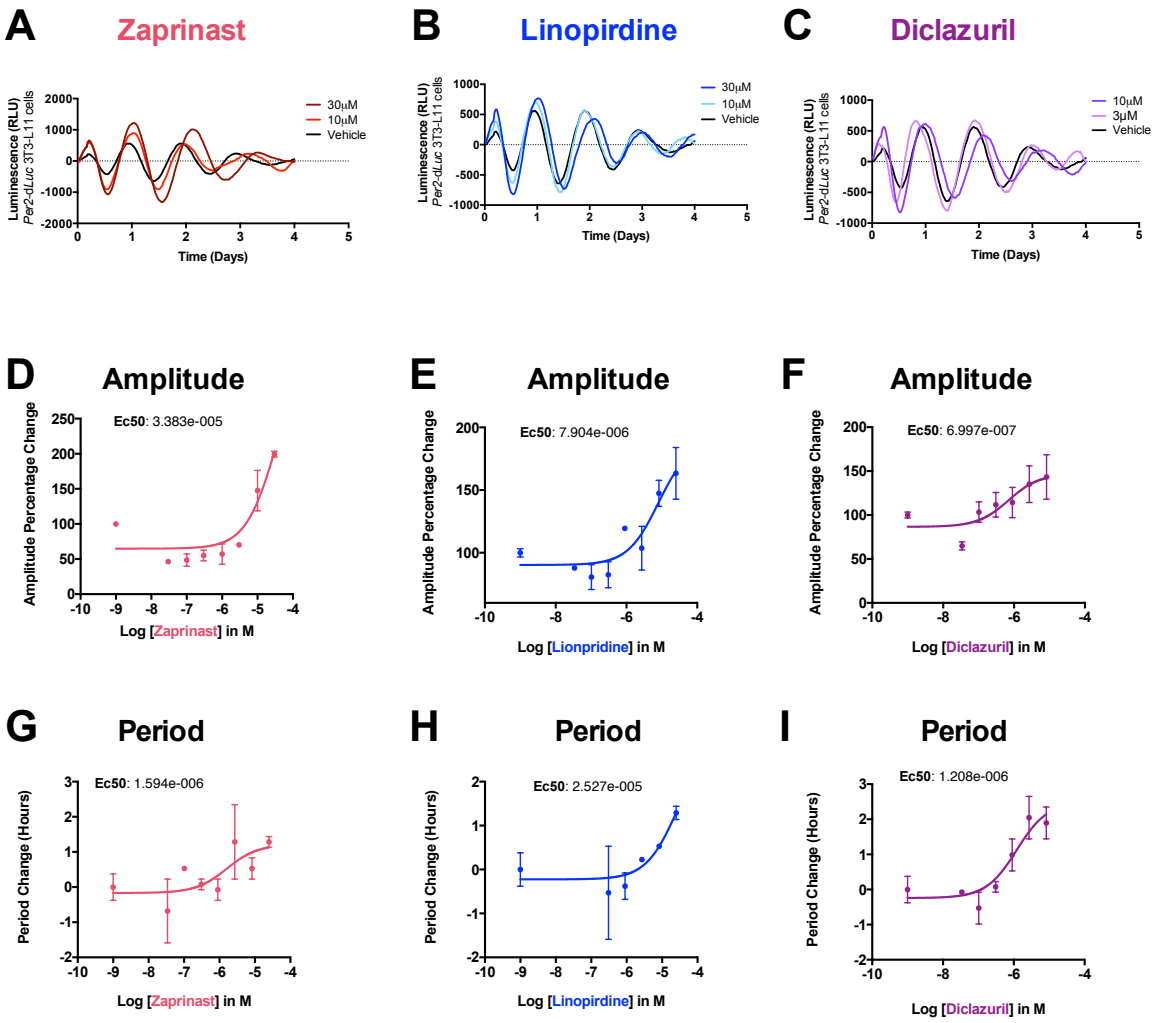


Figure 3.7b. The three leads from the drug screen increase amplitude of *Per2*-d*Luc* expression in 3T3-L1 preadipocytes: Undifferentiated *Per2*-d*Luc* 3T3-L1 cells were grown into confluency, synchronised, and then treated with increasing doses of Zaprinast, Linopirdine or Diclazuril and bioluminescence was measured in real-time. **A, B and C)** show representative traces. **D, E and F)** show analysis of amplitude percentage change of first day post-treatment. **G, H and I)** show period analysis post-treatment. Error bars represent ±SEM, N=3 (each).

3.2.2.2 Mouse embryonic fibroblasts:

For a second line of validation of the circadian modulatory effect of the 3 drug leads, increasing doses of all three drugs were administered on mouse embryonic fibroblasts cells (MEF) expressing PER2::LUC reporter (Figure 3.8). Contrary to U2OS and 3T3-L1 cells expressing promoter-luciferase reporters, these MEF cells express PER2-LUCIFERASE fusion protein, and therefore provide real-time monitoring of PER2 protein expression. Following synchronisation and drug treatment, amplitude effect of all three drugs was replicated in this cell-line. Zaprinast resulted in a maximal amplitude increase of 67.4±4.02%, Linopirdine increased amplitude by 25.2±1.6% and similarly Diclazuril resulted in a 22.3±2.43% increase in amplitude (±SEM) (Figure 3.8D).

However, in contrast to U2OS cells, these drugs showed a reduction in period of PER2::LUC expression, with Zaprinast reducing period by 1.4±0.11 hours, Linopirdine by 0.65±0.17 hours and Diclazuril by 1.3±0.186 hours (±SEM) (Figure 3.8E).

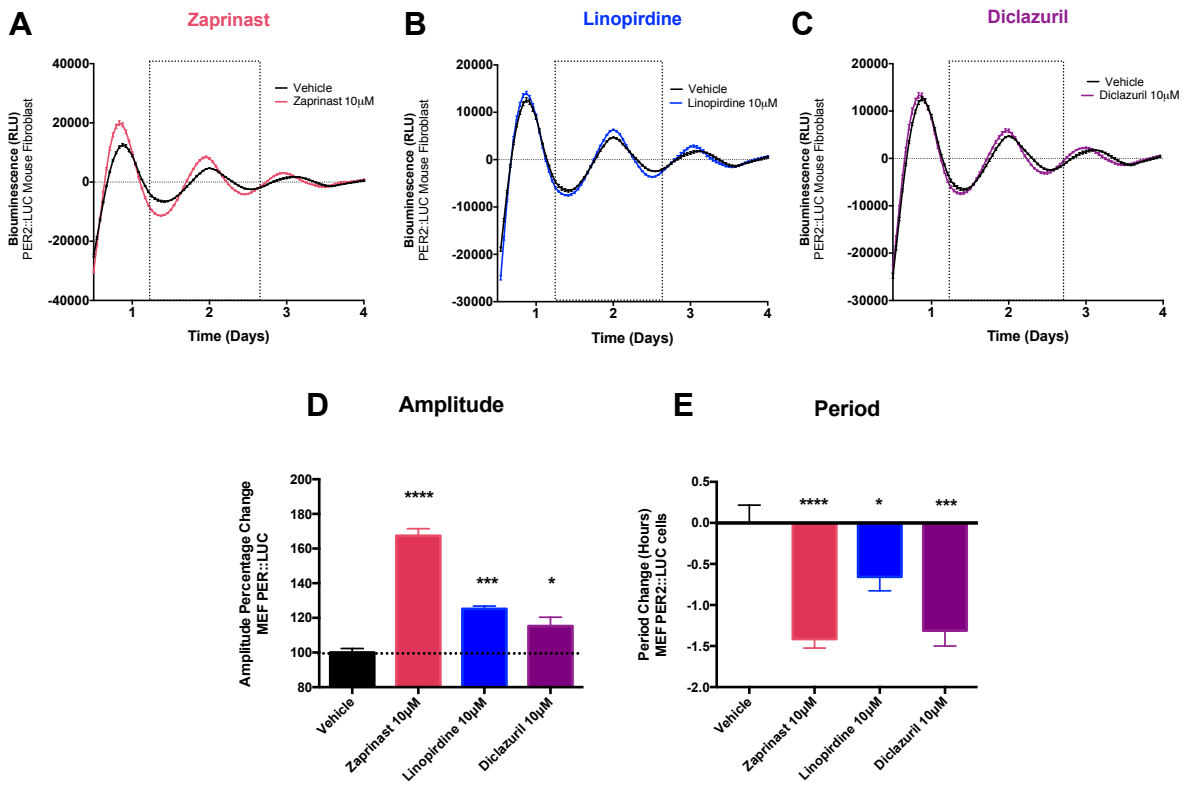


Figure 3.8. Key leads from drug screen increase amplitude of PER2 protein expression as reported in real time by PER2::LUC mouse embryonic fibroblasts (MEF): Following synchronisation, PER2::LUC MEF cells were treated with 10 μM Zaprinast (**A**), Linopirdine (**B**) or Diclazuril (**C**) and bioluminescence was recorded. All three drugs increase amplitude (**D**) and reduce period (**E**) of PER2 expression. Error bars represent ±SEM, N=6 (each) and repeated twice, significance determined by one-way ANOVA.

3.2.3 Validation of transcriptional change via mRNA

To further confirm the ability of these circadian modulators to increase circadian gene expression away from bioluminescent reporter cell-lines, mRNA quantification was carried out. To capture the first day amplitude effects that were observed in the circadian bioluminescence assays, U2OS cells were first synchronised, then treated with Zaprinast, Linopirdine or Diclazuril at 3 μM each (similar to the circadian luminescence reporter assays, at their corresponding ~EC75). 16 hours later mRNA was collected (time 0h), then 8 and 18 hours after that, and qPCR for *Per2* and *Bmal1* genes was performed. Figure 3.9A shows a schematic representation of mRNA collection times relative to bioluminescence assays. Zaprinast showed no effect on *Per2* gene expression at these time points, but resulted in a significant increase in *Bmal1* gene expression at 18h (Figure 3.9B-C). Linopirdine and Diclazuril both showed a significant increase in expression of *Per2* and *Bmal1* at 18h (Figure 3.9D-G).

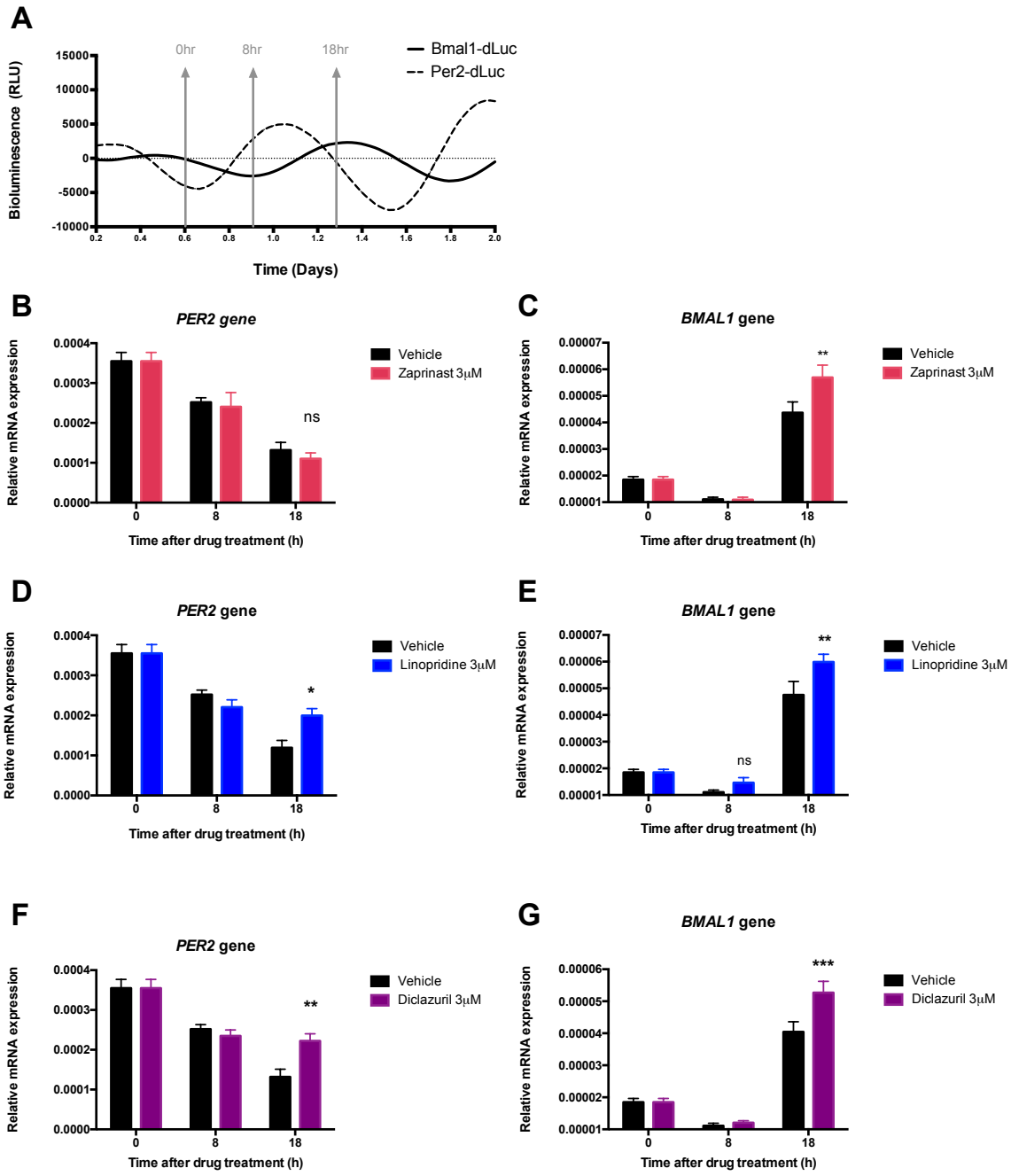


Figure 3.9. mRNA validation of *Per2* and *Bmal1* changes following drug administration in U2OS cells: U2OS cells were synchronised with Dexamethasone and then treated with drugs at the 3 μM concentration. mRNA was collected 16 hours after synchronisation (time 0), and at 8 and 18 hours thereafter. **A)** Schematic representation of mRNA collection times relative to bioluminescence assays. Quantification of relative mRNA levels of *Per2* (**B, D, F**) and *Bmal1* (**C, E, G**) was carried out using qPCR and data was normalised to two house-keeping genes: *β-Actin* and *Gapdh*. Error bars represent ±SEM, N=6. Significance determined by Two-way ANOVA

3.2.4 Investigating effects of lead circadian modulators on metabolic processes in adipocytes:

Metabolic syndrome (MetS) has been characterised by glucose intolerance, obesity, hypertension, and dyslipidaemia. As mentioned earlier, small molecules that increase amplitude of circadian clock genes, such as nobiletin, have been reported to ameliorate symptoms of MetS, particularly glucose intolerance and weight gain (He et al. 2016). To investigate this observation at a cellular level and help shed light on the mechanisms behind amplitude enhancement in adipocytes, *in vitro* metabolic screens focusing on glucose uptake (Figure 3.10), adipogenesis (Figures 3.11-3.12), lipolysis (Figure 3.13), and cellular bioenergetics (Figures 3.14-3.17), were optimised in mature adipocytes. These assays were used to examine the effects of the three key circadian modulators identified from the circadian screen, whose amplitude effects in mature adipocytes were validated (Figure 3.7a). All of the metabolic assays (except adipogenesis) were carried out following 24-hour treatment with the lead drugs, in order to allow time for full transcriptional effects of circadian amplitude enhancement (and any following post-translational actions) to occur over the subjective 24-hour cycle.

3.2.4.1 Glucose uptake

One of the key symptoms comprising MetS is the onset of hyperglycaemia as a result of glucose intolerance and/or insulin resistance (Eckel, Grundy, and Zimmet 2005). To investigate the effects of circadian modulators on glucose uptake, 3T3-L1 cells were differentiated into mature adipocytes (Figure 3.10A). The sensitivity of the assay to

detect glucose uptake by these cells was validated using increasing doses of insulin (Figure 3.10B), which showed 2.46±0.23 maximal fold increase at 100 nM insulin with an EC50 of 6.7 nM, similar to what is reported in literature (Weiland et al. 1991). Following 24-hour treatment with Zaprinast (10 μM, EC80) , Linopirdine (10 μM, EC70) or Diclazuril (3 μM, EC75), mature adipocytes were then glucose starved in the presence or absence of 100 nM insulin for 1 hour, then glucose uptake was quantified using 2-DeoxyGlucose (as mentioned in methods). 10 mM of metformin was used as a positive control for the assay. Interestingly, all three drugs showed a significant increase in basal glucose uptake (Zaprinast: 27±5.7% increase, Linopirdine: 58.75±8.7% increase, and Diclazruil:74.4±23.8% increase) (Figure 3.10C). On the other hand, neither Zaprinast nor Diclazuril had an effect on glucose uptake in the presence of 100 nM insulin, however, only Linopirdine resulted in a significant rise in insulin-stimulated glucose uptake compared to vehicle insulin-stimulated glucose uptake (20.68±5% , a= “p=0.02” unpaired t-test).

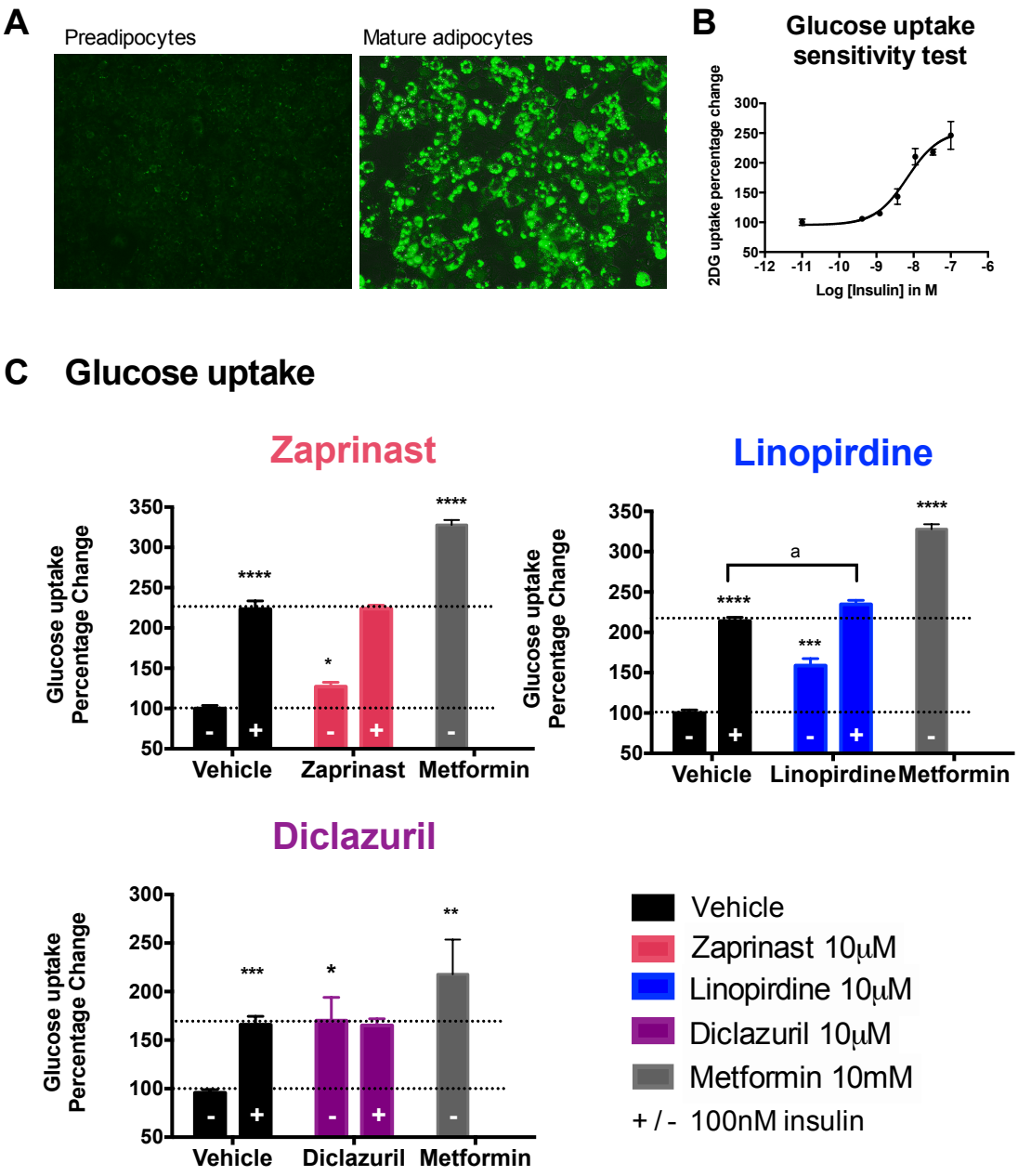


Figure 3.10. All 3 circadian amplitude enhancers increase glucose uptake in differentiated 3T3-L1 cells: (A) Lipid droplet accumulation of preadipocytes vs mature 3T3-L1 adipocytes stained using LipiTOX (magnification 40x). **(B)** Insulin dose-response on glucose uptake was used as a positive control for assay sensitivity (N= 3). **(C)** Following 24-hour treatment with Zaprinast (N=5), Linopirdine (N=5) and Diclazuril (N=4) in serum free media, mature adipocytes were glucose starved for an hour (with/without further treatment with 100 nM insulin), then glucose uptake assay was carried out. Metformin (without insulin treatment, N=5) was used as positive control. All experiments were repeated twice. Statistical significance determined by one-way ANOVA followed by Dunnett's multiple comparisons test against vehicle (-insulin). Unpaired t-test was done to compare vehicle and Linopirdine (+insulin), a represents p= 0.0207. Error bars represent ±SEM.

3.2.4.2 Adipogenesis

3.2.4.2.1 Lipid accumulation

To investigate how these circadian modulators affect adipocyte differentiation and maturation, 3T3-L1 preadipocytes were differentiated in the presence of Zaprinast, Linopirdine or Diclazuril, in two different conditions. *Experiment 1* (Figure 3.11a) involved induction of differentiation with IBMX, insulin, dexamethasone and Rosliglitazone (methods section 2.2.5). This protocol promotes maximal differentiation of preadipocytes into mature adipocytes, which would help assess any inhibitory effects of circadian modulators on adipocyte differentiation. In *experiment 2* (Figure 3.11b), 3T3-L1 cells were differentiated using a similar induction cocktail but without Rosliglitazone (IBMX, insulin and dexamethasone only), which results in 70.2±2.6% less differentiation (±SEM, Figure 3.11c). This therefore helps investigate any differentiation-enhancing effects of these circadian modulators and avoids masking effects of Rosiglitazone which is a very potent and critical inducer of 3T3-L1 differentiation (Zebisch et al. 2012). Lipid droplet staining using Nile Red was used a proxy for differentiation quantification.

Zaprinast showed a significant increase in lipid accumulation of mature adipocytes when differentiated in the absence of Rosiglitazone (70±18.2% increase Figure 3.11b,A-B) but no change in the presence of Rosiglitazone (Figure 3.11a,A-B), and no overall change in number of cells (Figures 3.11a,C, 3.11b,C).

On the other hand, Linopirdine showed significant decrease in lipid accumulation per cell in the presence of Rosiglitazone (60.9±2.03% decrease. Figure 3.11a,A-B) but had no effect in the absence of Rosiglitazone (Figure 3.11b,A-B). Interestingly, Linopirdine also resulted in a significant increase in cell number in both conditions (132.3±24.7% increase with Rosliglitazone (Figure 3.11a,C), and 32.8±4% increase without Rosliglitazone (Figure 3.11b,C). Finally, Diclazuril showed no change in lipid accumulation or cell number in either condition and therefore did not seem to affect adipocyte differentiation (Figure 3.11a-b).

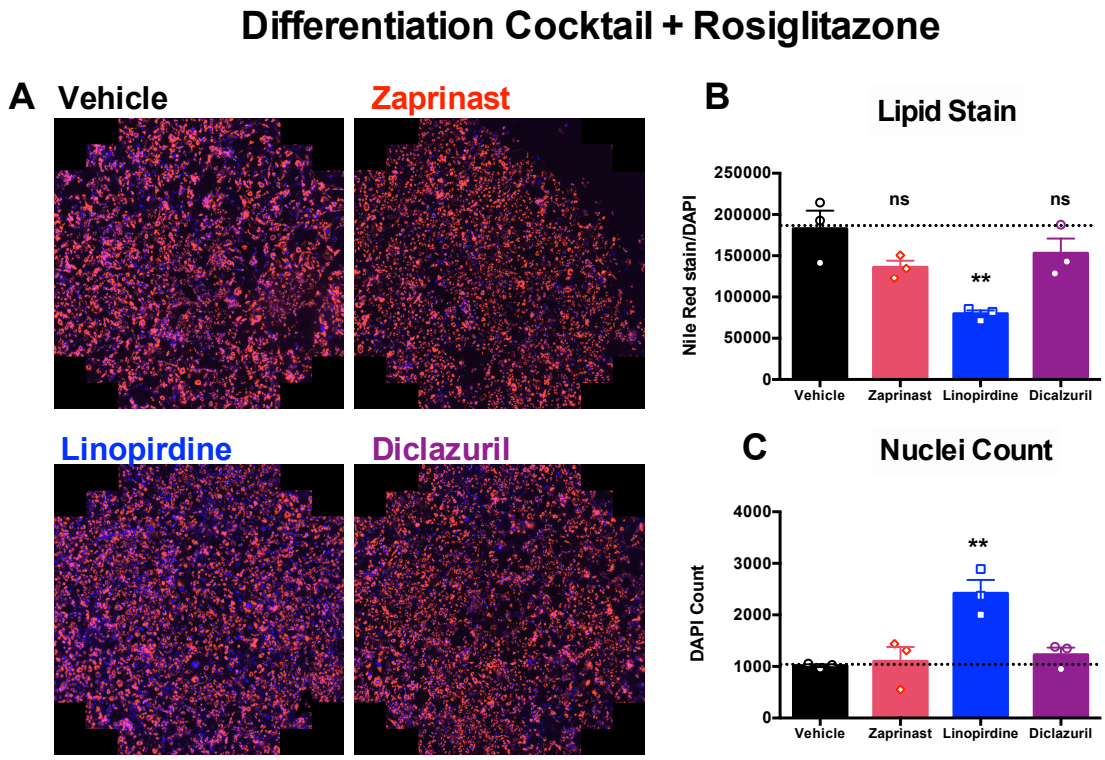


Figure 3.11a. ***Experiment 1*****- Screen for effect of drug leads on adipogenesis of 3T3-L1 cells using differentiation cocktail with 10 μM Rosiglitazone: A)** Microscope images (magnification 40x) of mature adipocytes differentiated in the presence of different treatments. Nile Red was used for staining lipid droplets and DAPI (blue) for nuclei. Quantification of lipid droplet accumulation **(B)** and cell number **(C)** following different treatments (N=3 each).

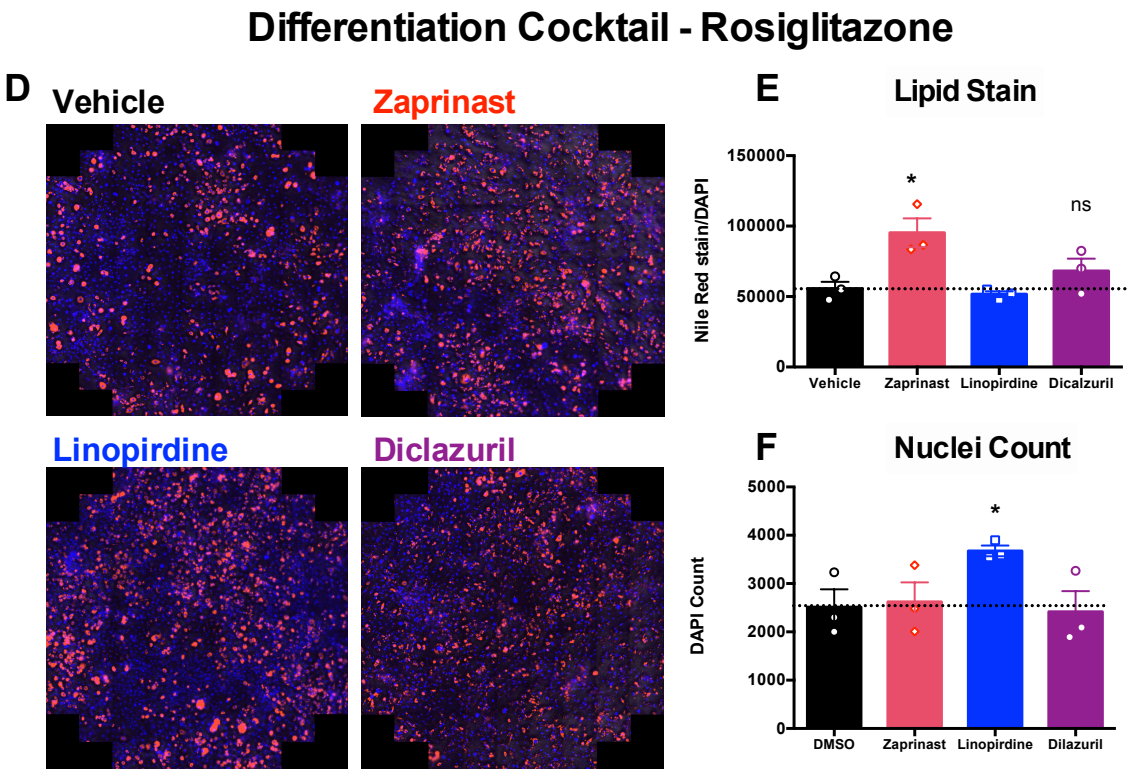


Figure 3.11b. ***Experiment 2*****- Screen for effect of drug leads on adipogenesis of 3T3-L1 cells using differentiation cocktail lacking Rosiglitazone: A)** Microscope images (magnification 40x) of mature adipocytes differentiated in the presence of different treatments. Nile Red was used for staining lipid droplets and DAPI (blue) for nuclei. Quantification of lipid droplet accumulation **(B)** and cell number **(C)** following different treatments (N=3 each).

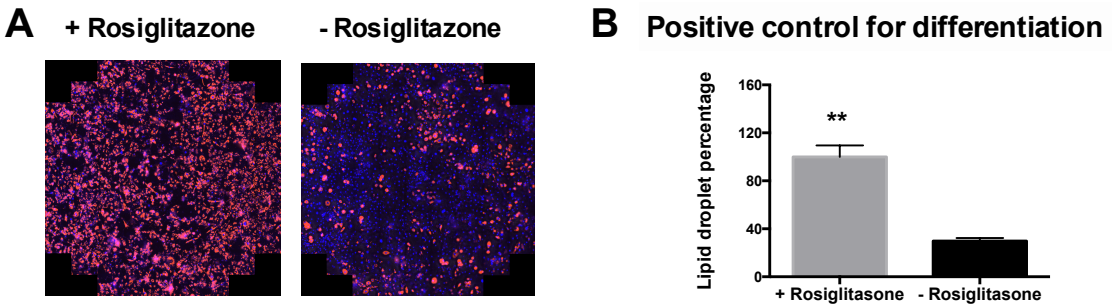


Figure 3.11c. Difference in lipid accumulation for ***Experiment 1*** **and** ***2*****: A)** Microscope images (magnification 40x) for mature 3T3-L1 following differentiation using Rosiglitazone-containing cocktail vs no Rosiglitazone. **B)** Quantification of lipid droplet accumulation normalised to cell number (N=3 each).

3.2.4.2.2 Quantification of WAT markers

To further explore the effects of these 3 circadian modulators on adipogenesis of 3T3-L1 cells, similar to *experiment 1*, preadipocytes were differentiated using Rosiglitazone-containing induction cocktail, in the presence of Zaprinast, Linopirdine or Diclazuril, and mRNA was collected. Quantification of key BAT and WAT markers was performed using qPCR. BAT markers like *UCP1* and *Prdm16* were undetectable while *Cidea* was poorly expressed but detectable, and showed no significance with any treatment (Figure 3.12a). WAT markers, on the other hand, showed significant changes with different drug treatments (Figure 3.12b). Zaprinast showed a significant reduction in *Ppary* and *Leptin* and a trend in reduction of *AdipoQ* mRNA (p=0.07). Linopirdine on the other hand, resulted in a significant increase in WAT markers *Fabp4*, *Leptin*, *AdipoQ* and *Glut4*, and showed a trend of increase in *Ppary* mRNA (t-test, p=0.04). Finally, Diclazuril showed slight discrepancy, reducing relative expression of *Ppary*, and *AdipoQ* but increasing *Leptin* mRNA.

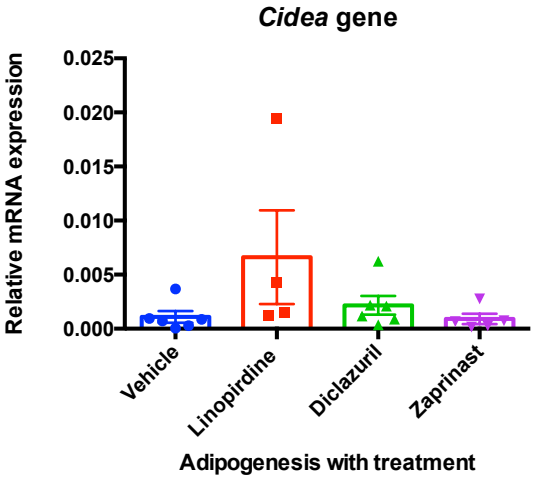


Figure 3.12a. mRNA quantification of BAT marker *Cidea*.

3T3-L1 cells were differentiated until maturity with IBMX, insulin, dexamethasone and Rosiglitazone (Experiment 1) in the presence of the mentioned treatments (all at 10 μM), and mRNA was collected. Brown marker Cidea was quantified using qPCR (normalised to house-keeping genes *Nono* and *β-Actin*).

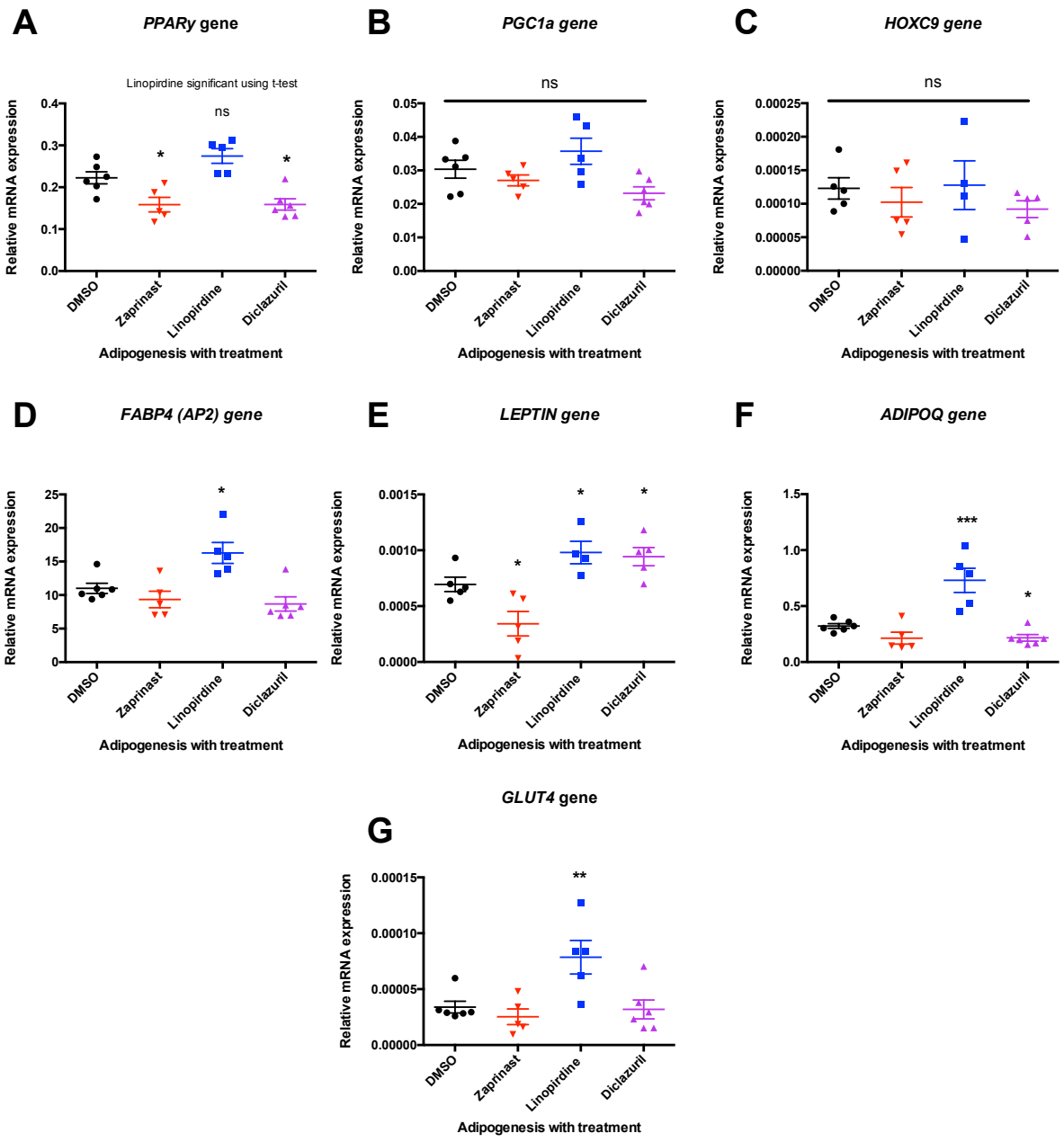


Figure 3.12b. mRNA quantification of WAT markers in mature 3T3-L1 adipocytes following differentiation in the presence of drug treatment:
Relative mRNA expression of WAT markers *Ppary*, *Pgc1a*, *Hoxc9*, *Fabp4*, *Leptin*, *Adiponectin*, *Glut4* (N=5-6) (A-G). Data was normalised to 2 housekeeping genes *Nono* and *β-Actin*. Statistical significance was calculated using one-way ANOVA.

3.2.4.3 Lipolysis

To follow up on how circadian modulators could ameliorate weight gain, lipolysis assay was carried out (Figure 3.13). 3T3-L1 cells were differentiated into maturity, and then treated for 24-hours with our key drug leads, before glycerol quantification. Isoprenaline (10 μM) was used as a positive control. It is a potent β-adrenergic agonist that induces PKA-mediated phosphorylation and translocation of Hormone-Sensitive Lipase (HSL) to the lipid droplet, promoting lipolysis (Clifford et al. 2000; Egan et al. 1992). Following 24-hour incubation, isoprenaline increased glycerol release by 46.7±14.9% (±SEM). Interestingly, Zaprinast and Diclazuril had no effect on stimulating lipolysis, whereas Linopirdine resulted in a 32.7±12.3% increase (±SEM).

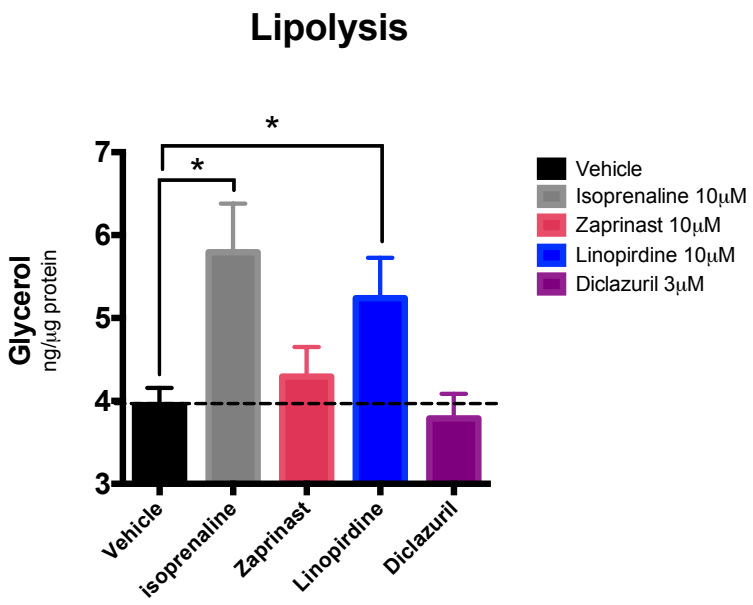


Figure 3.13. Linopirdine increases lipolysis in differentiated 3T3-L1 cells: Lipolysis assay following 24h pre-treatment with drugs, isoprenaline used as positive control (N=10 each). Error bars represent ±SEM.

3.2.4.4 Cellular bioenergetics

One way small molecules could protect against diet-induced obesity, could be to increase energy expenditure intracellularly. Furthermore, human and animal studies have shown obesity to be associated with a reduction in mitochondrial oxygen capacity (Choo et al. 2006; Xiao et al. 2014). To investigate how circadian modulators can affect the energy phenotype of mature adipocytes following drug treatment, and to monitor simultaneously any induced changes to mitochondrial respiration and glycolytic potential of these cells, seahorse assay was optimised and performed (Figure 3.14-3.17).

3.2.4.4.1 The PHD-inhibitor Molidustat shifts the bioenergetic phenotype of adipocytes towards glycolysis:.

An XF Extracellular Flux Analyzer was used to assess mitochondrial oxygen consumption rate (OCR) as well as extracellular acidification rate (ECAR) and Molidustat, a potent HIF1α stabiliser that mimics hypoxia (Beck et al. 2018), was used as a positive control (Figure 3.14). Similar to what is reported in literature regarding hypoxic conditions effects on cellular bioenergetics (Shih et al. 2018), Molidustat caused a dose-dependent reduction in mitochondrial ATP production (vehicle: 90.45±1.3, 3 μM: 58.5±2.05, 300 nM: 73.3±3.7 pmol ATP/min, Figure 3.14E), resulting in an energetic shift towards glycolytic pathways (vehicle: 0.29±0.02, 3 μM: 0.18±0.01, 300 nM: 0.22±0.01, mean±SEM, Figures 3.14D and 3.14B). In addition, it predictably caused a significant reduction in basal respiration (vehicle: 23.1±0.65, 3 μM: 15.04±0.96 , 300 nM:

19.7±1.06), ATP-linked respiration (vehicle: 15.43±0.76, 3 μM: 10.23±0.63, 300 nM: 13.0±0.71 maximal oxygen consumption rate (vehicle: 43.4±2.28, 3 μM: 21.04±1.04, 300 nM: 36.7±1.06), and spare capacity (vehicle: 24.8±1.23, 3 μM: 6.6±0.76, 300 nM: 16.9±1.05), without affecting proton leak (vehicle: 6.4±0.5, 3 μM: 5.3±0.4, 300 nM: 7.2±0.7) or non-mitochondrial respiration in these cells (vehicle: 37.36±2.16, 3 μM: 38.6±2.8, 300 nM: 43.25±3.87) (mean±SEM pmol O_2/min Figure 3.14C).

Furthermore, Molidustat resulted in a dose dependent reduction in the cell's ability to respond to energy demand, at a mitochondrial and a glycolytic level, denoted metabolic potential (Mitochondrial metabolic potential; vehicle: 136.9±3.5%, 3 μM: 114.9±4.1%, 300 nM: 127.9±2.8%, Glycolytic metabolic potential; vehicle: 134.3±2.2%, 3 μM: 120.3±1.5%, 300 nM: 127.6±1.1%, Figure 3.14F).

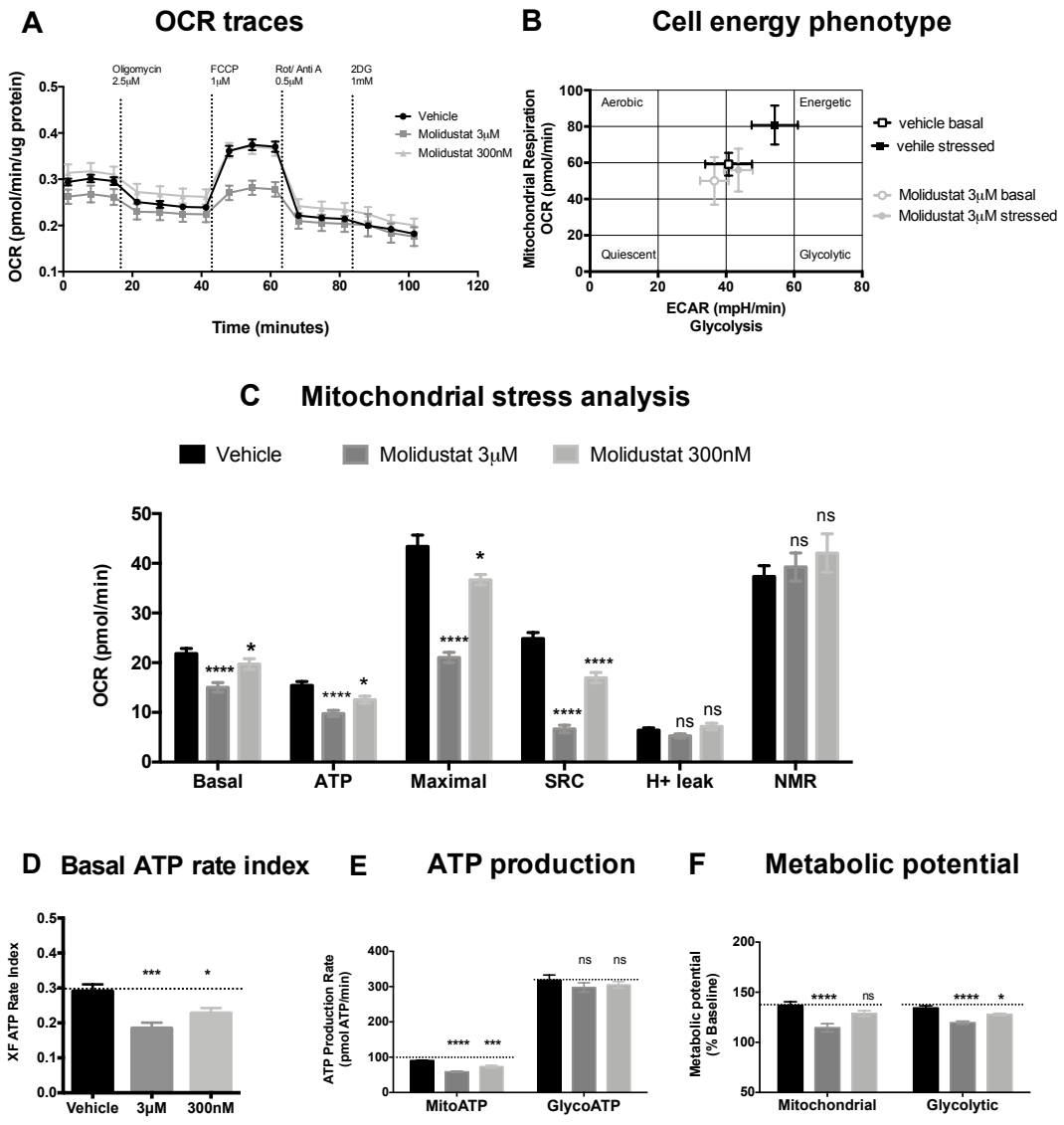


Figure 3.14. Molidustat shifts ATP rate index of differentiated 3T3-L1 cells towards glycolysis in a dose dependent manner:

A) OCR of mature 3T3-L1 adipocytes following 24-hour treatment with Molidustat 3 μM, 300 nM or vehicle and in response to the indicated mitochondrial inhibitors. **B)** The cellular energy phenotype of 3T3-L1 cells. Stressed indicates following administration of oligomycin and FCCP stressors that push cellular energetics to their maximum. **C)** Mitochondrial stress analysis derived from OCR traces. Basal: basal respiration, ATP: ATP-linked respiration, Maximal: Maximal respiratory capacity, SRC: spare respiratory capacity, H+ leak: proton leak, NMR: non-mitochondrial respiration.

D) Basal ATP Rate Index: Ratio of Mitochondrial ATP production rate and Glycolytic ATP production rate, both broken down in **(E).** Higher values of ATP Rate Index indicate greater oxidative phosphorylation.

F) The metabolic potential: the measure of cells' ability to meet an energy demand via respiration and glycolysis, denoted as percentage increase of stressed OCR over baseline OCR (Mitochondrial), and stressed ECAR over baseline ECAR (Glycolytic).

Each point represents the results of the mean ± standard error of the mean (SEM), with N= 7-9. Statistical significance was determined using one-way ANOVA followed by Dunnett's multiple comparisons test. Experiment repeated twice.

3.2.4.4.2 Zaprinast reduces glycolytic ATP production in 3T3-L1 cells without affecting other parameters:

The first circadian modulator tested, Zaprinast, showed no apparent shift in cellular energetics (Figure 3.15B, D) and no changes to mitochondrial parameters like, basal respiration, ATP-linked respiration, maximal respiratory capacity, spare respiratory capacity, proton leak or non-mitochondrial respiration (Figure 3.15C). However it did cause a significant reduction in the rate of Glycolytic ATP (vehicle: 310.8±113.8, 20 μM: 297.6±15.6, 10 μM: 306.0±9.3 , mean±SEM pmol ATP/min), and in Mitochondrial ATP at 20 μM (vehicle: 90.45±1.3, 20 μM: 58.5±2.04, 10 μM: 73.2±3.7, mean±SEM pmol ATP/min)(Figure 3.15 E).

3.2.4.4.3 Linopirdine shows no effects on cellular bioenergetics or mitochondrial function:

Similarly, Linopirdine also had no apparent shift in cellular bioenergetics (Figures 3.16 A, B and D), nor in any of the other mitochondrial or glycolytic parameters (Figures 3.16 C, E and F).

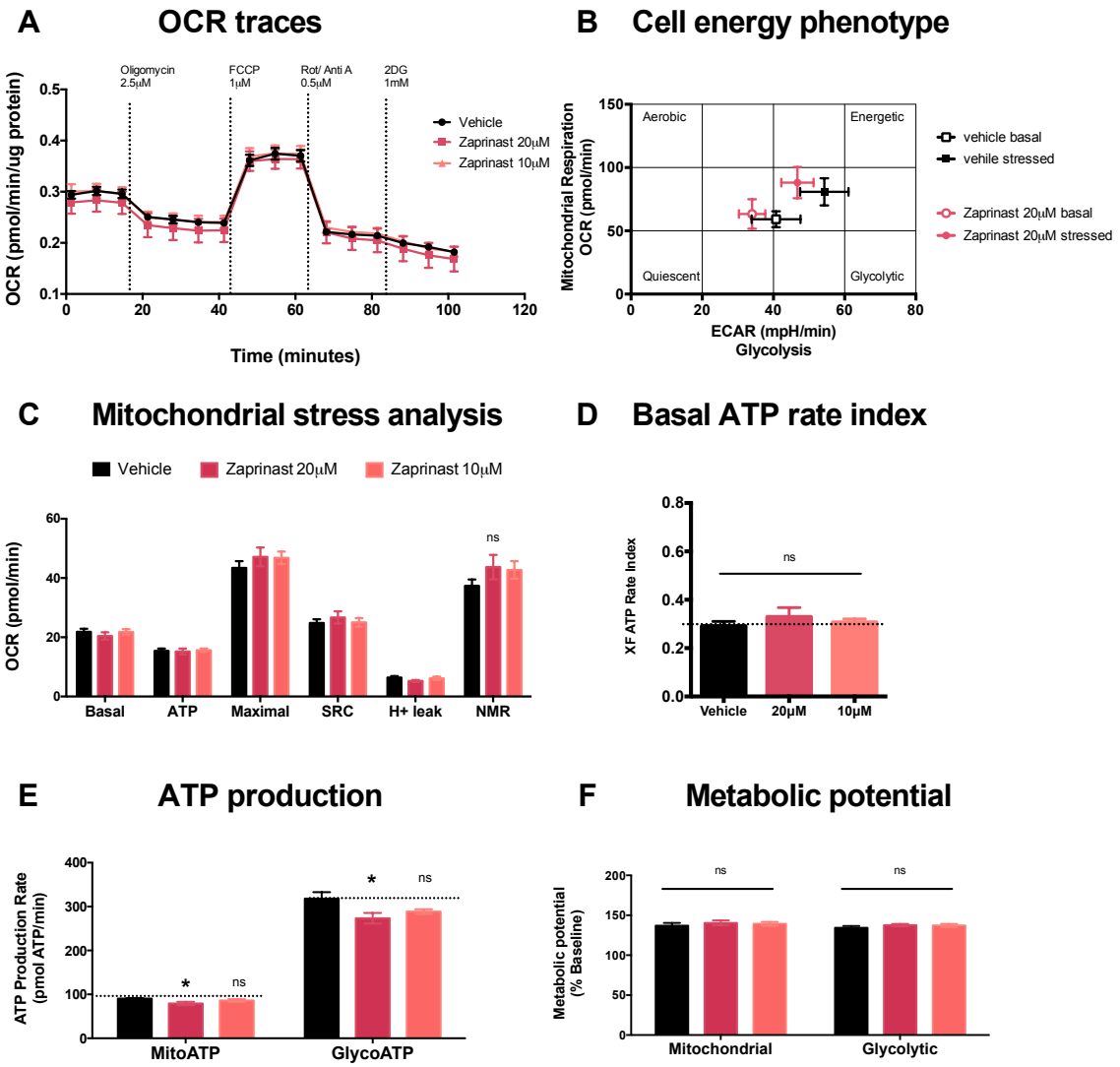


Figure 3.15. Real-time measurements of mitochondrial oxygen consumption rates (OCR) and effects of Zaprinast on mitochondrial bio-energetic profile:
A) OCR of mature 3T3-L1 adipocytes following 24-hour treatment with Zaprinast 20 μM, 10 μM or vehicle and in response to the indicated mitochondrial inhibitors. **B)** The cellular energy phenotype of 3T3-L1 cells. Stressed indicates following administration of oligomycin and FCCP stressors that push cellular energetics to their maximum. **C)** Mitochondrial stress analysis derived from OCR traces. Basal: basal respiration, ATP: ATP-linked respiration, Maximal: Maximal respiratory capacity, SRC: spare respiratory capacity, H+ leak: proton leak, NMR: non-mitochondrial respiration.
D) Basal ATP Rate Index: Ratio of Mitochondrial ATP production rate and Glycolytic ATP production rate, both broken down in **(E).** Higher values of ATP Rate Index indicate greater oxidative phosphorylation.
F) The metabolic potential: the measure of cells' ability to meet an energy demand via respiration and glycolysis, denoted as percentage increase of stressed OCR over baseline OCR (Mitochondrial), and stressed ECAR over baseline ECAR (Glycolytic).
Each point represents the results of the mean ± standard error of the mean (SEM), with N=7-9. Statistical significance was determined using one-way ANOVA followed by Dunnett's multiple comparisons test. Experiment repeated twice.

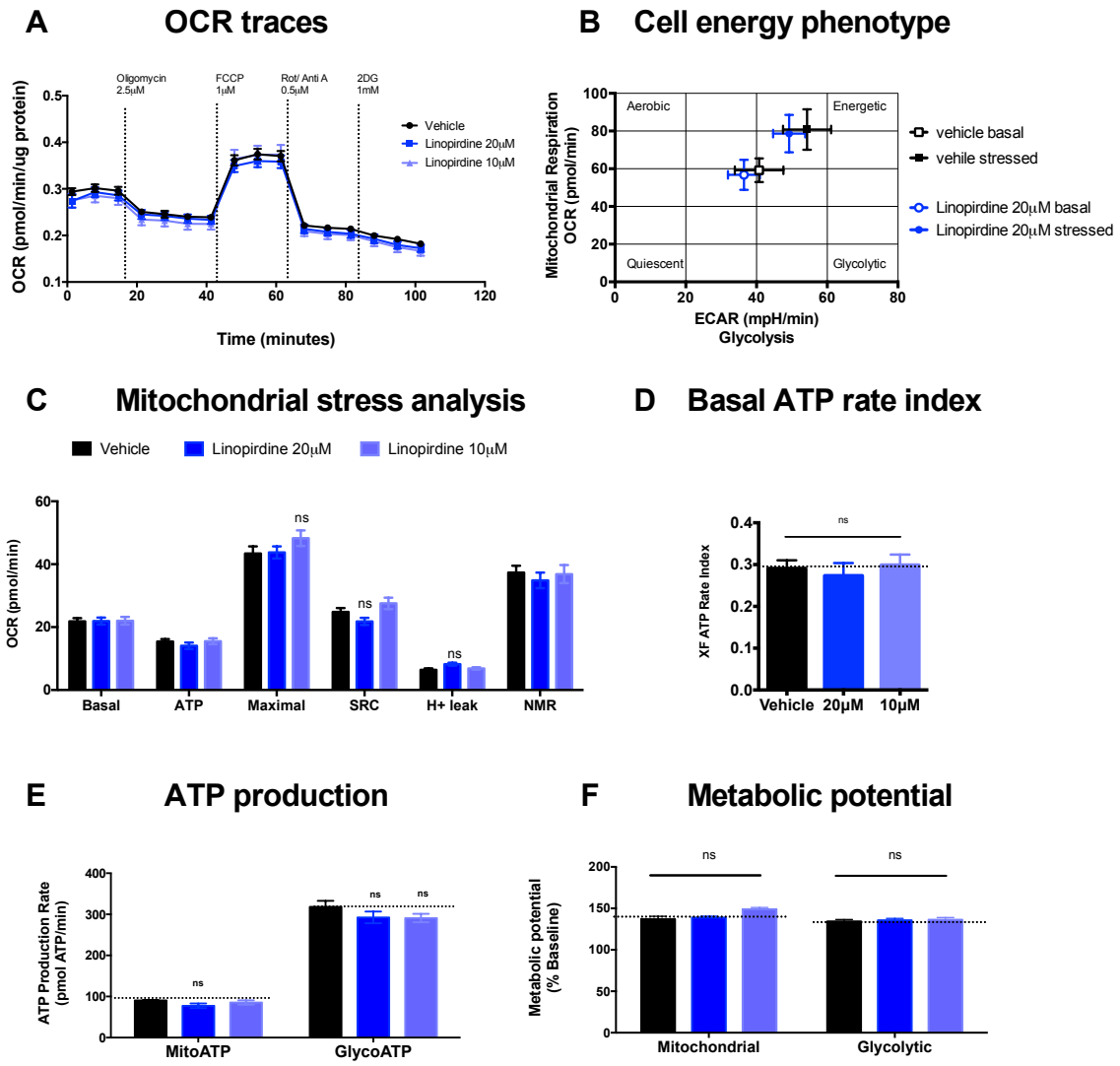


Figure 3.16. Real-time measurements of mitochondrial oxygen consumption rates (OCR) and effects of Linopirdine on mitochondrial bio-energetic profile:

A) OCR of mature 3T3-L1 adipocytes following 24-hour treatment with Linopirdine 20 μM, 10 μM or vehicle and in response to the indicated mitochondrial inhibitors. **B)** The cellular energy phenotype of 3T3-L1 cells. Stressed indicates following administration of oligomycin and FCCP stressors that push cellular energetics to their maximum. **C)** Mitochondrial stress analysis derived from OCR traces. Basal: basal respiration, ATP: ATP-linked respiration, Maximal: Maximal respiratory capacity, SRC: spare respiratory capacity, H+ leak: proton leak, NMR: non-mitochondrial respiration.

D) Basal ATP Rate Index: Ratio of Mitochondrial ATP production rate and Glycolytic ATP production rate, both broken down in **(E).** Higher values of ATP Rate Index indicate greater oxidative phosphorylation.

F) The metabolic potential: the measure of cells' ability to meet an energy demand via respiration and glycolysis, denoted as percentage increase of stressed OCR over baseline OCR (Mitochondrial), and stressed ECAR over baseline ECAR (Glycolytic).

Each point represents the results of the mean ± standard error of the mean (SEM), with N=7-9. Statistical significance was determined using one-way ANOVA followed by Dunnett's multiple comparisons test. Experiment repeated twice.

3.2.4.4.4 Diclazuril shifts ATP production in differentiated 3T3-L1 cells towards oxidative phosphorylation and enhances the cells' ability to respond to high energy demands:

Finally, Diclazuril was the only drug to shift the cellular bioenergetics towards more oxidative phosphorylation (vehicle: 0.29±0.01, 3 μM: 0.42±0.04, 1 μM: 0.35±0.04 , Figure 3.17B, D), primarily due to a dose-dependent reduction in glycolytic ATP production (vehicle: 328.5±16.8, 3 μM: 249.3±13.7, 1 μM: 271.4±13.4 pmol ATP/min, Figure 3.17E), but also possibly due to a slight but non-significant increase in mitochondrial ATP (vehicle: 90.4±1.3, 3 μM: 102.0±5.9 (p=0.07 t-test), 1 μM: 96.2±5.9 pmol ATP/min, Figure 3.17C). Diclazuril also showed no change in basal respiration, proton leak or non-mitochondrial respiration, but significantly increased maximal oxygen consumption rate (vehicle: 43.4±2.28, 3 μM: 56.1±2.9, 1 μM: 53.0±2.9 pmol O_2/min, Figure 3.17C) and spare capacity (vehicle: 24.8±1.23, 3 μM: 33.0±1.86, 1 μM: 29.8±1.6 pmol O_2/min, Figure 3.17C). As a result, the metabolic potential of 3T3-L1 cells, defined as their ability to respond to high energy demands, was significantly increased at the mitochondrial and glycolytic level (*Mitochondrial*; vehicle: 136.98±3.9%, 3 μM: 163.5±12.3%, 1 μM: 146.3±2.8% and *Glycolytic*; vehicle: 135.1±2.26%, 3 μM: 144.7±3.5%, 1 μM: 138.5±2.1%, Figure 3.17F).

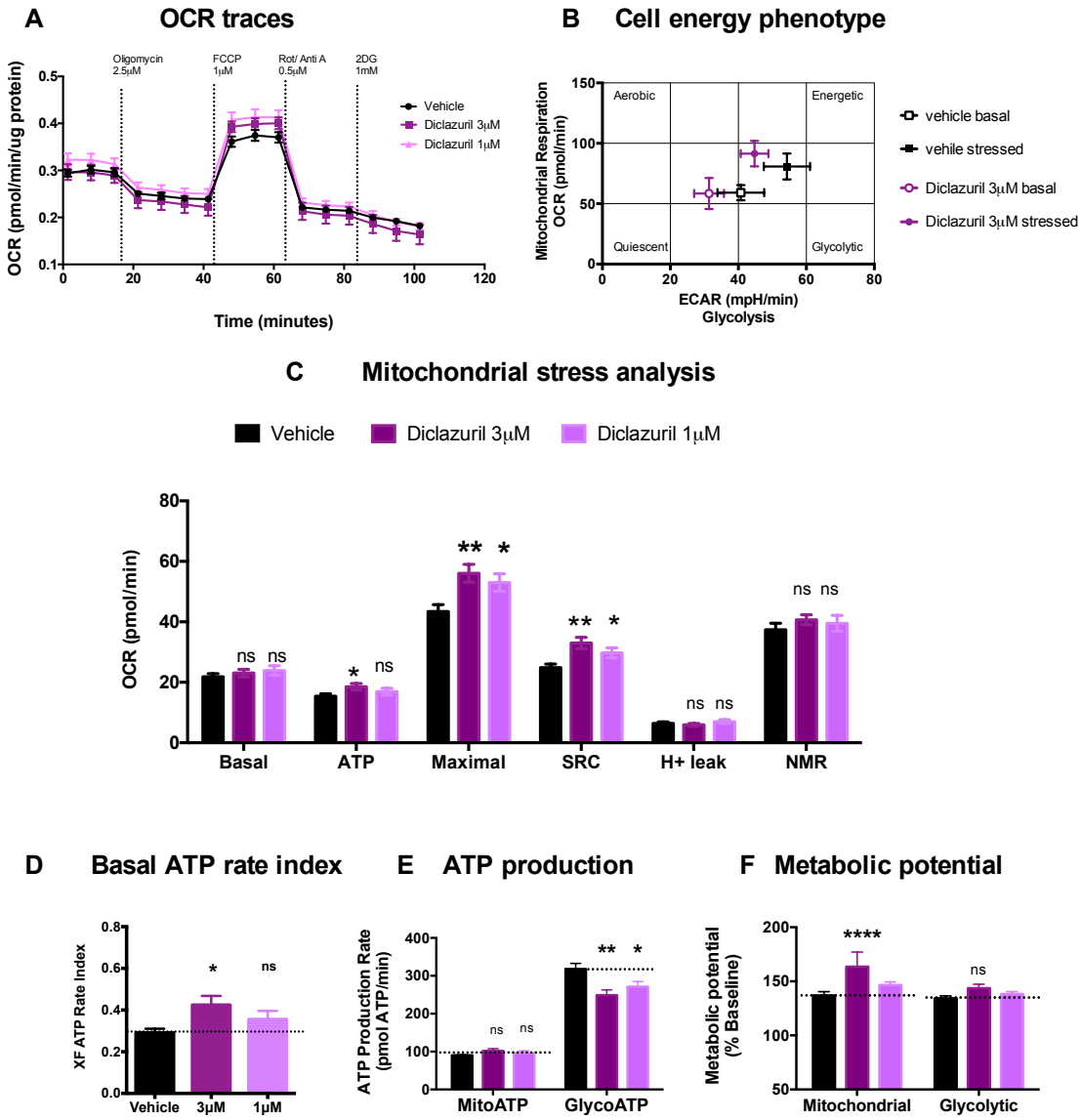


Figure 3.17. Real-time measurements of mitochondrial oxygen consumption rates (OCR) and effects of Diclazuril on mitochondrial bio-energetic profile:

A) OCR of mature 3T3-L1 adipocytes following 24-hour treatment with Linopirdine 20 μM, 10 μM or vehicle and in response to the indicated mitochondrial inhibitors. **B)** The cellular energy phenotype of 3T3-L1 cells. Stressed indicates following administration of oligomycin and FCCP stressors that push cellular energetics to their maximum**. C)** Mitochondrial stress analysis derived from OCR traces. Basal: basal respiration, ATP: ATP-linked respiration, Maximal: Maximal respiratory capacity, SRC: spare respiratory capacity, H+ leak: proton leak, NMR: non-mitochondrial respiration.

D) Basal ATP Rate Index: Ratio of Mitochondrial ATP production rate and Glycolytic ATP production rate, both broken down in **(E).** Higher values of ATP Rate Index indicate greater oxidative phosphorylation.

F) The metabolic potential: the measure of cells' ability to meet an energy demand via respiration and glycolysis, denoted as percentage increase of stressed OCR over baseline OCR (Mitochondrial), and stressed ECAR over baseline ECAR (Glycolytic). Each point represents the results of the mean ± standard error of the mean (SEM), with N=7-9. Statistical significance was determined using one-way ANOVA followed by Dunnett's multiple comparisons test. Experiment repeated twice

3.3 Discussion

3.3.1 Validation of the identified circadian modulators:

In the pursuit of novel potent circadian modulators, an extensive screening process utilising a range of cell lines expressing bioluminescent reporters of clock genes was carried out (summarised in Figure 3.1). Following this screen, three potent circadian amplitude enhancers that increase *Bmal1* and *Per2* in U2OS (Figures 3.5, 3.6) and differentiated 3T3-L1 cells (Figure 3.7a), respectively, were identified. Their amplitude enhancing effects across different cell lines was validated using mRNA quantification of *Bmal1* and *Per2* gene expression in U2OS cells (Figure 3.9), and via real-time quantification of PER2 protein expression in mouse embryonic fibroblasts (MEF)(Figure 3.8). The mRNA quantification in U2OS cells measured the key positive and negative arms of the clock at approximately their zenith and nadir of expression, while the MEFs expressing PER2::Luciferase fusion protein constructs helped track PER2 protein levels in real time via luminescent readings. Hence, taken together, these findings give confidence in the biological validity of the observed amplitude effects.

These drugs increased amplitude potently in all tested cell lines, however, it is important to note that there were differences in the period effects between these cell lines. All three drugs increased period in U2OS and 3T3-L1 cells at EC50s comparable to their amplitude effects (Figures 3.5, 3.6, 3.7). However, period shortening of PER2::LUC rhythms was observed in MEF cells (Figure 3.8). This could be associated with cell type-specific

functions of core clock genes. Indeed, Ramanthan et al have reporter similar divergent period phenotypes following *Per1*, *Per2* and *Per3* knockdown in different cell lines (Ramanathan et al. 2014). Furthermore, this period effect could also be attributed to a difference in stoichiometry of clock components, as MEF cells have been shown to express half the amount of PER1 and PER2 relative to BMAL1 and CLOCK whereas liver cells for example exhibit a 1:1 ratio (Lee et al. 2011), which could indicate more rapid elimination of PER in these cells.

However, given we hypothesize amplitude enhancement increases extent of expression of key downstream metabolic genes, the initiation of that expression by the positive arm of the clock (CLOCK-BMAL1 dimer), which later binds E-boxes and promotes downstream expression of CCG holds the greatest importance for our investigation. Furthermore, in adipocytes, which are the main model for our metabolic screening, both amplitude and period of expression are increased (Figure 3.7), allowing us to move past the divergent period shortening effects in MEF cells.

3.3.2 Different circadian amplitude enhancers diverge in their metabolic phenotypes:

To our surprise, enhancement of the 3T3-L1 clock expression using different molecules did not show a uniform metabolic phenotype. The three drugs, all sharing their amplitude enhancing ability, resulted in a significant increase in glucose uptake capacity of mature

adipocytes (Figure 3.10). However, they behaved very differently in the remaining metabolic assays. Table 3.2 summarises the metabolic phenotypes of all 3 drugs.

Table 3.2. A summary of the metabolic phenotypes of Zaprinsat, Linopirdine, Diclazuril on mature 3T3-L1 adipocytes

Metabolic change	Zaprinast	Linopirdine	Diclazuril
Glucose uptake	↑	↑	↑
Glycerol release	--	↑	--
Lipid accumulation (+ Rosiglitazone)	--	↓	--
Lipid accumulation (- Rosiglitazone)	↑	--	--
Key adipogenic markers (when adipogenesis induced with Rosiglitazone)	↓PPARy ↓Leptin ↓Adiponectin (p=0.07)	↑PPARy (t-test) ↑Leptin ↑Adiponectin ↑Ap2 ↑Glut4	↓PPARy ↑Leptin ↓Adiponectin
Energy phenotype	--	--	↑oxidative phosphorylation
Mitochondrial ATP	↓	--	Non-significant trend in ↑
Glycolytic ATP	↓	--	↓
Basal respiration	--	--	--
ATP-linked respiration	--	--	↑
Maximal respiration	--	--	↑
Reserve capacity	--	--	↑
Proton Leak	--	--	--
non-mitochondrial respiration	--	--	--
mitochondrial metabolic phenotype	--	--	↑
Glycolytic metabolic phenotype	--	--	↑

Arrows indicate increased (↑), unaltered (--), and decreased (↓) levels compared to controls.

3.3.2.1 Zaprinast

Zaprinast, is a phoshphodiesterase (PDE5,6) inhibitor that promotes accumulation of cyclic guanosine monophosphate (cGMP) (Turko et al. 1999). Following 24-hour incubation in adipocytes, Zaprinast increased glucose uptake (Figure 3.10), yet still resulted in a reduction in ATP production rates by these cells, both glycolytic and mitochondrial ATP (Figure 3.15E), without affecting the glycolytic-mitochondrial energy balance (Figure 3.15D). The reduction in mitochondrial ATP production rate could be explained by Zaprinast's well-established inhibition of mitochondrial pyruvate carrier (MPC), a key carrier that shuttles pyruvate from the cytosol to the mitochondria for oxidative phosphorylation to occur (Du et al. 2013). However, increasing glucose uptake is expected to increase glycolysis. The fact that glycolytic ATP production is reduced, suggests one of three scenarios; either an inhibitory effect of Zaprinast on one of the enzymes involved in glycolysis; or a promotion of glycogenesis, which promotes storage of glucose into glycogen; or might suggest an enhancement in the incorporation of glucose in *de novo* lipogenesis.

The adipogeneic profile of Zaprinast was not clear, but with reference to literature, was suggestive of browning (Mitschke et al. 2013; Haas et al. 2009). Zaprinast increased lipid accumulation when differentiated in the absence of the PPARγ agonist Rosiglitazone (Figure 3.11b), however had no effect in its presence (Figure 3.11a). This suggested a masking effect of Rosiglitazone on Zaprinast's adipogenic actions. Indeed, cGMP analogues have been shown to stimulate browning of WAT in a PKG-dependent

mechanism (Mitschke et al. 2013) while PPARγ agonists like Rosiglitazone have also been shown to activate PKG without changing cGMP levels (Yang et al. 2013), which suggests possible saturation of PKG pathways in the presence of Zaprinast and Rosiglitazone. Nonetheless, the observation that Zaprinast increases lipid accumulation could be indicative of browning (Figure 3.11b). Furthermore, the reduction in Leptin expression (and adiponectin to a smaller extent), two key markers of white adipose tissue, is indicative of a change in the adipocyte phenotype. However, mRNA markers for browning like *Prdm16*, *UCP1* and *Cidea* were not detectable in our assay, even when adipogenesis was induced with PPARγ agonist Rosiglitazone (expected to enhance beige-like properties of 3T3-L1 cells), and that is most likely due to the small concentrations of starting RNA that were used for the cDNA conversion (200 ng compared to 1-2 μg used by other studies (Xue et al. 2018; Wang et al. 2016).

Brown adipocytes help combat obesity through increasing energy expenditure via non-shivering thermogenesis, and also improve glucose tolerance (Bartelt and Heeren 2014). Therefore, at the level of adipocytes, Zaprinast could show benefit against symptoms of MetS through promoting glucose uptake, and possibly due to induction of browning as reported by similar acting cGMP analogues (Mitschke et al. 2013). Interestingly, Sildenafil, an analogous phosphodiesterase inhibitor, has been shown to protect against obesity and insulin resistance in HFD-mouse model (Ayala et al. 2007). There has also been reports of Sildenafil's direct effect on circadian behaviour, enhancing re-entrainment following phase advances (Agostino, Plano, and Golombek 2007). Hence,

cGMP accumulation, both *in vivo* and *in vitro* (at adipocyte level) seems to alter circadian clocks and also promote positive metabolic phenotypes. However, a link between the two observations has never been previously reported and poses a very exciting area to pursue.

3.3.2.2 Linopirdine

Linopirdine, is a potent KCNQ2/3 potassium channel blocker that was later tested as a cognitive enhancer for Alzheimer's, but failed in phase three clinical trials (Schnee and Brown 1998; Rockwood et al. 1997).

In adipocytes, Linopirdine increased glucose uptake and also enhanced insulin-mediated glucose uptake (Figure 3.10). It also promoted lipolysis following 24-hour treatment (Figure 3.13). At mRNA level and following differentiation of preadipocytes in the presence of Linopirdine, this drug seemed to increase WAT adipogenic markers, like *Leptin*, *adiponectin*, *Glut4* and *PPARy*, and even increased *Ap2*, a key marker of adipogenic progenitors (Figure 3.12b). This is indicative of an enhancement in the WAT properties of these cells. However, staining showed a reduction in lipid accumulation, with an increase in cell number, which could be explained by the combination of an increase in adipocyte number as well as enhancement of lipid breakdown by this drug at the time of staining. Linopirdine had no effect on the cellular bioenergetics of mature adipocytes following 24-hour treatment (Figure 3.16).

It is difficult to predict whether enhancement of adipogenesis and lipogenesis together pose a beneficial or determinantal effect on symptoms of metabolic syndrome at the level of an individual. Indeed, adipogenic expansion is crucial in cases of high calorie intake to protect against ectopic fat accumulation and its associated insulin resistance (Kim et al. 2014), yet at the same time, excessive adipogenesis results in exacerbation of obesity. Furthermore, breakdown of triglycerides in adipocyte lipid droplets by enhancement of lipolysis could further exacerbate insulin resistance due to NEFA-mediated lipotoxicity (Boden 2008). Interestingly, Linopirdine's action resembles the *in vitro* actions of nobiletin, the potent circadian amplitude enhancer that was reported to protect against metabolic disorders via its action on the clock. Nobiletin also increased both lipolysis and adipogenesis of 3T3-L1 cells (Saito, Abe, and Sekiya 2007) and enhanced glucose uptake in 3T3-F442A adipocytes (Onda et al. 2013). This similarity could be an indication of potential beneficial metabolic outcomes of Linopirdine treatment at an adipocyte level. However, given nobiletin's established increase in overall energy expenditure *in vivo* and possible alterations of circadian machinery centrally (He et al. 2016), its crucial to investigate Linopirdine's effects on neuronal and hormonal pathways involved in MetS and explore the extent of dominance of its metabolic effects *in vivo* before drawing any conclusions on its overall metabolic benefit. Nonetheless, these findings make Linopirdine an interesting candidate to pursue in a *in vivo* model of metabolic syndrome.

3.3.2.3 Diclazuril

Diclazuril has been primarily used in poultry and other animals as an antiprotozoal agent however its mechanism of action is unknown. Interestingly, in a report assessing the safety and efficacy of Diclazuril as an antiprotozoal treatment and food additive for chicken fattening, at specific doses, it was shown to prevent total body weight gain without affecting food intake and without any reported detrimental biochemical and haematological changes (European Food Safety Authority 2010). What was unfavourable for a chicken fattening study, was actually a very interesting observation indicating a possible protective role for Diclazuril against obesity in the presence of high-calorie intake challenges.

In adipocytes, differentiation with Diclazuril showed no effect on lipid accumulation, however it resulted in a reduction in mRNA of *PPARγ* and adiponectin, and an increase in *Leptin* mRNA (Figure 3.12b). It also had no effect on lipolysis following 24-hour treatment (Figure 3.13), but resulted in a significant increase in glucose uptake of adipocytes (Figure 3.10). What was most striking about Diclazuril compared to the other chrono-modulators was the shift in adipocyte energy phenotype observed, pushing these cells into a more aerobic phenotype (Figure 3.17B). This shift was primarily due to inhibition of glycolytic ATP-rates (Figure 3.17E). Although the mitochondrial-ATP rate showed no significance, it did increase ATP-linked respiration at 3 μM, suggesting an increase in overall mitochondrial ATP production as well, which might be driving the aerobic shift in energy phenotype. Furthermore, Diclazuril significantly increased

adipocyte's mitochondrial metabolic potential (Figure 3.17F), which is the mitochondria's ability to meet energy demand when stressed. This could be explained by the dose dependent rise in maximal respiration and reserve capacity observed with Diclazuril treatment (Figure 3.17C), which in turn might be indicative of either an increase in number of mitochondria in these cells, or an increase in mitochondrial activity.

Diclazuril's effect on adipocyte bioenergetics indicates and enhancement in mitochondrial bioenergetic capacity, possibly at the expense of glycolysis. Interestingly, obesity has been linked to a reduction in mitochondrial oxidative capacity of human subcutaneous depots (Chattopadhyay et al. 2011), independent of adipocyte hypertrophy (Xiao et al. 2014). The use of genetic or dietary mouse models of obesity have also shown a clear reduction in mitochondrial oxidative capacity of WAT (Choo et al. 2006; Wilson-fritch et al. 2003). Although it is still unclear whether this reduction is a cause or an outcome of other metabolic anomalies linked to obesity, like diabetes and insulin resistance, nonetheless, Jokinen and colleagues showed that higher mitochondrial capacity of subcutaneous adipose tissue (SAT) from human biopsies predicted good long term weight loss control in obese individuals (Jokinen et al. 2018). Hence, an intervention that could increase adipocyte mitochondrial capacity could be promising.

3.3.3 Role of the clock in the observed metabolic phenotypes:

Whether these observed effects are mediated by the clock or whether they are purely driven by target-specific clock-independent pathways is still unclear.

Given all three drugs are associated with an increase in glucose uptake, and similarly they all increase extent of clock gene expression, one could hypothesize a direct role of clock gene controlled expression of key factors associated with glucose uptake. Indeed, *Bmal1* knockout in skeletal muscles, which significantly dampens expression of all key clock genes, has been reported to reduce the extent of rhythmic expression of GLUT4 and HK2 proteins (Dyar et al. 2014). To validate the involvement of the clock, 24-hour mRNA or protein changes of these two key metabolic players could be quantified following drug treatment.

On the other hand, although all drugs have a clear action on the clock, they have different characterized targets, which could be driving the metabolic phenotypes completely independent of the clock. In the case of Zaprinast for example, it is well established as an inhibitor of PDE5 and 6 and hence induces accumulation of cGMP, analogues of which have been linked with browning of adipocytes, similar to what is observed with Zaprinast. However, cGMP has also been shown to mediate clock entrainment at the SCN level (Prosser, McArthur, and Gillette 1989), and therefore is likely to be driving the circadian phenotype observed. However, whether cGMP mediates these metabolic phenotypes in a clock-dependent or clock-independent manner has never been explored

and warrants investigation. Linopirdine on the other hand, is a potent KCNQ2/3-heteromer inhibitor, and has been reported to induce subtle changes on calcium channels and promote Ca^{2+} flux into cells (Dzhura, He, and Currie 2006). Although evidence supporting calcium's direct impact on the clock machinery of non-neuronal cells in mammals is still lacking, knockdown of Ca^{2+} pathways has been shown to affect periodicity of clock function in Drosophila in non-neuronal cells (Palacios-Muñoz and Ewer 2018). Furthermore, given the quiescent nature of U2OS and adipocytes and the relatively low expression of KCNQ2 (Uhlén et al. 2015), the possibility of a different target is also plausible and remains to be elucidated. Finally, Diclazuril has a completely unknown mechanism of action, introducing the clock as a possible candidate and making an investigation for its underlying mechanism even more interesting.

Given the gap in knowledge, it is crucial to validate the mechanisms via which these drugs are interacting with the clock. Following which, we can probe whether the metabolic phenotypes are target-specific, completely independent of the clock, or whether the mechanism via which the circadian clock is modulated poses a vital difference in the outcomes of gene expression. In line with that, chapters 4 and 5 will focus on exploring the mechanisms of action that underly the circadian phenotypes of these drugs. It's worth noting that although these circadian amplitude enhancers all had different metabolic phenotypes in adipocytes, they all showed plausible benefits in overcoming different aspects of metabolic syndrome. Given MetS is a global phenomenon, with influences from different organs and tissues, and inputs from hormones and neurotransmitters

associated with satiety, hunger and energy balance, testing these small molecules *in vivo* and then comparing their adipocyte metabolic profile with their overall outcome is imperative and an elegant way of understanding the role of circadian amplitude enhancement at different levels of biology. This will also allow us to identify which metabolic assays were most predictive of metabolic benefits *in vivo*, and will help understand the contribution of central vs peripheral circadian clocks in metabolic phenotypes. In line with that, Chapter 6 in this thesis will explore the effects of Linopirdine and Diclazuril in an *in vivo* model of diet-induced obesity (DIO) and metabolic syndrome, and the findings from both will be discussed extensively.

3.4 Conclusion

Evidence supporting amplitude enhancement *in vivo* seems compelling, while the details of mechanisms underpinning these processes is superficial. Further, we lack understanding of the metabolic changes that mediate these improvements at the adipocyte level. Finally as most studies have been done *in vivo*, there has been no distinction between central vs peripheral clock effecting these changes. Given the adipocytes are important metabolic organs at the heart of metabolic disorders, which are largely affected by shifts in energy expenditure and have direct influence on the pathogenesis of insulin resistance in obesity (Holzer et al. 2011; Kanda et al. 2006), and given the huge role the clock machinery plays in its metabolic pathways, understanding the effects of amplitude enhancement in these cells is key to identifying how pharmacological agents could be used therapeutically for combatting metabolic syndrome.

To date, there have been no phenotypic characterization of the effects of various circadian amplitude enhancers on adipocytes. While trying to characterize the metabolic phenotypes of 3 circadian amplitude enhancers, we uncovered major differences in their actions. This finding highlighted that enhancement of amplitude of the adipocyte autonomous circadian machinery is not enough to predict changes in metabolism in these cells. Furthermore, the changes in metabolic phenotypes do not seem to be linked to the extent of the amplitude enhancement; for instance, Zaprinast showed the biggest

amplitude effect in *Per2* rhythms of mature 3T3-L1 cells, but contrarily had the smallest effect on glucose uptake and a minor influence on energy dynamics of adipocytes. Given these drugs have different reported targets in literature, it seems the mechanism of action driving the amplitude enhancing effect is what plays the most significant role in their observed effects.

Hence, the next two chapters (4 and 5) will focus on identifying and validating the mechanisms of action through which Linopirdine-mediated amplitude enhancement is taking place, and then explore its actions in an *in vivo* model of metabolic disorder to shed light on its overall metabolic phenotype and help compare between its effects at adipocyte vs whole organism level. Chapter 6 on the other hand will focus on understanding the role of cGMP in regulating peripheral clocks. Due to time restrictions, Diclazuril will not be investigated in the scope of this thesis.

CHAPTER 4:

Investigating the Mechanism of Action of Linopirdine

4.1 Introduction

Linopirdine was identified as one of the key leads from our circadian screen (Chapter 3), owing to the potent increase in *Bmal1*-d*Luc* and subsequent increase in *Per2*-d*Luc* expression in U2OS cells as well as 3T3-L1 cells. Furthermore, in a phenotypic screen with mature adipocytes, Linopirdine demonstrated an increase in glucose uptake and lipolysis which would be deemed favourable in indications relating to metabolic dysfunction. However, given Linopirdine was administering both the circadian and metabolic changes via an unknown mechanism, it was decided to embark on identifying the downstream targets of Linopirdine. Unearthing the mechanism of action of Linopirdine indeed could shed light on pathways at the intersection of circadian clocks and metabolism.

4.1.1 Background on Linopirdine

Linopirdine (DuP 996) was originally developed as a putative cognitive enhancer, that promotes depolarization-induced release of various neurotransmitters, like Acetylcholine (Ach), dopamine and serotonin, without increasing basal efflux in unstimulated brain slices (Zaczek, Chorvat, and Brown 1997; Saletu, Darragh, Salmon, Coen 1989; Nickolson, Tam, and Myers 1989). It was shown to increase Ach release *in vivo* (Nickolson, Tam, and Myers 1990) and also exhibited promising cognitive enhancing effects in various animal models of learning and memory (Cook et al. 1990; DeNoble, et al., 1990). EEG studies on elderly participants showed promise of significant increase in

vigilance properties (Saletu et al. 1989). Consequently, it was taken forward as a possible novel cognitive adjuvant for Alzheimer's disease. Linopirdine despite being safe and well tolerated, only demonstrated modest improvements in cognitive function following 6 months of treatment, which was not deemed clinically meaningful (Rockwood et al. 1997). In light of this finding, Linopirdine was discontinued as a clinical candidate, limiting its use to a pharmacological tool.

Linopirdine primarily targets KCNQ potassium channels, blocking M-currents at the extracellular site with an IC50 of 3.4 μM (Lamas, Selyanko, and Brown 1997), but has also been reported to inhibit other voltage-gated potassium currents at a much lower potency. For instance, Linopirdine was reported to block delayed rectifier potassium channels at IC50 63 μM, transient currents at 69 μM, eag1 at 31 μM, erg1 at 53 μM and erg3 at 85 μM (Wang et al. 1998; Lamas, Selyanko, and Brown 1997). Potassium channels make up a big family of over 100 genes. Many of these are ubiquitous and play key roles in both excitable and non-excitable cells in controlling membrane potential, regulating cell volume and mediating salt, neurotransmitter and hormone secretion (Ko, Shi, and Ko 2009). KCNQ potassium channels, in specific, have 5 subtypes, KCNQ 2 and 3 in particular, are most prominently expressed in the brain and in sympathetic ganglia (Wang et al. 1998). However, U2OS cells and fibroblasts have also been shown to express KCNQ3 (Uhlén et al. 2015), making these channels key candidates behind Linopirdine's observed circadian and metabolic effects.

With that in mind, a role for KCNQ channels in peripheral tissues and whether they promote downstream circadian clock alterations has never been investigated. Interestingly, other subtypes of potassium channels have been associated with alterations of circadian rhythmicity in the SCN. For instance, mice lacking either *Kcna4* or *Kcnd2* voltage-gated K^+ channel pore-forming subunits that instruct A-type K^+ currents (IA), exhibit 0.5 hour shorter circadian periods in locomotor activity and SCN firing relative to wild-type mice (Granados-Fuentes et al. 2015) . Furthermore, loss of the *Kcnma1* gene, encoding the BK potassium channels, enhances behavioural arrhythmicity *in vivo* and alters amplitude and period of SCN rhythmic activity (Kent and Meredith 2008). However, there has been no elaborative investigation whether potassium channels in non-excitable cells could influence circadian clock machinery.

4.1.2 Could Linopirdine have a second target?

When comparing potencies of Linopirdine, an intriguing discrepancy was observed between the concentrations at which it mediates its circadian effects vs its reported affinity for KCNQ channel, for which it was originally developed. Linopirdine induced expression of *Bmal1*-d*Luc* at an EC50 of ~200 nM, 10 times more potently than its reported KCNQ blocking action (Lamas, Selyanko, and Brown 1997). Given the off-targets effects of many drugs, it seemed likely that Linopirdine could be engaging with the circadian machinery via alternative pathway/s. Indeed, in-silico mining, using the Similarity Ensemble Approach (or SEA) tool (Keiser et al. 2007), identified several

possible targets for Linopirdine which are summarised in Table 4.1. This chemo-centric approach quantitatively groups and links proteins based on the chemical similarity of their ligands, and then utilises the database to identify potential targets for small molecules based on their chemical structure. Further, the emerging literature on cross-talk between the circadian clock and hypoxia, coupled with the SEA analysis ranking, highlighted EGLN homolog 1, which represents Hypoxia-inducible factor prolyl hydroxylase 2 (PHD2), as a particular target of interest.

Table 4.1: SEA analysis results for Linopirdine:

Target ID	P-Value	Z-Score	Name	Description
5HT7R_CAVPO	6.53E-07	10.6537	HTR7	5-hydroxytryptamine receptor 7
CP2C9_HUMAN	1.15E-02	3.0298	CYP2C9	Cytochrome P450 2C9
CP2CJ_HUMAN	1.94E-01	0.7481	CYP2C19	Cytochrome P450 2C19
CP3A4_HUMAN	7.55E-02	1.5339	CYP3A4	Cytochrome P450 3A4
EGLN1_HUMAN	1.68E-22	38.644	EGLN1	Egl nine homolog 1
ELNE_HUMAN	8.38E-09	14.0507	ELANE	Neutrophil elastase
MURA_ECOLI	4.12E-09	14.6032	murA	UDP-N-acetylglucosamine 1-carboxyvinyltransferase
MURB_ECOLI	3.65E-07	11.1078	murB	UDP-N-acetylenolpyruvoylglucosamine reductase
MURB_STAAU	5.75E-19	32.2979	murB	UDP-N-acetylenolpyruvoylglucosamine reductase
PPOC_ORYSJ	2.25E-07	11.4838	PPOX1	Protoporphyrinogen oxidase, chloroplastic

4.1.3 Hypoxia and circadian signalling

Hypoxia is a state of severe oxygen deficiency in cells and tissues. At the cellular level, hypoxia is met by a transcriptional response that aims to restore oxygen deficiencies and minimise hypoxic injury. This cellular response is regulated by the hypoxia-inducible factor (HIF) family of transcription factors, which are DNA binding complexes known to be conserved in humans and all animal species (Semenza 2004). The transcription factor HIF is a heterodimer composed of an oxygen-sensing α subunit, and a constitutively expressed β subunit, two basic-helix-loop-helix proteins of the PAS family (Wang et al. 1995). HIF stability is highly oxygen dependent, and is mainly regulated by post-translational prolyl hydroxylation of it's α residues by the oxygen sensing PHD family of enzymes, first described 10 years after the discovery of HIF (Jaakkola et al. 2001; Epstein et al. 2001). In normoxic conditions, following hydroxylation by PHD, HIF1α is recognised and ubiquitinated by von Hippel-Lindau protein (pVHL) (Maxwell et al. 1999; Ohh et al. 2000; Kamura et al. 2000), hence preventing the HIF transcription heterodimer from forming. On the other hand, in hypoxic conditions, due to the scarcity of oxygen, PHD is inhibited, allowing HIF α and β to heterodimerise, and together with co-activators CBP/p300 (Arany et al. 1996; Bhattacharya et al. 1999), bind to HIF-response elements (HRE) in promoters within the genome, inducing transcription of a plethora of target genes to elicit a survival response, including activating transcription of; *EPO*, for erythropoietin production (Costa-Giomi P, Caro J 1990), *VEGF*, involved in angiogenesis (Shweiki et al. 1992), and *Glut1*, associated with enhanced glucose uptake (Changhu Chen et al. 2001; Ebert, Firth, and Ratcliffe 1995). Similarly, a second class of dioxygenase

enzymes, Factor-inhibiting HIF (FIH), also hydroxylates HIF1α in normoxia at an aspargine residue (Asn803 in human HIF-1α), preventing HIF1α from interacting with p300/CBP and reducing its transcriptional activity (Lando et al. 2002). This intricate cascade of events maintains protein levels of HIF1α under check under normal oxygen environment and mounts the hypoxic signalling cascade when needed. Figure 4.1 summarises this regulation of HIF under normoxic and hypoxic conditions.

Increasing evidence supports cross-talk between HIF and circadian machinery. For instance, hypoxic conditions have been shown to speed up mice entrainment to jet lag (Adamovich et al. 2017) and reported to increase PER1 and CLOCK protein levels in mice (Chilov et al. 2001). In addition, the circadian clocks have been shown to regulate oxygen consumption and glycolysis in skeletal muscles via regulation of HIF1α (Peek et al. 2017), reiterating the strong interaction between these pathways and their bidirectional involvement in metabolism as well. Finally, HIF1α expression has been shown to follow circadian regulation, both *in vivo* and *in vitro*, and has been shown to induce PER2 expression by directly binding to its promoter (Wu et al. 2017). Consequently, the notion that PHD2 could be a target of Linopirdine is worth pursuing.

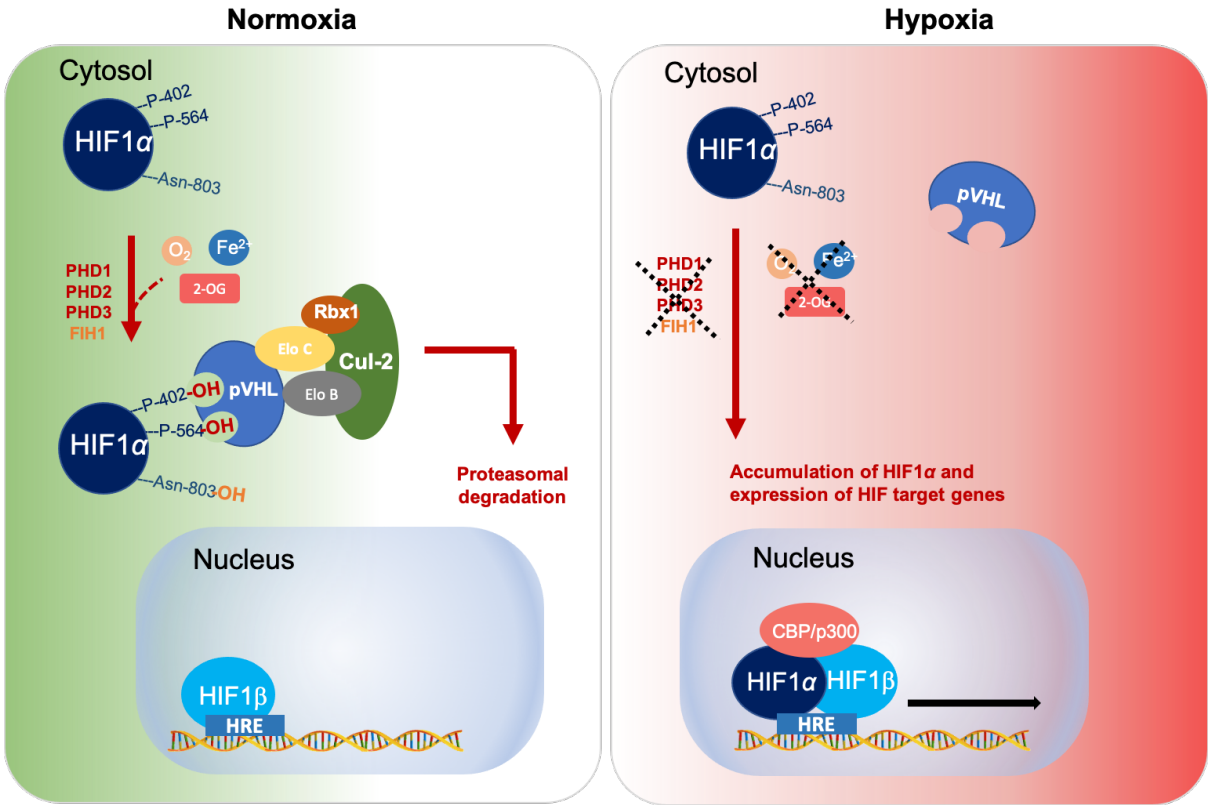


Figure 4.1: Schematic summary of the hypoxia-inducible pathway under normoxia (Left) and hypoxia (Right).

(Left) When oxygen levels are normal (normoxia), prolyl hydroxylases (PHD1-3) hydroxylate the HIF1α subunits at two specific proline residues (human Pro402 and 562) within its oxygen dependent degradation domain, utilising iron (Fe^{2+}), oxygen (O_2), 2-oxaloglutarate (2-OG- also known as a-ketoglutarate) as well as ascorbic acid (not shown) as co-substrates. This hydroxylation triggers the von Hippel Lindau tumor suppressor protein (pVHL) to recognize HIF1α. The ubiquitin ligase complex comprising pVHL, elongin (Elo) B and C, cullin-2 (Cul2) and RING-box protein (Rbx1), together, promotes proteasomal degradation of HIF1α. In addition, the factor inhibiting HIF (FIH1) also hydroxylates HIF1α at the asparagine residue (human- Asn803) which further prevents its interaction with the transcriptional co-activator histone acetyltransferase p300/CREB-binding protein (p300/CBP), therefore reducing the transcriptional activity of HIF.

(Right) On the other hand, when oxygen is scarce, PHD and FIH are incapable of hydroxylating HIF1α subunits, as a result, HIF1α accumulates, migrates to the nucleus, and consequently forms the HIF-complex with HIF1β -subunits, which then binds HIF-response elements (HRE) in the genome and drives transcription of a plethora of genes to counteract the hypoxic environment.

4.1.4 Aims

Through our circadian screen, we identified Linopirdine as a highly potent circadian modulator which also displayed interesting metabolic phenotypes in adipocytes. Understanding the mechanism underlying Linopirdine's circadian effect helps elaborate these findings and could give insight on new pathways via which the circadian clock could be manipulated. It could also help investigate whether its circadian effects correlate with the metabolic phenotypes observed and could shed light on potential novel pathways interlinking circadian clocks and metabolism. Hence, in this chapter, I aim to dissect the downstream players mediating Linopirdine's circadian effect, mainly focusing on potassium channels and PHD2 and its downstream pathways to understand how Linopirdine interacts with the clock.

4.2 Results

4.2.1 Is Linopirdine's amplitude enhancing effect mediated by KCNQ inhibition?

4.2.1.1 KCNQ agonist shows no effect on amplitude of Per2-dLuc cells

As mentioned earlier, Linopirdine is a potent KCNQ2/3 inhibitor (Lamas, Selyanko, and Brown 1997) and U2OS cells have been shown to express KCNQ3 (Uhlén et al. 2015). To validate the involvement of KCNQ channels in Linopirdine's circadian effect in U2OS cells, we explored whether an agonist of these channels would have a dampening effect on amplitude. To do that, retigabine, a potent anticonvulsant molecule that activates all KCNQ2-5 channels, was tested in *Per2*-d*Luc* U2OS cells (Figure 4.2A) (Tatulian et al. 2001; Gunthorpe, Large, and Sankar 2012). Retigabine significantly reduced cell viability at doses 10 μM- 1 mM (Figure 4.2B). Strikingly, it had no amplitude or period effects at doses that correspond to its EC50 of KCNQ activation , as reported by *Kumar et* al to be 3.3±0.8 μM (Kumar et al. 2016). On the other hand, retigabine resulted in significant amplitude dampening and period elongation at doses 300 μM and 1 mM (Figure 4.2C-D), which matched the significant reduction observed in cell viability at these concentrations (Figure. 4.2B). All together, it seemed KCNQ activation showed no circadian effects at non-toxic doses of retigabine.

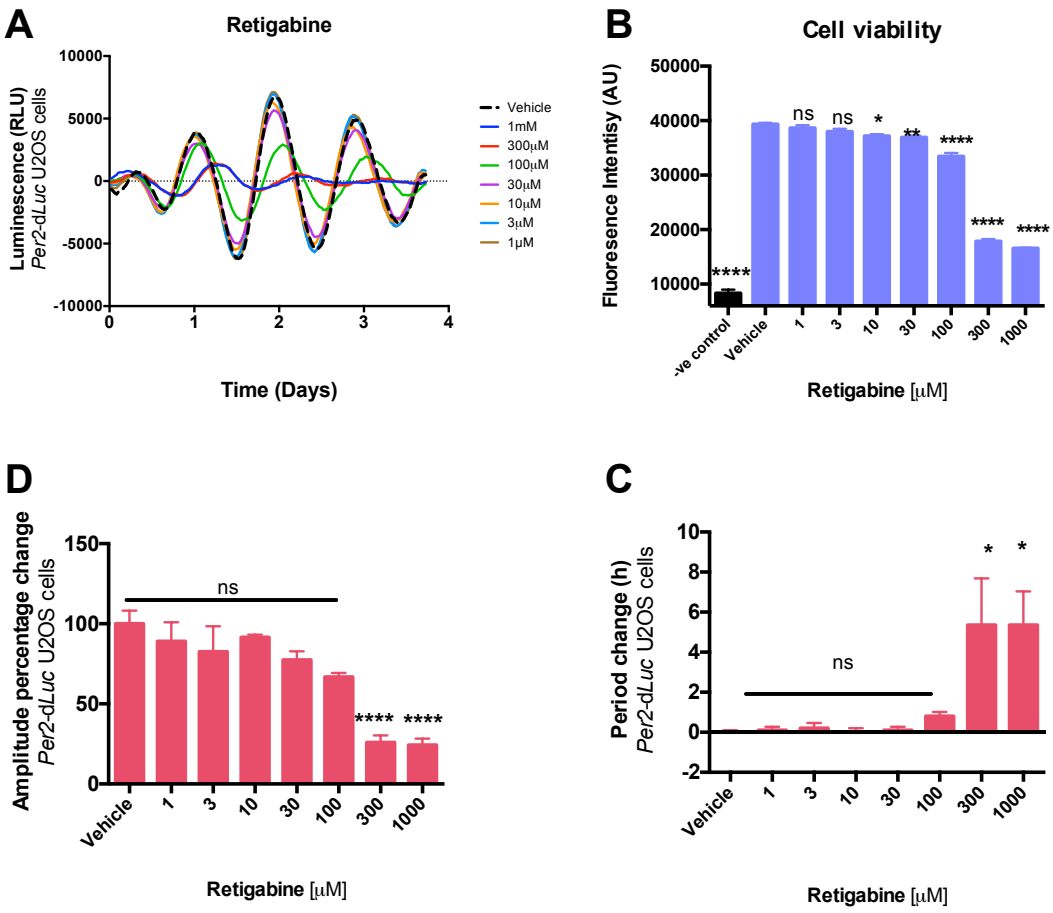


Figure 4.2. Effects of Retigabine on amplitude and period of *Per2*-d*Luc* U2OS cells: U2OS cells were grown to confluency, synchronised with dexamethasone and then treated with increasing doses of Retigabine. **A)** Representative luminescence traces in *Per2*-d*Luc* U2OS cells. **B)** Cell viability. **C)** Amplitude percentage change for the first day following treatment. **D)** Period analysis. Error bars represent ±SEM. N=3. Significance determined by One-way ANOVA.

4.2.1.2 Linopirdine's amplitude effect is unaffected by the KCNQ agonist retigabine

To further investigate the role of KCNQ channels, we wanted to see whether retigabine could reverse the amplitude effects of Linopirdine. Retigabine has been reported to reverse KCNQ2/3 inhibition by Linopirdine in PC12 and Chinese hamster ovary cells expressing KCNQ2/Q3 K^+ channels (Wickenden et al. 2000). Consequently, *Per2*-d*Luc* U2OS cells were treated with increasing doses of Linopirdine in the presence or absence of 5 μM Retigabine, which corresponded to its reported EC50 (Figure 4.3A). Linopirdine maintained its amplitude and period enhancing effects in the presence of 5 μM Retigabine (Figure 4.3B-D), with its overall amplitude effects being slightly enhanced (Figure 4.3D) but with no further effect on period (Figure 4.3B). Similar effects were observed in the presence of 50 μM Retigabine (~EC90, Figure 4.4). This suggested that KCNQ channels were not mediating Linopirdine's circadian effects in these cells.

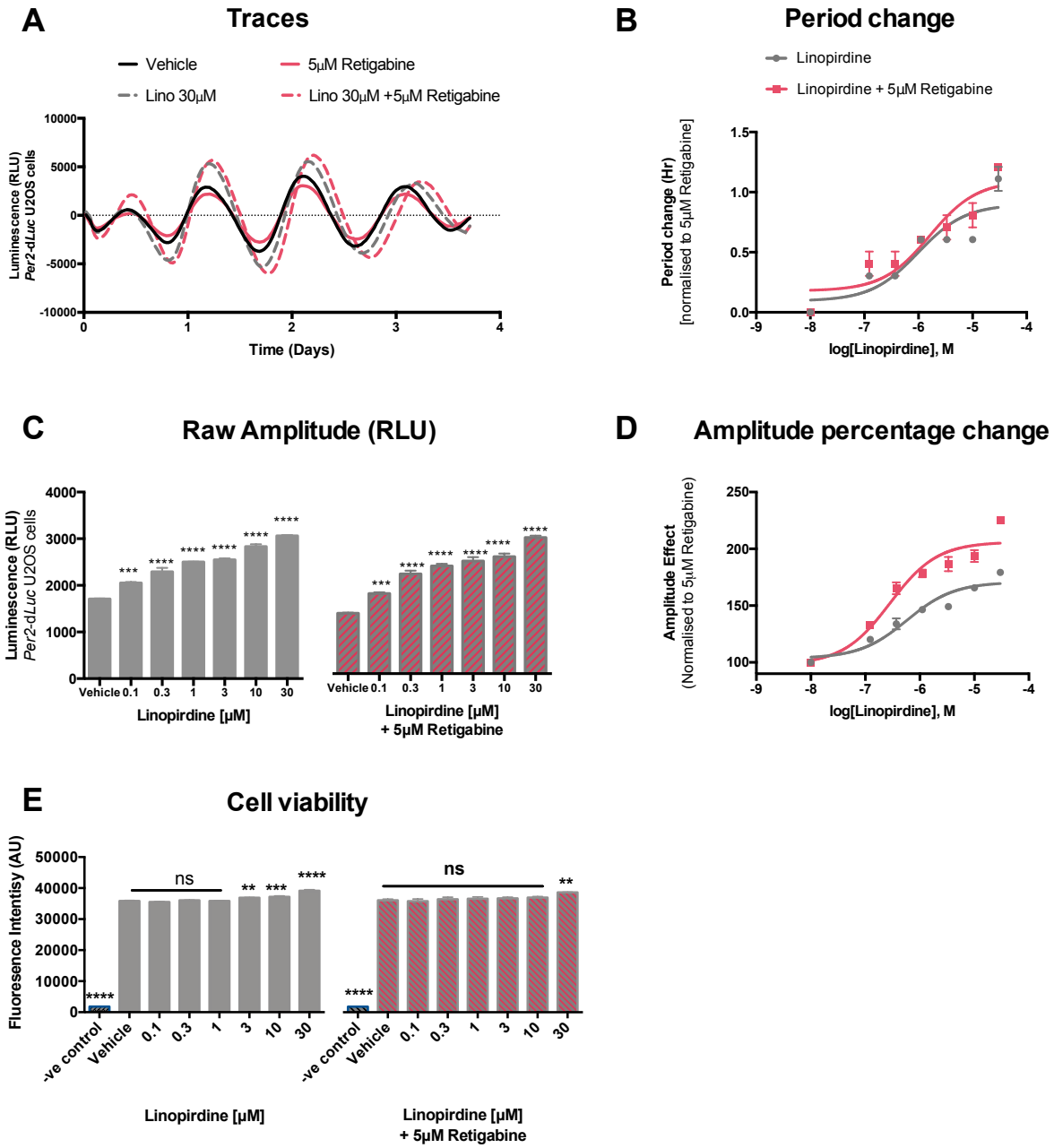


Figure 4.3. Effect of 5 μM Retigabine on Linopirdine's circadian phenotype:
Per2-d*Luc* U2OS cells synchronised with dexamethasone were treated with increasing doses of Linopirdine in the presence (red) or absence (grey) of 5 μM Retigabine. **(A)** Representative luminescence traces in *Per2*-d*Luc* U2OS cells. **(B)** Period change in the presence or absence of 5 μM retigabine. **(C)** Amplitude of luminescence following first day of treatment. **(D)** Normalised amplitude percentage change in the presence or absence of 5 μM retigabine. **(E)** Cell viability. Error bars represent ±SEM. N=3. Significance determined by One-way ANOVA.

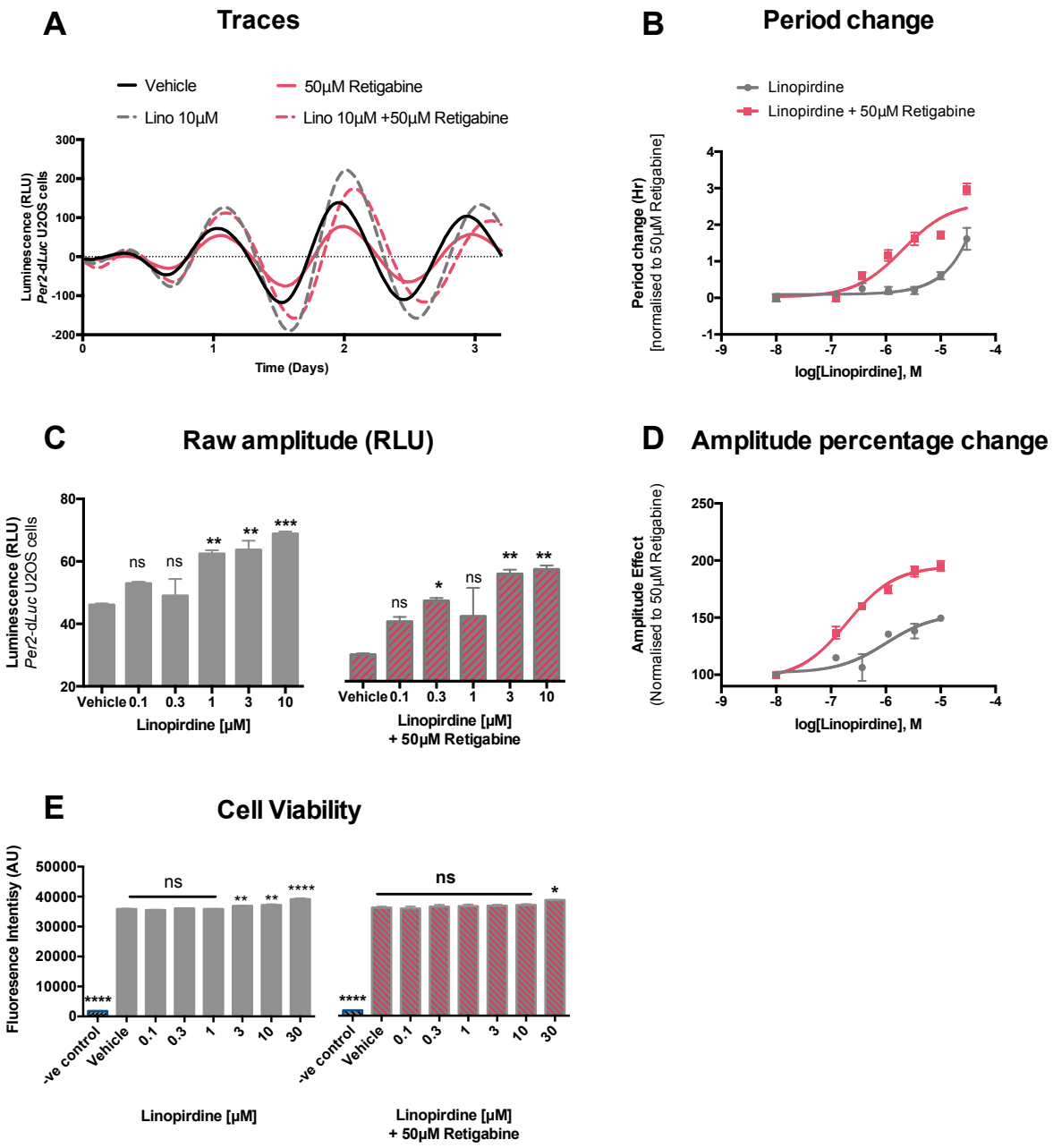


Figure 4.4. Effect of 50 μM Retigabine on Linopirdine's circadian phenotype:
Per2-d*Luc* U2OS cells synchronised with dexamethasone were treated with increasing doses of Linopirdine in the presence (red) or absence (grey) of 50 μM Retigabine. **(A)** Representative luminescence traces in *Per2*-d*Luc* U2OS cells. **(B)** Period change in the presence or absence of 50μM retigabine. **(C)** Amplitude of luminescence following first day of treatment. **(D)** Normalised amplitude percentage change in the presence or absence of 50 μM retigabine**. (E)** Cell viability. Error bars represent ±SEM. N=3. Significance determined by One-way ANOVA

4.2.1.3 Potassium channel inhibitors display no circadian effects on U2OS cells, while the structurally similar XE-991 phenocopies Linopirdine

Linopirdine has been shown to target potassium channels other than KCNQ, including EAG and ERG, but at much lower potency (Lamas, Selyanko, and Brown 1997; Wang et al. 1998). To investigate the possibility of other potassium channels mediating the amplitude effect, we tested 3 inhibitors, Nifekalant, Clofilium tosylate and XE-991, and monitored their circadian effects.

Nifekalant predominantly inhibits the inward rectifier potassium channel I_k (Sato et al. 1995). Clofilium tosylate has been shown to block numerous potassium channels at various potencies, including hERG (IC50 2.5 nM), hEAG (IC50 255 nM) (Gessner and Heinemann 2003), Kv1.5 (IC50 840 nM) (Malayev, Nelson, and Philipson 1995) and KCNQ1-KCNE1 (IC50 about 100 μM) (Honoré et al. 1991). Finally, XE-991 is structurally similar to Linopirdine (Figure 4.5C) and has similar KCNQ blocking action but at a higher potency (EC50 of 490 nM) (Zaczek et al. 1998) and with higher selectivity to KCNQ channels (Wang et al. 1998).

At doses that did not affect cell viability, Clofilium tosylate and Nifekalant failed to demonstrate any effect on *Bmal1*-d*Luc* (Figure 4.5A) and *Per2*-d*Luc* expression (Figure 4.5B). On the other hand, XE-991 resulted in a significant enhancement of amplitude of both *Bmal1*-d*Luc* (Figure 4.5A) and *Per2*-d*Luc* expression (Figure 4.5B), with an EC50 of 3.8 nM and 7.8 nM, and a maximal amplitude enhancement of 33.5±3.5% and 48.5± 7.7%,

respectively. XE-991 also resulted in a comparable increase in period in both cell lines, with a similar EC50 of 36 nM and 5.8 nM in *Bmal1*-d*Luc* and *Per2*-d*Luc* U2OS cells, respectively (Figure 4.6 A-B).

When comparing the structures of these potassium channel blockers, XE-991 and Linopirdine showed very high similarity, compared to the structurally distinct Clofilium tosylate and Nifekalant (Figure 4.5C). Therefore, to investigate the role of KCNQ channels in XE-991'S circadian phenotype, retigabine was used in parallel with XE-991. Strikingly, similar to what was observed with Linopirdine, retigabine also failed to eliminate the amplitude and period effects of XE-991 on *Per2*-d*Luc* U2OS cells (Figure 4.7).

Taken together, these findings suggested that the circadian effects observed with Linopirdine and XE-991 were potentially driven by a shared common target for both, and not via KCNQ, hEAG, hERG, or inward rectifier potassium channels.

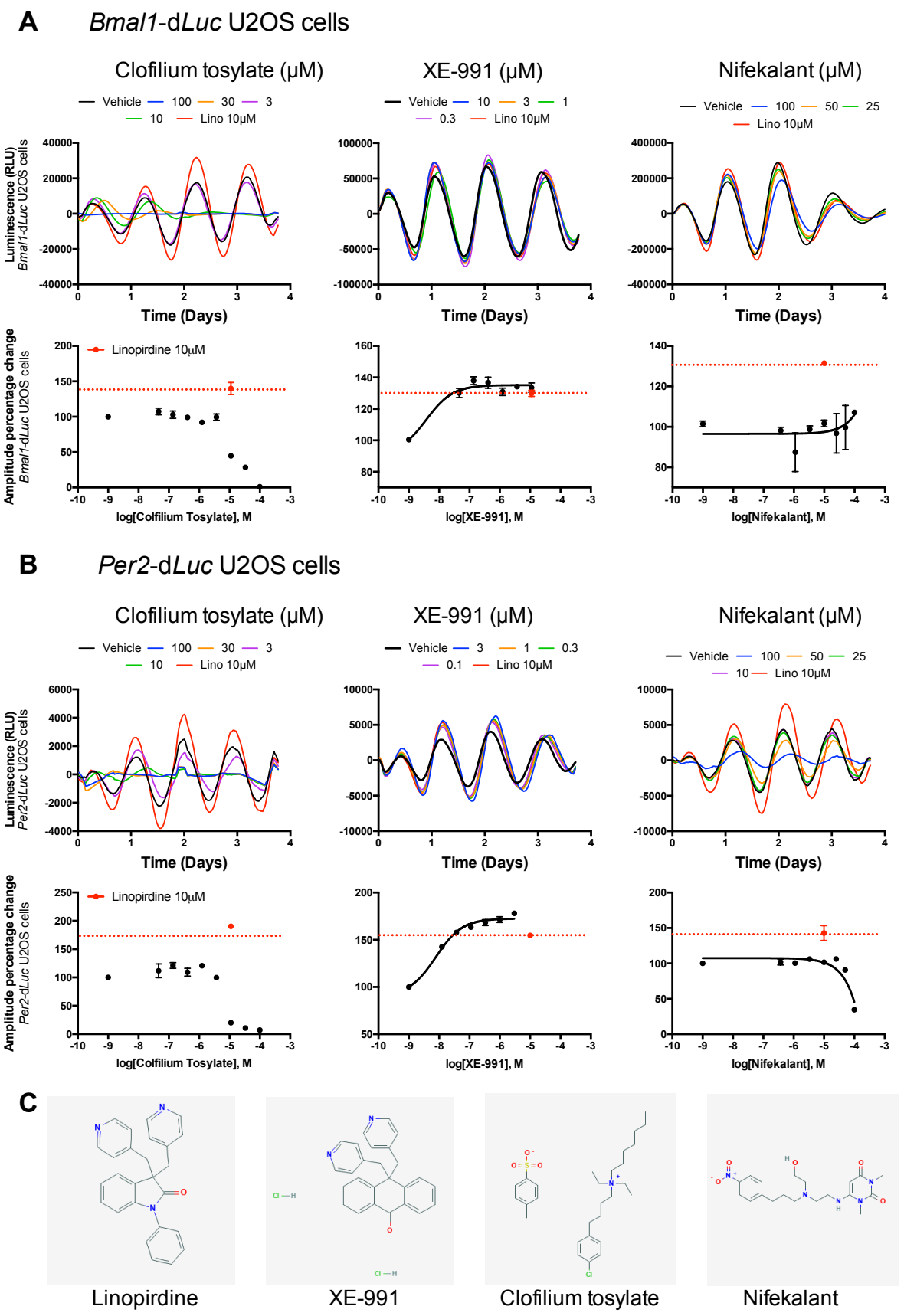

A
Bmal1-dLuc U2OS cells
Clofilium tosylate (μM)
XE-991 (μM)
Nifekalant (μM)
Vehicle 100 30 3 10 Lino 10μM
Vehicle 10 3 1 0.3 Lino 10μM
Vehicle 100 50 25 Lino 10μM
Luminescence (RLU) Bmal1-dLuc U2OS cells
Time (Days)
Linopirdine 10μM
Amplitude percentage change Bmal1-dLuc U2OS cells
log[Colfilium Tosylate], M
log[XE-991], M
log[Nifekalant], M
B
Per2-dLuc U2OS cells
Clofilium tosylate (μM)
XE-991 (μM)
Nifekalant (μM)
Vehicle 100 30 3 10 Lino 10μM
Vehicle 3 1 0.3 0.1 Lino 10μM
Vehicle 100 50 25 10 Lino 10μM
Luminescence (RLU) Per2-dLuc U2OS cells
Time (Days)
Linopirdine 10μM
Amplitude percentage change Per2-dLuc U2OS cells
log[Colfilium Tosylate], M
log[XE-991], M
log[Nifekalant], M
C
Linopirdine
XE-991
Clofilium tosylate
Nifekalant

Figure 4.5. Amplitude effects of 3 different potassium channel blockers on *Bmal1*-d*Luc* and *Per2*-d*Luc* U2OS cells:
A) Representative luminescence traces and corresponding amplitude percentage change analysis of first day following treatment of (left-right) Clofilium tosylate, XE-991 and Nifekalant compared to 10 μM Linopirdine (red), in *Bmal1*-d*Luc* U2OS cells**. B)** Representative luminescence traces and corresponding amplitude percentage change analysis of first day following treatment of of (left-right) Clofilium tosylate, XE-991 and Nifekalant compared to 10 μM Linopirdine (red), in *Per2*-d*Luc* U2OS cells. **C)** Chemical structures of the different potassium channel blockers used. Error bars represent ±SEM, N=3.

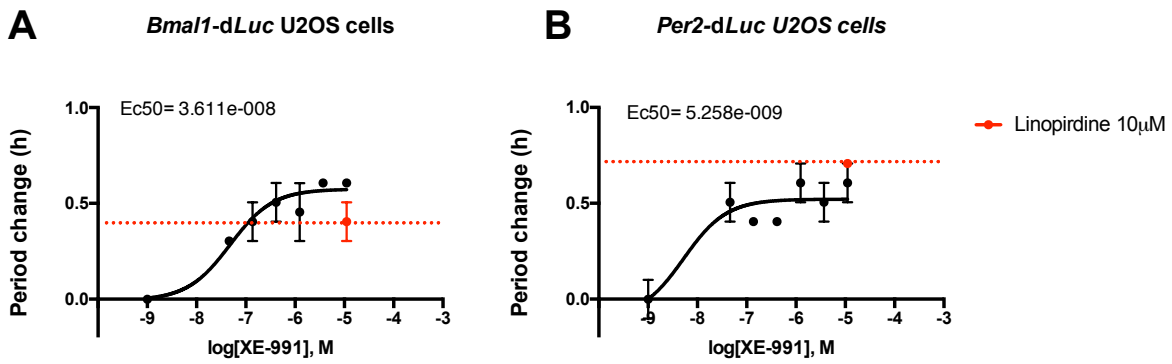


Figure 4.6. XE-991 Period change in *Bmal1*-d*Luc* and *Per2*-d*Luc* U2OS cells:
U2OS cells synchronised with dexamethasone were treated with increasing doses of XE-991. Period change following XE-991 treatment in **(A)** *Bmal1*-d*Luc* U2OS cells and **(B)** *Per2*-d*Luc* U2OS cells are shown with their corresponding EC50s. The red line represents the period change following 10 μM Linopirdine treatment for comparison. Error bars represent ±SEM. N=3.

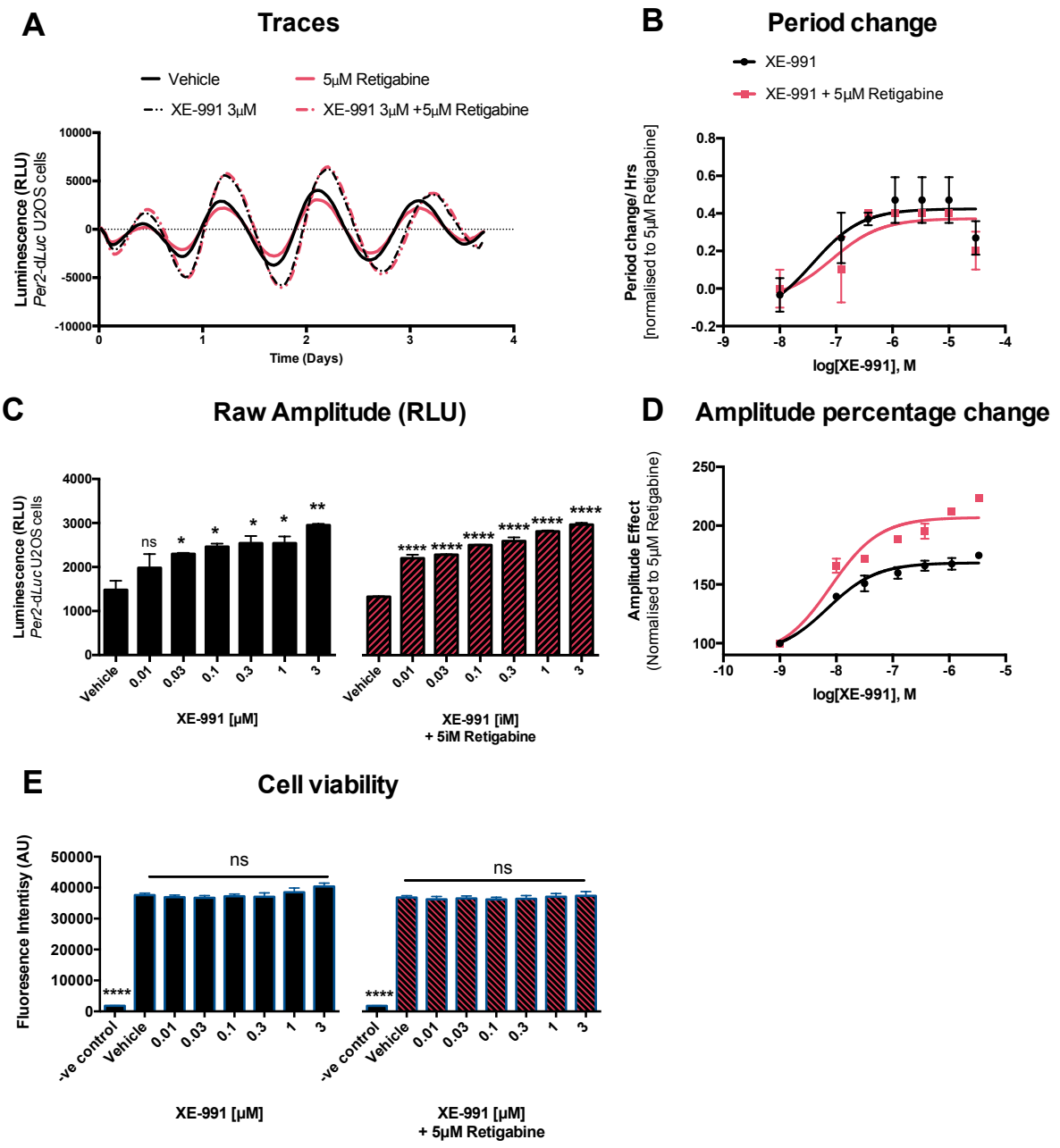


Figure 4.7. Effect of Retigabine on XE-991's circadian phenotype:
Per2-d*Luc* U2OS cells synchronised with dexamethasone were treated with increasing doses of XE-991 in the presence (red) or absence (black) of 5 μM Retigabine. **(A)** Representative luminescence traces in *Per2*-d*Luc* U2OS cells. **(B)** Period change in the presence or absence of 5 μM retigabine. **(C)** Amplitude of luminescence following first day of treatment. **(D)** Normalised amplitude percentage change in the presence or absence of 5 μM retigabine. **(E)** Cell viability. Error bars represent ±SEM. N=3. Significance determined by One-way ANOVA.

4.2.2 Investigating PHD2-linked pathways as possible targets for Linopirdine

4.2.2.1 PHD2 inhibitor Molidustat increases amplitude of Bmal1-dLuc U2OS cells and HRE-activation at a similar EC50

As mentioned earlier, SEA analysis reported chemical similarity between PHD2 ligands and Linopirdine. To explore the effects of PHD2 inhibition on circadian phenotype, synchronised *Bmal1*-d*Luc* and *Per2*-d*Luc* were treated with increasing doses of Molidustat, a potent PHD2 inhibitor. Molidustat resulted in a dose dependent increase in both amplitude and period of *Bmal1*-d*Luc* expression (Figure 4.8A-i). At 3 μM, it increased amplitude by 70.9±3% and period by 1.3 hours, with an EC50 of 917 nM (Figure 4.8A-ii) and 1.1 μM (Figure 4.8A-iii), respectively. On the other hand, Molidustat showed different effects on *Per2*-d*Luc* U2OS (Figure 4.8B-i), displaying a slight reduction in amplitude at 3 μM (Figure 4.8B-ii), and a small non-significant increase in period (Figure 4.8B-iii). Furthermore, to evaluate if the circadian phenotype conferred by Molidustat could be via PHD2 inhibition, plasmids expressing HRE-luciferase were transiently transfected in U2OS cells and increasing doses of Molidustat were administered. Intriguingly, Molidustat increased HRE-activity in a dose dependent manner (Figure 4.8C), with and EC50 of 863 nM (Figure 4.8C-iii) which was comparable to that of its amplitude effect on *Bmal1* promoter (917 nM), demonstrating a role for PHD2 inhibition in Molidustat's circadian effect, acting on *Bmal1* promoter in particular.

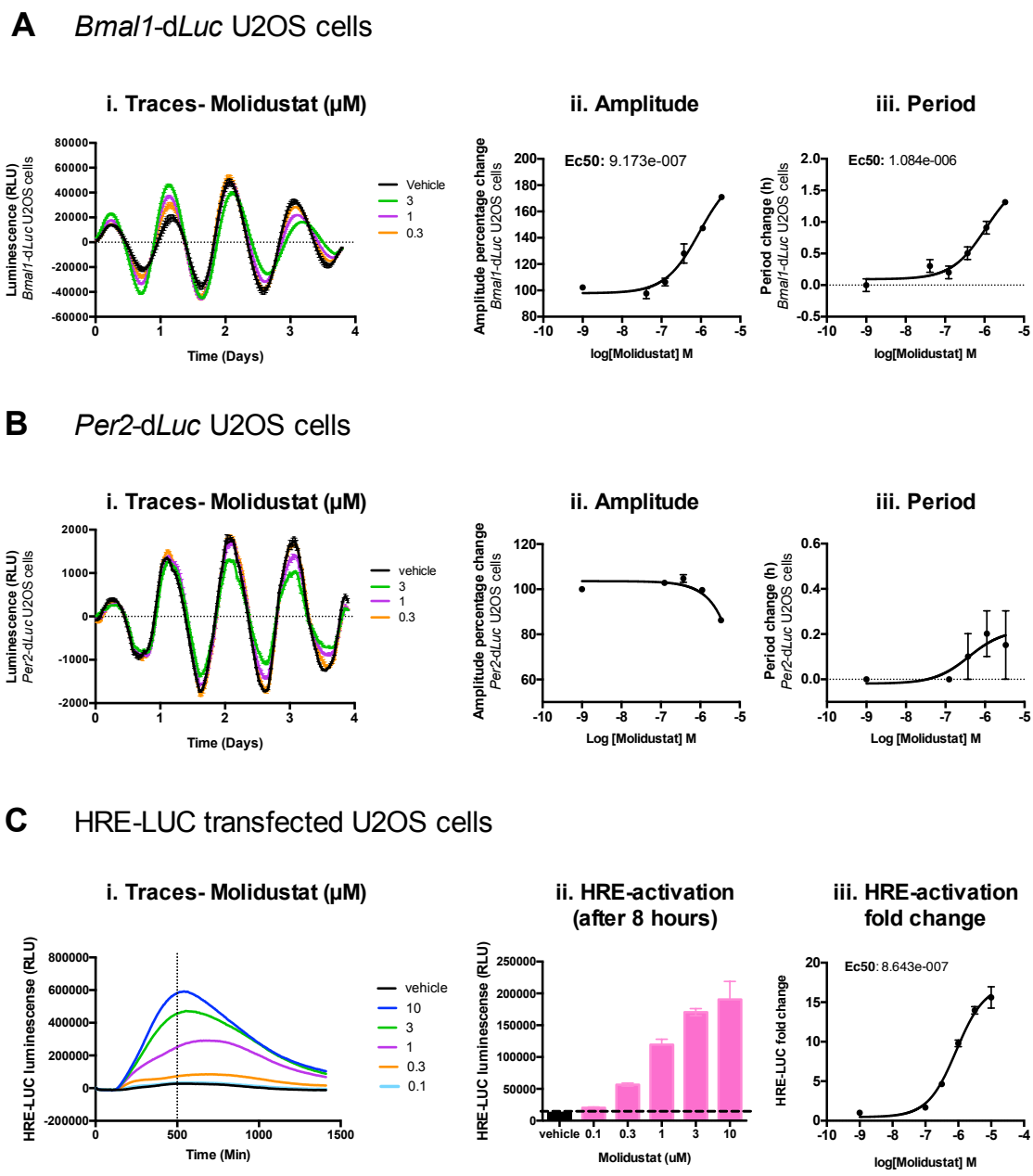


Figure 4.8. Effects of Molidustat on *Bmal1*-d*Luc* and *Per2*-d*Luc* U2OS cells, and HRE-LUC activation:

Bmal1-d*Luc* U2OS cells **(A)** and *Per2*-d*Luc* U2OS cells **(B)** synchronised with dexamethasone were treated with increasing doses of Molidustat and their representative luminescence traces **(i)** with their corresponding amplitude percentage change **(ii)** and period change analyses **(iii)** are shown (A and B, left to right). U2OS cells transiently transfected with HRE-LUC were also treated with increasing doses of Molidustat **(C).** The raw mean traces for HRE-LUC luminescence with increasing doses of Molidustat **(i)** and the representative bar charts for maximal HRE-activation following 8 hour of treatment **(ii)** and their corresponding fold change relative to vehicle **(iii)** are shown (C, left to right). N=3 for all. Error bars represent ±SEM.

4.2.2.2 Hypoxia increases amplitude and period of Bmal1-dLuc and Per2-dLuc U2OS cells

Given PHD2 is an oxygen dependent enzyme, its enzymatic ability is inhibited by hypoxia. To further validate the role of PHD2 inhibition on circadian effects and to investigate how hypoxia affects molecular circadian rhythms, we exposed *Bmal1*-d*Luc* and *Per2*-d*Luc* U2OS cells to 6 hours of hypoxia (1% O_2) and monitored luminescence in real time. Such hypoxic conditions, previously validated to increase in HIF1α protein levels via PHD2 inhibition (Peek et al. 2017), significantly increased hypoxia-response element (HRE) activation in U2OS cells transfected with the HRE-reporter luciferase (Figure 4.9A, C). Subsequently this exposure to 6h of 1% O_2 also resulted in a significant increase in amplitude and period of both *Bmal1*-d*Luc* and *Per2*-d*Luc* expression (Figure 4.9A, C). 6h of 1% O_2 resulted in a 144.2±45.4% increase in amplitude and 3.25±1.4 hour elongation in period of *Bmal1*-d*Luc* U2OS cells (Figure 4.9B). Similarly, 6h of 1% O_2 also increased amplitude and period of *Per2*-d*Luc* U2OS cells by 167.5±34.2% and 4.6±0.72 hours, respectively (Figure 4.9D). These findings supported a role for hypoxic pathways in enhancing circadian amplitude of expression, and given the lack of *Per2*-enhancing effects by the PHD2 inhibitor Molidustat, suggested that Linopirdine treatment is more analogous to hypoxia.

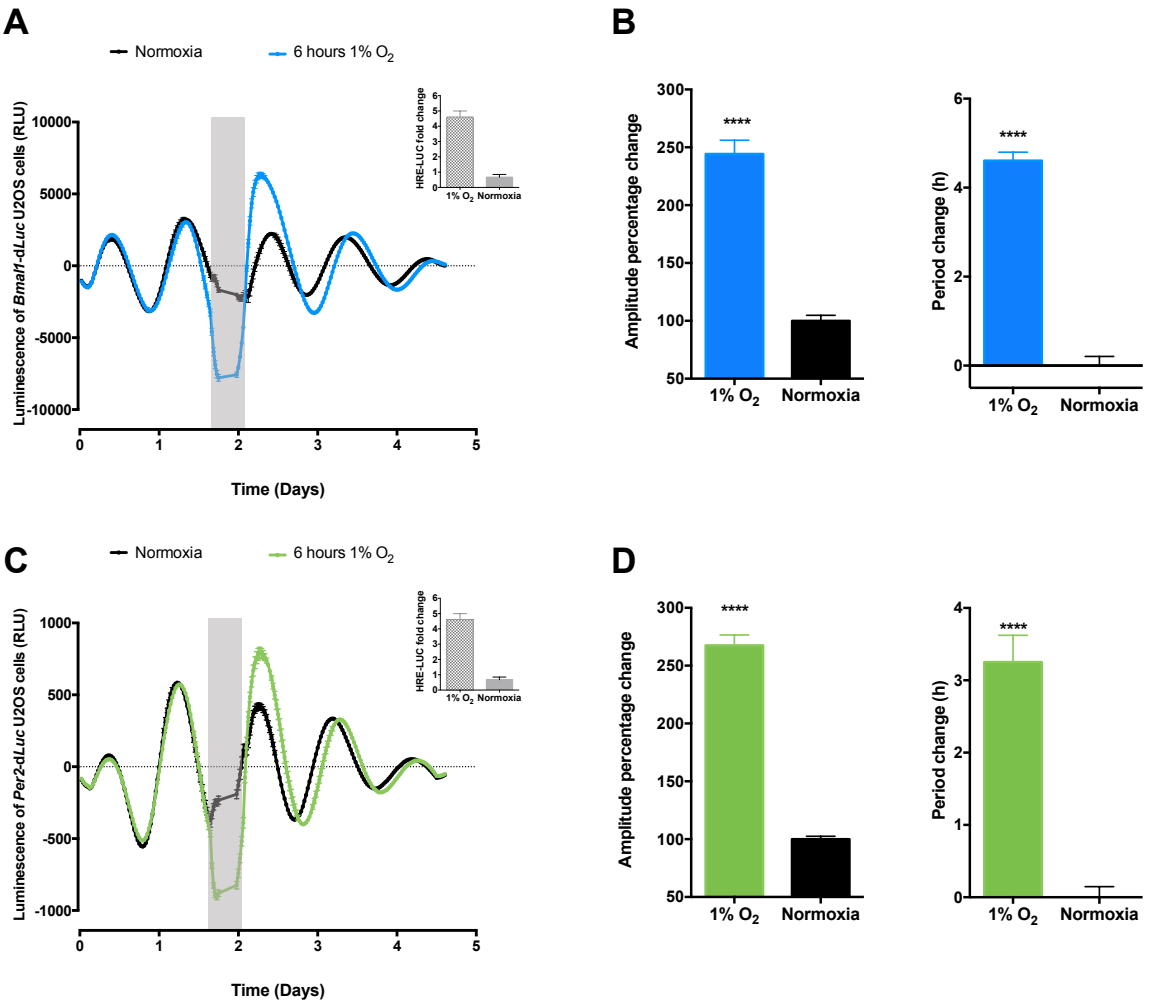


Figure 4.9. 6 hours of Hypoxia increases amplitude and period of *Bmal1*-d*Luc* and *Per2*-d*Luc* U2OS cells:
Real time luminescence measurements conducted in *Bmal1*-d*Luc* and *Per2*-d*Luc* U2OS cells, synchronised with dexamatheasone and exposed to 1% oxygen (hypoxia) or 20% oxygen (normoxia) for 6 hours. Representative traces of *Bmal1*-d*Luc* U2OS cells (N=6) **(A)** and their corresponding amplitude and period analysis **(B).** Representative traces of *Per2*-d*Luc* U2OS cells (N=6) **(C)** and their corresponding amplitude and period analysis **(D).** Grey rectangle represents the period of hypoxia/normoxia where luminescence was not measured. Right corner of **(A)** and **(C)** shows HRE-Luc fold change following the same conditions (N=3). All error bars represent ±SEM.

4.2.2.3 Linopirdine increases HRE-activation and expression of HIF1α downstream targets

From the previous experiments, it was clear that hypoxia directly influences the amplitude of circadian gene expression. However, how these pathways link to Linopirdine still required investigation. Therefore, to explore Linopirdine's actions on HIF pathways, HRE-luciferase plasmids were transiently transfected in U2OS cells. Remarkably, Linopirdine increased HRE-activity in a dose dependent manner (Figure 4.10A), with and EC50 of 471 nM (Figure 4.10B) which was comparable to that of its amplitude effect (187 nM in *Bmal1*-d*Luc* and 740 nM in *Per2*-d*Luc* U2OS cells, Figures 3.3 and 3.4 respectively). Furthermore, to further validate the biological relevance of HRE-promoter activation, mRNA of two key genes associated with the hypoxic response were quantified following Linopirdine treatment. As predicted, Linopirdine increased mRNA expression of vascular-endothelial growth factor (*Vegf*) in U2OS cells, at 4 and 6 hours following treatment, by 80.8±20.45% and 91.4±33.7% respectively (Figure 4.10C), and had a small insignificant increase in *Glut1* mRNA expression at 6 hours (62.1±47.2% increase, p=0.06, Figure 4.10D). Remarkably, these findings suggested a functional activation of HIF and its downstream targets by Linopirdine, which has not been reported before.

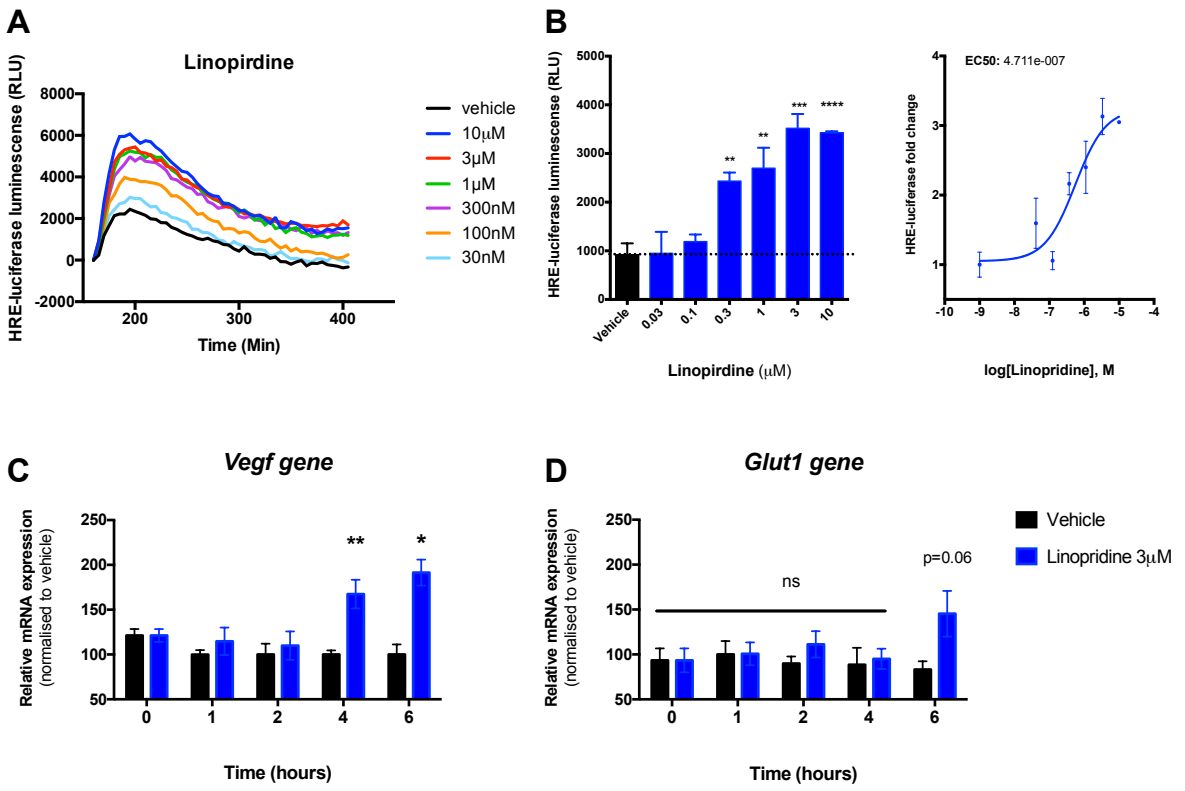


Figure 4.10. Linopirdine activates HRE and increases mRNA expression of VEGF in U2OS cells: A) Raw mean traces of HRE-LUC Luminescence in the presence of increasing doses of Linopirdine **B)** Representative normalised bar charts of HRE activation by linopirdine (Left) and their corresponding fold change relative to vehicle (Right) (N=3) Relative mRNA expression of **C)** *Vegf*, and **D)** *Glut1*, at 0, 1, 2, 4 and 6 hours following vehicle or linopirdine 3 μM treatment. All data normalised to *Gapdh* and *βActin* and each time point normalised to 0h (N=6 each). All error bars represent ±SEM. Vegf: vascular endothelial growth factor.

4.2.2.4 HRE-effect of Linopirdine is mimicked by XE-991, but not Clofilium tosylate.

We showed earlier that XE-991, a structurally similar molecule to Linopirdine significantly increased amplitude of both *Bmal1*-d*Luc* and *Per2*-d*Luc* U2OS cells. However, Clofilium tosylate, a potent potassium channel blocker which also targeted KCNQ channels, did not. To further investigate the role of potassium channels in the HRE-activation mediated by Linopirdine and to compare circadian phenotypes with HRE-activation, we tested both XE-991 and Clofilium tosylate for their HRE-activating abilities. Interestingly, XE-991 also induced a significant increase in HRE-luciferase expression, whereas Clofilium tosylate showed no effect (Figure 4.11A). Furthermore, XE-991-mediated HRE activation exhibited an EC50 of 10.3 nM (Figure 4.11B), which was very similar to its amplitude enhancing effects in *Bmal1*-d*Luc* and *Per2*-d*Luc* U2OS cells (3.8 nM and 7.8 nM respectively, Figure 4.5) and 40 folds lower than its KCNQ-blocking actions (Zaczek et al. 1998). Consequently, these findings eliminated a role for potassium channels in HRE-activation, and re-iterated the importance of the structure of Linopirdine and XE-991 in the observed circadian and HRE-activating effects, proposing a link between all three.

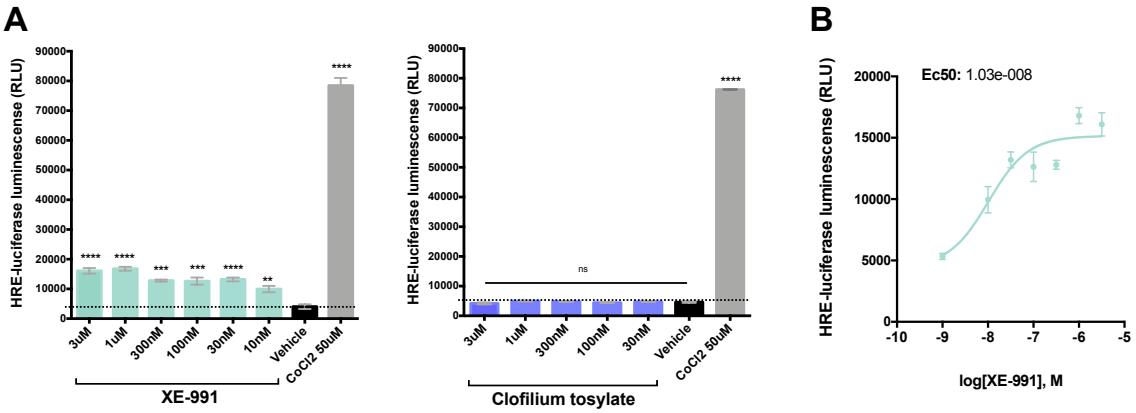


Figure 4.11. HRE-activation following XE-991 and Clofilium tosylate administration: A) Luminescence of HRE-luc activation in the presence of increasing doses of XE-991 (left) and Clofilium tosylate (right). **B)** Log-dose vs response analysis of XE-991-medited HRE activation. N=3 for all. Error bars represent ±SEM. One-way ANOVA used for calculating significance relative to vehicle ($p<0.05$).

4.2.2.5 HIF1α siRNA eliminates amplitude effect of Linopirdine in Bmal1-dLuc U2OS cells but not in Per2-dLuc U2OS cells:

Next, we speculated that HRE-activation was driving the circadian effects observed with Linopirdine. Given HRE are primarily driven by HIF transcription factor, and since HIF1α makes up the O_2 sensitive subunit, we hypothesized that knocking down HIF1α using siRNA would eliminate Linopirdine's amplitude and period effects on U2OS cells.

Interestingly, in *Bmal1*-d*Luc* U2OS cells, HIF1α knockdown (KD) completely abolished the amplitude enhancement usually observed with Linopirdine (Figure 4.12A). In the presence of non-targeting siRNA, Linopirdine increased amplitude by 29.2±4.9% whereas HIF1α siRNA resulted in a 3.7±12.5% amplitude change (Figure 4.12C). This was reiterated with Molidustat, who's amplitude and period effects were similarly

abolished (Figure4.12B), increasing amplitude by 26±3.8% when non-targeting siRNA was used, compared to -5.9±8.7% with HIF1α siRNA (Figure 4.12C). Intriguingly, HIF1α KD eliminated the period effects of Molidustat (Non-targeting Control: 0.4±0.15, HIF1α: -0.07±0.14 hours), and it also reduced Linopirdine-mediated period elongation in these cells (Non-targeting Control: 0.68±0.14, HIF1α: 0.45±0.14 hours relative to vehicle, p=0.039) but did not fully abolish it (Figure 4.12C). Nonetheless, these findings identified HIF1α as the key transcription factor mediating Linopirdine's amplitude enhancing effects in *Bmal1*-d*Luc* U2OS cells.

On the other hand, in *Per2*-d*Luc* U2OS cells, as expected, Molidustat showed no circadian effect, with amplitude and period of *Per2*-d*Luc* expression unaltered in the presence of non-targeting siRNA, and hence unaffected by HIF1α siRNA as well (Figure 4.13B-C). Furthermore, Linopirdine showed a predicted significant enhancement of both amplitude and period of *Per2*-d*Luc* expression (Figure 4.13A) with non-targeting siRNA control, which was reduced but not abolished by HIF1α knockdown (Amplitude-NTC: 75.45±3.3%, HIF1α: 52.1±2.6%; p=0.01, Period- NTC: 2.12±0.15, HIF1α: 1.79±0.14 hours, p=0.02 relative to vehicle). This finding suggested that a proportion of the *Per2*-expression is mediated via HIF1α driving *Bmal1* expression which later promotes *Per2* expression. However, the strong residual amplitude effect of Linopirdine on *Per2*-d*Luc* proposed the possibility of a second target independently inducing Linopirdine's circadian effects on *Per2* expression.

All together, my data confirms that Linopirdine drives *Bmal1*-d*Luc* expression in a HIF1α-dependent pathway.

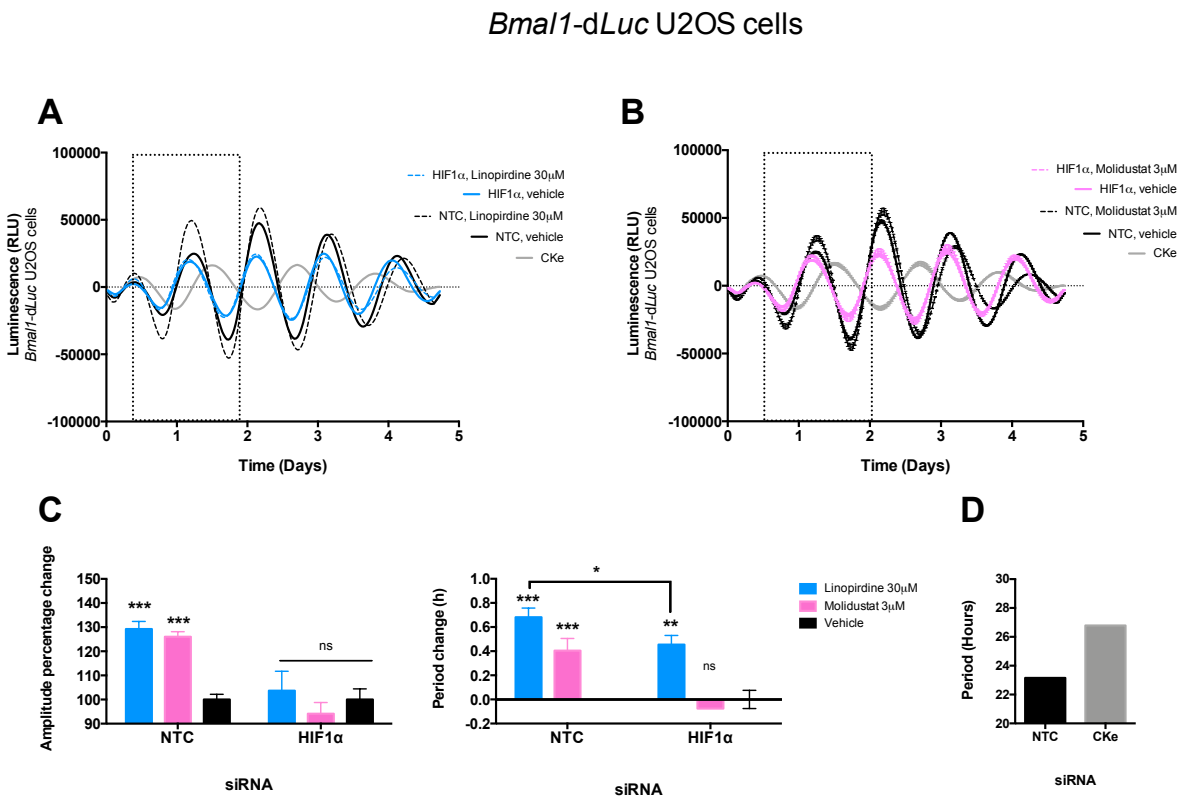


Figure 4.12. HIF1α siRNA knockdown eliminates Linopirdine and Molidustat effect on *Bmal1*-d*Luc* U2OS cells: A) Representative luminescence traces of *Bmal1*-d*Luc* U2OS cells treated with linopirdine (dashed lines) following HIF1α knockdown (Blue) or non-targeting siRNA control (Black). **B)** Representative luminescence traces of *Bmal1*-d*Luc* U2OS cells treated with Molidustat (dashed lines) following HIF1α knockdown (Pink) or non-targeting siRNA control (Black).**C)** Amplitude and Period analysis following Linopirdine and Molidustat. **D)** CKe siRNA was used as a positive control for transfection, and its period analysis is represented. NTC: non-targeting siRNA control, HIF1a: Hypoxia-inducible factor 1α siRNA, CKe: Casein Kinase ε. N=4, Error bars represent ±SEM.

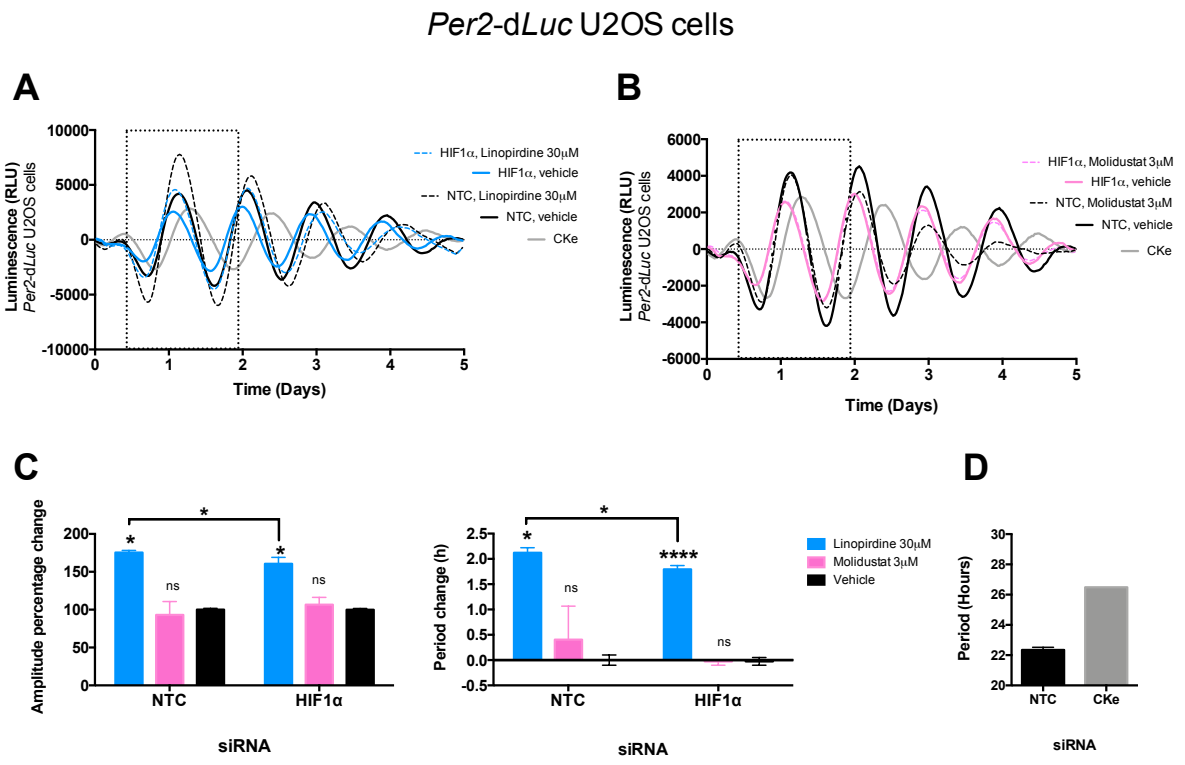


Figure 4.13. HIF1a siRNA knockdown shows no effect on Linopirdine 's circadian effects in *Per2*-d*Luc* U2OS cells:

A) Representative luminescence traces of *Per2*-d*Luc* U2OS cells treated with linopirdine (dashed lines) following HIF1α knockdown (Blue) or non-targeting siRNA control (Black). **B)** Representative luminescence traces of *Per2*-d*Luc* U2OS cells treated with Molidustat (dashed lines) following HIF1α knockdown (Pink) or non-targeting siRNA control (Black). **C)** Amplitude and Period analysis following Linopirdine and Molidustat. **D)** CKe siRNA was used as a positive control for transfection, and its period analysis is represented.

NTC: non-targeting siRNA control, HIF1α: Hypoxia-inducible factor 1α siRNA, CKe: Casein Kinase ε. N=4, Error bars represent ±SEM.

4.2.3 Investigating the mechanism mediating Per2 amplitude enhancement:

Given the prominent amplitude and period effects of Linopirdine on *Per2*-d*Luc* expression, we wanted to explore the other transcription factors involved in mediating these effects. Towards this, an unbiased transcription-factor screen was perfomed using barcoded synthetic tandem repeat promoter screening (dubbed BC-STAR-PROM) developed by Gosselin and colleagues (Gosselin et al. 2016) (Refer to methods section 2.3.4). BC-STAR-PROM consists of a library of ~3000 luciferase-expression vectors, each containing a *promoter* (made from 6 tandem repeats of synthetic random DNA) and a corresponding 20 base-pair *barcode* that lies withing the 3' untranslated mRNA region. Following transfection with the library, cells were treated with the small molecule under investigation (Linopirdine), and mRNAs were counted by next-generation sequencing of the barcodes, which allows tracking of the ~3000 synthetic promoters simultaneously.

4.2.3.1 Validation of BC-STAR-PROM

To validate the reproducibility of this technique and given each of the ~3000 vectors in the library expresses luciferase, BC-STAR-PROM plasmid library were transfected into U2OS cells and treated with 10 μM Forskolin (Adenylyl cyclase agonist) (Figure 4.14B) and with 100 nM Vinblastine (anti-tumour agent that inhibits mitosis through micro-tubule depolymerization) (Figure 4.14C) and luminescence was measured in real time. As expected, Forskolin and Vinblastine resulted in a significant enhancement of luciferase expression driven by their associated transcription factor activation (e.g. CREB

and SRF-MRTF pathways). Transfection efficiency was also tested using Green fluorescent protein (GFP) plasmid and showed high efficiency (Figure 4.14A).

Prior to treatment with Linopirdine or vehicle, bioluminescence of each well was measured to assess relative transfection efficiencies. Only wells with comparable luciferase expression that showed a coefficient of variation [CV]<12% were selected for further experiments. RNA was extracted 0, 2, 4 and 8 hours following Linopirdine and vehicle treatment and reverse transcribed into cDNA. The cDNA barcode regions were amplified using PCR, indexed appropriately, and then prepared for next-generation sequencing (NGS). Following NGS and normalisation of reads to baseline (0h), volcano plots were constructed to compare reproducibility of the two independent replicates. Replicates for all vehicle (Figure 4.14C) and Linopirdine (Figure 4.42D) time points showed strong correlation, with Pearson coefficients of correlation $\geqq 0.8$.

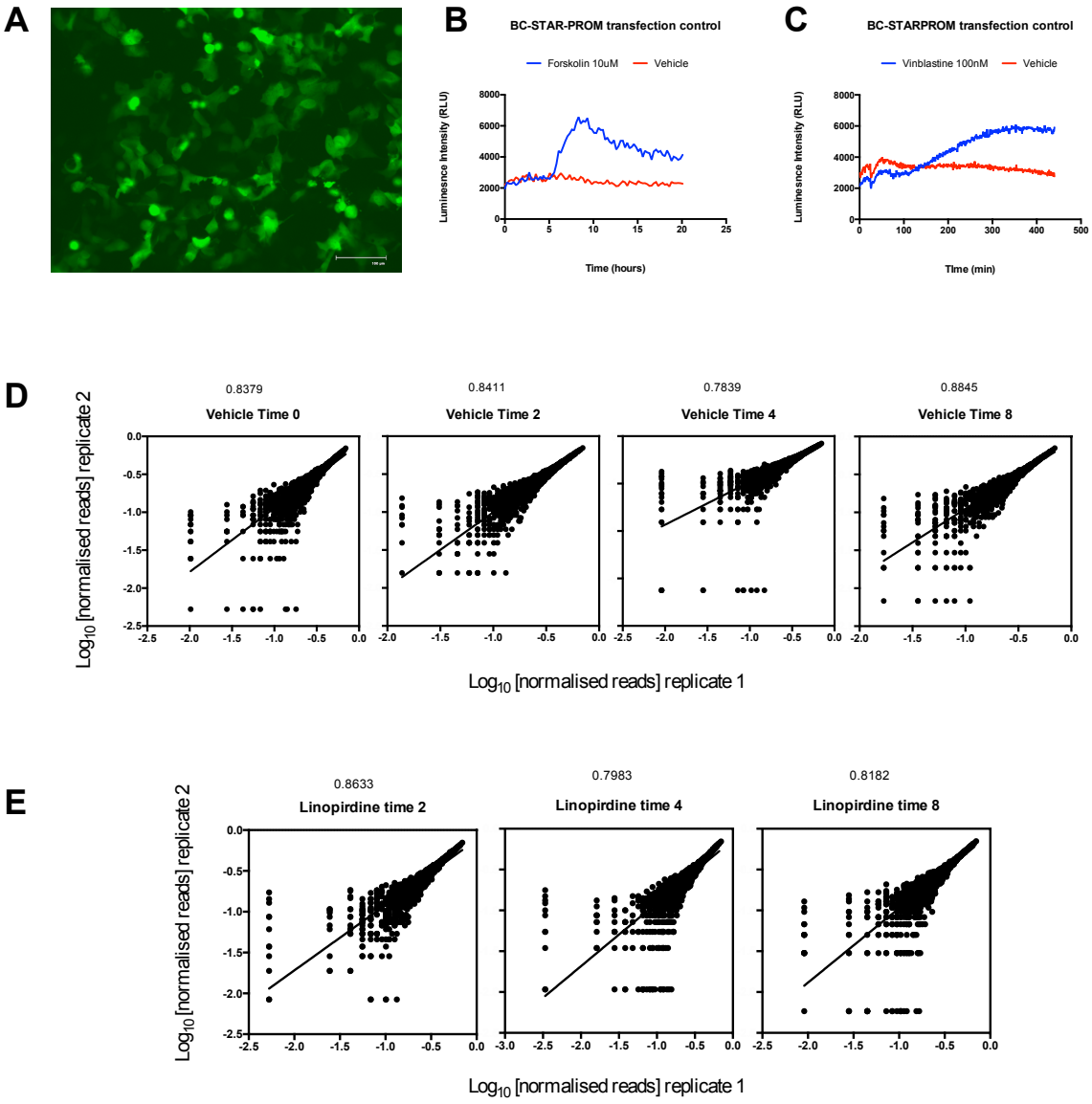
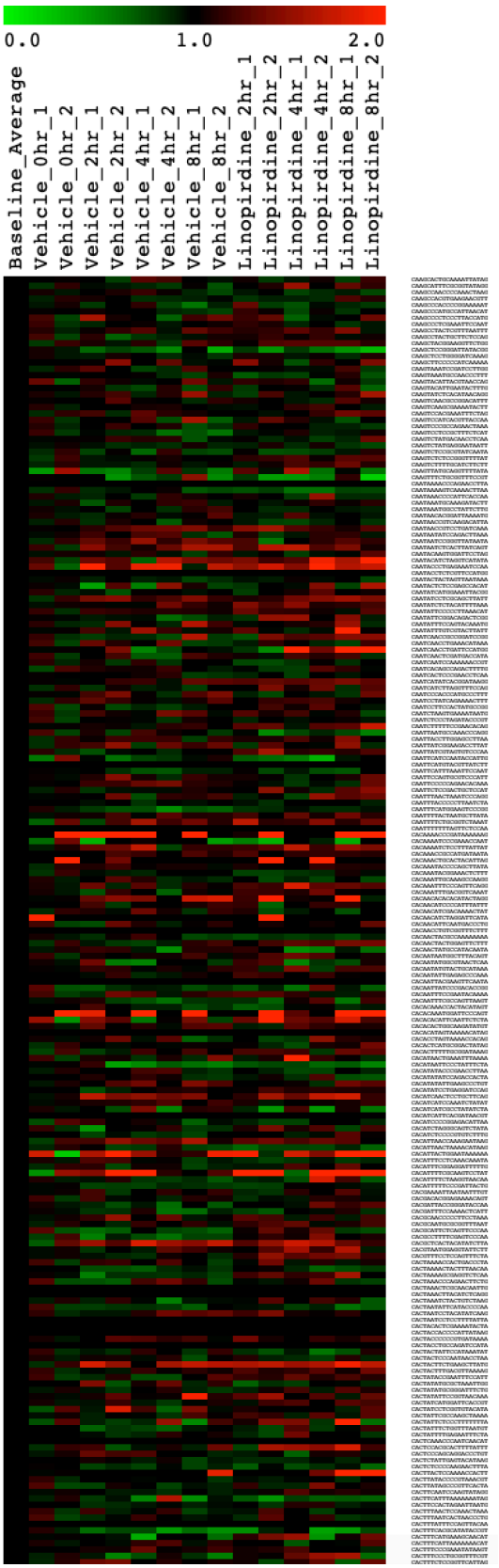


Figure 4.14. BC-STAR-PROM validation:
A) Image of GFP-transfected U2OS cells at magnification 40x. **B)** Representative traces of Forksolin 10 µM treatment following BC-STAR-PROM plasmid transfection. **C)** Representative traces of Vinblastine 100 nM treatment following BC-STAR-PROM plasmid transfection. **D)** Volcano plots comparing vehicle-treated replicates at different time points. Number on top of each figure represent their corresponding Pearson correlation coefficients. **E)** Volcano plots comparing Linopirdine-treated replicates at different time points. Number on top of each figure represent their corresponding coefficient of correlation.

4.2.3.2 BC-STAR-PROM identifies transcription factors potentially mediating Linopirdine's circadian effects.

Following Next-generation sequencing and analysis of upregulated sequences against known transcription factor motifs, a list of 26 transcription factors emerged as possible downstream signals of Linopirdine treatment (Figure 4.15).

To validate these transcription factors and investigate which one could be mediating Linopirdine's circadian effect on *Per2* promoter expression, an siRNA screen was used to knockdown each candidate in *Per2*-d*Luc* U2OS cells (Figures 4.16-4.19). Knockdown of some transcription factors (TFs) on their own had a circadian phenotype (Figure 4.16). Therefore, to examine the direct effects of TF knockdown on Linopirdine's circadian actions, amplitude and period were normalised to their corresponding vehicle treatment for each siRNA. The key candidates that showed significant reduction in Linopirdine's amplitude effect in order of their significant reduction were MEIS1 (Figure 4.19A), CELF6 (Figure 4.18A), PAX2, MAFG, MEIS3 and FXR1 (Figure 4.19A). Their representative traces are shown in Figure 4.20. Taking into account the extent of amplitude reduction (Amplitude reduction relative to Linopirdine control; MEIS1: 40.9±4.7%, CELF6: 34.9±2.1%, PAX2: 30+8.0%, MAFG:19.56+8.8%, MEIS3: 19.5±6.5%, FXR1: 18.5±4%) and the visible changes observed in the traces, MEIS1, MAFG and CELF6 emerged as the most plausible candidates.



	List of BC-STAR-PROM hits
1	RXRa
2	TBP3 (Tata box binding protein 3)
3	THRb1 (Thyroid hormone nuclear receptor beta variant 1)
4	Mef2d (Myocyte specific enhancer factor 2d)
5	Mafb2
6	CEBP/AP1
7	STAT2
8	STAT4
9	YY1
10	C3H transcription factor family Expressed protein
11	FHL1 (Four And A Half LIM Domains 1)
12	BRUNOL6 (RRM) (CELF6)
13	MBNL1 (Muscleblind Like Splicing Regulator 1) homosapiens
14	SP4
15	GFi1b (growth factor independent 1B, mus musculus)
16	HINFP (homosapiens)
17	RBM42 (RRM) RNA Binding Motif Protein 42, homosapien
18	Zinc finger protein 161 homolog (HIC1)
19	MYB88
20	Max2 (Protein Max)
21	Hes5 transcription factor
22	Hey2 (Hairy/enhancer-of-split related with YRPW motif protein 2, Homo sapiens) or CHF1 (cardiovascular helix-loop-helix factor 1)
23	Homeobox protein Meis1 (Homosapiens)
24	Transcription factor MafG
25	Paired box protein Pax-2
26	FXR1 (human)

Figure 4.15. BC-STAR-PROM hits:
Left- Representative heat map displaying some of the barcode counts upon Linopirdine treatment in time-course experiment. Each row represents a barcode, and each column represents the fold change calculated as the log2 of the barcode counts at a given time point (0, 2, 4, 8 hours) minus the log2 of the average barcode counts in the vehicle treated controls **Right**- Table listing the top transcription factor hits identified following Linopirdine stimulation.

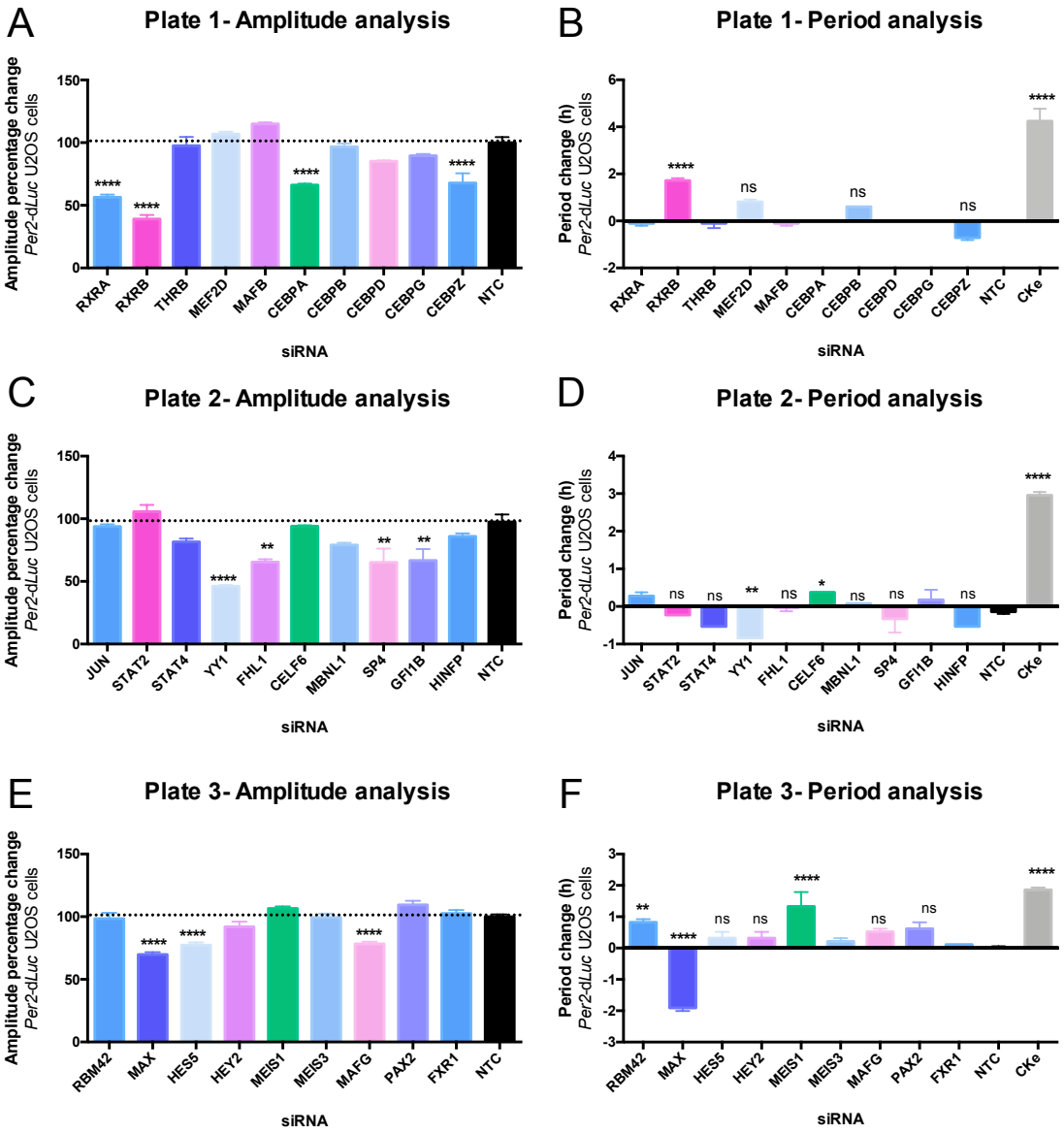


Figure 4.16. Amplitude and Period effects of siRNA knockdown of BC-STAR-PROM candidates in *Per2*-d*Luc* U2OS cells: The key candidates that were identified by BC-STAR-PROM following Linopirdine treatment were independently knocked down in *Per2*-d*Luc* U2OS cells in a 3-plate format, to assess their amplitude **(A, C, E)** and period **(B, D, F)** effects. Error bars represent ±SEM, N=3 (each). Significance determined by One-way ANOVA.

RXRA: Retinoid X Receptor Alpha, *RXRB*: Retinoid X Receptor Beta, *THRB*: Thyroid hormone nuclear receptor beta, *MEF2D*: Myocyte specific enhancer factor 2d, *MAFB*: MAF BZIP Transcription Factor B, *CEBPs*: CCAAT-enhancer-binding proteins (A: alpha, B: beta, D: delta, G: gamma, Z: zeta), *JUN*: c-Jun, *STAT2-4*: Signal Transducers and Activators of Transcription, *YY1*: Yin Yang 1, *FHL1*: Four And A Half LIM Domains 1, *CELF6*: CUG-BP, Elav-like factor 6 , *MBLN1*: Muscleblind Like Splicing Regulator 1 , *SP4*: Specificity protein 4, *GFI1B*: growth factor independent 1B, *HINFP*: Histone H4 Transcription Factor, *RBM42*: RNA Binding Motif Protein 42, *MAX*: myc-associated factor X, *HES5*: Hes Family BHLH Transcription Factor 5, *HEY2*: Hairy/enhancer-of-split related with YRPW motif protein 2 , *MEIS1*,3: Meis Homeobox 1,3 , *MAFG*: MAF BZIP Transcription Factor G, *PAX2*: Paired box protein 2, *FXR1*: Fragile X mental retardation syndrome-related protein 1, *NTC*: non-targeting siRNA control, *CKe*: Casein Kinase ε.

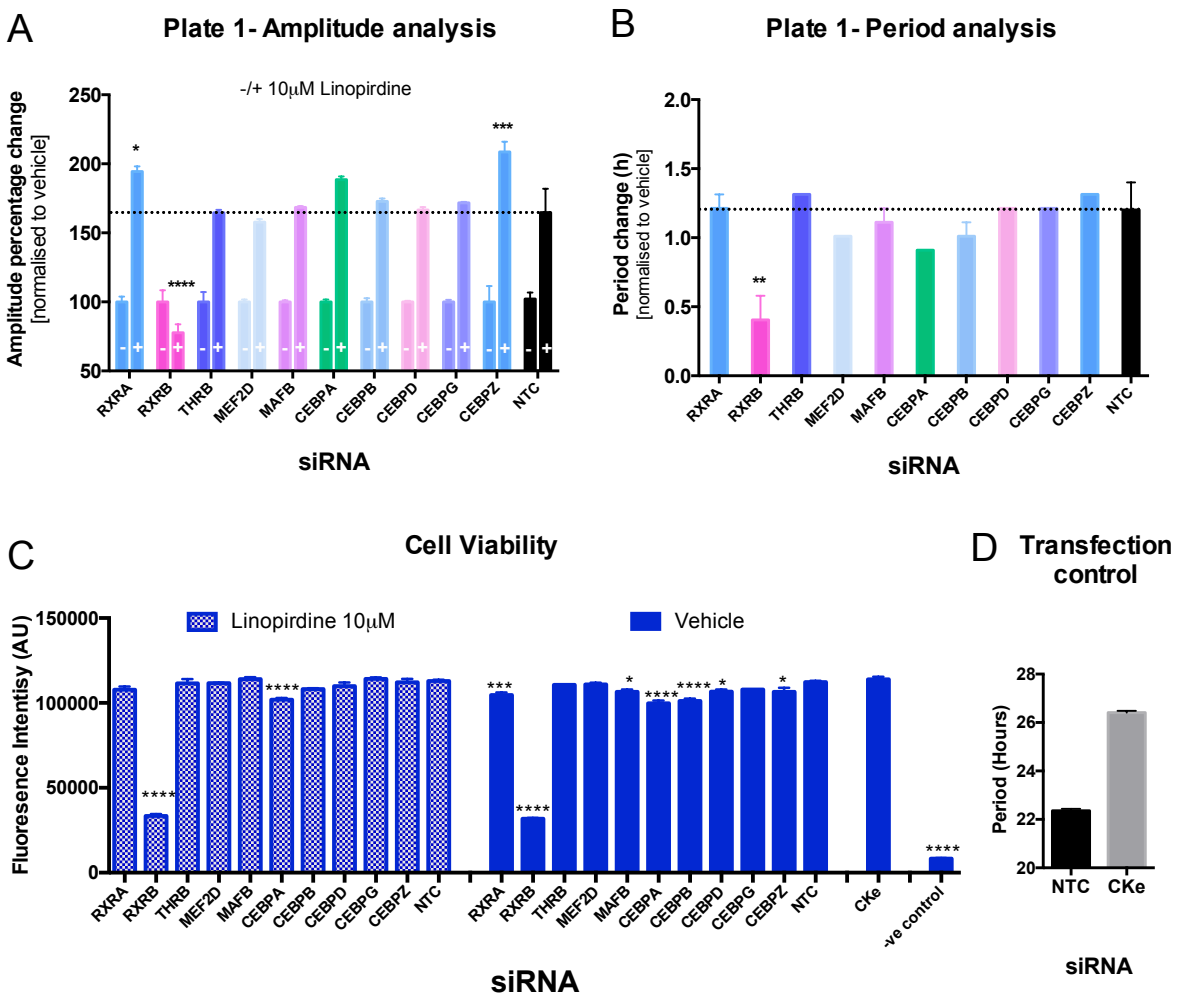


Figure 4.17. siRNA screen plate 1 in *Per2*-d*Luc* U2OS cells with Linopirdine treatment: A) Amplitude percentage change for vehicle (-) or with 10 μM Linopirdine (+), each normalised to its own vehicle. **B)** Period change following 10 μM Linopirdine treatment, each normalised to its own vehicle. **C)** Cell viability **D)** Transfection control. Error bars represent ±SEM, N=3.
RXRA: Retinoid X Receptor Alpha, *RXRB*: Retinoid X Receptor Beta, *THRB*: Thyroid hormone nuclear receptor beta, *MEF2D*: Myocyte specific enhancer factor 2d, *MAFB*: MAF BZIP Transcription Factor B, *CEBPs*: CCAAT-enhancer-binding proteins (A: alpha, B: beta, D: delta, G: gamma, Z: zeta), *NTC*: non-targeting siRNA control, *CKe*: Casein Kinase ε.

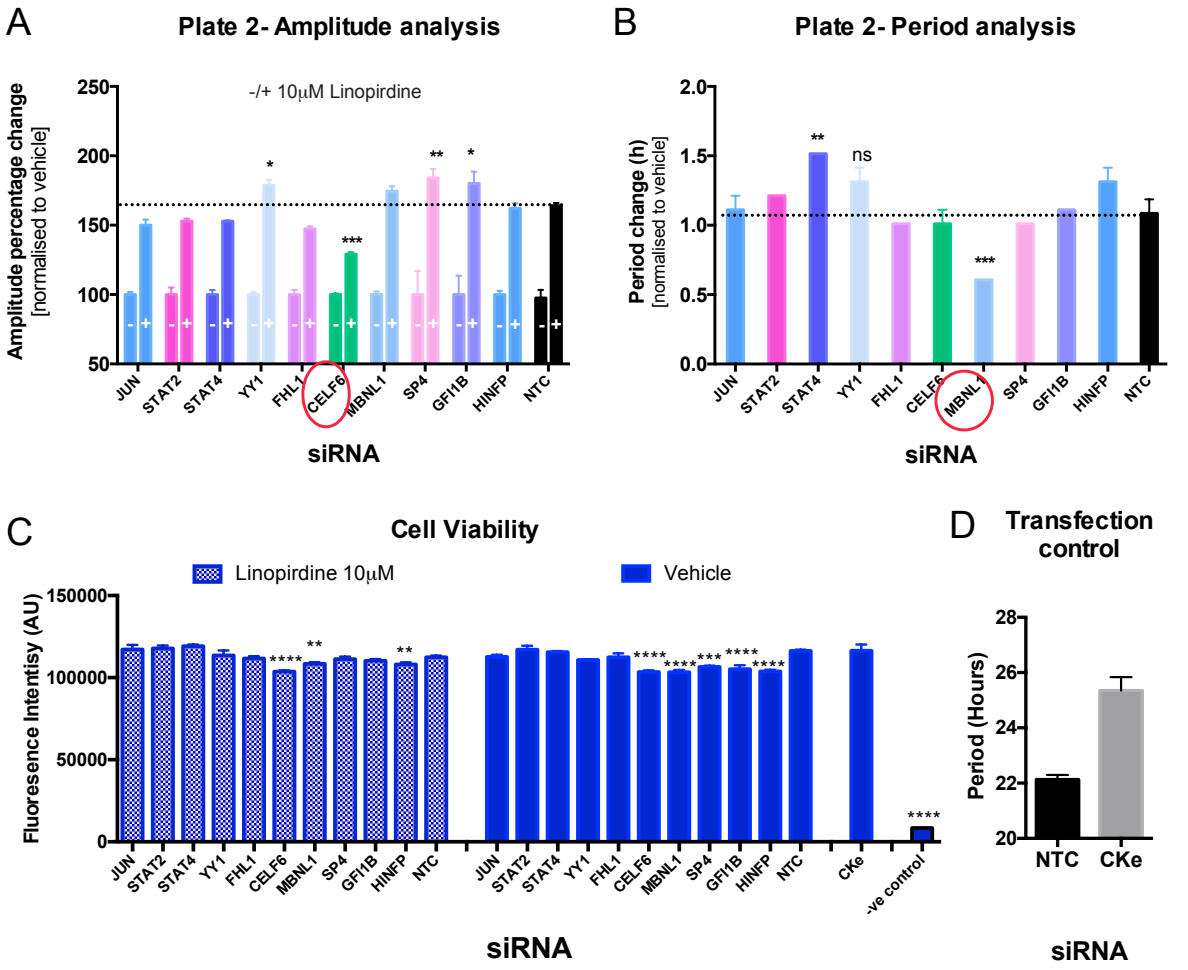


Figure 4.18. siRNA screen plate 2 in *Per2*-d*Luc* U2OS cells with Linopirdine treatment: A) Amplitude percentage change for vehicle (-) or with 10 μM Linopirdine (+), each normalised to its own vehicle. **B)** Period change following 10 μM Linopirdine treatment, each normalised to its own vehicle. **C)** Cell viability **D)** Transfection control. Error bars represent ±SEM, N=3.
JUN: c-Jun, *STAT2-4*: Signal Transducers and Activators of Transcription, *YY1*: Yin Yang 1, *FHL1*: Four And A Half LIM Domains 1, *CELF6*: CUG-BP, Elav-like factor 6 , *MBLN1*: Muscleblind Like Splicing Regulator 1 , *SP4*: Specificity protein 4, *GFI1B*: growth factor independent 1B, *HINFP*: Histone H4 Transcription Factor, *NTC*: non-targeting siRNA control, *CKe*: Casein Kinase ε.

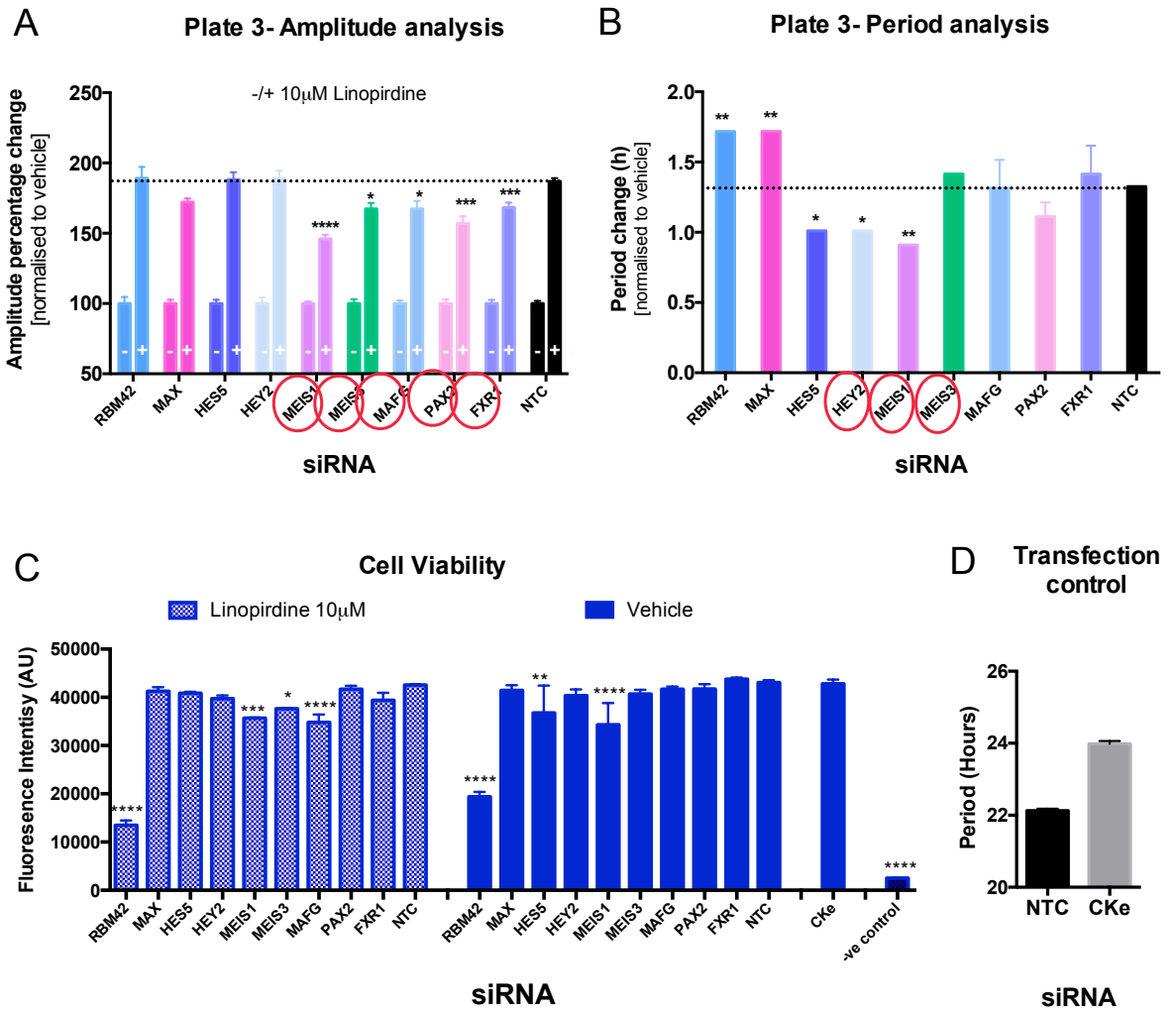


Figure 4.19. siRNA screen plate 3 in *Per2*-d*Luc* U2OS cells with Linopirdine treatment: A) Amplitude percentage change for vehicle (-) or with 10 μM Linopirdine (+), each normalised to its own vehicle. **B)** Period change following 10 μM Linopirdine treatment, each normalised to its own vehicle. **C)** Cell viability **D)** Transfection control. Error bars represent ±SEM, N=3.
RBM42: RNA Binding Motif Protein 42, *MAX*: myc-associated factor X, *HES5*: Hes Family BHLH Transcription Factor 5, *HEY2*: Hairy/enhancer-of-split related with YRPW motif protein 2 , *MEIS1*,3: Meis Homeobox 1,3 , *MAFG*: MAF BZIP Transcription Factor G, *PAX2*: Paired box protein 2, *FXR1*: Fragile X mental retardation syndrome-related protein 1, *NTC*: non-targeting siRNA control, *CKe*: Casein Kinase ε.

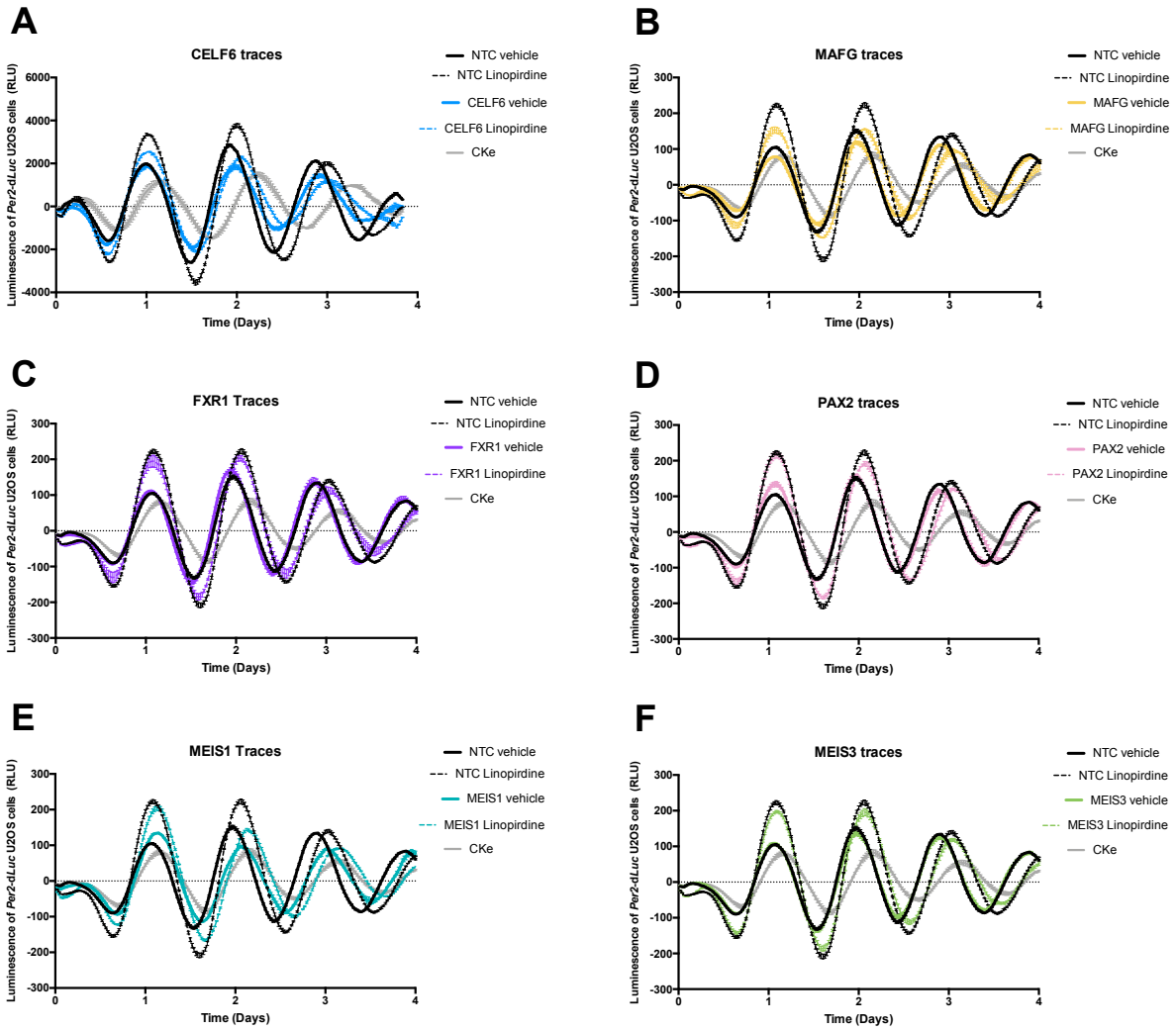


Figure 4.20. Representative traces for transcription factors showing most prominent effect on Linopirdine's circadian effect following their knockdown:
Dashed lines denote Linopirdine, Black solid lines non-targeting siRNA control (NTC) and grey solid line transfection control CKe. The figure displays traces for **A)** CELF6 **B)** MAFG **C)** FXR1 **D)** PAX2 **E)** MEIS1 **F)** MEIS3.
Error bars represent ±SEM, N=3.

4.2.3.3 Validation of BC-STARPROM candidates identifies MEIS1 as the candidate for Linopirdine's circadian effects:

Finally, we endeavoured to replicate the siRNA knockdown of the key targets, MEIS1, MAFG and CELF6, and examine their effects. However, to eliminate any oversaturating effects of Linopirdine at 10 μM and also to validate and replicate the previous finding, two doses of Linopirdine, 10 μM and 1 μM (a dose closer to its EC50) were used.

Interestingly, none of the transcription factors had an effect on Linopirdine's period elongation (Figure 4.21.i C,F,I). However, MEIS1 knockdown completely abolished Linopirdine's amplitude effect at both doses (NTC: 10 μM: 40±6.35%, 1 μM: 40.9±9.6% , vehicle:-0.1±2.25% ; MEIS1: 10 μM: 4.8±13.9% , 1 μM: -5.4±4.6% , vehicle: 0±7.6%, Figure 4.21.i B). On the other hand, CELF6 had no effect on Linopirdine's amplitude effect at 10 μM (Figure 4.21.i E, Traces in Figure 4.21.ii B). However, it reduced the percentage amplitude increase relative to its vehicle control at 1 μM, which was not significant in comparison to its corresponding NTC siRNA (NTC: 10 μM: 35.0±10%, 1 μM: 40.9±9.6% , vehicle: -0.1±2.25% ; CELF6: 10 μM: 47.8± 3.5% , 1 μM: 19.5±12.1%, vehicle: 0±6.1%, Figure 4.21.i E) . Finally, MAFG siRNA had no effect on Linopirdine's circadian effects, leaving its amplitude and period effects unchanged (Figure 4.21.i G-I). Hence, taken together, these findings identified MEIS1 as the key candidate behind Linopirdine's *Per2* expression in U2OS cells.

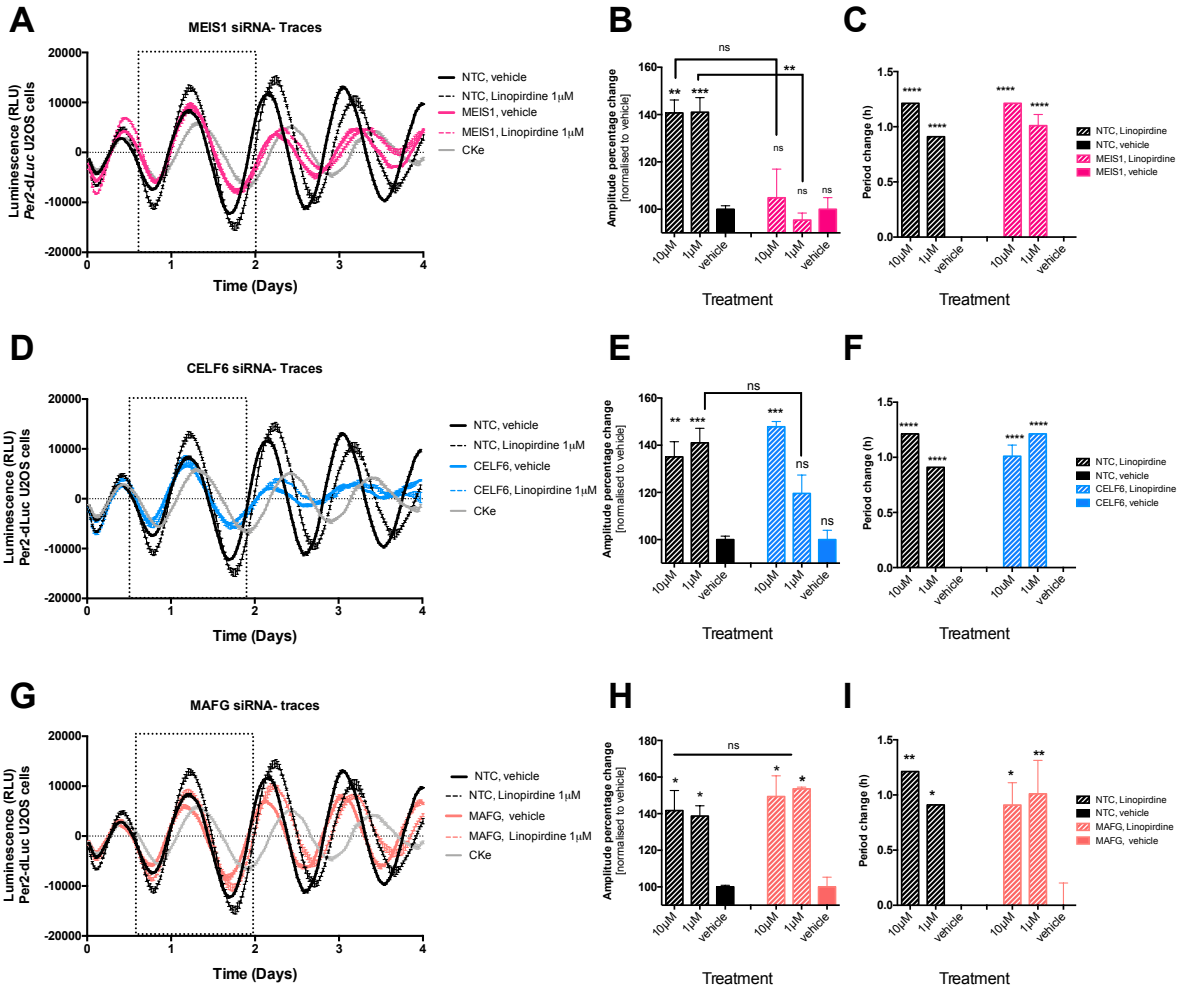


Figure 4.21.i. MEIS1 siRNA knockdown eliminates amplitude effect of Linopirdine in *Per2*-d*Luc* U2OS cells:

A) Representative traces for MEIS1 siRNA (pink) vs non-targeting control (black) in the presence or absence of Linopirdine (dashed lined). **B)** Amplitude analysis and **C)** period change comparison for Linopirdine following MEIS1 siRNA knockdown or non-targeting siRNA. **D)** Representative traces for CELF6 siRNA (blue) vs non-targeting control (black) in the presence or absence of Linopirdine (dashed lined). **E)** Amplitude analysis and **F)** period change comparison for Linopirdine following CELF6 siRNA knockdown or non-targeting siRNA. **G)** Representative traces for MAFG siRNA (orange) vs non-targeting control (black) in the presence or absence of Linopirdine (dashed lined). **H)** Amplitude analysis and **I)** period change comparison for Linopirdine following MAFG siRNA knockdown or non-targeting siRNA.

Error bars represent ±SEM, N=3.

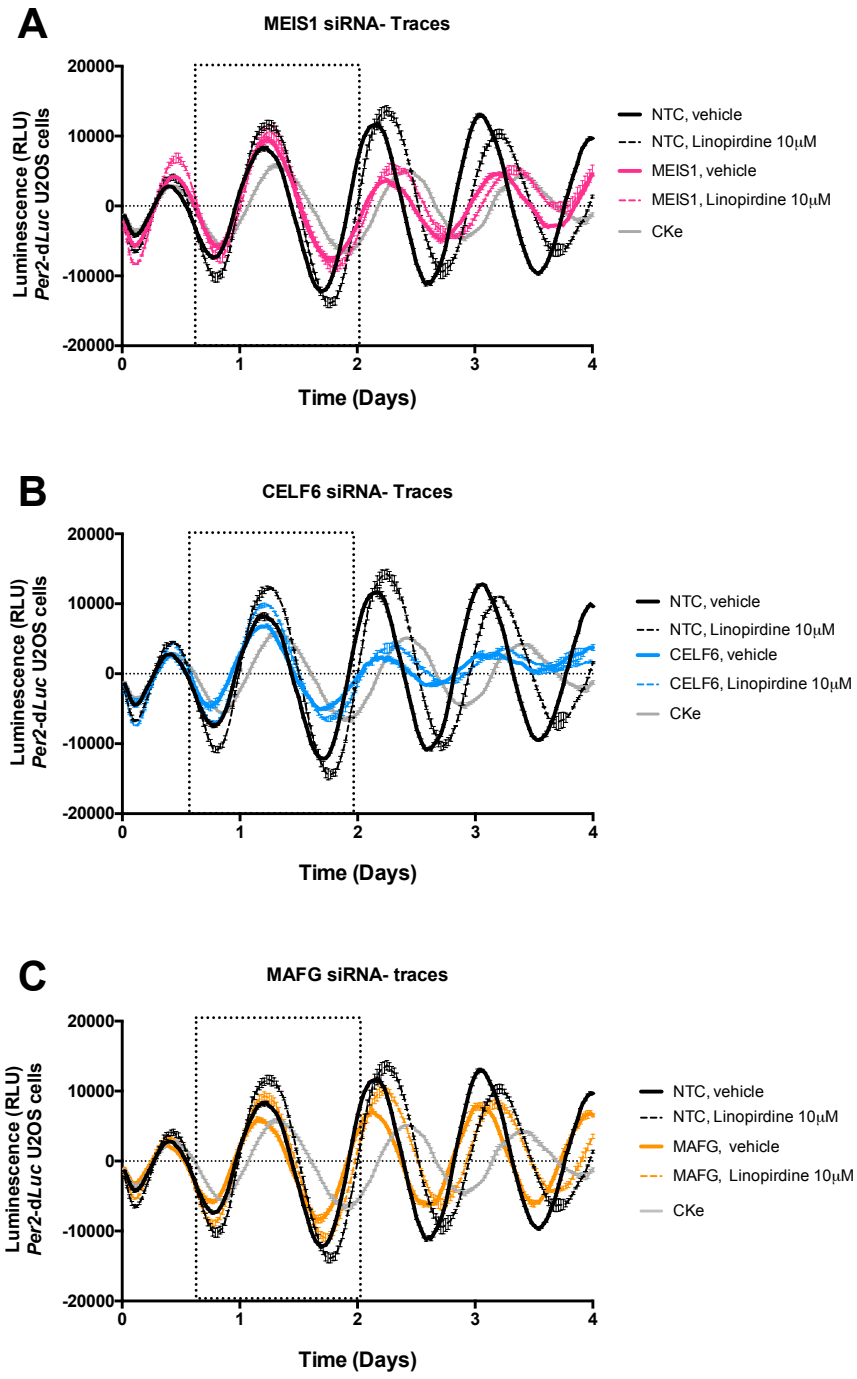


Figure 4.21.ii: Representative traces of *Per2*-d*Luc* U2OS cells for MEIS1, CELF6 and MAFG siRNA treated with 10 μM Linopirdine:
Following siRNA transfection, *Per2*-d*Luc* U2OS cells were synchronised and treated with 10 μM Linopirdine. Representative traces for **(A)** MEIS1 siRNA (pink), **(B)** CELF6 siRNA (blue), and **(C)** MAFG siRNA (orange) vs non-targeting control (black) in the presence or absence of Linopirdine (dashed lined). Error bars represent ±SEM, N=3. *NTC*: non-targeting control.

4.2.3.4 HIF1α mRNA precedes Bmal1 and Per2 mRNA expression following Linopirdine treatment:

Following the unbiased screen using BC-STAR-PROM, the main candidates mediating Linopirdine's circadian effect were MEIS1 and CELF6. Although both hits require further validation, reports from literature showed that HIF1α and HIF2α are key targets of MEIS1 (Kocabas et al. 2012). We therefore hypothesized, that MEIS1 upregulated in the first 8 hours following Linopirdine treatment, could be initiating the entire amplitude effect observed.

To test that, we wanted to explore whether HIF1α mRNA was elevated following Linopirdine treatment and how it corresponded to the timing of *Bmal1* and *Per2* mRNA expression, and hence the circadian phenotype replicated via luminescence. Towards this, mRNA was extracted 16 hours after synchronization (time 0h) and then 8 and 18 hours following that. Interestingly, *HIF1α* mRNA was significantly increased at 8h, and was later followed by the enhancement of *Bmal1* and Per2 mRNA at 18h (Figure 4.22), proposing that *HIF1α* expression preceded them and hence could be driving their expression.

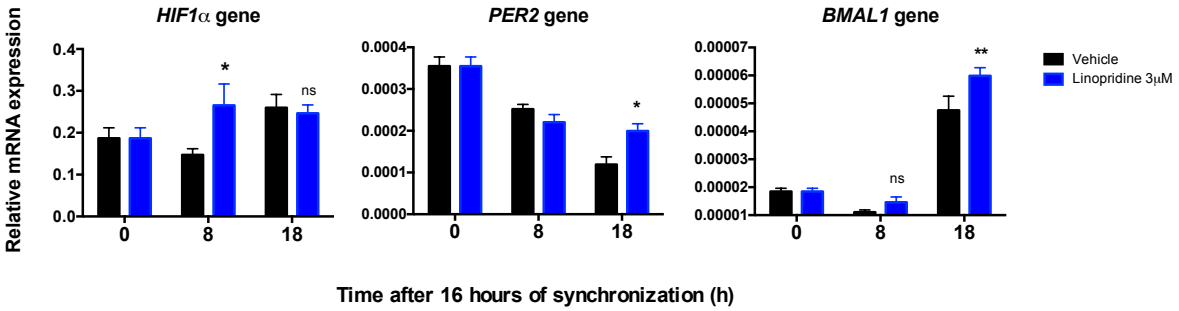


Figure 4.22. HIF1α mRNA precedes *Bmal1* and *Per2* mRNA expression following Linopirdine treatment:
U2OS cells were grown to confluency, synchronized with dexamethasone, and then treated with 3 μM of Linopirdine (blue) or vehicle (black). 16 hours later, mRNA was extracted (Time 0h) and then 8 and 18 hours thereafter. Relative mRNA expression of HIF1α **(A)**, Bmal1 **(B)** and Per2 **(C)** were quantified. All data normalised to *Gapdh* and *βActin*. Error bars represent.

4.3 Discussion

As the primary target reported for Linopirdine, KCNQ channels were expected to be driving the observed circadian phenotype. The use of retigabine, a highly potent activator of KCNQ2-4, with reported reversal of Linopirdine's effects on these channels (Wickenden et al. 2000), uncovered that KCNQ channels could not be mediating Linopirdine's circadian phenotype. Although retigabine did reduce amplitude of *Per2* expression in U2OS cells as would be expected with a counter mechanism to Linopirdine, the reduction however occurred at doses associated with significant cell death (Figure 4.2B). Furthermore, if Linopirdine promoted amplitude enhancement via blocking KCNQ channels, the presence of an agonist should have counteracted or shifted its potency. Remarkably, retigabine (at EC50, Figure 4.3 and EC90, Figure 4.4) did not block the circadian effects of Linopirdine or XE-991's (Figure 4.7). In addition, both Linopirdine and XE-991 promoted HRE-activation and circadian amplitude enhancement at EC50s approximately 10 and 40 folds lower than their reported KCNQ inhibiting actions (Lamas, Selyanko, and Brown 1997). Thus, altogether, these findings suggested that KCNQ channels are unlikely to be driving these observed phenotypes. Furthermore, other potassium channel blockers failed to promote any circadian phenotype in these cells (Figure 4.5). That, XE-991, a drug with high structural similarity to Linopirdine, phenocopies Linopirdine both at the level of HRE activation and circadian effects suggests the presence of a common pathway for these drugs, independent of their KCNQ blocking actions.

Indeed, the first indication of an additional target for Linopirdine came from the in silico Similarity Ensemble Approach (or SEA) developed by Keiser and colleagues, which used Linopirdine's chemical structure to identify targets with similar ligands (Keiser et al. 2007). SEA analysis identified prolyl hydroxylase (PHD2) as a possible candidate (Table 4.1), which lead us to an in-depth investigation of the hypoxic pathways in Linopirdine's circadian effects. Our findings revealed Linopirdine's potent ability to increase HRE-activation in a dose-dependent manner, which was interestingly at an EC50 similar to that of its *Bmal1*-promoter activation (Figure 4.8A-B). We further demonstrated that the HRE-activation was functional, with Linopirdine enhancing expression of HRE-driven downstream targets like VEGF (Figure 4.8C-D). In addition, *HIF1*α knockdown abolished Linopirdine's circadian effects on *Bmal1*-promoter and reduced the extent of *Per2*-promoter amplitude enhancement. Further, HRE sites were evident in the murine *Bmal1* promoter (Figure 4.23). Taken together, my data demonstrates that Linopirdine drives *Bmal1* promoter activation involving a *HIF1*α mediated pathway, which later partially contributes to the *Per2*-promoter activation. Indeed, *Bmal1* mRNA has been shown to be upregulated in the presence of $CoCl_2$ and with *HIF1*α overexpression (Yu et al. 2015), supporting a role for HIF1α in promoting *Bmal1* expression.

It is important to note that *HIF1*α knockdown eliminated the amplitude enhancing effects of Linopirdine in *Bmal1-dLuc* U2OS cells, however its period effects were significantly reduced but not eliminated. The period of the clock is predominately set by the stability and dimerization of the negative arms of the clock PER and CRY, and their feedback

inhibition of Bmal1/CLOCK's interaction with E-boxes (Jagannath et al. 2017). Therefore, the lack of period elimination could be associated with the mechanism via which Linopirdine enhances *Per2* expression, independently of HIF1α. Furthermore, although HIF1α seems to be the key initiator of *Bmal1* expression, other subtypes like HIF2α (also known as EPAS1) or HIF3α could be pitching in following HIF1α knockdown, and therefore could be involved with the remaining period effect.

Given *HIF1α* siRNA knockdown eliminated Linopirdine's enhancement of *Bmal1* promoter but not *Per2*, it became clear that a second pathway could be involved. Furthermore, Linopirdine induces a transcriptional effect, as it was shown to enhance expression of *Bmal1* and *Per2* mRNA (Figure 3.7). Therefore, we aimed to investigate the TF candidate mediating Linopirdine's circadian effects, and for that, we used BC-STAR-PROM to carry out an extended unbiased screen for TFs upregulated by Linopirdine. The BC-STAR-PROM library used consists of ~3000 luciferase-expression vectors, each containing a promoter and a unique barcode, with promoter sequences encompassing more than 400,000 base pairs (bp) of random DNA that generates a complexity sufficient to capture most transcription factors (TF) (Gosselin et al. 2016). The use of this approach relies on the observation that majority of TF-binding sites occur at high frequencies in random DNA (Reinke et al. 2008; Gerber et al. 2013) and utilises the robust interaction of TFs with promoters harbouring tandem repeats of its binding site. Therefore, promoters within the luciferase-vectors used were composed of 6 tandem repeats of synthetic random DNA, and each associated with a 20 base pair (bp) barcode within the

3’ untranslated mRNA region (3’UTR) (see Methods, Figure 2.3). This avoids the need for thousands of transfections of individual vectors and instead allows a single transfection of a pool of barcoded plasmids for a high-throughput investigation of TFs. When a TF is upregulated in response to Linopirdine, it binds to its corresponding motif within the barcoded promoter, thereby promoting expression and corresponding upregulation of the barcode, which is subsequently counted using next-generation sequencing.

The list of upregulated barcodes was generated following DESeq2 analysis (Love, Huber, and Anders 2014). The most common approach for differential analysis of transcriptomic data is to set a null hypothesis of the logarithmic fold change (LFC) for a gene of interest (or barcode in our case) between treatment and control to be exactly zero, suggesting no upregulation of the barcode by the treatment. This is then followed by multiple test adjustments and *p*-value rankings, to generate a list of candidate genes (or barcodes). However, this could be complicated by noisy LFC estimates for low count genes and low sample size. DESeq2 offers the advantage of a more quantitative analysis compared to other analysis models by using shrinkage estimators for dispersion and fold change. This means that the LFC estimates are dependent on available information for a particular gene, with higher shrinkage when little information is available, i.e when counts are low, dispersion is high, or degrees of freedom are few. Therefore, this approach helps facilitate ranking and visualisation of candidate genes based on better estimates of effect size or LFC, focusing on strength of differential expression rather than its mere presence. The reproducibility of the technique across independent experiments was verified by

comparing the Pearson correlation coefficients between both replicates, which is a statistical measure of how strong the relationship between these two variables is. Indeed, our replicates showed correlation coefficients greater than 0.8 across all time points (Figure 4.12), which suggested that for every positive increase in one replicate, there was a fixed proportional increase in the other. Next, all upregulated promoter sequences were analysed using Homer software (see methods section 2.3.4.8), which helps identify motifs and compares them to known bindings sites of TF. Upregulated motifs that showed statistical significance (adjusted *P*-value <0.1) relative to vehicle treated samples across different time points, and those that showed visible upregulation in heat map (example shown in Figure 4.15) were selected. From these, the motifs that represented relevant TFs expressed in mammalian tissues were identified, which consequently proposed a list of 22 TF hits. siRNA knockdown was subsequently carried out to verify the candidate TFs identified, and validate their involvement in Linopirdine's actions on *Per2* promoter activation (Figures 4.16-4.20). From this, CELF6 and MEIS1 emerged as interesting candidates.

CELF6, denoted CUG-BP Elav-like factor 6, belongs to a novel family of splicing regulators referred to as CELF proteins (Ladd, Charlet-B., and Cooper 2001). It is a poorly understood RNA-binding protein that is associated with regulation of pre-mRNA alternative splicing (Ladd et al. 2004). Alternative splicing helps generate multiple mRNA from a single gene, that tend to produce functionally distinct protein isoforms, and can also regulate the levels of different isoforms to meet cellular needs in a tissue-specific or

developmental-stage-specific manner. Despite the fact that more than a third of the human genome undergoes alternative splicing (Hanke et al. 1999), the mechanisms that regulate it are still poorly understand. Increasing evidence has been emerging supporting post-transcriptional regulations of circadian clocks, and recently, RNA binding proteins have been implicated with circadian clock regulation. The heterogeneous nuclear ribonucleoprotein Q (hnRNP Q) for example, has been shown to rhythmically bind to *Bmal1* mRNA 5'UTR and regulate its rhythmic expression. Furthermore, its depletion was associated with an increase in *Bmal1* protein levels and mRNA oscillations of *Bmal1*-regulated target genes (Jung et al. 2019). Therefore, a similar role for the RNA-binding protein CELF6 in regulating circadian clock genes is plausible. However, to date there has been no reports of CELF6 interacting with the circadian clock. Although the role for CELF6 in Linopirdine's circadian effect still requires further validation, particularly given its inability to reproducibly eliminate the circadian phenotype at 10 μM (Figures 4.17-4.18), it nonetheless, could potentially introduce the first line of evidence supporting a link between its mRNA splicing actions and post-transcriptional regulation of circadian clocks.

On the other hand, MEIS1, or the Myeloid ecotropic viral integrations site-1, is a member of the three amino acid loop extension (TALE) family of transcription factors. MEIS1 is ubiquitously expressed (Uhlén et al. 2015) and has been hugely associated with cell proliferation and development. In fact its expression has been deemed a necessary requirement to maintain cells in a proliferative stage (Calvo et al. 2001) and there is

emerging evidence of its role as an oncogene (Lawrence et al. 1999; Wong et al. 2007). Interestingly, a recent GWAS study on ~70,000 people has identified a correlation between SNPs in MEIS1 and low amplitude of circadian rhythms, as measured by accelerometers (Ferguson et al. 2018). Furthermore, similar genetic studies showed MEIS1 to have the strongest association signal with insomnia (Hammerschlag et al. 2017), which itself has been associated with circadian rhythm disruption. In addition, heterozygous MEIS1 knockout mice, particularly males, have been reported to exhibit circadian hyperactivity (Salminen et al. 2017), suggesting an association between MEIS1 and circadian pathways. However a direct link between the two has not been reported.

Interestingly, our findings support a role for MEIS1 in mediating Linopirdine's circadian phenotype. Although its direct implication requires further validation, several observations support its involvement. Firstly, MEIS1 knockdown was enough to eliminate Linopirdine's amplitude effect in *Per2*-d*Luc* U2OS cells (Figure 4.18). Indeed, MEIS1 targets the TGACAG consensus (Shen et al., 1997), which is evidently present within the *Per2* promoter (Figure 4.21), and hence could be promoting the enhancement in amplitude of *Per2* expression. Furthermore, HIF1α has been reported as a key target of MEIS1 upregulation, where expression of MEIS1 has been shown to drive expression of HIF1α-promoter and its inducible deletion has been associated with down regulation of HIF1α and HIF2α (Kocabas et al. 2012). Interestingly, our findings showed that HIF1α mRNA was significantly increased following Linopirdine treatment (Figure 4.19A) which could be an outcome of MEIS1 upregulation. In fact, the increase in HIF1α mRNA

following Linopirdine treatment preceded *Bmal1* and *Per2* expression (Figure 4.19A-C). Furthermore, following BC-STAR-PROM analysis over an 8 hour window, HRE-consensus was manually detectable in the list of upregulated barcodes, however, its upregulation was low and did not make the cut-off of significance compared to the identified hits (Figure 4.13). Hence, this could suggest that MEIS1's interaction with its target response elements, which was detectable within 8 hours of treatment, promoted *HIF1*α mRNA expression and hence preceded HRE-activation. Taken together, these findings propose the notion that MEIS1 could be driving Linopirdine's entire circadian effect on both *Bmal1* and *Per2* promoters.

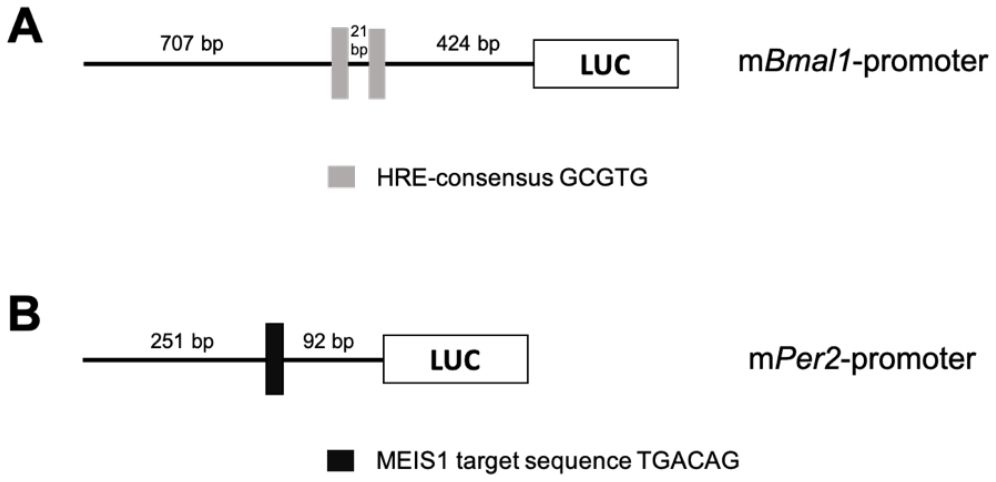


Figure 4.23. Representative diagram of *mBmal1*-d*Luc* and m*Per2*-d*Luc* promoters:
A) The mouse *Bmal1*-promoter used in our experiments contains the HRE-consensus at two different locations upstream of the luciferase gene.
B) The mouse *Per2*-promoter used in our experiments contains the MEIS1 target Ssequence.

On another note, MEIS1 has also been associated with iron metabolism (Sarayloo, Dion, and Rouleau 2019; Guo et al. 2017). siRNA knockdown of a MEIS1 ortholog in Caenorhabditis elegans, *Unc-62*, has been associated with higher expression of ferritin, a protein that stores intracellular excess iron (Catoire et al. 2011; Harrison and Arosio 1996). A similar observation was also made in autopsy cases from patients with Restless Legs syndrome (RLS), a neurological condition strongly correlated to decreased MEIS1 mRNA and protein expression (Catoire et al. 2011). This study reported an increase in mRNA expression of both ferritin (FTN) light and heavy chains as well as divalent metal transporter-1 (DMT-1) in the thalamus, which are involved in intracellular storage and uptake of iron, respectively. Interestingly, the content of cytoplasmic FTN is regulated by intracellular iron levels, where high iron levels have been shown to increase ferritin synthesis (at a transcriptional and post-translational level) (Aziz and Munro 1986; Rogers and Munro 1987; Cairo et al. 1985; Torti and Torti 2002). Therefore, upregulation of DMT-1 could be associated with an increase in iron uptake, while the increase in FTN could be a response to increased intracellular iron. Altogether, this would suggest MEIS1 downregulation in RLS patients correlates with a reduction in systemic iron levels, but an increase in intracellular iron. Indeed, human cells cultured under iron-deficient environments display reduced MEIS1 expression (Catoire et al. 2011). Therefore, if a cell's response to iron deficiency is to reduce MEIS1, that could in turn suggest that high MEIS1 activity reduces iron and in iron-deficient conditions, the cell tries to counteract that to retain its homeostasis. Given the oxygen sensing enzymes, PHD2 and FIH, require both oxygen and iron to function, it is possible that a reduction in iron within the cells

(following MEIS1 upregulation) could be associated with a hypoxic phenotype that might be aiding in Linopirdine's HIF1α stabilisation. Interestingly, a series of coimmunoprecipitation-based experiments done by Kobayashi and colleagues showed that PER2 protein directly interacted with HIF1α. Furthermore, overexpression of PER2 protein potentiated HIF1α recruitment to HRE-sites, enhancing its transcriptional activity, without affecting its mRNA or protein levels. More importantly, this enhancement of HRE activation only occurred under hypoxic conditions when HIF1α aspargine-803 (N803A) residue was un-hydroxylated (Kobayashi et al. 2017). FIH-1 is a key enzyme in regulating HIF transcription, which hydroxylates HIF1α at the aspargine-803 residue (N803A) in an oxygen and iron dependent manner (Figure 4.1), and as a result suppresses its transcriptional activity by inhibiting p300/CBP recruitment (Lando et al. 2002). Hence, if MEIS1 upregulation indeed reduces iron levels, that could subsequently inhibit FIH-1 hydroxylation of HIF1α, thereby enhancing PER2-mediated recruitment of HIF1α to its HRE-sites, which could further potentiate the HIF1α mediated *Bmal1* transcription, and might explain why Linopirdine's circadian phenotype and its HRE-activation are dissimilar to that of Molidustat. However, this hypothesis requires further investigation to validate the effects of Linopirdine and MEIS1 on iron levels *in vitro*.

Altogether, our study identified a novel mechanism of action underlying Linopirdine's circadian phenotype. A schematic summary of our proposed mechanism is displayed in Figure 4.24.

Going back to Linopirdine's metabolic phenotypes in adipocytes (Chapter 3), we reported several interesting observations, where Linopirdine increased glucose uptake and amplified adipocyte cell number during differentiation. Although a role of the circadian clock in these observed effects is not entirely clear, the involvements of MEIS1 and HIF1α seem likely. For instance, GLUT1 mRNA showed a trend of increase 6 hours following Linopirdine treatment (Figure 4.10D). Given Glut1 is one of the key target genes of HIF1α, it is possible that HIF1α could be enhancing glucose uptake via Glut1 upregulation. Furthermore, upregulation of MEIS1 could also be contributing to the observed adipocyte hyperplasia when differentiated with Linopirdine given MEIS1's vital role in maintaining cell proliferation and self-renewal (Calvo et al. 2001).

Linopirdine also resulted in enhancement of lipolysis and increase in adipogenic markers during differentiation, which do not correlate with HIF1α functions. Indeed, HIF1α has been associated with inhibition of adipogenesis, by repressing *PPARy2* gene expression and promoting expression of transcriptional repressors DEC1/Stra13 (Yun et al. 2002). However, HIF2α expression has been shown to increase early on during adipogenesis and enhance adipogenic potential in NIH-3T3 fibroblasts, while overexpression of a dominant negative form of HIF2α inhibited adipogenesis in 3T3-L1 cells (Shimba et al. 2004). Therefore, together this indicates opposing roles of HIF1α and HIF2α on adipogenesis of 3T3-L1 cells. Interestingly, loss of MEIS1 has been associated with a down-regulation of both HIF1α and HIF2α (Kocabas et al. 2012), suggesting both transcription factors are under MEIS1 regulation. Therefore, If Linopirdine, as a

consequence of MEIS1 activation, is upregulating HIF2α in parallel with the HIF1α upregulation, this could explain the enhancement in adipogenic markers and the reduction in lipid accumulation observed, respectively.

Finally, Linopirdine showed no effect on cellular bioenergetics, whereas the HIF1α stabiliser Molidustat exhibited dramatic modulation of mitochondrial function in adipocytes. On one hand, Molidustat shifted the cell's bioenergetics towards glycolysis (3.12B) and significantly reduced overall mitochondrial bioenergetics as shown by a reduction in mitochondrial ATP (Figure 3.12E), spare capacity and basal respiration without changing non-mitochondrial respiration in these cells (Figure 3.12C). On the other hand, Linopirdine showed no change in cellular bioenergetics or any of the mentioned parameters (Figure 3.14). As a selective PHD2 inhibitor and a HIF stabiliser, Molidustat's effects are in agreement with outcomes of hypoxia on oxygen consumption and mitochondrial bioenergetics (Shih et al. 2018), which would have suggested similar outcomes from Linopirdine. Nonetheless, MEIS1 knockdown has been shown to significantly reduce mitochondrial gene expression such as mitochondrial cytochrome-c oxidase subunits 1, 2 and 3 (MT-CO1, MT-CO2, MT-CO3), ATP synthase 6 and 8 and several NADH-ubiquinone oxidoreductase chains (Tomoeda et al. 2011), all key enzymes in the electron-transport chain which drives oxidative phosphorylation. This suggests that Linopirdine-mediated upregulation of MEIS1 (which enhances mitochondrial gene expression) could counteract the effects of HIF1α and could explain this discrepancy.

All in all, our findings help shed light on possible mechanisms underlying the metabolic phenotypes of Linopirdine, however more direct evidence linking HIF1 and MEIS1 to these metabolic phenotypes in adipocytes is yet to be explored.

4.4 Conclusion and future work:

In this chapter, we uncovered a novel pathway driving Linopirdine's circadian effect, which seems to be independent of its previously reported potassium channel blocking action. We postulate that Linopirdine interacts with the clock by promoting MEIS1 upregulation, via an intermediary target, which promotes *Per2* and *HIF1α* expression. The latter then would drive HRE-mediated *Bmal1* expression and could also contribute marginally to the enhancement in *Per2* expression (Figure 4.13). We also speculated that MEIS1 could also be contributing further to *HIF1α* stability through reduction in iron levels, which inhibit the dioxygenase enzymes responsible for its hydroxylation. A schematic representation of our hypothesis is summarised in Figure 4.24. This of course warrants further validation, which is beyond the scope of this thesis, but nonetheless introduces MEIS1 as a transcription factor associated with both circadian rhythms and hypoxic pathways.

In addition, our findings uncovered a novel pathway downstream of Linopirdine which has not been reported before. There are no small molecule up-regulators of MEIS1 known to date, and Linopirdine could be used as a novel pharmacological tool for such use. Furthermore, as mentioned previously, reduction in mRNA and protein levels of

MEIS1 have been linked to restless leg syndrome (RLS), a highly prevalent neurological disorder (Sarayloo, Dion, and Rouleau 2019; Xiong et al. 2009), and perhaps the use of Linopirdine could form an interesting new therapeutic intervention to explore.

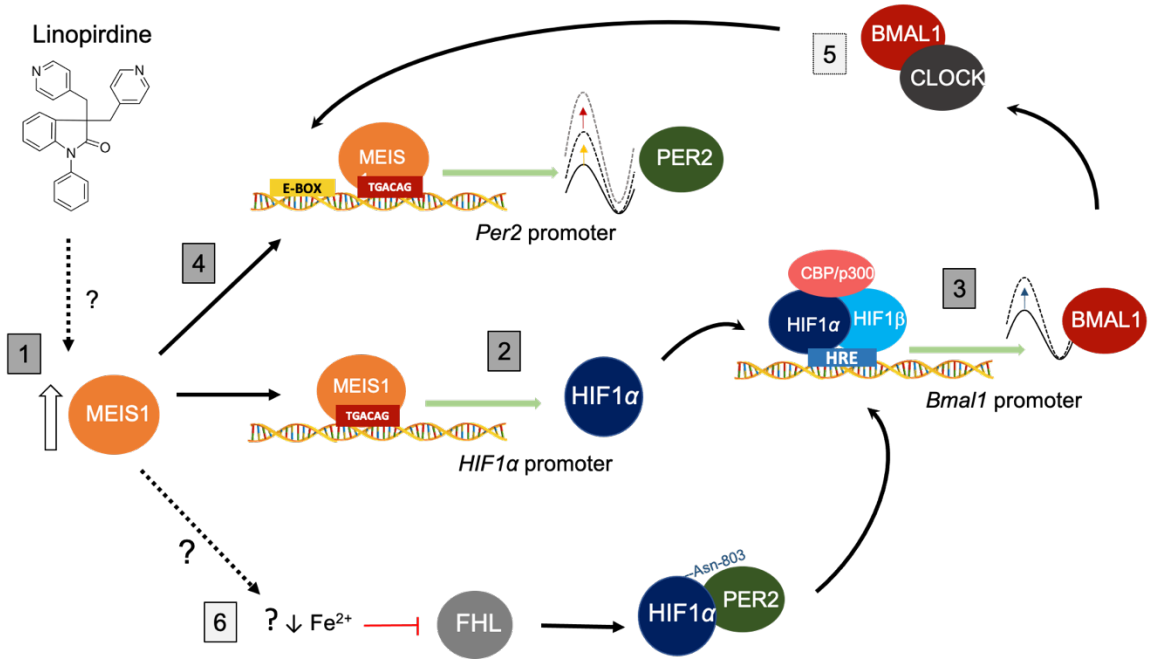


Figure 4.24. Schematic representation of the mechanism underlying Linopirdine's circadian phenotype in U2OS cells: Grey boxes represent experiments performed in our study, white boxes represent hypothesized contributions to Linopirdine's effect from literature.
1- BC-STAR-PROM identified MEIS1 as a possible target upregulated by Linopirdine.
2- HIF1α mRNA was shown to increase following Linopirdine treatment, and its expression precedes that of *Bmal1* and *Per2* genes.
3- HIF1α was shown to be necessary for Linopirdine's enhancement of *Bmal1* expression, where siRNA for *HIF1α* abolished amplitude effect in *Bmal1*-d*Luc* U2OS cells.
4- siRNA knockdown of MEIS1 was able to completely abolish Linopirdine amplitude effect on *Per2*-d*Luc* expression. Furthermore, MEIS1 targeting sequences are evident in murine *Per2* promoter.
5-The role of BMAL1/CLOCK heterodimer in promoting *Per2* expression via E-Boxes is well established. Given HIF1α knockdown reduced amplitude of *Per2* expression in U2OS cells, it seems plausible that *Bmal1* driven by HIF1α could be further contributing to Linopirdine's circadian effects in these cells.
6- Upregulation of MEIS1 is hypothesized to reduce iron, which in turn is known to inhibit FHL enzyme, thereby keeping the HIF-aspargine-803 residue unhydroxylated and capable of PER2 binding, which can enhance HIF-HRE binding.

CHAPTER 5:

Investigating Linopirdine's *in vivo* actions in a DIO-Model of Metabolic Syndrome

5.1 Introduction:

Metabolic syndrome (MetS) is portrayed by the concomitant occurrence of at least three of the following health conditions; hyperglycaemia, obesity, hypertension and/or dyslipidaemia (Alberti et al. 2009). The worldwide prevalence of MetS has been on the rise, with nearly 20-25% of the word's adult population estimated to suffer from it (Alberti, Zimmet, and Shaw 2006). Currently, combatting metabolic syndrome depends predominantly on lifestyle changes, like calorie restriction and increased exercise (see Chapter 1). Other approaches used clinically also include bariatric surgery and the use of pharmacological agents that reduce caloric harvesting from the gut. However, bariatric surgery is highly invasive and exhibits risk of post-operative complications, while current pharmacological agents in many cases fail to provide long term weight loss and subsequent improvement in metabolic health (Narayanaswami and Dwoskin 2017; Srivastava and Apovian 2018a). This, along with the increase in sedentary lifestyles of most MetS patients, calls for the development of new pharmacological interventions and strategies to tackle obesity and MetS.

The adipocyte is a vital tissue at the centre of metabolic disorder with obesity, one of the key hallmarks of MetS, believed to be reflected by adipose tissue hyperplasia (increase in number) as well as hypertrophy (increase in size) (Jo et al. 2009). In our previous studies, we have shown interesting metabolic phenotypes at the adipocyte level produced by one of our key leads Linopirdine. This small molecule acutely enhanced

glucose uptake and lipolysis within adipocytes, yet also promoted adipogenesis and preadipocyte hyperplasia following chronic treatment (Chapter 3). However, utilising these *in vitro* markers of adipogenesis and lipogenesis for predicting the drug outcomes in metabolic syndrome is difficult due to the multi-factorial and multi-organ nature of the disorder. On one hand, enhancing adipocyte hyperplasia could be protective against glucose intolerance. For instance, mice exhibiting lower white adipose hyperplastic potential have been shown to have higher susceptibility to insulin resistance (Kim et al. 2014). Furthermore, a number of animal and human studies have shown adipocyte hypertrophy to be predictive of metabolic diseases (Weyer et al. 2000; Kabir et al. 2011). This suggests that Linopirdine-mediated induction of lipolysis could prevent excess lipid accumulation in adipocytes, reducing hypertrophy and in combination with enhanced hyperplasia, could possibly improve insulin resistance. However, on the other hand, enhancing lipolysis might also increase plasma non-esterified fatty acids (NEFA), which in turn has been associated acutely with insulin resistance, at the level of peripheral glucose uptake (Shah et al. 2002; Boden et al. 1994) and hepatic gluconeogenesis (Staehr et al. 2003; Roden et al. 2000) and with poor outcome for glucose tolerance (Kruszynska et al. 1997).

That said, our previous studies also identified Linopirdine as a potent circadian modulator in different tissues, which strongly increases amplitude of expression of key clock genes like *Bmal1* and Per2 (Chapter 3, Figure 3.5, 3.6). As previously discussed, the clock genes have been implicated with glucose homeostasis and lipogenesis, and a

dysfunctional clock, caused as a result of jet lag, shift work (Bescos et al. 2018) or as a result of mutations to circadian genes has been linked to metabolic syndrome (Jagannath et al. 2017). Furthermore, there is increasing evidence supporting a role for amplitude enhancement being beneficial for development of metabolic disorders. One key study in support of that was the work done by He and colleagues (He et al. 2016). In this study, the small molecule nobiletin was shown to significantly enhance circadian gene expression and restore dampened rhythms in clock-mutant heterozygous mouse fibroblasts and simultaneously protect mice fed high-fat diet from obesity and symptoms of metabolic syndrome in a *Clock*-dependent mechanism. Interestingly, Linopirdine's metabolic phenotype in adipocytes resembles reported *in vitro* actions of nobiletin, which, similar to Linopirdine, has been shown to increase glucose uptake in 3T3-F442A adipocytes (Onda et al. 2013) and promote adipogenesis and lipolysis in 3T3-L1 cells (Saito, Abe, and Sekiya 2007), which proposes potential beneficial metabolic outcomes of Linopirdine treatment.

Our findings also proposed HIF stabilisation and mRNA expression as a key outcome of Linopirdine treatment, which plays a central role in its amplitude enhancing effects of *Bmal1*-promoter expression (Chapter 4). In obesity, adipocyte hypertrophy, together with reduced adipose tissue vascularisation, leads to zones of adipose tissue hypoxia (Pasarica et al. 2009), which is believed to cause adipose tissue dysfunction in obesity (Hosogai et al. 2007) and has been shown to compromise adipocyte insulin sensitivity (Regazzetti et al. 2009). In fact, contrary to what amplitude enhancement is hypothesized

to do, intermittent hypoxia (IH) has been associated with worsened metabolic outcomes. Several animal studies have shown exacerbation of obesity induced metabolic dysfunction, such as hyperinsulinemia and impaired glucose tolerance, in both diet-induced obese and leptin-deficient mice by IH (Polotsky et al. 2003; Drager et al. 2011). Similar observations were also seen clinically in healthy volunteers , where an acute protocol of 5 hour IH was associated with impaired insulin sensitivity, independent of compensatory insulin secretion (Louis and Punjabi 2009). Furthermore, *in vivo* inhibition of HIF1α pharmacologically (Sun et al. 2013) or using antisense oligonucleotides (Shin et al. 2012) have been associated with significant reduction in weight gain and hyperglycaemia associated with HFD, stressing that overall *in vivo* elevation of HIF could have detrimental effects on metabolic parameters. With a half-life of 3.2 hours and its validated action via HIF, we hypothesized Linopirdine could mimic intermittent hypoxia *in vivo*. However, given Linopirdine also potently promoted enhancement of peripheral circadian clocks, this begged the question: which pathway has a more pronounced effect *in vivo*, mimicking hypoxia via HIF induction, or increasing amplitude of clock genes via MEIS1 and HIF1α?

In line with our interest in metabolic disorders and for the purpose of understanding which downstream pathway holds stronger *in vivo* influence on Linopirdine's actions, we aimed to investigate Linopirdine's effects in a diet-induced obesity (DIO) mouse model, which is the closest representative model corresponding to environment-induced obesity and MetS, independent of genetic factors. Furthermore, investigating

Linopirdine's *in vivo* effects and comparing them to the data from our *in vitro* screens could shed light on the translatability of our adipocyte *in vitro* screening assays, and help pinpoint which *in vitro* phenotype could be the strongest predictor of metabolic benefit in a DIO-model of metabolic syndrome.

5.2 Results:

5.2.1 Acute treatment of Linopirdine in vivo reduces blood glucose levels

To begin with, we wanted to validate Linopirdine's metabolic effects *in vivo*. To do that, mice were administered Linopirdine for 3 hours, and their blood glucose levels were quantified. As predicted by our *in vitro* assay, Linopirdine significantly reduced fasting blood glucose levels (Figure 5.1A, *5 hour fasting*: vehicle: 11.9±1 Linopirdine: 9.4±1.03 mmol/L, $p<0.05$; *16hour fasting*: vehicle: 7.7±1.2, Linopirdine :6.06±0.6 mmol/L, $p<0.05$). Linopirdine also showed a significant decrease in glucose levels at t=0 (following 16hour fast) and t=15 min (Figure 5.1B), however, displayed no significant effect on glucose tolerance (Figure 5.1B) or on insulin tolerance (Figure 5.1C) following a glucose or insulin challenge, respectively, as represented by the area under curve (AUC) of glucose concentration vs time. This suggested an increase in glucose uptake induced by Linopirdine, without affecting insulin sensitivity in normoglycemic mice, which is reflective of the increase in glucose uptake observed in our *in vitro* assays (Figure 3.10C).

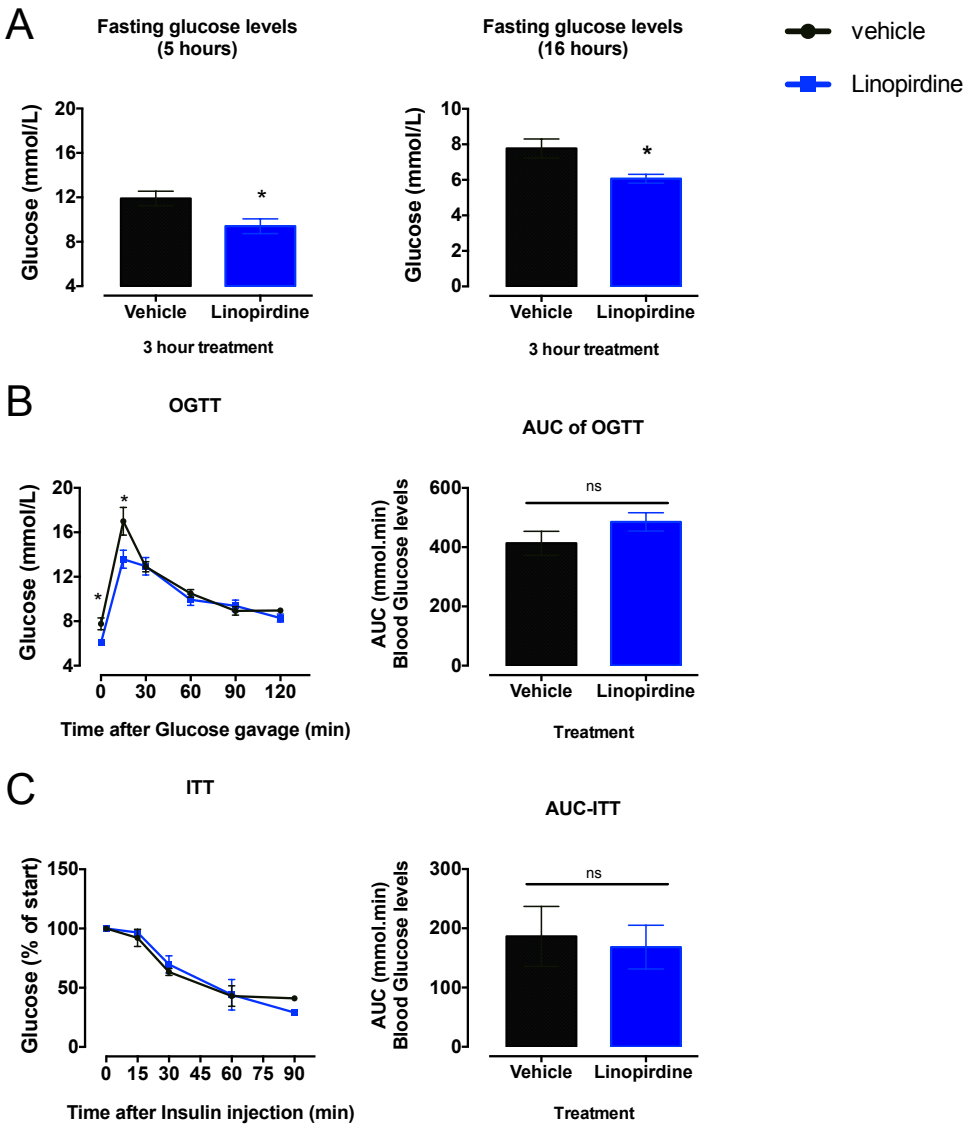


Figure 5.1 Linopirdine reduces fasting blood glucose levels *in vivo:*
A) C57BL/6 mice were fasted for 5 (left, N=3) and 16 hours (right, N=6) and then treated with Linopirdine (7.5mg/kg, blue) or vehicle (black) and blood glucose levels were quantified 3 hours later. **(B)** Oral glucose tolerance test (OGTT) following 3 hour Linopirdine or vehicle treatment (left) and its corresponding quantification represented as area under the curve (right), N=6 (internally controlled). **(C)** Insulin tolerance test (ITT) following 3 hour Linopirdine or vehicle treatment (left) and its corresponding quantification represented as area under the curve (right), N=3 (internally controlled).Error bars represent ±SEM.

5.2.2 Linopirdine exacerbates metabolic syndrome in DIO-mouse model

To investigate how Linopirdine affects development of metabolic disorder and in order to understand its *in vivo* effects, we endeavoured on a 10-week high-fat diet (HFD, 60% Kcal fat) feeding regimen alongside daily administration of Linopirdine or vehicle in C57BL/6 mice. Such feeding protocol is well-documented and widely used to promote significant weight gain and development of key hallmarks of metabolic disorder, such as glucose tolerance, insulin resistance, hyperlipidaemia and hypercholesterolemia (He et al. 2016). To eliminate experimental bias and to validate our findings, a third group was fed normal matched low fat control diet (balanced calories). This was used as an additional control alongside HFD fed mice receiving daily dose of the vehicle.

As predicted, mice on HFD developed worsened metabolic parameters and showed hallmarks of metabolic syndrome. Compared to Diet-control, mice on HFD exhibited significant weight gain (Figure 5.2A,B), worsened insulin resistance as evaluated using the homeostasis model assessment (Figure 5.2C, [HOMA; fasting insulin μU/mL x fasting glucose (mM)/22.5 (see (Matthews et al. 1985)]), impaired glucose and insulin tolerance (Figure 5.2D, E), and had higher levels of plasma total cholesterol, non-esterified free fatty acids (NEFA) and blood glucose levels (Figure 5.2F). Moreover, mice on HFD also showed higher lipid accumulation in liver (Figure 5.3A, B), suggestive of non-alcoholic fatty liver disease (NAFLD).

Strikingly, compared to vehicle-treated mice on HFD, Linopirdine significantly worsened most metabolic parameters. Linopirdine exacerbated weight gain from HFD (Figure 5.2 A,B *Week 10*; Linopirdine HFD: 41.6±3.5, vehicle HFD: 37.4±3.7, Diet-control: 28.9±2.3 g) without affecting glucose tolerance (Figure 5.2D). Moreover, Linopirdine significantly worsened insulin sensitivity (Figure 5.2E; Linopirdine HFD: 158.4±53.7, vehicle HFD: 285.1±95.9, Diet-control: 523.0±152.2 mmol.min) and also increased overall plasma insulin levels (Figure 5.2F; Linopirdine HFD:7.3±2.6, vehicle HFD: 3.18±0.93, Diet-control: 3.37±1.7) and increased HOMA index (Figure 5.2C; Linopirdine HFD: 1.83±1.09, vehicle HFD: 0.57±0.14 , Diet-control: 0.39± 0.1), suggesting exacerbated insulin resistance. Interestingly, compared to vehicle treated mice on HFD, Linopirdine reduced total cholesterol levels in plasma, without affecting NEFA and fasting glucose levels (Figure 5.2E, *Serum total cholesterol levels*; Linopirdine HFD: 475.3±112.8, vehicle HFD: 569.2±68.5, Diet-control: 235.1±34.9). Finally, plasma triglycerides in all three groups were similar (Figure 5.2E, ns). Taken together, these findings support an overall impairment in metabolic profile following Linopirdine treatment.

Furthermore, looking at the liver, Linopirdine significantly worsened the onset of hepatic steatosis on HFD. As reported by many studies (Eccleston et al. 2011; He et al. 2016), 10 weeks of HFD induces significant increase in hepatic lipid content in vehicle treated mice relative to diet-control mice. Interestingly, when compared to vehicle treated mice on HFD, Linopirdine significantly increased lipid accumulation in the liver (Figure 5.3A, B; Linopirdine HFD: 46.3±9.7%, vehicle HFD: 20.3±6.3%, Diet-control: 2.5±1.46%) and

increased liver weight (Figure 5.3C; Linopirdine HFD: 0.08±0.01, vehicle HFD: 0.068±0.01, Diet-control: 0.065±0.007 g/mm), hence exaggerating the manifestation of hepatic steatosis. This was likely due to a Linopirdine-induced increase in adipogenic profile of the liver, as indicated by the increase in fatty acid synthase (FASN) (Figure 5.3E; Linopirdine HFD: 0.012±0.003, vehicle HFD: 0.006±0.001, Diet-control: 0.005±0.002) and Peroxisome-proliferator-activated receptor y (PPARy) mRNA expression (Figure 5.3F; Linopirdine HFD: 0.002±0.0008, vehicle HFD: 0.001±0.0004, Diet-control: 0.0003±0.0001). Furthermore, Linopirdine also significantly enhanced platelet glycoprotein 4 (CD36) mRNA relative to its HFD control (Figure 5.3D), which indicates increase in lipid uptake by the liver (Figure 5.3D, Linopirdine HFD: 0.0098±0.003, vehicle HFD: 0.0048±0.002, Diet-control: 0.0014±0.0002), thus further contributing to the observed phenotype. On another note, Linopirdine significantly reduced DBP (named for albumin gene D-site binding protein) mRNA expression compared to both control groups (Figure 5.3G, Linopirdine HFD: 0.0066±0.003, vehicle HFD: 0.01±0.004, Diet-control: 0.011±0.003), which is a key output of the circadian clock that drives a multitude of downstream genes and clock outputs (Stratmann et al. 2012; Wuarin et al. 1992), therefore proposing possible alterations of liver clock function.

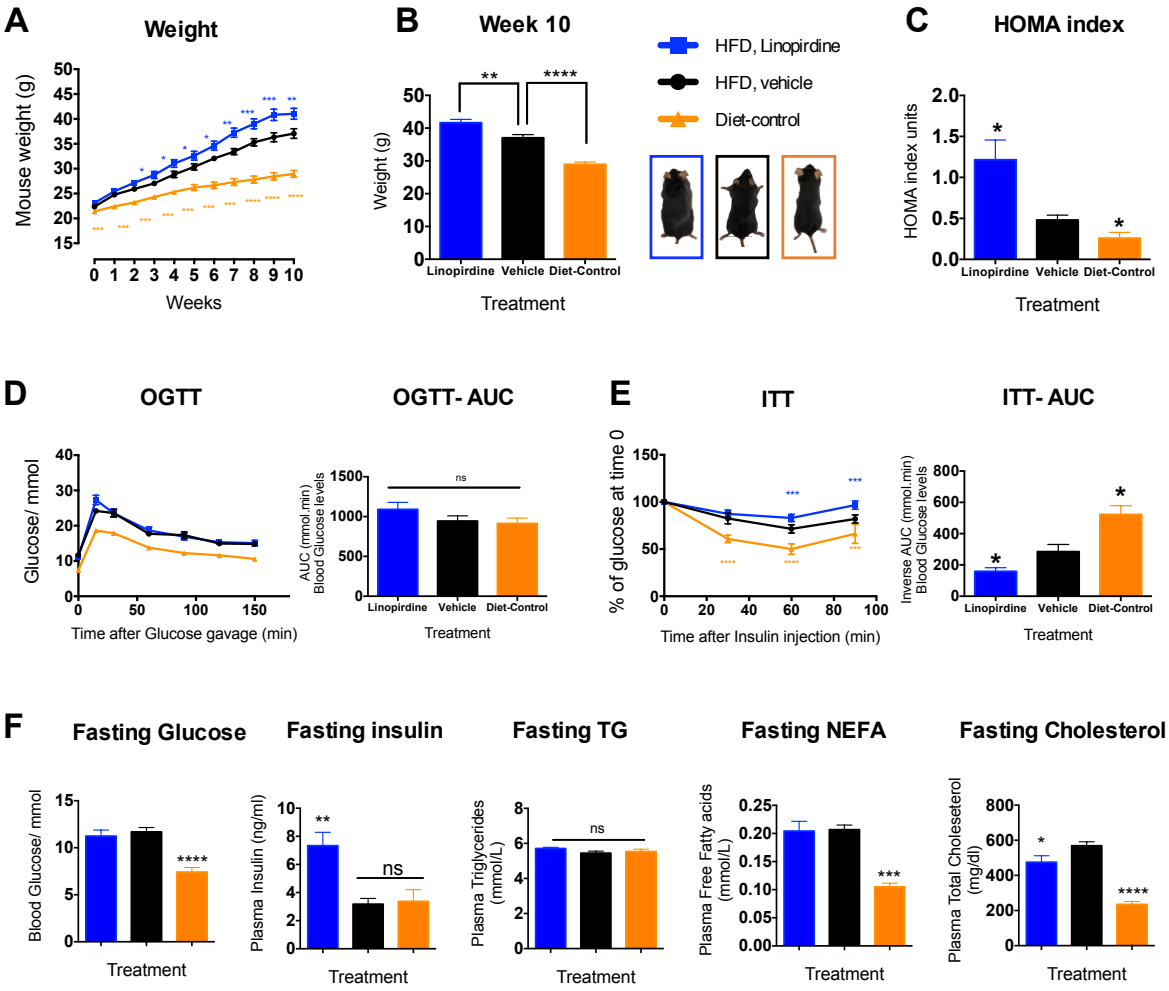


Figure 5.2. Linopirdine exacerbates metabolic syndrome in DIO-mouse model:
(A) Average body weight of C57BL/6 mice fed either high fat-diet and treated with vehicle (black) or Linopirdine (blue) (N=16) or fed diet-control (orange, N=12) for 10 weeks. **(B)** Average body weight and representative images at week 10 **(C)** HOMA index of insulin resistance. **(D)** Oral glucose tolerance test (OGTT) at week 10 and its corresponding quantification represented as area under the curve (right). **(E)** Insulin tolerance test (ITT) (left) and its corresponding quantification represented as area under the curve (right). **(F)** Quantification of fasting plasma total cholesterol, free fatty acids, triglycerides, blood glucose and plasma insulin levels at week 10.
Error bars represent ±SEM. *p<0.05, **p<0.01, ***p<0.001,****p<0.0001 Diet control and Linopirdine HFD vs vehicle HFD.

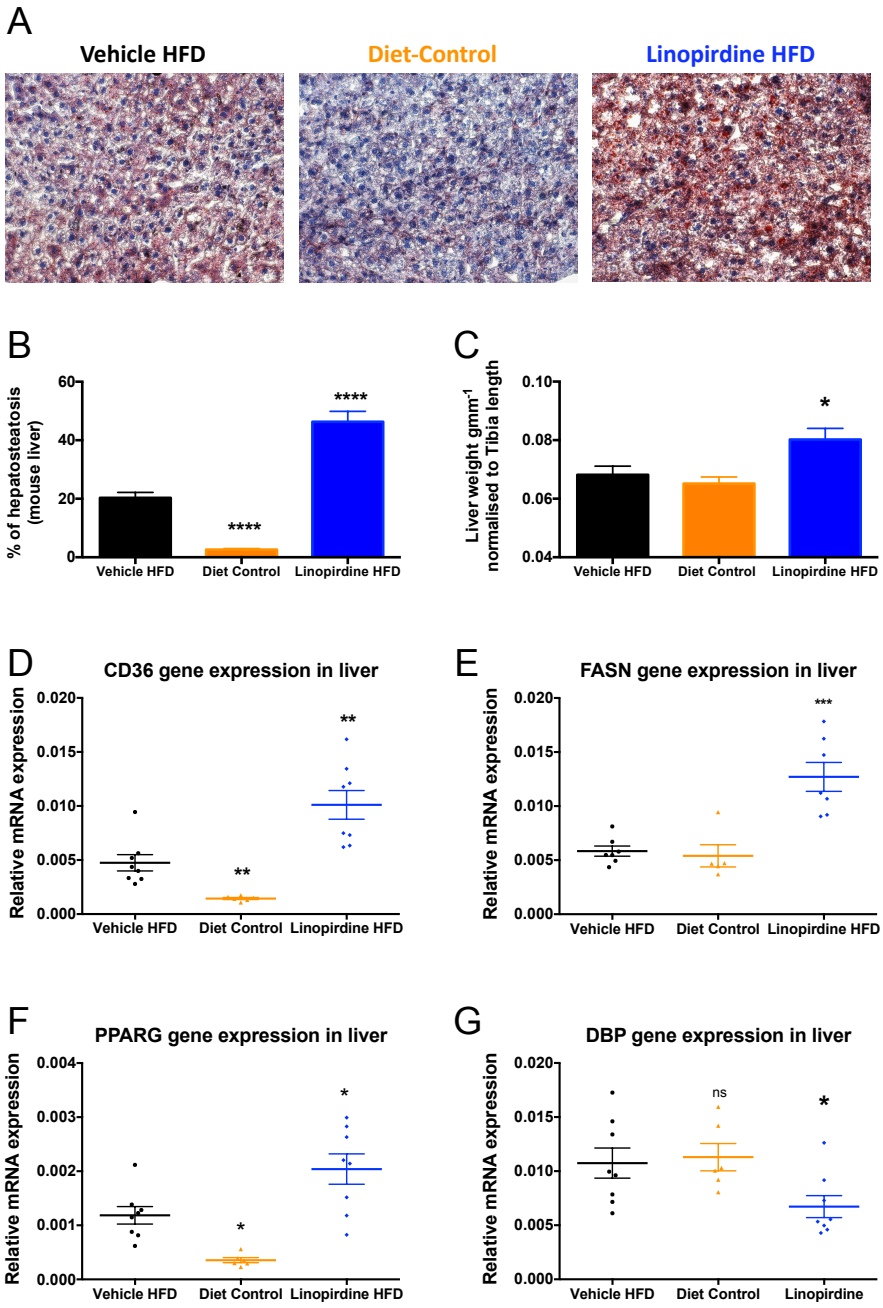


Figure 5.3. Linopirdine treatment exacerbates development of fatty liver in DIO-mouse model:**(A)** Oil Red-O staining of liver tissue following 10 weeks of HFD or diet-control. **(B)** Corresponding quantification of hepatosteatosis as percentage of lipid droplets accumulation in liver (N=8-12) **(C)** Liver weight (N=12-16). Relative mRNA expression of **(D)** *CD36*, **(E)** *FASN*, **(F)** *PPARG* and **(G)** *DBP* in liver, all genes normalised to *18S* and *Nono* housekeeping genes. *CD36:* platelet glycoprotein 4 , *FASN:* fatty acid synthase, *PPARG*: peroxisome proliferator-activated receptorsγ and *DBP*: D site of albumin promoter (albumin D-box) binding protein. Error bars represent ±SEM. *p<0.05, **p<0.01, ***p<0.001,****p<0.0001 Diet control and Linopirdine HFD vs vehicle HFD.

5.2.3 Linopirdine reduces XBP1s mRNA expression in hypothalamus:

When examining the feeding behaviour of our different groups, the diet-control group predictably consumed lower calories per day compared to the HFD-control group, however, Linopirdine showed significant increase in overall food consumption (Figure 5.4A), without a change in overall energy efficiency following 8 weeks of HFD, represented as weight gain per Kcal (Figure 5.4B, ns). This proposed that Linopirdine promoted weight gain without affecting energy expenditure or nutrient absorption.

As a result, this led us to hypothesize a possible onset of leptin resistance associated with this observed phenotype. Quantification of leptin mRNA in visceral fat showed no change in the Linopirdine treated group (Figure 5.5). Moreover, endoplasmic reticulum (ER) stress, defined as the imbalance between the load of unfolded proteins and the capacity of the ER to handle them, has been strongly coupled with leptin resistance as a result of diet-induced obesity (Lee et al. 2016; Ozcan et al. 2009). The long-term adaptation to ER stress entails a transcriptional increase in ER-protein folding machinery, in order to increase the capacity of the ER to handle the overload. Indeed, vehicle treated group on HFD displayed a significant increase in ER-stress markers like Heat Shock Protein Family A (Hsp70) Member 1A (HSPA1A) (Figure 5.6A) in the hypothalamus relative to Diet-control, without affecting expression of the pro-apoptotic DNA damage-inducible transcript 3 (Ddit3) (Figure 5.6C), also referred to as CCAAT/enhancer-binding protein-homologous protein (CHOP). However, Linopirdine showed XBP1s mRNA levels similar to diet control, and significantly lower than vehicle-treated HFD group, suggesting

decreased ER stress within the hypothalamus (Figure 5.6B). Taken together, these findings point away from leptin resistance.

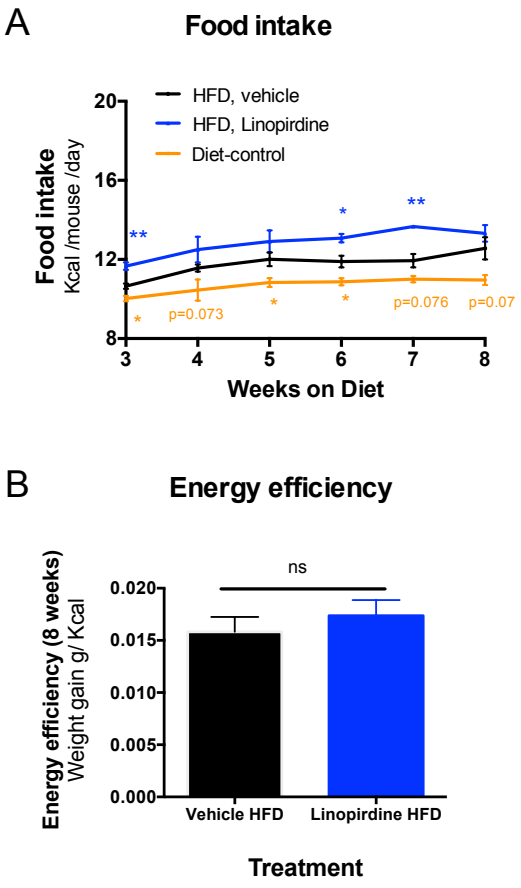


Figure 5.4. Linopirdine increases food intake without affecting energy efficiency of DIO-mice:

(A) Food intake of C57BL/6 mice fed HFD and treated with Linopirdine or vehicle or fed Diet-control over a period of 6 weeks

(B) Energy efficiency of mice over 8 weeks of HFD and daily treatment with vehicle or Linopirdine. N= 12-16. Error bars represent ±SEM. *p<0.05, **p<0.01, Diet control and Linopirdine HFD vs vehicle HFD.

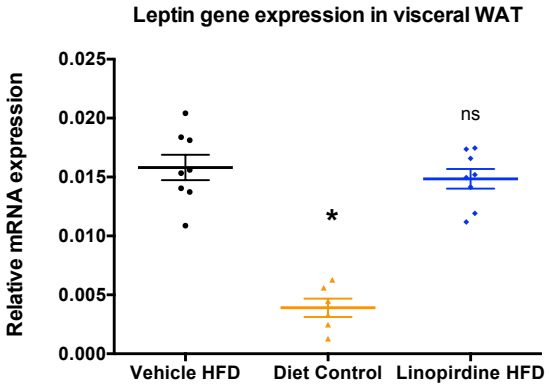


Figure 5.5. Linopirdine has no effect on Leptin expression in visceral WAT in DIO-mouse model:

Relative mRNA expression of *leptin* in visceral WAT after 10 weeks of HFD or diet-control and daily vehicle or Linopirdine gavage, normalised to *18S* and *Nono* housekeeping genes. Error bars represent ±SEM. *p<0.05, Diet control and Linopirdine HFD vs vehicle HFD.

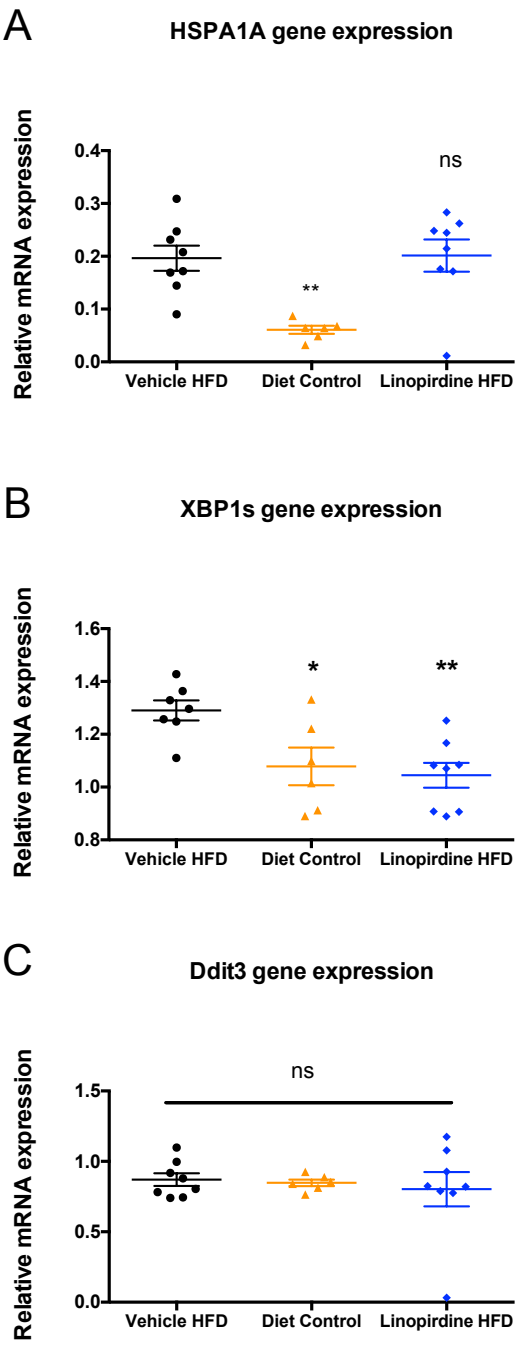


Figure 5.6. Linopirdine reduces HFD induced expression of ER-stress responsive gene Xbp1s:

Relative mRNA expression of markers of ER-stress in the PVN after 10 weeks of HFD or Diet control and daily vehicle or Linopirdine gavage.

(A) *HSPA1A*: Heat Shock Protein Family A (Hsp70) Member 1A

(B) *XBP1s*: spliced X-box binding protein 1

(C) *Ddit3*: DNA damage-inducible transcript 3, also referred to as CCAAT/enhancer-binding protein-homologous protein (CHOP).

All normalised to *β-Actin* and *GusB* housekeeping genes. Error bars represent ±SEM. *p<0.05,**p<0.01 Diet control and Linopirdine HFD vs vehicle HFD.

.

5.2.4 Linopirdine reduces markers of insulin sensitivity in visceral fat and liver, but significantly improves them in skeletal muscles:

To understand the mechanistic changes underlying the observed insulin resistance following *in vivo* Linopirdine treatment, we investigated changes in key candidates of glucose uptake and insulin responses in different tissues.

Interestingly, in the liver, Linopirdine worsened insulin responses (Figure 5.7). Although HFD on its own showed no change in insulin receptor substrate (*IRS*) 1 and 2 mRNA expression or *Glut1* and *Glut4* expression compared to diet control, Linopirdine significantly reduced relative mRNA expression of *IRS1* (Figure 5.7A, vehicle HFD: 0.32±0.1, Diet-control: 0.29±0.06 , Linopirdine HFD: 0.19±0.053, $x10^{-3}$)and *Glut4* (Figure 5.7D; vehicle HFD: 5.69±2.48, Diet-control: 7.078±4.34, Linopirdine HFD: 2.53±1.98, $x10^{-5}$) and showed a trend in *IRS2* reduction as well (Figure 5.7B; vehicle HFD: 3.8±2.88, Diet-control: 3.8±0.60, Linopirdine HFD: 1.6±0.68, $x10^{-3}$, *vehicle HFD vs Linopirdine HFD p=0.08, student t-test*). This suggested significant worsening in the liver's insulin response following chronic Linopirdine treatment.

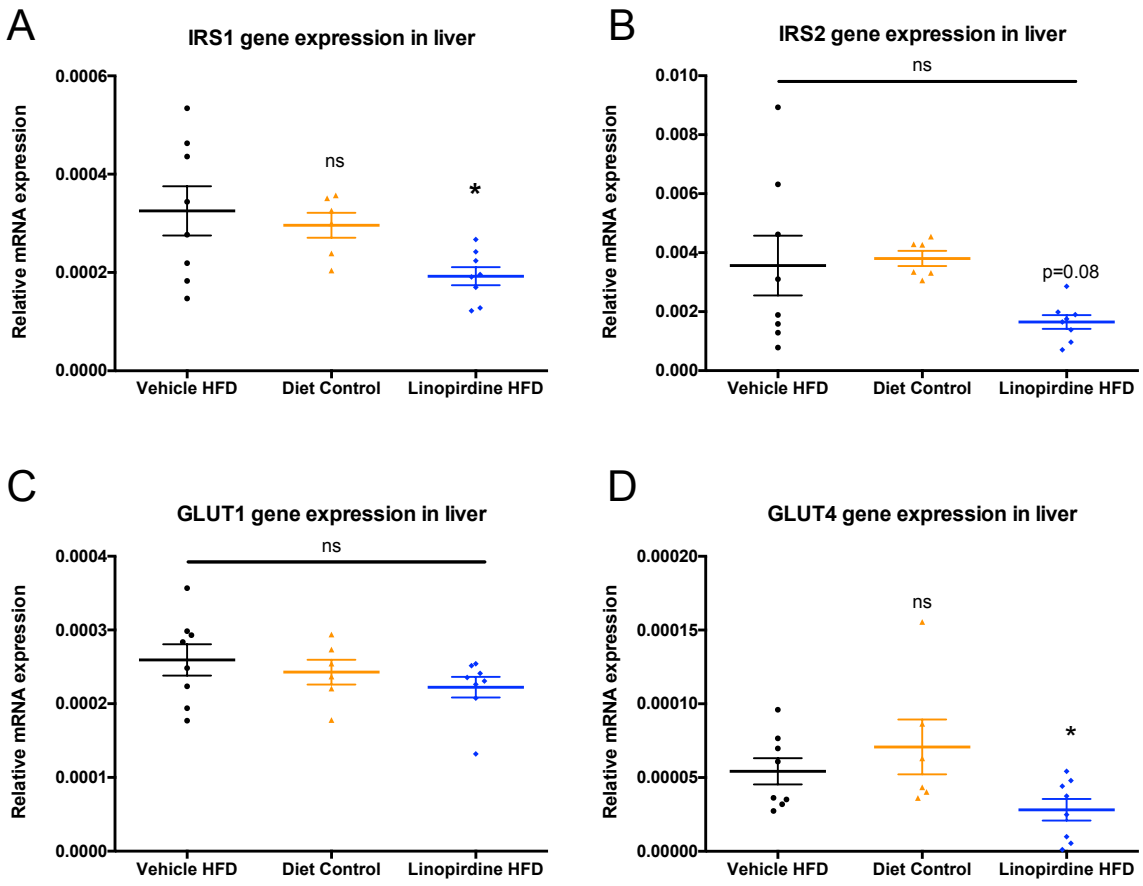


Figure 5.7. Linopirdine reduces markers of insulin sensitivity in liver of DIO-mice: Relative mRNA expression of markers of insulin resistance in liver after 10 weeks of HFD or Diet control and daily vehicle or Linopirdine gavage. **(A)** *IRS1:* Insulin receptor substrate 1. **(B)** *IRS2*: Insulin receptor substrate 2. **(C)** *GLUT1.* **(D)** *GLUT4*. All normalised to *18S* and *Nono* housekeeping genes. Error bars represent ±SEM. *p<0.05 Diet control and Linopirdine HFD vs vehicle HFD.

In visceral white adipocyte tissue (WAT), HFD on its own significantly reduced *IRS1* (Figure 5.8A; vehicle HFD: 13.35±5.15, Diet-control: 27.38±4.57) and *Glut4* (Figure 5.8D; vehicle HFD: 47.05±22.46, Diet-control: 106.05±44.99) mRNA expression compared to diet-control and increased *Glut1* expression (Figure 5.8C; vehicle HFD: 57.32±28.8, Diet-control: 31.57±13.2), suggesting reduced insulin sensitivity. Similar findings were observed in Linopirdine treated mice on HFD, which also worsened *Glut1* (Figure 5.8C; Diet-control: 31.57±13.2, Linopirdine HFD: 66.35±30.3, $x10^{-5}$) and *Glut4* (Figure 5.8D; Diet-control: 106.05±44.99, Linopirdine HFD: 30.6±13.1, $x10^{-5}$) compared to diet-control, but also significantly reduced *IRS1* mRNA expression compared to its vehicle control (Figure 5.8A, vehicle HFD: 13.35±5.15, Linopirdine HFD: 8.5±2.55, $x10^{-5}$), thus suggesting further deterioration of HFD-induced adipocyte insulin intolerance following Linopirdine treatment. *IRS2* mRNA expression was unchanged in all treatments (Figure 5.8B).

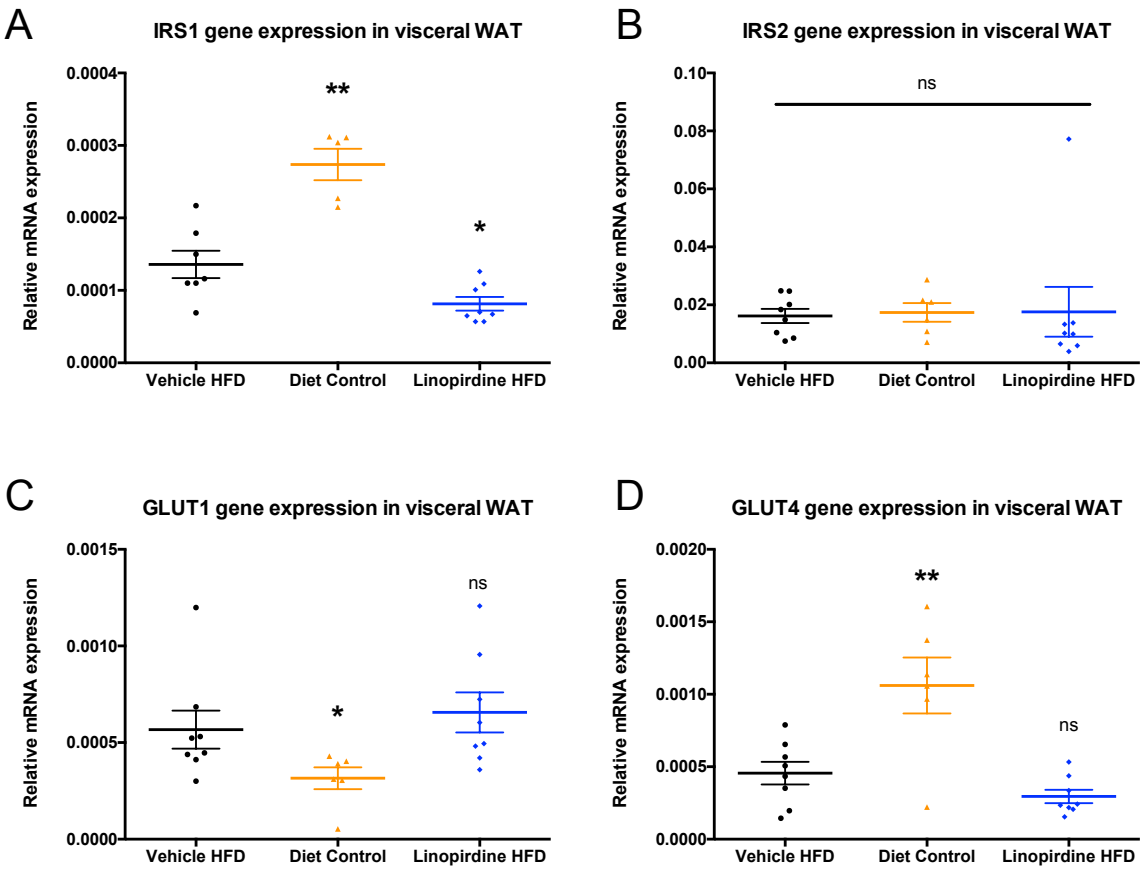


Figure 5.8. Linopirdine reduces IRS1 mRNA expression in visceral WAT of DIO-mice:
Relative mRNA expression of markers of insulin resistance in visceral WAT after 10 weeks of HFD or Diet control and daily vehicle or Linopirdine gavage. **(A)** *IRS1:* Insulin receptor substrate 1. **(B)** *IRS2*: Insulin receptor substrate 2. **(C)** *GLUT1.* **(D)** *GLUT4*. All normalised to *18S* and *Nono* housekeeping genes. Error bars represent ±SEM. *p<0.05,**p<0.01 Diet control and Linopirdine HFD vs vehicle HFD.

Interestingly, in skeletal muscles, Linopirdine showed significant improvement in markers of insulin responses. Unlike the vehicle control on HFD which significantly reduced markers of glucose uptake and insulin sensitivity like *IRS1, IRS2, Glut1*, *Glut4* and *INSR* (insulin receptor), Linopirdine treated DIO-mice showed significant increase in mRNA expression of these markers similar to what is observed in the diet-control group (Figure 5.9A-E). Linopirdine also increased expression of glucokinase (*GCK*) compared to diet-control as well (Figure 5.9G: vehicle HFD: 122.8±18.5, Diet-control: 133.1±17.1, Linopirdine HFD: 194.7±32.1, $x10^{-5}$), the enzyme that catalyses the rate limiting step in glucose metabolism, all of which suggested significant improvement in skeletal muscle insulin sensitivity and reversal of HFD-induced insulin intolerance in this tissue following Linopirdine treatment. Taken together, our data indicates that the Linopirdine's mediated insulin resistance is predominantly driven by its effects on liver.

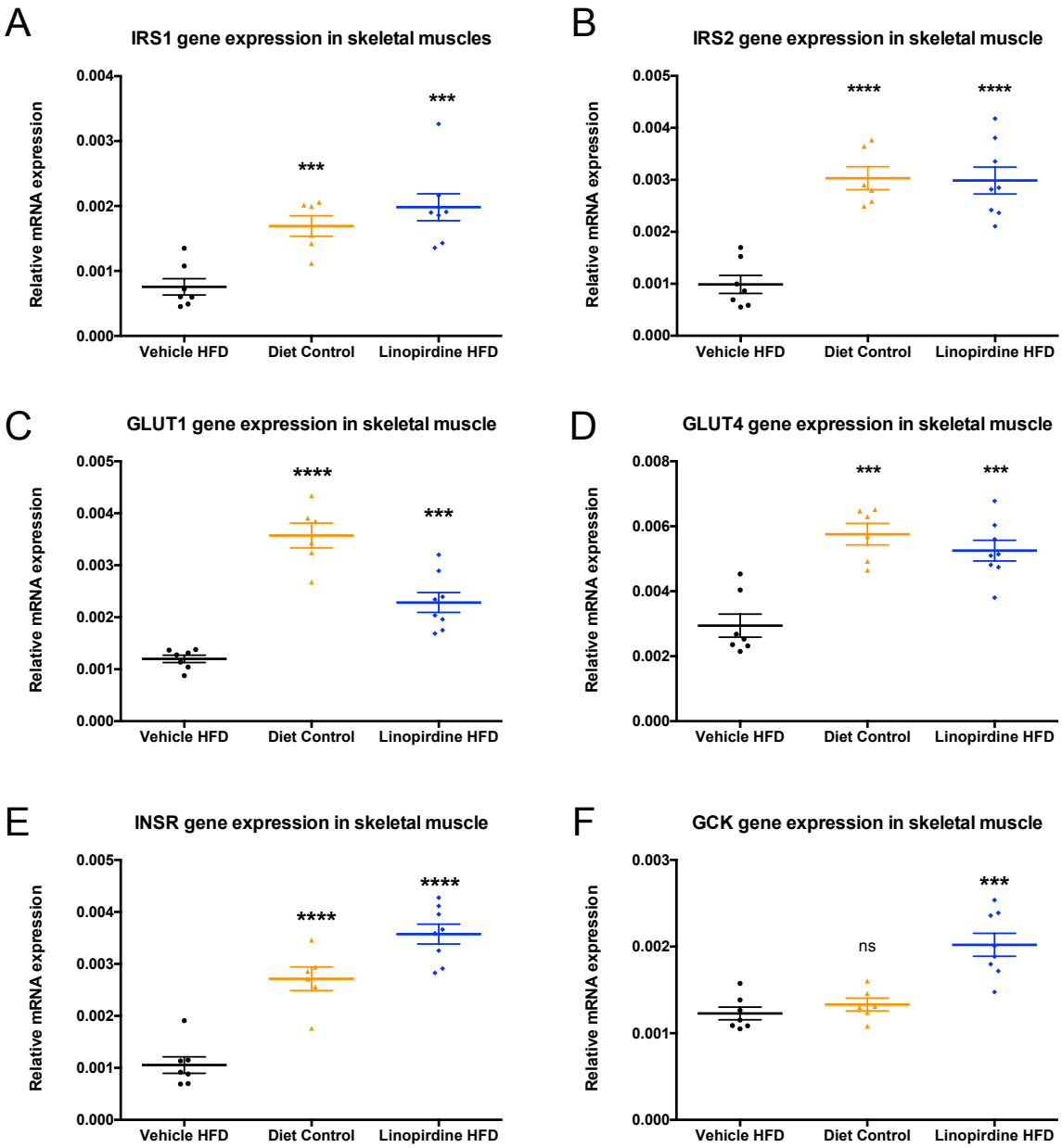


Figure 5.9. Linopirdine reverses HFD-induced reduction in markers of insulin sensitivity in skeletal muscles:
Relative mRNA expression of markers of insulin resistance in liver after 10 weeks of HFD or Diet control and daily vehicle or Linopirdine gavage. **(A)** *IRS1:* Insulin receptor substrate 1. **(B)** *IRS2*: Insulin receptor substrate 2 **(C)** *GLUT1.* **(D)** *GLUT4.* **(E)** *INSR:* Insulin receptor. **(F)** *GCK:* Glucokinase. All normalised to *18S* and *Nono* housekeeping genes. Error bars represent ±SEM. ***p<0.001,****p<0.0001 Diet control and Linopirdine HFD vs vehicle HFD.

5.2.5 Linopirdine exacerbates inflammation of visceral WAT in DIO-mice:

Adipocyte inflammation is a key hallmark of metabolic syndrome, characterized by secretion of inflammatory adipokines such as interleukin (IL-6), tumour necrosis factor-α (TNF-α), monocyte chemoattractant protein-1 (MCP-1), and resistin (Lafontan 2005) as well as a reduction in anti-inflammatory adipokine like adiponectin (AdipoQ) (Ouchi and Walsh 2007). In our study, 10 weeks of HFD showed no change in mRNA expression of IL6, MCP-1 or resistin (Figure 5.10A, C, E) in visceral WAT compared to diet-control, however significantly increased TNF-α (Figure 5.10B; vehicle HFD: 4.32±2.16, Diet-control: 1.24±0.74, Linopirdine HFD: 7.7±2.58, $x10^{-5}$) and reduced adiponectin expression (Figure 5.10D; vehicle HFD: 76.7±27.7, Diet-control: 135.6±39.4, Linopirdine HFD: 67.2±33.9, $x10^{-3}$). Linopirdine further increased TNF-α relative to vehicle HFD control without any changes to additional inflammatory markers (Figure 5.10B; vehicle HFD: 4.32±2.16, Linopirdine HFD: 7.7±2.58, $x10^{-5}$), suggesting potentially exacerbated adipocyte inflammatory response.

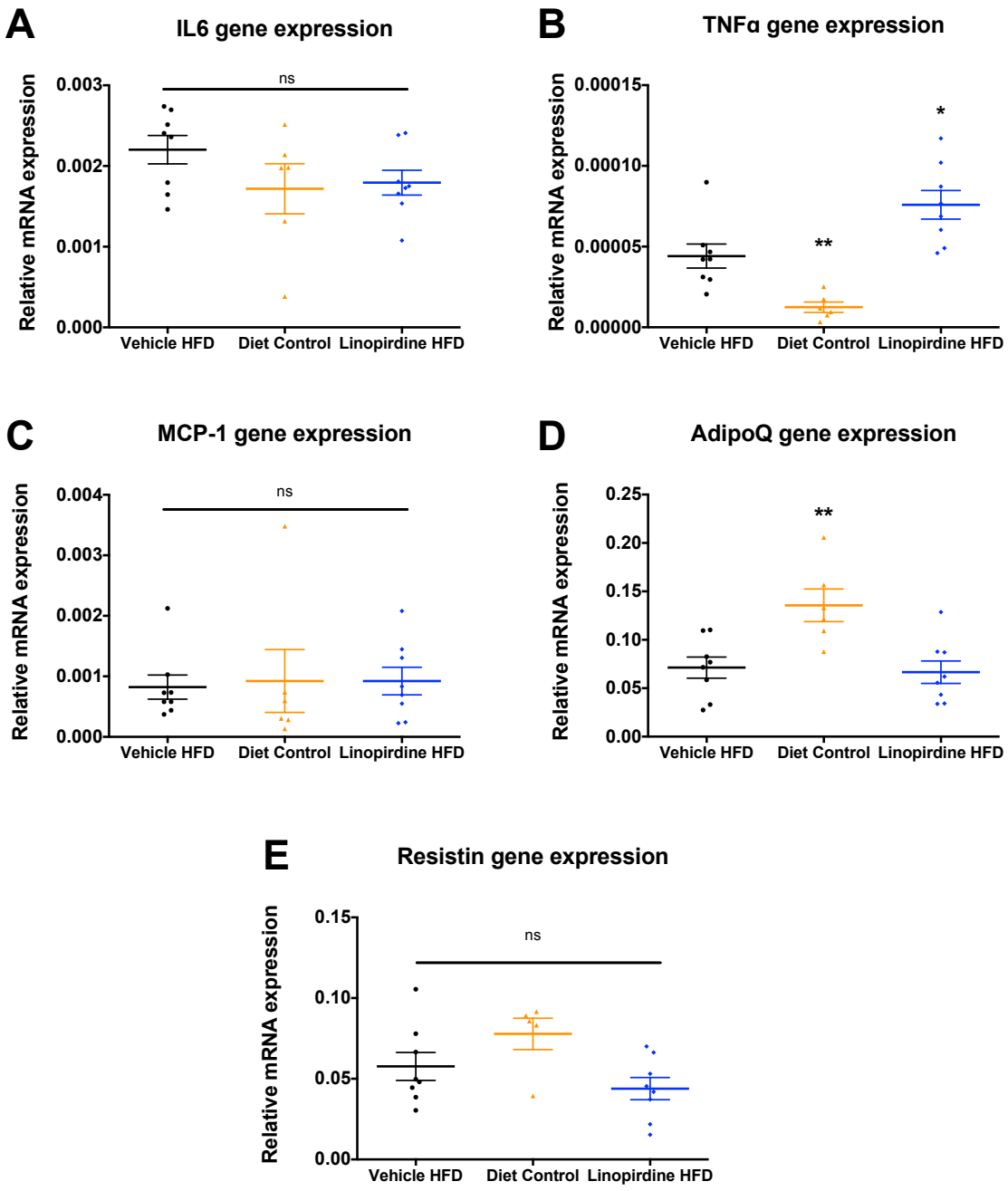


Figure 5.10. Linopirdine increases TNF α expression in visceral WAT of DIO-mice: Relative mRNA expression of markers of major inflammatory adipokines in visceral white adipose tissue after 10 weeks of HFD or Diet control and daily vehicle or Linopirdine gavage. **(A)** *IL6:* Interleukin 6 **(B)** *TNFα:* Tumour necrosis factor *α* **(C)** *MCP-1:* monocyte chemoattractant protein-1 **(D)** *AdipoQ:* Adiponectin **(E)** *Resistin.* All normalised to *18S* and *Nono* housekeeping genes. Error bars represent ±SEM. *p<0.05, **p<0.01, Diet control and Linopirdine HFD vs vehicle HFD.

5.2.6 Linopirdine treatment does not cause peripheral clock desynchrony:

Given Linopirdine shortened period in MEF PER::LUC cells (Figure 3.8) but increased it in *Per2*-d*Luc* U2OS (Figure 3.6) and 3T3L1 cells (Figure 3.7), we hypothesized that the worsened metabolic phenotype could be linked to circadian desynchrony. Therefore to investigate that, we tested Linopirdine's actions on the master clock using *ex-vivo* SCN cultures from PER2::LUC transgenic mice. SCN slices were synchronized and luminescence was monitored in real time for 2-4 days before Linopirdine or vehicle treatment. Linopirdine was administered at CT4-8 (subjective day) or CT 16-20 (subjective night). Interestingly, at both time points, Linopirdine showed no change in period or phase of SCN PER2 expression (Figures 5.11 and 5.12, respectively), suggesting that its main action lies in peripheral cells.

Following that, we then investigated whether *in vivo* administration of Linopirdine could affect phase of circadian clock in different tissues. To do that, Linopirdine was administered via gavage to PER2::LUC transgenic mice maintained under 12/12 hour light/dark (LD) cycles at ZT4. 3 hours later, *ex vivo* slices of SCN, lung and kidney were collected rapidly and their bioluminescence directly recorded in real-time in a plate reader. Representative traces for SCN, lung and kidney are shown in Figure 5.13A, B and C respectively. Interestingly, following phase analysis, attributed as the peak time from ZT0 (or lights on), Linopirdine showed no change in phase in any of the assessed tissues relative to vehicle (Figure 5.13D). This shows Linopirdine does not induce circadian desynchrony, and by extension fails to reject the null hypothesis.

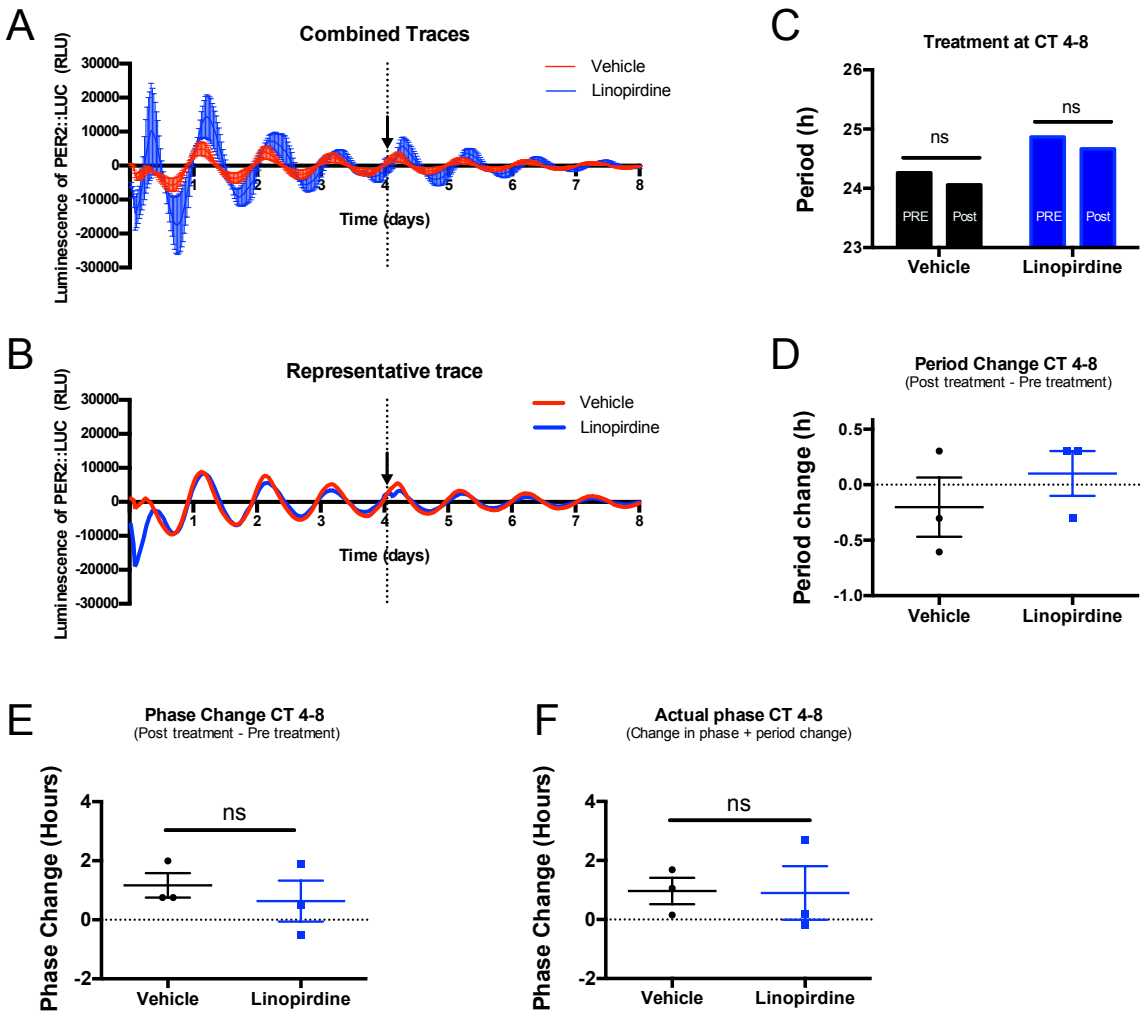


Figure 5.11. Linopirdine treatment of *ex-vivo* SCN slices at subjective day (~CT 4-8) causes no change in period or phase:
A) Combined bioluminescence traces for 3 SCN slices from PER2::LUC transgenic mice, treated with vehicle (red) or 10 µM Linopirdine (blue) at CT 4-8 (as pointed by arrow). (N=3). **B)** Representative bioluminescence traces for single trace showing lack of Linopirdine effect on SCN. **C)** SCN period (in hours) before (PRE) and after (post) vehicle or Linopirdine treatment **D)** Calculated period change (post treatment- pre treatment) **E)** Calculated phase change for vehicle and Linopirdine represented as post treatment-pre treatment. **F)** Actual phase, denoted as change in phase + period change, following vehicle and Linopirdine treatment.
Error bars represent ±SEM. N=3 (unless stated otherwise).

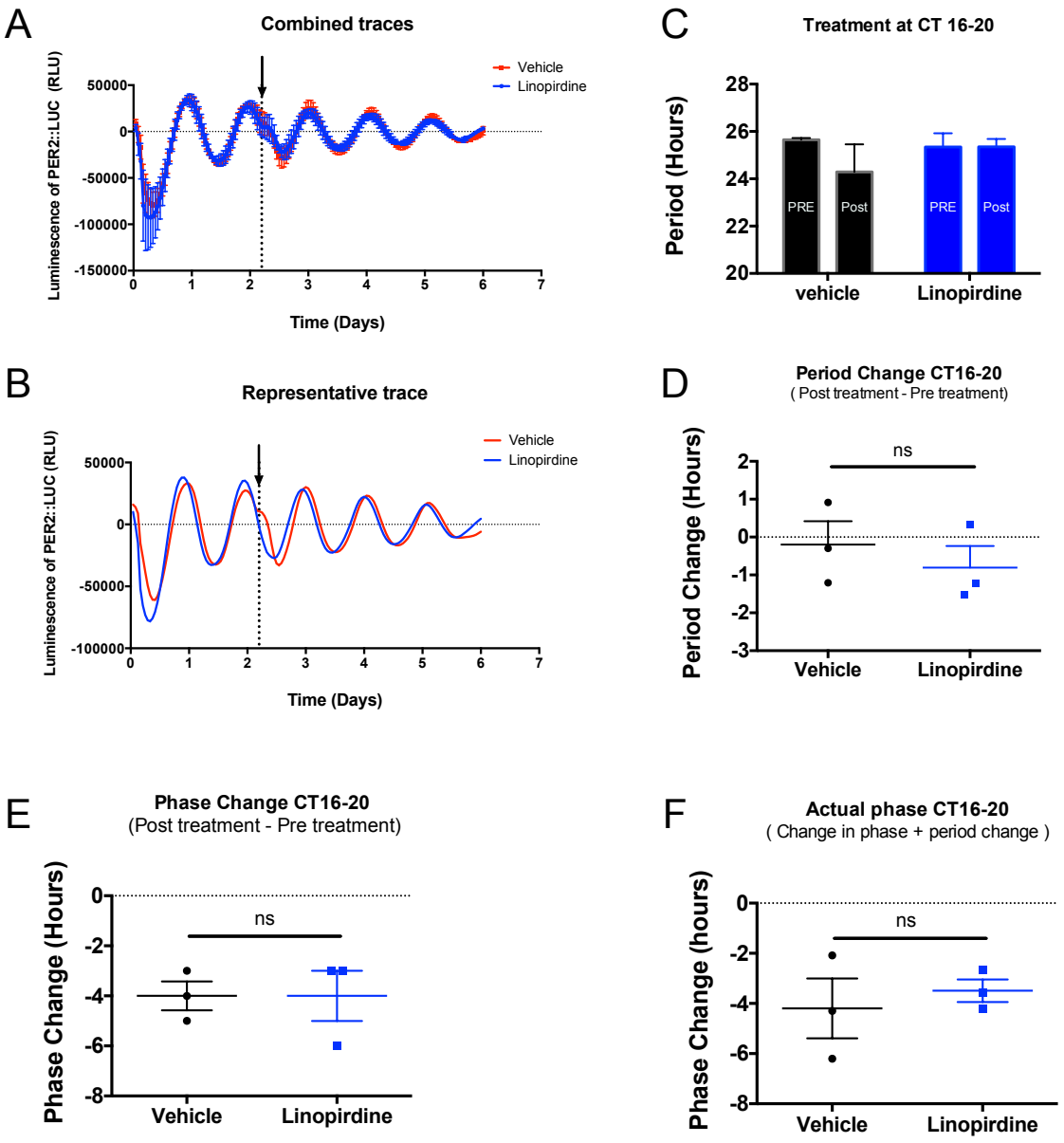


Figure 5.12. Linopirdine treatment of *ex-vivo* SCN slices at subjective day (~CT 16-20) causes no change in period or phase:
A) Combined bioluminescence traces for 3 SCN slices from PER2::LUC transgenic mice, treated with vehicle (red) or 10 µM Linopirdine (blue) at CT 16-20 (as pointed by arrow). (N=3) **B)** Representative bioluminescence traces for single trace showing lack of Linopirdine effect on SCN. **C)** SCN period (in hours) before (PRE) and after (post) vehicle or Linopirdine treatment **D)** Calculated period change (post treatment- pre treatment) **E)** Calculated phase change for vehicle and Linopirdine represented as post treatment- pre treatment. **F)** Actual phase, denoted as change in phase + period change, following vehicle and Linopirdine treatment. Error bars represent ±SEM. N=3 (unless stated otherwise).

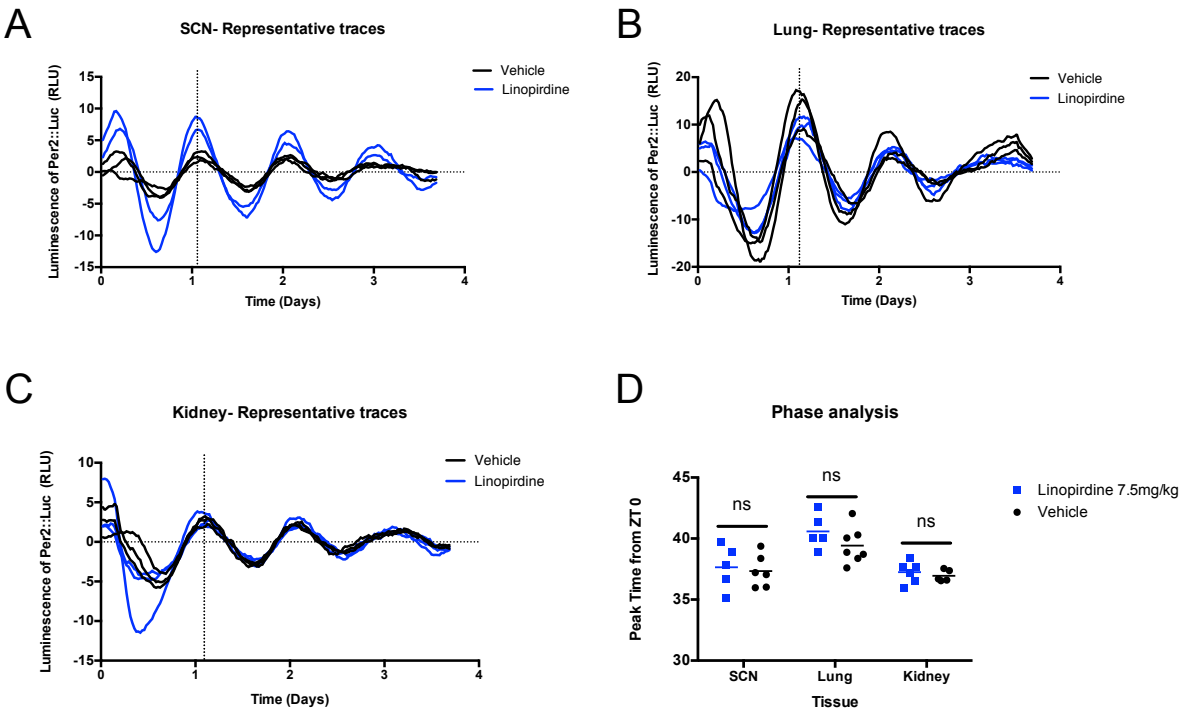


Figure 5.13. Acute *in vivo* administration of Linopirdine does not induce circadian misalignment:
Transgenic PER2::LUC mice housed at 12/12 LD cycles were gavaged with Linopirdine (7.5mg/kg, blue) or vehicle (black) at ZT4. 3 hours later, SCN, Lung and kidney were harvested, sliced, and relative bioluminescence was quantified in real time. Representative traces for technical replicates of SCN **(A)**, Lung **(B)** and Kidney **(C)** are shown. **(D)** Phase analysis following treatment was quantified, represented as peak time from ZT 0. N=5-7 biological replicates. Error bars represent ±SEM.

5.2.7 Linopirdine treatment increases markers of MEIS1 upregulation in different tissues:

Previous RNA-seq studies have reported a positive correlation between MEIS1 and mRNA expression of squalene epoxidase (SQLE), a key enzyme in cholesterol synthesis and a reported oncogene for NAFLD-induced hepatocellular carcinoma (Howe et al. 2017). In addition, a recent study by Liu et al showed that overexpression of MEIS1 has also been shown to induce squalene epoxidase (SQLE) mRNA and protein expression in two hepatic cell-lines LO-2 and HKCL-2 (Liu et al. 2018). Therefore, to investigate the role of MEIS1 in Linopirdine's *in vivo* effects, we quantified mRNA of SQLE in liver following Linopirdine treatment. Furthermore, to validate our *in vitro* investigation (Chapter 4) and explore the target effect of Linopirdine *in vivo,* we also quantified expression of HIF1α in the three main metabolic organs; muscle, liver and WAT. Indeed, following Linopirdine treatment, expression of HIF1α was significantly increased in WAT and skeletal muscle (Figure 5.14A, B) but remained unchanged in the liver (Figure 5.14C). Furthermore, Linopirdine treatment showed a trend of increase in SQLE mRNA expression in the liver (Figure 5.14D, student t-test p=0.07). Taken together, these findings support our *in vitro* findings, proposing Linopirdine upregulates MEIS1 and HIF1α *in vivo* as well.

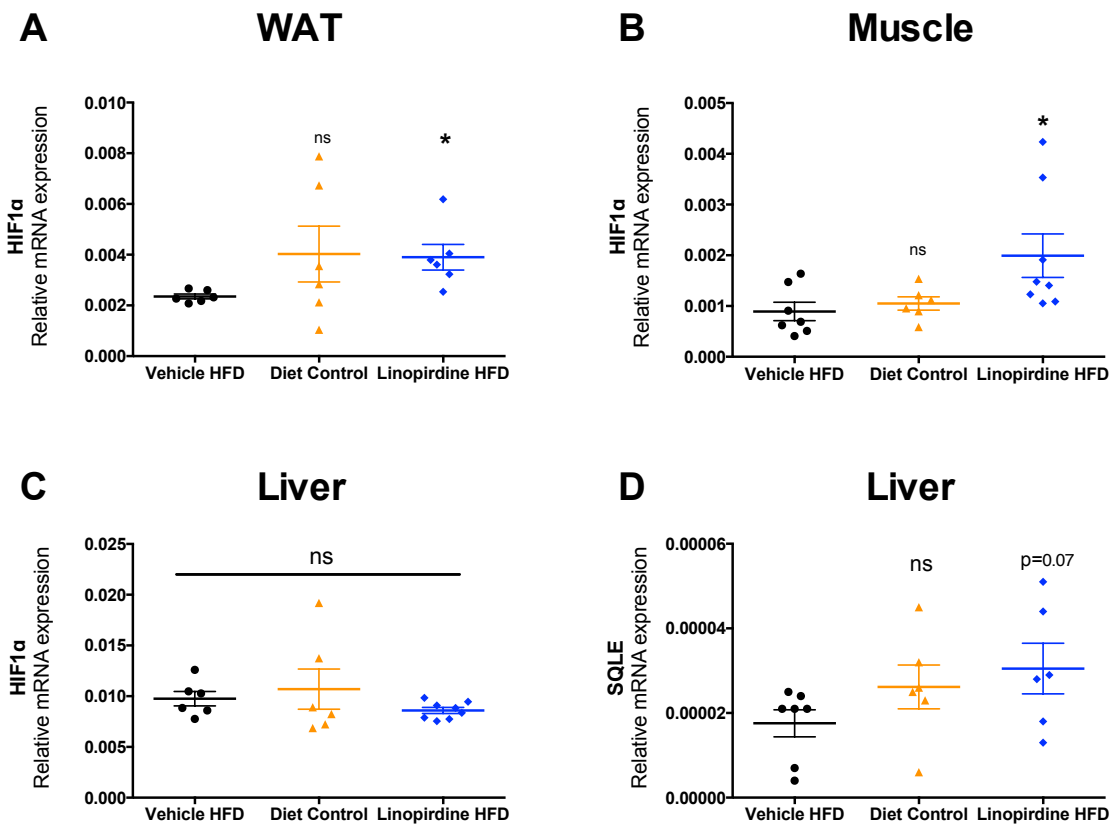


Figure 5.14. mRNA expression of MEIS1 markers in different tissues:
Relative mRNA expression after 10 weeks of HFD or Diet control and daily vehicle or Linopirdine gavage for *HIF1α* in **(A)** WAT**, (B)** skeletal muscle and, **(C)** liver, and for **(D)** *SQLE* (squalene epoxidase) in liver. All normalised to *18S* and *Nono* housekeeping genes. Error bars represent ±SEM. *p<0.05, Diet control and Linopirdine HFD vs vehicle HFD.

5.3 Discussion:

The goal of this study was to examine the *in vivo* effects of chronic Linopirdine treatment in a diet-induced mouse model of metabolic syndrome. Linopirdine exacerbated metabolic impairment associated with diet-induced obesity. On one hand, Linopirdine promoted hyperphagia (Figure 5.4) and significantly increased weight gain (Figure 5.2A). Linopirdine also worsened HFD-induced insulin resistance, as shown by an increase in insulin serum levels (Figure 5.2F), an increase in the HOMA index (Figure 5.2C) as well as impaired glucose reuptake following insulin injection (ITT) (Figure 5.2E) and also exacerbated progression of hepatic steatosis in this model (Figure 5.3 A-C).

Numerous dietary approaches and genetic models that induce/display metabolic syndrome have been reported. These include dietary approaches like high-fat, high sucrose, high fructose, and combination diets, or genetic models like leptin deficient (*ob/ob*) mice, leptin-receptor deficient (*db/db*) mice, Zucker fatty (ZF) rats and Zucker diabetic fatty (ZDF) rats (Wong et al. 2016). Although genetic mice models provide great insight into the pathogenesis of MetS associated with specific genetic factors, diet-induced obesity (DIO) animal models provide the closest representation for the mechanisms promoting obesity and MetS in humans, given one of the greatest drivers of MetS remains to be poor diet and lifestyle choices. These models therefore help investigate the role of diet, pathophysiology and aetiology of MetS. However, results could be discrepant based on diet compositions and animal model used, with different

diets offering distinct advantages and disadvantages (Nilsson et al., 2012). For example, the cafeteria diet is one feeding regime in which animals have a choice of several palatable energy-dense food items in addition to their standard non-purified chow (Rothwell and Stock 1988). This diet offers the advantage of being more similar to the human diet situation and shows a higher propensity of overeating than with predefined high-fat diets therefore inducing significant weight gain (Rothwell and Stock 1988). However, it is difficult to standardize nutritional content and deficiencies in protein or essential vitamins have been reported (Moore 1987). Similarly, the choice of mouse strain also plays a key role. For instance, mice strains like S5B/PI or A/J are resistant to diet-induced obesity (Nilsson et al. 2012), while C57BL6/J mice naturally develop obesity over their lifetime even on standard diets, which resembles what occurs in humans (Madsen et al. 2010; Surwit et al. 1995). Therefore, the choice of a standardized diet and the appropriate mouse strain is key. The modern human diet is generally composed of high levels of carbohydrates and fat. Based on work by Hu and colleagues, intake of dietary fat (not protein or sucrose) increased adiposity in mice (Hu et al. 2018). On the other hand, several studies have shown fructose in diet to be important in development of MetS, since it is associated with insulin resistance and leptin resistance as well that could lead to weight gain (Aydin et al. 2014; Sheludiakova, Rooney, and Boakes 2012). C57BL6/J mice on HFD, similar to what has been used in our study, have been well documented to display symptoms of metabolic syndrome including obesity, insulin resistance and hepatic steatosis (Chen, Zhang, and Huang 2010; He et al. 2016; Henderson et al. 2016), therefore providing an excellent model for understanding

development of metabolic syndrome. Furthermore, our *in vivo* data replicates previous findings using this DIO-model, thereby supporting the reproducibility of this model. In addition, our choice of diet (*refer to Methods*) consists of 20% Kcal protein, 60% fat and 20% carbohydrates, of which 7% is sucrose, and our data was analysed against a low fat diet-control with equivalent 20% protein and vitamin contents but with 10% fat and 70% carbohydrate content that is matched for sucrose levels. Therefore, this set up provides a well-controlled reproducible model that conveys effects of dietary fat intake on development of metabolic syndrome, focusing primarily on increased adiposity and controlling for sucrose and fructose contents. Consequently, this helps assess the effects of Linopirdine on development of MetS associated with increased adiposity in situations of positive energy balance.

Interestingly, our *in vivo* metabolic data was indeed in complete agreement with our *in vitro* studies demonstrating HIF1α upregulation and stabilisation being the primary mechanism for mediating the circadian effects of our drug. Firstly, similar to our *in vitro* findings, Linopirdine increased mRNA expression of HIF1α in both WAT and skeletal muscle (Figure 5.14A-B). Moreover, Linopirdine-induced insulin resistance was associated with a significant reduction in insulin-sensitivity markers in white adipose tissue (Figure 5.8), with a striking significant improvement in skeletal muscle insulin sensitivity (Figure 5.9). This is particularly interesting, given HIF overexpression in adipocytes and skeletal muscles has similar reported tissue-specific actions: 1) adipocyte-specific overexpression of HIF1α has been associated with increase in body

weight and insulin resistance (Halberg et al. 2009; Jun et al. 2017) while adipocyte-specific knockdown or dominant negative HIF1α overexpression have been linked to the opposite effects *in vivo* (Jiang et al. 2011; Krishnan et al. 2012; Sun et al. 2013; Lee et al. 2014). 2) Similar to Linopirdine, chronic hypoxia has been shown to increase insulin-stimulated glucose uptake in mouse skeletal muscles (Gamboa, Garcia-Cazarin, and Andrade 2011), and 3) HIF1α upregulation by hypoxia has been directly implicated in increase in insulin response and glucose uptake in skeletal muscles (Görgens et al. 2017). Thus, suggesting a strong correlation of HIF1α stabilisation with Linopirdine's observed effects.

The observed exacerbation of hepatic steatosis following Linopirdine treatment (Figure 5.3A-B) correlates with upregulation of HIF and MEIS1. Indeed, both HIF1α and HIF2α overexpression can induce hepatic steatosis. Evidence from disruption of VHL (Kucejova et al. 2011), PHD2 (Luo et al. 2018) or PHD3 (Minamishima et al. 2009) at the hepatocyte-level, all of which promote oxygen-independent upregulation of HIF1α and HIF2α, have been shown to promote onset of hepatic steatosis. In addition, while overexpression of hepatocyte HIF1α significantly exaggerates ethanol-induced hepatic steatosis, targeted HIF1α disruption in the liver improves chronic-induced hepatosteatosis (Nath et al. 2011). Furthermore, in our studies, chronic Linopirdine treatment was shown to promote hepatocyte *de novo* lipogenesis, and increase fatty acid synthesis and uptake in the liver, by upregulating gene expression of PPARy, fatty acid synthase (FASN) and CD36, respectively, which is similar to what has been observed previously with

hepatocyte-specific upregulation of HIF2α (Qu et al. 2011), a key target of MEIS1 upregulation. Oral administration of Linopirdine could have also further contributed to hepatic steatosis, given activation of intestinal HIF2α during obesity has been shown to aggravate progression of hepatic steatosis and non-alcoholic fatty liver disease (NAFLD) (Xie et al. 2017). A direct link could be investigated by quantifying ceramide levels in the serum, given it has been shown to correlate with HIF2α-NEU3-ceramide salvage pathway, which itself has been linked to NAFLD. Neu3, encoding sialidase 3 (NEU3) is a vital enzyme in the ceramide salvage pathway generating ceramide (Miyagi et al. 2008), and has been validated as a target of HIF2α in the intestines (Xie et al. 2017). Selective inhibitors of NEU3 as well as HIF2α (Xie et al. 2017; 2018) have been shown to ameliorate development of HFD-induced NAFLD, therefore establishing the HIF2α a-NEU3-ceramide pathway as an important contributor in the development of hepatic steatosis and metabolic disease, and proposing quantification of serum ceramide levels following Linopirdine treatment as a form of validation worth pursuing. Furthermore, other than MEIS1-mediated upregulation of HIF1α and HIF2α by Linopirdine, upregulation of MEIS1 on its own could also contribute to this phenotype, as it has been reported to induce squalene epoxidase (SQLE) mRNA and protein expression, a key enzyme in cholesterol synthesis and a reported oncogene for NAFLD-induced hepatocellular carcinoma (Liu et al. 2018). Moreover, our findings support this notion and show a similar trend in SQLE mRNA in the liver following Linopirdine treatment (Figure 5.14D). Taken together, MEIS1 and HIF upregulation and stabilisation by Linopirdine seem to predominate its *in vivo* actions.

Contrary to our expectations, Linopirdine's metabolic phenotypes do not seem to correlate with enhancement of clock gene function. As discussed in Chapter 1, several human and mouse studies have stressed the link between clock gene mutations and metabolic syndrome. For example, conditional knockdown of the *Clock* gene in pancreatic β-cells has been shown to trigger diabetes mellitus (Marcheva et al. 2010). Furthermore, islets from T2DM patients reportedly display reduced circadian amplitude and impaired *in vitro* synchronisation capacity compared to their non-diabetic controls, and treating patient islets with nobiletin increases their amplitude and significantly improves insulin secretion (Petrenko et al. 2020). Given Linopirdine treatment induces worsened symptoms of metabolic syndrome, particularly insulin resistance, its effects as a chrono-modulator and as an enhancer of clock gene expression seems less prevalent than its HIF stabilising actions. This indeed suggests that the mechanism via which the circadian effects are mediated are of prime importance.

Furthermore, Linopirdine's metabolic phenotype was not due to circadian misalignment. Linopirdine exerted no effect on SCN (Figure 5.11, 5.12), and therefore seems to predominantly act on peripheral clocks (as shown in U2OS, 3T3L1 and MEF cells, Figures 3.6, 3.7 and 3.8, respectively). In addition, acute *in vivo* administration of Linopirdine caused no change to the phase of lung or kidney relative to vehicle (Figure 5.13). On the other hand, low oxygen pulses have been previously shown to accelerate mice adaptation to phase advances and delays in a HIF1α-dependent manner (Adamovich et al. 2017), suggesting HIF1α is required for and capable of circadian clock resetting *in vivo*.

Furthermore, our *ex-vivo* peripheral cultures did not reproduce recent findings from Manella et al, that showed significant peripheral clock misalignment following hypoxia (Manella et al. 2020). However, unlike hypoxia on its own, these discrepancies could be attributed to the dual action of Linopirdine on both MEIS1 and HIF and their cumulative enhancement of amplitude of clock gene expression, which is believed to reduce susceptibility of circadian clocks to phase shifts (Lakin-Thomas, Brody, and Cote 1991; Jewett, Kronauer, and Czeisler 1994). However, it is important to note that data from organotypic slices should be interpreted cautiously, due to possible confounding effects associated with tissue handling, *ex vivo* culture, and temperature changes. Nonetheless, they are broadly acceptable in the field (Yamazaki and Takahashi 2005).

Further evidence supporting the involvement of HIF in Linopirdine's metabolic phenotype can be obtained from its acute actions on lean mice (Figure 5.1A), independently of HFD-induced hypoxic niches within adipocytes as a result of obesity. Indeed, acute Linopirdine treatment rapidly reduced fasting serum glucose levels, without affecting insulin sensitivity (Figure 5.1C), a finding similar to what has been reported by Polotsky et al following short term hypoxia in lean mice, where fasting glucose levels were reduced without any observed changes in fasting insulin levels (Polotsky et al. 2003). Linopirdine is also a validated KCNQ channel blocker, however, although mice lacking functional KCNQ1 channels have also been associated with a reduction in overall serum glucose concentrations, these mice also displayed significant reduction in serum insulin levels and showed enhanced insulin sensitivity in response to

intraperitoneal insulin injection (Boini et al. 2009), which was not observed in our studies. This again reinforces the role of HIF in Linopirdine's observed actions.

Linopirdine significantly increased food intake across the 10-week period compared to vehicle treated mice on HFD (Figure 5.4A), without affecting energy efficiency (Figure 5.4B). Among the main causes of hyperphagia is leptin resistance (Coleman 1978), with the latter being strongly associated with a significant increase in ER stress (Lee et al. 2016; Ozcan et al. 2009). Therefore, to explore the possible manifestation of leptin resistance retrospectively, we investigated and compared changes in mRNA expression of ER chaperones in the hypothalamus (Figure 5.6). The ER membrane in mammals contains sensors that can monitor rising levels of unfolded proteins in the ER and consequently induce the unfolding protein response (UPR) or the ER stress response to mitigate the burden of unfolded proteins (Ron and Walter 2007). One adaptation driven by UPR is the upregulation of targets that function as part of the ER protein-folding apparatus; these sensors are the PKR-like ER-resistance kinase (PERK), the activating transcription factor 6 (ATF6) and the inositol requiring enzyme (IRE1). The x-box binding protein 1 (Xbp1) is a key transcription factor that regulates the expression of downstream effectors that help mitigate ER stress. Its splice variant, XBP1s is a strong marker of ER stress, as its pre-mRNA XBP1 does not accumulate following UPR and is predominantly cleaved following stress-induced induction of IRE1 (Yoshida et al. 2001; Calfon et al. 2002). XBP1s then binds ER-stress response elements (ERSE) and promotes transcription of ER chaperons (Yoshida et al. 2003), including the pro-apoptotic DNA

damage-inducible transcript 3 (*Ddit3*, also known as C/EBP homologous protein CHOP) (Kim, Xu, and Reed 2008). Other markers of ER stress include the heat shock 70KDa protein 1 (HSPA1A/HSP70) cellular chaperone, which reportedly increases in the early stages of ER stress (Bertolotti et al. 2000). Indeed, vehicle treated HFD group showed a significant increase in *Xbp1s* and *HSPA1A* mRNA expression compared to diet-control, with no change in *Ddit3*, suggestive of HFD-induced ER stress (Figure 5.6A-C). However, to the contrary, although Linopirdine resulted in a comparable increase in *HSPA1A* mRNA expression following HFD, it however reverted the increase in *Xbp1s* mRNA expression and displayed similar expression to diet-control group. Therefore, this suggests that Linopirdine did not exacerbate ER stress in the hypothalamus, but instead displays trend of decrease, all of which provides a strong argument against worsened leptin resistance mediating the observed hyperphagia. Furthermore, hypoglycaemia on its own has been associated with an increase in food intake mediated by glucocorticoids and independent of leptin. Perry et al have shown that rats consumed 4 times as many calories following insulin-mediated hypoglycaemia, majority of which was predominantly driven by hypercorticosteronemia, without changes to plasma leptin concentrations (Perry et al. 2019). Given acute Linopirdine triggers acute hypoglycaemia following treatment (Figure 5.1A), daily gavage could induce corresponding short-term hypoglycaemia sparks that can promote hyperphagia. Ghrelin is another key hormone in regulating food intake, and quantifying its levels following Linopirdine treatment could also shed more light on the cause of the observed hyperphagia.

The exacerbation of insulin resistance following Linopirdine treatment could be attributed to several outcomes. First, Linopirdine significantly increased expression of TNFα in visceral WAT (Figure 5.10B), indicating increased inflammation within adipocytes, an observation that has been strongly associated with adipocyte dysfunction and insulin resistance (Ouchi et al. 2011; Cooke et al. 2016). Indeed, TNFα has been shown to inhibit tyrosine phosphorylation of the IRS1, thereby decreasing insulin sensitivity (Hotamisligil, Shargill, and Spiegelman 1993; Hotamisligil et al. 1996), which was also reflected with the significant reduction in overall insulin sensitivity markers in adipocytes following Linopirdine treatment (Figure 5.8). Furthermore, intermittent hypoxia has been shown to promote a pro-inflammatory response via induction of the nuclear factor–kapa B (NF-kB), the master transcriptional regulator of inflammatory responses which induces expression of various pro-inflammatory facilitators , including TNFα among others (Ryan, Taylor, and McNicholas 2005; 2006; Greenberg et al. 2006). Hence, this again supports Linopirdine's exacerbation of hypoxic responses in the adipocyte. It is important to note that mice on HFD, both vehicle and Linopirdine treated, showed no change in IL6, MCP-1 or Resistin mRNA expression compared to diet-control (Figure 5.10), however both resulted in a similar significant reduction in adiponectin expression in visceral WAT. This suggests that 10 weeks of HFD promote visceral WAT inflammation via an increase in the pro-inflammatory TNFα and a reduction in the anti-inflammatory adiponectin.

In addition, Linopirdine significantly reduced markers of insulin sensitivity in liver as well (Figure 5.7) but significantly improved them in skeletal muscles (Figure 5.9). Interestingly, skeletal muscles are believed to account for up to 80% of postprandial plasma glucose uptake in healthy individuals (Thiebaud et al. 1982). Nonetheless, since Linopirdine-mediated insulin resistance was accompanied with improvement of insulin sensitivity in muscles but impairment in liver and adipocytes, this stresses that dysregulation of adipocyte and liver functionality can outweigh skeletal muscle benefits in an impaired obese system and is an observation worth noting for future phenotypic *in vitro* screening.

5.4 Conclusion:

In conclusion, chronic *in vivo* administration of Linopirdine in a DIO-mouse model significantly exacerbated metabolic syndrome, increasing weight (Figure 5.2A), and worsening insulin resistance (Figure 5.2C, E) and hepatic steatosis (Figure 5. A-C) associated with this model. Contrary to what we had hoped, Linopirdine's *in vivo* actions seem to be predominated by its HIF and MEIS1 upregulation, irrespective of its circadian modulation and in the absence of any peripheral clock misalignment (Figure 5.13). This therefore emphasises the importance of the mechanism of action via which circadian modulation occurs. The target via which the clock is modulated should be taken into account and must be given priority over its observed circadian modulatory effects. Furthermore, tissue-specific actions should also be considered. For example, as

discussed, localising HIF1α mRNA expression can have a huge impact on the observable outcomes, given its upregulation displays diverse physiological effects in different tissues. Finally, the impact of liver and adipocyte functionality in glucose homeostasis and development of insulin resistance was clearly observed, where even though skeletal muscle insulin sensitivity was significantly improved (Figure 5.9), the dysfunction within the liver and adipocyte drastically outweighed it. Therefore, it would be useful to further investigate how the adipocyte structure changed with Linopirdine treatment, exploring possible hypertrophy vs hyperplasia, then comparing it with the *in vitro* adipocyte phenotypes, to pinpoint patterns and make predictions on which observation *in vitro* holds strongest *in vivo* outcome in progression of metabolic disorders. In addition, setting up hepatocyte-specific metabolic assays could be another way forward for screening molecules for potential benefit against glucose intolerance and insulin resistance.

CHAPTER 6:

Investigating the Mechanism of Action of Zaprinast

6.1 Introduction

It is commonly acknowledged that sleep and circadian rhythm disruptions (SCRD) are associated with a wide range of physiological disorders (Jagannath et al. 2017). Misalignments in the orchestration of clock gene expression among various tissues can lead to functional asynchrony. Extensive work has been done to understand how circadian clocks maintain their synchrony and achieve entrainment to external environmental cues. Cyclic guanosine monophosphate (cGMP) has been strongly implicated in SCN phase shifts and is an important second messenger underlying a myriad of physiological functions. PKG has been acknowledged to play a key role in cGMP's observed circadian modulation within the SCN, however, the pathway downstream remains elusive (Golombek et al. 2004) and whether cGMP has a circadian role with peripheral clocks remains unexamined. Our unbiased in-house circadian-drug screen identified Zaprinast as a strong circadian modulator, which is also a selective cGMP-stabiliser. Therefore, as Zaprinast selectively elevates endogenous cGMP levels, we set out to investigate the underlying pathways for its observed chrono-modulatory effects in peripheral cells, focusing on the role of CREB, and using Zaprinast as a tool to understand cGMP regulation of peripheral clocks.

6.1.1 Background on Zaprinast

Zaprinast is a well-validated competitive inhibitor of cyclic guanosine monophosphate (cGMP)-specific phosphodiesterases (PDEs) that increases cGMP availability by inhibiting its PDE-mediated degradation (Turko et al. 1999). In chapter 3, I reported the potent circadian-modulatory actions of Zaprinast, increasing amplitude of *Bmal1*-promoter expression by 65.3% and *Per2* expression by 15.2%, at an EC50 of 1.08 μM and 2.8 μM respectively. To date, 11 PDE families have been characterized in mammals, based on substrate specificity, amino acid sequences, pharmacological properties, and endogenous/exogenous ligands. These include: PDE1 (Ca^{2+}/Calmodulin-stimulated), PDE2 (cGMP-activated), PDE3 (cyclic adenosine monophosphate (cAMP)-selective, cGMP-inhibited), PDE4 (cAMP-selective, cGMP-insensitive), PDE5 (cGMP-selective), PDE6 (cGMP-specific and photoreceptor), PDE7-8 (both dual substrates exhibiting higher affinity to cAMP), PDE9 (exhibits higher affinity to cGMP), and PDE10-11 (both dual substrates) (Keravis and Lugnier 2012). Zaprinast has been shown to potently inhibit PDE5 and PDE6 (cell-free IC50 values of 150 and 760 nM, respectively). It also weakly inhibits PDE9 at IC50 of 35 μM and PDE11 at Ic50 11-33 μM (Christensen and Torphy 1994; Nakamizo et al. 2003), and therefore is predominantly cGMP-selective.

6.1.2 Role of cGMP and cAMP in the circadian machinery:

cGMP is a key second messenger mediating various physiological processes in different cell types and tissues. Unlike cAMP, which was discovered as a second messenger following knowledge of various functions, the cGMP molecule was identified first and its

functional role was later put into biological context within the NO signalling pathway, awarding Ferid Murad, Robert F. Furchgott, and Louis J. Ignarro the nobel prize of Physiology or Medicine in 1998 (Smith 1998).

cGMP signalling is an intricate pathway with a vast array of physiological responses and associated pathologies. As seen in Figure 6.1, cGMP production is triggered by guanylyl cyclase (GC) activation. Two subtypes of GCs are evident; the soluble guanylyl cyclase (sGC) usually stimulated by nitric oxide (NO) formed from L-arginine by NO synthases (NOS) and accompanied with the stoichiometric formation of citrulline, or the particulate subtypes (pGC) mainly activated by natriuretic peptides (atrial natriuretic peptide (ANP), or B and C-type natriuretic peptides (BNP and CNP) (Silberbach and Roberts 2001). Three isoforms of NOS exist, endothelial, neuronal, and inducible (eNOS, nNOS and iNOS, respectively). eNOS and nNOS are constitutive in nature, and their activation is Ca^{2+}-dependent. On the other hand, iNOS is inducible, independently of Ca^{2+} levels, generally upregulated promptly following immunological stimulation (Ding et al. 1994; Watanabe et al. 1995; Melo, Golombek, and Ralph 1997b; Agostino et al. 2004). Moreover, cGMP targets several identified effectors, like ion channels, phosphodiesterases (PDEs), and cGMP-regulated protein kinases (denoted PKGs), the latter regulating an array of transcription factors and enzymes and hence partaking a crucial role in cGMP's downstream effects (Friebe, Sandner, and Schmidtko 2020; Francis, Busch, and Corbin 2010). Furthermore, cGMP can strongly influence gene transcription, by modulating activation status of various transcription factors, such as

CREB, AP-1, ATF1, etc. (summarised in table 6.1) and its signalling cascade is terminated via cGMP hydrolysis by PDEs and/or via cGMP export by ABC transporters (also referred to as multidrug resistance proteins) (Giacomini et al. 2010; Friebe, Sandner, and Schmidtko 2020).

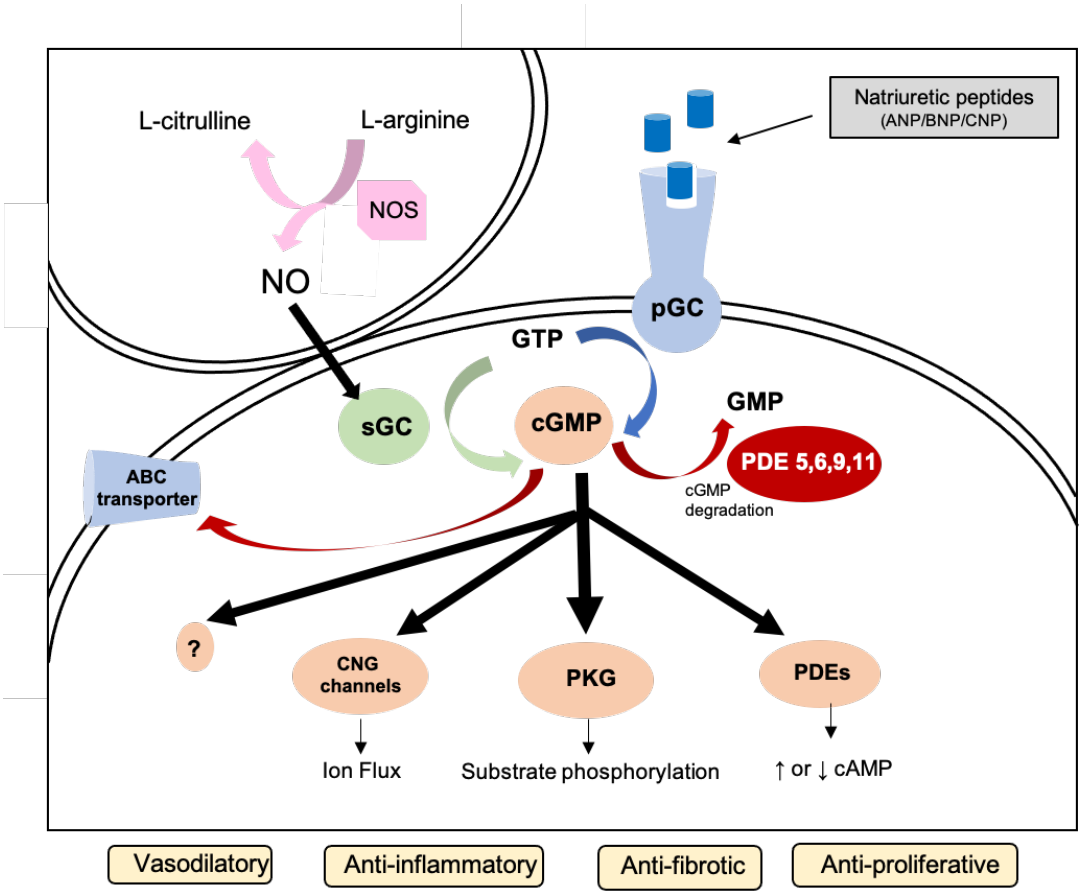


Figure 6.1. Basic principles of cGMP signalling:
Nitric oxide (NO) is generated by Nitric oxide synthase (NOS) in nearby cell from L-arginine (ex: inducible NOS stimulated by cytokines, or Ca2+ activated endothelial NOS), which then diffuses across cell membrane into target adjacent cell (ex: platelet or vascular smooth muscle cell). NO interacts with the Fe^{2+} of the heme group in soluble guanylyl cyclase (sGC), inducing global cGMP generation within the cytosol. On the other hand, natriuretic peptides bind to particulate GC (pGC) within the membrane and trigger generation of local cGMP microdomains near the plasma membrane. cGMP exerts a wide range of physiological functions, by targeting several protein effectors, mainly cGMP-regulated protein kinases (PKGs), phosphodiesterases (PDEs), cyclic nucleotide-gated cation channels (CNG) or through other targets. Elimination of cGMP is carried out by PDE-mediated hydrolysis to 5-GMP, and via excretion through plasma-membrane bound transporters, such as the ABC transporters. cGMP can also regulate cAMP levels by modulating PDE activity, either enhancing or inhibiting cAMP degradation as a consequence. Through its different effectors, cGMP can play major roles in physiology, promoting vasodilatory, anti-inflammatory, anti-fibrotic, and even anti-proliferative effects in different cell lines.

Table 6.1. Transcription factors modulated by cGMP

TRANSCRIPTION FACTOR	CELL TYPE	MECHANISM OF REGULATION	OUTCOME OF cGMP	REFERENCES
AP-1 (C-FOS, JUN B)	BHK REF52, thyroid cells, Neuronal cells, others	CREB-dependent ↑ in transcription	↑ transcription (in serum-starved cells) ↑ mRNA ↑ AP-1 DNA-binding	(Pilz et al. 1995) (Thiriet et al. 1997; J. Wu et al. 2000)
ATF-1	VSMCs BHK	PKG-dependent ↑ ATF-1 phosphorylation	↑ transcription	(Sauzeau et al. 2003) (Gudi et al. 2000)
CREB	Neuronal cells VSMCs	Direct or indirect PKG-mediated ↑ in CREB Ser-133 phosphorylation	↑ transcription	(Ciani et al. 2002)(Lu, Kandel, and Hawkins 1999) (Sauzeau et al. 2003)
EGR-1	Neuronal cells	↑ transcription	↑ transcription ↑ mRNA ↑ DNA-binding	(Esteve et al. 2001), (Thiriet et al. 1997) (Cibelli et al. 2002)
GAX	VSMCs	?	↑ mRNA	(Yamashita et al. 1997)
NF-KB	Cardiomyocytes T-lymphocytes Endothelial cells, hepatocytes	P50/p65 phosphorylation IkB phosphorylation/destabilisation IkB stabilisation	↑ transcription ↑ transcription ↓ cytokine-induced DNA binding	(Kalra et al. 2000) (Bin He and Weber 2003) (Kiemer, Weber, and Vollmar 2002) (Kiemer et al. 2002)
NF/AT	Cardiomyocytes	↓ Ca^{2+} influx ↓ Calcineurin action	↓ nuclear translocation ↓ transcription	(Fiedler et al. 2002)
SRF	Cardiomyocytes, VSMCs	↓ Rho-dependent activation	↓ SRF-associated transcription (SRF on the *fos* and *egr-1* promoters insensitive to Rho signalling)	(Gudi et al. 2002)(Murai and Treisman 2002)
TFII-I	BHK, COS-7, C2C12	PKG-mediated phosphorylation of TFII-I	↑ transcription	(Casteel et al. 2002)

BHK: Baby hamster kidney cells, *VSMC*: Vascular smooth muscle cells, *REF52*: Rat-spontaneously immortalised quiescent cells, *COS*-7: Monkey African green kidney SV 40 transformed, *C2C12*: myoblasts.

Interestingly, the involvement of cGMP in regulation of circadian machinery has been well documented, particularly within the SCN master clock. SCN synchronises its phase by various pathways that relay environmental cues through the retinal hypothalamic tract. Its phase shifts in response to light are gated (*reviewed* in Chapter 1), with a light-unaffected "deadzone" during the subjective day, a light-induced phase delay during the early night, and a light-induced phase advance (CT14) in response to light stimulus in the late night (CT18-19) (Watanabe, Deboer, and Meijer 2001; Best et al. 1999; Takahashi et al. 1984). cGMP signalling seems to be heavily involved in mediating light and glutamate-mediated phase advances. For example*, in vitro*, cGMP analogues have been shown to reset the SCN clock and induce stable phase shifts (advance) when administered during the subjective night (CT18-19) but not during the subjective day (CT7) (Prosser, McArthur, and Gillette 1989). Similarly, the muscarinic agonist carbachol, which upregulates cGMP and activates PKGs, has also been shown to promote phase shifts in SCN cultures in a cGMP-mediated mechanism (Liu and Gillette 1996; Liu et al. 1997). Moreover, *in vivo* administration of NOS inhibitor L-NAME, the PKG inhibitor KT5823, and the GC inhibitor ODQ have been shown to block light-mediated phase advances in hamster (Ferreyra and Golombek 2001; Mathur, Golombek, and Ralph 1996; Melo, Golombek, and Ralph 1997a). Similarly, the cGMP-specific PDE5 inhibitor, sildenafil, has been shown to enhance light induced phase advance when administered to mice during their subjective night (CT18; phase advance) and also speed up mice re-entrainment time following phase advances of their light/dark cycles (Agostino, Plano, and Golombek 2007). However, similar to *in vitro* studies, sildenafil showed no effect on phase delays

when administered at CT14. Thus, cGMP seems to be a key signalling molecule directly influencing circadian clock gene expression, gated by a clear phase specificity to the subjective night, or the biological equivalent of dawn in the physical world.

On the other hand, cAMP, which has been identified as a core component of the circadian machinery (O'Neill et al. 2009), shows opposing effects to cGMP on circadian clock resetting (schematic comparison displayed in Figure 6.2). Firstly, cAMP and cGMP-mediated phase shifts are in anti-phase, where contrary to cGMP, cAMP has been shown to promote maximal electrical phase shifts in SCN during the subjective day only (at CT6-7) and no effects during the subjective night (Prosser and Gillette 1989). Furthermore, cAMP analogues have been shown to enhance glutamate-induced phase delays, and block glutamate-induced phase advances. This was further validated with PKA inhibitors, which contrarily potentiated glutamate-phase advances and inhibited delays (Tischkau et al. 2000). Altogether, this proposes that cAMP seems to be predominantly involved in induction of phase delays and that late night elevation of cAMP could be inhibitory for cGMP-mediated phase advances.

Interestingly, although the role of second messengers in general has been extensively investigated in the SCN, very little work has been done to elucidate the downstream signalling cascade following cGMP generation, and equally the role of cGMP is largely unexplored in regulating peripheral circadian clocks.

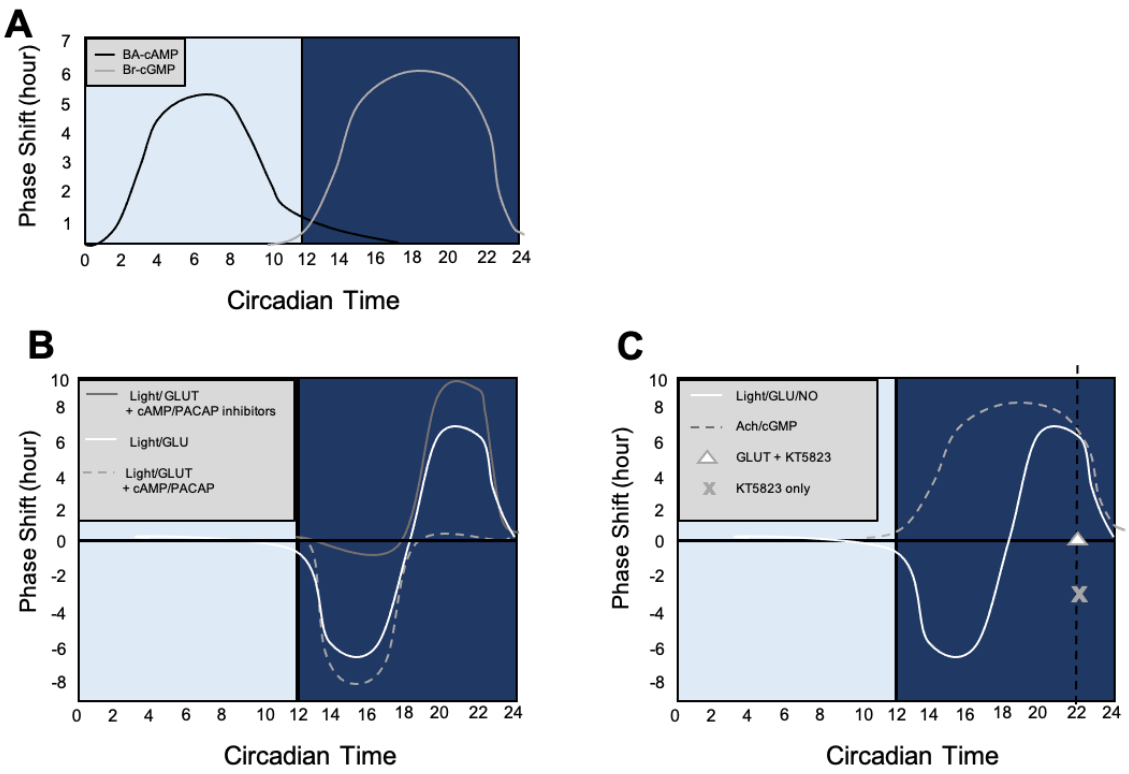


Figure 6.2. Effect of cAMP and cGMP on phase shifting of circadian clocks in SCN:
A) Phase response curve displaying SCN clock sensitivity to resetting by cAMP and cGMP analogues administered at different circadian time points. The figure shows SCN phase shifts (in hours) following 1 hour exposure to the corresponding analogue initiated at the denoted circadian time. cAMP and cGMP show antiphase responses, with the domain of clock sensitivity to 8-Bromo-cAMP (BA-cAMP) (black) occurring during the subjective day, while that for 8-Bromo-cGMP (Br-cGMP) occurs during subjective night. (Data charted from (Prosser, McArthur, and Gillette 1989; Prosser and Gillette 1989))
B) Schematic representation of the modulatory effects of cAMP and pituitary adenylyl cyclase activating peptides (PACAP) on the SCN neuronal activity induced by light or glutamate (GLU). Although cAMP analogues and PACAP have no effect on their own when administered in subjective night, they however enhance GLU-mediated phase advances in the late night. PACAP and cAMP inhibitors, on the other hand, block GLU-induced phase delays in early night, and further potentiate phase advances in late night. (Data redrawn from (Tischkau et al. 2000)).
C) Schematic phase response curve comparing the effects of cGMP and ACh agonists on phase shifting (grey dashed line) relative to light, glutamate or NO-induced phase shifts (white). Within the subjective night, light and glutamate can promote NMDA receptor activation with the resultant release of NO, which seem to act on different targets in early and late night, generating phase delays and phase advances, respectively. On the other hand, throughout the night-time domain, muscarinic receptor activation that promotes CO release and cGMP elevation, promotes phase advances (Liu et al. 1997; Hu and El-Fakahany 1993). Phase advances induced by glutamate are completely abolished with administration of the PKG inhibitor KT5823 (Δ) while KT5823 administration on its own has an opposite effect to glutamate or cGMP analogues, inducing a phase delay of ~3.5 hours (X) (Tischkau et al. 2004).

6.1.3 CREB- a key transcription factor regulating circadian rhythms

CREB, or the Ca^{2+}/cAMP response element binding protein, is an interesting prototypical stimulus-inducible transcription factor that plays major roles in circadian regulation and phase resetting. CREB belongs to the bZIP superfamily of transcriptions factors, which include other members like ATF-1 and CREM (Mayr and Montminy 2001). CREB regulates transcription of a wide array of genes through interaction with cAMP response elements (CRE) within the genome. CRE is comprised of the palindromic consensus sequence TGACGTCA, with CREB binding sites almost always harbouring the CGTCA core sequence (Mayr and Montminy 2001; Shaywitz and Greenberg 1999). While the bZIP domains regulate DNA binding, CREB transcription is regulated tightly through interaction of co-activators with its other functional domains; the two glutamine rich domains Q1 and Q2/CAD (constitutively active domain) and the kinase inducible domain (KID). The KID residues contain the critical Serine-133 residue, which when phosphorylated in response to a stimulus, allows recruitment of the CREB binding protein CBP into the KID domain (Chrivia et al. 1993; Kwok et al. 1994) via the former's CREB-binding domain (KIX) (Parker et al. 1996; Radhakrishnan et al. 1997). It is believed that this stimulus-triggered domain interaction promotes the CREB-mediated inducible gene expression. The Q2/CAD domain on the other hand interacts with other basal transcription components, like Transcription factor IID, IIB, and TATA-binding protein (TBP) and promotes stimulus-independent CRE-mediated gene expression (Ferreri, Gill, and Montminy 1994; Xing, Gopal, and Quinn 1995). Remarkably, CREB phosphorylation and CRE-mediated gene expression have been shown to follow a circadian pattern within

the SCN, with phospho-CREB (Ser-133) levels peaking during the mid-to late subjective night followed by maximal CRE-reporter gene expression occurring from late-subjective night to mid-subjective day (Obrietan et al. 1999; O'Neill et al. 2009). Furthermore, CRE-elements have been identified in *Per1* and *Per2* promoters (Travnickova-Bendova et al. 2002), whose transcription can initiate phase advances and delays, respectively (Albrecht et al. 2001; 1997). Moreover, nocturnal light as well as glutamate treatment, both known to promote SCN phase shifting, have been shown to induce CREB phosphorylation in the SCN (at both Ser-133 and Ser-142 sites) (Ding et al. 1997; Gau et al. 2002). Similarly, CREB-Ser-133 (Wheaton et al. 2018) and CREB-Ser-142 (Gau et al. 2002) mouse mutants have been shown to exhibit attenuated light-induced phase shifts. Taken together, CREB seems to be a key transcription factor in relaying external cues to circadian clocks.

Besides its strong role in circadian regulation, CREB is a well-documented common downstream target of both cGMP as well as cAMP-cascades (Gonzalez and Montminy 1989; Lueptow, Zhan, and O'Donnell 2016; Gudi et al. 1996). However, given their opposing effects on circadian phase shifting, and the inferred inhibitory action of cAMP-signalling on cGMP-mediated phase advances, it is highly unlikely that both cAMP and cGMP impose their circadian effects via CREB activation. Indeed, both early and late night stimuli (at CT14 and CT18) promote induction of CREB-phosphorylation in the SCN (Von Gall et al. 1998), which resembles cAMP elevation post glutamate treatment at these time points (Tischkau et al. 2000). Moreover, although both PKG and PKA can promote CREB

phosphorylation at Ser-133 residues, PKG-mediated CREB activation occurs at a slower kinetic rate compared to PKA, and with lower efficiency of CRE-activation, almost 10 folds lower (Collins and Uhler 1999; Gudi et al. 1996; 2000). Indeed, cAMP analogues on their own have been shown to promote CREB phosphorylation at Ser-133 site (Kornhauser et al. 2002) and potently induce CRE activation (Gudi et al. 1996). On the other hand, cGMP analogues fail to promote CREB phosphorylation and CRE activation at basal condition, but only do so in cells overexpressing GC and PKG (Gudi et al. 2000; Sauzeau et al. 2003; Gudi et al. 1996). Given induction of CREB-phosphorylation in the SCN occurs following both early and late night stimuli (Von Gall et al. 1998), which links to phase delays and advances, respectively, this overall suggests that a gate upstream of CREB is vital for gating nocturnal phase shifting, but also makes it unlikely for both cAMP and cGMP to be engaging with the clock via the same mechanism, i.e CREB.

To date, there has been no direct investigation of how cGMP elicits its circadian effects. Although PKG involvement in the SCN is evident (Oster et al. 2003; Tischkau et al. 2004), the downstream effect of PKG still remains unclear. Furthermore, most studies so far have focused on cGMP phase-resetting in the SCN, without investigating amplitude or period, and with no reported investigations in peripheral tissues. In chapter 3, we identified the cGMP-selective PDE inhibitor Zaprinast as a potent enhancer of amplitude and period of circadian clocks of peripheral cells in culture, including fibroblasts, adipocytes and U2OS osteosarcoma cells (Figures 3.5-3.8). This finding sheds light on a novel role for cGMP in enhancing amplitude of clock gene expression, and in regulating

circadian clocks within peripheral tissues. The use of stably-transfected circadian reporter cell lines, similar to those used in Chapter 3, can provide a very useful tool for investigating the mechanism underlying cGMP's circadian phenotype. This model enables real-time monitoring and analysis of changes in amplitude and period of circadian gene expression of peripheral clocks, and helps dissect the downstream signalling of cGMP via pharmacological and molecular manipulations. Furthermore, cAMP modifying drugs are generally associated with various side effects (Boswell-Smith, Spina, and Page 2006), however, cGMP-selective drugs like sildenafil exhibit less adverse effects and are regularly used in clinics. Hence, following further exploration, the cGMP signalling cascade provides an interesting target for developing drugs that reset the clock in a safe manner, which consequently holds promise for ameliorating symptoms of jet lag or other conditions associated with sleep and circadian rhythm disorders (SCRD).

6.1.4 Aims:

Following the unbiased identification of Zaprinast as a potent circadian modulator, we intended to use this molecule as a tool for *in vitro* investigation of the underlying mechanism behind cGMP's chrono-modulatory effects. The role of CREB as an effector mediating cGMP's circadian action remains elusive. U2OS cells expressing *Bmal1* and *Per2* promoters allow real-time monitoring of circadian rhythms and provide an elegant model for molecular and pharmacological manipulations and mechanistic investigations. Hence, in this study, we aimed to utilise this model to:

- Validate the involvement of cGMP in Zaprinast's circadian actions
- Evaluate the role of cGMP in peripheral circadian rhythms
- Dissect the role of CREB as the mediating transcription factor and investigate other downstream targets of cGMP signalling like ERK and mTOR to explore their possible association with clock gene regulation.

6.2 Results:

U2OS cells were used to evaluate the effects of pharmacologically and molecularly targeting the cGMP cascade and CREB on Zaprinast's circadian actions, in order to address the mechanism underlying its circadian phenotype and shed light on the role of CREB in cGMP-dependent circadian modulation, as well as other possible pathways.

6.2.1 Zaprinast showed high specificity for cGMP:

We have shown previously in Chapter 3 that the PDE inhibitor Zaprinast induced significant amplitude and period enhancement of core clock gene expression. Therefore, to understand the mechanism underlying Zaprinast's circadian phenotype, we first wanted to validate its selectivity for cGMP. To do so, U2OS cells were transiently transfected with luminescence-based GloSensors selective for cAMP or cGMP, and Zaprinast's actions were evaluated. The Nitric oxide donor sodium-nitroprusside (SNP) (Figure 6.3A) and the adenylyl cyclase activator Forskolin (Figure 6.3B) were used as positive controls for cGMP and cAMP level potentiation, respectively. Zaprinast administration resulted in a dose dependent increase in cGMP levels (Figure 6.3C, E), without affecting cAMP (Figure 6.3D, F). Indeed, 100 μM Zaprinast induced a 25.9±2.2 fold increase in cGMP levels compared to 0.95±0.17 fold increase in cAMP. This was similar for the PDE5-selective inhibitor Sildenafil (100 μM), which increased cGMP levels by 25.6±0.06 folds compared to 0.9±0.28 folds for cAMP (Figure 6.3G). These findings supported the selectivity of Zaprinast for cGMP-sensitive PDE in these cell lines.

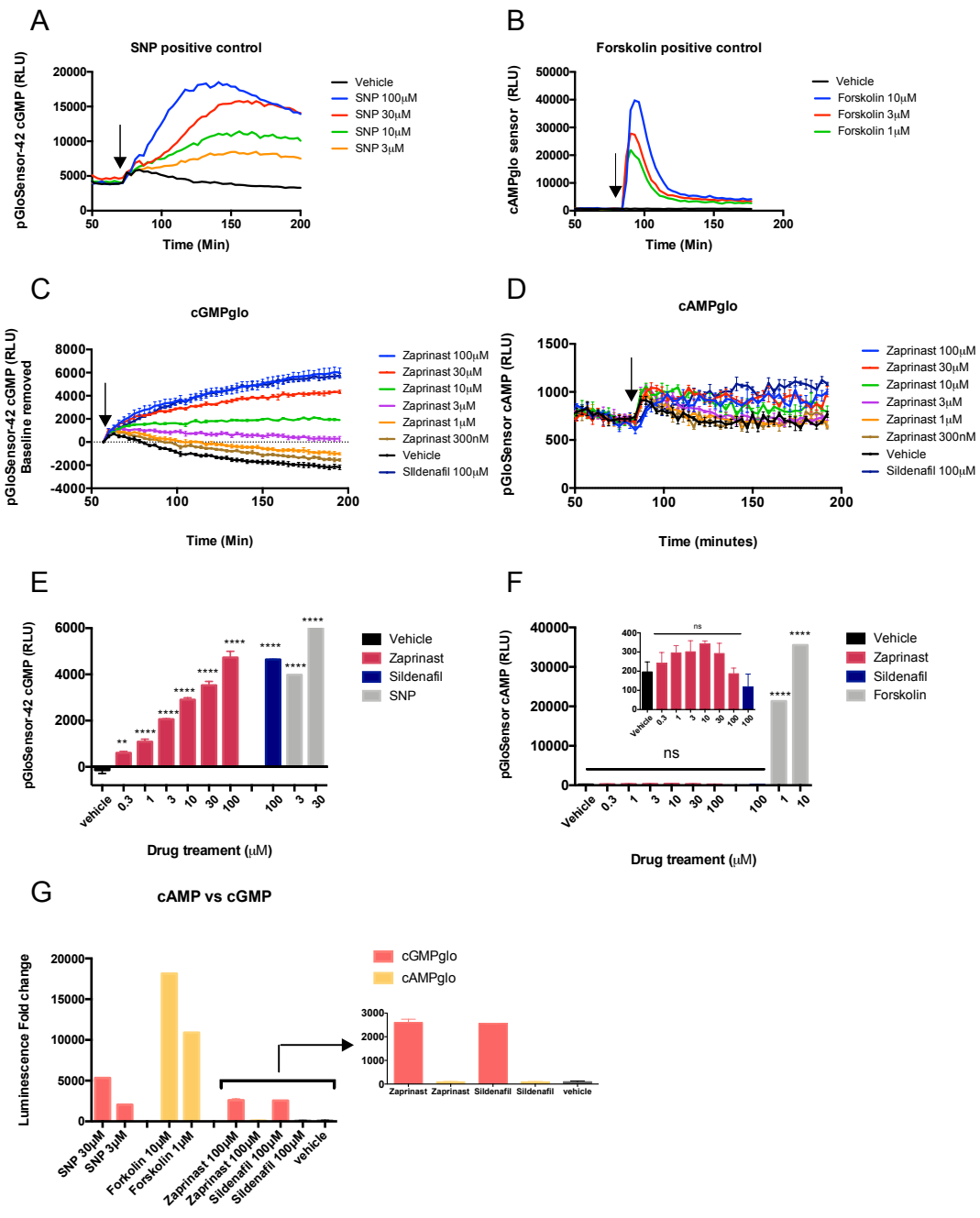


Figure 6.3. Zaprinast selectively targets cGMP specific PDE's; increasing cGMP intracellularly without affecting cAMP levels in U2OS cells: Raw luminescence traces following increasing doses of SNP **(A)** and Forskolin **(B)** were used as positive controls for cGMP and cAMP glosensors, respectively. **(C)** Baseline-corrected traces of cGMP GloSensors following increasing doses of Zaprinast, vehicle and 100 μM Sildenafil. **(D)** Quantification of cGMP levels. **(E)** Raw luminescence of cAMP GloSensor following increasing doses of Zaprinast, vehicle, and 100 μM Sildenafil. **(F)** Quantification of cAMP levels. **(G)** Comparison between cAMP and cGMP fold change following SNP (30 μM, 3 μM), Forskolin (10 μM, 1 μM), Zaprinast (100 μM), and Sildenafil (100 μM) treatments. Error bars represent ±SEM. N=3. *SNP*: Sodium nitroprusside.

6.2.2 cGMP elevation induces Bmal1-promoter expression and period elongation:

In order to validate the functionality of PDE-inhibition and cGMP elevation in Zaprinast's circadian phenotype, we tested a second PDE5 selective inhibitor for its circadian effect. Interestingly, Sildenafil resulted in a similar amplitude enhancing effect as Zaprinast, producing a maximal enhancement of *Bmal1* promoter expression of 38.9±11% (Figure 6.4A-B) at an EC50 of 2.4 μM. Sildenafil also showed 15.15±9.3 minutes period elongation as well, at a similar EC50 (3.9 μM) (Figure 6.4C). To further validate how endogenous cGMP elevation affects circadian clocks, the C-type natriuretic peptide (CNP) was used to activate the membrane-bound GC (GC-B or NPR2). Similar to PDE inhibition, CNP also increasd amplitude of *Bmal1* expression by 13±2.1% at an EC50 of 208 nM (Figure 6.4D-F), comparable to that of its reported GC activation *in vitro* (Shuhaibar et al. 2017; 2016). Taken together, these findings support the notion that stimulating endogenous elevation of cGMP induces a reproducible circadian phenotype and encourages the use of Zaprinast as a pharmacological tool for understanding cGMP-mediated circadian modulation.

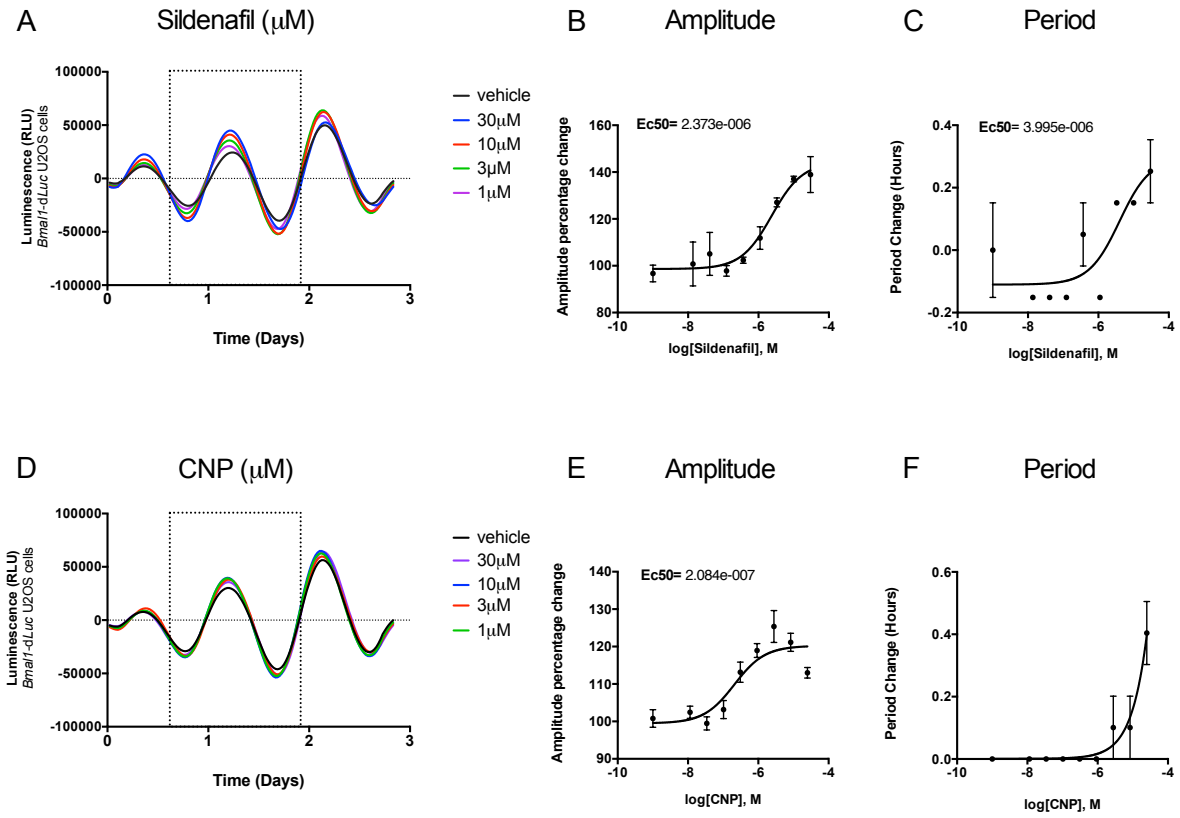


Figure 6.4. Sildenafil and CNP increase amplitude of Bmal1 expression in *Bmal1*-d*Luc* U2OS cells: (A) Representative luminescence traces for Sildenafil. **(B)** Amplitude percentage change analysis for first day following Sildenafil treatment. **(C)** Period change following sildenafil. **(D)** Representative luminescence traces for CNP. **(B)** Amplitude percentage change analysis for first day following CNP treatment. **(C)** Period change following CNP. Error bars represent ±SEM. N=3. *CNP*: C-type natriuretic peptide

6.2.3 Zaprinast's circadian phenotype was attenuated by PKG inhibition:

One of the key targets of cGMP signalling is the cGMP-sensitive kinase PKG. In order to assess the mechanism via which cGMP elevation promotes enhancement of *Bmal1* expression, the PKG-selective inhibitor KT5823 was used. A concentration of 3 μM KT5823 (Figure 6.5A), shown to inhibit PKG selectively, avoiding inhibition of other kinases like PKC and PKA (Gadbois et al. 1992) was used. Interestingly, KT5823 significantly reduced Zaprinast's amplitude enhancing effect by approximately 40.7±2% (Figure 6.5B) and completely abolished and even strikingly reversed its period effect on *Bmal1* promoter expression (Figure 6.5D), without affecting cell viability (Figure 6.5C). This suggested PKG, downstream of cGMP elevation, is necessary for Zaprinast's circadian phenotype.

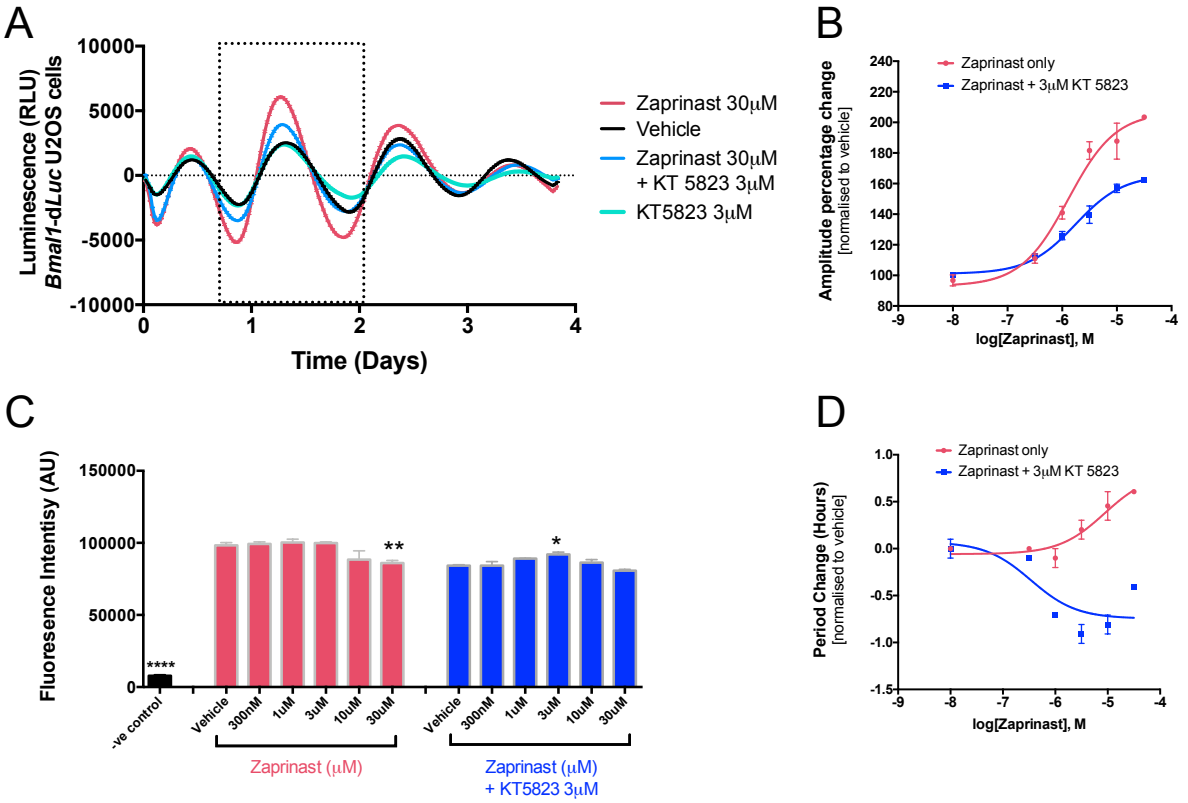


Figure 6.5. PKG inhibitor KT 5823 significantly reduces circadian effect of Zaprinast in *Bmal1*-d*Luc* U2OS cells: *Bmal1*-d*Luc* U2OS cells were treated with increasing doses of Zaprinast, alone or in the presence of 3 μM KT5823. **(A)** Representative luminescence traces of *Bmal1*-d*Luc* U2OS cells following treatment with 30 μM Zaprinast, in the presence or absence of 3 μM KT5823. **(B)** Amplitude percentage change analysis for Zaprinast in the presence and absence of the inhibitor. **(C)** Cell viability. **(D)** Period change. Error bars represent ±SEM. N=3.

6.2.4 Zaprinast's circadian phenotype was unaffected by blocking CREB phosphorylation:

$CREB^{S133A}$ (referred as mCREB or CREB-M) is a mutant CREB that contains a point mutation within its Ser-133 residue, preventing phosphorylation at that critical site that allows its interaction with CBP, hence rendering the protein insensitive to kinase-inducible activation (Barco and Marie 2011). In our study, overexpression of $CREB^{S133A}$ completely abolished Forskolin-mediated CRE-activation (Figure 6.6A-C) without affecting cell viability (Figure 6.6D). Moreover, in *Bmal1*-d*Luc* U2OS cells, similar overexpression of $CREB^{S133A}$ significantly reduced amplitude of *Bmal1*-promoter expression (Figure 6.6E-F) also without affecting cell viability (Figure 6.6G), thus validating the significance of Ser-133 phosphorylation in basal circadian gene expression. Remarkably, Zaprinast's circadian phenotype seemed unaffected by $CREB^{S133A}$ (Figure 6.7A-B), with its amplitude and period enhancing effects retained and its EC50 unaffected (Figure 6.7C-E). In addition, unlike Forskolin which significantly increased CREB-phosphorylation at Ser-133 site by 72.2±28.7%, acute treatment of U2OS cells with Zaprinast (alone and in the presence of PKG inhibitor KT5823) showed no change in protein levels of phosphor-CREB (Ser-133) (Figure 6.8). Together, these findings provided the first comprehensive line of evidence untangling CREB from cGMP and PKG's -mediated circadian phenotypes.

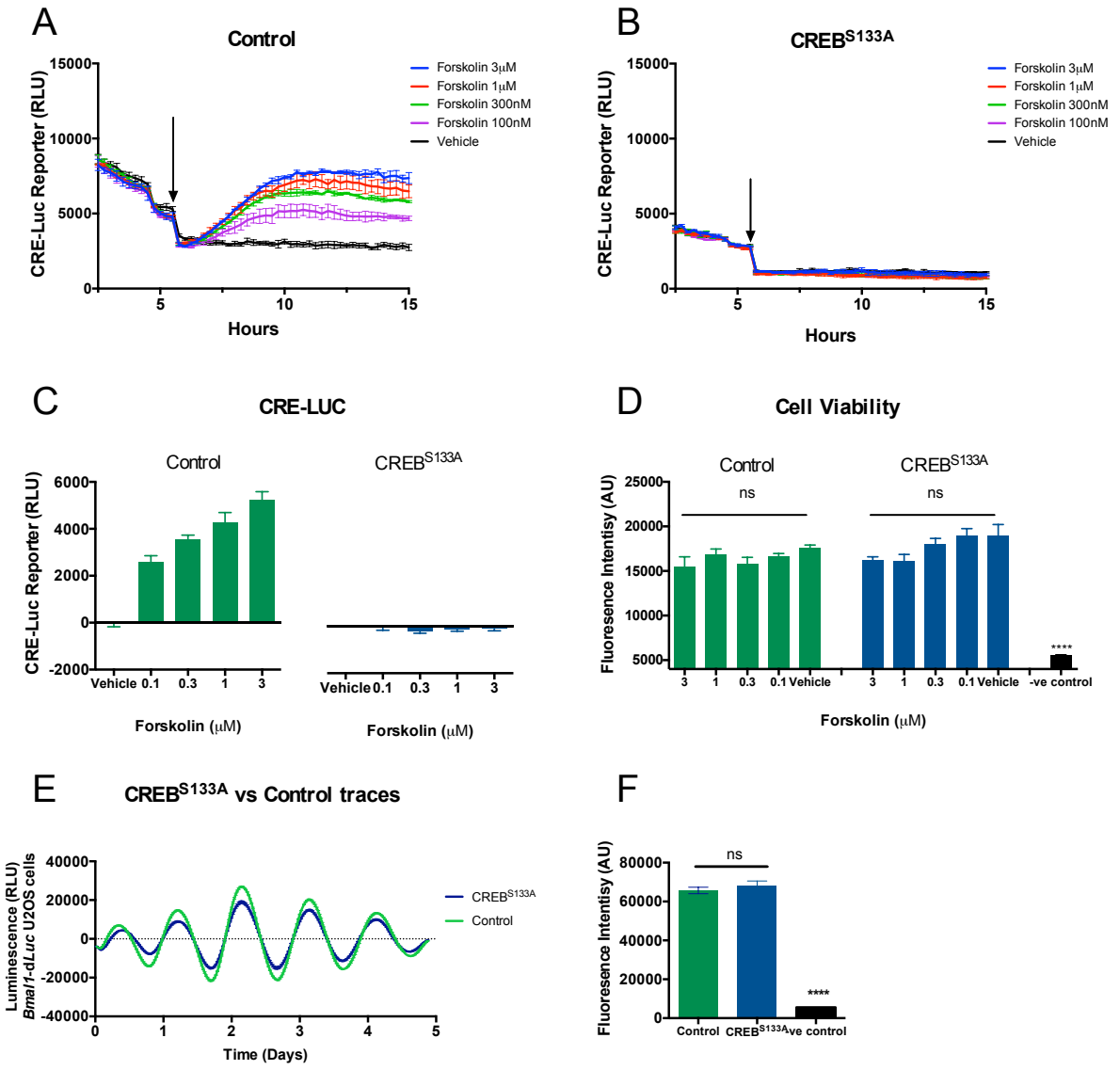


Figure 6.6. Overexpression of CREB^{S133A} completely abolishes Forskolin-mediated CRE activation and reduces amplitude of *Bmal1* promoter expression: U2OS cells were transiently co-transfected with CRE-Luc reporter and Control vector **(A)** or CREB^{S133A} **(B)** and then treated with increasing doses of Forskolin. Their raw traces are shown in A and B respectively. **(C)** Quantification of CRE-activation following Forskolin treatment in Control-transfected (left) and CREB^{S133A} transfected cells (right). **(D)** Cell viability following Forskolin treatment**. (E)** Representative traces for *Bmal1*-d*Luc* U2OS cells transfected with CREB^{S133A} or control vector **(F)** Amplitude of luminescence of *Bmal1*-promoter expression with CREB^{S133A} or control vector **(G)** Cell viability of *Bmal1*-d*Luc* U2OS cell. Error bars represent ±SEM. N=3.

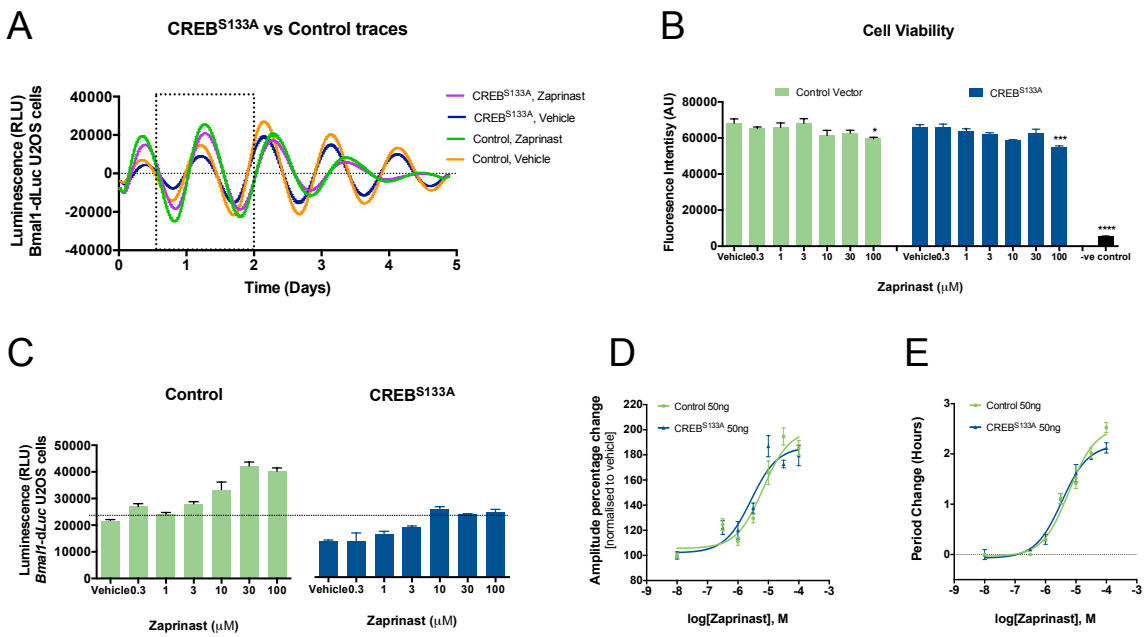


Figure 6.7. Overexpression of mutant CREB^{S133A} shows no effect on Zaprinast's circadian effect in *Bmal1*-d*Luc* U2OS cells: (A) Representative traces for 30 μM Zaprinast vs vehicle of *Bmal1*-d*Luc* U2OS cells transiently transfected with mutant CREB^{S133A} or control plasmid. **(B)** Corresponding cell viability following drug treatment and plasmid transfection. **(C)** Amplitude percentage change for first day following synchronization. **(D)** Period change. **(E)** Amplitude of luminescence of control (left) and mutant CREB^{S133A} (right) transfected *Bmal1*-d*Luc* U2OS cells. Error bars represent ±SEM. N=3.

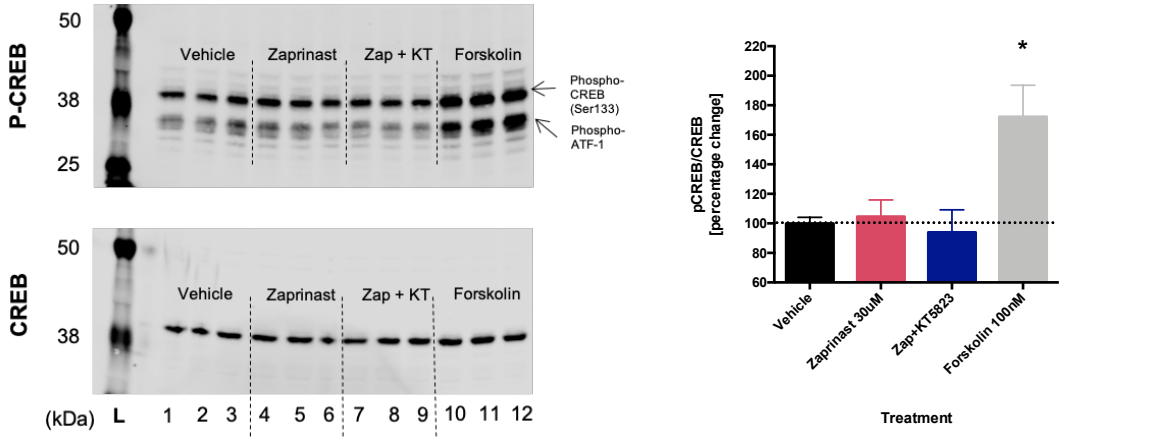


Figure 6.8. Zaprinast does not induce phosphorylation of CREB at Ser-133:
(Left) Western blot bands for Phospho-CREB and CREB following 1 hour treatment of U2OS cells with vehicle (1-3), Zaprinast 30 μM (4-6), Zaprinast 30 μM + KT5823 3 μM (7-9) or Forskolin 100 nM, ***L***= Molecular weight ladder, *ATF-1*: Activating transcription factor 1 **(Right)** Percentage change of phosphorylated CREB as a ratio of total CREB following drug treatment. Error bars represent ±SEM. N=3. *=p<0.05

CREB transcriptional activity can also be modulated through phosphorylation of its Ser-142 residue. Indeed, in the SCN, light at night induced phosphorylation of CREB at 142 site, and mutating that site inhibited *Per1* elevation to light and also removed phase delay and reduced phase advance (Oster et al. 2003). To further investigate how Zaprinast could modulate CREB phosphorylation, overexpression of the $CREB^{S142A}$ mutant was carried out. Similar to the previous findings, Zaprinast's enhancement of amplitude and period of *Bmal1*-promoter expression was independent of CREB phosphorylation at that site (Figure 6.9A-D). Zaprinast resulted in a maximal amplitude enhancement of 82±8.5 and 73.6±25.2% and a period elongation of 2.5±0.1 and 2.0±0.1 hours at 100 and 30 μM, respectively. On the other hand, in cells overexpressing $CREB^{S142A}$, the same concentrations of Zaprinast still induced an increase of 56±3.5 and 65.9±30.9% and period elongation of 1.97±0.17 and 2.3±0.52 hours, at 100 μM and 30 μM Zaprinast (Figure 6.9B-C), even when cell viability was reduced at these concentrations (Figure 6.9D). These findings again eliminate a role for cGMP-mediated CREB regulation in Zaprinast's circadian effects.

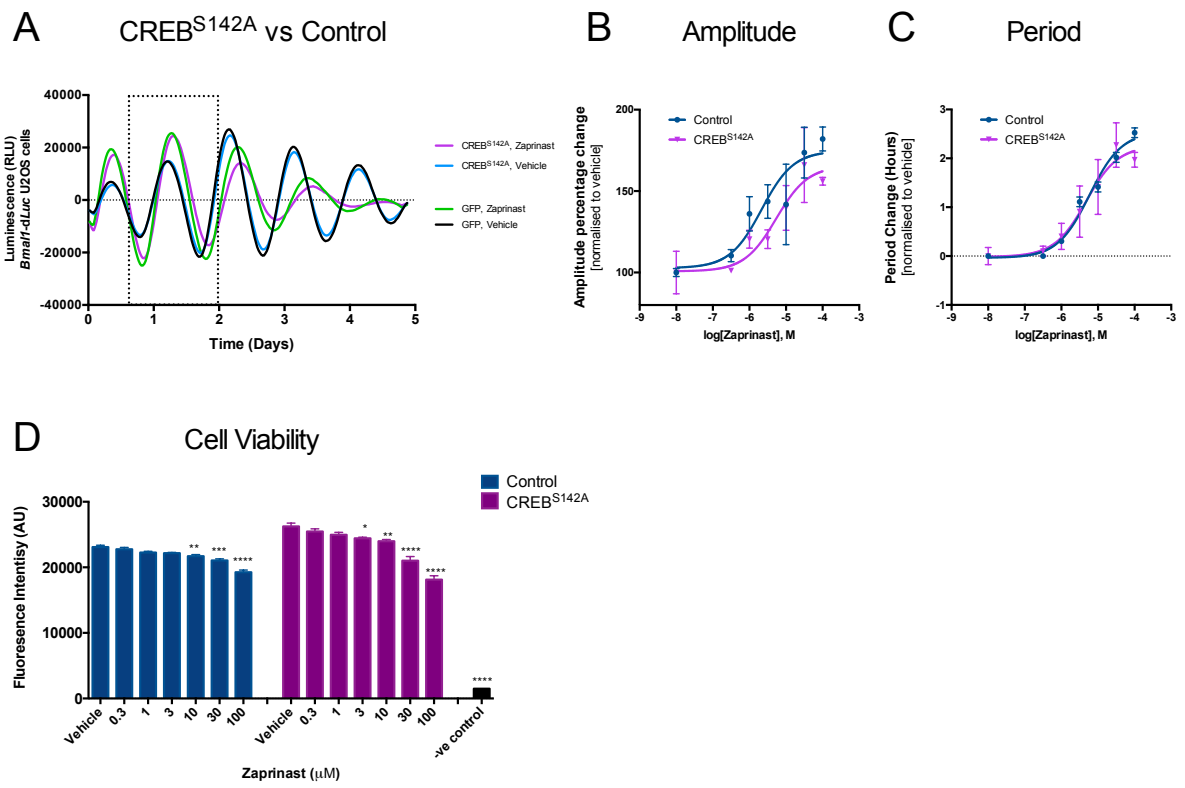


Figure 6.9. Overexpression of mutant CREB^{S142A} shows no effect on Zaprinast's circadian effect in *Bmal1*-d*Luc* U2OS cells: (A) Representative traces for 30 μM Zaprinast vs vehicle in *Bmal1*-d*Luc* U2OS cells transiently transfected with mutant CREB^{S142A} or control plasmid. **(B)** Amplitude percentage change for first day following synchronization. **(C)** Period change. **(D)** Cell viability. Error bars represent ±SEM. N=3.

6.2.5 Zaprinast's circadian phenotype was unaffected by inhibition of CREB DNA binding:

As an extra layer of validation for the lack of CREB involvement, K-CREB mutant was used to investigate CREB DNA binding. This mutant exhibits a point mutation within CREB's DNA binding domain, hence making it sensitive to phosphorylation and co-activator regulation, but rendering it incapable of DNA binding (Walton et al. 1992). Indeed, K-CREB overexpression significantly reduced Forskolin's CRE-activation (Figure 6.10A-C) without affecting cell viability (Figure 6.10D). However, when overexpressed in *Bmal1*-d*Luc* U2OS cells, K-CREB resulted in no change in Zaprinast's circadian phenotype (Figure 6.11), again re-iterating the lack of CREB involvement.

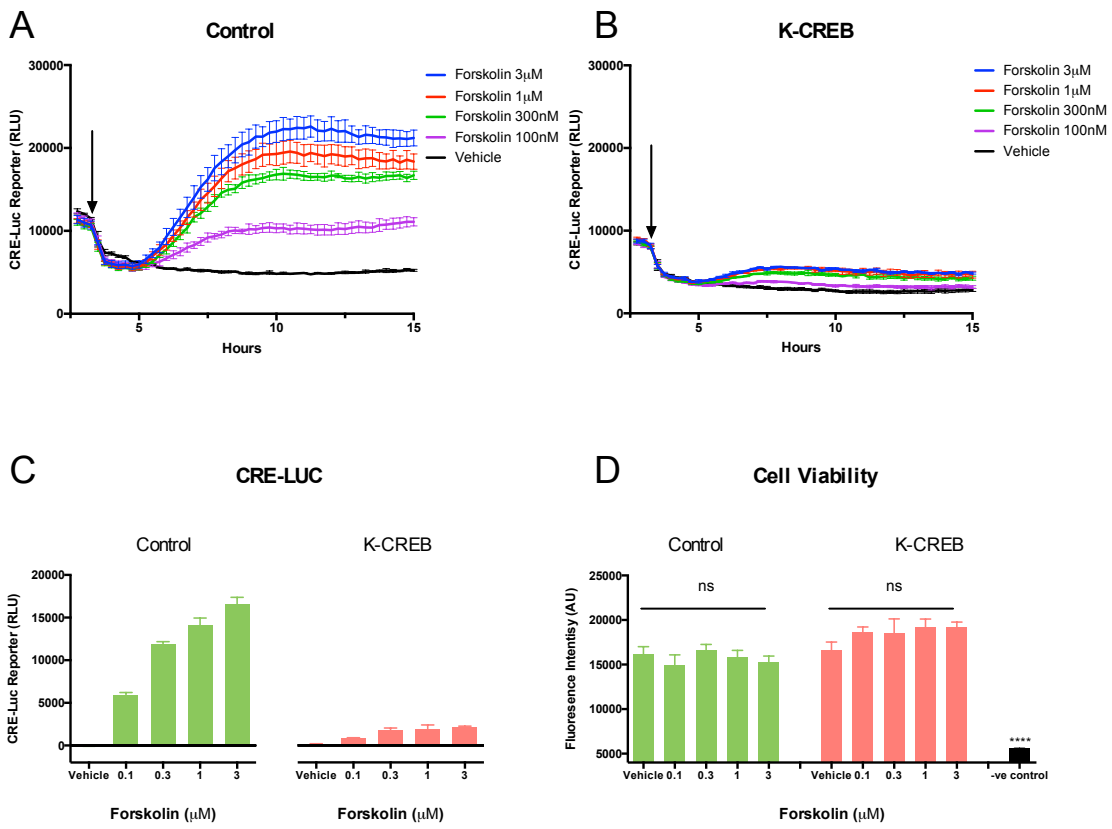


Figure 6.10. Overexpression of mutant K-CREB significantly reduces Forskolin-mediated CRE activation: U2OS cells were transiently co-transfected with CRE-Luc reporter and Control vector **(A)** or mutant K-CREB **(B)** and then treated with increasing doses of Forskolin. Their raw traces are shown in A and B respectively. **(C)** Quantification of CRE-activation following Forskolin treatment in Control-transfected (left) and mutant-K-CREB transfected cells (right). **(D)** Cell viability. Error bars represent ±SEM. N=3.

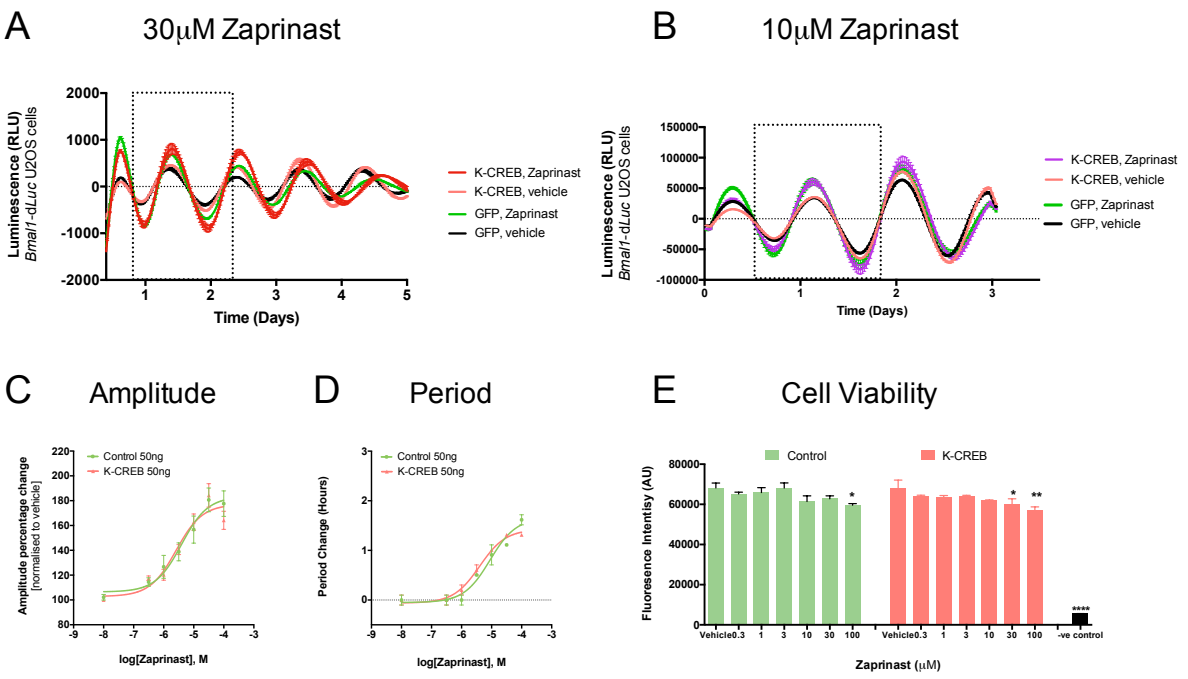


Figure 6.11. Overexpression of mutant K-CREB reduces Zaprinast's amplitude of *Bmal1* expression but leaves period unchanged in *Bmal1*-d*Luc* U2OS cells: (A) Representative traces for 30 μM Zaprinast vs vehicle of *Bmal1*-d*Luc* U2OS cells transiently transfected with mutant K-CREB or control plasmid (N=3). **(B)** and **(C)** represent amplitude percentage change for first day following synchronization (N=6) and period change analysed from two independent experiments in *Bmal1*-d*Luc* U2OS cells (N=6). **(D)** Corresponding cell viability following drug treatment and plasmid transfection (N=3). Error bars represent ±SEM.

6.2.6 Zaprinast showed no effect on CRE activation

Finally, CREB transcription factor has been shown to promote gene transcription predominantly via binding with CREB-response elements (CRE) within gene promoters. To assess how Zaprinast affects CRE-activation, U2OS cells were transiently transfected with CRE-luciferase reporter plasmids and then treated with increasing doses of Zaprinast (Figure 6.12A). Interestingly, within the normal 6-hour window of maximal CRE-activation following treatment with established cAMP elevators like Forskolin,

Zaprinast showed no effect on CRE-activation. Similarly, Zaprinast also had no effect on Forskolin-mediated CRE-activation (Figure 6.12B-C). Consequently, taken together, these findings support our hypothesis that cGMP-mediated clock modulation occurs independently of CREB.

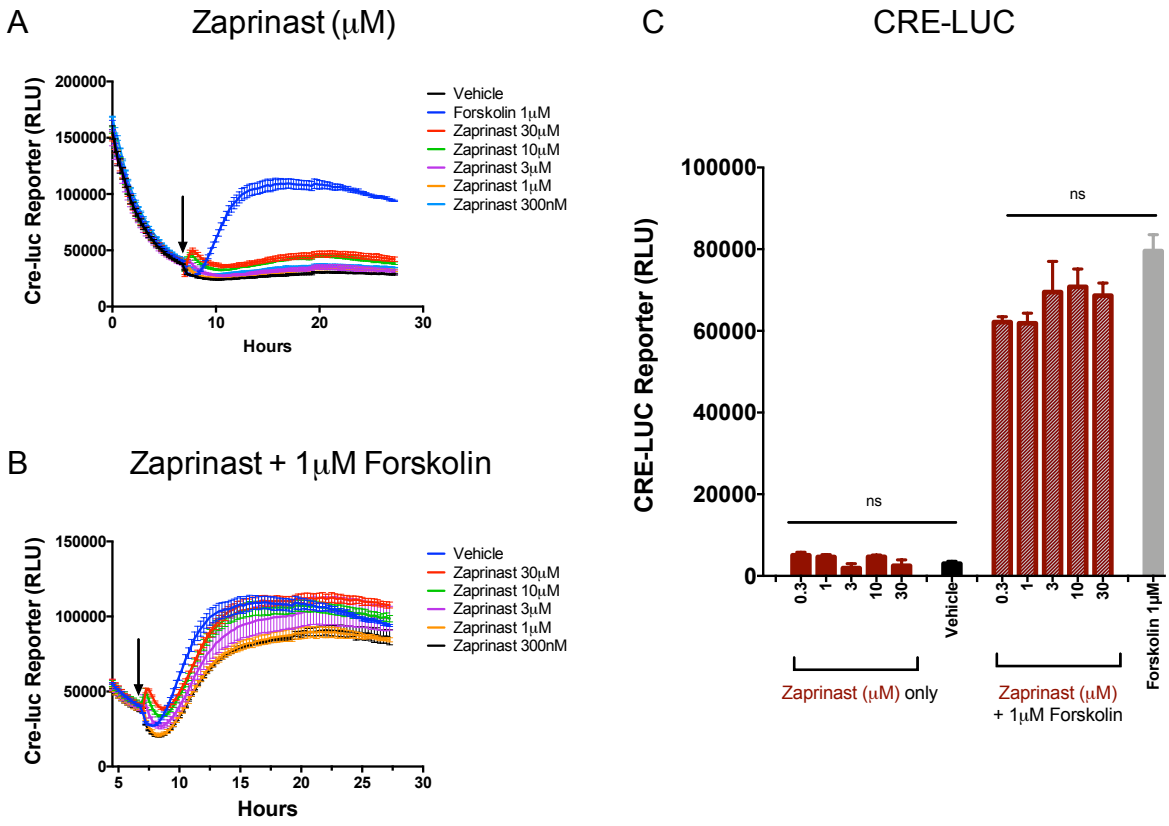


Figure 6.12. Zaprinast does not induce CRE activation: U2OS cells were transiently transfected with CRE-LUC reporter and effects of Zaprinast were assessed. Raw CRE-LUC reporter traces following treatment with **(A)** increasing doses of Zaprinast or **(B)** Zaprinast in the presence of 1 μM Forskolin. **(C)** Quantification of CRE-LUC reporter activation. Error bars represent ±SEM. N=3. Significance determined by one-way Anova.

6.2.7 mTOR inhibition reduced Zaprinast's period elongation without affecting Bmal1-promoter expression:

We have previously shown, in line with literature, that Zaprinast significantly increased adipogenesis of 3T3-L1 cells (Chapter 3, Figure 3.11b). Interestingly, the browning phenotype of cGMP was shown to be mediated through PKG phosphorylation of Raptor at Serine-791 , that results in activation of the mechanistic target of Rapamycin complex or mTORC1 (Liu, Ceddia, and Collins 2018). Furthermore, in peripheral clock models of adipocytes, inhibition of the protein kinase mTOR (mechanistic target of rapamycin) has been shown to dampen amplitude of clock gene expression (Ramanathan et al. 2018). Hence, we hypothesized that elevation of cGMP by Zaprinast could be acting via mTOR activation. To test that, we investigated the circadian effects of mTOR inhibition on *Bmal1*-d*Luc* U2OS cells and explored whether it counteracts Zaprinast's observed phenotype. Interestingly, the mTOR inhibitor Rapamycin resulted in a reduction in amplitude of *Bmal1* promoter expression on their own (Figure 6.13A), in line with the possibility of mTOR activation enhancing amplitude. However, rapamycin failed to eliminate Zaprinast's amplitude enhancement phenotype (Figure 6.13D) but nonetheless significantly reduced the period elongation elicited by Zaprinast (Figures 6.13E, 6.13D). The same observations were replicated following treatment with a second selective mTOR inhibitor Torin1 (Figure 6.14A-C). Therefore, taken together, these findings suggested that mTOR activation could partly contribute to cGMP-mediated period elongation.

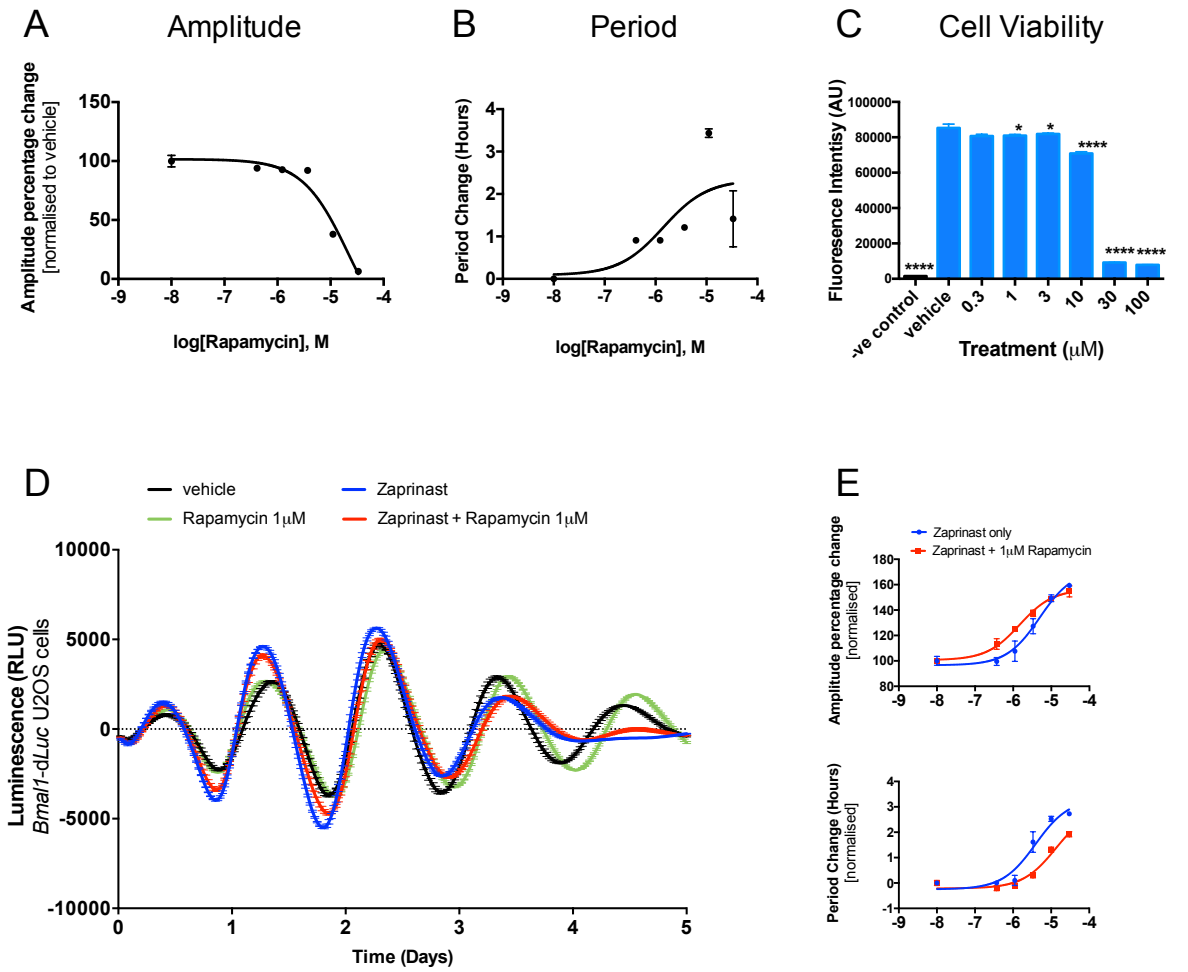


Figure 6.13. Inhibition of mTOR by Rapamycin has no effect on Zaprinast's circadian phenotype in *Bmal1*-d*Luc* U2OS cells: *Bmal1*-d*Luc* U2OS cells were treated with increasing doses of Rapamycin **(A-C)** or Zaprinast in the presence or absence of 1 μM Rapamycin **(D-E)**. **(A)** Amplitude percentage change for first day following synchronisation and Rapamycin treatment **(B)** Period change. **(C)** Cell viability. **(D)** Representative traces for Zaprinast (30 μM) alone or with 1 μM Rapamycin in *Bmal1*-d*Luc* U2OS cells. **(E)** Corresponding amplitude percentage change (top) and period change (bottom) for Zaprinast in the presence or absence of 1 μM Rapamycin.

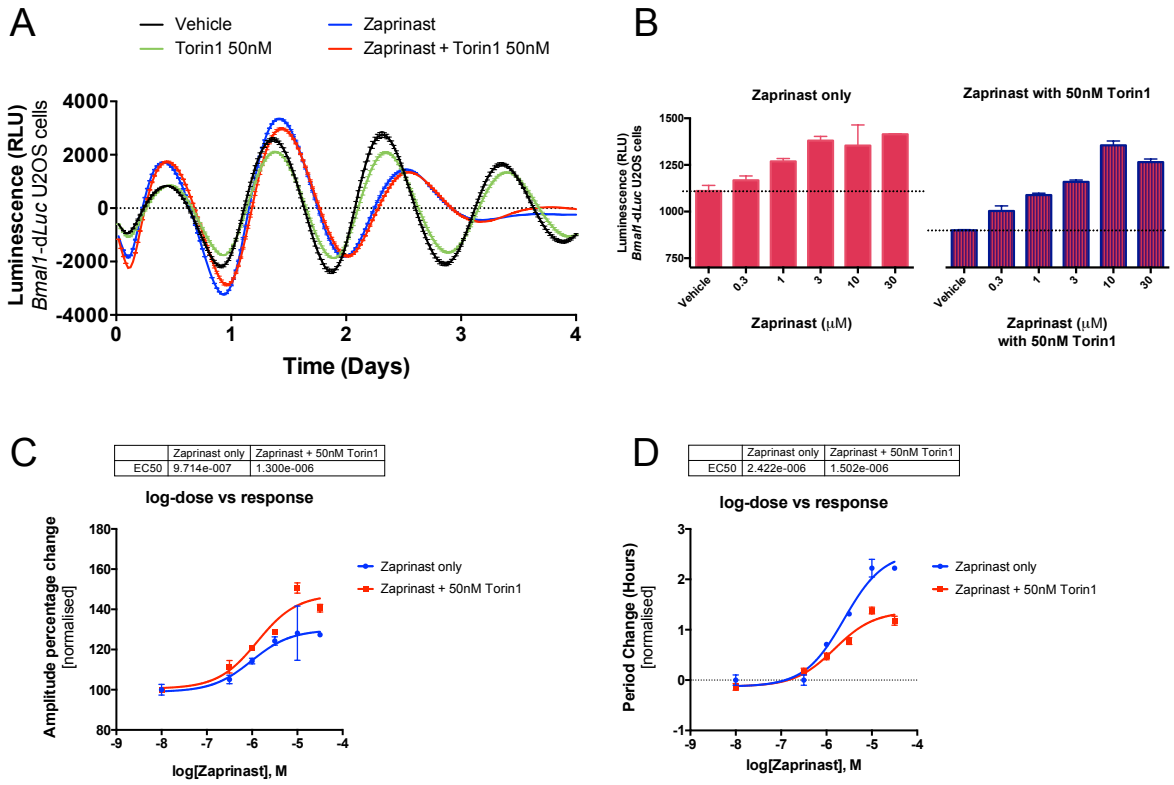


Figure 6.14. Inhibition of mTOR by Torin1 has no effect on Zaprinast's circadian phenotype in *Bmal1*-d*Luc* U2OS cells: *Bmal1*-d*Luc* U2OS cells were treated with increasing doses of Zaprinast in the presence or absence of 50 nM Torin1. **(A)** Representative traces for Zaprinast (30 μM) alone or with 50 nM Torin1. **(B)** Corresponding raw amplitude of luminescence. **(C)** Amplitude percentage change for first day following synchronisation and Rapamycin treatment. **(D)** Period change. Error bars represent ±SEM. N=3.

6.2.8 ERK inhibition potentiated Zaprinast's amplitude effect in Bmal1-dLuc U2OS cells but reduced its period elongation:

Another key pathway downstream of PKG is the extracellular signal-regulated kinase (ERK) cascade (or MAP-kinase signalling). Interestingly, PKG has been shown to both inhibit or activate ERK pathways in different cell lines (Sang et al. 2012; Komalavilas et al. 1999; Mitani et al. 2000). Therefore, to investigate how ERK could be involved, and

guided by studies that have shown cGMP-mediated increase in MAP-kinase phosphatase-1 (MKP-1) mRNA expression, independent of ERK activation (Suhasini et al. 1998), we investigated how Zaprinast treatment influences MKP-1 expression in our cell lines. Indeed, similar to what has been reported, Zaprinast resulted in a significant increase in MKP-1 mRNA, which was interestingly preceding *Bmal1* expression (Figure 6.15). To delve deeper into that, we targeted ERK pharmacologically using the selective MEK inhibitor PD98059 and the ERK1/2 selective inhibitor SCH772984. Interestingly, inhibiting the MEK/ERK cascade in both cases resulted in a significant reduction in amplitude of *Bmal1*-promoter expression (Figures 6.16C, 6.17C), supporting a role for ERK activation in enhancing circadian gene expression. However, strikingly, both could not eliminate Zaprinast's amplitude enhancing effect. Instead, when data was normalised to eliminate the amplitude inhibitory effect of MEK and ERK inhibition, both drugs resulted in a significant increase in *Bmal1*-promoter expression mediated by Zaprinast (Figures 6.16D, 6.17D). On the other hand, similar to mTOR inhibition, blocking the ERK signalling cascade significantly reduced Zaprinast's period elongation. Taken together, these findings suggested that Zaprinast could be enhancing amplitude of clock gene expression via a pathway that is generally inhibited by ERK, however at the same time proposed that the period effect, particularly those observed at high Zaprinast concentrations (>10 μM) could be somewhat associated with ERK activation.

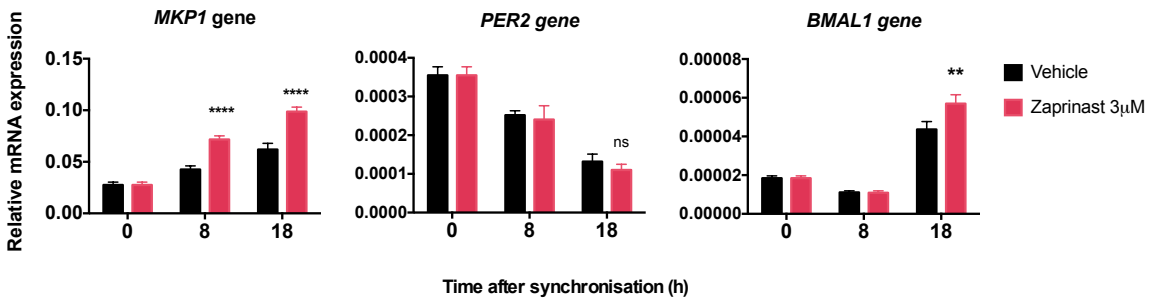


Figure 6.15. Zaprinast increases MKP1 mRNA expression: Relative mRNA expression for *MKP-1*, *PER2* and *BMAL1* genes at 0, 8, and 18 hours following synchronization. All genes normalised *to Gapdh and b-Actin. Error* bars represent ±SEM. N=3. *MPK1*: Mitogen-activated Protein Kinase Phosphatase 1.

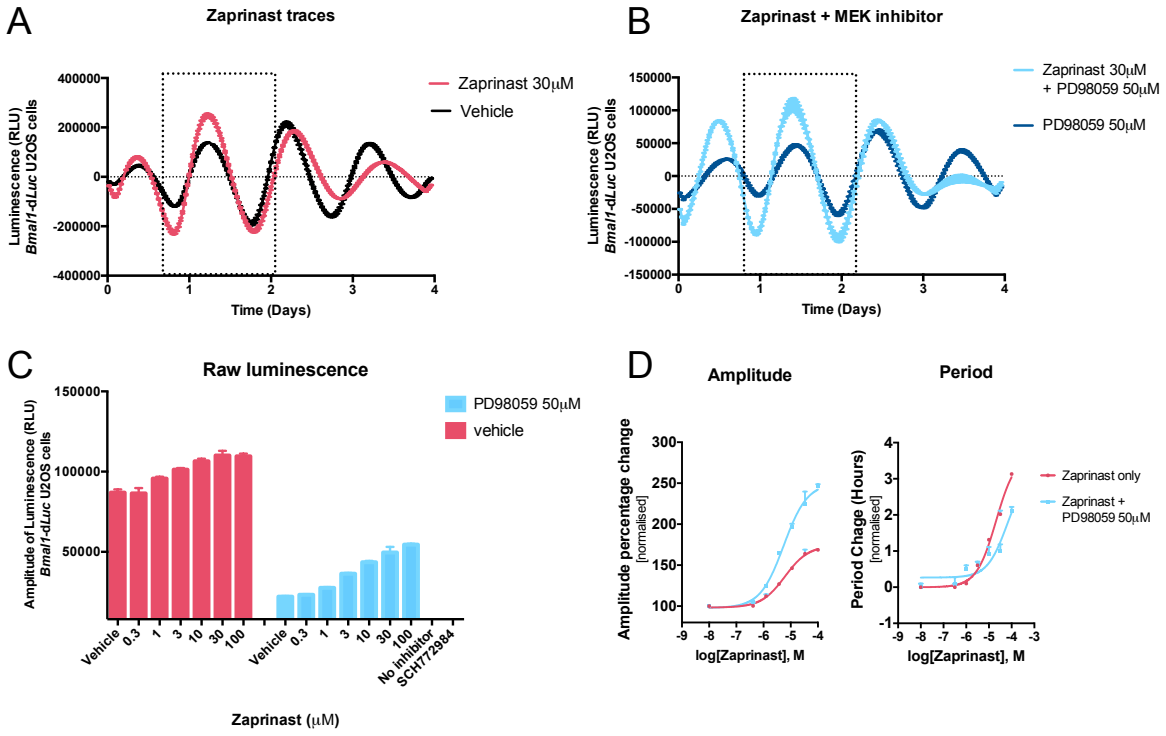


Figure 6.16. MEK inhibitor PD98059 reduces overall amplitude of *Bmal1* expression but potentiates Zaprinast's circadian phenotype in *Bmal1*-d*Luc* U2OS cells: (A) Representative traces for 30 μM Zaprinast. **(B)** Representative traces for 30 μM Zaprinast with 50 μM PD98059. **(C)** Corresponding raw amplitude of luminescence comparing both conditions. **(D)** Amplitude percentage change for first day following synchronisation (left) and Period change (right). Error bars represent ±SEM. N=3.

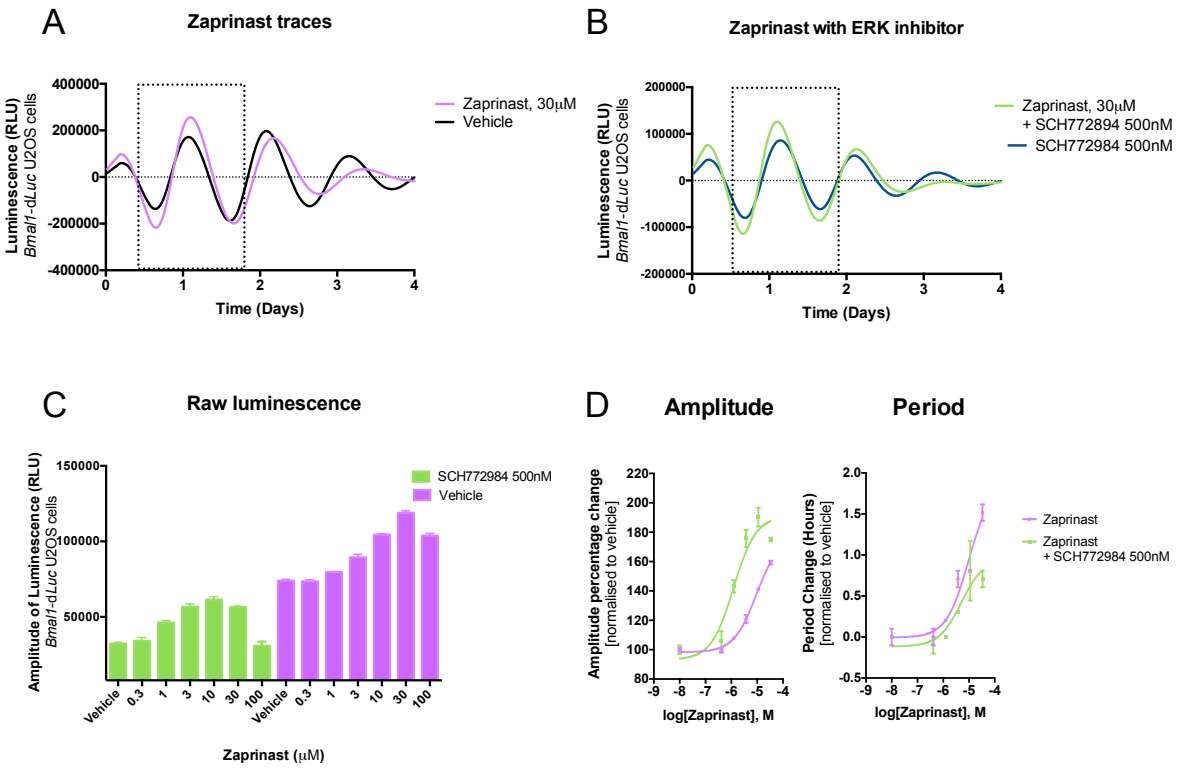


Figure 6.17. ERK1/2 inhibitor SCH772894 reduces overall amplitude of *Bmal1* expression but potentiates Zaprinast's circadian phenotype in *Bmal1*-d*Luc* U2OS cells: (A) Representative traces for 30 μM Zaprinast. **(B)** Representative traces for 30 μM Zaprinast with 500 nM SCH772894. **(C)** Corresponding raw amplitude of luminescence comparing both conditions. **(**D) Amplitude percentage change for first day following synchronisation (left) and period change (right). Error bars represent ±SEM. N=3.

6.3 Discussion:

The original motivation for our investigation was threefold: 1) to investigate the involvement of cGMP in Zaprinast's circadian phenotype, 2) Evaluate the role of cGMP in peripheral circadian rhythms, and 3) Study the role of CREB in mediating these effects.

Contrary to the conceived notion (Golombek et al. 2004; Gillette and Mitchell 2002), our study demonstrated that cGMP-elevation in response to PDE-inhibition by Zaprinast induces circadian amplitude and period enhancement in a CREB-independent pathway. Zaprinast showed selectivity for cGMP stabilisation and its circadian effect was partly dependent on PKG activity. Moreover, Zaprinast failed to phosphorylate CREB or activate CRE-elements and its circadian effects were broadly unaffected by multiple forms of dominant negative mutants of CREB. By investigating the role of ERK and mTOR, we uncovered what seemed to be a complex mechanism underlying the circadian effects of cGMP and by extension Zaprinast. This investigation has been crucial in elucidating components of the downstream pathway behind cGMP's circadian phenotype, by dismissing CREB and proposing a contributing role for mTOR in cGMP's observed effects in *Bmal1*-d*Luc* U2OS cells. Nonetheless, the cGMP effector responsible for the circadian modulation remains to be identified, setting the scene for an interesting future investigation.

6.3.1 Significance of cGMP signalling in peripheral circadian clocks:

In line with our hypothesis, our findings have shown that enhancing endogenous cGMP levels regardless of the different mechanisms can promote significant circadian effects in peripheral cells. Firstly, inhibition of PDEs by Zaprinast (Chapter 3, Figure 3.5) or Sildenafil (Figure 6.5A-C) resulted in a significant enhancement of *Bmal1* promoter expression and period elongation in U2OS cells and a similar but smaller circadian phenotype was observed with the membrane-bound guanylyl cyclase (GC-B or NRP2) activator, C-type Natriuretic Peptide (CNP). Although Zaprinast was shown to elicit a greater amplitude enhancement compared to Sildenafil, this was possibly due to its inhibitory action on all 3 PDEs (5, 6, and 9) relative to the more selective PDE5 inhibitor Sildenafil, as all three are expressed in U2OS cells (Uhlén et al. 2015). Similarly, the modest increase in amplitude of *Bmal1* expression by CNP could also be linked to low GC expression in U2OS cells (Uhlén et al. 2015) and pathway-specific compartmentalisation which is believed to generate localised elevation of cGMP near the plasma membrane (Fischmeister et al. 2006). Furthermore, our findings on Zaprinast's similar amplitude enhancing phenotype in preadipocytes, mature adipocytes, and mouse embryonic fibroblasts (Chapter 3, Figures 3.7a-b and 3.8 respectively), emphasises the significance of cGMP's circadian modulatory role in different peripheral cells. It is important to note that these findings were limited by the use of promoter-driven luciferase reporters. However, given Zaprinast significantly and selectively increased endogenous cGMP (Figure 6.3), and at the same time, was associated with a significant increase in mRNA expression of *Bmal1* (Chapter 3, Figure 3.9) and an enhancement of PER2-LUC fusion

protein expression (Chapter 3, Figure 3.8), its modulation of the clock seems clearly evident. Taken together, these observations predict that cGMP could modulate circadian rhythms in most if not all peripheral tissues, particularly through increasing amplitude.

cGMP regulates physiology mainly via targeting PDEs, PKG, or CNG (Friebe, Sandner, and Schmidtko 2020; Francis, Busch, and Corbin 2010). Similar to previous reports (Oster et al. 2003; Liu et al. 1997), our data proposed a role for PKG as a key downstream effector contributing to cGMP's circadian effects. The use of the PKG-selective inhibitor KT5823 significantly reduced the enhancement of *Bmal1*-promoter expression observed with Zaprinast and reversed its period effect (Figure 6.5). In addition, accumulating evidence supported a role for PKG in cGMP-mediated circadian effects. For instance, inhibition of PKG-II by selective antisense oligodeoxynucleotides has been shown to induce phase delays in *Bmal1* mRNA expression, supporting a role for PKG in enhancement of *Bmal1*-promoter expression (Tischkau et al. 2004). Furthermore, inhibition of PKG in the SCN using pharmacological agents and antisense oligodeoxynucleotides induced phase delays *in vitro* in the SCN, suggestive of a reversal of the cGMP-mediated phase advances usually observed following light or glutamate treatment (Tischkau et al. 2003). Similarly, *in vivo* studies also showed that mice deficient in PKG-II were insensitive to circadian clock resetting following light pulses (Oster et al. 2003). Although KT5823 reduced *Bmal1*-promoter expression by 40%, this could have been a result of incomplete inhibition of PKG by this molecule. Indeed, KT5823, although claimed as one of the most selective PKG-inhibitors available, has not always been shown to successfully inhibit PKG

(Burkhardt et al. 2000). Furthermore, KT5823 has been reported to weakly inhibit other protein kinases like PKC and PKA at IC50 of 4 μM and >10 μM, respectively (Gadbois et al. 1992). However, using 3 μM of KT5823 in our study reduced the risk of off-target inhibition given its below their threshold. Nonetheless, to fully eliminate the risk of non-specificity, the use of selective PKA and PKC inhibitors could shed more light on the involvement of cAMP and Ca^{2+} in Zaprinast's circadian effect, and seems worth exploring.

Another explanation for the incomplete reduction of Zaprinast's amplitude enhancing effects by KT5823 could be the involvement of a second pathway downstream of cGMP, independent of PKG. Indeed, cGMP has been shown to activate different ion channels, such as the big conductance Ca^{2+} activated potassium channels (BK_{Ca}) (Schubert and Nelson 2001), which in turn have been shown to regulate spontaneous rhythmicity of the SCN (Kent and Meredith 2008) and play a role in SCN daytime-gating (Whitt, Montgomery, and Meredith 2016). Nevertheless, since U2OS cells are quiescent in nature, changes in ion influx seems less likely to play a role in the observed circadian changes. Indeed, our previous findings showing lack of circadian effects of the KCNQ agonist retigabine and the potassium channel blockers Nifekalant and Clofilium tosylate in U2OS cells supports this statement (Chapter 4, Figure 4.5).

6.3.2 The mechanisms underlying cGMP's circadian modulation:

The main goal of our investigation was to assess the role of CREB in cGMP-mediated circadian regulation. Although both cGMP and CREB have both been strongly implicated in regulation of circadian machinery, and CREB is one of the downstream effectors of cGMP-PKG cascade, whether CREB drives the transcriptional enhancement of clock gene expression following cGMP elevation has not been investigated. Using U2OS cells expressing *Bmal1*-luciferase promoters and Zaprinast as a validated pharmacological tool for elevating cGMP levels and driving circadian gene expression in these cells, we studied the role of CREB as the downstream effector. Unlike the general belief that CREB could be the candidate behind cGMP's circadian modulation, our study showed Zaprinast's circadian phenotype to be independent of CREB.

Firstly, Zaprinast did not induce CREB-phosphorylation of its Ser-133 residue (Figure 6.8), which has been shown to be a vital step in CBP binding and induction of CREB-mediated gene transcription (Chrivia et al. 1993; Kwok et al. 1994). Similarly, Zaprinast's circadian effect did not seem to be dependent on CREB phosphorylation at neither its Ser-133 nor its 142 sites (Figures 6.7, 6.9), the two most established sites for regulating CREB-activation (Mayr and Montminy 2001). Interestingly, overexpression of the mutant $CREB^{S133A}$ significantly reduced amplitude of *Bmal1*-promoter expression on its own (Figure 6.7), therefore supporting a role for CREB in regulating clock gene transcription. Nonetheless, although it abolished Forskolin-mediated CRE activation as predicted (Figure 6.6), it failed to eliminate Zaprinast's circadian amplitude or period

effects (Figure 6.7). This proposed that CREB phosphorylation at the Ser-133 site was unnecessary for cGMP-mediated actions on the clock.

Furthermore, CRE elements were unresponsive to Zaprinast treatment, even when basal cAMP and activated CREB levels were boosted with Forskolin (Figure 6.12). CRE has been shown to be expressed in *Per1* and *Per2* promoters (Travnickova-Bendova et al. 2002) and is the main response element associated with CREB-mediated gene transcription (Mayr and Montminy 2001; Shaywitz and Greenberg 1999). The CRE-LUC plasmid used in our experiments contains CREB's canonical response element and therefore should show high responsiveness to CREB-binding, as shown with forskolin (Figure 6.12). Thus, the lack of CRE activation strongly supported lack of CREB DNA-binding following Zaprinast treatment. This was further reiterated with the use of the K-CREB mutant which also failed to counteract Zaprinast's circadian phenotype (Figure 6.11). As mentioned previously, this dominant negative mutant contains a point mutation within its K304 residue that mediates its interaction with Mg^{2+}, therefore preventing its DNA-binding. It also heterodimerises with wild type CREB, therefore does not only rely on competitive inhibition, but can also quench other members of the CREB transcription family (Walton et al. 1992). Hence, further eliminating a role for other members of the CREB transcription family, like ATF-1, and CREM in Zaprinast's circadian phenotype.

Interestingly, evidence from several studies supports our observations. Indeed, activating cGMP-cascade in several peripheral cell lines, like Baby Hamster Kidney cells

(BHK) or fibroblasts showed no induction of CREB phosphorylation and CRE activation when investigated at native GC and PKG expression (Gudi et al. 2000; Sauzeau et al. 2003; Gudi et al. 1996) (as opposed to over expression), which resembled the conditions of our experiment, and is more representative of the natural state of a cell. Finally, we have shown in our previous work (Chapter 3, Figure 3.5, 3.6) that Zaprinast predominantly increased amplitude of *Bmal1*-promoter expression (60%) but had a much smaller effect on the CRE-containing *Per2*-promoter in U2OS cells (Travnickova-Bendova et al. 2002), again reinforcing the CRE-LUC data and reiterating the lack of CREB involvement in this cell line.

Interestingly, Gudi *et al* and Sauzeau *et al* both showed that cGMP analogues do elicit CREB phosphorylation in the previously mentioned peripheral cells, but only when allowed to overexpress GC or PKG (or both) (Gudi et al. 2000; Sauzeau et al. 2003). Hence, this proposes the existence of cell-type specific differences in the underlying mechanism of cGMP-mediated circadian clock modulation based on the level of expression of the regulatory molecules within the cascade in different cells. As a result, reproducing our findings in other cell types, as well as in the SCN, is of importance to understand the role of cGMP as a chrono-modulatory second messenger. This would help us comprehend the mechanistic pathways of cGMP-dependent phase advances in the SCN vs amplitude enhancements in peripheral circadian clocks. On a similar note, since the amplitude of clock gene expression has been associated with resistance to phase shifts as verified by both experimental as well as mathematical modelling studies (Lakin-Thomas, Brody, and

Cote 1991; Jewett, Kronauer, and Czeisler 1994), it suggests that endogenous cGMP elevation in peripheral clocks could be associated with a reduction in peripheral cells' response to mis-cued stimuli (e.g. wrongly timed food, relative to time of the day). This is particularly important, given misalignment between feeding cues and light stimuli can re-entrain peripheral clocks and uncouple peripheral clocks from SCN phase (Damiola et al. 2000) and such circadian disruption has been strongly linked to symptoms of metabolic disorder, like hypertension, obesity, and diabetes (*see* Chapter 1).

Following the dismissal of CREB's role in mediating Zaprinast's circadian phenotype, and in efforts to explore the underlying mechanism downstream of cGMP elevation, our study further investigated two possible signalling cascades that have reported cross-talk with cGMP; mTOR and ERK.

Interestingly, the mTOR inhibitor Rapamycin decreased amplitude and increased period of *Bmal1*-d*Luc* U2OS cells, similar to what has been reported in other cell lines harbouring the *Per2*-d*Luc* reporter (Ramanathan et al. 2018). Together with evidence linking mTOR activation with cGMP-dependent adipocyte browning (Liu, Ceddia, and Collins 2018), this proposed mTOR activation via Zaprinast as a possible mechanism. However, both mTOR inhibitors Rapamycin and Torin1 could not completely counteract the circadian amplitude enhancing effects of Zaprinast. Nonetheless, both inhibitors significantly reduced Zaprinast's period elongation in *Bmal1*-d*Luc* U2OS cells. Taken together, this suggested a definitive role for mTOR activation in Zaprinast's period effect.

Since our data represented expression of *Bmal1*-promoter expression, an increase in period without affecting amplitude of expression can only be explained with a post-transcriptional modification or stabilisation of the BMAL1 or PER2 proteins over several days. Interestingly, Lipton *et al* have shown that elevation of mTOR activity *in vivo*, in mice expressing mutants of the key inhibitors of mTOR, *tsc1* and *tsc2*, resulted in higher rate of BMAL1 protein production and reduction in its degradation rate, most importantly without affecting its mRNA expression (Lipton et al. 2017), therefore supporting a role for mTOR activation in the period elongation elicited by Zaprinast. Nonetheless, additional lines of evidence are needed to confirm mTORs pathway being the sole mediator of Zaprinast's effects in this cell line and to apprehend how cGMP promotes enhancement of *Bmal1* expression.

As the cGMP pathway has been linked to the ERK pathway, for completeness, we targeted the ERK pathway to investigate its involvement in driving Zaprinast's amplitude enhancing effect. Interestingly, MEK and ERK inhibition on their own elicited a significant reduction in amplitude of *Bmal1*-promoter expression. However, in the presence of Zaprinast, they significantly potentiated its amplitude effect. This suggested that Zaprinsat could be targeting a pathway that is generally inhibited by ERK activation, providing a clue for the actual pathway mediating cGMP's effects. One such pathway, at the intersection between ERK inhibition, cGMP, and circadian regulation is the IRS/pAKT pathway. For example, activated ERK has been shown to inhibit phosphorylation of the insulin-receptor substrate (pIRS) (by activating mTOR) (Winter, Jefferson, and Kimball

2011; Guertin and Sabatini 2005) and also inhibit protein kinase B (pAKT) activation (Kiyatkin et al. 2006). In addition, insulin, which actively enhances IRS1/pAKT, has been shown to reduce phosphorylated REVERBα activity and eliminate its repressing actions on *Bmal1* mRNA expression (Mukherji et al. 2015), hence could suggest a link between pAKT activation and the increase in amplitude of expression of the latter. On a similar note, NO and Sildenafil have both been shown to enhance pAKT and IRS1 signalling pathway *in vitro* and when insulin-stimulated *in vivo*, respectively (Rizzo et al. 2010), which has been replicated in various cell lines (Kawasaki et al. 2003; Ciani et al. 2002). Taken together, this could introduce cGMP-mediated enhancement of pAKT pathways as a possible mechanism worth investigating, and also proposes a role for PI3K-mTOR pathway where pAKT lies in the middle of this signalling cascade. However, although this might be the case in peripheral tissues, this pathway may not be of relevance in cGMP-mediated phase shifts within the SCN. Indeed, light-induced phosphorylation of AKT has not been detected in the SCN, indicating a minimal level of Akt involvement (Cao et al. 2012). More importantly, the SCN has been shown to be insensitive to food-driven phase resetting (Damiola et al. 2000), and work by Crosby and colleagues have verified a lack of SCN response to insulin, a key postprandial hormone and an important activator of PI3K/Akt signalling, which was attributed to the strong network coupling in this region (Crosby et al. 2019).

Furthermore, although MEK/ERK inhibition potentiated Zaprinast's amplitude enhancing effect, they however significantly reduced its period enhancing effect, similar

to mTOR inhibition. This is particularly interesting since ERK and mTOR pathways cross-talk, where ERK has been shown to cross-activate mTORC1 signalling (Mendoza, Er, and Blenis 2011). For instance, Ras activation (which leads to MEK and ERK activation) inhibits the suppressive actions of *TSC2* on mTOR thereby increasing its activity (Roux et al. 2004). Therefore, this suggests MEK/ERK inhibition could lead to mTOR inhibition, again pointing towards an mTOR-mediated period elongation. Hence, investigating the activation of validated mTOR targets like phosphorylated S6 Kinase (S6K1) following Zaprinast treatment is one way of probing mTOR involvement, and is key in authenticating its interaction further.

All things considered, the mechanism via which cGMP mediates its circadian phenotype is a complex one that has not been resolved yet. Given Zaprinast resulted in a transcriptional increase in *Bmal1* mRNA (Chapter 3, Figure 3.9), another unbiased line of investigation that could be worth pursuing is BC-STAR-PROM that we previously utilised with Linopirdine in Chapter 4. This powerful unbiased screen could shed light on all upregulated transcription factors downstream of cGMP and provide key leads to understand the signalling cascade involved.

6.4 Conclusion:

In conclusion, although its known that cGMP and PKG play a role in photic entrainment of the SCN, the exact mechanistic pathways that relays their effects remains elusive. Furthermore, whether cGMP plays a role in peripheral clocks has not been previously reported. In our study, we have presented the cGMP cascade as a robust circadian modulator in peripheral cells, acting via PKG. The mechanism via which cGMP interacts with the clock is complex and possibly involves several converging pathways. Contrary to what was believed in the SCN, our study showed that cGMP elevation interacts with the U2OS clock in a CREB-independent manner. Furthermore, we propose that the observed amplitude enhancement and period elongation possibly occur via distinct and accumulative pathways. The underlying mechanism driving cGMP's circadian modulation remains unresolved, but the mTOR pathway has the hallmarks of being a pathway of interest, thus providing an exciting area for future investigations. Understanding the molecular signal transductions behind endogenous chrono-modulators is important as it helps improve our understanding of known molecular feedback loops of clock genes and their products and also provides clues as to how the clock keeps track with our environments.

CHAPTER 7:

General Discussion

Metabolic syndrome (MetS) embodies a clustering of different metabolic abnormalities affecting approximately 25% of the world's population, as estimated by the International Diabetes Federation (IDF) (O'Neill and O'Driscoll 2015). It exhibits a multifaceted pathophysiology, many aspects of which coincide with physiological abnormalities as a result of circadian disruption. The circadian clock governs major aspects of metabolism, including key pathways involved in the pathophysiology of MetS, like glucose homeostasis and lipid metabolism. Obesity, on the other hand, has been associated with a reduction in clock gene expression in key metabolic genes. Therefore, targeting the circadian clocks is emerging as an interesting area for pharmacological intervention. Indeed, a handful of small molecules targeting the clock have shown metabolic benefit in MetS, however, which direction of chrono-modulation is beneficial remains unclear. For instance, small molecules that increase amplitude and period (like the ROR agonist nobiletin), or reduce amplitude (like REV-ERB and CRY agonists) have both been shown to ameliorate symptoms of MetS. This stresses the grave influence of the circadian clock on metabolism and metabolic disorders, but also demonstrates the need for further investigations to understand this influence, not only to increase our knowledge of how circadian clocks and metabolism converge, but also to guide more promising drug discovery efforts.

7.1 Understanding Linopirdine's mechanism of action- a novel circadian enhancing molecule

In the search for novel chrono-modulators and circadian-enhancing molecules, and following a multi-step medium-throughput screen, Linopirdine was identified as one of the key leads of our circadian screen (see Chapter 3), owing to its potent ability to increase expression of *Bmal1* and *Per2* promoters in different cell lines (Figures 3.5-3.8). Despite being developed as a KCNQ channel blocker, Linopirdine's circadian phenotype was not mediated by that pathway. Instead, using in silico mining and cutting-edge unbiased transcription factor screening (BC-STAR-PROM), our study demonstrated a novel pathway underlying Linopirdine's circadian phenotype (see Chapter 4, Figures 4.12, 4.21, 4.22). Indeed, we identified Linopirdine as a novel MEIS1 activator and HIF up-regulator. On one hand, the ability of Linopirdine to enhance *Bmal1* promoter expression in a HIF-dependent mechanism (Figure 4.12) reaffirms the role of HIF in circadian regulation. On the other hand, the identification of MEIS1 transcription factor as the mediator behind Linopirdine's circadian effect supports the involvement of MEIS1 in circadian regulation. Indeed, a recent GWAS study proposed a correlation between low amplitude of human circadian rhythms and SNPs in MEIS1 (Ferguson et al. 2018). In addition, heterozygous MEIS1 knockout mice, particularly males, have been reported to display circadian hyperactivity (Salminen et al. 2017). Hence, an association between MEIS1 and circadian pathways has been previously reported in literature, but our study provides the first direct link between MEIS1 and *Per2* promoter upregulation. As MEIS1 is highly associated with cell proliferation and development that maintains cells in a

proliferative stage (Calvo et al. 2001), identifying an input pathway of this transcription factor into the circadian clock machinery is particularly important as it could guide our understanding of how the proliferative stage of a cell can feedback into the circadian clock. Indeed, peripheral circadian rhythms have been implicated in the regulation of the cell cycle. Expression of several key genes in cell-cycle progression were found to be under CLOCK-BMAL1 transcriptional regulation, while livers following partial hepatectomy were shown to regenerate much slower in *Cry1*/2 double KO mice compared to wild-type (Matsuo et al. 2003). Furthermore, individual cells have been shown to maintain rhythmic protein expression during cell division and the onset of their cell-division is gated by the circadian clock (Nagoshi et al. 2004). However, apart from transcription silencing that occurs during mitosis that is bound to impact the transcriptional feedback loops regulating the clock (Gottesfeld and Forbes 1997), there is very little evidence for cell cycle-dependent control of the circadian clock (Feillet et al. 2015). Therefore, investigating the role of MEIS1 in circadian regulation and cell proliferation can shed light on the cross-talk between both pathways.

Furthermore, to date and to the best of our knowledge, there are no reported small molecules that increase MEIS1 activity. Interestingly, reduction in mRNA and protein levels of MEIS1 have been linked to restless leg syndrome (RLS), a highly prevalent neurological disorder, estimated to vary between 3.9% and 14.3% in general populations (Ohayon et al. 2012; Sarayloo et al. 2019; Xiong et al. 2009). This proposes the use of Linopirdine as an investigative tool in understanding the role of MEIS1 in the

pathophysiology of this condition, and perhaps as an interesting new therapeutic intervention to explore.

7.2 Role of cGMP in peripheral clock regulation:

SCN-based investigations have reported an important role of cGMP in light-induced phase advances both *in vivo* and *in vitro* (Golombek et al. 2004; Agostino, Plano, and Golombek 2007) , however little was known about its role in peripheral clocks. Following an unbiased circadian screen, we identified the cGMP-selective PDE inhibitor Zaprinast as a potent chrono-modulator and helped shed light on this interesting pathway. Our findings provided the first evidence of cGMP-mediated regulation of clock gene expression in peripheral tissues. This suggests that the signalling cascades in SCN and peripheral tissues overlap and emphasises the importance of this pathway in regulating circadian clocks in different tissues.

The role of PKG in the SCN phase advances is evident (Gudi et al. 1996; Liu et al. 1997), however, its actions in the SCN are predominantly attributed to CREB phosphorylation and *Per* transcription (Albrecht et al., 1997; Albrecht et al., 2001; Gillette & Mitchell, 2002; Golombek et al., 2004). In our study, we demonstrated a lack of CREB effect on cGMP-driven circadian clock gene expression in peripheral cells (Chapter 6, Figures 6.7-6.12) and a more prominent increase in *Bmal1* mRNA expression and amplitude following cGMP stabilisation (Chapter 3, Figures 3.5,3.6). Furthermore, our findings proposed that the observed amplitude enhancement and period elongation possibly

occur via distinct and accumulative pathways, and introduces ERK and mTOR as two interlinking pathways potentially involved in cGMP's circadian function (Chapter 6, Figures 6.13-6.17).

In light of this, further investigation of the role of these molecules is of great interest and worth exploration, as it will improve our understanding of how cGMP and the circadian clock interact. Furthermore, replicating these findings in the SCN can shed light on a fundamental mechanism underlying light-induced phase advances. In addition, most cAMP stabilisers have failed as therapeutic candidates because of their broad side effects (Boswell-Smith, Spina, and Page 2006), while cGMP-selective PDE like Sildenafil are safe and frequently prescribed, which proposes the cGMP-cascade as an interesting and potentially useable druggable pathway for chrono-modulation and phase resetting.

7.3 *In vitro* and *in vivo* metabolic investigations of circadian modulators:

As the adipocyte is a key metabolic organ with a robust autonomous clock that regulates various aspect of its metabolism, one of our key aims was to investigate how novel chrono-modulators that enhance the adipocyte clock influence this tissue's metabolic profile. To do that, several *in vitro* assays that correlate to various aspects of metabolic syndrome at the adipocyte level were set up, and the main leads from our in-house medium-throughput screen were tested. While trying to characterize the metabolic phenotypes of our 3 lead circadian amplitude enhancers, we uncovered major differences in their adipogenic (Figures 3.11-3.12), lipolytic (Figure 3.13) and

bioenergetic profiles (Figures 3.14-3.17). Furthermore, the changes in metabolic phenotypes observed did not correlate with the extent of amplitude enhancement; for instance, Zaprinast showed the biggest amplitude effect in *Per2* rhythms of mature 3T3-L1 cells (Figure 3.8), but contrarily had the smallest effect on glucose uptake (Figure 3.10) and a minor influence on energy dynamics of adipocytes (Figure 3.15). This highlighted that enhancement of amplitude of the adipocyte autonomous circadian machinery alone is not enough to predict physiological and metabolic changes. Indeed, although an extensive metabolic screen of different adipocyte clock-enhancing molecules has not been reported before, discrepancies in the effects of different circadian modulators on adipogenesis have been previously described. For instance, the amplitude enhancing ROR agonist, nobiletin, has been shown to increase adipogenesis in 3T3-L1 adipocytes (Saito, Abe, and Sekiya 2007), while REV-ERB agonists that reduce amplitude have shown similar effects (Kumar et al. 2010). Furthermore, metformin whose mechanism of action is partly attributed to AMPK activation, has been shown to induce phase advances and suppress *Clock* gene expression in liver, but promote phase delays and increase *Clock* gene expression in muscle. However, its metabolic effects on both tissues are similar (Barnea et al. 2012). Therefore, these findings demonstrate the complexity of metabolic pathways and stress the importance of the mechanistic targets of these drugs in predicting physiological outcomes.

Another aim of our study was to investigate the influence of target vs clock effects in ameliorating the development of MetS. To address that, Linopirdine was administered

daily in a DIO-mouse model and the progression of metabolic anomalies were assessed. Linopirdine profoundly exacerbated the development of various aspects of the metabolic syndrome, like weight gain, insulin resistance (Chapter 5, Figure 5.2) and hepatic steatosis (Figure 5.3). As we validated Linopirdine to increase HIF activity (Chapter 4, Figure 4.10), we hypothesized it would mimic intermittent hypoxia *in vivo*, which has been reported to exacerbate outcomes of metabolic syndrome (Polotsky et al. 2003; Drager et al. 2011). Remarkably, our *in vivo* metabolic data was indeed in complete agreement with our *in vitro* studies demonstrating HIF1α stabilisation as the primary mechanism underlying Linopirdine's circadian effects. Indeed, Linopirdine replicated HIF stabilisation and over-expression studies linking adipocyte-specific overexpression of HIF1α with increase in body weight and insulin resistance (Halberg et al. 2009; Jun et al. 2017), hypoxia with increase in skeletal muscle insulin-stimulated glucose uptake (Gamboa, Garcia-Cazarin, and Andrade 2011) and hepatocyte-specific disruption of VHL, PHD2 or PHD3 with onset of hepatic steatosis (Kucejova et al. 2011; Luo et al. 2018; Minamishima et al. 2009). This was particularly interesting as it provides to the best of our knowledge the first evidence of a HIF-stabilising small molecule in a DIO *in vivo* model, which supports HIF-overexpression and knockout studies, but avoids complications linked to genetic redundancies. Furthermore, it sheds light on the role of HIF in diet-induced obesity outside of hypoxic environments, since low oxygen could interact with pathways other than HIF, including alteration of enzymatic activity (Lushchak et al., 1998; O'Dwyer et al., 1994), impairment of oxidative phosphorylation (Fuhrmann and Brüne 2017; Gnaiger and Kuznetsov 2002) and risk of reactive oxygen

species (ROS) accumulation (Chandel et al., 1998; Patel et al., 2019). For example, hypoxia and $CoCl_2$ have both been shown to increase ROS, however they activate transcription via different pathways, emphasizing that hypoxia and pharmacological inhibition of HIF cascades are not identical (Chandel et al., 1998). Taken together, our study demonstrates a detrimental role of HIF hyperactivation in the development of metabolic syndrome. As HIF stabilisers like Molidustat are currently being developed for the treatment of severe anaemia (Macdougall et al., 2019; Zhong, Zhou, Li, & Zhong, 2018), these molecules should be administered with caution or alongside mindful feeding regimens to avoid detrimental metabolic phenotypes.

Moreover, in our *in vivo* investigation, Linopirdine predominantly displayed effects of HIF stabilisation and MEIS1 upregulation. This suggested dominance of its HIF stabilising effects, which outweighed its amplitude enhancing outcomes. While addressing our aim of understanding the importance of the target via which we facilitate circadian modulation, we conclude that understanding the mechanisms and signalling cascades underlying the circadian phenotypic outcomes of the drug in question is of uttermost importance, and likely plays the dominant role. Furthermore, the use of unbiased phenotypic circadian screens is a very useful approach that can help shed light on novel sites of circadian interactions and points of input that improve our knowledge of the circadian machinery and its accessory pathways. Indeed, our identification of MEIS1 (Chapter 4) and cGMP (Chapter 6) is a good example of that. In addition, other groups have identified novel sites of circadian regulation successfully using similar approaches.

For instance, Hirota and colleagues have identified GSK-3beta as a key enzyme in regulating circadian period using similar chemical biology techniques (Hirota et al. 2008), which highlights the effectiveness of such unbiased pharmacological screening in investigating unidentified mechanisms of the circadian clock.

On another note, our *in vivo* investigation demonstrated the development of profound hyperinsulinemia and insulin resistance (Chapter 5, Figure 5.2) in Linopirdine-treated DIO mice, despite the improvements to insulin sensitivity markers in the skeletal muscles (Figure 5.9). Linopirdine also caused a significant reduction in insulin sensitivity markers in liver and adipose tissue (Figures 5.7-5.8). Although skeletal muscles are believed to account for up to 80% of postprandial plasma glucose uptake in healthy individuals (Thiebaud et al. 1982), our data shows the influence of impaired liver and adipocyte insulin signalling (as a result of high fat diet) outweighs the benefit of any improvement in insulin sensitivity within the skeletal muscle in conditions of high-energy abundance. This is not surprising, as the liver is the main site for glycogenesis and gluconeogenesis (Han et al., 2016), and dysfunction in its insulin sensitivity will significantly impair glucose homeostasis (Sharabi et al., 2015). Nonetheless, this observation stresses the importance of tissue-specific effects of pharmacological intervention and emphasises the impact of liver insulin signalling pathways in development of metabolic syndrome.

Furthermore, the adipocyte *in vitro* assays on their own were not enough to predict *in vivo* outcomes, however they significantly contributed to our understanding of

Linopirdine's *in vivo* actions and helped shed light on the advantages and drawbacks of using different metabolic screening assays in adipocytes. For instance, although Linopirdine improved glucose uptake in adipocytes *in vitro* (Chapter 3, Figure 3.10), and in lean mice *in vivo* (Chapter 5, Figure 5.1), it still resulted in worsened overall insulin resistance under high fat diet (Chapter 5, Figure 5.2). This suggests that the *in vitro* adipocyte glucose uptake assay is predictive of glucose uptake in a healthy lean model. However, it does not apply in pathological conditions (under HFD) where adipocytes are inflamed and hypertrophic, thereby necessitating the development of a newer model for investigating the effects of drugs on glucose uptake in conditions of high energy abundance or pathological adipocytic phenotypes. Furthermore, *in vitro*, the lipolysis assay showed increase in glycerol release from mature adipocytes (Chapter 3, Figure 3.13), which did not correlate with plasma triglycerides levels, that remained unchanged despite the profound increase in overall weight (Chapter 5, Figure 5.2). This could have been attributed to the increase in hepatic fatty acid uptake and onset of hepatic steatosis (Chapter 5, Figure 5.3), thereby again stressing the influence of the liver in maintaining lipid homeostasis. Interestingly, the adipogenesis assay seemed to be the most predictive of these metabolic assays, where the *in vitro* increase in preadipocyte number (Chapter 3, Figure 3.11a) and WAT adipogenic markers (Chapter 3, Figure 3.12b) following Linopirdine treatment correlated with a significant increase in body weight (Chapter 5, Figure 5.2) and fat mass *in vivo*, highlighting this assay as a key asset for future *in vitro* screening protocols.

Therefore, given these observations and the multifaceted pathophysiology of the MetS, one key learning outcome would be to incorporate other tissues in the metabolic screen for future drug discovery efforts. Indeed, the effects of different chrono-modulators that have shown benefit against metabolic syndrome have been reported in hepatocyte or muscle cultures. As previously discussed, CRY agonists for example, have been shown to inhibit glucagon-induced gluconeogenesis in primary hepatocytes (Hirota et al. 2012) and improve insulin sensitivity *in vivo* (Humphries et al. 2016). In skeletal muscles, REV-ERB agonist SR9009 has been shown to modulate gene networks controlling mitochondrial function and number, and as a result improve muscle oxidative function (Woldt et al. 2013). Similar *in vivo* REV-ERB activation was paralleled with a significant increase in energy expenditure and reduction in obesity in DIO-mouse model (Solt et al. 2012). In addition, adipocyte *in vitro* models have also been beneficial, where the amplitude enhancing small molecule nobiletin, that also ameliorates onset of MetS, was shown to enhance glucose uptake and adipogenesis in 3T3-L1 cells (Onda et al. 2013; Saito, Abe, and Sekiya 2007). Therefore, one way of taking this forward is to follow up the circadian phenotypic screen with multiple tissue-specific screens. For example, testing molecules for their effects on glycogen homeostasis in hepatocytes, cellular bioenergetics in skeletal muscles, adipogenic effects in adipocytes, and glucose uptake effects in all three tissues. This would likely provide a better prediction of their overall metabolic benefit away from humoral inputs, and if accompanied with a mechanistic understanding of its signalling cascade, could hold greater potential of positive metabolic outcomes.

7.4 Final overviews:

Returning to the original aims we set out to inspect, the work presented contributes several novel findings to both the fields of circadian rhythms and metabolic syndrome research, and in the advancement of drug discovery at the intersection of these two fields.

On one hand, we identified 3 novel chrono-modulators and shed light on two interesting pathways interacting with the circadian machinery as a consequence. We uncovered a novel mechanism of action for one of our lead chrono-modulators, Linopirdine, as a MEIS1 activator and HIF up-regulator, and in the process demonstrated the first evidence supporting a direct role for MEIS1 in circadian clock regulation. Furthermore, our work also provided the first *in vivo* investigation of a HIF enhancing molecule in the development of metabolic syndrome, which supports findings from genetic and hypoxic approaches, away from genetic redundancies and low oxygen effects. Furthermore, we also unearthed a new role for cGMP in regulation of peripheral circadian clocks, independent of CREB.

On the other hand, we were one of the first groups to carry out a phenotypic characterization of various circadian amplitude enhancers on adipocytes, thereby demonstrating a lack of correlation between pharmacological amplitude enhancement of adipocyte clock and metabolic phenotypes, and consequently excluding adipocyte-clock enhancement as a mechanism that justifies discrepancies between different directions of chrono-modulation. Instead, our findings emphasised the importance of

understanding the mechanisms and signalling cascades underlying the circadian phenotypic outcomes of the drug and proposed the drug target as the dominant predictor of *in vivo* effects.

Overall, our work sheds light on novel pathways of circadian clock regulation, provides original insight into the use of small molecule chrono-modulators in the treatment of metabolic syndrome, and highlights key experimental learning outcomes, which could pave the way for more efficient future drug discovery efforts.

References:

Abe, Michikazu, Erik D Herzog, Shin Yamazaki, Marty Straume, Hajime Tei, Yoshiyuki Sakaki, Michael Menaker, and Gene D Block. 2002. "Circadian Rhythms in Isolated Brain Regions." *The Journal of Neuroscience* 22 (1): 350 LP – 356. https://doi.org/10.1523/JNEUROSCI.22-01-00350.2002.

Abrahamson, E E, and R Y Moore. 2001. "Suprachiasmatic Nucleus in the Mouse: Retinal Innervation, Intrinsic Organization and Efferent Projections." *Brain Research* 916 (1–2): 172–91. https://doi.org/10.1016/s0006-8993(01)02890-6.

Adamovich, Y, L Rousso-Noori, Z Zwighaft, A Neufeld-Cohen, M Golik, J Kraut-Cohen, M Wang, X Han, and G Asher. 2014. "Circadian Clocks and Feeding Time Regulate the Oscillations and Levels of Hepatic Triglycerides." *Cell Metabolism* 19: 319–30.

Adamovich, Yaarit, Benjamin Ladeuix, Marina Golik, Maarten P. Koeners, and Gad Asher. 2017. "Rhythmic Oxygen Levels Reset Circadian Clocks through HIF1α." *Cell Metabolism* 25 (1): 93–101. https://doi.org/10.1016/j.cmet.2016.09.014.

Agostino, P. V., S. A. Plano, and D. A. Golombek. 2007. "Sildenafil Accelerates Reentrainment of Circadian Rhythms after Advancing Light Schedules." *Proceedings of the National Academy of Sciences* 104 (23): 9834–39. https://doi.org/10.1073/pnas.0703388104.

Agostino, Patricia V, Gabriela A Ferreyra, Alejandro D Murad, Yasuo Watanabe, and Diego A Golombek. 2004. "Diurnal, Circadian and Photic Regulation of Calcium/Calmodulin-Dependent Kinase II and Neuronal Nitric Oxide Synthase in the Hamster Suprachiasmatic Nuclei." *Neurochemistry International* 44 (8): 617–25. https://doi.org/https://doi.org/10.1016/j.neuint.2003.09.005.

Akashi, Makoto, and Toru Takumi. 2005. "The Orphan Nuclear Receptor RORalpha Regulates Circadian Transcription of the Mammalian Core-Clock Bmal1." *Nature Structural & Molecular Biology* 12 (5): 441–48. https://doi.org/10.1038/nsmb925.

Akashi, Makoto, Yoshiki Tsuchiya, Takao Yoshino, and Eisuke Nishida. 2002. "Control of Intracellular Dynamics of Mammalian Period Proteins by Casein Kinase I Epsilon (CKIepsilon) and CKIdelta in Cultured Cells." *Molecular and Cellular Biology* 22 (6): 1693–1703. https://doi.org/10.1128/mcb.22.6.1693-1703.2002.

Akhtar, Ruth A, Akhilesh B Reddy, Elizabeth S Maywood, Jonathan D Clayton, Verdun M King, Andrew G Smith, Timothy W Gant, et al. 2002. "Circadian Cycling of the Mouse Liver Transcriptome , as Revealed by CDNA Microarray , Is Driven by the Suprachiasmatic Nucleus." *Current Biology* 12 (02): 540–50.

Alberti, K. G.M.M., Robert H. Eckel, Scott M. Grundy, Paul Z. Zimmet, James I. Cleeman,

Karen A. Donato, Jean Charles Fruchart, W. Philip T. James, Catherine M. Loria, and Sidney C. Smith. 2009. “Harmonizing the Metabolic Syndrome: A Joint Interim Statement of the International Diabetes Federation Task Force on Epidemiology and Prevention; National Heart, Lung, and Blood Institute; American Heart Association; World Heart Federation; International .” *Circulation* 120 (16): 1640–45. https://doi.org/10.1161/CIRCULATIONAHA.109.192644.

Alberti, K. G.M.M., Paul Z. Zimmet, and Reuben J Shaw. 2006. “The IDF Consensus Worldwide Definition of the Metabolic Syndrome. Brussels: International Diabetes Federation.”

Alberti, K.G.M.M., and P Z Zimmet. 1998. “Definition, Diagnosis and Classification of Diabetes Mellitus and Its Complications. Part 1: Diagnosis and Classification of Diabetes Mellitus. Provisional Report of a WHO Consultation.” *Diabetic Medicine* 15 (7): 539–53. https://doi.org/10.1002/(SICI)1096-9136(199807)15:7<539::AID-DIA668>3.0.CO;2-S.

Alberti, K George M M, Paul Zimmet, and Jonathan Shaw. 2005. “The Metabolic Syndrome--a New Worldwide Definition.” *Lancet (London, England)* 366 (9491): 1059–62. https://doi.org/10.1016/S0140-6736(05)67402-8.

Albrecht, Urs, Zhong Sheng Sun, Gregor Eichele, and Cheng Chi Lee. 1997. “A Differential Response of Two Putative Mammalian Circadian Regulators, Mper1 and Mper2, to Light.” *Cell* 91 (7): 1055–64. https://doi.org/10.1016/S0092-8674(00)80495-X.

Albrecht, Urs, Binhai Zheng, David Larkin, Zhong Sheng Sun, and Cheng Chi Lee. 2001. “MPer1 and MPer2 Are Essential for Normal Resetting of the Circadian Clock.” *Journal of Biological Rhythms* 16 (2): 100–104. https://doi.org/10.1177/074873001129001791.

Alenghat, T, K Meyers, S E Mullican, K Leitner, A Adeniji-Adele, J Avila, M Bucan, R S Ahima, K H Kaestner, and M A Lazar. 2008. “Nuclear Receptor Corepressor and Histone Deacetylase 3 Govern Circadian Metabolic Physiology.” *Nature* 456: 997–1000.

Ando, Hitoshi, Masafumi Kumazaki, Yuya Motosugi, Kentarou Ushijima, Tomohiro Maekawa, Eiko Ishikawa, and Akio Fujimura. 2011. “Impairment of Peripheral Circadian Clocks Precedes Metabolic Abnormalities in Ob/Ob Mice.” *Endocrinology* 152 (4): 1347–54. https://doi.org/10.1210/en.2010-1068.

Arany, Z, L E Huang, R Eckner, S Bhattacharya, C Jiang, M A Goldberg, H F Bunn, and D M Livingston. 1996. “An Essential Role for P300/CBP in the Cellular Response to Hypoxia.” *Proceedings of the National Academy of Sciences of the United States of America* 93 (23): 12969–73. https://doi.org/10.1073/pnas.93.23.12969.

Arasaradnam, M P, L Morgan, J Wright, and R Gama. 2002. “Diurnal Variation in Lipoprotein Lipase Activity.” *Annals of Clinical Biochemistry* 39 (Pt 2): 136–39.

https://doi.org/10.1258/0004563021901883.

Aronne, Louis J, Thomas A Wadden, Craig Peterson, David Winslow, Sarah Odeh, and Kishore M Gadde. 2013. "Evaluation of Phentermine and Topiramate versus Phentermine/Topiramate Extended-Release in Obese Adults." *Obesity (Silver Spring, Md.)* 21 (11): 2163–71. https://doi.org/10.1002/oby.20584.

Aronoff, S. L., K. Berkowitz, B. Shreiner, and L. Want. 2004. "Glucose Metabolism and Regulation: Beyond Insulin and Glucagon." *Diabetes Spectrum* 17 (3): 183–90. https://doi.org/10.2337/diaspect.17.3.183.

Aschoff, J. 1965. "A Self-Sustained Oscillator with an Inherent Frequency Underlies Human 24-Hour Periodicity." *Science* 148: 1427.

Asher, Gad, David Gatfield, Markus Stratmann, Hans Reinke, Charna Dibner, Florian Kreppel, Raul Mostoslavsky, Frederick W Alt, and Ueli Schibler. 2008. "SIRT1 Regulates Circadian Clock Gene Expression through PER2 Deacetylation." *Cell* 134 (2): 317–28. https://doi.org/http://doi.org/10.1016/j.cell.2008.06.050.

Aubert, H, C Frère, M F Aillaud, P E Morange, I Juhan-Vague, and M C Alessi. 2003. "Weak and Non-Independent Association between Plasma TAFI Antigen Levels and the Insulin Resistance Syndrome." *Journal of Thrombosis and Haemostasis* 1 (4): 791–97. https://doi.org/10.1046/j.1538-7836.2003.00147.x.

Avenell, A, J Broom, T J Brown, A Poobalan, L Aucott, S C Stearns, W C S Smith, R T Jung, M K Campbell, and A M Grant. 2004. "Systematic Review of the Long-Term Effects and Economic Consequences of Treatments for Obesity and Implications for Health Improvement." *Health Technology Assessment (Winchester, England)* 8 (21): iii—iv, 1—182. https://doi.org/10.3310/hta8210.

Ayala, Julio E, Deanna P Bracy, Brianna M Julien, Jeffrey N Rottman, Patrick T Fueger, and David H Wasserman. 2007. "Chronic Treatment With Sildenafil Improves Energy Balance and Insulin Action in High Fat–Fed Conscious Mice." *Diabetes* 56 (April): 1025–33. https://doi.org/10.2337/db06-0883.2.

Aydin, Suleyman, Aziz Aksoy, Suna Aydin, Mehmet Kalayci, Musa Yilmaz, Tuncay Kuloglu, Cihan Citil, and Zekiye Catak. 2014. "Today's and Yesterday's of Pathophysiology: Biochemistry of Metabolic Syndrome and Animal Models." *Nutrition* 30 (1): 1–9. https://doi.org/10.1016/j.nut.2013.05.013.

Aziz, N, and H N Munro. 1986. "Both Subunits of Rat Liver Ferritin Are Regulated at a Translational Level by Iron Induction." *Nucleic Acids Research* 14 (2): 915–27. https://doi.org/10.1093/nar/14.2.915.

Back, Sung Hoon, and Randal J Kaufman. 2012. "Endoplasmic Reticulum Stress and Type 2 Diabetes." *Annual Review of Biochemistry* 81: 767–93. https://doi.org/10.1146/annurev-biochem-072909-095555.

Bae, Kiho, Xiaowei Jin, Elizabeth S. Maywood, Michael H. Hastings, Steven M. Reppert, and

David R. Weaver. 2001. “Differential Functions of MPer1, MPer2, and MPer3 in the SCN Circadian Clock.” *Neuron* 30 (2): 525–36. https://doi.org/10.1016/S0896-6273(01)00302-6.

Baggs, Julie E, and Carla B Green. 2003. “Nocturnin, a Deadenylase in Xenopus Laevis Retina: A Mechanism for Posttranscriptional Control of Circadian-Related MRNA.” *Current Biology : CB* 13 (3): 189–98. https://doi.org/10.1016/s0960-9822(03)00014-9.

Bajaj, Mandeep, and Mary Ann Banerji. 2004. “Type 2 Diabetes in South Asians: A Pathophysiologic Focus on the Asian-Indian Epidemic.” *Current Diabetes Reports* 4 (3): 213–18. https://doi.org/10.1007/s11892-004-0026-4.

Balkau, B. 1999. “Comment on the Provisional Report from the WHO Consultation. European Group for the Study of Insulin Resistance (EGIR).” *Diabet Med* 16: 442–43. https://doi.org/10.1046/j.1464-5491.1999.00059.x.

Balsalobre, A. 2002. “Clock Genes in Mammalian Peripheral Tissues.” *Cell and Tissue Research*, no. 309: 193–99.

Balsalobre, A, S A Brown, L Marcacci, F Tronche, C Kellendonk, H M Reichardt, G Schütz, and U Schibler. 2000. “Resetting of Circadian Time in Peripheral Tissues by Glucocorticoid Signaling.” *Science (New York, N.Y.)* 289 (5488): 2344–47. https://doi.org/10.1126/science.289.5488.2344.

Balsalobre, A, F Damiola, and U Schibler. 1998. “A Serum Shock Induces Circadian Gene Expression in Mammalian Tissue Culture Cells.” *Cell* 93 (6): 929–37. https://doi.org/10.1016/s0092-8674(00)81199-x.

Barco, Angel, and Hélène Marie. 2011. “Genetic Approaches to Investigate the Role of CREB in Neuronal Plasticity and Memory.” *Molecular Neurobiology* 44 (3): 330–49. https://doi.org/10.1007/s12035-011-8209-x.

Barnea, Maayan, Liyan Haviv, Roee Gutman, Nava Chapnik, Zecharia Madar, and Oren Froy. 2012. “Metformin Affects the Circadian Clock and Metabolic Rhythms in a Tissue-Specific Manner.” *Biochimica et Biophysica Acta - Molecular Basis of Disease* 1822 (11): 1796–1806. https://doi.org/10.1016/j.bbadis.2012.08.005.

Bartelt, Alexander, and Joerg Heeren. 2014. “Adipose Tissue Browning and Metabolic Health.” *Nature Reviews Endocrinology* 10 (1): 24–36. https://doi.org/10.1038/nrendo2013204.

Batsis, J. A., R. E. Nieto-Martinez, and F. Lopez-Jimenez. 2007. “Metabolic Syndrome: From Global Epidemiology to Individualized Medicine.” *Clinical Pharmacology and Therapeutics* 82 (5): 509–24. https://doi.org/10.1038/sj.clpt.6100355.

Baumann, C A, V Ribon, M Kanzaki, D C Thurmond, S Mora, S Shigematsu, P E Bickel, J E Pessin, and A R Saltiel. 2000. “CAP Defines a Second Signalling Pathway Required for Insulin-Stimulated Glucose Transport.” *Nature* 407 (6801): 202–7.

https://doi.org/10.1038/35025089.

Beck, Hartmut, Mario Jeske, Kai Thede, Friederike Stoll, Ingo Flamme, Metin Akbaba, Jens-Kerim Ergüden, et al. 2018. "Discovery of Molidustat (BAY 85-3934): A Small-Molecule Oral HIF-Prolyl Hydroxylase (HIF-PH) Inhibitor for the Treatment of Renal Anemia." *ChemMedChem* 13 (10): 988–1003. https://doi.org/10.1002/cmdc.201700783.

Bedogni, Giorgio, Lucia Miglioli, Flora Masutti, Claudio Tiribelli, Giulio Marchesini, and Stefano Bellentani. 2005. "Prevalence of and Risk Factors for Nonalcoholic Fatty Liver Disease: The Dionysos Nutrition and Liver Study." *Hepatology (Baltimore, Md.)* 42 (1): 44–52. https://doi.org/10.1002/hep.20734.

Bell-Pedersen, Deborah, Vincent M. Cassone, David J. Earnest, and Mark J. Zoran. 2005. "Circadian Rhythms from Multiple Oscillators: Lessons from Diverse Organisms." *Nature Reviews Drug Discovery* 4 (2): 544–56. https://doi.org/10.1038/nrd1633.

Benoit, Stephen C, Christopher J Kemp, Carol F Elias, William Abplanalp, James P Herman, Stephanie Migrenne, Anne-Laure Lefevre, et al. 2009. "Palmitic Acid Mediates Hypothalamic Insulin Resistance by Altering PKC-Theta Subcellular Localization in Rodents." *The Journal of Clinical Investigation* 119 (9): 2577–89. https://doi.org/10.1172/JCI36714.

Berson, David M, Felice A Dunn, and Motoharu Takao. 2002. "Phototransduction by Retinal Ganglion Cells That Set the Circadian Clock." *Science* 295 (5557): 1070–73. https://doi.org/10.1126/science.1067262.

Bertolotti, A, Y Zhang, L M Hendershot, H P Harding, and D Ron. 2000. "Dynamic Interaction of BiP and ER Stress Transducers in the Unfolded-Protein Response." *Nature Cell Biology* 2 (6): 326–32. https://doi.org/10.1038/35014014.

Bescos, R., M. J. Boden, M. L. Jackson, A. J. Trewin, E. C. Marin, I. Levinger, A. Garnham, et al. 2018. "Four Days of Simulated Shift Work Reduces Insulin Sensitivity in Humans." *Acta Physiologica* 223 (2). https://doi.org/10.1111/apha.13039.

Best, Jonathan D., Elizabeth S. Maywood, Karen L. Smith, and Michael H. Hastings. 1999. "Rapid Resetting of the Mammalian Circadian Clock." *Journal of Neuroscience* 19 (2): 828–35. https://doi.org/10.1523/jneurosci.19-02-00828.1999.

Bhattacharya, S, C L Michels, M K Leung, Z P Arany, A L Kung, and D M Livingston. 1999. "Functional Role of P35srj, a Novel P300/CBP Binding Protein, during Transactivation by HIF-1." *Genes & Development* 13 (1): 64–75. https://doi.org/10.1101/gad.13.1.64.

Björntorp, P. 1996. "The Regulation of Adipose Tissue Distribution in Humans." *International Journal of Obesity and Related Metabolic Disorders : Journal of the International Association for the Study of Obesity* 20 (4): 291–302.

Björntorp, P, B Hood, A Martinsson, and B Persson. 1966. "The Composition of Human

Subcutaneous Adipose Tissue in Obesity." *Acta Medica Scandinavica* 180 (1): 117–21. https://doi.org/10.1111/j.0954-6820.1966.tb02815.x.

Boden, Guenther. 2008. "Obesity and Free Fatty Acids." *Endocrinology and Metabolism Clinics of North America* 37 (3): 635–ix. https://doi.org/10.1016/j.ecl.2008.06.007.

Boden, Guenther, Xinhua Chen, Jose Ruiz, John V. White, and Luciano Rossetti. 1994. "Mechanisms of Fatty Acid-Induced Inhibition of Glucose Uptake." *Journal of Clinical Investigation* 93 (6): 2438–46. https://doi.org/10.1172/JCI117252.

Boini, Krishna M., Dirk Graf, Anita M. Hennige, Saisudha Koka, Daniela S. Kempe, Kan Wang, Teresa F. Ackermann, et al. 2009. "Enhanced Insulin Sensitivity of Gene-Targeted Mice Lacking Functional KCNQ1." *American Journal of Physiology - Regulatory Integrative and Comparative Physiology* 296 (6): 22–26. https://doi.org/10.1152/ajpregu.90839.2008.

Bolli, G B, P De Feo, S De Cosmo, G Perriello, M M Ventura, F Calcinaro, C Lolli, P Campbell, P Brunetti, and J E Gerich. 1984. "Demonstration of a Dawn Phenomenon in Normal Human Volunteers." *Diabetes* 33 (12): 1150–53. https://doi.org/10.2337/diab.33.12.1150.

Boswell-Smith, Victoria, Domenico Spina, and Clive P. Page. 2006. "Phosphodiesterase Inhibitors." *British Journal of Pharmacology* 147 (SUPPL. 1): 252–57. https://doi.org/10.1038/sj.bjp.0706495.

Bouatia-Naji, Nabila, Amélie Bonnefond, Christine Cavalcanti-Proença, Thomas Sparsø, Johan Holmkvist, Marion Marchand, Jérôme Delplanque, et al. 2009. "A Variant near MTNR1B Is Associated with Increased Fasting Plasma Glucose Levels and Type 2 Diabetes Risk." *Nature Genetics* 41 (1): 89–94. https://doi.org/10.1038/ng.277.

Brancaccio, Marco, Andrew P Patton, Johanna E Chesham, Elizabeth S Maywood, and Michael H Hastings. 2017. "Astrocytes Control Circadian Timekeeping in the Suprachiasmatic Nucleus via Glutamatergic Signaling." *Neuron* 93 (6): 1420-1435.e5. https://doi.org/10.1016/j.neuron.2017.02.030.

Brown, Steven A., Dieter Kunz, Amelie Dumas, Pål O. Westermark, Katja Vanselow, Amely Tilmann-Wahnschaffe, Hanspeter Herzel, and Achim Kramer. 2008. "Molecular Insights into Human Daily Behavior." *Proceedings of the National Academy of Sciences of the United States of America* 105 (5): 1602–7. https://doi.org/10.1073/pnas.0707772105.

Brown, Steven a, Gottlieb Zumbrunn, Fabienne Fleury-Olela, Nicolas Preitner, and Ueli Schibler. 2002. "Rhythms of Mammalian Body Temperature Can Sustain Peripheral Circadian Clocks." *Current Biology : CB* 12 (18): 1574–83. http://www.ncbi.nlm.nih.gov/pubmed/12372249.

Bunger, M K, L D Wilsbacher, S M Moran, C Clendenin, L A Radcliffe, J B Hogenesch, M C Simon, J S Takahashi, and C A Bradfield. 2000. "Mop3 Is an Essential Component of

the Master Circadian Pacemaker in Mammals." *Cell* 103 (7): 1009–17. https://doi.org/10.1016/s0092-8674(00)00205-1.

Bünning, E. 1971. "Symptoms, Problems, and Common Features of Circadian Rhythms in Plants and Animals." *Proc Int Symp Circadian Rhythmicity, Wageningen*, 11–31.

Burkhardt, M, M Glazova, S Gambaryan, T Vollkommer, E Butt, B Bader, K Heermeier, T M Lincoln, U Walter, and A Palmetshofer. 2000. "KT5823 Inhibits CGMP-Dependent Protein Kinase Activity in Vitro but Not in Intact Human Platelets and Rat Mesangial Cells." *The Journal of Biological Chemistry* 275 (43): 33536–41. https://doi.org/10.1074/jbc.M005670200.

Cahill, A L, and C F Ehret. 1981. "Circadian Variations in the Activity of Tyrosine Hydroxylase, Tyrosine Aminotransferase, and Tryptophan Hydroxylase: Relationship to Catecholamine Metabolism." *Journal of Neurochemistry* 37 (5): 1109—1115. https://doi.org/10.1111/j.1471-4159.1981.tb04660.x.

Cailotto, Cathy, Jun Lei, Jan van der Vliet, Caroline van Heijningen, Corbert G van Eden, Andries Kalsbeek, Paul Pévet, and Ruud M Buijs. 2009. "Effects of Nocturnal Light on (Clock) Gene Expression in Peripheral Organs: A Role for the Autonomic Innervation of the Liver." *PLOS ONE* 4 (5): e5650. https://doi.org/10.1371/journal.pone.0005650.

Cairo, G, L Bardella, L Schiaffonati, P Arosio, S Levi, and A Bernelli-Zazzera. 1985. "Multiple Mechanisms of Iron-Induced Ferritin Synthesis in HeLa Cells." *Biochemical and Biophysical Research Communications* 133 (1): 314–21. https://doi.org/10.1016/0006-291x(85)91877-7.

Caldelas, I, V.-J Poirel, B Sicard, P Pvet, and E Challet. 2003. "Circadian Profile and Photic Regulation of Clock Genes in the Suprachiasmatic Nucleus of a Diurnal Mammal Arvicanthis Ansorgei." *Neuroscience* 116 (2): 583–91. https://doi.org/http://dx.doi.org/10.1016/S0306-4522(02)00654-1.

Calfon, Marcella, Huiqing Zeng, Fumihiko Urano, Jeffery H. Till, Stevan R. Hubbard, Heather P. Harding, Scott G. Clark, and David Ron. 2002. "IRE1 Couples Endoplasmic Reticulum Load to Secretory Capacity by Processing the XBP-1 MRNA (Nature (2002) 415 (92-96))." *Nature* 420 (6912): 202. https://doi.org/10.1038/nature01193.

Calvo, Katherine R, Paul S Knoepfler, David B Sykes, Martina P Pasillas, and Mark P Kamps. 2001. "Meis1a Suppresses Differentiation by G-CSF and Promotes Proliferation by SCF: Potential Mechanisms of Cooperativity with Hoxa9 in Myeloid Leukemia." *Proceedings of the National Academy of Sciences* 98 (23): 13120 LP – 13125. https://doi.org/10.1073/pnas.231115398.

Canaple, Laurence, Juliette Rambaud, Ouria Dkhissi-Benyahya, Béatrice Rayet, Nguan Soon Tan, Liliane Michalik, Franck Delaunay, Walter Wahli, and Vincent Laudet.

2006. “Reciprocal Regulation of Brain and Muscle Arnt-Like Protein 1 and Peroxisome Proliferator-Activated Receptor α Defines a Novel Positive Feedback Loop in the Rodent Liver Circadian Clock.” *Molecular Endocrinology* 20 (8): 1715–27. https://doi.org/10.1210/me.2006-0052.

Cannon, Barbara, and Jan Nedergaard. 2004. “Brown Adipose Tissue: Function and Physiological Significance.” *Physiological Reviews* 84 (1): 277–359. https://doi.org/10.1152/physrev.00015.2003.

Cantó, Carles, and Johan Auwerx. 2013. “Caloric Restriction , SIRT1 and Longevity” 20 (7): 325–31. https://doi.org/10.1016/j.tem.2009.03.008.Caloric.

Cao, Ruifeng, Frances E Anderson, Yeon-Joo Jung, Heather Dziema, and Karl Obrietan. 2012. “Circadian Reglator of MTOR Signaling in the Mouse SCN.” *Nacional Institutes of Health* 181 (614): 79–88. https://doi.org/10.1016/j.neuroscience.2011.03.005.Circadian.

Carling, David. 2005. “AMP-Activated Protein Kinase : Balancing the Scales” 87: 87–91. https://doi.org/10.1016/j.biochi.2004.10.017.

Carskadon, M A, S E Labyak, C Acebo, and R Seifer. 1999. “Intrinsic Circadian Period of Adolescent Humans Measured in Conditions of Forced Desynchrony.” *Neuroscience Letters* 260 (2): 129—132. https://doi.org/10.1016/s0304-3940(98)00971-9.

Casteel, Darren E, Shunhui Zhuang, Tanima Gudi, Julian Tang, Milena Vuica, Stephen Desiderio, and Renate B Pilz. 2002. “CGMP-Dependent Protein Kinase I Beta Physically and Functionally Interacts with the Transcriptional Regulator TFII-I.” *The Journal of Biological Chemistry* 277 (35): 32003–14. https://doi.org/10.1074/jbc.M112332200.

Castel, M, M Belenky, S Cohen, O P Ottersen, and J Storm-Mathisen. 1993. “Glutamate-like Immunoreactivity in Retinal Terminals of the Mouse Suprachiasmatic Nucleus.” *The European Journal of Neuroscience* 5 (4): 368—381. https://doi.org/10.1111/j.1460-9568.1993.tb00504.x.

Castelló, A, A Gumá, L Sevilla, M Furriols, X Testar, M Palacín, and A Zorzano. 1995. “Regulation of GLUT5 Gene Expression in Rat Intestinal Mucosa: Regional Distribution, Circadian Rhythm, Perinatal Development and Effect of Diabetes.” *Biochemical Journal* 309 (1): 271–77. https://doi.org/10.1042/bj3090271.

Catoire, Hélène, Patrick A. Dion, Lan Xiong, Mourabit Amari, Rebecca Gaudet, Simon L. Girard, Anne Noreau, et al. 2011. “Restless Legs Syndrome-Associated MEIS1 Risk Variant Influences Iron Homeostasis.” *Annals of Neurology* 70 (1): 170–75. https://doi.org/10.1002/ana.22435.

Caton, P W, J Kieswich, M M Yaqoob, M J Holness, and M C Sugden. 2011. “Metformin Opposes Impaired AMPK and SIRT1 Function and Deleterious Changes in Core Clock Protein Expression in White Adipose Tissue of Genetically-Obese Db/Db Mice.”

Diabetes, Obesity and Metabolism 13 (12): 1097–1104. https://doi.org/10.1111/j.1463-1326.2011.01466.x.

Chandel NS, Maltepe E, Goldwasser E, Mathieu CE, Simon MC, Schumacker PT. 1998. "Mitochondrial Reactive Oxygen Species Trigger Hypoxia-." *Proceedings of the National Academy of Sciences of the United States of America* 95 (September): 11715–20.

Charlton, Michael, Raghavakaimal Sreekumar, Deborah Rasmussen, Keith Lindor, and K Sreekumaran Nair. 2002. "Apolipoprotein Synthesis in Nonalcoholic Steatohepatitis." *Hepatology (Baltimore, Md.)* 35 (4): 898–904. https://doi.org/10.1053/jhep.2002.32527.

Chattopadhyay, Mrittika, Ishita Guhathakurta, Prajna Behera, Kumar Rajeev Ranjan, Manoj Khanna, Satinath Mukhopadhyay, and Sasanka Chakrabarti. 2011. "Mitochondrial Bioenergetics Is Not Impaired in Nonobese Subjects with Type 2 Diabetes Mellitus." *Metabolism: Clinical and Experimental* 60 (12): 1702–10. https://doi.org/10.1016/j.metabol.2011.04.015.

Chen, Changhu, Nabendu Pore, Alireza Behrooz, Faramarz Ismail-Beigi, and Amit Maity. 2001. "Regulation of Glut1 MRNA by Hypoxia-Inducible Factor-1: Interaction between H-Ras and Hypoxia." *Journal of Biological Chemistry* 276 (12): 9519–25. https://doi.org/10.1074/jbc.M010144200.

Chen, Chunhua, Yuebo Zhang, and Cheng Huang. 2010. "Berberine Inhibits PTP1B Activity and Mimics Insulin Action." *Biochemical and Biophysical Research Communications* 397 (3): 543–47. https://doi.org/https://doi.org/10.1016/j.bbrc.2010.05.153.

Chen, Dong, Gordon F Buchanan, Jian M Ding, Jens Hannibal, and Martha U Gillette. 1999. "Pituitary Adenylyl Cyclase-Activating Peptide: A Pivotal Modulator of Glutamatergic Regulation of the Suprachiasmatic Circadian Clock." *Proceedings of the National Academy of Sciences* 96 (23): 13468 LP – 13473. https://doi.org/10.1073/pnas.96.23.13468.

Chiang, Shian Huey, Christian A. Baumann, Makoto Kanzaki, Debbie C. Thurmond, Robert T. Watson, Cheryl L. Neudauer, Ian G. Macara, Jeffrey E. Pessin, and Alan R. Saltiel. 2001. "Insulin-Stimulated GLUT4 Translocation Requires the CAP-Dependent Activation of TC10." *Nature* 410 (6831): 944–48. https://doi.org/10.1038/35073608.

Chilov, D, T Hofer, C Bauer, R H Wenger, and M Gassmann. 2001. "Hypoxia Affects Expression of Circadian Genes PER1 and CLOCK in Mouse Brain." *FASEB Journal* 15 (14): 2613–22. https://doi.org/10.1096/fj.01-0092com.

Choi, Sarah M., David F. Tucker, Danielle N. Gross, Rachael M. Easton, Lisa M. DiPilato, Abigail S. Dean, Bob R. Monks, and Morris J. Birnbaum. 2010. "Insulin Regulates

Adipocyte Lipolysis via an Akt-Independent Signaling Pathway." *Molecular and Cellular Biology* 30 (21): 5009–20. https://doi.org/10.1128/mcb.00797-10.

Choo, H. J., J. H. Kim, O. B. Kwon, C. S. Lee, J. Y. Mun, S. S. Han, Y. S. Yoon, G. Yoon, K. M. Choi, and Y. G. Ko. 2006. "Mitochondria Are Impaired in the Adipocytes of Type 2 Diabetic Mice." *Diabetologia* 49 (4): 784–91. https://doi.org/10.1007/s00125-006-0170-2.

Christensen, Siegfried B, and Theodore J Torphy. 1994. "Isozyme-Selective Phosphodiesterase Inhibitors as Antiasthmatic Agents." In , edited by James A B T - Annual Reports in Medicinal Chemistry Bristol, 29:185–94. Academic Press. https://doi.org/https://doi.org/10.1016/S0065-7743(08)60732-0.

Chrivia, J C, R P Kwok, N Lamb, M Hagiwara, M R Montminy, and R H Goodman. 1993. "Phosphorylated CREB Binds Specifically to the Nuclear Protein CBP." *Nature* 365 (6449): 855–59. https://doi.org/10.1038/365855a0.

Chua, S C Jr, W K Chung, X S Wu-Peng, Y Zhang, S M Liu, L Tartaglia, and R L Leibel. 1996. "Phenotypes of Mouse Diabetes and Rat Fatty Due to Mutations in the OB (Leptin) Receptor." *Science (New York, N.Y.)* 271 (5251): 994–96. https://doi.org/10.1126/science.271.5251.994.

Ciani, Elisabetta, Sandra Guidi, Renata Bartesaghi, and Antonio Contestabile. 2002. "Nitric Oxide Regulates CGMP-Dependent CAMP-Responsive Element Binding Protein Phosphorylation and Bcl-2 Expression in Cerebellar Neurons: Implication for a Survival Role of Nitric Oxide." *Journal of Neurochemistry* 82 (5): 1282–89. https://doi.org/10.1046/j.1471-4159.2002.01080.x.

Cibelli, Giuseppe, Vincenza Policastro, Oliver G Rössler, and Gerald Thiel. 2002. "Nitric Oxide-Induced Programmed Cell Death in Human Neuroblastoma Cells Is Accompanied by the Synthesis of Egr-1, a Zinc Finger Transcription Factor." *Journal of Neuroscience Research* 67 (4): 450–60. https://doi.org/10.1002/jnr.10141.

Clifford, G M, C Londos, F B Kraemer, R G Vernon, and S J Yeaman. 2000. "Translocation of Hormone-Sensitive Lipase and Perilipin upon Lipolytic Stimulation of Rat Adipocytes." *The Journal of Biological Chemistry* 275 (7): 5011–15. https://doi.org/10.1074/jbc.275.7.5011.

Coleman, D L. 1978. "Obese and Diabetes: Two Mutant Genes Causing Diabetes-Obesity Syndromes in Mice." *Diabetologia* 14 (3): 141–48. https://doi.org/10.1007/BF00429772.

Collins, Sean P., and Michael D. Uhler. 1999. "Cyclic AMP- and Cyclic GMP-Dependent Protein Kinases Differ in Their Regulation of Cyclic AMP Response Element-Dependent Gene Transcription." *Journal of Biological Chemistry* 274 (13): 8391–8404. https://doi.org/10.1074/jbc.274.13.8391.

Consoli, A., F. Kennedy, J. Miles, and J. Gerich. 1987. "Determination of Krebs Cycle Metabolic Carbon Exchange in Vivo and Its Use to Estimate the Individual

Contributions of Gluconeogenesis and Glycogenolysis to Overall Glucose Output in Man." *Journal of Clinical Investigation* 80 (5): 1303–10. https://doi.org/10.1172/JCI113206.

Cook, Leonard, Victor J Nickolson, George F Steinfels, Kenneth W Rohrbach, and Victor J Denoble. 1990. "Cognition Enhancement by the Acetylcholine Releaser DuP 996" 314: 301–14.

Cooke, Aoife A, Ruth M Connaughton, Claire L Lyons, Aoibheann M McMorrow, and Helen M Roche. 2016. "Fatty Acids and Chronic Low Grade Inflammation Associated with Obesity and the Metabolic Syndrome." *European Journal of Pharmacology* 785 (August): 207–14. https://doi.org/10.1016/j.ejphar.2016.04.021.

Costa-Giomi P, Caro J, Weinmann R. 1990. "Enhancement by Hypoxia of Human Erythropoietin Gene Transcription in Vitro." *J Biol Chem* 265 (10185).

Crosby, Priya, Ryan Hamnett, Marrit Putker, Nathaniel P. Hoyle, Martin Reed, Carolyn J. Karam, Elizabeth S. Maywood, et al. 2019. "Insulin/IGF-1 Drives PERIOD Synthesis to Entrain Circadian Rhythms with Feeding Time." *Cell* 177 (4): 896-909.e20. https://doi.org/10.1016/j.cell.2019.02.017.

Cuninkova, Ludmila, and Steven A Brown. 2008. "Peripheral Circadian Oscillators: Interesting Mechanisms and Powerful Tools." *Annals of the New York Academy of Sciences* 1129: 358–70. https://doi.org/10.1196/annals.1417.005.

Czeisler, C A, J F Duffy, T L Shanahan, E N Brown, J F Mitchell, D W Rimmer, J M Ronda, et al. 1999. "Stability, Precision, and near-24-Hour Period of the Human Circadian Pacemaker." *Science (New York, N.Y.)* 284 (5423): 2177–81. https://doi.org/10.1126/science.284.5423.2177.

Daan, Serge, and Colin S. Pittendrigh. 1976. "A Functional Analysis of Circadian Pacemakers in Nocturnal Rodents - II. The Variability of Phase Response Curves." *Journal of Comparative Physiology ■ A* 106 (3): 253–66. https://doi.org/10.1007/BF01417857.

Dallmann, R, A U Viola, L Tarokh, C Cajochen, and S A Brown. 2012. "The Human Circadian Metabolome." *PNAS* 109: 2625–29.

Dallongeville, Jean, Nicole Helbecque, Dominique Cottel, Philippe Amouyel, and Aline Meirhaeghe. 2003. "The Gly16→Arg16 and Gln27→Glu27 Polymorphisms of B2-Adrenergic Receptor Are Associated with Metabolic Syndrome in Men." *The Journal of Clinical Endocrinology & Metabolism* 88 (10): 4862–66. https://doi.org/10.1210/jc.2003-030173.

Damiola, F., N. Le Minli, N. Preitner, B. Kornmann, F. Fleury-Olela, and U. Schibler. 2000. "Restricted Feeding Uncouples Circadian Oscillators in Peripheral Tissues from the Central Pacemaker in the Suprachiasmatic Nucleus." *Genes and Development* 14 (23): 2950–61. https://doi.org/10.1101/gad.183500.

Damiola, Francesca, Nguyet Le Minh, Nicolas Preitner, Fabienne Fleury-olela, and Ueli Schibler. 2000. "Restricted Feeding Uncouples Circadian Oscillators in Peripheral Tissues from the Central Pacemaker in the Suprachiasmatic Nucleus," 2950–61. https://doi.org/10.1101/gad.183500.moral.

Davies, Melanie J, Richard Bergenstal, Bruce Bode, Robert F Kushner, Andrew Lewin, Trine Vang Skjøth, Arne Haahr Andreasen, Christine Bjørn Jensen, and Ralph A DeFronzo. 2015. "Efficacy of Liraglutide for Weight Loss Among Patients With Type 2 Diabetes: The SCALE Diabetes Randomized Clinical Trial." *JAMA* 314 (7): 687–99. https://doi.org/10.1001/jama.2015.9676.

DeBruyne, Jason P, David R Weaver, and Steven M Reppert. 2007. "CLOCK and NPAS2 Have Overlapping Roles in the Suprachiasmatic Circadian Clock." *Nature Neuroscience* 10 (5): 543–45. https://doi.org/10.1038/nn1884.

DeCoursey, P J, J R Krulas, G Mele, and D C Holley. 1997. "Circadian Performance of Suprachiasmatic Nuclei (SCN)-Lesioned Antelope Ground Squirrels in a Desert Enclosure." *Physiology & Behavior* 62 (5): 1099–1108. https://doi.org/10.1016/s0031-9384(97)00263-1.

DeCoursey, P J, J K Walker, and S A Smith. 2000. "A Circadian Pacemaker in Free-Living Chipmunks: Essential for Survival?" *Journal of Comparative Physiology. A, Sensory, Neural, and Behavioral Physiology* 186 (2): 169–80. https://doi.org/10.1007/s003590050017.

DeFronzo, R A, and E Ferrannini. 1991. "Insulin Resistance. A Multifaceted Syndrome Responsible for NIDDM, Obesity, Hypertension, Dyslipidemia, and Atherosclerotic Cardiovascular Disease." *Diabetes Care* 14 (3): 173–94. https://doi.org/10.2337/diacare.14.3.173.

DeNoble, V. J., K. F. DeNoble, K. R. Spencer, L. C. Johnson, L. Cook, M. J. Myers, and R. M. Scribner. 1990. "Comparison of DuP 996 with Physostigmine, THA and 3,4-DAP on Hypoxia-Induced Amnesia in Rat." *Pharmacol. Biochem. Behav* 36: 957–61.

Dentin, Renaud, Yi Liu, Seung-Hoi Koo, Susan Hedrick, Thomas Vargas, Jose Heredia, John Yates, and Marc Montminy. 2007. "Insulin Modulates Gluconeogenesis by Inhibition of the Coactivator TORC2." *Nature* 449 (7160): 366–69. https://doi.org/10.1038/nature06128.

Dibner, C, and U Schibler. 2018. "Body Clocks: Time for the Nobel Prize." *Acta Physiologica* 222 (2): e13024. https://doi.org/10.1111/apha.13024.

Ding, J M, D Chen, E T Weber, L E Faiman, M A Rea, and M U Gillette. 1994. "Resetting the Biological Clock: Mediation of Nocturnal Circadian Shifts by Glutamate and NO." *Science* 266 (5191): 1713 LP – 1717. https://doi.org/10.1126/science.7527589.

Ding, Jian M., Lia E. Faiman, William J. Hurst, Liana R. Kuriashkina, and Martha U. Gillette. 1997. "Resetting the Biological Clock: Mediation of Nocturnal CREB Phosphorylation

via Light, Glutamate, and Nitric Oxide." *Journal of Neuroscience* 17 (2): 667–75. https://doi.org/10.1523/jneurosci.17-02-00667.1997.

Doi, Ryosuke, Katsutaka Oishi, and Norio Ishida. 2010. "CLOCK Regulates Circadian Rhythms of Hepatic Glycogen Synthesis through Transcriptional Activation of Gys2." *Journal of Biological Chemistry* 285 (29): 22114–21. https://doi.org/10.1074/jbc.M110.110361.

Donnelly, Kerry L, Coleman I Smith, Sarah J Schwarzenberg, Jose Jessurun, Mark D Boldt, and Elizabeth J Parks. 2005. "Sources of Fatty Acids Stored in Liver and Secreted via Lipoproteins in Patients with Nonalcoholic Fatty Liver Disease." *The Journal of Clinical Investigation* 115 (5): 1343–51. https://doi.org/10.1172/JCI23621.

Drager, Luciano F., Jianguo Li, Christian Reinke, Shannon Bevans-Fonti, Jonathan C. Jun, and Vsevolod Y. Polotsky. 2011. "Intermittent Hypoxia Exacerbates Metabolic Effects of Diet-Induced Obesity." *Obesity* 19 (11): 2167–74. https://doi.org/10.1038/oby.2011.240.

Du, Jianhai, Whitney M. Cleghorn, Laura Contreras, Ken Lindsay, Austin M. Rountree, Andrei O. Chertov, Sally J. Turner, et al. 2013. "Inhibition of Mitochondrial Pyruvate Transport by Zaprinast Causes Massive Accumulation of Aspartate at the Expense of Glutamate in the Retina." *Journal of Biological Chemistry* 288 (50): 36129–40. https://doi.org/10.1074/jbc.M113.507285.

Dyar, Kenneth A., Stefano Ciciliot, Lauren E. Wright, Rasmus S. Biensø, Guidantonio M. Tagliazucchi, Vishal R. Patel, Mattia Forcato, et al. 2014. "Muscle Insulin Sensitivity and Glucose Metabolism Are Controlled by the Intrinsic Muscle Clock." *Molecular Metabolism* 3 (1): 29–41. https://doi.org/10.1016/j.molmet.2013.10.005.

Dzhura, Elvira V, Wenjuan He, and Kevin P M Currie. 2006. "Linopirdine Modulates Calcium Signaling and Stimulus- Secretion Coupling in Adrenal Chromaffin Cells by Targeting M-Type K." *Pharmacology* 316 (3): 1165–74. https://doi.org/10.1124/jpet.105.095570.G.

Ebert, B. L., J. D. Firth, and P. J. Ratcliffe. 1995. "Hypoxia and Mitochondrial Inhibitors Regulate Expression of Glucose Transporter-1 via Distinct Cis-Acting Sequences." *Journal of Biological Chemistry* 270 (49): 29083–89. https://doi.org/10.1074/jbc.270.49.29083.

Eccleston, Heather B, Kelly K Andringa, Angela M Betancourt, Adrienne L King, Sudheer K Mantena, Telisha M Swain, Heather N Tinsley, et al. 2011. "Chronic Exposure to a High-Fat Diet Induces Hepatic Steatosis, Impairs Nitric Oxide Bioavailability, and Modifies the Mitochondrial Proteome in Mice." *Antioxidants & Redox Signaling* 15 (2): 447–59. https://doi.org/10.1089/ars.2010.3395.

Eckel-Mahan, Kristin, and Paolo Sassone-Corsi. 2013. "Metabolism and the Circadian Clock Converge." *Physiological Reviews* 93 (1): 107–35.

https://doi.org/10.1152/physrev.00016.2012.

Eckel, R H. 1989. “Lipoprotein Lipase. A Multifunctional Enzyme Relevant to Common Metabolic Diseases.” *The New England Journal of Medicine* 320 (16): 1060–68. https://doi.org/10.1056/NEJM198904203201607.

Eckel, Robert H, Scott M Grundy, and Paul Z Zimmet. 2005. “The Metabolic Syndrome.” *Lancet.* 365 (9501): 1415–28. https://doi.org/10.1016/S0140-6736(05)67780-X.

Egan, J J, A S Greenberg, M K Chang, S A Wek, M C Moos Jr, and C Londos. 1992. “Mechanism of Hormone-Stimulated Lipolysis in Adipocytes: Translocation of Hormone-Sensitive Lipase to the Lipid Storage Droplet.” *Proceedings of the National Academy of Sciences of the United States of America* 89 (18): 8537–41. https://doi.org/10.1073/pnas.89.18.8537.

El-Haschimi, K, D D Pierroz, S M Hileman, C Bjørbaek, and J S Flier. 2000. “Two Defects Contribute to Hypothalamic Leptin Resistance in Mice with Diet-Induced Obesity.” *The Journal of Clinical Investigation* 105 (12): 1827–32. https://doi.org/10.1172/JCI9842.

Englund, Ani, Leena Kovanen, Sirkku T Saarikoski, Jari Haukka, Antti Reunanen, Arpo Aromaa, Jouko Lönnqvist, and Timo Partonen. 2009. “NPAS2 and PER2 Are Linked to Risk Factors of the Metabolic Syndrome.” *Journal of Circadian Rhythms* 7: 5. https://doi.org/10.1186/1740-3391-7-5.

Epstein, A C, J M Gleadle, L A McNeill, K S Hewitson, J O’Rourke, D R Mole, M Mukherji, et al. 2001. “C. Elegans EGL-9 and Mammalian Homologs Define a Family of Dioxygenases That Regulate HIF by Prolyl Hydroxylation.” *Cell* 107 (1): 43–54. https://doi.org/10.1016/s0092-8674(01)00507-4.

Esposito, Katherine, Raffaele Marfella, Miryam Ciotola, Carmen Di Palo, Francesco Giugliano, Giovanni Giugliano, Massimo D’Armiento, Francesco D’Andrea, and Dario Giugliano. 2004. “Effect of a Mediterranean-Style Diet on Endothelial Dysfunction and Markers of Vascular Inflammation in the Metabolic Syndrome: A Randomized Trial.” *JAMA* 292 (12): 1440–46. https://doi.org/10.1001/jama.292.12.1440.

Esseveldt, K E van, M N Lehman, and G J Boer. 2000. “The Suprachiasmatic Nucleus and the Circadian Time-Keeping System Revisited.” *Brain Research. Brain Research Reviews* 33 (1): 34–77. https://doi.org/10.1016/s0165-0173(00)00025-4.

Esteve, Laurent, Pierre Lutz, Nathalie Thiriet, Marie Odile Revel, Dominique Aunis, and Jean Zwiller. 2001. “Cyclic GMP-Dependent Protein Kinase Potentiates Serotonin-Induced Egr-1 Binding Activity in PC12 Cells.” *Cellular Signalling* 13 (6): 425–32. https://doi.org/10.1016/S0898-6568(01)00163-2.

European Food Safety Authority. 2010. “Scientific Opinion on the Safety and Efficacy of Koffogran (Nicarbazin) as a Feed Additive for Chickens for Fattening.” *The EFSA Journal* 8 (3): 1–40. https://doi.org/10.2903/j.efsa.2010.1551.

Expert-Panel. 1998. “Executive Summary of the Clinical Guidelines on the Identification, Evaluation, and Treatment of Overweight and Obesity in Adults.” *Archives of Internal Medicine* 158 (17): 1855–67. https://doi.org/10.1001/archinte.158.17.1855.

———. 2001. “Executive Summary of The Third Report of The National Cholesterol Education Program (NCEP) Expert Panel on Detection, Evaluation, And Treatment of High Blood Cholesterol In Adults (Adult Treatment Panel III).” *JAMA* 285 (19): 2486–97. https://doi.org/10.1001/jama.285.19.2486.

FDA. 2007. “Developing Products for Weight Management (Draft Guidance).” http://www.fda.gov/cder/guidance/index.htm%0AU.S.

Feillet, Celine, Gijsbertus T J van der Horst, Francis Levi, David A Rand, and Franck Delaunay. 2015. “Coupling between the Circadian Clock and Cell Cycle Oscillators: Implication for Healthy Cells and Malignant Growth.” *Frontiers in Neurology* 6: 96. https://doi.org/10.3389/fneur.2015.00096.

Ferguson, Amy, Laura M. Lyall, Joey Ward, Rona J. Strawbridge, Breda Cullen, Nicholas Graham, Claire L. Niedzwiedz, et al. 2018. “Genome-Wide Association Study of Circadian Rhythmicity in 71,500 UK Biobank Participants and Polygenic Association with Mood Instability.” *EBioMedicine* 35: 279–87. https://doi.org/10.1016/j.ebiom.2018.08.004.

Ferreri, K, G Gill, and M Montminy. 1994. “The CAMP-Regulated Transcription Factor CREB Interacts with a Component of the TFIID Complex.” *Proceedings of the National Academy of Sciences* 91 (4): 1210 LP – 1213. https://doi.org/10.1073/pnas.91.4.1210.

Ferreyra, Gabriela A, and Diego A Golombek. 2001. “Rhythmicity of the CGMP-Related Signal Transduction Pathway in the Mammalian Circadian System.” *American Journal of Physiology-Regulatory, Integrative and Comparative Physiology* 280 (5): R1348–55. https://doi.org/10.1152/ajpregu.2001.280.5.R1348.

Fidler, Meredith C, Matilde Sanchez, Brian Raether, Neil J Weissman, Steven R Smith, William R Shanahan, and Christen M Anderson. 2011. “A One-Year Randomized Trial of Lorcaserin for Weight Loss in Obese and Overweight Adults: The BLOSSOM Trial.” *The Journal of Clinical Endocrinology and Metabolism* 96 (10): 3067–77. https://doi.org/10.1210/jc.2011-1256.

Fiedler, Beate, Suzanne M. Lohmann, Albert Smolenski, Stephan Linnemüller, Burkert Pieske, Frank Schröder, Jeffery D. Molkentin, Helmut Drexler, and Kai C. Wollert. 2002. “Inhibition of Calcineurin-NFAT Hypertrophy Signaling by CGMP-Dependent Protein Kinase Type I in Cardiac Myocytes.” *Proceedings of the National Academy of Sciences of the United States of America* 99 (17): 11363–68. https://doi.org/10.1073/pnas.162100799.

Filiano, A N, T Millender-Swain, R Johnson, M E Young, K L Gamble, and S M Bailey. 2013.

"Chronic Ethanol Consumption Disrupts the Core Molecular Clock and Diurnal Rhythms of Metabolic Genes in the Liver without Affecting the Suprachiasmatic Nucleus." *PLoS ONE* 8: e71684.

Fischmeister, Rodolphe, Liliana R.V. Castro, Aniella Abi-Gerges, Francesca Rochais, Jonas Jurevičius, Jérôme Leroy, and Grégoire Vandecasteele. 2006. "Compartmentation of Cyclic Nucleotide Signaling in the Heart: The Role of Cyclic Nucleotide Phosphodiesterases." *Circulation Research* 99 (8): 816–28. https://doi.org/10.1161/01.RES.0000246118.98832.04.

Flak, Jonathan N, and Martin G Jr Myers. 2016. "Minireview: CNS Mechanisms of Leptin Action." *Molecular Endocrinology (Baltimore, Md.)* 30 (1): 3–12. https://doi.org/10.1210/me.2015-1232.

Fleur, S E La, A Kalsbeek, J Wortel, and R M Buijs. 1999. "A Suprachiasmatic Nucleus Generated Rhythm in Basal Glucose Concentrations." *Journal of Neuroendocrinology* 11 (8): 643–52. https://doi.org/10.1046/j.1365-2826.1999.00373.x.

Fleur, Susanne E La, Andries Kalsbeek, Joke Wortel, Madelon L Fekkes, and Ruud M Buijs. 2001. "A Daily Rhythm in Glucose Tolerance." *Diabetes* 50: 1237–43.

Foran, Patrick G.P., Laura M. Fletcher, Paru B. Oatey, Nadiem Mohammed, J. Oliver Dolly, and Jeremy M. Tavaré. 1999. "Protein Kinase B Stimulates the Translocation of GLUT4 but Not GLUT1 or Transferrin Receptors in 3T3-L1 Adipocytes by a Pathway Involving SNAP-23, Synaptobrevin-2, and/or Cellubrevin." *Journal of Biological Chemistry* 274 (40): 28087–95. https://doi.org/10.1074/jbc.274.40.28087.

Fowler, S D, and P Greenspan. 1985. "Application of Nile Red, a Fluorescent Hydrophobic Probe, for the Detection of Neutral Lipid Deposits in Tissue Sections: Comparison with Oil Red O." *The Journal of Histochemistry and Cytochemistry : Official Journal of the Histochemistry Society* 33 (8): 833–36. https://doi.org/10.1177/33.8.4020099.

Francis, Sharron H., Jennifer L. Busch, and Jackie D. Corbin. 2010. "CGMP-Dependent Protein Kinases and CGMP Phosphodiesterases in Nitric Oxide and CGMP Action." *Pharmacological Reviews* 62 (3): 525–63. https://doi.org/10.1124/pr.110.002907.

Frank, Laura Lewis, Bess E Sorensen, Yutaka Yasui, Shelley S Tworoger, Robert S Schwartz, Cornelia M Ulrich, Melinda L Irwin, et al. 2005. "Effects of Exercise on Metabolic Risk Variables in Overweight Postmenopausal Women: A Randomized Clinical Trial." *Obesity Research* 13 (3): 615–25. https://doi.org/10.1038/oby.2005.66.

Frederich, Robert C, Andreas Hamann, Stephen Anderson, Bettina Löllmann, Bradford B Lowell, and Jeffrey S Flier. 1995. "Leptin Levels Reflect Body Lipid Content in Mice: Evidence for Diet-Induced Resistance to Leptin Action." *Nature Medicine* 1 (12): 1311–14. https://doi.org/10.1038/nm1295-1311.

Friebe, Andreas, Peter Sandner, and Achim Schmidtko. 2020. "CGMP: A Unique 2nd

Messenger Molecule – Recent Developments in CGMP Research and Development." *Naunyn-Schmiedeberg's Archives of Pharmacology* 393 (2): 287–302. https://doi.org/10.1007/s00210-019-01779-z.

Fuhrmann, Dominik C., and Bernhard Brüne. 2017. "Mitochondrial Composition and Function under the Control of Hypoxia." *Redox Biology* 12 (February): 208–15. https://doi.org/10.1016/j.redox.2017.02.012.

Fumeron, Frédéric, Roberte Aubert, Afshan Siddiq, Dina Betoulle, Frank Péan, Samy Hadjadj, Jean Tichet, et al. 2004. "Adiponectin Gene Polymorphisms and Adiponectin Levels Are Independently Associated with the Development of Hyperglycemia during a 3-Year Period: The Epidemiologic Data on the Insulin Resistance Syndrome Prospective Study." *Diabetes* 53 (4): 1150–57. https://doi.org/10.2337/diabetes.53.4.1150.

Gaal, L F Van, J I Broom, G Enzi, and H Toplak. 1998. "Efficacy and Tolerability of Orlistat in the Treatment of Obesity: A 6-Month Dose-Ranging Study. Orlistat Dose-Ranging Study Group." *European Journal of Clinical Pharmacology* 54 (2): 125–32. https://doi.org/10.1007/s002280050433.

Gadbois, D M, H A Crissman, R A Tobey, and E M Bradbury. 1992. "Multiple Kinase Arrest Points in the G1 Phase of Nontransformed Mammalian Cells Are Absent in Transformed Cells." *Proceedings of the National Academy of Sciences of the United States of America* 89 (18): 8626–30. https://doi.org/10.1073/pnas.89.18.8626.

Gall, Charlotte Von, Giles E. Duffield, Michael H. Hastings, Michael D.A. Kopp, Faramarz Dehghani, Horst Werner Korf, and Jörg H. Stehle. 1998. "CREB in the Mouse SCN: A Molecular Interface Coding the Phase-Adjusting Stimuli Light, Glutamate, PACAP, and Melatonin for Clockwork Access." *Journal of Neuroscience* 18 (24): 10389–97. https://doi.org/10.1523/jneurosci.18-24-10389.1998.

Gamboa, J. L., Mary L. Garcia-Cazarin, and Francisco H. Andrade. 2011. "Chronic Hypoxia Increases Insulin-Stimulated Glucose Uptake in Mouse Soleus Muscle." *American Journal of Physiology - Regulatory Integrative and Comparative Physiology* 300 (1): 85–91. https://doi.org/10.1152/ajpregu.00078.2010.

Gasquet, P De, S Griglio, E Pequignot-Planche, and M I Malewiak. 1977. "Diurnal Changes in Plasma and Liver Lipids and Lipoprotein Lipase Activity in Heart and Adipose Tissue in Rats Fed a High and Low Fat Diet." *The Journal of Nutrition* 107 (2): 199–212. https://doi.org/10.1093/jn/107.2.199.

Gau, Daniel, Thomas Lemberger, Charlotte Von Gall, Oliver Kretz, Nguyet Le Minh, Peter Gass, Wolfgang Schmid, Ueli Schibler, Horst W Korf, and Gü Nther Schü Tz. 2002. "Phosphorylation of CREB Ser142 Regulates Light-Induced Phase Shifts of the Circadian Clock Being the Day-Night Cycle. Indeed, Light Pulses Applied during Early or Late Subjective Night Result in Phase de-Lays or Advances, Respectively, While

Light Pulses ." *Neuron* 34: 245–53. https://ac.els-cdn.com/S0896627302006566/1-s2.0-S0896627302006566-main.pdf?_tid=5529a694-b679-4c40-a25f-c65dd17cea02&acdnat=1541367489_e2d740db0827dc705494f4a81cd87985.

Gekakis, N, D Staknis, H B Nguyen, F C Davis, L D Wilsbacher, D P King, J S Takahashi, and C J Weitz. 1998. "Role of the CLOCK Protein in the Mammalian Circadian Mechanism." *Science (New York, N.Y.)* 280 (5369): 1564–69. https://doi.org/10.1126/science.280.5369.1564.

Gerber, Alan, Cyril Esnault, Gregory Aubert, Richard Treisman, François Pralong, and Ueli Schibler. 2013. "Blood-Borne Circadian Signal Stimulates Daily Oscillations in Actin Dynamics and SRF Activity." *Cell* 152 (3): 492–503. https://doi.org/10.1016/j.cell.2012.12.027.

Gessner, Guido, and Stefan H Heinemann. 2003. "Inhibition of HEAG1 and HERG1 Potassium Channels by Clofilium and Its Tertiary Analogue LY97241." *British Journal of Pharmacology* 138 (1): 161–71. https://doi.org/10.1038/sj.bjp.0705025.

Giacomini, Kathleen M., Shiew Mei Huang, Donald J. Tweedie, Leslie Z. Benet, Kim L.R. Brouwer, Xiaoyan Chu, Amber Dahlin, et al. 2010. "Membrane Transporters in Drug Development." *Nature Reviews Drug Discovery* 9 (3): 215–36. https://doi.org/10.1038/nrd3028.

Gillette, Martha U., and Jennifer W. Mitchell. 2002. "Signaling in the Suprachiasmatic Nucleus: Selectively Responsive and Integrative." *Cell and Tissue Research* 309 (1): 99–107. https://doi.org/10.1007/s00441-002-0576-1.

Gloston, Gabrielle F, Seung-hee Yoo, and Zheng Jake Chen. 2017. "Clock-Enhancing Small Molecules and Potential Applications in Chronic Diseases and Aging" 8 (March): 1–12. https://doi.org/10.3389/fneur.2017.00100.

Gnaiger, E., and A. V. Kuznetsov. 2002. "Mitochondrial Respiration at Low Levels of Oxygen and Cytochrome C." *Biochemical Society Transactions*, 252–58. https://doi.org/10.1042/0300-5127.

Godinho, Sofia I H, Elizabeth S Maywood, Linda Shaw, Valter Tucci, Alun R Barnard, Luca Busino, Michele Pagano, et al. 2007. "The After-Hours Mutant Reveals a Role for Fbxl3 in Determining Mammalian Circadian Period." *Science* 316 (5826): 897–900. https://doi.org/10.1126/science.1141138.

Goldstein, J L, R A DeBose-Boyd, and M S Brown. 2006. "Protein Sensors for Membrane Sterols." *Cell* 124: 35–46.

Golombek, Diego A., Patricia V. Agostino, Santiago A. Plano, and Gabriela A. Ferreyra. 2004. "Signaling in the Mammalian Circadian Clock: The NO/CGMP Pathway." *Neurochemistry International* 45 (6): 929–36. https://doi.org/10.1016/j.neuint.2004.03.023.

Gonzalez, Gustavo A, and Marc R Montminy. 1989. "Cyclic AMP Stimulates Somatostatin

Gene Transcription by Phosphorylation of CREB at Serine 133." *Cell* 59 (4): 675–80. https://doi.org/https://doi.org/10.1016/0092-8674(89)90013-5.

Görgens, Sven W., Tim Benninghoff, Kristin Eckardt, Christian Springer, Alexandra Chadt, Anita Melior, Jakob Wefers, et al. 2017. "Hypoxia in Combination With Muscle Contraction Improves Insulin Action and Glucose Metabolism in Human Skeletal Muscle via the HIF-1α Pathway." *Diabetes* 66 (11): 2800–2807. https://doi.org/10.2337/db16-1488.

Gosselin, Pauline, Gianpaolo Rando, Fabienne Fleury-olela, and Ueli Schibler. 2016. "Unbiased Identification of Signal-Activated Transcription Factors by Barcoded Synthetic Tandem Repeat Promoter Screening." *Genes & Development*, 1895–1907. https://doi.org/10.1101/gad.284828.116.

Gottesfeld, J M, and D J Forbes. 1997. "Mitotic Repression of the Transcriptional Machinery." *Trends in Biochemical Sciences* 22 (6): 197–202. https://doi.org/10.1016/s0968-0004(97)01045-1.

Granados-Fuentes, Daniel, Tracey O. Hermanstyne, Yarimar Carrasquillo, Jeanne M. Nerbonne, and Erik D. Herzog. 2015. "IA Channels Encoded by Kv1.4 and Kv4.2 Regulate Circadian Period of Per2 Expression in the Suprachiasmatic Nucleus." *Journal of Biological Rhythms* 30 (5): 396–407. https://doi.org/10.1177/0748730415593377.

Green, Carla B, Nicholas Douris, Shihoko Kojima, Carl A Strayer, Joseph Fogerty, David Lourim, Susanna R Keller, and Joseph C Besharse. 2007. "Loss of Nocturnin , a Circadian Deadenylase , Confers Resistance to Hepatic Steatosis and Diet-Induced Obesity" 104 (23).

Green, D J, and R Gillette. 1982. "Circadian Rhythm of Firing Rate Recorded from Single Cells in the Rat Suprachiasmatic Brain Slice." *Brain Research* 245 (1): 198–200. https://doi.org/10.1016/0006-8993(82)90361-4.

Green, Howard, and Olaniyi Kehinde. 1974. "Sublines of Mouse 3T3 Cells That Accumulate Lipid." *Cell* 1 (3): 113–16. https://doi.org/https://doi.org/10.1016/0092-8674(74)90126-3.

———. 1975. "An Established Preadipose Cell Line and Its Differentiation in Culture II. Factors Affecting the Adipose Conversion." *Cell* 5 (1): 19–27. https://doi.org/https://doi.org/10.1016/0092-8674(75)90087-2.

Greenberg, Harly, Xiaobing Ye, David Wilson, Aung K Htoo, Todd Hendersen, and Shu Fang Liu. 2006. "Chronic Intermittent Hypoxia Activates Nuclear Factor-KappaB in Cardiovascular Tissues in Vivo." *Biochemical and Biophysical Research Communications* 343 (2): 591–96. https://doi.org/10.1016/j.bbrc.2006.03.015.

Greenspan, P, E P Mayer, and S D Fowler. 1985. "Nile Red: A Selective Fluorescent Stain for Intracellular Lipid Droplets." *The Journal of Cell Biology* 100 (3): 965–73.

https://doi.org/10.1083/jcb.100.3.965.
Groop, Leif. 2005. “Genetics of the Metabolic Syndrome.” *British Journal of Nutrition*, 401–50. https://doi.org/10.1002/0470011327.ch13.
Grundy, Scott M, James I Cleeman, Stephen R Daniels, Karen A Donato, Robert H Eckel, Barry A Franklin, David J Gordon, et al. 2005. “Diagnosis and Management of the Metabolic Syndrome: An American Heart Association/National Heart, Lung, and Blood Institute Scientific Statement.” *Circulation* 112 (17): 2735–52. https://doi.org/10.1161/CIRCULATIONAHA.105.169404.
Gudi, Tanima, Darren E. Casteel, Charles Vinson, Gerry R. Boss, and Renate B. Pilz. 2000. “NO Activation of Fos Promoter Elements Requires Nuclear Translocation of G-Kinase I and CREB Phosphorylation but Is Independent of Map Kinase Activation.” *Oncogene* 19 (54): 6324–33. https://doi.org/10.1038/sj.onc.1204007.
Gudi, Tanima, Jeffrey C. Chen, Darren E. Casteel, Tammy M. Seasholtz, Gerry R. Boss, and Renate B. Pilz. 2002. “CGMP-Dependent Protein Kinase Inhibits Serum-Response Element-Dependent Transcription by Inhibiting Rho Activation and Functions.” *Journal of Biological Chemistry* 277 (40): 37382–93. https://doi.org/10.1074/jbc.M204491200.
Gudi, Tanima, Ivana Huvar, Matthias Meinecke, Suzanne M Lohmann, Gerry R Boss, and Renate B Pilz. 1996. “Regulation of Gene Expression by CGMP-Dependent Protein Kinase.” *The Journal of Biological Chemistry* 271 (9): 4597–4600. https://doi.org/10.1016/S0959-437X(96)80046-3.
Guertin, David A., and David M. Sabatini. 2005. “An Expanding Role for MTOR in Cancer.” *Trends in Molecular Medicine* 11 (8): 353–61. https://doi.org/10.1016/j.molmed.2005.06.007.
Guillaumond, Fabienne, Hugues Dardente, Vincent Giguère, and Nicolas Cermakian. 2005. “Differential Control of Bmal1 Circadian Transcription by REV-ERB and ROR Nuclear Receptors.” *Journal of Biological Rhythms* 20 (5): 391–403. https://doi.org/10.1177/0748730405277232.
Gunthorpe, Martin J, Charles H Large, and Raman Sankar. 2012. “The Mechanism of Action of Retigabine (Ezogabine), a First-in-Class K+ Channel Opener for the Treatment of Epilepsy.” *Epilepsia* 53 (3): 412–24. https://doi.org/10.1111/j.1528-1167.2011.03365.x.
Guo, Shiyi, Jinsha Huang, Haiyang Jiang, Chao Han, Jie Li, Xiaoyun Xu, Guoxin Zhang, Zhicheng Lin, Nian Xiong, and Tao Wang. 2017. “Restless Legs Syndrome: From Pathophysiology to Clinical Diagnosis and Management.” *Frontiers in Aging Neuroscience* 9 (JUN): 1–14. https://doi.org/10.3389/fnagi.2017.00171.
Guo, Z, D D Hensrud, C M Johnson, and M D Jensen. 1999. “Regional Postprandial Fatty Acid Metabolism in Different Obesity Phenotypes.” *Diabetes* 48 (8): 1586–92.

https://doi.org/10.2337/diabetes.48.8.1586.

Haas, Bodo, Peter Mayer, Katja Jennissen, Daniela Scholz, Mauricio Berriel Diaz, Wilhelm Bloch, Stephan Herzig, Reinhard Fässler, and Alexander Pfeifer. 2009. "Protein Kinase G Controls Brown Fat Cell Differentiation and Mitochondrial Biogenesis-Supplimentary Materials." *Science Signaling* 2 (99). https://doi.org/10.1126/scisignal.2000511.

Hajduch, E, D R Alessi, B A Hemmings, and H S Hundal. 1998. "Constitutive Activation of Protein Kinase B Alpha by Membrane Targeting Promotes Glucose and System A Amino Acid Transport, Protein Synthesis, and Inactivation of Glycogen Synthase Kinase 3 in L6 Muscle Cells." *Diabetes* 47 (7): 1006 LP – 1013. https://doi.org/10.2337/diabetes.47.7.1006.

Halberg, Nils, Tayeba Khan, Maria E. Trujillo, Ingrid Wernstedt-Asterholm, Alan D. Attie, Shariq Sherwani, Zhao V. Wang, et al. 2009. "Hypoxia-Inducible Factor 1α Induces Fibrosis and Insulin Resistance in White Adipose Tissue." *Molecular and Cellular Biology* 29 (16): 4467–83. https://doi.org/10.1128/mcb.00192-09.

Hammerschlag, Anke R, Sven Stringer, Christiaan A de Leeuw, Suzanne Sniekers, Erdogan Taskesen, Kyoko Watanabe, Tessa F Blanken, et al. 2017. "Genome-Wide Association Analysis of Insomnia Complaints Identifies Risk Genes and Genetic Overlap with Psychiatric and Metabolic Traits." *Nature Genetics* 49 (11): 1584–92. https://doi.org/10.1038/ng.3888.

Hampp, Gabriele, Jürgen A Ripperger, Thijs Houben, Isabelle Schmutz, Christian Blex, Stéphanie Perreau-Lenz, Irene Brunk, et al. 2008. "Regulation of Monoamine Oxidase A by Circadian-Clock Components Implies Clock Influence on Mood." *Current Biology : CB* 18 (9): 678–83. https://doi.org/10.1016/j.cub.2008.04.012.

Han, Hye-Sook, Geon Kang, Jun Seok Kim, Byeong Hoon Choi, and Seung-Hoi Koo. 2016. "Regulation of Glucose Metabolism from a Liver-Centric Perspective." *Experimental & Molecular Medicine* 48 (3): e218–e218. https://doi.org/10.1038/emm.2015.122.

Hanke, Jens, Dave Brett, Inga Zastrow, Atakan Aydin, Sebastian Delbrück, Gerrit Lehmann, Friedrich Luft, Jens Reich, and Peer Bork. 1999. "Alternative Splicing of Human Genes: More the Rule than the Exception?" *Trends in Genetics* 15 (10): 389–90. https://doi.org/10.1016/S0168-9525(99)01830-2.

Harms, Matthew, and Patrick Seale. 2013. "Brown and Beige Fat: Development, Function and Therapeutic Potential." *Nature Medicine* 19 (10): 1252–63. https://doi.org/10.1038/nm.3361.

Harrison, Pauline M., and Paolo Arosio. 1996. "The Ferritins: Molecular Properties, Iron Storage Function and Cellular Regulation." *Biochimica et Biophysica Acta - Bioenergetics* 1275 (3): 161–203. https://doi.org/10.1016/0005-2728(96)00022-9.

Hastings, Michael H., Akhilesh B. Reddy, and Elizabeth S. Maywood. 2003. “A Clockwork Web: Circadian Timing in Brain and Periphery, in Health and Disease.” *Nature Reviews Neuroscience* 4 (8): 649–61. https://doi.org/10.1038/nrn1177.

Hattar, S, H.-W. Liao, M Takao, D M Berson, and K.-W. Yau. 2002. “Melanopsin-Containing Retinal Ganglion Cells: Architecture, Projections, and Intrinsic Photosensitivity.” *Science* 295 (5557): 1065–70. https://doi.org/10.1126/science.1069609.

He, Baokun, Kazunari Nohara, Noheon Park, Joseph S Takahashi, Seung-hee Yoo, Zheng Chen, Baokun He, et al. 2016. “The Small Molecule Nobiletin Targets the Molecular Oscillator to Enhance Circadian Rhythms and Protect against Metabolic Syndrome Article The Small Molecule Nobiletin Targets the Molecular Oscillator to Enhance Circadian Rhythms and Protect against Metabo.” *Cell Metabolism* 23 (4): 610–21. https://doi.org/10.1016/j.cmet.2016.03.007.

He, Bin, and Georg F. Weber. 2003. “Phosphorylation of NF-KB Proteins by Cyclic GMP-Dependent Kinase: A Noncanonical Pathway to NF-KB Activation.” *European Journal of Biochemistry* 270 (10): 2174–85. https://doi.org/10.1046/j.1432-1033.2003.03574.x.

Hegele, Robert A. 2003. “Monogenic Forms of Insulin Resistance: Apertures That Expose the Common Metabolic Syndrome.” *Trends in Endocrinology and Metabolism: TEM* 14 (8): 371—377. https://doi.org/10.1016/s1043-2760(03)00142-5.

Henderson, S J, A Konkar, D C Hornigold, J L Trevaskis, R Jackson, M Fritsch Fredin, R Jansson-Löfmark, et al. 2016. “Robust Anti-Obesity and Metabolic Effects of a Dual GLP-1/Glucagon Receptor Peptide Agonist in Rodents and Non-Human Primates.” *Diabetes, Obesity and Metabolism* 18 (12): 1176–90. https://doi.org/10.1111/dom.12735.

Hirota, Tsuyoshi, Jae Wook Lee, Peter C. St. John, Mariko Sawa, Keiko Iwaisako, Takako Noguchi, Pagkapol Y. Pongsawakul, et al. 2012. “Identification of Small Molecule Activators of Cryptochrome.” *Science* 337 (6098): 1094–97. https://doi.org/10.1126/science.1223710.

Hirota, Tsuyoshi, Jae Wook Lee, Peter C St John, Mariko Sawa, Keiko Iwaisako, Takako Noguchi, Pagkapol Y Pongsawakul, et al. 2012. “Identification of Small Molecule Activators of Cryptochrome.” *Science (New York, N.Y.)* 337 (6098): 1094–97. https://doi.org/10.1126/science.1223710.

Hirota, Tsuyoshi, Warren G Lewis, Andrew C Liu, Jae Wook Lee, Peter G Schultz, and Steve A Kay. 2008. “A Chemical Biology Approach Reveals Period Shortening of the Mammalian Circadian Clock by Specific Inhibition of GSK-3beta.” *Proceedings of the National Academy of Sciences of the United States of America* 105 (52): 20746–51. https://doi.org/10.1073/pnas.0811410106.

Hirsch, J, and J L Knittle. 1970. “Cellularity of Obese and Nonobese Human Adipose

Tissue." *Federation Proceedings* 29 (4): 1516–21.
Hofman, M A, E Fliers, E Goudsmit, and D F Swaab. 1988. "Morphometric Analysis of the Suprachiasmatic and Paraventricular Nuclei in the Human Brain: Sex Differences and Age-Dependent Changes." *Journal of Anatomy* 160 (October): 127–43. https://pubmed.ncbi.nlm.nih.gov/3253251.
Holzer, Ryan G, Eek-Joong Park, Ning Li, Helen Tran, Monica Chen, Crystal Choi, Giovanni Solinas, and Michael Karin. 2011. "Saturated Fatty Acids Induce C-Src Clustering within Membrane Subdomains, Leading to JNK Activation." *Cell* 147 (1): 173–84. https://doi.org/10.1016/j.cell.2011.08.034.
Honma, Sato, Takeshi Kawamoto, Yumiko Takagi, Katsumi Fujimoto, Fuyuki Sato, Mitsuhide Noshiro, Yukio Kato, and Ken Ichi Honma. 2002. "Dec1 and Dec2 Are Regulators of the Mammalian Molecular Clock." *Nature* 419 (6909): 841–44. https://doi.org/10.1038/nature01123.
Honoré, E, B Attali, G Romey, C Heurteaux, P Ricard, F Lesage, M Lazdunski, and J Barhanin. 1991. "Cloning, Expression, Pharmacology and Regulation of a Delayed Rectifier K+ Channel in Mouse Heart." *The EMBO Journal* 10 (10): 2805–11. https://pubmed.ncbi.nlm.nih.gov/1655403.
Hoogerwerf, W A, H L Hellmich, G Cornelissen, F Halberg, V B Shahinian, J Bostwick, T C Savidge, and V M Cassone. 2007. "Clock Gene Expression in the Murine Gastrointestinal Tract: Endogenous Rhythmicity and Effects of a Feeding Regimen." *Gastroenterology* 133: 1250–60.
Horst, G. T. J. van der, M. Muijtjens, K. Kobayashi, R. Takano, and A. Yasui. 1999. "Mammalian Cry1 and Cry2 Are Essential for Maintenance of Circadian Rhythms." *Nature* 389 (6728): 627–30.
Hosogai, Naomi, Atsunori Fukuhara, Kazuya Oshima, Yugo Miyata, Sachiyo Tanaka, Katsumori Segawa, Shigetada Furukawa, et al. 2007. "Adipose Tissue Hypoxia in Obesity and Its Impact on Adipocytokine Dysregulation." *Diabetes* 56 (4): 901–11. https://doi.org/10.2337/db06-0911.
Hotamisligil, Gökhan S., Pascal Peraldi, Adriane Budavari, Ramsey Ellis, Morris F. White, and Bruce M. Spiegelman. 1996. "IRS-1-Mediated Inhibition of Insulin Receptor Tyrosine Kinase Activity in TNF-α- and Obesity-Induced Insulin Resistance." *Science* 271 (5249): 665–68. https://doi.org/10.1126/science.271.5249.665.
Hotamisligil, Gökhan S., Narinder S. Shargill, and Bruce M. Spiegelman. 1993. "Adipose Expression of Tumor Necrosis Factor-α: Direct Role in Obesity-Linked Insulin Resistance." *Science* 259 (5091): 87–91. https://doi.org/10.1126/science.7678183.
Howe, Vicky, Laura J Sharpe, Anika V Prabhu, and Andrew J Brown. 2017. "New Insights into Cellular Cholesterol Acquisition: Promoter Analysis of Human HMGCR and SQLE, Two Key Control Enzymes in Cholesterol Synthesis." *Biochimica et Biophysica*

Acta (BBA) - Molecular and Cell Biology of Lipids 1862 (7): 647–57. https://doi.org/https://doi.org/10.1016/j.bbalip.2017.03.009.

Hu, Jingru, and Esam E El-Fakahany. 1993. "Role of Intercellular and Intracellular Communication by Nitric Oxide in Coupling of Muscarinic Receptors to Activation of Guanylate Cyclase in Neuronal Cells." *Journal of Neurochemistry* 61 (2): 578–85. https://doi.org/10.1111/j.1471-4159.1993.tb02161.x.

Hu, Sumei, Lu Wang, Dengbao Yang, Li Li, Jacques Togo, Yingga Wu, Quansheng Liu, et al. 2018. "Dietary Fat, but Not Protein or Carbohydrate, Regulates Energy Intake and Causes Adiposity in Mice." *Cell Metabolism*, 415–31. https://doi.org/10.1016/j.cmet.2018.06.010.

Humphries, Paul S., Ross Bersot, John Kincaid, Eric Mabery, Kerryn McCluskie, Timothy Park, Travis Renner, et al. 2016. "Carbazole-Containing Sulfonamides and Sulfamides: Discovery of Cryptochrome Modulators as Antidiabetic Agents." *Bioorganic and Medicinal Chemistry Letters* 26 (3): 757–60. https://doi.org/10.1016/j.bmcl.2015.12.102.

Ingalls, A M, M M Dickie, and G D Snell. 1950. "Obese, a New Mutation in the House Mouse." *The Journal of Heredity* 41 (12): 317–18. https://doi.org/10.1093/oxfordjournals.jhered.a106073.

Inoue, Ikuo, Yuichi Shinoda, Masaaki Ikeda, Kenji Hayashi, Kenta Kanazawa, Masahiko Nomura, Toshiyuki Matsunaga, et al. 2005. "CLOCK/BMAL1 Is Involved in Lipid Metabolism via Transactivation of the Peroxisome Proliferator-Activated Receptor (PPAR) Response Element." *Journal of Atherosclerosis and Thrombosis* 12 (3): 169–74. https://doi.org/10.5551/jat.12.169.

Inouye, S T, and H Kawamura. 1979. "Persistence of Circadian Rhythmicity in a Mammalian Hypothalamic 'Island' Containing the Suprachiasmatic Nucleus." *Proceedings of the National Academy of Sciences of the United States of America* 76 (11): 5962–66. https://doi.org/10.1073/pnas.76.11.5962.

Ishida, Atsushi, Tatsushi Mutoh, Tomoko Ueyama, Hideki Bando, Satoru Masubuchi, Daiichiro Nakahara, Gozoh Tsujimoto, and Hitoshi Okamura. 2005. "Light Activates the Adrenal Gland: Timing of Gene Expression and Glucocorticoid Release." *Cell Metabolism* 2 (5): 297–307. https://doi.org/10.1016/j.cmet.2005.09.009.

Ishikawa, K., and T. Shimazu. 1980. "Circadian Rhythm of Liver Glycogen Metabolism in Rats: Effects of Hypothalamic Lesions." *American Journal of Physiology - Endocrinology and Metabolism* 1 (1): 21–25. https://doi.org/10.1152/ajpendo.1980.238.1.e21.

Ishikawa, K, and T Shimazu. 1976. "Daily Rhythms of Glycogen Synthetase and Phosphorylase Activities in Rat Liver: Influence of Food and Light." *Life Sciences* 19 (12): 1873–78. https://doi.org/10.1016/0024-3205(76)90119-3.

Isidor, Marie S., Sally Winther, Astrid L. Basse, M. Christine H. Petersen, Barbara Cannon, Jan Nedergaard, and Jacob B. Hansen. 2016. “An SiRNA-Based Method for Efficient Silencing of Gene Expression in Mature Brown Adipocytes.” *Adipocyte* 5 (2): 175–85. https://doi.org/10.1080/21623945.2015.1111972.

Izumo, Mariko, Carl Hirschie Johnson, and Shin Yamazaki. 2003. “Circadian Gene Expression in Mammalian Fibroblasts Revealed by Real-Time Luminescence Reporting: Temperature Compensation and Damping.” *Proceedings of the National Academy of Sciences of the United States of America* 100 (26): 16089–94. https://doi.org/10.1073/pnas.2536313100.

Jaakkola, Panu, David R Mole, Ya-Min Tian, Michael I Wilson, Janine Gielbert, Simon J Gaskell, Alexander von Kriegsheim, et al. 2001. “Targeting of HIF-α to the von Hippel-Lindau Ubiquitylation Complex by O₂-Regulated Prolyl Hydroxylation.” *Science* 292 (5516): 468 LP – 472. https://doi.org/10.1126/science.1059796.

Jagannath, Aarti, Lewis Taylor, Zeinab Wakaf, Sridhar R. Vasudevan, and Russell G. Foster. 2017. “The Genetics of Circadian Rhythms, Sleep and Health.” *Human Molecular Genetics* 26 (R2): R128–38. https://doi.org/10.1093/hmg/ddx240.

James, W P, A Avenell, J Broom, and J Whitehead. 1997. “A One-Year Trial to Assess the Value of Orlistat in the Management of Obesity.” *International Journal of Obesity and Related Metabolic Disorders : Journal of the International Association for the Study of Obesity* 21 Suppl 3 (June): S24-30.

Jewett, Megan E., Richard E. Kronauer, and Charles A. Czeisler. 1994. “Phase-Amplitude Resetting of the Human Circadian Pacemaker via Bright Light: A Further Analysis.” *Journal of Biological Rhythms* 9: 295–314. https://doi.org/10.1177/074873049400900310.

Jiang, Changtao, Aijuan Qu, Tsutomu Matsubara, Tatyana Chanturiya, William Jou, Oksana Gavrilova, Yatrik M. Shah, and Frank J. Gonzalez. 2011. “Disruption of Hypoxia-Inducible Factor 1 in Adipocytes Improves Insulin Sensitivity and Decreases Adiposity in High-Fat Diet-Fed Mice.” *Diabetes* 60 (10): 2484–95. https://doi.org/10.2337/db11-0174.

Jo, Junghyo, Oksana Gavrilova, Stephanie Pack, William Jou, Shawn Mullen, Anne E. Sumner, Samuel W. Cushman, and Vipul Periwal. 2009. “Hypertrophy and/or Hyperplasia: Dynamics of Adipose Tissue Growth.” *PLoS Computational Biology* 5 (3). https://doi.org/10.1371/journal.pcbi.1000324.

Jokinen, R., R. Rinnankoski-Tuikka, S. Kaye, L. Saarinen, S. Heinonen, M. Myöhänen, E. Rappou, et al. 2018. “Adipose Tissue Mitochondrial Capacity Associates with Long-Term Weight Loss Success.” *International Journal of Obesity* 42 (4): 817–25. https://doi.org/10.1038/ijo.2017.299.

Jud, Corinne, Isabelle Schmutz, Gabriele Hampp, Henrik Oster, and Urs Albrecht. 2005. “A Guideline for Analyzing Circadian Wheel-Running Behavior in Rodents under Different Lighting Conditions.” *Biological Procedures Online* 7 (1): 101–16. https://doi.org/10.1251/bpo109.

Julia, Steinberger, Daniels Stephen R., Eckel Robert H., Hayman Laura, Lustig Robert H., McCrindle Brian, and Mietus-Snyder Michele L. 2009. “Progress and Challenges in Metabolic Syndrome in Children and Adolescents.” *Circulation* 119 (4): 628–47. https://doi.org/10.1161/CIRCULATIONAHA.108.191394.

Jun, Jonathan C., Ronald Devera, Dileep Unnikrishnan, Mi Kyung Shin, Shannon Bevans-Fonti, Qiaoling Yao, Aman Rathore, et al. 2017. “Adipose HIF-1α Causes Obesity by Suppressing Brown Adipose Tissue Thermogenesis.” *Journal of Molecular Medicine* 95 (3): 287–97. https://doi.org/10.1007/s00109-016-1480-6.

Jung, Youngseob, Hye Guk Ryu, Sung Wook Kim, Kyung Ha Lee, Sohyun Gu, Hee Yi, Hyun Ok Ku, Sung Key Jang, and Kyong Tai Kim. 2019. “The RNA-Binding Protein HnRNP Q Represses Translation of the Clock Gene Bmal1 in Murine Cells.” *Journal of Biological Chemistry* 294 (19): 7682–91. https://doi.org/10.1074/jbc.RA118.006947.

Kabir, Morvarid, Darko Stefanovski, Isabel R. Hsu, Malini Iyer, Orison O. Woolcott, Dan Zheng, Karyn J. Catalano, et al. 2011. “Large Size Cells in the Visceral Adipose Depot Predict Insulin Resistance in the Canine Model.” *Obesity* 19 (11): 2121–29. https://doi.org/10.1038/oby.2011.254.

Kallen, C B, and M A Lazar. 1996. “Antidiabetic Thiazolidinediones Inhibit Leptin (Ob) Gene Expression in 3T3-L1 Adipocytes.” *Proceedings of the National Academy of Sciences of the United States of America* 93 (12): 5793–96. https://doi.org/10.1073/pnas.93.12.5793.

Kalló, Imre, Theodosis Kalamatianos, Nzinga Wiltshire, Sanbing Shen, W John Sheward, Anthony J Harmar, and Clive W Coen. 2004. “Transgenic Approach Reveals Expression of the VPAC2 Receptor in Phenotypically Defined Neurons in the Mouse Suprachiasmatic Nucleus and in Its Efferent Target Sites.” *European Journal of Neuroscience* 19 (8): 2201–11. https://doi.org/10.1111/j.0953-816X.2004.03335.x.

Kalra, Dinesh, Georg Baumgarten, Ziad Dibbs, Yukihiro Seta, Natarajan Sivasubramanian, and Douglas L. Mann. 2000. “Nitric Oxide Provokes Tumor Necrosis Factor-α Expression in Adult Feline Myocardium through a CGMP-Dependent Pathway.” *Circulation* 102 (11): 1302–7. https://doi.org/10.1161/01.CIR.102.11.1302.

Kalsbeek, A, E Fliers, M A Hofman, D F Swaab, and R M Buijs. 2010. “Vasopressin and the Output of the Hypothalamic Biological Clock.” *Journal of Neuroendocrinology* 22 (5): 362–72. https://doi.org/10.1111/j.1365-2826.2010.01956.x.

Kamura, Takumi, Shigeo Sato, Kazuhiro Iwai, Maria Czyzyk-Krzeska, Ronald C Conaway,

and Joan Weliky Conaway. 2000. “Activation of HIF1α Ubiquitination by a Reconstituted von Hippel-Lindau (VHL) Tumor Suppressor Complex.” *Proceedings of the National Academy of Sciences* 97 (19): 10430 LP – 10435. https://doi.org/10.1073/pnas.190332597.

Kanda, Hajime, Sanshiro Tateya, Yoshikazu Tamori, Ko Kotani, Ken-ichi Hiasa, Riko Kitazawa, Sohei Kitazawa, et al. 2006. “MCP-1 Contributes to Macrophage Infiltration into Adipose Tissue, Insulin Resistance, and Hepatic Steatosis in Obesity.” *The Journal of Clinical Investigation* 116 (6): 1494–1505. https://doi.org/10.1172/JCI26498.

Kang, Jun Goo, and Cheol Young Park. 2012. “Anti-Obesity Drugs: A Review about Their Effects and Safety.” *Diabetes and Metabolism Journal* 36 (1): 13–25. https://doi.org/10.4093/dmj.2012.36.1.13.

Kaplan, Norman M. 1989. “The Deadly Quartet: Upper-Body Obesity, Glucose Intolerance, Hypertriglyceridemia, and Hypertension.” *Archives of Internal Medicine* 149 (7): 1514–20. https://doi.org/10.1001/archinte.1989.00390070054005.

Kapuscinski, J. 1995. “DAPI: A DNA-Specific Fluorescent Probe.” *Biotechnic & Histochemistry : Official Publication of the Biological Stain Commission* 70 (5): 220–33. https://doi.org/10.3109/10520299509108199.

Kawasaki, Koh, Robert S. Smith, Chung-Ming Hsieh, Jianxin Sun, Julie Chao, and James K. Liao. 2003. “Activation of the Phosphatidylinositol 3-Kinase/Protein Kinase Akt Pathway Mediates Nitric Oxide-Induced Endothelial Cell Migration and Angiogenesis.” *Molecular and Cellular Biology* 23 (16): 5726–37. https://doi.org/10.1128/mcb.23.16.5726-5737.2003.

Keiser, Michael J, Bryan L Roth, Blaine N Armbruster, Paul Ernsberger, John J Irwin, and Brian K Shoichet. 2007. “Relating Protein Pharmacology by Ligand Chemistry.” *Nature Biotechnology* 25 (2): 197–206. https://doi.org/10.1038/nbt1284.

Kelley, David E, Jing He, Elizabeth V Menshikova, and Vladimir B Ritov. 2002. “Dysfunction of Mitochondria in Human Skeletal Muscle in Type 2 Diabetes.” *Diabetes* 51 (10): 2944–50. https://doi.org/10.2337/diabetes.51.10.2944.

Kelly, T, W Yang, C-S Chen, K Reynolds, and J He. 2008. “Global Burden of Obesity in 2005 and Projections to 2030.” *International Journal of Obesity (2005)* 32 (9): 1431–37. https://doi.org/10.1038/ijo.2008.102.

Kent, Jack, and Andrea L. Meredith. 2008. “BK Channels Regulate Spontaneous Action Potential Rhythmicity in the Suprachiasmatic Nucleus.” *PLoS ONE* 3 (12). https://doi.org/10.1371/journal.pone.0003884.

Keravis, Thérèse, and Claire Lugnier. 2012. “Cyclic Nucleotide Phosphodiesterase (PDE) Isozymes as Targets of the Intracellular Signalling Network: Benefits of PDE Inhibitors in Various Diseases and Perspectives for Future Therapeutic

Developments." *British Journal of Pharmacology* 165 (5): 1288–1305. https://doi.org/10.1111/j.1476-5381.2011.01729.x.

Kersten, S, B Desvergne, and W Wahli. 2000. "Roles of PPARs in Health and Disease." *Nature* 405 (6785): 421–24. https://doi.org/10.1038/35013000.

Kida, K, T Nishio, T Yokozawa, K Nagai, H Matsuda, and H Nakagawa. 1980. "The Circadian Change of Gluconeogenesis in the Liver in Vivo in Fed Rats." *Journal of Biochemistry* 88 (4): 1009–13. https://doi.org/10.1093/oxfordjournals.jbchem.a133051.

Kiemer, Alexandra K., Alexander L. Gerbes, Manfred Bilzer, and Angelika M. Vollmar. 2002. "The Atrial Natriuretic Peptide and CGMP: Novel Activators of the Heat Shock Response in Rat Livers." *Hepatology* 35 (1): 88–94. https://doi.org/10.1053/jhep.2002.30080.

Kiemer, Alexandra K., Nina C. Weber, and Angelika M. Vollmar. 2002. "Induction of IκB: Atrial Natriuretic Peptide as a Regulator of the NF-KB Pathway." *Biochemical and Biophysical Research Communications* 295 (5): 1068–76. https://doi.org/10.1016/S0006-291X(02)00807-0.

Kim, Dae Hyun, German Perdomo, Ting Zhang, Sandra Slusher, Sojin Lee, Brett E Phillips, Yong Fan, et al. 2011. "FoxO6 Integrates Insulin Signaling With Gluconeogenesis in the Liver." *Diabetes* 60 (11): 2763–74. https://doi.org/10.2337/db11-0548.

Kim, Inki, Wenjie Xu, and John C Reed. 2008. "Cell Death and Endoplasmic Reticulum Stress: Disease Relevance and Therapeutic Opportunities." *Nature Reviews Drug Discovery* 7 (12): 1013–30. https://doi.org/10.1038/nrd2755.

Kim, Soo M., Mingyue Lun, Mei Wang, Samuel E. Senyo, Christelle Guillermier, Parth Patwari, and Matthew L. Steinhauser. 2014. "Loss of White Adipose Hyperplastic Potential Is Associated with Enhanced Susceptibility to Insulin Resistance." *Cell Metabolism* 20 (6): 1049–58. https://doi.org/10.1016/j.cmet.2014.10.010.

Kim, Young-Bum, Gerald I Shulman, and Barbara B Kahn. 2002. "Fatty Acid Infusion Selectively Impairs Insulin Action on Akt1 and Protein Kinase C Lambda /Zeta but Not on Glycogen Synthase Kinase-3." *The Journal of Biological Chemistry* 277 (36): 32915–22. https://doi.org/10.1074/jbc.M204710200.

King, D P, Y Zhao, A M Sangoram, L D Wilsbacher, M Tanaka, M P Antoch, T D Steeves, et al. 1997. "Positional Cloning of the Mouse Circadian Clock Gene." *Cell* 89 (4): 641–53. https://doi.org/10.1016/s0092-8674(00)80245-7.

Kiyatkin, Anatoly, Edita Aksamitiene, Nick I. Markevich, Nikolay M. Borisov, Jan B. Hoek, and Boris N. Kholodenko. 2006. "Scaffolding Protein Grb2-Associated Binder 1 Sustains Epidermal Growth Factor-Induced Mitogenic and Survival Signaling by Multiple Positive Feedback Loops." *Journal of Biological Chemistry* 281 (29): 19925–38. https://doi.org/10.1074/jbc.M600482200.

Ko, Gladys Y.P., Liheng Shi, and Michael L. Ko. 2009. "Circadian Regulation of Ion Channels

and Their Functions." *Journal of Neurochemistry* 110 (4): 1150–69. https://doi.org/10.1111/j.1471-4159.2009.06223.x.

Kobayashi, Minoru, Akiyo Morinibu, Sho Koyasu, Yoko Goto, Masahiro Hiraoka, and Hiroshi Harada. 2017. "A Circadian Clock Gene, PER2, Activates HIF-1 as an Effector Molecule for Recruitment of HIF-1α to Promoter Regions of Its Downstream Genes." *FEBS Journal* 284 (22): 3804–16. https://doi.org/10.1111/febs.14280.

Kocabas, Fatih, Junke Zheng, Suwannee Thet, Neal G Copeland, Nancy A Jenkins, Ralph J DeBerardinis, Chengcheng Zhang, and Hesham A Sadek. 2012. "Meis1 Regulates the Metabolic Phenotype and Oxidant Defense of Hematopoietic Stem Cells." *Blood* 120 (25): 4963–72. https://doi.org/10.1182/blood-2012-05-432260.

Kohsaka, Akira, Aaron D Laposky, Kathryn Moynihan Ramsey, Carmela Estrada, Corinne Joshu, Yumiko Kobayashi, Fred W Turek, and Joseph Bass. 2007. "High-Fat Diet Disrupts Behavioral and Molecular Circadian Rhythms in Mice," no. November: 414–21. https://doi.org/10.1016/j.cmet.2007.09.006.

Koike, Nobuya, Seung-Hee Yoo, Hung-Chung Huang, Vivek Kumar, Choogon Lee, Tae-Kyung Kim, and Joseph S Takahashi. 2012. "Transcriptional Architecture and Chromatin Landscape of the Core Circadian Clock in Mammals." *Science* 338 (6105): 349–54. https://doi.org/10.1126/science.1226339.

Komalavilas, Padmini, Paras K. Shah, Hanjoong Jo, and Thomas M. Lincoln. 1999. "Activation of Mitogen-Activated Protein Kinase Pathways by Cyclic GMP and Cyclic GMP-Dependent Protein Kinase in Contractile Vascular Smooth Muscle Cells." *Journal of Biological Chemistry* 274 (48): 34301–9. https://doi.org/10.1074/jbc.274.48.34301.

Kornhauser, Jon M, Christopher W Cowan, Adam J Shaywitz, Ricardo E Dolmetsch, Eric C Griffith, Linda S Hu, Chia Haddad, Zhengui Xia, and Michael E Greenberg. 2002. "CREB Transcriptional Activity in Neurons Is Regulated by Multiple, Calcium-Specific Phosphorylation Events." *Neuron* 34 (2): 221–33. https://doi.org/https://doi.org/10.1016/S0896-6273(02)00655-4.

Kral, John G., and Erik Näslund. 2007. "Surgical Treatment of Obesity." *Nature Clinical Practice Endocrinology and Metabolism* 3 (8): 574–83. https://doi.org/10.1038/ncpendmet0563.

Kris-Etherton, P, R H Eckel, B V Howard, S St Jeor, and T L Bazzarre. 2001. "AHA Science Advisory: Lyon Diet Heart Study. Benefits of a Mediterranean-Style, National Cholesterol Education Program/American Heart Association Step I Dietary Pattern on Cardiovascular Disease." *Circulation* 103 (13): 1823–25. https://doi.org/10.1161/01.cir.103.13.1823.

Krishnan, Jaya, Carsten Danzer, Tatiana Simka, Josef Ukropec, Katharina Manuela Walter, Susann Kumpf, Peter Mirtschink, et al. 2012. "Dietary Obesity-Associated Hif1α

Activation in Adipocytes Restricts Fatty Acid Oxidation and Energy Expenditure via Suppression of the Sirt2-NAD+ System." *Genes and Development* 26 (3): 259–70. https://doi.org/10.1101/gad.180406.111.

Kruszynska, Yolanta T, Mim I Mulford, Joseph G Yu, Debra A Armstrong, and Jerrold M Olefsky. 1997. "Effects of Nonesterified Fatty Acids on Glucose Metabolism After Glucose Ingestion." *Diabetes* 46 (October).

Kucejova, B., N. E. Sunny, A. D. Nguyen, R. Hallac, X. Fu, S. Pẽa-Llopis, R. P. Mason, et al. 2011. "Uncoupling Hypoxia Signaling from Oxygen Sensing in the Liver Results in Hypoketotic Hypoglycemic Death." *Oncogene* 30 (18): 2147–60. https://doi.org/10.1038/onc.2010.587.

Kumar, Manoj, Nicholas Reed, Ruiting Liu, Elias Aizenman, Peter Wipf, and Thanos Tzounopoulos. 2016. "Synthesis and Evaluation of Potent KCNQ2/3-Specific Channel Activators." *Molecular Pharmacology* 89 (6): 667–77. https://doi.org/10.1124/mol.115.103200.

Kumar, Naresh, Laura A Solt, Yongjun Wang, Pamela M Rogers, Gargi Bhattacharyya, Theodore M Kamenecka, Keith R Stayrook, et al. 2010. "Regulation of Adipogenesis by Natural and Synthetic REV-ERB Ligands." *Endocrinology* 151 (7): 3015–25. https://doi.org/10.1210/en.2009-0800.

Kume, K, M J Zylka, S Sriram, L P Shearman, D R Weaver, X Jin, E S Maywood, M H Hastings, and S M Reppert. 1999. "MCRY1 and MCRY2 Are Essential Components of the Negative Limb of the Circadian Clock Feedback Loop." *Cell* 98 (2): 193–205. https://doi.org/10.1016/s0092-8674(00)81014-4.

Kwok, Kelvin H.M., Karen S.L. Lam, and Aimin Xu. 2016. "Heterogeneity of White Adipose Tissue: Molecular Basis and Clinical Implications." *Experimental and Molecular Medicine* 48 (3). https://doi.org/10.1038/emm.2016.5.

Kwok, R P, J R Lundblad, J C Chrivia, J P Richards, H P Bächinger, R G Brennan, S G Roberts, M R Green, and R H Goodman. 1994. "Nuclear Protein CBP Is a Coactivator for the Transcription Factor CREB." *Nature* 370 (6486): 223–26. https://doi.org/10.1038/370223a0.

Kylin, E. 1923. "Studien Ueber Das Hypertonie-Hyperglykamie-Hyperurikamiesyndrom." *Zentralblatt Für Innere Medizin*, no. 44: 105–27.

Ladd, Andrea N., Nicolas Charlet-B., and Thomas A. Cooper. 2001. "The CELF Family of RNA Binding Proteins Is Implicated in Cell-Specific and Developmentally Regulated Alternative Splicing." *Molecular and Cellular Biology* 21 (4): 1285–96. https://doi.org/10.1128/mcb.21.4.1285-1296.2001.

Ladd, Andrea N., Nicole H. Nguyen, Kavin Malhotra, and Thomas A. Cooper. 2004. "CELF6, a Member of the CELF Family of RNA-Binding Proteins, Regulates Muscle-Specific Splicing Enhancer-Dependent Alternative Splicing." *Journal of Biological Chemistry*

279 (17): 17756–64. https://doi.org/10.1074/jbc.M310687200.

Lafontan, Max. 2005. “FAT CELLS: Afferent and Efferent Messages Define New Approaches to Treat Obesity.” *Annual Review of Pharmacology and Toxicology* 45 (1): 119–46. https://doi.org/10.1146/annurev.pharmtox.45.120403.095843.

Lakin-Thomas, Patricia L., Stuart Brody, and Gary G Cote. 1991. “Amplitude Model for the Effects of Mutations and Temperature on Period and Phase Resetting of the Neurospora Circadian Oscillator.” *Journal of Biological Rhythms* 6 (4): 281–97.

Lamas, J. Antonio, A. A. Selyanko, and D. A. Brown. 1997. “ Effects of a Cognition-Enhancer, Linopirdine (DuP 996), on M-Type Potassium Currents (I K(M)) Some Other Voltage- and Ligand-Gated Membrane Currents in Rat Sympathetic Neurons .” *European Journal of Neuroscience* 9 (3): 605–16. https://doi.org/10.1111/j.1460-9568.1997.tb01637.x.

Lamia, Katja A., Stephanie J. Papp, Ruth T. Yu, Grant D. Barish, N. Henriette Uhlenhaut, Johan W. Jonker, Michael Downes, and Ronald M. Evans. 2011. “Cryptochromes Mediate Rhythmic Repression of the Glucocorticoid Receptor.” *Nature* 480 (7378): 552–56. https://doi.org/10.1038/nature10700.

Lamia, Katja A., Kai Florian Storch, and Charles J. Weitz. 2008. “Physiological Significance of a Peripheral Tissue Circadian Clock.” *Proceedings of the National Academy of Sciences of the United States of America* 105 (39): 15172–77. https://doi.org/10.1073/pnas.0806717105.

Lamia, Katja A, Uma M Sachdeva, Luciano Ditacchio, Elliot C Williams, Jacqueline G Alvarez, Daniel F Egan, Debbie S Vasquez, et al. 2009. “AMPK Regulates the Circadian Clock by Cryptochrome Phosphorylation and Degradation.” *Science*, no. October: 437–41.

Landgraf, Dominic, Lexie L Wang, Tanja Diemer, and David K Welsh. 2016. “NPAS2 Compensates for Loss of CLOCK in Peripheral Circadian Oscillators.” *PLoS Genetics* 12 (2): e1005882. https://doi.org/10.1371/journal.pgen.1005882.

Lando, David, Daniel J. Peet, Jeffrey J. Gorman, Dean A. Whelan, Murray L. Whitelaw, and Richard K. Bruick. 2002. “FIH-1 Is an Asparaginyl Hydroxylase Enzyme That Regulates the Transcriptional Activity of Hypoxia-Inducible Factor David.” *Genes & Development* 16: 11466–71. https://doi.org/10.1101/gad.991402.1466.

Lawrence, H J, S Rozenfeld, C Cruz, K Matsukuma, A Kwong, L Kömüves, A M Buchberg, and C Largman. 1999. “Frequent Co-Expression of the HOXA9 and MEIS1 Homeobox Genes in Human Myeloid Leukemias.” *Leukemia* 13 (12): 1993–99. https://doi.org/10.1038/sj.leu.2401578.

Lee, Jaemin, Junli Liu, Xudong Feng, Mario Andrés Salazar Hernández, Patrick Mucka, Dorina Ibi, Jae Won Choi, and Umut Ozcan. 2016. “Withaferin A Is a Leptin Sensitizer with Strong Antidiabetic Properties in Mice.” *Nature Medicine* 22 (9): 1023–32.

https://doi.org/10.1038/nm.4145.

Lee, SoJung, Ian Janssen, and Robert Ross. 2004. "Interindividual Variation in Abdominal Subcutaneous and Visceral Adipose Tissue: Influence of Measurement Site." *Journal of Applied Physiology (Bethesda, Md.: 1985)* 97 (3): 948–54. https://doi.org/10.1152/japplphysiol.01200.2003.

Lee, Yongjin, Rongmin Chen, Hyeong Min Lee, and Choogon Lee. 2011. "Stoichiometric Relationship among Clock Proteins Determines Robustness of Circadian Rhythms." *Journal of Biological Chemistry* 286 (9): 7033–42. https://doi.org/10.1074/jbc.M110.207217.

Lee, Yun Sok, Jung-whan Kim, Olivia Osborne, Da Young Oh, Roman Sasik, Simon Schenk, Ai Chen, et al. 2014. "Increased Adipocyte O 2 Consumption Triggers HIF-1 a , Causing Inflammation and Insulin Resistance in Obesity." *Cell* 157 (6): 1339–52. https://doi.org/10.1016/j.cell.2014.05.012.

Lefebvre, Philippe, Giulia Chinetti, Jean-charles Fruchart, and Bart Staels. 2006. "Sorting out the Roles of PPAR α in Energy Metabolism and Vascular Homeostasis" 116 (3): 571–80. https://doi.org/10.1172/JCI27989.symptoms.

Lettéron, Philippe, Angela Sutton, Abdellah Mansouri, Bernard Fromenty, and Dominique Pessayre. 2003. "Inhibition of Microsomal Triglyceride Transfer Protein: Another Mechanism for Drug-Induced Steatosis in Mice." *Hepatology (Baltimore, Md.)* 38 (1): 133–40. https://doi.org/10.1053/jhep.2003.50309.

Lewy, A J, and S P Markey. 1978. "Analysis of Melatonin in Human Plasma by Gas Chromatography Negative Chemical Ionization Mass Spectrometry." *Science* 201 (4357): 741 LP – 743. https://doi.org/10.1126/science.675255.

Li, Xinghai, Bobby Monks, Qingyuan Ge, and Morris J Birnbaum. 2007. "Akt/PKB Regulates Hepatic Metabolism by Directly Inhibiting PGC-1α Transcription Coactivator." *Nature* 447 (7147): 1012–16. https://doi.org/10.1038/nature05861.

Lipton, Jonathan O., Lara M. Boyle, Elizabeth D. Yuan, Kevin J. Hochstrasser, Fortunate F. Chifamba, Ashwin Nathan, Peter T. Tsai, Fred Davis, and Mustafa Sahin. 2017. "Aberrant Proteostasis of BMAL1 Underlies Circadian Abnormalities in a Paradigmatic MTOR-Opathy." *Cell Reports* 20 (4): 868–80. https://doi.org/10.1016/j.celrep.2017.07.008.

Liu, Andrew C., Hien G. Tran, Eric E. Zhang, Aaron A. Priest, David K. Welsh, and Steve A. Kay. 2008. "Redundant Function of REV-ERBα and β and Non-Essential Role for Bmal1 Cycling in Transcriptional Regulation of Intracellular Circadian Rhythms." *PLoS Genetics* 4 (2). https://doi.org/10.1371/journal.pgen.1000023.

Liu, Chang, Siming Li, Tiecheng Liu, Jimo Borjigin, and Jiandie D Lin. 2007. "Transcriptional Coactivator PGC-1 a Integrates the Mammalian Clock and Energy Metabolism" 447 (May): 477–82. https://doi.org/10.1038/nature05767.

Liu, Chen, Jian M. Ding, Lia E. Faiman, and Martha U. Gillette. 1997. "Coupling of Muscarinic Cholinergic Receptors and CGMP in Nocturnal Regulation of the Suprachiasmatic Circadian Clock." *Journal of Neuroscience* 17 (2): 659–66. https://doi.org/10.1523/jneurosci.17-02-00659.1997.

Liu, Chen, and Martha U. Gillette. 1996. "Cholinergic Regulation of the Suprachiasmatic Nucleus Circadian Rhythm via a Muscarinic Mechanism at Night." *Journal of Neuroscience* 16 (2): 744–51. https://doi.org/10.1523/jneurosci.16-02-00744.1996.

Liu, D., C. C. Wong, L. Fu, H. Chen, L. Zhao, C. Li, Y. Zhou, et al. 2018. "Squalene Epoxidase Drives NAFLD-Induced Hepatocellular Carcinoma and Is a Pharmaceutical Target." *Science Translational Medicine* 10 (460): 1–15. https://doi.org/10.1126/scitranslmed.aav4522.

Liu, Dianxin, Ryan P. Ceddia, and Sheila Collins. 2018. "Cardiac Natriuretic Peptides Promote Adipose 'Browning' through MTOR Complex-1." *Molecular Metabolism* 9 (January): 192–98. https://doi.org/10.1016/j.molmet.2017.12.017.

Liu, Junli, Jaemin Lee, Mario Andres Salazar Hernandez, Ralph Mazitschek, and Umut Ozcan. 2015. "Treatment of Obesity with Celastrol." *Cell* 161 (5): 999–1011. https://doi.org/10.1016/j.cell.2015.05.011.

Louis, Mariam, and Naresh M. Punjabi. 2009. "Effects of Acute Intermittent Hypoxia on Glucose Metabolism in Awake Healthy Volunteers." *Journal of Applied Physiology* 106 (5): 1538–44. https://doi.org/10.1152/japplphysiol.91523.2008.

Love, Michael I., Wolfgang Huber, and Simon Anders. 2014. "Moderated Estimation of Fold Change and Dispersion for RNA-Seq Data with DESeq2." *Genome Biology* 15 (12): 1–21. https://doi.org/10.1186/s13059-014-0550-8.

Lowrey, P L, K Shimomura, M P Antoch, S Yamazaki, P D Zemenides, M R Ralph, M Menaker, and J S Takahashi. 2000. "Positional Syntenic Cloning and Functional Characterization of the Mammalian Circadian Mutation Tau." *Science (New York, N.Y.)* 288 (5465): 483–92. https://doi.org/10.1126/science.288.5465.483.

Lu, Yun Fei, Eric R. Kandel, and Robert D. Hawkins. 1999. "Nitric Oxide Signaling Contributes to Late-Phase LTP and CREB Phosphorylation in the Hippocampus." *Journal of Neuroscience* 19 (23): 10250–61. https://doi.org/10.1523/jneurosci.19-23-10250.1999.

Luca, Carl de, Timothy J Kowalski, Yiying Zhang, Joel K Elmquist, Charlotte Lee, Manfred W Kilimann, Thomas Ludwig, Shun-Mei Liu, and Streamson C Jr Chua. 2005. "Complete Rescue of Obesity, Diabetes, and Infertility in Db/Db Mice by Neuron-Specific LEPR-B Transgenes." *The Journal of Clinical Investigation* 115 (12): 3484–93. https://doi.org/10.1172/JCI24059.

Lucas, R J, S Hattar, M Takao, D M Berson, R G Foster, and K-W Yau. 2003. "Diminished

Pupillary Light Reflex at High Irradiances in Melanopsin-Knockout Mice." *Science (New York, N.Y.)* 299 (5604): 245–47. https://doi.org/10.1126/science.1077293.

Lueptow, Lindsay M, Chang-Guo Zhan, and James M O'Donnell. 2016. "Cyclic GMP-Mediated Memory Enhancement in the Object Recognition Test by Inhibitors of Phosphodiesterase-2 in Mice." *Psychopharmacology* 233 (3): 447–56. https://doi.org/10.1007/s00213-015-4129-1.

Lumeng, Carey N, and Alan R Saltiel. 2011. "Inflammatory Links between Obesity and Metabolic Disease." *The Journal of Clinical Investigation* 121 (6): 2111–17. https://doi.org/10.1172/JCI57132.

Luo, Beibei, Dao Xiang, Die Wu, Changcheng Liu, Yiqun Fang, Peijie Chen, and Yi-Ping Hu. 2018. "Hepatic PHD2/HIF-1α Axis Is Involved in Postexercise Systemic Energy Homeostasis." *The FASEB Journal* 32 (9): 4670–80. https://doi.org/10.1096/fj.201701139R.

Lushchak, V I, T V Bahnjukova, and K B Storey. 1998. "Effect of Hypoxia on the Activity and Binding of Glycolytic and Associated Enzymes in Sea Scorpion Tissues." *Brazilian Journal of Medical and Biological Research* 31: 1059–67. http://www.scielo.br/scielo.php?script=sci_arttext&pid=S0100-879X1998000800005&nrm=iso.

Lyssenko, Valeriya, Cecilia L.F. Nagorny, Michael R. Erdos, Nils Wierup, Anna Jonsson, Peter Spégel, Marco Bugliani, et al. 2009. "Common Variant in MTNR1B Associated with Increased Risk of Type 2 Diabetes and Impaired Early Insulin Secretion." *Nature Genetics* 41 (1): 82–88. https://doi.org/10.1038/ng.288.

Macdougall, Iain C, Tadao Akizawa, Jeffrey S Berns, Thomas Bernhardt, and Thilo Krueger. 2019. "Effects of Molidustat in the Treatment of Anemia in CKD." *Clinical Journal of the American Society of Nephrology : CJASN* 14 (1): 28–39. https://doi.org/10.2215/CJN.02510218.

Madsen, Andreas Nygaard, Gitte Hansen, Sarah Juel Paulsen, Kirsten Lykkegaard, Mads Tang-Christensen, Harald S Hansen, Barry E Levin, et al. 2010. "Long-Term Characterization of the Diet-Induced Obese and Diet-Resistant Rat Model: A Polygenetic Rat Model Mimicking the Human Obesity Syndrome." *The Journal of Endocrinology* 206 (3): 287–96. https://doi.org/10.1677/JOE-10-0004.

Maemura, K, S M de la Monte, M T Chin, M D Layne, C M Hsieh, S F Yet, M A Perrella, and M E Lee. 2000. "CLIF, a Novel Cycle-like Factor, Regulates the Circadian Oscillation of Plasminogen Activator Inhibitor-1 Gene Expression." *The Journal of Biological Chemistry* 275 (47): 36847–51. https://doi.org/10.1074/jbc.C000629200.

Mai, J K, O Kedziora, L Teckhaus, and M V Sofroniew. 1991. "Evidence for Subdivisions in the Human Suprachiasmatic Nucleus." *Journal of Comparative Neurology* 305 (3): 508–25. https://doi.org/10.1002/cne.903050312.

Mairan, J. J. D. De. 1729. “Observation Botanique.” *Hist. Acad. Roy. Sci.*, 35–36.

Malayev, A A, D J Nelson, and L H Philipson. 1995. “Mechanism of Clofilium Block of the Human Kv1.5 Delayed Rectifier Potassium Channel.” *Molecular Pharmacology* 47 (1): 198 LP – 205. http://molpharm.aspetjournals.org/content/47/1/198.abstract.

Manella, Gal, Rona Aviram, Nityanand Bolshette, Sapir Muvkadi, Marina Golik, David F. Smith, and Gad Asher. 2020. “Hypoxia Induces a Time- And Tissue-Specific Response That Elicits Intertissue Circadian Clock Misalignment.” *Proceedings of the National Academy of Sciences of the United States of America* 117 (1): 779–86. https://doi.org/10.1073/pnas.1914112117.

Marchesini, G, M Brizi, G Bianchi, S Tomassetti, E Bugianesi, M Lenzi, A J McCullough, S Natale, G Forlani, and N Melchionda. 2001. “Nonalcoholic Fatty Liver Disease: A Feature of the Metabolic Syndrome.” *Diabetes* 50 (8): 1844–50. https://doi.org/10.2337/diabetes.50.8.1844.

Marchesini, G, M Brizi, A M Morselli-Labate, G Bianchi, E Bugianesi, A J McCullough, G Forlani, and N Melchionda. 1999. “Association of Nonalcoholic Fatty Liver Disease with Insulin Resistance.” *The American Journal of Medicine* 107 (5): 450–55. https://doi.org/10.1016/s0002-9343(99)00271-5.

Marcheva, Biliana, Kathryn Moynihan Ramsey, Ethan D Buhr, Yumiko Kobayashi, Hong Su, Caroline H Ko, Ganka Ivanova, et al. 2010. “Disruption of the Clock Components CLOCK and BMAL1 Leads to Hypoinsulinemia and Diabetes.” *Nature* 466 (7306): 627–31. https://doi.org/10.1038/nature09253.

Marcheva, Biliana, Kathryn Moynihan Ramsey, Ethan D Buhr, Yumiko Kobayashi, Hong Su, Caroline H Ko, Ganka Ivanova, et al. 2010. “Disruption of the Clock Components CLOCK and BMAL1 Leads to Hypoinsulinaemia and Diabetes.” *Nature* 466 (7306): 627–31. http://dx.doi.org/10.1038/nature09253.

Martelot, G Le, T Claudel, D Gatfield, O Schaad, B Kornmann, G Lo Sasso, A Moschetta, and U Schibler. 2009. “REV–ERBα Participates in Circadian SREBP Signaling and Bile Acid Homeostasis.” *PLoS Biology* 7: e1000181.

Mathur, A, D A Golombek, and M R Ralph. 1996. “CGMP-Dependent Protein Kinase Inhibitors Block Light-Induced Phase Advances of Circadian Rhythms in Vivo.” *American Journal of Physiology-Regulatory, Integrative and Comparative Physiology* 270 (5): R1031–36. https://doi.org/10.1152/ajpregu.1996.270.5.R1031.

Matsuno, T, N Kobayashi, F Hariguchi, T Okamoto, Y Okada, and T Hayashi. 1996. “Investigation for the Characteristic Anticoccidial Activity of Diclazuril in Battery Trials.” *The Journal of Veterinary Medical Science* 58 (2): 129–33. https://doi.org/10.1292/jvms.58.129.

Matsuo, Takuya, Shun Yamaguchi, Shigeru Mitsui, Aki Emi, Fukuko Shimoda, and Hitoshi Okamura. 2003. “Control Mechanism of the Circadian Clock for Timing of Cell

Division in Vivo." *Science* 302 (5643): 255–59. https://doi.org/10.1126/science.1086271.

Matthews, D R, J P Hosker, A S Rudenski, B A Naylor, D F Treacher, and R C Turner. 1985. "Homeostasis Model Assessment: Insulin Resistance and Beta-Cell Function from Fasting Plasma Glucose and Insulin Concentrations in Man." *Diabetologia* 28 (7): 412–19. https://doi.org/10.1007/BF00280883.

Mattson, Mark P. 2010. "Perspective: Does Brown Fat Protect against Diseases of Aging?" *Ageing Research Reviews* 9 (1): 69–76. https://doi.org/10.1016/j.arr.2009.11.004.

Maury, Eleonore, Kathryn Moynihan Ramsey, and Joseph Bass. 2010. "Circadian Rhythms and Metabolic Syndrome: From Experimental Genetics to Human Disease." *Circulation Research* 106 (3): 447–62. https://doi.org/10.1161/CIRCRESAHA.109.208355.

Maxwell, P H, M S Wiesener, G W Chang, S C Clifford, E C Vaux, M E Cockman, C C Wykoff, C W Pugh, E R Maher, and P J Ratcliffe. 1999. "The Tumour Suppressor Protein VHL Targets Hypoxia-Inducible Factors for Oxygen-Dependent Proteolysis." *Nature* 399 (6733): 271–75. https://doi.org/10.1038/20459.

Mayr, Bernhard, and Marc Montminy. 2001. "Transcriptional Regulation by the Phosphorylation-Dependent Factor Creb." *Nature Reviews Molecular Cell Biology* 2 (8): 599–609. https://doi.org/10.1038/35085068.

McCracken, Emma, Monica Monaghan, and Shiva Sreenivasan. 2018. "Pathophysiology of the Metabolic Syndrome." *Clinics in Dermatology* 36 (1): 14–20. https://doi.org/10.1016/j.clindermatol.2017.09.004.

Melnikova, Irena, and David Wages. 2006. "Anti-Obesity Therapies." *Nature Reviews Drug Discovery* 5 (5): 369–70. https://doi.org/10.1038/nrd2037.

Melo, Lucy, Diego A Golombek, and Martin R Ralph. 1997a. "Regulation of Circadian Photic Responses by Nitric Oxide." *Journal of Biological Rhythms* 12 (4): 319–26. https://doi.org/10.1177/074873049701200404.

———. 1997b. "Regulation of Circadian Photic Responses by Nitric Oxide." *Journal of Biological Rhythms* 12 (4): 319–26. https://doi.org/10.1177/074873049701200404.

Mendoza, Michelle C., E. Emrah Er, and John Blenis. 2011. "The Ras-ERK and PI3K-MTOR Pathways: Cross-Talk and Compensation." *Trends in Biochemical Sciences* 36 (6): 320–28. https://doi.org/10.1016/j.tibs.2011.03.006.

Minamishima, Yoji Andrew, Javid Moslehi, Robert F. Padera, Roderick T. Bronson, Ronglih Liao, and William G. Kaelin. 2009. "A Feedback Loop Involving the Phd3 Prolyl Hydroxylase Tunes the Mammalian Hypoxic Response In Vivo." *Molecular and Cellular Biology* 29 (21): 5729–41. https://doi.org/10.1128/mcb.00331-09.

Minh, N Le, F Damiola, F Tronche, G Schütz, and U Schibler. 2001. "Glucocorticoid

Hormones Inhibit Food-Induced Phase-Shifting of Peripheral Circadian Oscillators." *The EMBO Journal* 20 (24): 7128–36. https://doi.org/10.1093/emboj/20.24.7128.

Mitani, Yoshihide, Syed H E Zaidi, Pascale Dufourcq, Karen Thompson, and Marlene Rabinovitch. 2000. "Nitric Oxide Reduces Vascular Smooth Muscle Cell Elastase Activity through CGMP-Mediated Suppression of ERK Phosphorylation and AML1B Nuclear Partitioning." *The FASEB Journal* 14 (5): 805–14. https://doi.org/10.1096/fasebj.14.5.805.

Mitschke, Michaela M, Linda S Hoffmann, Thorsten Gnad, Daniela Scholz, Katja Kruithoff, Peter Mayer, Bodo Haas, et al. 2013. "Increased CGMP Promotes Healthy Expansion and Browning of White Adipose Tissue Oil Red O Staining" 27 (4): 1621–30. https://doi.org/10.1096/fj.12-221580.

Miyagi, Taeko, Tadashi Wada, Kazunori Yamaguchi, Keiko Hata, and Kazuhiro Shiozaki. 2008. "Plasma Membrane-Associated Sialidase as a Crucial Regulator of Transmembrane Signalling." *The Journal of Biochemistry* 144 (3): 279–85. https://doi.org/10.1093/jb/mvn089.

Moller-Levet, C. S., S. N. Archer, G. Bucca, E. E. Laing, A. Slak, R. Kabiljo, J. C. Y. Lo, et al. 2013. "Effects of Insufficient Sleep on Circadian Rhythmicity and Expression Amplitude of the Human Blood Transcriptome." *Proceedings of the National Academy of Sciences* 110 (12): E1132–41. https://doi.org/10.1073/pnas.1217154110.

Moore, Barbara J. 1987. "The Cafeteria Diet—An Inappropriate Tool for Studies of Thermogenesis." *The Journal of Nutrition* 117 (2): 227–31. https://doi.org/10.1093/jn/117.2.227.

Moore, R Y, and V B Eichler. 1972. "Loss of a Circadian Adrenal Corticosterone Rhythm Following Suprachiasmatic Lesions in the Rat." *Brain Research* 42 (1): 201–6. https://doi.org/10.1016/0006-8993(72)90054-6.

Mrosovsky, N, K Edelstein, M H Hastings, and E S Maywood. 2001. "Cycle of Period Gene Expression in a Diurnal Mammal (Spermophilus Tridecemlineatus): Implications for Nonphotic Phase Shifting." *Journal of Biological Rhythms* 16 (5): 471–78. https://doi.org/10.1177/074873001129002141.

Mukherji, Atish, Ahmad Kobiita, Manohar Damara, Nisha Misra, Hamid Meziane, Marie France Champy, and Pierre Chambon. 2015. "Shifting Eating to the Circadian Rest Phase Misaligns the Peripheral Clocks with the Master SCN Clock and Leads to a Metabolic Syndrome." *Proceedings of the National Academy of Sciences of the United States of America* 112 (48): E6691–98. https://doi.org/10.1073/pnas.1519807112.

Murai, Kasumi, and Richard Treisman. 2002. "Interaction of Serum Response Factor (SRF) with the Elk-1 B Box Inhibits RhoA-Actin Signaling to SRF and Potentiates Transcriptional Activation by Elk-1." *Molecular and Cellular Biology* 22 (20): 7083–

92. https://doi.org/10.1128/mcb.22.20.7083-7092.2002.

Nagoshi, Emi, Camille Saini, Christoph Bauer, Thierry Laroche, Felix Naef, and Ueli Schibler. 2004. "Circadian Gene Expression in Individual Fibroblasts: Cell-Autonomous and Self-Sustained Oscillators Pass Time to Daughter Cells." *Cell* 119 (5): 693–705. https://doi.org/10.1016/j.cell.2004.11.015.

Nakahata, Yasukazu, Milota Kaluzova, Benedetto Grimaldi, Saurabh Sahar, Jun Hirayama, Danica Chen, Leonard P Guarente, and Paolo Sassone-Corsi. 2008. "The NAD+-Dependent Deacetylase SIRT1 Modulates CLOCK-Mediated Chromatin Remodeling and Circadian Control." *Cell* 134 (2): 329–40. https://doi.org/http://doi.org/10.1016/j.cell.2008.07.002.

Nakamizo, Tomoki, Jun Kawamata, Kohei Yoshida, Yuko Kawai, Rie Kanki, Hideyuki Sawada, Takeshi Kihara, et al. 2003. "Phosphodiesterase Inhibitors Are Neuroprotective to Cultured Spinal Motor Neurons." *Journal of Neuroscience Research* 71 (4): 485–95. https://doi.org/10.1002/jnr.10483.

Namikawa, Chikako, Zhang Shu-Ping, John Raynor Vyselaar, Yasuko Nozaki, Yoshihisa Nemoto, Masafumi Ono, Naoaki Akisawa, et al. 2004. "Polymorphisms of Microsomal Triglyceride Transfer Protein Gene and Manganese Superoxide Dismutase Gene in Non-Alcoholic Steatohepatitis." *Journal of Hepatology* 40 (5): 781–86. https://doi.org/10.1016/j.jhep.2004.01.028.

Narayanaswami, Vidya, and Linda P. Dwoskin. 2017. "Obesity: Current and Potential Pharmacotherapeutics and Targets." *Pharmacology and Therapeutics* 170: 116–47. https://doi.org/10.1016/j.pharmthera.2016.10.015.

Nath, Bharath, Ivan Levin, Timea Csak, Jan Petrasek, Christian Mueller, Karen Kodys, Donna Catalano, Pranoti Mandrekar, and Gyongyi Szabo. 2011. "Hepatocyte-Specific Hypoxia-Inducible Factor-1α Is a Determinant of Lipid Accumulation and Liver Injury in Alcohol-Induced Steatosis in Mice." *Hepatology* 53 (5): 1526–37. https://doi.org/10.1002/hep.24256.

Nedergaard, Jan, Tore Bengtsson, and Barbara Cannon. 2007. "Unexpected Evidence for Active Brown Adipose Tissue in Adult Humans." *American Journal of Physiology - Endocrinology and Metabolism* 293 (2): 444–52. https://doi.org/10.1152/ajpendo.00691.2006.

Nickolson, V. J., S. W. Tam, M. J. Myers, and L. Cook. 1989. "DuP 996 Enhances the K - Stimulated Release of Acetyicholine in Rat Braiin Vitro and in Vivo." *FASEB Journal* 3 (A931).

Nickolson, V. J., S. W. Tam, M. J. Myers, and L. Cook. 1990. "DuP 996 (3,3-Bis(4-Pyrindinylmethyl)-1-Phenylindolin-2-One) Enhances the Stimulus-Induced Release of Acetylcholine from Rat Brain in Vitro and in Vivo." *Drug Dev. Res* 19: 285–300.

Nilsson, Cecilia, Kirsten Raun, Fei Fei Yan, Marianne O. Larsen, and Mads Tang-

Christensen. 2012. “Laboratory Animals as Surrogate Models of Human Obesity.” *Acta Pharmacologica Sinica* 33 (2): 173–81. https://doi.org/10.1038/aps.2011.203.

O’Dwyer, P. J., K. S. Yao, P. Ford, A. K. Godwin, and M. Clayton. 1994. “Effects of Hypoxia on Detoxicating Enzyme Activity and Expression in HT29 Colon Adenocarcinoma Cells.” *Cancer Research* 54 (12): 3082–87.

O’Neill, John S, Elizabeth S Maywood, Johanna E Chesham, Joseph S Takahashi, and Michael H Hastings. 2009. “CAMP-Dependent Signalling as a Core Component of the Mammalian Circadian Pacemaker” 320 (5878): 949–53. https://doi.org/10.1126/science.1152506.cAMP-Dependent.

O’Neill, S, and L O’Driscoll. 2015. “Metabolic Syndrome: A Closer Look at the Growing Epidemic and Its Associated Pathologies.” *Obesity Reviews : An Official Journal of the International Association for the Study of Obesity* 16 (1): 1–12. https://doi.org/10.1111/obr.12229.

Obrietan, Karl, Soren Impey, Dave Smith, Jaime Athos, and Daniel R. Storm. 1999. “Circadian Regulation of CAMP Response Element-Mediated Gene Expression in the Suprachiasmatic Nuclei.” *Journal of Biological Chemistry* 274 (25): 17748–56. https://doi.org/10.1074/jbc.274.25.17748.

Ohayon, Maurice M, Ruth O’Hara, and Michael V Vitiello. 2012. “Epidemiology of Restless Legs Syndrome: A Synthesis of the Literature.” *Sleep Medicine Reviews* 16 (4): 283–95. https://doi.org/10.1016/j.smrv.2011.05.002.

Ohh, M, C W Park, M Ivan, M A Hoffman, T Y Kim, L E Huang, N Pavletich, V Chau, and W G Kaelin. 2000. “Ubiquitination of Hypoxia-Inducible Factor Requires Direct Binding to the Beta-Domain of the von Hippel-Lindau Protein.” *Nature Cell Biology* 2 (7): 423–27. https://doi.org/10.1038/35017054.

Oishi, Katsutaka, Hidenori Shirai, and Norio Ishida. 2005. “CLOCK Is Involved in the Circadian Transactivation of Peroxisome-Proliferator-Activated Receptor α (PPARα) in Mice.” *Biochemical Journal* 386 (3): 575–81. https://doi.org/10.1042/BJ20041150.

Oliver, P, J Ribot, A M Rodríguez, J Sánchez, C Picó, and A Palou. 2006. “Resistin as a Putative Modulator of Insulin Action in the Daily Feeding/Fasting Rhythm.” *Pflugers Archiv : European Journal of Physiology* 452 (3): 260–67. https://doi.org/10.1007/s00424-005-0034-5.

Onda, Kenji, Natsumi Horike, Tai Ichi Suzuki, and Toshihiko Hirano. 2013. “Polymethoxyflavonoids Tangeretin and Nobiletin Increase Glucose Uptake in Murine Adipocytes.” *Phytotherapy Research* 27 (2): 312–16. https://doi.org/10.1002/ptr.4730.

Oster, Henrik, Sebastian Damerow, Silke Kiessling, Vladimira Jakubcakova, Diya Abraham, Jiong Tian, Matthias W Hoffmann, and Gregor Eichele. 2006. “The

Circadian Rhythm of Glucocorticoids Is Regulated by a Gating Mechanism Residing in the Adrenal Cortical Clock." *Cell Metabolism* 4 (2): 163–73. https://doi.org/10.1016/j.cmet.2006.07.002.

Oster, Henrik, Claudia Werner, Maria Chiara Magnone, Helmut Mayser, Robert Feil, Mathias W. Seeliger, Franz Hofmann, and Urs Albrecht1. 2003. "CGMP-Dependent Protein Kinase II Modulates MPer1 and MPer2 Gene Induction and Influences Phase Shifts of the Circadian Clock." *Current Biology* 13: 725–33. https://doi.org/10.1016/S.

Ouchi, Noriyuki, Jennifer L. Parker, Jesse J. Lugus, and Kenneth Walsh. 2011. "Adipokines in Inflammation and Metabolic Disease." *Nature Reviews Immunology* 11 (2): 85–97. https://doi.org/10.1038/nri2921.

Ouchi, Noriyuki, and Kenneth Walsh. 2007. "Adiponectin as an Anti-Inflammatory Factor." *Clinica Chimica Acta; International Journal of Clinical Chemistry* 380 (1–2): 24–30. https://doi.org/10.1016/j.cca.2007.01.026.

Ozaki, Noritsugu, Mitsuhide Noshiro, Takeshi Kawamoto, Ayumu Nakashima, Kiyomasa Honda, Urara Fukuzaki-Dohi, Sato Honma, et al. 2012. "Regulation of Basic Helix-Loop-Helix Transcription Factors Dec1 and Dec2 by RORα and Their Roles in Adipogenesis†." *Genes to Cells* 17 (2): 109–21. https://doi.org/10.1111/j.1365-2443.2011.01574.x.

Ozcan, Lale, Ayse Seda Ergin, Allen Lu, Jason Chung, Sumit Sarkar, Duyu Nie, Martin G. Myers, and Umut Ozcan. 2009. "Endoplasmic Reticulum Stress Plays a Central Role in Development of Leptin Resistance." *Cell Metabolism* 9 (1): 35–51. https://doi.org/10.1016/j.cmet.2008.12.004.

Ozcan, Umut, Qiong Cao, Erkan Yilmaz, Ann-Hwee Lee, Neal N Iwakoshi, Esra Ozdelen, Gürol Tuncman, Cem Görgün, Laurie H Glimcher, and Gökhan S Hotamisligil. 2004. "Endoplasmic Reticulum Stress Links Obesity, Insulin Action, and Type 2 Diabetes." *Science (New York, N.Y.)* 306 (5695): 457–61. https://doi.org/10.1126/science.1103160.

Palacios-Muñoz, Angelina, and John Ewer. 2018. "Calcium and CAMP Directly Modulate the Speed of the Drosophila Circadian Clock." *PLoS Genetics* 14 (6): 1–21. https://doi.org/10.1371/journal.pgen.1007433.

Pan, X, and M M Hussain. 2009. "Clock Is Important for Food and Circadian Regulation of Macronutrient Absorption in Mice." *Journal of Lipid Research* 50: 1800–1813.

Pan, X, Y Zhang, L Wang, and M M Hussain. 2010. "Diurnal Regulation of MTP and Plasma Triglyceride by CLOCK Is Mediated by SHP." *Cell Metabolism* 12: 174–86.

Panda, Satchidananda, Marina P Antoch, Brooke H Miller, Andrew I Su, Andrew B Schook, Marty Straume, Peter G Schultz, Steve a Kay, Joseph S Takahashi, and John B Hogenesch. 2002. "Coordinated Transcription of Key Pathways in the Mouse by the

Circadian Clock." *Cell* 109 (3): 307–20. http://www.ncbi.nlm.nih.gov/pubmed/12015981.

Pardini, L, B Kaeffer, A Trubuil, A Bourreille, and J P Galmiche. 2005. "Human Intestinal Circadian Clock: Expression of Clock Genes in Colonocytes Lining the Crypt." *Chronobiology International* 22: 951–61.

Parker, D, K Ferreri, T Nakajima, V J LaMorte, R Evans, S C Koerber, C Hoeger, and M R Montminy. 1996. "Phosphorylation of CREB at Ser-133 Induces Complex Formation with CREB-Binding Protein via a Direct Mechanism." *Molecular and Cellular Biology* 16 (2): 694–703. https://doi.org/10.1128/mcb.16.2.694.

Pasarica, Magdalena, Olga R. Sereda, Leanne M. Redman, Diana C. Albarado, David T. Hymel, Laura E. Roan, Jennifer C. Rood, David H. Burk, and Steven R. Smith. 2009. "Reduced Adipose Tissue Oxygenation in Human Obesity Evidence for Rarefaction, Macrophage Chemotaxis, and Inflammation without an Angiogenic Response." *Diabetes* 58 (3): 718–25. https://doi.org/10.2337/db08-1098.

Paschos, Georgios K, Salam Ibrahim, Wen-Liang Song, Takeshige Kunieda, Gregory Grant, Teresa M Reyes, Christopher A Bradfield, et al. 2012. "Obesity in Mice with Adipocyte-Specific Deletion of Clock Component Arntl." *Nature Medicine* 18 (12): 1768–77. https://doi.org/10.1038/nm.2979.

Paschos, P., and K. Paletas. 2009. "Non Alcoholic Fatty Liver Disease and Metabolic Syndrome." *Hippokratia* 13 (1): 9–19.

Patel, Manish Kumar, Sonika Pandey, David J. Burritt, and Lam Son Phan Tran. 2019. "Plant Responses to Low-Oxygen Stress: Interplay between ROS and NO Signaling Pathways." *Environmental and Experimental Botany* 161 (February): 134–42. https://doi.org/10.1016/j.envexpbot.2019.02.013.

Peek, Clara Bien, Daniel C. Levine, Jonathan Cedernaes, Akihiko Taguchi, Yumiko Kobayashi, Stacy J. Tsai, Nicolle A. Bonar, Maureen R. McNulty, Kathryn Moynihan Ramsey, and Joseph Bass. 2017. "Circadian Clock Interaction with HIF1α Mediates Oxygenic Metabolism and Anaerobic Glycolysis in Skeletal Muscle." *Cell Metabolism* 25 (1): 86–92. https://doi.org/10.1016/j.cmet.2016.09.010.

Perelis, Mark, Biliana Marcheva, Kathryn Moynihan Ramsey, Matthew J. Schipma, Alan L. Hutchison, Akihiko Taguchi, Clara Bien Peek, et al. 2015. "Pancreatic β Cell Enhancers Regulate Rhythmic Transcription of Genes Controlling Insulin Secretion." *Science* 350 (6261). https://doi.org/10.1126/science.aac4250.

Peret, J, M Chanez, and G Pascal. 1976. "Schedule of Protein Ingestion and Circadian Rhythm of Certain Hepatic Enzyme Activities Involved in Glucose Metabolism in the Rat." *Nutrition and Metabolism* 20 (2): 143–57. https://doi.org/10.1159/000175698.

Perry, Rachel J., Jon M. Resch, Amelia M. Douglass, Joseph C. Madara, Aviva Rabin-Court,

Hakan Kucukdereli, Chen Wu, Joongyu D. Song, Bradford B. Lowell, and Gerald I. Shulman. 2019. "Leptin's Hunger-Suppressing Effects Are Mediated by the Hypothalamic–Pituitary–Adrenocortical Axis in Rodents." *Proceedings of the National Academy of Sciences of the United States of America* 116 (27): 13670–79. https://doi.org/10.1073/pnas.1901795116.

Petersen, Kitt Falk, Douglas Befroy, Sylvie Dufour, James Dziura, Charlotte Ariyan, Douglas L Rothman, Loretta DiPietro, Gary W Cline, and Gerald I Shulman. 2003. "Mitochondrial Dysfunction in the Elderly: Possible Role in Insulin Resistance." *Science (New York, N.Y.)* 300 (5622): 1140–42. https://doi.org/10.1126/science.1082889.

Petersen, Kitt Falk, Sylvie Dufour, Douglas Befroy, Rina Garcia, and Gerald I Shulman. 2004. "Impaired Mitochondrial Activity in the Insulin-Resistant Offspring of Patients with Type 2 Diabetes." *The New England Journal of Medicine* 350 (7): 664–71. https://doi.org/10.1056/NEJMoa031314.

Petrenko, Volodymyr, Nikhil R. Gandasi, Daniel Sage, Anders Tengholm, Sebastian Barg, and Charna Dibner. 2020. "In Pancreatic Islets from Type 2 Diabetes Patients, the Dampened Circadian Oscillators Lead to Reduced Insulin and Glucagon Exocytosis." *Proceedings of the National Academy of Sciences of the United States of America* 117 (5): 2484–95. https://doi.org/10.1073/pnas.1916539117.

Pevet, Paul, and Etienne Challet. 2011. "Melatonin: Both Master Clock Output and Internal Time-Giver in the Circadian Clocks Network." *Journal of Physiology Paris* 105 (4–6): 170–82. https://doi.org/10.1016/j.jphysparis.2011.07.001.

Piggins, H D, M C Antle, and B Rusak. 1995. "Neuropeptides Phase Shift the Mammalian Circadian Pacemaker." *The Journal of Neuroscience* 15 (8): 5612 LP – 5622. https://doi.org/10.1523/JNEUROSCI.15-08-05612.1995.

Pilz, R B, M Suhasini, S Idriss, J L Meinkoth, and G R Boss. 1995. "Nitric Oxide and CGMP Analogs Activate Transcription from AP-1-Responsive Promoters in Mammalian Cells." *The FASEB Journal* 9 (7): 552–58. https://doi.org/10.1096/fasebj.9.7.7737465.

Pol, Anthony N van den. 1980. "The Hypothalamic Suprachiasmatic Nucleus of Rat: Intrinsic Anatomy." *Journal of Comparative Neurology* 191 (4): 661–702. https://doi.org/10.1002/cne.901910410.

Polotsky, Vsevolod Y., Jianguo Li, Naresh M. Punjabi, Arnon E. Rubin, Philip L. Smith, Alan R. Schwartz, and Christopher P. O'Donnell. 2003. "Intermittent Hypoxia Increases Insulin Resistance in Genetically Obese Mice." *Journal of Physiology* 552 (1): 253–64. https://doi.org/10.1113/jphysiol.2003.048173.

Prokopenko, Inga, Claudia Langenberg, Jose C. Florez, Richa Saxena, Nicole Soranzo, Gudmar Thorleifsson, Ruth J.F. Loos, et al. 2009. "Variants in MTNR1B Influence

Fasting Glucose Levels." *Nature Genetics* 41 (1): 77–81. https://doi.org/10.1038/ng.290.

Proper, Karin I, Daniëlla Van De Langenberg, Wendy Rodenburg, Roel C H Vermeulen, Allard J Van Der Beek, Harry Van Steeg, and Linda W M Van Kerkhof. 2016. "The Relationship Between Shift Work and Metabolic Risk Factors." *American Journal of Preventive Medicine* 50 (5): e147–57. https://doi.org/10.1016/j.amepre.2015.11.013.

Prosser, R. A., and M. U. Gillette. 1989. "The Mammalian Circadian Clock in the Suprachiasmatic Nuclei Is Reset in Vitro by CAMP." *Journal of Neuroscience* 9 (3): 1073–81. https://doi.org/10.1523/jneurosci.09-03-01073.1989.

Prosser, R a, a J McArthur, and M U Gillette. 1989. "CGMP Induces Phase Shifts of a Mammalian Circadian Pacemaker at Night, in Antiphase to CAMP Effects." *Proceedings of the National Academy of Sciences of the United States of America* 86 (17): 6812–15. https://doi.org/10.1073/pnas.86.17.6812.

Provencio, Ignacio, Howard M Cooper, and Russell G Foster. 1998. "Retinal Projections in Mice with Inherited Retinal Degeneration: Implications for Circadian Photoentrainment." *Journal of Comparative Neurology* 395 (4): 417–39. https://doi.org/10.1002/(SICI)1096-9861(19980615)395:4<417::AID-CNE1>3.0.CO;2-4.

Puri, Puneet, and Arun J. Sanyal. 2012. "Nonalcoholic Fatty Liver Disease: Definitions, Risk Factors, and Workup." *Clinical Liver Disease* 1 (4): 99–103. https://doi.org/10.1002/cld.81.

Qu, Aijuan, Matthew Taylor, Xiang Xue, Tsutomu Matsubara, Daniel Metzger, Pierre Chambon, Frank J. Gonzalez, and Yatrik M. Shah. 2011. "Hypoxia-Inducible Transcription Factor 2α Promotes Steatohepatitis through Augmenting Lipid Accumulation, Inflammation, and Fibrosis." *Hepatology* 54 (2): 472–83. https://doi.org/10.1002/hep.24400.

Radhakrishnan, I, G C Pérez-Alvarado, D Parker, H J Dyson, M R Montminy, and P E Wright. 1997. "Solution Structure of the KIX Domain of CBP Bound to the Transactivation Domain of CREB: A Model for Activator:Coactivator Interactions." *Cell* 91 (6): 741–52. https://doi.org/10.1016/s0092-8674(00)80463-8.

Radziuk, J, and S Pye. 2006. "Diurnal Rhythm in Endogenous Glucose Production Is a Major Contributor to Fasting Hyperglycaemia in Type 2 Diabetes. Suprachiasmatic Deficit or Limit Cycle Behaviour?" *Diabetologia* 49 (7): 1619–28. https://doi.org/10.1007/s00125-006-0273-9.

Ralph, M R, R G Foster, F C Davis, and M Menaker. 1990. "Transplanted Suprachiasmatic Nucleus Determines Circadian Period." *Science (New York, N.Y.)* 247 (4945): 975–78. https://doi.org/10.1126/science.2305266.

Ramanathan, Chidambaram, Nimish D. Kathale, Dong Liu, Choogon Lee, David A. Freeman, John B. Hogenesch, Ruifeng Cao, and Andrew C. Liu. 2018. "MTOR Signaling Regulates Central and Peripheral Circadian Clock Function." *PLoS Genetics* 14 (5): 1–21. https://doi.org/10.1371/journal.pgen.1007369.

Ramanathan, Chidambaram, Haiyan Xu, Sanjoy K. Khan, Yang Shen, Paula J. Gitis, David K. Welsh, John B. Hogenesch, and Andrew C. Liu. 2014. "Cell Type-Specific Functions of Period Genes Revealed by Novel Adipocyte and Hepatocyte Circadian Clock Models." *PLoS Genetics* 10 (4). https://doi.org/10.1371/journal.pgen.1004244.

Reaven, G M. 1988. "Banting Lecture 1988. Role of Insulin Resistance in Human Disease." *Diabetes* 37 (12): 1595–1607. https://doi.org/10.2337/diab.37.12.1595.

Reddy, Akhilesh B, Natasha a Karp, Elizabeth S Maywood, Elizabeth a Sage, Michael Deery, John S O'Neill, Gabriel K Y Wong, et al. 2006. "Circadian Orchestration of the Hepatic Proteome." *Current Biology : CB* 16 (11): 1107–15. https://doi.org/10.1016/j.cub.2006.04.026.

Reed, H E, A Meyer-Spasche, D J Cutler, C W Coen, and H D Piggins. 2001. "Vasoactive Intestinal Polypeptide (VIP) Phase-Shifts the Rat Suprachiasmatic Nucleus Clock in Vitro." *The European Journal of Neuroscience* 13 (4): 839—843. https://doi.org/10.1046/j.0953-816x.2000.01437.x.

Regazzetti, Claire, Pascal Peraldi, Thierry Grémeaux, Rosanna Najem-Lendom, Issam Ben-Sahra, Mireille Cormont, Frédéric Bost, Yannick Le Marchand-Brustel, Jean François Tanti, and Sophie Giorgetti-Peraldi. 2009. "Hypoxia Decreases Insulin Signaling Pathways in Adipocytes." *Diabetes* 58 (1): 95–103. https://doi.org/10.2337/db08-0457.

Reinke, Hans, Camille Saini, Fabienne Fleury-Olela, Charna Dibner, Ivor J Benjamin, and Ueli Schibler. 2008. "Differential Display of DNA-Binding Proteins Reveals Heat-Shock Factor 1 as a Circadian Transcription Factor." *Genes & Development* 22 (3): 331–45. https://doi.org/10.1101/gad.453808.

Rhoads, David B., David H. Rosenbaum, Hilal Unsal, Kurt J. Isselbacher, and Lynne L. Levitsky. 1998. "Circadian Periodicity of Intestinal Na+/Glucose Cotransporter 1 MRNA Levels Is Transcriptionally Regulated." *Journal of Biological Chemistry* 273 (16): 9510–16. https://doi.org/10.1074/jbc.273.16.9510.

Ribon, Vered, Roman Herrera, Brian K. Kay, and Alan R. Saltiel. 1998. "A Role for CAP, a Novel, Multifunctional Src Homology 3 Domain- Containing Protein in Formation of Actin Stress Fibers and Focal Adhesions." *Journal of Biological Chemistry* 273 (7): 4073–80. https://doi.org/10.1074/jbc.273.7.4073.

Ribon, Vered, and Alan R Saltiel. 1997. "Insulin Stimulates Tyrosine Phosphorylation of the Proto-Oncogene Product of c-Cbl in 3T3-L1 Adipocytes." *Biochemical Journal* 324 (3): 839–46. https://doi.org/10.1042/bj3240839.

Rice, B, I Janssen, R Hudson, and R Ross. 1999. “Effects of Aerobic or Resistance Exercise and/or Diet on Glucose Tolerance and Plasma Insulin Levels in Obese Men.” *Diabetes Care* 22 (5): 684–91. https://doi.org/10.2337/diacare.22.5.684.

Ripperger, Jürgen A, Corinne Jud, and Urs Albrecht. 2011. “The Daily Rhythm of Mice.” *FEBS Letters* 585 (10): 1384–92. https://doi.org/10.1016/j.febslet.2011.02.027.

Rizzo, Norma O., Ezekiel Maloney, Matilda Pham, Ian Luttrell, Hunter Wessells, Sanshiro Tateya, Guenter Daum, Priya Handa, Michael W. Schwartz, and Francis Kim. 2010. “Reduced NO-CGMP Signaling Contributes to Vascular Inflammation and Insulin Resistance Induced by High-Fat Feeding.” *Arteriosclerosis, Thrombosis, and Vascular Biology* 30 (4): 758–65. https://doi.org/10.1161/ATVBAHA.109.199893.

Rockwood, K, B L Beattie, M R Eastwood, H Feldman, E Mohr, W Pryse-Phillips, and S Gauthier. 1997. “A Randomized, Controlled Trial of Linopirdine in the Treatment of Alzheimer’s Disease.” *The Canadian Journal of Neurological Sciences Le Journal Canadien Des Sciences Neurologiques* 24 (2): 140–45. https://doi.org/10.1017/S031716710002148X.

Roden, Michael, Harald Stingl, Visvanathan Chandramouli, William C. Schumann, Astrid Hofer, Bernard R. Landau, Peter Nowotny, Werner Waldhäusl, and Gerald I. Shulman. 2000. “Effects of Free Fatty Acid Elevation on Postabsorptive Endogenous Glucose Production and Gluconeogenesis in Humans.” *Diabetes* 49 (5): 701–7. https://doi.org/10.2337/diabetes.49.5.701.

Rodgers, R. John, Matthias H. Tschöp, and John P.H. Wilding. 2012. “Anti-Obesity Drugs: Past, Present and Future.” *DMM Disease Models and Mechanisms* 5 (5): 621–26. https://doi.org/10.1242/dmm.009621.

Rogers, J, and H Munro. 1987. “Translation of Ferritin Light and Heavy Subunit MRNAs Is Regulated by Intracellular Chelatable Iron Levels in Rat Hepatoma Cells.” *Proceedings of the National Academy of Sciences of the United States of America* 84 (8): 2277–81. https://doi.org/10.1073/pnas.84.8.2277.

Romanatto, Talita, Maristela Cesquini, Maria E Amaral, Érika A Roman, Juliana C Moraes, Márcio A Torsoni, Ariovaldo P Cruz-Neto, and Lício A Velloso. 2007. “TNF-α Acts in the Hypothalamus Inhibiting Food Intake and Increasing the Respiratory Quotient—Effects on Leptin and Insulin Signaling Pathways.” *Peptides* 28 (5): 1050–58. https://doi.org/https://doi.org/10.1016/j.peptides.2007.03.006.

Ron, David, and Peter Walter. 2007. “Signal Integration in the Endoplasmic Reticulum Unfolded Protein Response.” *Nature Reviews Molecular Cell Biology* 8 (7): 519–29. https://doi.org/10.1038/nrm2199.

Rothwell, N. J., and M. J. Stock. 1988. “The Cafetaria Diet as a Tool for Studies of Thermogenesis.” *Journal of Nutrition* 118 (8): 925–28. https://doi.org/10.1093/jn/118.8.925.

Roux, Philippe P., Bryan A. Ballif, Rana Anjum, Steven P. Gygi, and John Blenis. 2004. "Tumor-Promoting Phorbol Esters and Activated Ras Inactivate the Tuberous Sclerosis Tumor Suppressor Complex via P90 Ribosomal S6 Kinase." *Proceedings of the National Academy of Sciences of the United States of America* 101 (37): 13489–94. https://doi.org/10.1073/pnas.0405659101.

Ruderman, N, D Chisholm, X Pi-Sunyer, and S Schneider. 1998. "The Metabolically Obese, Normal-Weight Individual Revisited." *Diabetes* 47 (5): 699–713. https://doi.org/10.2337/diabetes.47.5.699.

Rudic, R Daniel, Peter Mcnamara, Anne-maria Curtis, Raymond C Boston, Satchidananda Panda, John B Hogenesch, and Garret A Fitzgerald. 2004. "BMAL1 and CLOCK , Two Essential Components of the Circadian Clock , Are Involved in Glucose Homeostasis." *PLOS Biology* 2 (11). https://doi.org/10.1371/journal.pbio.0020377.

Ruiter, Marieke, Susanne E La Fleur, Caroline van Heijningen, Jan van der Vliet, Andries Kalsbeek, and Ruud M Buijs. 2003. "The Daily Rhythm in Plasma Glucagon Concentrations in the Rat Is Modulated by the Biological Clock and by Feeding Behavior." *Diabetes* 52 (7): 1709–15. https://doi.org/10.2337/diabetes.52.7.1709.

Rutter, Jared, Martin Reick, Leeju C Wu, and Steven L McKnight. 2001. "Regulation of Clock and NPAS2 DNA Binding by the Redox State of NAD Cofactors." *Science* 293 (5529): 510 LP – 514. http://science.sciencemag.org/content/293/5529/510.abstract.

Ryan, Silke, Cormac T Taylor, and Walter T McNicholas. 2005. "Selective Activation of Inflammatory Pathways by Intermittent Hypoxia in Obstructive Sleep Apnea Syndrome." *Circulation* 112 (17): 2660–67. https://doi.org/10.1161/CIRCULATIONAHA.105.556746.

———. 2006. "Predictors of Elevated Nuclear Factor-KappaB-Dependent Genes in Obstructive Sleep Apnea Syndrome." *American Journal of Respiratory and Critical Care Medicine* 174 (7): 824–30. https://doi.org/10.1164/rccm.200601-066OC.

Saito, Takeshi, Daigo Abe, and Keizo Sekiya. 2007. "Nobiletin Enhances Differentiation and Lipolysis of 3T3-L1 Adipocytes." *Biochemical and Biophysical Research Communications* 357 (2): 371–76. https://doi.org/10.1016/j.bbrc.2007.03.169.

Saletu, B., Darragh, A., Salmon, P. & Coen, R. 1989. "Topographic Pharmaco-EEG Brain Mapping Following Administration of a New Acetyl Choline Releasing Drug: A New Methodological Approach." *Lancet.*

Saletu, B, A Darragh, P Salmon, and R Coen. 1989. "EEG Brain Mapping in Evaluating the Time-Course of the Central Action of DUP 996-a New Acetylcholine Releasing Drug." *Br. J. Clin. Pharmac* 28: 1–16.

Salminen, Aaro V., Lillian Garrett, Barbara Schormair, Jan Rozman, Florian Giesert, Kristina M. Niedermeier, Lore Becker, et al. 2017. "Meis1: Effects on Motor

Phenotypes and the Sensorimotor System in Mice." *DMM Disease Models and Mechanisms* 10 (8): 981–91. https://doi.org/10.1242/dmm.030080.

Saltiel, Alan R, and C. Ronald Kahn. 2001. "Insulin Signalling and the Regulation of Glucose and Lipid Metabolism." *Nature* 414 (December): 1–8. http://www.medgen.med.umich.edu/labs/saltiel/.

Samuel, Varman T, Zhen-Xiang Liu, Xianqin Qu, Benjamin D Elder, Stefan Bilz, Douglas Befroy, Anthony J Romanelli, and Gerald I Shulman. 2004. "Mechanism of Hepatic Insulin Resistance in Non-Alcoholic Fatty Liver Disease." *The Journal of Biological Chemistry* 279 (31): 32345–53. https://doi.org/10.1074/jbc.M313478200.

Sang, Jianrong, Yongchang Chen, Lu Jiang, Yan Tao, Yan Wu, Ying Wang, Yueying Li, Ting Lan, and Genbao Shao. 2012. "Type II CGMP-Dependent Protein Kinase Inhibits ERK/JNK-Mediated Activation of Transcription Factors in Gastric Cancer Cells." *Molecular Medicine Reports* 6 (5): 1190–94. https://doi.org/10.3892/mmr.2012.1050.

Sanyal, Arun J. 2005. "Mechanisms of Disease: Pathogenesis of Nonalcoholic Fatty Liver Disease." *Nature Clinical Practice. Gastroenterology & Hepatology* 2 (1): 46–53. https://doi.org/10.1038/ncpgasthep0084.

Sarayloo, Faezeh, Patrick A Dion, and Guy A Rouleau. 2019. "MEIS1 and Restless Legs Syndrome: A Comprehensive Review." *Frontiers in Neurology* 10 (August): 935. https://doi.org/10.3389/fneur.2019.00935.

Sato, R., S. I. Koumi, I. Hisatome, H. Takai, Y. Aida, M. Oyaizu, S. Karasaki, H. Mashiba, and R. Katori. 1995. "A New Class III Antiarrhythmic Drug, MS-551, Blocks the Inward Rectifier Potassium Channel in Isolated Guinea Pig Ventricular Myocytes." *Journal of Pharmacology and Experimental Therapeutics* 274 (1): 469–74.

Sato, Trey K, Satchidananda Panda, Loren J Miraglia, Teresa M Reyes, Radu D Rudic, Peter McNamara, Kinnery A Naik, Garret A FitzGerald, Steve A Kay, and John B Hogenesch. 2004. "A Functional Genomics Strategy Reveals Rora as a Component of the Mammalian Circadian Clock." *Neuron* 43 (4): 527–37. https://doi.org/10.1016/j.neuron.2004.07.018.

Sato, Trey K, Rikuhiro G Yamada, Hideki Ukai, Julie E Baggs, Loren J Miraglia, Tetsuya J Kobayashi, David K Welsh, Steve A Kay, Hiroki R Ueda, and John B Hogenesch. 2006. "Feedback Repression Is Required for Mammalian Circadian Clock Function." *Nature Genetics* 38 (3): 312–19. https://doi.org/10.1038/ng1745.

Sauzeau, Vincent, Malvyne Rolli-Derkinderen, Céline Marionneau, Gervaise Loirand, and Pierre Pacaud. 2003. "RhoA Expression Is Controlled by Nitric Oxide through CGMP-Dependent Protein Kinase Activation." *Journal of Biological Chemistry* 278 (11): 9472–80. https://doi.org/10.1074/jbc.M212776200.

Scheer, Frank A J L, Michael F Hilton, Christos S Mantzoros, and Steven A Shea. 2009.

"Adverse Metabolic and Cardiovascular Consequences of Circadian Misalignment." *Proceedings of the National Academy of Sciences* 106 (11): 4453–58. https://doi.org/10.1073/pnas.0808180106.

Schlierf, G, and E Dorow. 1973. "Diurnal Patterns of Triglycerides, Free Fatty Acids, Blood Sugar, and Insulin during Carbohydrate-Induction in Man and Their Modification by Nocturnal Suppression of Lipolysis." *Journal of Clinical Investigation* 52: 732–40.

Schnee, Michael E., and Barry S. Brown. 1998. "Selectivity of Linopirdine (DuP 996), a Neurotransmitter Release Enhancer, in Blocking Voltage-Dependent and Calcium-Activated Potassium Currents in Hippocampal Neurons." *Journal of Pharmacology and Experimental Therapeutics* 286 (2): 709–17.

Schoenhard, John A, Layton H Smith, Corrie A Painter, Mesut Eren, Carl H Johnson, and Douglas E Vaughan. 2003. "Regulation of the PAI-1 Promoter by Circadian Clock Components: Differential Activation by BMAL1 and BMAL2." *Journal of Molecular and Cellular Cardiology* 35 (5): 473–81. https://doi.org/10.1016/s0022-2828(03)00051-8.

Schroeder, Analyne M, and Christopher S Colwell. 2013. "How to Fix a Broken Clock." *Trends in Pharmacological Sciences* 34 (11): 605–19. https://doi.org/https://doi.org/10.1016/j.tips.2013.09.002.

Schubert, Rudolf, and Mark T Nelson. 2001. "Protein Kinases: Tuners of the BK-Ca Channel in Smooth Muscle." *Trends in Pharmacological Sciences* 22 (10): 505–12. https://doi.org/10.1016/S0165-6147(00)01775-2.

Schweiger, Martina, Thomas O Eichmann, Ulrike Taschler, Robert Zimmermann, Rudolf Zechner, and Achim Lass. 2014. "Measurement of Lipolysis." *Methods Enzymol* 538 (1): 171–93. https://doi.org/10.1016/B978-0-12-800280-3.00010-4.Measurement.

Scott, E M, A M Carter, and P J Grant. 2007. "Association between Polymorphisms in the Clock Gene, Obesity and the Metabolic Syndrome in Man." *Int J Obes* 32 (4): 658–62. http://dx.doi.org/10.1038/sj.ijo.0803778.

Semenza, Gregg L. 2004. "Hydroxylation of HIF-1: Oxygen Sensing at the Molecular Level." *Physiology* 19 (4): 176–82. https://doi.org/10.1152/physiol.00001.2004.

Shah, Pankaj, Adrian Vella, Ananda Basu, Rita Basu, Aron Adkins, W. Frederick Schwenk, C. Michael Johnson, K. Sreekumaran Nair, Michael D. Jensen, and Robert A. Rizza. 2002. "Effects of Free Fatty Acids and Glycerol on Splanchnic Glucose Metabolism and Insulin Extraction in Nondiabetic Humans." *Diabetes* 51 (2): 301–10. https://doi.org/10.2337/diabetes.51.2.301.

Sharabi, Kfir, Clint D.J. Tavares, Amy K. Rines, and Pere Puigserver. 2015. "Molecular Pathophysiology of Hepatic Glucose Production." *Molecular Aspects of Medicine* 46: 21–33. https://doi.org/10.1016/j.mam.2015.09.003.

Shaywitz, A J, and M E Greenberg. 1999. “CREB: A Stimulus-Induced Transcription Factor Activated by a Diverse Array of Extracellular Signals.” *Annual Review of Biochemistry* 68: 821–61. https://doi.org/10.1146/annurev.biochem.68.1.821.

Shearman, L P, X Jin, C Lee, S M Reppert, and D R Weaver. 2000. “Targeted Disruption of the MPer3 Gene: Subtle Effects on Circadian Clock Function.” *Molecular and Cellular Biology* 20 (17): 6269–75. https://doi.org/10.1128/mcb.20.17.6269-6275.2000.

Shearman, L P, M J Zylka, S M Reppert, and D R Weaver. 1999. “Expression of Basic Helix-Loop-Helix/Pas Genes in the Mouse Suprachiasmatic Nucleus.” *Neuroscience* 89 (2): 387–97. https://doi.org/https://doi.org/10.1016/S0306-4522(98)00325-X.

Sheludiakova, Anastasia, Kieron Rooney, and Robert A. Boakes. 2012. “Metabolic and Behavioural Effects of Sucrose and Fructose/Glucose Drinks in the Rat.” *European Journal of Nutrition* 51 (4): 445–54. https://doi.org/10.1007/s00394-011-0228-x.

Shepherd, P R, B T Navé, and K Siddle. 1995. “Insulin Stimulation of Glycogen Synthesis and Glycogen Synthase Activity Is Blocked by Wortmannin and Rapamycin in 3T3-L1 Adipocytes: Evidence for the Involvement of Phosphoinositide 3-Kinase and P70 Ribosomal Protein-S6 Kinase.” *Biochemical Journal* 305 (1): 25–28. https://doi.org/10.1042/bj3050025.

Shibata, Shigenobu, and Robert Y Moore. 1993. “Tetrodotoxin Does Not Affect Circadian Rhythms in Neuronal Activity and Metabolism in Rodent Suprachiasmatic Nucleus in Vitro.” *Brain Research* 606 (2): 259–66. https://doi.org/https://doi.org/10.1016/0006-8993(93)90993-W.

Shibata, Shigenobu, Yutaka Oomura, Hitoshi Kita, and Kiichi Hattori. 1982. “Circadian Rhythmic Changes of Neuronal Activity in the Suprachiasmatic Nucleus of the Rat Hypothalamic Slice.” *Brain Research* 247 (1): 154–58. https://doi.org/https://doi.org/10.1016/0006-8993(82)91041-1.

Shih, Cheng Ping, Jen Tin Lee, Hang Kang Chen, Yi Chun Lin, Hsin Chien Chen, Yuan Yung Lin, Chao Yin Kuo, Yu Ting Chen, and Chih Hung Wang. 2018. “Comparison of Changes in Mitochondrial Bioenergetics between Keratinocytes in Human External Auditory Canal Skin and Cholesteatomas from Normoxia to Hypoxia.” *Scientific Reports* 8 (1): 1–11. https://doi.org/10.1038/s41598-017-18536-y.

Shimba, Shigeki, Norimasa Ishii, Yuki Ohta, Toshiharu Ohno, Yuichi Watabe, Mitsuaki Hayashi, Taira Wada, Toshinori Aoyagi, and Masakatsu Tezuka. 2005. “Brain and Muscle Arnt-Like Protein-1 (BMAL1), a Component of the Molecular Clock, Regulates Adipogenesis.” *Proceedings of the National Academy of Sciences* 102 (34): 12071–76. http://www.jstor.org/stable/3376400?seq=1#page_scan_tab_contents.

Shimba, Shigeki, Taira Wada, Shuntaro Hara, and Masakatsu Tezuka. 2004. “EPAS1 Promotes Adipose Differentiation in 3T3-L1 Cells.” *Journal of Biological Chemistry* 279 (39): 40946–53. https://doi.org/10.1074/jbc.M400840200.

Shin, Mi Kyung, Luciano F. Drager, Qiaoling Yao, Shannon Bevans-Fonti, Doo Young Yoo, Jonathan C. Jun, Susan Aja, Sanjay Bhanot, and Vsevolod Y. Polotsky. 2012. "Metabolic Consequences of High-Fat Diet Are Attenuated by Suppression of HIF-1α." *PLoS ONE* 7 (10): 1–10. https://doi.org/10.1371/journal.pone.0046562.

Shostak, A, J Meyer-Kovac, and H Oster. 2013. "Circadian Regulation of Lipid Mobilization in White Adipose Tissues." *Diabetes* 62: 2195–2203.

Shuhaibar, Leia C, Jeremy R Egbert, Aaron B Edmund, Tracy F Uliasz, Deborah M Dickey, Siu-Pok Yee, Lincoln R Potter, and Laurinda A Jaffe. 2016. "Dephosphorylation of Juxtamembrane Serines and Threonines of the NPR2 Guanylyl Cyclase Is Required for Rapid Resumption of Oocyte Meiosis in Response to Luteinizing Hormone." *Developmental Biology* 409 (1): 194–201. https://doi.org/https://doi.org/10.1016/j.ydbio.2015.10.025.

Shuhaibar, Leia C, Jerid W Robinson, Giulia Vigone, Ninna P Shuhaibar, Jeremy R Egbert, Valentina Baena, Tracy F Uliasz, et al. 2017. "Dephosphorylation of the NPR2 Guanylyl Cyclase Contributes to Inhibition of Bone Growth by Fibroblast Growth Factor." *ELife* 6 (December): e31343. https://doi.org/10.7554/eLife.31343.

Shweiki, Dorit, Ahuva Itin, Dov Soffer, and Eli Keshet. 1992. "Vascular Endothelial Growth Factor Induced by Hypoxia May Mediate Hypoxia-Initiated Angiogenesis." *Nature* 359 (6398): 843–45. https://doi.org/10.1038/359843a0.

Siepka, Sandra M., and Joseph S. Takahashi. 2005. "Methods to Record Circadian Rhythm Wheel Running Activity in Mice." *Methods in Enzymology* 393 (05): 230–39. https://doi.org/10.1016/S0076-6879(05)93008-5.

Silberbach, Michael, and Charles T Roberts. 2001. "Natriuretic Peptide Signalling: Molecular and Cellular Pathways to Growth Regulation." *Cellular Signalling* 13 (4): 221–31. https://doi.org/https://doi.org/10.1016/S0898-6568(01)00139-5.

Sinturel, Flore, Anne-Marie Makhlouf, Patrick Meyer, Christel Tran, Zoltan Pataky, Alain Golay, Guillaume Rey, et al. 2019. "Cellular Circadian Period Length Inversely Correlates with HbA(1c) Levels in Individuals with Type 2 Diabetes." *Diabetologia* 62 (8): 1453–62. https://doi.org/10.1007/s00125-019-4907-0.

Sjöström, Lars, Kristina Narbro, C David Sjöström, Kristjan Karason, Bo Larsson, Hans Wedel, Ted Lystig, et al. 2007. "Effects of Bariatric Surgery on Mortality in Swedish Obese Subjects." *New England Journal of Medicine* 357 (8): 741–52. https://doi.org/10.1056/NEJMoa066254.

Sladek, M, M Rybova, Z Jindrakova, Z Zemanova, L Polidarova, L Mrnka, J O'Neill, J Pacha, and A Sumova. 2007. "Insight into the Circadian Clock within Rat Colonic Epithelial Cells." *Gastroenterology* 133: 1240–49.

Smith, Orla. 1998. "Nobel Prize for NO Research." *Nature Medicine* 4 (11): 1215. https://doi.org/10.1038/3182.

Smith, Sidney C., Emelia J. Benjamin, Robert O. Bonow, Lynne T. Braun, Mark A. Creager, Barry A. Franklin, Raymond J. Gibbons, et al. 2011. "AHA/ACCF Secondary Prevention and Risk Reduction Therapy for Patients with Coronary and Other Atherosclerotic Vascular Disease: 2011 Update: A Guideline from the American Heart Association and American College of Cardiology Foundation." *Circulation* 124 (22): 2458–73. https://doi.org/10.1161/CIR.0b013e318235eb4d.

Solt, Laura A., Yongjun Wang, Subhashis Banerjee, Travis Hughes, Douglas J. Kojetin, Thomas Lundasen, Youseung Shin, et al. 2012. "Regulation of Circadian Behaviour and Metabolism by Synthetic REV-ERB Agonists." *Nature* 485 (7396): 62–68. https://doi.org/10.1038/nature11030.

Sookoian, Silvia, Carolina Gemma, Tomas Fernández Gianotti, Adriana Burgueño, Gustavo Castaño, and Carlos Jose Pirola. 2008. "Genetic Variants of Clock Transcription Factor Are Associated with Individual Susceptibility to Obesity." *American Journal of Clinical Nutrition* 87 (6): 1606–15. https://doi.org/87/6/1606 [pii].

Spalding, Kirsty L., Erik Arner, Pål O. Westermark, Samuel Bernard, Bruce A. Buchholz, Olaf Bergmann, Lennart Blomqvist, et al. 2008. "Dynamics of Fat Cell Turnover in Humans." *Nature* 453 (7196): 783–87. https://doi.org/10.1038/nature06902.

Spiegel, Karine, Rachel Leproult, and Eve Van Cauter. 1999. "Early Report Impact of Sleep Debt on Metabolic and Endocrine Function" 354: 1435–39.

Srivastava, Gitanjali, and Caroline Apovian. 2018a. "Future Pharmacotherapy for Obesity: New Anti-Obesity Drugs on the Horizon." *Current Obesity Reports* 7 (2): 147–61. https://doi.org/10.1007/s13679-018-0300-4.

Srivastava, Gitanjali, and Caroline M Apovian. 2018b. "Current Pharmacotherapy for Obesity." *Nature Reviews. Endocrinology* 14 (1): 12–24. https://doi.org/10.1038/nrendo.2017.122.

Staehr, Peter, Ole Hother-Nielsen, Bernard R. Landau, Visvanathan Chandramouli, Jens Juul Holst, and Henning Beck-Nielsen. 2003. "Effects of Free Fatty Acids per Se on Glucose Production, Gluconeogenesis, and Glycogenolysis." *Diabetes* 52 (2): 260–67. https://doi.org/10.2337/diabetes.52.2.260.

Stavinoha, M A, J W Rayspellicy, M L Hart-Sailors, H J Mersmann, M S Bray, and M E Young. 2004. "Diurnal Variations in the Responsiveness of Cardiac and Skeletal Muscle to Fatty Acids." *American Journal of Physiology. Endocrinology and Metabolism* 287: E878–87.

Stephan, F K, and I Zucker. 1972. "Circadian Rhythms in Drinking Behavior and Locomotor Activity of Rats Are Eliminated by Hypothalamic Lesions." *Proceedings of the National Academy of Sciences of the United States of America* 69 (6): 1583–86. https://doi.org/10.1073/pnas.69.6.1583.

Stokkan, Karl-arne, Shin Yamazaki, and Hajime Tei. 1999. “Entrainment of the Circadian Clock in the Liver by Feeding.”

Storch, Kai-Florian, Ovidiu Lipan, Igor Leykin, N Viswanathan, Fred C Davis, Wing H Wong, and Charles J Weitz. 2002. “Extensive and Divergent Circadian Gene Expression in Liver and Heart.” *Nature* 417 (6884): 78–83. http://dx.doi.org/10.1038/nature744.

Stratmann, Markus, David Michael Suter, Nacho Molina, Felix Naef, and Ueli Schibler. 2012. “Circadian Dbp Transcription Relies on Highly Dynamic BMAL1-CLOCK Interaction with E Boxes and Requires the Proteasome.” *Molecular Cell* 48 (2): 277–87. https://doi.org/10.1016/j.molcel.2012.08.012.

Stubblefield, Jeremy J., Peng Gao, Gokhul Kilaru, Bilal Mukadam, Jeremy Terrien, and Carla B. Green. 2018. “Temporal Control of Metabolic Amplitude by Nocturnin.” *Cell Reports* 22 (5): 1225–35. https://doi.org/10.1016/j.celrep.2018.01.011.

Suhasini, Modem, Hien Li, Suzanne M. Lohmann, Gerry R. Boss, and Renate B. Pilz. 1998. “Cyclic-GMP-Dependent Protein Kinase Inhibits the Ras/Mitogen-Activated Protein Kinase Pathway.” *Molecular and Cellular Biology* 18 (12): 6983–94. https://doi.org/10.1128/mcb.18.12.6983.

Sun, K., N. Halberg, M. Khan, U. J. Magalang, and P. E. Scherer. 2013. “Selective Inhibition of Hypoxia-Inducible Factor 1 Ameliorates Adipose Tissue Dysfunction.” *Molecular and Cellular Biology* 33 (5): 904–17. https://doi.org/10.1128/mcb.00951-12.

Surwit, R S, M N Feinglos, J Rodin, A Sutherland, A E Petro, E C Opara, C M Kuhn, and M Rebuffé-Scrive. 1995. “Differential Effects of Fat and Sucrose on the Development of Obesity and Diabetes in C57BL/6J and A/J Mice.” *Metabolism: Clinical and Experimental* 44 (5): 645–51. https://doi.org/10.1016/0026-0495(95)90123-x.

Takahashi, J S, P J DeCoursey, L Bauman, and M Menaker. 1984. “Spectral Sensitivity of a Novel Photoreceptive System Mediating Entrainment of Mammalian Circadian Rhythms.” *Nature* 308 (5955): 186–88. https://doi.org/10.1038/308186a0.

Takahashi, Joseph S. 2017. “Transcriptional Architecture of the Mammalian Circadian Clock.” *Nature Reviews Genetics* 18 (3): 164–79. https://doi.org/10.1038/nrg.2016.150.

Tanaka, Masaki, Yukio Ichitani, Hitoshi Okamura, Yoshifumi Tanaka, and Yasuhiko Ibata. 1993. “The Direct Retinal Projection to VIP Neuronal Elements in the Rat SCN.” *Brain Research Bulletin* 31 (6): 637–40. https://doi.org/https://doi.org/10.1016/0361-9230(93)90134-W.

Tanaka, S, C Horimai, and F Katsukawa. 2003. “Ethnic Differences in Abdominal Visceral Fat Accumulation between Japanese, African-Americans, and Caucasians: A Meta-Analysis.” *Acta Diabetologica* 40 Suppl 1 (October): S302-4. https://doi.org/10.1007/s00592-003-0093-z.

Taniguchi, Cullen M., Brice Emanuelli, and C. Ronald Kahn. 2006. “Critical Nodes in Signalling Pathways: Insights into Insulin Action.” *Nature Reviews Molecular Cell Biology* 7 (2): 85–96. https://doi.org/10.1038/nrm1837.

Tasaka, Yoshimasa, Sachiko Inoue, Koji Maruno, and Yukimasa Hirata. 1980. “Twenty-Four-Hour Variations of Plasma Pancreatic Polypeptide, Insulin and Glucagon in Normal Human Subjects.” *Endocrinologia Japonica* 27 (4): 495–98. https://doi.org/10.1507/endocrj1954.27.495.

Tatulian, L., P. Delmas, F. C. Abogadie, and D. A. Brown. 2001. “Activation of Expressed KCNQ Potassium Currents and Native Neuronal M-Type Potassium Currents by the Anti-Convulsant Drug Retigabine.” *Journal of Neuroscience* 21 (15): 5535–45. https://doi.org/10.1523/jneurosci.21-15-05535.2001.

Thaler, Joshua P, Chun-Xia Yi, Ellen A Schur, Stephan J Guyenet, Bang H Hwang, Marcelo O Dietrich, Xiaolin Zhao, et al. 2012. “Obesity Is Associated with Hypothalamic Injury in Rodents and Humans.” *The Journal of Clinical Investigation* 122 (1): 153–62. https://doi.org/10.1172/JCI59660.

Thiebaud, D, E Jacot, R A DeFronzo, E Maeder, E Jequier, and J P Felber. 1982. “The Effect of Graded Doses of Insulin on Total Glucose Uptake, Glucose Oxidation, and Glucose Storage in Man.” *Diabetes* 31 (11): 957–63. https://doi.org/10.2337/diacare.31.11.957.

Thiriet, Nathalie, Laurent Esteve, Dominique Aunis, and Jean Zwiller. 1997. “Immediate Early Gene Induction by Natriuretic Peptides in PC12 Phaeochromocytoma and C6 Glioma Cells.” *NeuroReport* 8 (2). https://journals.lww.com/neuroreport/Fulltext/1997/01200/Immediate_early_gene_induction_by_natriuretic.3.aspx.

Tilg, Herbert, and Alexander R. Moschen. 2006. “Adipocytokines: Mediators Linking Adipose Tissue, Inflammation and Immunity.” *Nature Reviews Immunology* 6 (10): 772–83. https://doi.org/10.1038/nri1937.

Tischkau, S. A., E. A. Gallman, G. F. Buchanan, and M. U. Gillette. 2000. “Differential CAMP Gating of Glutamatergic Signaling Regulates Long-Term State Changes in the Suprachiasmatic Circadian Clock.” *Journal of Neuroscience* 20 (20): 7830–37. https://doi.org/10.1523/jneurosci.20-20-07830.2000.

Tischkau, Shelley A., Jennifer W. Mitchell, Laura A. Pace, Jessica W. Barnes, Jeffrey A. Barnes, and Martha U. Gillette. 2004. “Protein Kinase G Type II Is Required for Night-to-Day Progression of the Mammalian Circadian Clock.” *Neuron* 43 (4): 539–49. https://doi.org/10.1016/j.neuron.2004.07.027.

Tischkau, Shelley A, E Todd Weber, Sabra M Abbott, Jennifer W Mitchell, and Martha U Gillette. 2003. “Circadian Clock-Controlled Regulation of CGMP-Protein Kinase G in the Nocturnal Domain.” *The Journal of Neuroscience* 23 (20): 7543 LP – 7550.

https://doi.org/10.1523/JNEUROSCI.23-20-07543.2003.

Tomoeda, Miki, Michiko Yuki, Chiaki Kubo, Hidenori Yoshizawa, Masanori Kitamura, Shigenori Nagata, Yasuko Nishizawa, and Yasuhiko Tomita. 2011. "Role of Meis1 in Mitochondrial Gene Transcription of Pancreatic Cancer Cells." *Biochemical and Biophysical Research Communications* 410 (4): 798–802. https://doi.org/https://doi.org/10.1016/j.bbrc.2011.06.066.

Torti, Frank M., and Suzy V. Torti. 2002. "Regulation of Ferritin Genes and Protein." *Blood* 99 (10): 3505–16. https://doi.org/10.1182/blood.V99.10.3505.

Travnickova-Bendova, Zdenka, Nicolas Cermakian, Steven M Reppert, and Paolo Sassone-Corsi. 2002. "Bimodal Regulation of MPeriod Promoters by CREB-Dependent Signaling and CLOCK/BMAL1 Activity." *Proceedings of the National Academy of Sciences* 99 (11): 7728–33. https://doi.org/10.1073/pnas.102075599.

Trayhurn, P, and J H Beattie. 2001. "Physiological Role of Adipose Tissue: White Adipose Tissue as an Endocrine and Secretory Organ." *The Proceedings of the Nutrition Society* 60 (3): 329–39. https://doi.org/10.1079/pns200194.

Tsai, J Y, P C Kienesberger, T Pulinilkunnil, M H Sailors, D J Durgan, C Villegas-Montoya, A Jahoor, R Gonzalez, M E Garvey, and B Boland. 2010. "Direct Regulation of Myocardial Triglyceride Metabolism by the Cardiomyocyte Circadian Clock." *Journal of Biological Chemistry* 285: 2918–29.

Tuomilehto, Jaakko, Jaanna Lindstrom, Johan G. Eriksson, Timo T. Valle, and Matti Uusitupa. 2001. "Prevention of Type 2 Diabetes Mellitus By Changes in Lifestyle Among Subjects With Impaired Glucose Tolerance." *N Engl J Med* 344 (18): 1343–50.

Turek, Fred W, Corinne Joshu, Akira Kohsaka, Emily Lin, Ganka Ivanova, Aaron Laposky, Sue Olson, et al. 2005. "Obesity and Metabolic Syndrome in Circadian Clock Mutant Mice." *Science* 308 (5724): 1043–45. https://doi.org/10.1126/science.1108750.Obesity.

Turko, Illarion V., Stephen A. Ballard, Sharron H. Francis, and Jackie D. Corbin. 1999. "Inhibition of Cyclic GMP-Binding Cyclic GMP-Specific Phosphodiesterase (Type 5) by Sildenafil and Related Compounds." *Molecular Pharmacology* 56 (1): 124–30. https://doi.org/10.1124/mol.56.1.124.

Ueda, Hiroki R, Wenbin Chen, Akihito Adachi, Hisanori Wakamatsu, Satoko Hayashi, Tomohiro Takasugi, Mamoru Nagano, et al. 2002. "A Transcription Factor Response Element for Gene Expression during Circadian Night." *Nature* 418 (6897): 534–39. https://doi.org/10.1038/nature00906.

Ueki, Kohjiro, Ritsuko Yamamoto-Honda, Yasushi Kaburagi, Toshimasa Yamauchi, Kazuyuki Tobe, Boudewijn M.Th Burgering, Paul J. Coffer, et al. 1998. "Potential Role of Protein Kinase B in Insulin-Induced Glucose Transport, Glycogen Synthesis, and

Protein Synthesis." *Journal of Biological Chemistry* 273 (9): 5315–22. https://doi.org/10.1074/jbc.273.9.5315.

Uhlén, Mathias, Linn Fagerberg, Björn M Hallström, Cecilia Lindskog, Per Oksvold, Adil Mardinoglu, Åsa Sivertsson, et al. 2015. "Proteomics. Tissue-Based Map of the Human Proteome." *Science (New York, N.Y.)* 347 (6220): 1260419. https://doi.org/10.1126/science.1260419.

Um, Jee Hyun, Shutong Yang, Shin Yamazaki, Hyeog Kang, Benoit Viollet, Marc Foretz, and Jay H Chung. 2007. "Activation of 5'-AMP-Activated Kinase with Diabetes Drug Metformin Induces Casein Kinase Iepsilon (CKIepsilon)-Dependent Degradation of Clock Protein MPer2." *The Journal of Biological Chemistry* 282 (29): 20794–98. https://doi.org/10.1074/jbc.C700070200.

Versteyhe, Soetkin, Christophe Blanquart, Cornelia Hampe, Shaukat Mahmood, Nevena Christeff, Pierre De Meyts, Steven G Gray, and Tarik Issad. 2010. "Insulin Receptor Substrates-5 and -6 Are Poor Substrates for the Insulin Receptor." *Molecular Medicine Reports* 3 (1): 189–93. https://doi.org/10.3892/mmr_00000239.

Vgontzas, A N, D A Papanicolaou, E O Bixler, A Lotsikas, K Zachman, A Kales, P Prolo, et al. 1999. "Circadian Interleukin-6 Secretion and Quantity and Depth of Sleep." *The Journal of Clinical Endocrinology and Metabolism* 84 (8): 2603–7. https://doi.org/10.1210/jcem.84.8.5894.

Vgontzas, A N, M Zoumakis, D A Papanicolaou, E O Bixler, P Prolo, H-M Lin, A Vela-Bueno, A Kales, and G P Chrousos. 2002. "Chronic Insomnia Is Associated with a Shift of Interleukin-6 and Tumor Necrosis Factor Secretion from Nighttime to Daytime." *Metabolism: Clinical and Experimental* 51 (7): 887–92. https://doi.org/10.1053/meta.2002.33357.

Vieira, Elaine, Elena G. Ruano, Ana Lucia C. Figueroa, Gloria Aranda, Dulce Momblan, Francesc Carmona, Ramon Gomis, Josep Vidal, and Felicia A Hanzu. 2014. "Altered Clock Gene Expression in Obese Visceral Adipose Tissue Is Associated with Metabolic Syndrome." *PLOS ONE* 9 (11): e111678. https://doi.org/10.1371/journal.pone.0111678.

Vitaterna, M H, C P Selby, T Todo, H Niwa, C Thompson, E M Fruechte, K Hitomi, et al. 1999. "Differential Regulation of Mammalian Period Genes and Circadian Rhythmicity by Cryptochromes 1 and 2." *Proceedings of the National Academy of Sciences of the United States of America* 96 (21): 12114–19. https://doi.org/10.1073/pnas.96.21.12114.

Vujovic, Nina, Alec J Davidson, and Michael Menaker. 2008. "Sympathetic Input Modulates, but Does Not Determine, Phase of Peripheral Circadian Oscillators." *American Journal of Physiology. Regulatory, Integrative and Comparative Physiology* 295 (1): R355-60. https://doi.org/10.1152/ajpregu.00498.2007.

Wahren, J, P Felig, and L Hagenfeldt. 1978. “Physical Exercise and Fuel Homeostasis in Diabetes Mellitus.” *Diabetologia* 14 (4): 213–22. https://doi.org/10.1007/BF01219419.

Walton, Kevin M, Janis E Lochner, Robert P Rehfuss, Richard H Goodman, and C Chrivia. 1992. “A Dominant Repressor of Cyclic Protein Activity Inhibits the CAMP- Mediated Induction of the Somatostatin Promoter in Viva.” *Molecular Endocrinology*, no. August: 12–14.

Wang, G L, B H Jiang, E A Rue, and G L Semenza. 1995. “Hypoxia-Inducible Factor 1 Is a Basic-Helix-Loop-Helix-PAS Heterodimer Regulated by Cellular O2 Tension.” *Proceedings of the National Academy of Sciences of the United States of America* 92 (12): 5510–14. https://doi.org/10.1073/pnas.92.12.5510.

Wang, Hong, Libin Liu, Jean Z. Lin, Tamar R. Aprahamian, and Stephen R. Farmer. 2016. “Browning of White Adipose Tissue with Roscovitine Induces a Distinct Population of UCP1+ Adipocytes.” *Cell Metabolism* 24 (6): 835–47. https://doi.org/10.1016/j.cmet.2016.10.005.

Wang, Hong Sheng, Zongming Pan, Wenmei Shi, Barry S. Brown, Randy S. Wymore, Ira S. Cohen, Jane E. Dixon, and David McKinnon. 1998. “KCNQ2 and KCNQ3 Potassium Channel Subunits: Molecular Correlates of the M-Channel.” *Science* 282 (5395): 1890–93. https://doi.org/10.1126/science.282.5395.1890.

Wang, Qiong A, Caroline Tao, Rana K Gupta, and Philipp E Scherer. 2013. “Tracking Adipogenesis during White Adipose Tissue Development, Expansion and Regeneration.” *Nature Medicine* 19 (10): 1338–44. https://doi.org/10.1038/nm.3324.

Wang, X-S, M E G Armstrong, B J Cairns, T J Key, and R C Travis. 2011. “Shift Work and Chronic Disease: The Epidemiological Evidence.” *Occupational Medicine (Oxford, England)* 61 (2): 78–89. https://doi.org/10.1093/occmed/kqr001.

Wannamethee, S G, and A G Shaper. 2001. “Physical Activity in the Prevention of Cardiovascular Disease: An Epidemiological Perspective.” *Sports Medicine (Auckland, N.Z.)* 31 (2): 101–14. https://doi.org/10.2165/00007256-200131020-00003.

Watanabe, Akihito, Michiko Ono, Shigenobu Shibata, and Shigenori Watanabe. 1995. “Effect of a Nitric Oxide Synthase Inhibitor, N-Nitro-l-Arginine Methylester, on Light-Induced Phase Delay of Circadian Rhythm of Wheel-Running Activity in Golden Hamsters.” *Neuroscience Letters* 192 (1): 25–28. https://doi.org/https://doi.org/10.1016/0304-3940(95)11599-R.

Watanabe, Kazuto, Tom Deboer, and Johanna H. Meijer. 2001. “Light-Induced Resetting of the Circadian Pacemaker: Quantitative Analysis of Transient versus Steady-State Phase Shifts.” *Journal of Biological Rhythms* 16 (6): 564–73.

https://doi.org/10.1177/074873001129002259.
Weaver, D. R. 1998. “The Suprachiasmatic Nucleus: A 25-Year Retrospective.” *Journal of Biological Rhythms*, no. 13: 100–112.
Wehrli, Natasha E, Gonca Bural, Mohamed Houseni, Khaled Alkhawaldeh, Abass Alavi, and Drew A Torigian. 2007. “Determination of Age-Related Changes in Structure and Function of Skin, Adipose Tissue, and Skeletal Muscle with Computed Tomography, Magnetic Resonance Imaging, and Positron Emission Tomography.” *Seminars in Nuclear Medicine* 37 (3): 195–205. https://doi.org/10.1053/j.semnuclmed.2007.02.002.
Wei, Enhui, Yassine Ben Ali, James Lyon, Huajin Wang, Randy Nelson, Vernon W Dolinsky, Jason R B Dyck, Grant Mitchell, Gregory S Korbutt, and Richard Lehner. 2010. “Loss of TGH/Ces3 in Mice Decreases Blood Lipids, Improves Glucose Tolerance, and Increases Energy Expenditure.” *Cell Metabolism* 11 (3): 183–93. https://doi.org/10.1016/j.cmet.2010.02.005.
Weiland, M., F. Bahr, M. Höuhne, A. Schürmann, D. Ziehm, and H. G. Joost. 1991. “The Signaling Potential of the Receptors for Insulin and Insulin-like Growth Factor I (IGF-I) in 3t3-l1 Adipocytes: Comparison of Glucose Transport Activity, Induction of Oncogene C-fos, Glucose Transporter MRNA, and DNA-synthesis.” *Journal of Cellular Physiology* 149 (3): 428–35. https://doi.org/10.1002/jcp.1041490311.
Weintraub, M, P R Sundaresan, M Madan, B Schuster, A Balder, L Lasagna, and C Cox. 1992. “Long-Term Weight Control Study. I (Weeks 0 to 34). The Enhancement of Behavior Modification, Caloric Restriction, and Exercise by Fenfluramine plus Phentermine versus Placebo.” *Clinical Pharmacology and Therapeutics* 51 (5): 586–94. https://doi.org/10.1038/clpt.1992.69.
Weitzman, E D, D Fukushima, C Nogeire, H Roffwarg, T F Gallagher, and L Hellman. 1971. “Twenty-Four Hour Pattern of the Episodic Secretion of Cortisol in Normal Subjects.” *The Journal of Clinical Endocrinology and Metabolism* 33 (1): 14–22. https://doi.org/10.1210/jcem-33-1-14.
Welsh, David K, Joseph S Takahashi, and Steve A Kay. 2010. “Suprachiasmatic Nucleus: Cell Autonomy and Network Properties.” *Annual Review of Physiology* 72: 551–77. https://doi.org/10.1146/annurev-physiol-021909-135919.
Weyer C, Foley J.E, Borgadus C, Tataranni P.A, and Pratley R.E. 2000. “Enlarged Subcutaneous Adbominal Adipocyte Size, but Not Obesity Itself, Predicts Type II Diabetes Independent of Insulin Resistance.” *Diabetologia* 43: 1498–1506.
Wheaton, Kelin L., Katelin F. Hansen, Sydney Aten, Kyle A. Sullivan, Hyojung Yoon, Kari R. Hoyt, and Karl Obrietan. 2018. “The Phosphorylation of CREB at Serine 133 Is a Key Event for Circadian Clock Timing and Entrainment in the Suprachiasmatic Nucleus.” *Journal of Biological Rhythms* 33 (5): 497–514.

https://doi.org/10.1177/0748730418791713.

White, Morris F. 2003. “Insulin Signaling in Health and Disease.” *Science (New York, N.Y.)* 302 (5651): 1710–11. https://doi.org/10.1126/science.1092952.

Whitt, Joshua P., Jenna R. Montgomery, and Andrea L. Meredith. 2016. “BK Channel Inactivation Gates Daytime Excitability in the Circadian Clock.” *Nature Communications* 7: 1–13. https://doi.org/10.1038/ncomms10837.

Wickenden, Alan D., Weifeng Yu, Anrou Zou, Tim Jegla, and P. Kay Wagoner. 2000. “Retigabine, a Novel Anti-Convulsant, Enhances Activation of KCNQ2/Q3 Potassium Channels.” *Molecular Pharmacology* 58 (3): 591–600. https://doi.org/10.1124/mol.58.3.591.

Williams, Kevin W, Tiemin Liu, Xingxing Kong, Makoto Fukuda, Yingfeng Deng, Eric D Berglund, Zhuo Deng, et al. 2014. “Xbp1s in Pomc Neurons Connects ER Stress with Energy Balance and Glucose Homeostasis.” *Cell Metabolism* 20 (3): 471–82. https://doi.org/10.1016/j.cmet.2014.06.002.

Wilson-fritch, Leanne, Alison Burkart, Gregory Bell, Karen Mendelson, John Leszyk, Sarah Nicoloro, Michael Czech, and Silvia Corvera. 2003. “Mitochondrial Biogenesis and Remodeling during... [Mol Cell Biol. 2003] - PubMed - NCBI” 23 (3): 1085–94. https://doi.org/10.1128/MCB.23.3.1085.

Winter, Jeremiah N., Leonard S. Jefferson, and Scot R. Kimball. 2011. “ERK and Akt Signaling Pathways Function through Parallel Mechanisms to Promote MTORC1 Signaling.” *American Journal of Physiology - Cell Physiology* 300 (5): 1172–80. https://doi.org/10.1152/ajpcell.00504.2010.

Woldt, Estelle, Yasmine Sebti, Laura A Solt, Christian Duhem, Steve Lancel, Jérôme Eeckhoute, Matthijs K C Hesselink, et al. 2013. “Rev-Erb-α Modulates Skeletal Muscle Oxidative Capacity by Regulating Mitochondrial Biogenesis and Autophagy.” *Nature Medicine* 19 (8): 1039–46. https://doi.org/10.1038/nm.3213.Rev-erb-.

Wong, Piu, Masayuki Iwasaki, Tim C.P. Somervaille, Chi Wai Eric So, and Michael L. Cleary. 2007. “Erratum: Meis1 Is an Essential and Rate-Limiting Regulator of MLL Leukemia Stem Cell Potential (Genes and Development (2007) 21, (2762-2774)).” *Genes and Development* 21 (22): 3017. https://doi.org/10.1101/gad.1602107.nate.

Wong, Sok Kuan, Kok Yong Chin, Farihah Hj Suhaimi, Ahmad Fairus, and Soelaiman Ima-Nirwana. 2016. “Animal Models of Metabolic Syndrome: A Review.” *Nutrition and Metabolism* 13 (1): 1–12. https://doi.org/10.1186/s12986-016-0123-9.

Woon, Peng Y, Pamela J Kaisaki, José Bragança, Marie-Thérèse Bihoreau, Jonathan C Levy, Martin Farrall, and Dominique Gauguier. 2007. “Aryl Hydrocarbon Receptor Nuclear Translocator-like (BMAL1) Is Associated with Susceptibility to Hypertension and Type 2 Diabetes.” *Proceedings of the National Academy of Sciences* 104 (36): 14412–17. https://doi.org/10.1073/pnas.0703247104.

Wu, J, L Fang, Q Lin, and W D Willis. 2000. “Fos Expression Is Induced by Increased Nitric Oxide Release in Rat Spinal Cord Dorsal Horn.” *Neuroscience* 96 (2): 351–57. https://doi.org/https://doi.org/10.1016/S0306-4522(99)00534-5.

Wu, Yaling, Dingbin Tang, Na Liu, Wei Xiong, Huanwei Huang, Yang Li, Zhixiong Ma, et al. 2017. “Reciprocal Regulation between the Circadian Clock and Hypoxia Signaling at the Genome Level in Mammals.” *Cell Metabolism* 25 (1): 73–85. https://doi.org/10.1016/j.cmet.2016.09.009.

Wuarin, J., E. Falvey, D. Lavery, D. Talbot, E. Schmidt, V. Ossipow, P. Fonjallaz, and U. Schibler. 1992. “The Role of the Transcriptional Activator Protein DBP in Circadian Liver Gene Expression.” *Journal of Cell Science* 103 (SUPPL. 16): 123–27. https://doi.org/10.1242/jcs.1992.supplement_16.15.

Xiao, Yin X., Ian R. Lanza, James M. Swain, Michael G. Sarr, K. Sreekumaran Nair, and Michael D. Jensen. 2014. “Adipocyte Mitochondrial Function Is Reduced in Human Obesity Independent of Fat Cell Size.” *Journal of Clinical Endocrinology and Metabolism* 99 (2): 209–16. https://doi.org/10.1210/jc.2013-3042.

Xie, Cen, Xiaoxia Gao, Dongxue Sun, Youbo Zhang, Kristopher W. Krausz, Xuemei Qin, and Frank J. Gonzalez. 2018. “Metabolic Profiling of the Novel Hypoxia-Inducible Factor 2α Inhibitor PT2385 in Vivo and in Vitro.” *Drug Metabolism and Disposition* 46 (4): 336–45. https://doi.org/10.1124/dmd.117.079723.

Xie, Cen, Tomoki Yagai, Yuhong Luo, Xianyi Liang, Tao Chen, Qiong Wang, Dongxue Sun, et al. 2017. “Activation of Intestinal Hypoxia-Inducible Factor 2α during Obesity Contributes to Hepatic Steatosis.” *Nature Medicine* 23 (11): 1298–1308. https://doi.org/10.1038/nm.4412.

Xing, L, V K Gopal, and P G Quinn. 1995. “CAMP Response Element-Binding Protein (CREB) Interacts with Transcription Factors IIB and IID.” *The Journal of Biological Chemistry* 270 (29): 17488–93. https://doi.org/10.1074/jbc.270.29.17488.

Xiong L, Catoire H, Dion P, Gaspar C, Lafreniere RG, Girard SL, et al. 2009. “MEIS1 Intronic Risk Haplotype Associated with Restless Legs Syndrome Affects Its MRNA and Protein Expression Levels.” *HumMol Genet* 18: 1065–74.

Xue, Huiling, Zhe Wang, Yongjie Hua, Shanshan Ke, Yao Wang, Junpeng Zhang, Yi Hsuan Pan, Wenjie Huang, David M. Irwin, and Shuyi Zhang. 2018. “Molecular Signatures and Functional Analysis of Beige Adipocytes Induced from in Vivo Intra-Abdominal Adipocytes.” *Science Advances* 4 (7). https://doi.org/10.1126/sciadv.aar5319.

Yamashita, Jun, Hiroshi Itoh, Yoshihiro Ogawa, Naohisa Tamura, Kazuhiko Takaya, Toshio Igaki, Kentaro Doi, et al. 1997. “Opposite Regulation of Gax Homeobox Expression by Angiotensin II and C- Type Natriuretic Peptide.” *Hypertension* 29 (1 II): 381–87. https://doi.org/10.1161/01.hyp.29.1.381.

Yamazaki, S, R Numano, M Abe, A Hida, R Takahashi, M Ueda, G D Block, Y Sakaki, M

Menaker, and H Tei. 2000. “Resetting Central and Peripheral Circadian Oscillators in Transgenic Rats.” *Science (New York, N.Y.)* 288 (5466): 682–85. https://doi.org/10.1126/science.288.5466.682.

Yamazaki, Shin, and Joseph S Takahashi. 2005. “Real-Time Luminescence Reporting of Circadian Gene Expression in Mammals.” In *Circadian Rhythms*, edited by Michael W B T - Methods in Enzymology Young, 393:288–301. Academic Press. https://doi.org/https://doi.org/10.1016/S0076-6879(05)93012-7.

Yang, Han Mo, Baek Kyung Kim, Ju Young Kim, Yoo Wook Kwon, Sooryeonhwa Jin, Joo Eun Lee, Hyun Jai Cho, et al. 2013. “PPARγ Modulates Vascular Smooth Muscle Cell Phenotype via a Protein Kinase G-Dependent Pathway and Reduces Neointimal Hyperplasia after Vascular Injury.” *Experimental and Molecular Medicine* 45 (11): 1–9. https://doi.org/10.1038/emm.2013.112.

Yildiz, Bulent O, Marc A Suchard, Ma-Li Wong, Samuel M McCann, and Julio Licinio. 2004. “Alterations in the Dynamics of Circulating Ghrelin, Adiponectin, and Leptin in Human Obesity.” *Proceedings of the National Academy of Sciences of the United States of America* 101 (28): 10434–39. https://doi.org/10.1073/pnas.0403465101.

Yin, Lei, Nan Wu, Joshua C Curtin, Mohammed Qatanani, Nava R Szwergold, G Bruce Wisely, and Mitchell A Lazar. 2007. “Rev-Erba, a Heme Sensor That Coordinates Metabolic and Circadian Pathways.” *Sience*, no. December: 1786–90.

Yoo, Seung-Hee, Shin Yamazaki, Phillip L Lowrey, Kazuhiro Shimomura, Caroline H Ko, Ethan D Buhr, Sandra M Siepka, et al. 2004. “PERIOD2::LUCIFERASE Real-Time Reporting of Circadian Dynamics Reveals Persistent Circadian Oscillations in Mouse Peripheral Tissues.” *Proceedings of the National Academy of Sciences of the United States of America* 101 (15): 5339–46. https://doi.org/10.1073/pnas.0308709101.

Yoshida, Hiderou, Toshie Matsui, Nobuko Hosokawa, Randal J Kaufman, Kazuhiro Nagata, and Kazutoshi Mori. 2003. “A Time-Dependent Phase Shift in the Mammalian Unfolded Protein Response.” *Developmental Cell* 4 (2): 265–71. https://doi.org/10.1016/S1534-5807(03)00022-4.

Yoshida, Hiderou, Toshie Matsui, Akira Yamamoto, Tetsuya Okada, and Kazutoshi Mori. 2001. “XBP1 MRNA Is Induced by ATF6 and Spliced by IRE1 in Response to ER Stress to Produce a Highly Active Transcription Factor.” *Cell* 107 (7): 881–91. https://doi.org/10.1016/S0092-8674(01)00611-0.

Yu, Chao, Sheng Li Yang, Xiefan Fang, Jian Xin Jiang, Cheng Yi Sun, and Tao Huang. 2015. “Hypoxia Disrupts the Expression Levels of Circadian Rhythm Genes in Hepatocellular Carcinoma.” *Molecular Medicine Reports* 11 (5): 4002–8. https://doi.org/10.3892/mmr.2015.3199.

Yun, Zhong, Heather L. Maecker, Randall S. Johnson, and Amato J. Giaccia. 2002. “Inhibition of PPARγ2 Gene Expression by the HIF-1-Regulated Gene DEC1/Stra13:

A Mechanism for Regulation of Adipogenesis by Hypoxia." *Developmental Cell* 2 (3): 331–41. https://doi.org/10.1016/S1534-5807(02)00131-4.

Zaczek, R, R J Chorvat, J A Saye, M E Pierdomenico, C M Maciag, A R Logue, B N Fisher, D H Rominger, and R A Earl. 1998. "Two New Potent Neurotransmitter Release Enhancers, 10,10-Bis(4-Pyridinylmethyl)-9(10H)-Anthracenone and 10,10-Bis(2-Fluoro-4-Pyridinylmethyl)-9(10H)-Anthracenone: Comparison to Linopirdine." *Journal of Pharmacology and Experimental Therapeutics* 285 (2): 724 LP – 730. http://jpet.aspetjournals.org/content/285/2/724.abstract.

Zaczek, Robert, Robert J Chorvat, and Barry S Brown. 1997. "Linopirdine : Pharmacology of a Neurotransmitter Release Enhancer." *CNS Drug Reviews* 3 (2): 103–19.

Zebisch, Katja, Valerie Voigt, Martin Wabitsch, and Matthias Brandsch. 2012. "Protocol for Effective Differentiation of 3T3-L1 Cells to Adipocytes." *Analytical Biochemistry* 425 (1): 88–90. https://doi.org/https://doi.org/10.1016/j.ab.2012.03.005.

Zhang, Eric E., Yi Liu, Renaud Dentin, Pagkapol Y. Pongsawakul, Andrew C. Liu, Tsuyoshi Hirota, Dmitri A. Nusinow, et al. 2010. "Cryptochrome Mediates Circadian Regulation of CAMP Signaling and Hepatic Gluconeogenesis." *Nature Medicine* 16 (10): 1152–56. https://doi.org/10.1038/nm.2214.

Zhang, Ray, Nicholas F Lahens, Heather I Ballance, Michael E Hughes, and John B Hogenesch. 2014. "A Circadian Gene Expression Atlas in Mammals: Implications for Biology and Medicine." *Proceedings of the National Academy of Sciences of the United States of America* 111 (45): 16219–24. https://doi.org/10.1073/pnas.1408886111.

Zhang, Xiaoqing, Guo Zhang, Hai Zhang, Michael Karin, Hua Bai, and Dongsheng Cai. 2008. "Hypothalamic IKKbeta/NF-KappaB and ER Stress Link Overnutrition to Energy Imbalance and Obesity." *Cell* 135 (1): 61–73. https://doi.org/10.1016/j.cell.2008.07.043.

Zhang, Yiying, Ricardo Proenca, Margherita Maffei, Marisa Barone, Lori Leopold, and Jeffrey M Friedman. 1994. "Positional Cloning of the Mouse Obese Gene and Its Human Homologue." *Nature* 372 (6505): 425–32. https://doi.org/10.1038/372425a0.

Zhong, Hongzhen, Tianbiao Zhou, Hongyan Li, and Zhiqing Zhong. 2018. "The Role of Hypoxia-Inducible Factor Stabilizers in the Treatment of Anemia in Patients with Chronic Kidney Disease." *Drug Design, Development and Therapy* 12: 3003–11. https://doi.org/10.2147/DDDT.S175887.

Zvonic, Sanjin, Andrey A. Ptitsyn, Steven A. Conrad, L. K. Scott, Z. E. Floyd, Gail Kilroy, Xiying Wu, Brian C. Goh, Randall L. Mynatt, and Jeffrey M. Gimble. 2006. "Characterization of Peripheral Circadian Clocks in Adipose Tissues." *Diabetes* 55 (4): 962–70. https://doi.org/10.2337/diabetes.55.04.06.db05-0873.